VOL. I OF II
DOE-NDC-23
NEANDC(US)-209
INDC(USA)-85

PROCEEDINGS OF THE CONFERENCE ON NUCLEAR DATA EVALUATION METHODS AND PROCEDURES

HELD AT
BROOKHAVEN NATIONAL LABORATORY
UPTON, NEW YORK 11973
September 22-25, 1980

March 1981

INFORMATION ANALYSIS CENTER REPORT

NATIONAL NUCLEAR DATA CENTER
BROOKHAVEN NATIONAL LABORATORY
UPTON, NEW YORK 11973

BNL-NCS-51363 VOL. I OF II
DOE/NDC 23
NEANDC(US)-209
INDC(USA)-85
UC-80
(General Reactor Technology - TIC-4500)

PROCEEDINGS OF THE CONFERENCE ON NUCLEAR DATA EVALUATION METHODS AND PROCEDURES

HELD AT
BROOKHAVEN NATIONAL LABORATORY
UPTON, NEW YORK 11973
September 22-25, 1980

Conference Chairman:
R.J. Howerton
Lawrence Livermore National Laboratory

Proceedings Editors:
B.A. Magurno and S. Pearlstein
Brookhaven National Laboratory

March 1981

JOINTLY SPONSORED BY THE DIVISION OF HIGH ENERGY AND NUCLEAR PHYSICS,
DIVISION OF REACTOR RESEARCH AND TECHNOLOGY, AND OFFICE OF FUSION ENERGY
OF THE UNITED STATES DEPARTMENT OF ENERGY,
AND BY THE
ELECTRIC POWER RESEARCH INSTITUTE

NATIONAL NUCLEAR DATA CENTER

BROOKHAVEN NATIONAL LABORATORY

ASSOCIATED UNIVERSITIES, INC

UNITED STATES DEPARTMENT OF ENERGY

PREFACE

The Conference on Nuclear Data Evaluation Methods and Procedures organized under the auspices of the Division of High Energy and Nuclear Physics, the Division of Reactor Research and Technology, and the Office of Fusion Energy, of the U.S. Department of Energy and the Electric Power Research Institute (EPRI) was held at Brookhaven National Laboratory, Sept. 22-25, 1980. The Proceedings are presented in these volumes. The Conference was held in the format of a workshop in which review papers were presented by particularly knowledgeable persons in each aspect of nuclear data evaluation. Following each review paper there was a discussion period which proved, in most cases, to be lively.

Both written versions of the reviews and transcribed versions of the discussion periods are included in this report. It is hoped that it will serve the double purpose of describing the state-of-the-art and of providing a handbook of methods that can be referred by both experienced and new evaluators.

The organization and implementation of this conference required a large amount of work on the part of many persons. Quite clearly, the success of the effort depended primarily upon the reviewers who provided the technical substance. The organizing committee, made up of the session chairman, selected the reviewers so an acknowledgment of their efforts is likewise appropriate. A special word of thanks is due to Dr. J.J. Schmidt of the IAEA Nuclear Data Section who provided a masterful summary of each day's discussion as the last item on the day's program.

On the first evening of the meeting there was a "mixer" and a banquet was held at the end of the second day. Our after-dinner speaker, Professor H.H. Barschall, recounted his personal experiences during the early days of discovery of the fission process and his subsequent experiences with the Manhatten District Project.

The National Nuclear Data Center of Brookhaven National Laboratory was the host organization for the conference. Dr. Sol Pearlstein, Director of the NNDC, and his staff provided excellent support to the participants by taking care of the details of travel and housing, by insuring that the session were taped and by obtaining the use of the excellent auditorium in Berkner Hall.

Finally, I extend my personal thanks and those of the organizing committee to Mr. Benjamin Magurno of the NNDC. He handled the myriad of tasks associated with announcing the conference, pre-registration, organization of the banquet, and editing and expediting the publication of these proceedings.

Robert J. Howerton, Chairman
Livermore, California

TABLE OF CONTENTS

ORGANIZING COMMITTEE

R.J. Howerton, Chairman	LLNL
T.R. England	LANL
H. Henryson, II	ANL
S.F. Mughabghab	BNL
R.W. Peelle	ORNL
R.E. Schenter	HEDL
F. Schmittroth	HEDL
A.B. Smith	ANL
P.G. Young	LANL

LIST OF ATTENDEES

R.A. Anderl, EG&G
E.D. Arthur, LANL
H.H. Barschall, WIS
M.R. Bhat, BNL
R.C. Block, RPI
R.L. Bunting, EG&G
R.F. Chrien, BNL
L. Carter, HEDL
P. Collins, ANL
C.L. Cowan, GE-SU
C.L. Dunford, BNL
C. Durston, BNL
T.R. England, LANL
F. Froehner, KFK
C.Y. Fu, ORNL
M.A. Gardner, LLNL
Y. Gohar, ANL
L. Greenwood, ANL
H. Gruppelaar, ECN
F.T. Guenther, ANL
G.H. Hale, LANL
H. Henryson, II., ANL
R.J. Howerton, LLNL
G. Kegel, U of Lowell
Ch. Lagrange, BRC
D. Larson, ORNL
H. Lemmel, IAEA
H. Liou, BNL
R.C. Little, LANL
M.A. Lone, CRC
C.R. Lubitz, KAPL
R. MacFarlane, LANL
B.A. Magurno, BNL
D.G. Madland, LANL
J.H. Marable, ORNL
M. Mattes, USTUT
E. Menapace, CNEN
G.H. Miley, UI
P.A. Moldauer, ANL
M.S. Moore, LANL
S.F. Mughabghab, BNL
D. Nethaway, LLNL
D. Oberg, HEDL
O. Ozer, EPRI
B. Patrick, HAR
S. Pearlstein. BNL
R.W. Peelle, ORNL
F.G.J. Perey, ORNL
C. Philis, BRC
W.P. Poenitz, ANL
P. Reeder, BNWL
C.W. Reich, EG&G
B.F. Rider, GE-V
J. Rowlands, WIN
J.J. Schmidt, IAEA
F. Schmittroth, HEDL
R. Sher, STAN
A.B. Smith, ANL
L. Stewart, ORNL
H. Takahashi, BNL
N. Tubbs, NEADB
R.J. Tuttle, RI-AI
H. Vonach, IRK
H. Weigmann, CBNM
L. Weston, ORNL
N. Yamamuro, TIT
P.G. Young, LANL

SESSION I

PROCESSING NEEDS AND CONSTRAINTS
Chairman: H. Henryson, II. ANL

This session was presented in a panel format followed by a question and answer period. The panelists were:

Y. Gohar	ANL
R. MacFarlane	LANL
L. Carter	HEDL
O. Ozer	EPRI
J. Rowlands	WIN

Written summaries from the panelists* and the question and answer period follow.

*No written contribution from Y. Gohar, ANL.

PROCESSING NEEDS AND CONSTRAINTS: NEUTRON DATA PROCESSING

R. E. MacFarlane

Los Alamos Scientific Laboratory, University of California
Theoretical Division
Los Alamos, New Mexico 87545

ABSTRACT

New applications for processed data and increased accuracy requirements have generated needs for change in the Evaluated Nuclear Data Files (ENDF). Some constraints must be removed to allow this growth to take place, but other strong constraints must remain to protect existing users.

ENDF/B started life as a system oriented toward reactor applications, and this philosophy produced a very compact and useful set of files. Its success attracted more applications, and it grew more complex. Although some users find the current version too large, there are three forces acting which will cause the growth of the files to continue. First, the need for increased accuracy (e.g., heating, iron deep penetration); second, new applications (e.g., particle-beam therapy, fusion reactor radiation damage); and third, advanced evaluation methods based on nuclear models which produce more complete, detailed, and consistent information. Our problem during the next few years will be to remove enough constraints to allow ENDF to meet these needs without destroying the usefulness of the files for the old users.

These constraints can be divided into three classes. The first class is the "bookkeeping" constraints such as a maximum of 5000 energy points per section or a maximum of 20 Legendre coefficients for an angular distribution. These rules are designed to protect the memory allocation of the processing codes. Even with sophisticated memory management techniques such as paging, dynamic storage allocation, and parallel data streams, some such restrictions are needed. An apparent need to violate one of

these restrictions may result from an inappropriate representation (e.g., point cross sections instead of reasonance parameters) or reflect the need for a new representation (e.g., for diffraction scattering at 20 MeV).

The second class is the "representation" constraints. These are the much more important limitations resulting from the inability to describe a physical process using an ENDF/B format. Sometimes such limitations can be circumvented. An example is the use of "pseudo levels" to represent continuous energy-angle distributions for inelastic scattering. But if ENDF is to meet the needs of the next few years, some of the existing constraints are going to have to be removed by defining new formats. Some of the important problems are discussed below.

Fission Spectrum — A new representation is now available for the energy distribution of fission neutrons as a function of incident neutron energy. The spectrum could be approximated with Watt parameters, entered as a large tabulation, or represented by a new "law." The results should be very important for fission reactors.

Interpolation of Distributions — Two-dimensioned interpolation along the E and E' axes of an energy distribution often gives poor results unless many closely spaced E values are used. A contour scheme or a transformation to better axes might solve the problem.

Energy-Angle Distributions — The correlation of the energy and angle of secondary particles can be measured or estimated using model codes which account for direct processes. Since this effect is important for fast neutron transport, heating, and radiation damage, methods to incorporate energy-angle effects into ENDF should be developed.

Resonance Scattering — Current ENDF/B resonance parameters cannot be used to compute the angular distributions of elastically scattered neutrons. The introduction of an amplitude format might solve this problem and improve the calculation of the transport of fission-spectrum neutrons through iron, nickel, and chromium.

Unresolved Resonance Cross Sections and Covariances — This region is very important for fast reactors, but the cross sections are difficult to compute, and the covariances are not currently defined. Changing to a probability table representation would solve these problems and also improve the consistency between multigroup and Monte Carlo.

Diffraction Scattering — At high energies, elastic and discrete-inelastic angular distributions show strong diffraction

patterns, and many Legendre coefficients are required to represent the distributions. This causes severe problems for multigroup processing codes. Perhaps a new representation could be found which would remove the diffraction part of the scattering and treat it separately, leaving a well-behaved remainder to be represented by the Legendre expansion.

Distributions for Charged Particles — The modern model codes often produce spectra for each product of a neutron reaction, and the distribution of recoils can sometimes be deduced. Most of this information is now lost. If formats for these distributions were added to ENDF, improved heating, damage, and biomedical calculations would be possible.

The third class of constraints is the "judgment" constraints. These are the constraints that can't be quantified and force the evaluator to make tradeoffs between conflicting demands. They can be stated as three rules designed to ensure that ENDF remains an application oriented system.

THE RULE OF CHANGE

Don't make a change in data or formats unless test calculations show that the change will lead to a significant improvement for at least one of the important ENDF applications.

THE RULE OF SIZE

Always use the most compact repesentation available, and don't add detail unless test calculations show that it is needed for one of the important applications.

THE RULE OF CONSISTENCY

Try to satisfy conservation principles, sum rules, and ratio tests. If an answer can be obtained using two different combinations of data from the file, the results should be as equivalent as possible.

Observing these rules will lead to more work for evaluators, processors, and data testors. But it will help to protect the user; after all, "THE CUSTOMER IS KING."

POINT MONTE CARLO DATA NEEDS AND CONSTRAINTS

L. L. Carter

Hanford Engineering Development Laboratory
Westinghouse Hanford Company
Richland, Washington 99352, U.S.A.

ABSTRACT

The utilization of neutron and photon cross section data in pointwise Monte Carlo codes is discussed. As nuclear data files become more prolific, memory requirements for typical problems can exceed that available on modern computers. Evaluators and processors of the cross sections must work together to provide high quality cross sections for the user community without exceeding memory requirements.

INTRODUCTION

General purpose Monte Carlo computer codes are routinely being used to solve a wide variety of neutron and photon transport problems [1-9]. Pointwise cross section libraries based upon reliable nuclear data files, such as ENDF/B and ENDL, makes possible the confident utilization of these codes. The fine structure detail included in the data files, the large number of nuclei for which rather complete neutron cross section information exists, and the overall accuracy allows one standard library (a pointwise Monte Carlo library derived using ENDF/B and ENDL) to satisfy a large user community. The ideal is to minimize concerns about the cross sections so that the users can focus their effort upon the important engineering and physics problems.

The flexibility and reliability introduced by the recent ENDF/B-V master data file is not free from user difficulties, however. A pointwise library based upon an accurate representation of ENDF/B-V is impractical if a typical problem will not fit into the available memory of the modern computer. Furthermore, the larger the data base, the more difficult and time consuming is the checking of the data. This limitation applies not only to the experimenters, evaluators, and guardians of the ENDF/B data base, but also to those who develop and use the cross section processor and Monte Carlo computer codes. While simple integral checks with

the Monte Carlo code are very important, they are not sufficient in themselves to verify that the data being used in the final product are a satisfactory representation of the ENDF/B data and are being used correctly.

In addition to the sheer size of current libraries, users of pointwise Monte Carlo computer codes experience other nuclear data limitations. For nuclear heat deposition from neutron and photon interactions, the calculation depends upon consistent energy balances so that neutron KERMA factors and gamma production cross sections adequately conserve energy. From a Monte Carlo code user viewpoint, energy balances are often inadequate [9] even for cross section libraries derived from ENDF/B-V [10]. Another problem brought to my attention is related to the prescribed interpolation and extrapolation of data in the ENDF/B files--specifically, $S(\alpha,\beta)$ data. Of course, users continue to experience the usual limitations, and perhaps always will, in the experimental accuracy and/or availability of the nuclear data for their particular application.

A constant source of frustration is the long lapse of time between the measurement or sophisticated calculation of cross section information and the actual availability of the data in the pointwise Monte Carlo cross section library. Large, accurate nuclear data bases often seem to mitigate against the rapid use of new or revised data to solve current engineering problems.

The following sections expand upon these limitations and user frustrations. Although this is intended to be a constructive criticism, it fails to adequately address the positive aspects. The user community is indebted to those who labor faithfully to assure that the nuclear data base and the codes that use this data base are of the highest quality that is practical within budget constraints.

PROLIFERATION OF DATA

Discussion

In many problems the user of a Monte Carlo code could attain sufficient accuracy with a rather small amount of nuclear data. Fine structure detail in the cross section data base and an accurate treatment of the energy-angle distributions at collisions may be unnecessary. However, the user typically does not have the time and may not have the expertise to verify that a collapsed cross section set is appropriate. Thus, the availability of a large pointwise cross section library satisfies broad needs even though computer memory requirements tend to be excessive.

Practical considerations demand a balance between an unrestrained increase in the size of the nuclear data base on the one hand and overrestriction on the other. This balance was addressed in the literature years ago for Monte Carlo utilization of ENDF/B-III and ENDL data [11]. Here I summarize some recent

experience at Los Alamos Scientific Laboratory (LASL) in the generation of a pointwise cross section library from ENDF/B-V for use in the MCNP [4] Monte Carlo code. My thanks to Dr. Bob Seamon and Dr. Pat Soran of Group X-6 and Dr. Bob MacFarlane of Group T-2 at LASL for supplying this information.

Example of Pointwise Library from ENDF/B-V

A pointwise library encompassing 68 nuclides was generated using a module of the NJOY processor code [12]. The 68 nuclides, the ENDF/B MAT numbers, the number of energies for the linear-linear cross section tabulation, and the length (decimal) of each cross section set in the pointwise library are given in the first four columns of Table I. The total length of the pointwise library, as given by the sum of column four, is 3,130,345 decimal words. This total length is disturbing in the sense that typical problems utilizing ten to twenty-five of these nuclides will not directly fit into rather large computer memories; for example, large and small core on a CDC-7600. Hence, we are forced to either (1) thin the data, (2) use a computer with a larger memory, (3) pack more than one cross section per computer word, (4) resort to multigroup averaging, or (5) utilize an older data base.

Of the above possibilities, option (2) is expensive and is only available to users at a few laboratories; option (3) is possible although it introduces a variety of complications; and option (5) is clearly undesirable as a long term solution. Unfortunately, option (1), thinning the data, takes out some of the fine structure that evaluators and experimenters have worked so hard to put in the ENDF/B-V files. Since this thinning must be done for most of the 68 nuclides, an automated method is needed to thin in contrast to careful tailoring of the thinning to each nuclide--a budgetary limitation. This is a practical dilemma and is one reason why too much detail in the files is sometimes self-defeating.

Before addressing the results of a thinning procedure, the ENDF/B-V based pointwise cross section file is compared to an older (primarily ENDF/B-IV and ENDL based) pointwise file with lengths summarized in the fifth column of Table I. Length comparisons between columns four and five of Table I are summarized in Table II with major conclusions as follows:

- There are eight nuclides of total length 454,490 which were not available on the old file. However, there are 17 materials on the old file for which there are no corresponding cross section sets on the new file--a total length increase of -179,706 words. Hence, it is apparent that the total length increase going from old to new of 2,239,598 words is not dominated by differing nuclides on the files.
- Natural Eu and Gd have been replaced by isotopic representations on the new file with a net increase of 503,218 words.
- There are seven nuclides whose cross section representations increased in length by a factor of ten or more producing a

total length increase of 458,746 words.

- There are five nuclides which increased in length by a factor of five to ten with a total length increase of 248,294 words.
- There are six nuclides which increased in length by a factor of three to five with a total length increase of 442,558 words.
- There are eight nuclides which increased in length by a factor of two to three with a total length increase of 209,943 words.
- There are twenty-three nuclides which increased in length by factors of less than two for a total length increase of 102,055 words.

It is clear from the above that the large increase in the length of the new ENDF/B-V based pointwise Monte Carlo library is not due to just a few nuclides. Rather there is a general across-the-board increase, although certain isotopes are more crucial than others. The elaborate resonance parameterization in the newer ENDF/B data bases results in many points when the data are presented in tabular form. To further compound the problem, the angular distributions continue to increase in size.

The NJOY code was also used with a thinning algorithm to thin cross sections in such a way that the resonance integral of ENDF/B-V was changed by no more than one-half a percent. Angular distributions were also thinned. The result of the thinning is shown in the seventh column of Table I. The total file length after thinning is 1,076,418 which compares favorably with the length of the older file. However, the penalty is that one is now inflicted with the concern that inaccuracies may have been introduced for some user applications and this thinned cross section file has strayed away somewhat from the ENDF/B-V data base. Nevertheless practicality must play a role in such decisions.

We mentioned previously that another possible option is to resort to multigroup averaging. This option has also been exercised at LASL and is shown in the last column of Table I for a 240 energy group structure. This is actually a hybrid between a pointwise and a pure multigroup treatment in that the cross sections are collapsed into groups, but the angular distributions and inelastic energy laws are treated in a continuous energy fashion. Of course, multigrouping has definite limitations for problems where the resonance structure is important [13].

The 1979 version of the ENDL library is more compact than ENDF/B-V so that length considerations of pointwise libraries generated from ENDL are not such a problem. Nuclide lengths of a pointwise library generated from the 1979 ENDL tended to be even shorter than the corresponding thinned pointwise library based on ENDF/B-V.

Data Checking

As library files increase in length the manpower and computer effort required to adequately check the reliability of these

libraries also increases. Pointwise Monte Carlo libraries must be compared with the original ENDF/B or ENDL data base using both differential and integral checks. It is possible to make rather powerful integral checks by running simple problems with the Monte Carlo code. For example, in the regime of nuclear heat deposition, coupled neutron-gamma problems in an infinite one-nuclide media with monoenergetic neutron sources can be made to compare nuclear heat deposition to that obtained by mass and energy balances. However, there is a practical limit to the number of such integral tests that can be made so differential data checking must play a dominant role. A good summary is presented on pages 34-38 of Reference 14 for differential data checking techniques utilized with the MCNP code libraries.

NUCLEAR HEAT DEPOSITION

Energy balance problems within ENDF/B are being addressed and options are being provided in processor codes [10] to provide the Monte Carlo user with the best possible data. In recent cross section evaluations special care has been taken to assure adequate energy balances. A recent iron evaluation provides a good example [15]. It is important that evaluators and code developers continue to work together to resolve this energy balance problem.

In the context of appropriate energy balances within the microscopic data base, I would like to quote from page 44 of Reference 16 stating a philosophy for ENDL:

> "Since the difference between total energy deposit and local energy deposit represents the energy carried away by gamma rays, there is clearly a close relationship between the nonlocal energy deposit and the photon production data. To insure calculational consistency between these quantities, energy deposits are used as input data for calculating the photon production cross sections and spectra."

EXTENDING THE SCOPE OF ENDF/B

Fission reactor design provided much of the incentive for improvements in the nuclear data base for neutron energies below ~10 MeV. Fusion reactor research has subsequently provided the need to improve cross sections at somewhat higher energies culminating in ENDF/B-V for neutron energies up to 20 MeV. For many years there has been some interest in extending the energy regime of ENDF/B even higher. Neutronics [9] for the Fusion Materials Irradiation Test (FMIT) facility [17] has recently led to a renewed interest in neutron cross sections up to ~50 MeV (see Proceedings of a Symposium on Neutron Cross Sections from 10-50 MeV held at Brookhaven National Laboratory, May 12-14, 1980). This accelerator-based facility, now in the early stages of construction at Hanford,

will provide high fluences in a fusion-like radiation environment for the testing of materials.

SPECIFIC CROSS SECTION NEEDS

While a comprehensive discussion of cross section needs is beyond the scope of this paper, I will mention a few that have come to my attention.

Table I shows the nuclides for which photon production data exists in ENDF/B-V. Clearly the absence of photon production data for 22 out of these 68 nuclides is a definite limitation in some user applications.

The Mathematical Applications Group, Inc. (MAGI) would like to see some more work on the $S(\alpha,\beta)$ files and clarification of their use.* Specifically, for extreme values of α and β the tabulation is too coarse and interpolation rules are not adequate. There is also a singularity at $\alpha=0$, $\beta=0$ for which extrapolation rules should be provided.

The long string of interfaces

Experimentalists (measure cross sections)
↓
Evaluators (calculate and prepare cross sections for ENDF/B
↓ or ENDL)
Master File Guardians (OK cross sections for ENDF/B or ENDL
↓ and maintain file)
Code Processors (generate pointwise Monte Carlo library)
↓
Pointwise File Guardians (check data in pointwise file and
↓ OK data)
Monte Carlo Code Developers (adapt Monte Carlo code to cross
↓ section format and check code)
User

before the user can apply the original data from experimentalists and/or evaluators on current engineering problems implies a long time span. Efforts should be made to reduce this time span and provide short cuts prior to releases of new ENDF/B versions.

ACKNOWLEDGMENTS

My thanks to Dr. Bob Seamon, Dr. Pat Soran and Dr. Bob MacFarlane for supplying information on their experience in the generation of pointwise cross section libraries from ENDF/B-V. I would also like to thank Dr. Herb Steinberg for his comments on the $S(\alpha,\beta)$ data in ENDF/B.

*Telephone conversation with Dr. Herb Steinberg.

REFERENCES

1. L. L. CARTER et al., "Monte Carlo Applications at Hanford Engineering Development Laboratory", HEDL-SA-2072, Proceedings of a Seminar-Workshop on Theory and Application of Monte Carlo Methods, held at Oak Ridge, Tennessee, April 21-23, 1980. Published as ORNL/RSIC-44.

2. L. L. CARTER, "General Purpose Monte Carlo Codes and Applications", Trans. Am. Nucl. Soc., 27, 366 (1977).

3. L. L. CARTER and E. D. CASHWELL, "Particle Transport Simulation with the Monte Carlo Method", TID-26607, ERDA Critical Review Series, U. S. Energy Research and Development Administration, Technical Information Center, Oak Ridge, TN (1975).

4. LASL GROUP X-6, "MCNP - A General Monte Carlo Code for Neutron and Photon Transport", LA-7396-M, Los Alamos Scientific Laboratory, Los Alamos, NM (Revised November 1979).

5. R. N. BLOMQUIST, R. M. LELL, and E. M. GELBARD, "VIM - A Continuous Energy Monte Carlo Code at ANL", Proceedings of a Seminar-Workshop on Theory and Application of Monte Carlo Methods, held at Oak Ridge, Tennessee, April 21-23, 1980. Published as ORNL/RSIC-44.

6. H. STEINBERG and E. S. TROUBETZKOY, "Monte Carlo Methodology as Implemented in SAM-CE", Proceedings of a Seminar-Workshop on Theory and Application of Monte Carlo Methods, held at Oak Ridge, Tennessee, April 21-23, 1980. Published as ORNL/RSIC-44.

7. W. L. THOMPSON and E. D. CASHWELL, "The Status of Monte Carlo at Los Alamos", Proceedings of a Seminar-Workshop on Theory and Application of Monte Carlo Methods, held at Oak Ridge, Tennessee, April 21-23, 1980. Published as ORNL/RSIC-44.

8. A. BAUR et al., "Overview of TRIPOLI 2", Proceedings of a Seminar-Workshop on Theory and Application of Monte Carlo Methods, held at Oak Ridge, Tennessee, April 21-23, 1980. Published as ORNL/RSIC-44.

9. L. L. CARTER, R. J. MORFORD, and A. D. WILCOX, "Nuclear Data Relevant to Shield Design of FMIT Facility", HEDL-SA-2146. An invited review paper, Proceedings of a Symposium on Neutron Cross Sections from 10-50 MeV, held at Brookhaven National Laboratory, May 12-14, 1980.

10. R. E. MACFARLANE, "Energy Balance of ENDF/B-V", Trans. Am. Nucl. Soc., 33, 681 (1979).

11. E. D. CASHWELL and E. F. PLECHATY, "Specification and Testing of Nuclear Data Required for Monte Carlo Transport Calculations", Nucl. Sci. Eng., 49, 394 (1972).

12. R. E. MACFARLANE et al., "The NJOY Nuclear Data Processing System: User's Manual", LA-7584-M, Los Alamos Scientific Laboratory, Los Alamos, NM (December 1978).

13. J. S. HENDRICKS and L. L. CARTER, "Computational Benchmark for Neutron Penetration in Iron", accepted by Nuclear Science and Engineering for publication.

14. P. D. SORAN, Editor, "X-6 Activity Report July-December 1979", LA-8232-PR, Los Alamos Scientific Laboratory, Los Alamos, NM (February 1980).

15. E. D. ARTHUR and P. G. YOUNG, "Evaluation of Neutron Cross Sections to 40 MeV for ^{54,56}Fe", Proceedings of a Symposium on Neutron Cross Sections from 10-50 MeV, held at Brookhaven National Laboratory, May 12-14, 1980.

16. R. J. HOWERTON et al., "The LLL Evaluated Nuclear Data Library (ENDL): Evaluation Techniques, Reaction Index, and Description of Individual Evaluations", UCRL-50400, Vol. 15, Part A, Lawrence Livermore Laboratory (September 1975).

17. E. W. POTTMEYER, JR., "The Fusion Materials Irradiation Test Facility at Hanford", Journal of Nuclear Materials, 85 & 86, 463-465 (1979).

TABLE I

LENGTHS OF POINTWISE MONTE CARLO LIBRARIES

Material or Nuclide	ENDF/B-V MAT No.	Number Energy Points	Length (ENDF/B-V)	Length (ENDF/B-IV and ENDL)	Gamma Production	Length Thinned (ENDF/B-V)	Length with 240 Groups (ENDF/B-V)
H-1	1301	244	2,532	2,459	Yes	2,532	2,511
H-2	1302	214	3,736	3,007	Yes	3,666	3,950
H-3	1169	184	2,418	2,114	No	2,383	2,695
He-3	1146	229	1,834	1,517	No	1,824	1,916
He-4	1270	345	3,102	2,407	No	2,682	3,829
Li-6	1303	373	8,827	8,294	Yes	8,105	6,951
Li-7	1272	343	4,496	3,751	Yes	4,496	3,647
Be-9	1304	329	8,528	7,883	Yes	7,654	7,965
B-10	1305	514	13,563	9,241	Yes	12,206	7,241
B-11	1160	487	4,324	5,134	No	4,132	2,629
C-	1306	875	19,902	8,309	Yes	19,578	13,263
N-14	1275	1,196	30,048	21,553	Yes	29,959	17,363
O-16	1276	1,390	29,820	21,823	Yes	29,836	17,231
F-19	1309	1,568	26,955	24,464	Yes	24,419	11,189
Na-23	1311	2,702	45,916	6,816	Yes	42,539	20,847
Mg-	1312	2,429	48,805	3,771	Yes	42,080	9,792
Al-27	1313	2,028	31,144	32,517	Yes	30,433	9,968
Si-	1314	2,440	58,369	21,632	Yes	48,769	25,124

TABLE I (continued)

Material or Nuclide	ENDF/B-V MAT No.	Number Energy Points	Length (ENDF/B-V)	Length (ENDF/B-IV and ENDL)	Gamma Production	Length Thinned (ENDF/B-V)	Length with 240 Groups (ENDF/B-V)
P-31	1315	326	4,536	2,842	Yes	4,536	4,044
S-32	1316	363	4,895	3,252	Yes	4,887	3,962
Cl-	1149	1,498	19,190	38,371	Yes	17,098	7,382
K-	1150	1,241	16,583	7,436	Yes	13,724	7,165
Ca-	1320	2,394	39,830	24,085	Yes	31,820	11,197
Ti-	1322	4,434	44,858	10,644	Yes	24,570	6,562
V-	1323	2,265	26,823	6,456	Yes	23,427	5,264
Cr-	1324	11,050	125,671	38,240	Yes	49,196	27,793
Mn-55	1325	12,524	100,046	3,586	Yes	21,579	7,179
Fe-	1326	10,957	105,390	54,104	Yes	65,090	25,205
Co-59	1327	14,501	109,979	*	Yes	21,847	6,816
Ni-	1328	8,926	122,084	35,192	Yes	80,918	17,852
Zr-	1340	7,944	51,941	10,312	No	16,693	5,166
Nb-93	1189	17,278	125,234	29,725	Yes	10,958	6,281
Mo-	1321	4,260	31,894	5,715	Yes	6,400	3,755
Cd-	1281	2,981	19,595	7,690	No	6,615	2,809
Ba-138	1353	292	4,079	2,606	Yes	4,067	3,854

TABLE 1 (continued)

Material or Nuclide	ENDF/B-V MAT No.	Number Energy Points	Length (ENDF/B-V)	Length (ENDF/B-IV and ENDL)	Gamma Production	Length Thinned (ENDF/B-V)	Length with 240 Groups (ENDF/B-V)
Eu-151	1357	5,465	54,275	3,133	Yes	12,236	6,015
Eu-152	1292	4,553	39,836		No	9,009	4,776
Eu-153	1359	4,636	42,461		Yes	10,539	6,345
Eu-154	1293	4,030	32,289		No	8,952	4,702
Gd-152	1362	3,285	25,793	3,206	No	10,473	5,574
Gd-154	1364	7,167	49,130		No	11,040	5,609
Gd-155	1365	6,314	44,576		No	11,491	6,185
Gd-156	1366	3,964	33,310		No	10,542	5,698
Gd-157	1367	5,370	38,592		No	10,941	6,016
Gd-158	1368	15,000	95,568		No	11,626	5,522
Gd-160	1370	8,229	53,727		No	9,719	4,760
Ta-181	1285	6,341	49,246	18,114	Yes	10,051	5,964
Au-197	1379	23,563	145,013	19,844	No	12,187	4,675
Pb-	1382	1,186	29,858	21,052	Yes	24,331	16,568
Th-232	1390	17,901	149,980	31,235	Yes	14,534	8,566
Pa-233	1391	2,915	19,560	*	No	5,682	3,609
U-233	1393	2,293	18,856	7,945	No	7,754	4,059
U-234	1394	12,430	89,474	3,008	No	6,467	4,720
U-235	1395	5,724	56,283	18,385	Yes	21,619	7,834
U-236	1396	19,473	138,756	3,153	No	7,343	4,725
U-237	8237	3,293	28,794	2,478	Yes	6,666	4,456
U-238	1398	9,285	85,721	32,895	Yes	20,591	12,890

TABLE I (continued)

Material or Nuclide	ENDF/B-V MAT No.	Number Energy Points	Length (ENDF/B-V)	Length (ENDF/B-IV and ENDL)	Gamma Production	Length Thinned (ENDF/B-V)	Length with 240 Groups (ENDF/B-V)
Np-237	1337	8,519	63,264	*	No	9,787	5,154
Pu-238	1338	2,301	18,804	2,588	No	6,108	5,291
Pu-239	1399	7,808	71,109	25,417	Yes	15,952	9,020
Pu-240	1380	6,548	56,476	41,821	Yes	12,700	6,510
Pu-241	1381	3,744	34,412	3,443	Yes	9,227	6,967
Pu-242	1342	7,635	66,983	*	Yes	11,273	7,622
Am-241	1361	4,419	38,771	*	Yes	9,065	6,218
Am-242m**	1369	323	6,539	5,777	Yes	6,453	6,329
Am-243	1363	11,920	87,625	*	Yes	9,297	6,961
Cm-242	8642	3,112	26,650	*	Yes	5,520	4,152
Cm-244	1344	4,918	41,658	*	Yes	6,515	4,680
TOTALS			3,130,345	890,747		1,076,418	528,569

* Not available on older file.

** Cross sections for Am-242m, the metastable isomer of Am-242, with half-life ≈152 years.

TABLE II

LENGTH INCREASES ENCOUNTERED WITH ENDF/B-V

Source of Increase	Increase
New Nuclides	454,490
Eu + Gd Isotopic Instead of Elemental	503,218
Nuclide Length Increase Factor >10	458,746
Nuclide Length Increase Factor 5-10	248,294
Nuclide Length Increase Factor 3-5	442,558
Nuclide Length Increase Factor 2-3	209,943
Nuclide Length Increase Factor <2	102,055
Missing Nuclides	-179,706
	2,239,598 Words

COMPATIBILITY OF DETAILED EVALUATIONS WITH LWR APPLICATIONS

O. Ozer

Electric Power Research Institute
Palo Alto, California 94304

In typical Light Water Reactor (LWR) applications detailed evaluated data files are only used after a considerable amount of data reduction and processing. Evaluated files are processed into a multigroup library in general containing of the order of 100 groups. The selection of the weighting spectrum, energy grid structure and the preparation of resonance shielding factors make such multi-group libraries optimized for thermal reactor applications but not necessarily limited to a single type of reactor such as a BWR or a PWR. For a particular reactor, the multi-group data is further averaged over space, collapsed in energy and parameterized as a function of burnup, temperature, proximity of control rods, moderator characteristics, etc.

The accuracy of reactor calculations is dependent on the data reduction procedures as much as it is dependent on the basic data itself.

The data reduction procedure, can be considered to be a "second order evaluation" providing a bridge between the basic "detailed" evaluation and the expected end use. It requires intimate knowledge of the basic evaluation features and a determination of the importance of these features on the expected application. An example of such an effort can be seen in the Los Alamos work by T. England et. al., in which the very extensive fission product information contained in the last two versions of ENDF/B was reduced into a dozen linearized chains shown to be adequate for a wide range of LWR applications.

This two-level approach requires the basic evaluated data files to be prepared as an application-independent, general purpose master data library that will provide sufficient amount of detail in energy ranges and data types of interest to many different types of applications. Recent advances in computer efficiency and storage capabilities make the imposition of arbitrary size limitations unnecessary for the master data libraries. However more flexible reduction programs may be

required to eliminate the detail considered to be insignificant for a particular range of applications, while preserving the more important features.

The amount of detail and the extent of information provided in the ENDF/B version V library seem to be adequate for most LWR needs. However the presence of detail does not necessarily imply accuracy. A number of questions relating to the use of ENDF/B-V as a production library for fuel cycle optimization, reload licensing and accident analysis remain.

USE OF EVALUATED DATA FILES IN CROSS-SECTION ADJUSTMENT

J L Rowlands

United Kingdom Atomic Energy Authority
Atomic Energy Establishment
Winfrith, Dorchester, England

ABSTRACT

Cross-section adjustment is a way of predicting reactor properties taking into account both differential cross-section and integral nuclear data measurements. The differential cross-section measurements are evaluated first and then adjusted to fit the two types of data.

Evaluation of uncertainties is an essential requirement for cross-section adjustment and prediction of reactor properties. These depend on reactor neutron spectrum averaged values of cross-sections (although the spectrum shape itself depends on detailed aspects of cross-sections). For many cross-sections it is sufficient to know the uncertainties in the average values in broad energy intervals, in the dispersions about the averages (such as mean resonance parameters and cross-section minima) and in the broad energy gradients of cross-sections.

Some integral measurements might best be taken into account in the derivation of evaluated data files. These include measurements of single reactions in well defined spectra, measurements for single substances and measurements which give information about cross-section fine structure. More general types of integral data might best be used to adjust an applications orientated cross-section library.

The paper discusses the requirements for deriving cross-section adjustments and how these should be incorporated in cross-section libraries.

INTRODUCTION

By cross-section adjustment we mean taking into account both differential cross-section and integral nuclear data measurements in the derivation of a cross-section library. An alternative to deriving such an adjusted cross-section library is to correct calculations made using an unadjusted library (ie one based on differential cross-section measurements alone). The corrections can be bias factors obtained by analysing measurements of properties similar to the ones being predicted, or they can be calculated from the first order estimates of the cross-section adjustments required to fit a wider range of integral measurements (using the cross-section sensitivities for the property being predicted to calculate the correction). However, it is more accurate, and more convenient, to derive the adjusted set, iterating, if necessary, to obtain a converged fit. The accuracy of predictions can then be evaluated both by comparing measured and calculated values of integral properties and by combining the calculated covariance matrix for the adjusted cross-sections with the cross-section sensitivities for the predicted properties.

Carrying out a cross-section adjustment study also tests the consistency of the measurements. The whole range of different types of integral measurement can be included in an analysis and so it is possible to detect errors in integral measurement techniques, assembly composition data and modelling approximations. As the accuracy of the differential cross-section measurements and the reliability of uncertainty estimation improve so the impact of these on the assessment of consistency and accuracy of predictions will increase.

Before integral measurements can be taken into account in the production of a combined differential and integral nuclear data based library, energy dependent cross-section curves must be derived which include the detailed fine structure required in the final cross-sections. These curves are usually based on nuclear theory and differential cross-section measurements. These "evaluated cross-sections" are then adjusted to take account of the integral measurements (and, possibly, additional differential cross-section measurements). The integral measurements might indicate the need to revise the fine structure, as well as the average infinite dilute cross-sections, and it might be necessary to iterate because of the linearisation of equations in the adjustment process.

The distinction between "evaluated" and "adjusted" cross-sections is not clearly defined in practice. Certain simple types of integral measurement are sometimes taken into account in deriving "evaluated data files". These include, for example, thermal Maxwellian spectrum averages and resonance integrals. There is also no precise definition of "integral measurements". For example, should we class broad resolution thick sample transmission measurements as integral or differential measurements? In the fourth section of the paper different types of integral measurement are summarised and those appropriate for inclusion in "first stage" or "evaluated data files" are proposed. The evaluation of the differential cross-section data can also proceed in stages, with an "a priori" cross-section curve (which has been derived, for example, from a nuclear model calculation) being adjusted to fit differential cross-section measurements. An example of this approach has been given by Schmittroth and Schenter [1].

The main reason for producing evaluated nuclear data libraries is to predict integral properties. It is appropriate, therefore, to take account of integral measurements when producing these, provided that the uncertainties in the analysis of the integral measurements can be assessed reliably. This question is discussed in the fifth section. If, however, an evaluated library must be processed before it is used in applications, an intermediate processed library might be the more appropriate level at which to take into account the more general types of integral data. This is discussed in the second section. An adjusted nuclear data library should include integral measurements relating to all possible applications: thermal reactor, fast reactor, shielding, dosimetry, general criticality and fusion blankets. This is preferable to the development of specific application libraries, which is the usual approach at present. However, it would be a formidable undertaking to include the whole range of integral measurements in a single adjustment exercise. Therefore possible separations of the adjustments, by substance, reaction type and energy range, should be considered.

Procedures for combining differential and integral data have been developed and reviewed, and the philosophy of cross-section adjustment discussed, by number of authors. Comprehensive reviews have been published in recent years by Bobkov et al [2], Chao [3], Dragt et al [4], Gandini and Salvatores [5], Kuroi and Mitani [6], Pazy et al [7], Pearlstein [8] and Weisbin et al [9]. The methods involve the calcula-

tion of the sensitivities of integral properties to cross-section changes and estimation of the uncertainties in both the reference differential cross-sections and the integral measurements (and analysis). Although the mathematical equations can be expressed in terms of cross-section variations which are continuous functions of energy, it is the practice to reduce the number of variable cross-section parameters, most usually, by treating as the variables, factors applied in broad energy groups. This is appropriate because the integral measurements only provide information about averages over broad energy intervals. The factors can then be fitted by smooth curves before applying them to the differential cross-sections. The uncertainty information which is required consists of the variances in the values of cross-sections averaged over the energy groups and the covariances both between groups and between different reactions. Alternatively, for some reactions or energy ranges, other parameters can be chosen as the variables. The uncertainty information must then relate to these parameters. In the earlier applications of the cross-section adjustment procedure the covariances were often little better than guesses. The adjustments were nevertheless successful, for two reasons: firstly, the accuracy of predictions of reactor properties depended primarily on the integral data and was not so sensitive to the uncertainties in the differential cross-section data; secondly, the broad resolution of the integral measurements resulted in adjustments to most cross-sections which were slowly varying functions of energy (independently of the assumed energy covariances). Few cross-sections were changed by more than the assumed standard deviations (only U_{238} capture and fission in the UK studies). However, the uncertainties estimated for the cross-sections did have important effects in constraining adjustments, indicating inconsistences between integral measurements and the presence of additional sources of uncertainty (such as the moisture content of graphite, which first appeared, in our studies, as an adjustment to the carbon cross-section).

In the last few years methods have been devised for calculating cross-section uncertainties, and formats have been designed for storing the uncertainty data in files which can be processed conveniently. In particular, the work of Perey [10], Peelle [11] and Drischler and Weisbin [12] has been an important contribution, laying the foundations for the development of cross-section uncertainty evaluation and producing much valuable data.

The objectives of the continuing programmes of differential cross-section measurements and evaluation, and of integral measurements and analysis, are improving the accuracy of prediction of integral properties, and assessing the accuracy of predictions. Evaluating the uncertainties in the data is as important as improving the data, because the design margins must cover the assessed uncertainties. Some views on the requirements for cross-section uncertainty information are given in the third section of the paper. The aim should be to meet the requirements as simply as possible, taking into account the energy resolution requirements, the aspects of the cross-sections which are important (resonance structure, thresholds, energy gradients), the sources of uncertainty (normalisation, reference cross-sections), the reliability of the assumptions involved in the derivation and use of the uncertainty data (eg assumption of normal distributions of errors) and the incompleteness of the information on uncertainties in measurements.

FORMS OF CROSS-SECTION LIBRARY WHICH CAN BE ADJUSTED

A distinction between "evaluated" and "adjusted" cross-sections could be made for one of the following reasons:

(a) By choosing the primary cross-section library to be based on evaluations of differential cross-section measurements and nuclear theory the uncertainties in the evaluation of differential cross-sections are separated from those in the integral measurements and analysis. This is convenient because the uncertainties in the two types of data have different characteristics. However, integral measurements which give information about the fine structure of cross-sections and about individual reactions (without introducing complex correlations) are probably best included in the derivation of the primary library.

(b) Cross-section adjustments derived from an analysis of general integral data usually relate to an applications orientated cross-section library, like the MC^2 library, which has been derived from a basic "evaluated cross-section library" like ENDF/B. Simplifications and approximations are made in deriving the applications cross-section library and the adjustments might partly compensate for these approximations. The adjustments

might, therefore, only be valid for this library and should be incorporated in a library of the same type. Another consideration is that it is generally more convenient to make broad energy range adjustments to such a library (although fine structure adjustments are best made to the basic library). The applications library must be sufficiently general for all the required applications.

(c) In some applications the cross-sections are adjusted to compensate for approximations in the calculation methods as well as for the nuclear data uncertainties. This can be an effective way of improving the accuracy of prediction using a particular method, as has been shown by Pearlstein [8]. The adjusted cross-sections are parameters which fit the integral measurements and they have no application other than for interpolation within the range of this set of integral measurements calculated using this method. This approach is limited to applications where the approximations are the same in the methods used to analyse the measurements as those used to make predictions. For this reason it cannot be used in the analysis of fast reactor criticals because the cell heterogeneity calculation methods are different from those used to treat the power reactors for which predictions are to be made.

The adjusted cross-section library FGL5 was produced in fine group form from an unadjusted fine group library, called FGL5U [13], which was derived from evaluations of differential cross-section measurements. The integral properties were calculated using the fine group library but the adjustment parameters were factors applied in ten broad energy ranges (followed by a smooth fit to these factors). The adjustments were made in stages. The only cross-sections for which the fine structure was changed were for U_{238} in the resonance region (below 25 KeV). The resonance parameters were changed by reducing $\Gamma\gamma$ in the resolved region and revising all parameters in the unresolved region. These adjusted U_{238} cross-sections were generated in the basic evaluated library form. The bias introduced by this revision of the U_{238} cross-sections, relative to the evaluation of the differential cross-section measurements, was taken into account in the next stage of calculation of the cross-section adjustments. This next set of adjustments was applied to the fine group cross-sections. A further

cycle of very small adjustments was made to correct for non-linear effects found in the values calculated using the intermediate adjusted set.

The fine group libraries have a sufficiently detailed structure for them to be suitable for a wide range of applications. They are not spectrum dependent. The approximations made are:

i a sub group representation of resonance structure within fine groups.

ii a pseudo discrete level representation of inelastic scattering to the continuum.

iii the anisotropy of the angular distribution of secondary neutrons is approximated as P1 (or by the transport approximation), although more information about the anisotropy is contained in the library (in the secondary energy distributions).

In some studies the cross-section adjustments are applied to broad group sets. In these cases the adjustments could be more dependent on the approximations introduced by group averaging and could limit the range of integral measurements which can reliably be fitted and systems for which predictions can be made.

CROSS-SECTION UNCERTAINTY REQUIREMENTS

Information about the fine structure of cross-sections is only required when this affects neutron spectra, which, in fast reactor spectra, is for materials present in significant proportions, such as C, O, Na, Cr, Fe, Ni, U_{238}, Pu_{239} and Pu_{240}. For other substances, such as individual fission products, higher actinides and many activation reactions, the uncertainties in broad spectrum averaged values, and in the energy gradients of the cross-sections over broad energy intervals, are sufficient for fast reactor applications. In thermal reactor spectra shielding in individual low energy resonances can be significant for these substances and reactions.

Uncertainties in the average energy gradients over broad energy ranges (perhaps a decade in energy) are required to estimate uncertainties in the differences between reaction rates in different spectra, and to permit adjustments to be made to fit measurements made in different spectra. Effects such as fast reactor sodium voiding reactivities depend on the differences between relative reaction rates averaged

in the normal and in the sodium voided reactor spectra. It is also necessary to specify uncertainties in cross-section shapes to ensure that adjustments to fit integral measurements are consistent with nuclear theory and the differential cross-section measurements. For reactions with a threshold we need to know the uncertainties in the threshold energy and in the average gradient up to the plateau.

Neutron transmission through shields is sensitive to cross-section values in minima and so uncertainty information is required for these. The uncertainty in the transmission depends on uncertainties in the average values of quantities like $(1/\sigma)$.

We can separate the types of cross-section structure for which there are uncertainty requirements into the following categories:

(a) Individual resonances and cross-section minima. These are perhaps best characterised by the uncertainties in the resonance parameters and the correlations (both between the parameters of each resonance and between resonances).

(b) Average resonance structure in an interval. This might be characterised by uncertainties in average resonance parameters and their distributions. Alternatively the uncertainties in some other parameters representing the distribution of cross-section values might be sufficient (parameters in shielding factors being one possibility). A simple parametrisation should be sufficient to represent uncertainties.

(c) Intermediate structure. This could be represented by components of the uncertainties in the average resonance properties, or average cross-sections, which are uncorrelated between the energy intervals in which the resonance parameters are averaged.

(d) Threshold regions. The uncertainties in the effective threshold energy, the average energy gradient up to the plateau and values on the plateau are required. For reactions with thresholds above about 3MeV the uncertainties in the fission spectrum averaged values might suffice.

(e) Smooth cross-sections and the shapes of cross-sections averaged over the resonance structure and intermediate structure. The requirements are for the uncertainties in the average values and the average energy gradients over broad

energy ranges. Possible averages for which the uncertainties could be given are:

(i) Thermal Maxwellian

(ii) Variation of the thermal Maxwellian average with temperature

(iii) Resonance integral

(iv) Resonance integrals for lattices (resonance structure), including temperature dependence

(v) Energy averages over intervals of about 1 lethargy, 2 to 20 or decade intervals, depending on the importance of the cross-section. Correlations between the uncertainties in the averages in different intervals are also required

(vi) Average energy gradients over intervals and the correlations between intervals

(vii) Fission spectrum

(viii) Defined fast reactor spectrum (for less important reactions)

Several of these requirements could be met by representing the uncertainties by an energy dependent factor to be applied to the cross-section. For example, the factor could be a polynomial function of energy, $(1 + a + bE)$, or higher order, and the uncertainties in 'a' and 'b' would be specified. This polynomial can be simpler than the polynomial required to represent the shape of the cross-section. This would be a possible form for the cross-sections of hydrogen, B10 (below 1 MeV), carbon (below 1 MeV, with resonance parameters above), Cr, Fe, Ni (below about 100 eV with resonance parameters above, and average parameters above about 100 KeV). For cross-section curves which are averages over the resonance structure a similar parametrisation over selected energy ranges might be a suitable way to represent uncertainties.

Representing the uncertainties in terms of a few parameters (such as the thermal value and the energy gradient, or the values at a few energy points, with the shapes between these points being adjusted by a spline fit to the adjustments to the point values) enables the covariances between cross-section values at different energies to be calculated as continuously varying functions of energy. However, such a representation could require new processing codes to generate energy group covariances, or to transform the sensitivities to relate to these parameters.

Separating out independent uncertainty parameters, such as normalisation uncertainties and broad gradient uncertainties, enables the number of variables in an adjustment study to be reduced and also permits the fitted values of these parameters to be calculated directly. This was the approach adopted in Ref [14] to the representation of uncertainties in both differential nuclear data and integral measurement analysis. It is equivalent to transforming the variance-covariance matrix to a diagonal form and treating these independent parameters as the variables in the adjustment. The matrix of sensitivity coefficients is transformed to relate to these parameters and the fitting procedure then involves fewer matrix operations because the variance matrix is diagonal.

The particular form chosen to represent cross-section covariances should be the one which evaluators find most convenient because any form can be handled by those carrying out adjustment calculations. We should perhaps re-emphasise, though, that the requirements are for the uncertainties in average values, the fluctuations about the averages (including resonances and minima) and the energy gradients over broad energy intervals, to be calculated from the covariance data.

Importance of uncertainty estimates for mean resonance parameters

Calculations have been made to show the importance of allowing for changes in resonance shielding factors, as well as infinite dilute cross-sections, in adjustment studies. The quantities calculated are infinite dilute and shielded U_{238} capture cross sections averaged over the energy range 0.5 to 25 KeV using a fixed fast reactor spectrum and average resonance parameters. The shielded cross-sections are calculated for four temperatures, with a background scattering cross-section of 30 barns. Five sets of average resonance parameters are used, the reference set and sets with changes made to Γ_γ, D, S_0 and S_1 separately (keeping the other quantities fixed). These are given in Table 1. The resulting average capture cross-sections are shown in Table II and the percentage changes relative to the standard values in Table III. Measurements in fast reactor critical assemblies with compositions similar to a power fast reactor give information only about the shielded cross-section averaged over broad energy ranges (similar to the range used in the present study). If these measurements show a need for a 10% change in the capture cross-section in this energy range the change

in the infinite dilute cross-section could vary between 7% and 18%, depending on the resonance parameters adjusted. There are large differences in the Doppler effects calculated using the different possible resonance parameter adjustments as is seen from Table IV. Estimates of the uncertainties in mean resonance parameters, and of the covariances between them, are required, and these parameters (or related variables) should be treated as variables in an adjustment study. Similar conclusions have been reached by Greenspan et al [15]. The integral data should be chosen to provide information for different degrees of resonance shielding and ideally should include measurements of Doppler effects. Temperature dependent broad resolution thick sample transmission and self-indication measurements could meet this requirement. Adjustments to take such measurements into account might best be made separately from a general integral data adjustment exercise.

TYPES OF INTEGRAL MEASUREMENT AND THEIR USE IN CROSS-SECTION ADJUSTMENT

Different types of integral measurement for single reactions and substances are summarised in Table V and for mixtures in Table VI.

Measurements which give information about individual reactions and substances should be used to adjust the data for these separately. Some measurements are relative to a reference reaction (or other item of nuclear data) or made in a spectrum which depends on other data. It is still appropriate to adjust these separately if the uncertainties associated with the reference reaction and the spectrum are relatively small. This could be the case for the reaction rate and reactivity worth measurements made in reactor spectra for individual fission products, higher actinides and activation reactions (which do not contribute significantly to the reactor neutron balance and spectrum shape). Simultaneous evaluation of all the data involved is probably not warranted. Spectrum measurements which give information about details of cross-section structure (such as resonances, minima and thresholds), are also best taken into account separately. The detail of the spectrum shape in a small energy interval is not much influenced by errors in other cross-sections and energy ranges which affect the overall shape of the spectrum. A two-stage interpretation of spectrum measurements should be considered, separating the

fine structure information from the broad spectrum shape (averages over broad energy intervals).

There are broad energy ranges for which it might be possible to carry out the adjustments separately (but taking into account the revised covariance matrix at each stage). These energy ranges are thermal Maxwellian, resonance region (to about 1 KeV), fast reactor core (1 KeV to 1 MeV, for reactions other than threshold reactions), shield transmission (10 KeV to 10 MeV) and fission spectra (above 1 MeV). Measurements in benchmark fields can overlap these ranges.

Adjusting a cross-section which has a complex structure, such as the U_{238} capture cross-section in the resonance region, can be a lengthy procedure and if the requirements of integral measurements can be anticipated when selecting the representation for the detailed structure this can reduce the number of stages of iteration required to fit both the differential and integral measurements. However, the bias which has been introduced into the reference cross-section, (or the difference between this cross-section and the value which would be obtained by fitting only the differential cross-section measurements) must be allowed for in an adjustment study, and the uncertainties for an evaluation of the differential cross-section measurements alone must be used.

UNCERTAINTIES IN INTEGRAL MEASUREMENTS AND ANALYSIS

At present, the uncertainties calculated for the predicted values of many reactor properties depend mainly on the uncertainties estimated for the related integral measurements used in the derivation of the adjusted cross-sections. Consequently it is most important that these uncertainties are reliably estimated. Attention must be given to possible systematic errors which could affect all the measurements of a particular type of property. These systematic errors could be associated with the measurement technique, the material components used in a series of assemblies or the methods of analysis. Some systematic errors affect both different measurements in the same assembly and measurements in different assemblies. For example, approximations in the methods used to calculate cell heterogeneity affect U_{238} fission and capture and Pu_{239} fission and capture in related ways and the combined effect results in an error in Keff. The errors will be related in different assemblies but they will not be the same because of different cell structures and spectra. An

approximation which is made is to assume that between assemblies having a similar type of cell structure, the cell heterogeneity uncertainties consist of a fully correlated component and a random component, (rather than attempting to relate the systematic uncertainty to the changes in cell structure and spectra). The uncertainties are difficult to estimate and it has been hoped that by including measurements made with different types of cell heterogeneity the effects of these uncertainties would be removed. In the British facility, ZEBRA, measurements have been made using both plate and pin geometry cells and using plutonium metal plates and mixed uranium-plutonium oxide plates. In the French facility, MASURCA, the fuel is in rodded form. In the Argonne, German and Japanese facilities the plate fuel has a different composition to the British plate fuel, and measurements have also been made using fuel in pin form.

Monte Carlo calculations have been made to evaluate the cell calculation methods used at Argonne and these have given encouraging results [16]. However, both the type of heterogeneity and the method of analysis used for ZEBRA plutonium plate cells are different from the Argonne cells and methods. A number of measurements made in ZEBRA indicate differences between measurements made with plate and pin geometry cells, and using metal and oxide fuel, which are larger than the estimated uncertainties. There are measured differences in Keff of about 1% between plate and pin cells which are calculated to have the same value of Keff. This compares with typical calculated Keff heterogeneity effects of 1.4% and 0.4% for plate and pin cells, a difference of 1%. (However these are the net effects of several components, some of which tend to cancel). The pin cell results are more consistent with the measurements made in the Swiss facility PROTEUS (which uses oxide fuel in pin form), [17] and with the critical data for the UK Prototype Fast Reactor at Dounreay. It is clearly necessary both to improve the accuracy of cell calculation methods and to include the widest possible range of cell types when deriving cross-section adjustments.

It is interesting to note that the adjustment study made by Marable et al [18] (which was based on measurements of Keff and reaction rate ratios in four Argonne critical assemblies and reaction rate ratios in a benchmark field) gave similar standard deviations for predictions of fast power reactor Keff and breeding performance to those assessed for the adjusted cross-section library FGL5 [13], which included a wider range of integral measurements. This suggests that a

few accurately defined complementary integral measurements could provide a sufficient basis for prediction of these properties, although a wider range is desirable both to average out possible systematic errors and to provide data which can predict other properties. The accuracy of predicting Keff and breeding performance following fitting to integral measurement is about a factor of 5 higher than using unadjusted data.

The adjustments obtained by Marable et al to be applied to ENDF/B-IV calculations made for a reference 1200 MW(e) LMFBR model are +1.4% (±0.5%) for Keff and -5.5% (±2.0%) for the breeding ratio (without K reset). This compares with differences between calculations made using the FGL5 set and ENDF/B-IV (MC^2) for an international intercomparison benchmark model [19] of +2.9% for Keff and -2.5% for the total breeding ratio. This benchmark model had a high fuel density and low fissile enrichment, which could partly explain the greater difference in Keff, because the correction to U_{238} capture would have a larger effect. It is also consistent with a possible systematic error in our analysis of ZEBRA plutonium metal plate cell assemblies (the method of analysis being different from that used at Argonne). Although integral measurements made in other types of cell were used in the production of the FGL5 adjusted library this type had most influence on the adjustments which relate to the prediction of Keff in plutonium fuelled assemblies. However, the fitted ZPR-3/48 Keff values are similar in both studies.

CONCLUSIONS

It is usual to take account of integral measurements when predicting many reactor properties because these improve the accuracy of predictions significantly. This can be done by adjusting cross-sections, the advantages being that it is possible to take into account a wide range of integral measurements, consistently with the differential measurements and nuclear theory, to test the consistency of all the data and to evaluate uncertainties in predictions. It is important to have reliable evaluations of the uncertainties in the analyses of the integral measurements because systematic errors could introduce an undetected bias into predictions. Analysis of cell heterogeneity effects are still not completely satisfactory, particularly for some plate cell geometries, and improved methods are being developed. It is important

to include measurements made using different cell geometries in an adjustment exercise.

Estimates of the uncertainties in evaluations of the differential cross-section measurements are an important requirement, both for adjustment of cross-sections and for evaluating the accuracy of predictions. The requirements are for the uncertainties in averages over broad energy ranges, in the short and long range fluctuations about the averaged cross-sections (resonances, minima and intermediate structure) and in the average energy gradients. Separate identification of normalisation uncertainties, inter-relationships between cross-sections and uncertainties in simple parametric representations could be a convenient way to represent uncertainties.

The way in which integral measurements should be taken into account depends on the type of measurement. Simple integral measurements which relate to a single reaction or substance could be taken into account in deriving a basic evaluated data library like ENDF/B. Integral measurements which give information about cross-section fine structure (resonances, minima and thresholds) might also be best taken into account at this stage. Broad resolution data for mixtures might best be taken into account in an applications cross-section library.

It is a worthwhile aim to try to produce an adjusted library suitable for all applications, thermal reactor, fast reactor, criticality, shielding and fusion blankets. However, to achieve this, separating the integral data into energy ranges and groups of substances and making the adjustments in stages might be the most practical method.

REFERENCES

1. F. Schmittroth and R. E. Schenter, "Finite Element Basis in Data Adjustment," Nucl. Sci. Eng. 74 168 (1980).

2. Y. G. Bobkov et al., "The Adjustment of Group Constants on the Basis of Evaluated Integral Experiments and the Latest Evaluated Microscopic Nuclear Data," Third Kiev Conference, CONF-750555 (1975).

3. Y. A. Chao, "A New Approach to the Adjustment of Group Cross-Sections Fitting Integral Measurements," Nucl. Sci. Eng 72.1 (1979) and 75 60 (1980).

4. J. B. Dragt et al., "Methods of Adjustment and Error Evaluation of Neutron Capture Cross-Sections; Application to Fission Product Nuclides," Nucl. Sci. Eng. 62 117 (1977).

5. A. Gandini (and M. Salvatores for Part 3), "Nuclear Data and Integral Measurements Correlation for Fast Reactors," Parts 1, 2, 3 and 4. CNEN Reports RT/F1(73)5, RT/F1(73)22, RT/F1(74)3 and RT/F1(78)10 (1973, 1974 and 1978). M. Salvatores, "Recent Developments in Cross-Section Adjustment Procedures," Proc. ANS. Topical Meeting on Advances in Reactor Physics, CONF-780401 p 269 Gatlinburg (April 1978).

6. H. Kuroi and H. Mitani, "Adjustment of Cross-Section Data to fit Integral Experiments by Least Squares Method," J. Nucl. Sci. Technol. 12 (11) 663 (1975).

7. A. Pazy et al., "The Role of Integral Data in Neutron Cross-Section Evaluation," Nucl. Sci. Eng. 55 280 (1974).

8. S. Pearlstein, "Interrelating Differential and Integral Nuclear Data," Nucl. Sci. Eng. 74 215 (1980).

9. C. R. Weisbin et al., "Application of Sensitivity and Uncertainty Methodology to Fast Reactor Integral Experiment Analysis," Nucl. Sci. Eng. 66 307 (1978).

10. F. G. Perey, "The Data Covariance Files for ENDF/B-V" ORNL/TM-5938, ENDF-249 (1977).

11. R. W. Peelle, "Requirements on Experiment Reporting to meet Evaluation Needs," ANL-76-90, NEANDC(US)-199/L Proc. NEANDC/NEACRP Specialists Meeting on Fast Neutron Fission Cross-Sections of U-233, U-235, U-238 and Pu-239, P 421 Argonne National Laboratory (June 1976).

12. J. D. Drischler and C. R. Weisbin, "Compilation of Multigroup Cross-Section Covariance Matrices for Several Important Reactor Materials," ORNL-5319, ENDF-235 (October 1977).

13. J. L. Rowlands et al., "The Production and Performance of the Adjusted Cross-Section Set FGL5," Proc. Int. Symp. Physics of Fast Reactors p 1133 Tokyo (October 1973).

14. C. G. Campbell and J. L. Rowlands, "The Relationship of Microscopic and Integral Data," Proc. 2nd Int. Conf. Nuclear Data for Reactors Helsinki (June 1970).

15 E. Greenspan, Y. Kami and D. Gilai, "High Order Effects in Cross-Section Sensitivity Analyses," Proc. Seminar Workshop on the Theory and Applications of Sensitivity and Uncertainty Analysis," ORNL/RSIC-42 Oak Ridge (February 1979).

16. D. C. Wade, "Monte Carlo Based Validation of the ENDF/MC^2-II/SDX Cell Homogenisation Path," Proc. Specialists Meeting on Homogenisation Methods in Reactor Physics IAEA-TECDOC-231 p 137 Lugano (November 1978).

17. S. Seth et al., "GCFR Lattices with K_∞ Close to Unity. Comparison of Measured and Calculated Integral Data," ANS Trans. 26 533 (June 1977) [and later publications].

18. J. H. Marable, C. R. Weisbin and G. de Saussure, "Uncertainty in the Breeding Ratio of a Large Liquid-Metal Fast Breeder Reactor: Theory and Results," Nucl. Sci. Eng. 75 30 (1980).

19. L. G. Lesage et al., "Assessment of Evaluated Nuclear Data Files via Benchmark Calculations - A Preliminary Report on the NEACRP/IAEA International Comparison Calculation of a Large LMFBR," Proc. ANS Topical Meeting on Advances in Reactor Physics CONF-780401 p 1 Gatlinburg (April 1978).

TABLE I

U_{238} average resonance parameters used in the calculations

Parameter	Standard Value	Changed Value	Per Cent Change
$\Gamma\gamma$	23 mV	24 mV	+ 4.3
D	22.5 eV	20 eV	- 11.1
S_0	0.9289×10^{-4}	1.1611×10^{-4}	+ 25%
S_1	1.729×10^{-4}	1.9788×10^{-4}	+ 14.4%

TABLE II

The U_{238} capture cross-section averaged over the energy range 0.5 to 25 KeV

Parameter Set	Infinite Dilution	Shielded cross-sections			
		300°K	1500°K	2700°K	3900°K
Standard	2.5221	0.9392	1.2450	1.3915	1.4933
Γ_γ changed	2.5849	0.9577	1.2701	1.4198	1.5238
D changed	2.6990	1.0299	1.3750	1.5390	1.6525
S_0 changed	2.6507	0.9657	1.2967	1.4631	1.5819
S_1 changed	2.5901	0.9703	1.2781	1.4251	1.5270

TABLE III

Percentage changes from the values calculated using the standard parameter set (0.5-25 KeV)

Parameter changed		Cross-sections		Doppler Changes		
	Percent	Infinite dilute	300°K shielded	300 -1500°K	1500 -2700°K	2700 -3900°K
$\Gamma\gamma$	4.3	2.5	2.0	2.2	2.3	2.2
1/D	12.5	7.0	9.7	12.9	12.0	11.5
S_0	25.0	5.1	2.8	8.2	13.6	16.7
S_1	14.4	2.7	3.3	0.7	0.3	0.1

TABLE IV

Percentage changes corresponding to a 1% increase in the 300°K shielded cross-section (0.5-25 KeV)

Parameter changed		Infinite dilute	Doppler changes		
	Percent		300 -1500°K	1500 -2700°K	2700 -3900°K
$\Gamma\gamma$	2.2	1.3	1.1	1.1	1.1
1/D	1.3	0.7	1.3	1.2	1.2
S_0	8.9	1.8	2.9	4.9	6.0
S_i	4.4	0.8	0.2	0.1	0.0

TABLE V

INTEGRAL MEASUREMENTS FOR SINGLE SUBSTANCES

A. MEASUREMENTS IN AN INDEPENDENT SPECTRUM

Reaction Rates and Reaction Rate Ratios

Thermal maxwellian
Resonance integrals
Fission spectra
Standard benchmark fields
Reactor spectra

Reactivity Worths and Worth Ratios

Thermal maxwellian eta values
Small sample reactivity worths

B. SPECTRUM DETERMINED BY THE SUBSTANCE

Thick Samples and Heated Samples

Broad resolution transmission
Broad resolution self-indication
Resonance integrals
Reactivity worths and reaction rates

Large Blocks

Transmission spectra
Age to the indium resonance
Exponential experiments

TABLE VI

INTEGRAL MEASUREMENTS FOR MIXTURES

C. SIMPLE GEOMETRY ASSEMBLIES

Type:
- Null-reactivity test zone
- Region with measured buckling
- Uniform core and reflector
- Regular lattices

Measurements:
- Critical parameters
- Principal reaction rate ratios
- Neutron spectra
- Unit cell reactivity worth
- Component reactivity worths
- Reference reactivity worths
- Reaction rate distributions
- Reactivity worth distributions

D. MOCK UP ASSEMBLIES AND POWER REACTORS

- Critical dimensions
- Control rod worths
- Power and reaction rate distributions
- Large region sodium voiding reactivities
- Temperature and power coefficients
- Burn-up reactivity changes
- Compositions of irradiated materials

TABLE VII

TYPES OF INTEGRAL MEASUREMENT WHICH COULD BE TAKEN INTO ACCOUNT IN A BASIC EVALUATION

Spectrum Averaged Reaction Rate Measurements

(a) Well defined spectra (eg thermal maxwellian)

(b) Reactor spectrum measurements (eg material activation and higher actinides)

Single Substance Measurements

(c) Reactivity measurements
  (i) Thermal spectrum eta values
  (ii) Measurements in reactor spectra (eg individual fission products)

(d) Thick sample broad resolution measurements (Average resonance data)

(e) Large block transmission spectra (Resonance data and minima)

General Integral Data

(f) If used to guide selection of evaluation then record in the file the consequent bias relative to the evaluation of differential data alone. (Give variance-covariance relative to the latter).

Processing Needs and Constraints Discussion

Henryson

The presentations of our panel have raised questions about the size and detail of evaluated files. On the one hand, too much detail causes significant processing problems (e.g., point energy Monte Carlo) and tends to be lost in the processing step. On the other hand the detailed data are available and have application. Is there a concensus on how to deal with this dichotomy?

Carter

I'm afraid that I have no solution although there is clearly a problem. From the perspective of point Monte Carlo, it is highly desirable to have the detail but there is a practical problem in that the burden is placed on the processor codes and until computer memory and speed increase substantially, such processing is very expensive.

MacFarlane

Evaluated files have a wide variety of applications and complete detail is certainly required by someone. The only solution is to preprocess the data for applied users. The problems occur in fields where algorithms are not available to perform the processing. For example, in thinning the ENDF/B-V data for our point energy Monte Carlo applications, the processed data become application dependent in that the thinning algorithms were biased toward high energy applications.

Orer

It is important to retain detail in evaluated data files and keep the burden of the use of the files out of the hands of the evaluators. As a consequence it is essential to stress the importance of data processing. There is nothing wrong with application oriented processed files, but the data reduction step is the key. For example, in processing ENDF/B-V for LWR Monte Carlo applications, the structural materials initially take more space than the fertile and fissile materials which certainly is not consistent with the importance of the data for LWR applications.

Henryson

I am concerned with these responses in that I feel that we the users are copping out. We seem to be saying to the evaluators, run your model codes, put in all the detail you want and we won't

provide any guidance. I feel that the success of evaluated files world wide has been the fact that users use them. As we put more processing between the evaluated file and the application file, the relationship between the two becomes more tenuous and the usefulness of the evaluation then becomes more questionable.

Rowlands

I agee with others that the basic evaluated file should not be application oriented but believe that it should be possible to obtain an intermediate file which has wide application - thermal reactor, fast reactor, criticality, shielding. For such an intermediate library probability table representation of resonances or pseudo discrete inelastic levels are applicable but such representation should not be used in the basic file.

Gohar

It is fine to speak of details and fine structure, but let us first fill the gaps where data do not exist or where large uncertainties impact design applications. The lack of data is the real problem particularly in applications such as CTR shield design.

Henryson

We have been in the data evaluation field for many years, yet we still talk today about evaluation needs. Does anyone see any end to data evaluation? Is there some point at which we can say we've gone as far as we need to go?

Poentiz

Reactor designers have design goals for the accuracy of such parameters as breeding ratio, critically, etc. These translate to required accuracies (uncertainties) in cross sections. It appears that the measurements and evaluations effort would be concluded if these goals are met. This is not yet the case.

Smith

(i) Can user disciplines define guidelines for definition of evaluation, particularly detail, in particular user areas? (ii) Why is not more use made of theoretical representations i.e, Briet-Hopkins for H(n,n) or few R matrix parameters instead of hundreds of data points as for the carbon evaluation?

Rowlands

Addressing the question of detail, I would suggest that one wants quite accurate cross sections but less detail in the uncertainty data. In the resonance data we have problems at present in reconciling integral and differential data. This may be a consequence of resonance detail but it is quite difficult to generalize.

MacFarlane

On the representation question, we are certainly in agreement that one can trade off bulky tabulated representations of data against compact algorithms. Dave Madland's fission spectrum representation and Gerry Hale's R matrix parameters for charged particle scattering are examples. The problem is that there are a large number of processing codes with a great deal of money invested in their development, and one must consider representations which impact on such codes very carefully. Great coordination among Laboratories is required. For high energy applications where there are so many reaction channels open, such representations will be essential.

Dunford

In planning for future versions of an evaluated nuclear data file one must balance stability of the reference file against having the file reflect current values. How does the panel feel about these conflicting requirements? What should be the balance of increase in file size and the introduction of more compact data representations (i.e., new formats?)

Rowlands

One can't adopt a new library too often. There is an enormous amount of work in evaluating the performance of a new library (criticals reevaluation, design calculation bais, etc.). In view of the need for continuity, I would say that new libraries might be valuable every five to ten years.

Carter

I raised the issue in my talk although I have no answer. There is need for a stable and accurate data base, but these needs are in conflict. If stable, one cannot respond quickly to new measurements and evaluations. As a user I am constantly being asked "Why aren't you using these new data?" and it remains an important issue, particularly in those areas where data are not available in the sanctioned versions of the evaluated files.

Ozer

We must concentrate our efforts on areas of importance where fine tuning has benefits but without new library releases which break continuity of program and often make it impossible to build on what we have done in the past. On the representation issue I would remind everyone that ENDF is a compromise representation which has been found acceptable to users and evaluators. Any changes in representation for one without seriously considering the impact on the other would be a mistake. Changes in representation must not be taken lightly.

Pearlstein (Comment)

The biggest problem in any kind of data evaluation is the potential influence of systematic errors. They are difficult to determine unless data are measured in many different ways. John Rowlands said that inconsistencies between integral and differential data for Carbon led to discovering an error in core composition. Is the burden of proof on differential data, integral data, or both? When do we stop looking? When there is no discrepancy, or more accurately, no apparent discrepancy. I suggest that even when there is no apparent discrepancy that we continue through sensitivity studies to record alternate combinations that are equally likely to produce the same result so that we will not be lulled into a false sense of understanding.

Peelle

For which nuclides must we evaluate neutron reaction cross sections for radioactive nuclides for CTR applications? Is it primarily reaction products of first wall materials?

Gohar

In one of my viewgraphs I presented a list of materials which are of use in CTR applications. We must consider the 14 MeV neutron reactions which include (n,α) and (n,p) reactions. All of the isotopes of iron and nickel are important. We must look at those materials in the design and understand their radioactivity chains. The most important are in the blanket, but the magnet and shield materials also see 14 MeV neutrons.

Young

How good are the methods? For example, is there a concensus on how well k_{eff} can be calculated?

Henryson

At ANL we believe that the methods uncertainty in the k_{eff} calculation of a ZPR or ZPPR system is 0.2 to 0.5%. The major causes of uncertainty are the heterogeneity and streaming treatments in the plate lattices. It is my understanding that the British are now questioning whether the uncertainties in the heterogeneities of their criticals are not larger than those I have quoted. I would point out that just as there have been advances in data evaluation, there have also been enormous advances in data processing. We have reached the point where such small methods uncertainties are quoted with great confidence.

MacFarlane

It is important to distinguish between benchmark level codes such as those used at ANL in the analysis of criticals and design or application level codes. If you include the latter then uncertainties even in k_{eff} calculations are measured in percent rather than fractions of a percent. For plutonium production and reaction rate ratios, the situation is even worse.

Rowlands

It is important to consider a wide range of combinations to separate out systematic errors. This is certainly true of data adjustment studies. In fast reactors one should look at plate criticals, pin criticals, mixed oxide plates, Pu and U metal plates, and criticals from different countries. With all these input data we have evidence that there is a discrepancy for plate criticals.

Young (Comment)

Evaluators need more guidance as to detail and accuracy required in data e.g., how accurately do covariances need to be specified to do meaningful data adjustment? With regard to an earlier discussion on CTR needs, I encourage users to make their needs known to people in a position to support evaluation efforts. This have been a problem in the past

Vonach

What detail does the user really want in the uncertainty data?

Rowlands

One needs data in broad energy ranges. Most integral properties are sensitive to the uncertainties for broad energy ranges. It is necessary to get uncertainty information not only for the average cross section, but also the average gradiant and the average fine structure, a measure of the dispersion about the average.

SESSION II

USE OF UNCERTAINTIES AND CORRELATIONS
Chairman: R.W. Peelle ORNL

LOGICAL INFERENCE AND EVALUATION

F. G. Perey

Oak Ridge National Laboratory
Oak Ridge, Tennessee 37830, U.S.A.

ABSTRACT

Most methodologies of evaluation currently used are based upon the theory of statistical inference. It is generally perceived that this theory is not capable of dealing satisfactorily with what are called systematic errors. Theories of logical inference should be capable of treating all of the information available, including that not involving frequency data. A theory of logical inference is presented as an extension of deductive logic via the concept of plausibility and the application of group theory. Some conclusions, based upon the application of this theory to evaluation of data, are also given.

I. INTRODUCTION

As the Cross Section Evaluation Working Group (CSEWG) was about to release ENDF/B-III, a subcommittee was formed, under the chairmanship of Marvin Drake, to make recommendations concerning the manner and format in which the "estimated errors" in the evaluated cross sections could be reported. It was felt that users of the data should have easy access to this information, which until then had been given, if at all, in the final documentation. The introduction of summary documentation had partially remedied the problem that final documentation was often not issued, or was very late coming in. It was felt that the "estimated errors" in the evaluated data were not properly addressed in the summary documentation. The outgrowth of that concern was the appearance in ENDF/B-IV of some "Data Covariance Files" for a few of the cross sections of the carbon, nitrogen and oxygen evaluations. In the recently released ENDF/B-V the number of such files has increased greatly, but most of the cross sections in the library do not have associated with them "Covariance Files."

The subject of "Covariance Files" has always been somewhat controversial in the CSEWG. Most evaluators are somewhat reluctant to generate Covariance Files. They claim that it requires a

considerable amount of time for which they do not get much credit. This is so because these files were not requested by users and most users today do not know what to do with this information. Some of us in the CSEWG felt that it was our duty to communicate the covariances in the evaluated data since we could not conceive of users who would not be interested in knowing the reliability of the data they were using in their application. In fact, the Covariance Files were created because in their absence some users had to make assumptions as to how good the data were, and we were aware that in many instances their assumptions were not consistent with the information upon which the evaluated data had been established. This was true for those who believed that there were small uncertainties in the data and used the data as such. This was also true for those concerned about meeting target accuracies in the predictions of some nuclear systems performances and who were making some guesses as to the quality of the data in ENDF/B. Another major objection to the Covariance Files by evaluators is that the numbers placed into them are largely arbitrary, or at least much more so than the ones placed in the data files. Most people do not think that the numbers in the Data Covariance Files should be trusted to within a factor of two.

On the assumption that everybody knew that the Covariance Files of ENDF/B contained the "estimated errors" in the data, the organizing committee of this workshop wanted to devote one session to these files and limit the discussion to the use of these files. I presume that the idea was to assess from their utilization how much effort should be put into generating them and the degree of detail they should contain compared to the data files themselves.

Having been associated with the formulation of these Covariance Files, I was asked to address in this session the question of their uses. I was very reluctant to do so because I am not a "user" of ENDF/B in the sense we usually associate with the word "user." That is to say, I do not have a goal to accomplish where I find it convenient to use ENDF/B as input data and am concerned about the extent and quality of the data in the Covariance Files. From the titles of their talks, I am sure that the next four speakers will discuss this aspect of the files in connection with solving their problems. It was suggested to me that I address the topic: "The Use of Detailed Uncertainty Data in Cross Section Evaluations." From the title of his talk, I believe that W. P. Poenitz will give tomorrow exactly such a talk, and therefore I thought I could in this talk address a subject which does not appear to be covered explicitly at this conference but is implicit in all of our discussions at this workshop.

Until now in the CSEWG, and other similar groups elsewhere, we have mostly been preoccupied with generating what we call "evaluated" microscopic cross sections. Lately we have been concerned about the "estimated errors," but our major preoccupation has been in the area of formats to represent them and in what detail. After considerable reflection in the last two years, I have become convinced that many of our problems in the area of

evaluation, at least most of mine, occur because we tend to use some concepts and an associated method of reasoning to solve all our problems because it has been found useful to solve some specific types of problems. What I am referring to, as will be evident in all the presentations at this workshop, I believe, is that we tend to use the concepts and the language of the mathematical theory of statistics for all of our reasoning when we perform evaluations. I do not deny the usefulness of some of the results we obtain using the theory of statistics, but as is well known to all of you it is incapable, or rather it is not perceived to be useful, to deal with the concept of what we call "systematic errors."

What I will do in this talk is share with you some thoughts and conclusions on a "unified theory" which deals with the notions one usually associates with "systematic" and "statistical" errors. I cannot in the time allotted to me do more than explain some of the fundamental ideas behind this "unified theory" which I have been studying for some two years now. I have applied this theory to solve many problems which we will discuss at this workshop, and these details will be published elsewhere.[1] If I appear to stray from the subject of this workshop at times, please bear with me since I hope it will become clear later why.

II. HISTORICAL PERSPECTIVE

The basic idea of the approach is rather old. It seems to have been clearly stated by Liebnitz more than 300 years ago (1669) when he, according to Keynes,[2] wrote: "I have said more than once that we should have a new kind of logic, which would treat of degrees of probability." The new kind of logic Leibnitz alludes to is what we call now inductive logic. It is interesting to note that a mathematical theory of inductive logic was developed extensively more than fifty years (Laplace, 1795) before the first attempt at establishing a mathematical theory of deductive logic (Boole, 1847) was made. I guess the reason is that it is fairly easy to carry out and recognize a deductive reasoning without the help of a mathematical symbolism. This does not appear to be the case for most inductive reasoning, although, fortunately for us, there are quite a few situations where the reasoning is, as we say, a matter of elementary common sense. Laplace did not develop singlehandedly this "mathematical theory of common sense," as he called it, which owes much to many eighteenth century thinkers, in particular the Bernoullis. I shall not pursue in detail the history of the theory of inductive logic which is a fascinating and very colorful one involving many great mathematicians and philosophers of the last three centuries. My main purpose for pointing out the long history of the approach to our problems, which I will present, is that the concepts upon which it is based have been very extensively investigated and we are aware of their power and limitations. This has the enormous advantage, well

known to all of you, that we have as a result very many "benchmark experiments," as we call them in the CSEWG, which are in this case "logical problems," which any theory of inductive logic, or logical inference as it is sometimes called, must cope with.

Laplace's theory was essentially discarded about 100 years ago when it was discovered to give rise to paradoxes when used to solve some of these "logical problems." Laplace's theory was replaced by the mathematical theory of statistics, strangely enough not because it was capable of solving these problems, but because it could not be used to try to solve them!! The theory of statistics was, however, designed to reproduce many of the results of Laplace's theory, if not all, in some types of problems where it was felt that the results were very useful. To use a language familiar to you, this situation existed when there were a lot of "statistics" and no "systematic errors."

I became interested in Laplace's theory when I realized that through this approach one could cope with situations where we say today there are large "systematic errors." What was intriguing is that the "failure" of the theory had long been identified with one of the fundamental principles of the theory and that it may be possible to "fix" the theory if one could substitute for this principle another one which would serve the same purpose but would be less ambiguous so as not to lead to paradoxes. I believe that this has now been accomplished to the extent that is needed for our purposes in dealing with the magnitude of what we call physical quantities. I have been influenced by several contemporary authors, but most of all by E. T. Jaynes. In fact, to a large degree the theory which I will introduce to you in this talk is one which E. T. Jaynes has been advocating for some years now. A key paper of Jaynes' which has influenced me most was published in 1968 on "prior" probabilibies.[3] An interesting thing which I realized is that it was not necessary at all to introduce the notions of "a priori" probabilities nor the notion of "errors in measurements." The concept of "errors" in measurements has been a central one when dealing with uncertainties about the magnitude of physical quantities since it was introduced by Thomas Simpson[4] in 1755. It has been the cornerstone upon which most applications of the old theory of probability and the theory of statistics are based. There is a decided advantage today in not using the notion of "errors" when talking about the magnitude of physical quantities since this forces us to focus more sharply upon what we are doing and frees us from the constraints of habits. I vaguely perceived this ten years ago, and that is the major reason why the "Covariance Files" are no longer called the "Error Files" as they used to be at the beginning.

III. THE BASIC IDEAS

Our goal is to develop a theory which is designed to provide us with the feeling of having coped with the uncertainty we have

about the magnitude of physical data. We use the infinitive "to cope" in the sense of: "to contend or strive, especially on even terms or with success." This forces us to depart from a long tradition when dealing with what we call a "physical problem." We will look at it from our point of view — what we want to accomplish and what we know — rather than what "physical reality" is.

Why we must do so when dealing with uncertainty is simply a consequence of what we mean by the word "uncertainty" since it has the meaning of: "the condition of being in doubt; lack of certainty." Accordingly, the word uncertainty is used to describe the state of mind in which an individual finds himself under some circumstances. When we say we are uncertain about the magnitude of a physical quantity we imply two things: the physical quantity has a definite magnitude, and we are not totally ignorant of what it may be. Uncertainty is not a physical attribute or property of objects or things in the sense that, for example, length may be. For our purposes here, the magnitude of a physical quantity is a number that expresses the amount or quantity of a physical property which, in the context we use it, it is meaningful for us to say an object or thing possesses. When we say we are uncertain about the magnitude of a physical quantity, we state the fact that for our purposes it is useful to think that there is a number which expresses the value of this quantity, but that our relevant information is such that we cannot deduce what this value is.

The above situation, in which we find ourselves frequently, is only a problem when it prevents us from accomplishing something which we think we could achieve if we knew what the correct value was. This implies that we have a goal, and we believe we could be successful in meeting it if we knew what the correct value was. It must be that, for whatever reason, we think we are in a situation where we could predict what will happen. Without the correct value of the physical quantity, but with only the knowledge of a range of values which the physical quantity could have, there is a range of possibilities for the outcome, and we believe the correct value will prevail in determining the outcome which we could predict if we knew the correct value. The dilemma we are in is that we must choose a particular value, among all possible ones, and act as if it were the correct one (i.e., the true value). The painful thing is that we can only play once at this game, and we cannot ever win since at best the value we choose is the correct one, and our goal will be met. If the correct value is different from what we choose, then the outcome will differ in some fashion from what we are trying to accomplish. This can only be perceived to be a negative consequence, and in common language we say there is a risk involved in choosing any value as the correct one.

The above is, of course, well known to all of us who must face such decision problems constantly, not only in our professional life but in every aspect of our daily life. Having survived long enough to attend this workshop, we must have more or less successfully solved a great number of such decision problems. In many simple situations what we perceive we should do seems obvious,

and we say it is a matter of common sense. We have the feeling of having coped with the uncertainties about the situation. We think that anyone not doing what we have done in the circumstances should be suspected of lacking seriously in some capacity for logical reasoning or of being a wreckless individual who subjects himself, and possibly others, to unnecessary risks. In many situations, particularly new ones of the type we face in performing what we call "evaluations," it frequently does not seem clear to us that there is any way of coping with the uncertainty about the data. We may not perceive there is a unique answer to our problem and that we fully understand the implications of our limited knowledge. It is then not easy for us to provide all of the assumptions we are making, nor can we explain satisfactorily the rationale which led us to make a particular decision. We are then reduced to expressing an opinion, the basis for which is not clear and therefore may not be entirely rational, nor do we feel it to be a compelling one. I fully anticipate we will hear quite a few at this workshop.

The idea that one could develop a mathematical theory which might be useful to deal with complex situations, where what to do is not perceived to be a question of common sense, is very old, as we have already pointed out. By a mathematical theory we mean a body of deductions, from a set of well identified definitions, axioms and rules assumed to be true, that involve a quantification of some sort. If we think about it, this idea is a puzzling one because it means that we will try to develop a deductive theory to solve problems which by their nature cannot be solved by deduction! It obviously means that we interpret the infinitive "to solve" in two different ways depending upon the context we are in, as we shall later explain. As we have mentioned, developing such a theory was a concern of many people we tend to think of as physical scientists in the seventeenth and eighteenth centures and culminated in the work of Laplace.[5] For various reasons we will not go into here, these concerns were no longer actively pursued by many physicists toward the end of the nineteenth century. They found usually adequate to verbalize the solution to such problems in terms of the mathematical theory of statistics, in particular concerning the "errors" in measurements. The work of Gauss on the least-squares method[6] became the classic source for the method of choice in handling what we now call the "statistical errors" in the data. This is so because Gauss in this work restricted himself strictly to "statistical errors." To a large degree the concerns of developing a theory that would replace Laplace's theory, and therefore deal also with problems not addressed by the theory of statistics, became those of a class of people who we might refer to as logicians and philosophers worried about problems of epistemology.

Since the 1940's, mostly because of rapid and profound technological changes, a number of problems arose dealing with our physical environment which formally look very similar to the preoccupations of the eighteenth century "physicists." As a result,

a number of theories were developed to deal with them with interesting names such as: operations research, information theory, decision theory and now risk theory. Equally profound changes occurred in our own field, but it seems to me few people perceive that they may have upset to some degree a delicate balance which calls for a reassessment. It is a fact that the professional "evaluator," in the sense we use the word in this workshop, was born roughly during the last twenty years or so. The task of evaluating data was not new, but it used to be carried out by the same individual who made the measurements and used the data, or within a very closely knit community of providers and users of data. In some very specific ways the modern "data evaluator" is neither and both a provider and user of data. He does not decide what the experimental facts are and has often no access to them. This is done by measurers who often are interested in the facts to draw conclusions regarding questions of interest to them which are different from those the evaluators have. In the case of the CSEWG, at least, where we maintain the notion of "application independent evaluations," the evaluator is not the user, and he must make a choice of a "recommended value" without knowing what the goal of the user is, or rather independent of what the user seeks. As anybody who does evaluations soon learns, this is a very risky business to engage in, and there is no way you can win. The title of our workshop seems to reflect this fact since it says "evaluation methods and procedures" in the plural, possibly suggesting that what we produce is not and cannot be unique. It has often been said that evaluation is an art and not a science, and few people at this workshop I think would seriously challenge this. I read into this saying a connotation that it is not an entirely rational activity. What I have sought during the last few years is a general theory, or point of view, according to which this would not be the case. The hope was that this theory might provide a rational description of what we often do and thereby make clear the assumptions needed to justify them as purely logical actions. The theory could be tested if we found that these often unstated assumptions were largely valid when we were satisfied with our decisions but would be largely invalid when we are dissatisfied with them. The theory would be useful if in this latter case it suggested a rational decision consistent with our state of knowledge, which would yield results substantially different from those we perceive now to be unsatisfactory.

IV. A THEORY OF LOGICAL INFERENCE

We cannot develop here in any detail this theory of logical inference; this has been done elsewhere.[7] However, we will briefly indicate the fundamental concepts whereby the theory can be viewed as a simple extension of deductive logic. Although not the simplest way to go about it, we shall explain the ideas in the context of performing an evaluation since it is the business of

this workshop. It may therefore not be clear at first sight that this theory is extremely general and could be useful in many applications.

As an evaluator we would consider it almost ideal if having collected all of the experimentally observed facts relevant to our data of interest we could, on the basis of some fundamental relationships existing between the experimentally observed facts and the data whose values we seek, derive what are the true values of the data. By that we mean that we could set up a system of equations which would admit a unique solution for the data of interest. As we all perceive, this may not be possible in principle when dealing with physical data. Sometimes, even in our field, this situation exists, because the domain of possible solutions for the system of equations is so small that for any practical application for which the data might be used, the outcome would not be distinguishable from the predictions made from any value inside the permissible domain of values. It is even better if our experimental facts can be divided into several independent subsets related to the data values we seek by independent relations and all of the independent systems of equations produce the same results. In this fashion we acquire confidence that no mistakes have been made.

The above situation was intended to be a description of the application of deductive logic to perform an evaluation. There are several essential elements in it: every quantity we deal with has, as we say, a true value; every relationship we use is an equality which holds true for the true values of the quantities entering in them; a subset of the facts and relationships between them and the quantities we seek is adequate to determine them if we have made no mistakes. Where we run into difficulty (and why we are holding this workshop) is when, having collected all of the observed experimental facts, we cannot complete the above deductions because we are missing one or more elements to carry it out. It is immaterial to us here which specific ones these missing elements are. To deduce the values of the quantities of interest we may need more observable facts to use in connection with those we have in some equalities we know hold true for the true values, or instead of equalities we have some inequalities. The problem is now called an ill-posed one of deductive logic, or an underdetermined one, since we cannot prove that a specific assertion: "The quantities of interest have such and such values" is true. The best we can do using deductive logic on the basis of only what we know is true, and the assumption that we have made no mistake, is end up with a mutually exclusive set of assertions "the quantities of interest have such and such values," differing only in the numbers we substitute for the word "values," which could be true. If we have learned anything from the observed facts and our relations connecting them to our quantities of interest, it is because the set of assertions we end up with is a subset of all the assertions we were considering as possibly true before our deductions based upon them. We are then, according to its definition, uncertain about the values of the quantities of interest. We shall not

be concerned in this talk about the fact that we are often dealing with "continuous" sets and will assume that we have "discretized" the set of assertions in some fashion, as we did in our first example.

We know from some simple situations of the above type in everyday life where, given an exhaustive and mutually exclusive set of assertions derived from some specific facts, the human mind is capable of performing some assessment of logical degree of truth among these assertions, and we have the concept of plausibility, or probability, to indicate this capability of the human mind. We say that on the basis of the specific facts available, or considered, it is more or less probable that some of the assertions, in the subset of possibly true values obtained from deductive logic, are true, or that one particular assertion is more probably true than some other one. This is very well known to all of you and it is this aspect of the human mind which, at least in some simple cases, seems to be able to carry logical reasoning beyond deductive logic, as we define it today, which is referred to as inductive logic or the capacity for drawing logical inferences. This notion of probability as some measure of degree of logical relationship between assertions such that if one is true another one is more or less true, when we know by deduction it must either be true or false, is very different from the one we use when we apply the theory of statistics. In this latter case it is defined as the ratio of the number of outcomes in an exhaustive set of equally likely outcomes that produce a given event to the total number of possible outcomes, or some other similar definitions. An interesting aspect of this second concept is that it always identifies in some way probability as a frequency of some sort, but also always includes a reference to the other concept of probability. In the above specific definition this is to be found in the word "equally likely." The concept of probability as some measure of degree of logical relationship between assertions is applicable to all assertions, whether a frequency element is involved or not. Through this concept we may therefore be able to deal in a logical fashion with both what we call today the "systematic" and the "statistical" errors. The human mind does not appear to be often capable of performing much more than a semiquantitative or relative assessment of probability. The idea of developing a theory where probabilities in the sense of degree of logical relationship between assertions are given a numerical measure is what mathematical theories of logical inference are about. Such theories are not in any way "explanations" of how the human mind works nor should work. But if we succeed in comparing the predictions of the theory with what we often do and feel quite confident about, but find disagreement with it when we are not confident about what we do, nothing is to prevent us from considering as an alternative what the theory says. Such theories should therefore be relevant to the work we call evaluation in the sense that they provide methods and procedures for performing them. All of the methods and procedures which we will hear about in this

workshop can be viewed as theories of logical inferences being advocated by their proponents. We are therefore entitled to ask whether they are consistent or not, on what form of logic or assumptions they are based and in what sense they can be called the solution to an ill-posed problem of deductive logic, etc.

The theory of logical inference we advocate, because we have found it very useful[7] and believe solves satisfactorily the logical problems which we know of and were the downfall of earlier theories of logical inference,[8] includes all of the laws of deductive logic to which have been added a fundamental definition and a principle. The fundamental definition is the one for probability which we take as a scalar to provide a measure of the logical degree of truth of an assertion conditional upon the truth of another related assertion. This definition introduces the concept of quantification for what we will call plausibility. We now require at least one axiom to assign this scalar which, following Jaynes,[3] we call "the desideratum of consistency" and we phrase as follows: "In two different problems given the same information we shall assign the same probability." Other definitions and rules are eventually required to extend the theory, but the above ones are the cornerstones upon which we extend what we call deductive logic. The desideratum of consistency we argue is a simple consequence of the definition of probability used since it merely asserts that whatever the context, the different problems, probability is a syntactical measure relating assertions. Therefore given the same information (i.e., the same set of assertions), as true, we should assign the same measure to various assertions which are related syntactically in an identical fashion to our givens. This idea is the same one used in deductive logic where we assign in Boolean algebra the same truth value to every assertion which is true.

A major objection has often been raised on philosophical grounds against theories of probabilities where the definition of probability, as in this theory, is not an observable quantity, even in principle. They are called Bayesian theories in which probabilities not being observable quantities are said to be subjective probabilities. This adjective is useful to distinguish these theories from others where probabilities being defined as frequencies, which are measurable quantities, are said to use objective probabilities. We do not fully understand what these philosophical considerations are, but note that unfortunately these adjectives of "objective" and "subjective" tend to create what appears to be some confusion because they are also used to describe emotional attributes. No one at least at this workshop would, I believe, think it is very descriptive to call quantum mechanics a subjective theory because one of its fundamental concepts, a state wave function, is not a physically measurable quantity. It is in this very same sense that we must view in this theory of logical inference the concept of probability. However, as in quantum mechanics, the "subjective" concept of probability must lead to observable effects and it is from the comparison of

the predictions of these observables with the results of observations that we can judge the usefulness of the theory.

This theory, by virtue of the desideratum of consistency used to assign probabilities, has also another analogy with modern theoretical physics. The desideratum of consistency is phrased in such a way as to cause the probabilities to be assigned by "a transformation group method," like that which plays such a large role in modern theoretical physics and whose power is well known to the participants of this workshop.

In fact it is possible to view this theory of logical inference as merely an extension of what we call deductive logic via the concept of probability by means of group theory. All of the relevant information provided in the statement of the problem defines a transformation group and the probability used is related to the irreducible representation of this transformation group This has the advantage that the solution, in this case the probability assignment for the logical degree of truth of the assertions, is entirely and uniquely given by what we are told in the statement of the problem which is therefore known to us and does not depend in any way whatsoever upon what we are not told and would have made the problem one of deductive logic. It is in this sense that one must define the solution to a problem of logical inference by virtue of the fact that it is the unique answer which can be provided based only upon what we are given in the statement of the problem.

It is possibly because of our perceived need to rely upon logical reasoning only for our conclusions in the sciences and because today we feel this is ensured only by the use of deductive logic that, when faced with a problem of logical inference, we very often transform it into a problem of deductive logic by means of what we call assumptions. This forces us to take as the solution to our problem the solution of another problem which we know how to solve. In the case of experimental measurements of physical quantities we have come to accept as the solution to the problem: on the basis of the observations made, what can we conclude about the true values of the quantities of interest, the answer to the problem: if we assume our results to be a random sample of results from some distributions, what can we say about the mean of the results we might observe if we were to repeat the measurements indefinitely? This transformation of the problem was to our knowledge first suggested by Thomas Simpson* in 1755, and since we know how to answer this second problem, and the result is fairly independent of any assumed distribution if our sample is fairly large, we have come to accept it as the answer to our original problem. If we view the second problem, there is an inherent uncertainty because we do not know what assumptions to make and if our observations are a random sample. In the theory of logical inference we advocate, beyond accepting the concept of probability we use and its associated desideratum of consistency for all problems which are ill-posed ones of deductive logic, if we are certain of the facts in the statement of the problem because they

have been observed to occur in the measurement, or are deduced from them, we are just as certain of the assignment of the probabilities. The theory is fully objective in the sense that every individual using it must reach the same conclusions because all and only the information provided in the statement of the problem is used and is therefore available to all.

There is no uncertainty data in this theory, neither as input nor as output. Uncertainty is a concept related to the notions of deductive logic. In a well-posed problem of deductive logic we can prove that one and only one of a set of assertions is true. Real life problems are always ill-posed ones of deductive logic, but we know from experience in simple situations that they have a unique solution in the sense that a particular course of action is preferable to any other if we are trying to accomplish a goal. We tend to view the problem as one of trying to know what the true values of the physical quantities of interest are. In this theory of logical inference this is not done. In a first step we determine first an intermediate "object," called probability density function, which summarizes what all of the facts we are considering in the statement of the problem tell us about the true value of these quantities. This *conditional probability density function* is then used to make a decision in which enters other considerations based upon what we are trying to accomplish with this decision. To push the analogy with quantum mechanics, what we are trying to accomplish determines the operator which acts upon the probability density function to produce a decision which is an observable of the theory. We do not have time here to develop this aspect of the theory and show how this operator is generated and can be identified with the "loss function" used in some decision theories. This is a "user problem" which we are not considering at this workshop.

V. EVALUATIONS

Having analyzed a number of problems during the last two years, I think that this theory should impact significantly what we do in evaluation work today. Rather than provide some examples here which would require a development of the theory, that I cannot carry out here, I will now summarize some conclusions which I have come to from using it[7] and will provide elsewhere a detailed justification for them.

A lot of what we do in data evaluation is not entirely rational and I believe we could make a much more efficient job of it than we are now doing. We are far more influenced by what we think we are doing than most of us perceive. This is reflected largely in the way we organize the evaluation work, the information we seek to utilize, what and how we communicate to the measurers, theoreticians and users. We therefore tend to lose a lot of information which is relevant to our work and the work of others. However, as many of you perceive, in the nuclear data community we do a far better job of it than most other fields I am aware of.

Many of the issues that we think are rather fundamental which we have discussed for years in and out of the CSEWG, some of them will no doubt be raised at this conference (representations, covariances, details in the file, adjustments and biases, standards, special purpose files, consistency, etc.), do not appear fundamental at all from the point of view of this theory and therefore I believe could be easily resolved to everyones satisfaction. Many of these issues are semantic problems which arise because of the way we verbalize what it is that we do. This often forces us to focus on trying to answer some questions which have only marginal bearing on the issues we are concerned about.

There is, however, I think, very little confusion in what we are trying to accomplish. We have now considerable experience at many of the things we do in data evaluation and, since our numbers keep on being used by many people, much of what we do could not be all that wrong. Any theory which would produce the conclusion that much of what we do is seriously wrong would have to be judged to be inconsistent with the facts at hand. I am therefore happy to say that this theory leads me to conclude that much of what we do is right in the sense of being consistent with what we take to be the facts and the goals we seek.

In my opinion, this theory is most useful because it points out some serious deficiencies in several areas and makes some concrete suggestions on how we could remove them. Although the theory does correctly identify some areas which we are concerned about today without its use, it does point out others where we tend to think what we do is reasonably correct. It should possibly come as no surprise to anyone that many of these areas of concern are related to what we identify today as being affected by "systematic errors."

We have some difficulties with what is to be used as "input data." Many of our "input data" come from the general literature where the experiments were performed to answer some specific questions often related to theoretical considerations and/or previous experimental results. As it should be, the experiments are designed and the observations treated so as to have most bearing upon the questions being addressed. Very frequently what are reported as "data" are not what was observed but rather conclusions relevant to the questions being addressed in the paper. This usually means that the data reduction, as we call it, contains in it the consideration of the "loss function" for the particular application it was intended to serve. In the usual language, various biases and systematic errors are introduced for convenience since they have little or no bearing upon the answers to the specific questions being addressed. The consequence is that what we take as "experimental data" are not what we should use, but we are not given sufficient information to recover from them what we need for our own applications. These "experimental results" as we call them are only relevant for a limited time period since we are no longer interested in conclusions based upon assumptions which we no longer consider valid. This is the major reason why often, but

certainly not always, old data are not perceived to be as useful as new. There are in general difficulties with the treatment of observations of relative values and the role of ratio measurements and "standard cross sections."

There is often poor treatment of theoretical information in the use of models and of so-called correction factors in both experimental papers and evaluation work. This is again due to the fact that these do introduce, as we say, systematic errors and biases.

We have often some difficulties with the treatment of angular distributions and energy spectra. We are aware of it since some of our most trusted formulae, for instance obtained from the least-squares method, sometimes produce negative cross sections and fluxes. Lately[9] the "logarithmic least-squares method" has been extensively used to avoid just such problems; often the theory says that this is not the proper way of doing it. We have great difficulties in dealing with uncertainties in these quantities and this is largely due to the fact that we have little or no frequency data in some angular and energy ranges. This problem, according to the theory, is closely related to several other ones which today we do not perceive clearly to be connected. Some of these are: what is the uncertainty on the uncertainty? How do we prevent our data files from blowing up with all the information we attempt to put in them? Why are we reluctant to allow some cross sections to be adjusted but not some others? When reevaluating a cross section we feel we must go back and consider all the data again; why can we not start from the old evaluation and add the new data? How do we rationally deal with the "oddball" result? Unfortunately, I cannot go into details here and explain why we only get limited guidance from the theory of statistics in these areas and why they are all closely connected with the concept of the probability of a probability. As I have pointed out earlier, the observable facts and the deductions obtained from them determine uniquely the probability density functions for the quantities of interest. What I did not go into is that the nature of these facts determines also a certain rigidity to this probability density function. We can tell from the nature of the information how likely are our conclusions subject to change if we are given more information of certain types. Lawyers are well aware of this and talk of the evidence for a conclusion and the weight of this evidence. We also have this notion in data evaluation work but do not know how to quantify and use it. We perceive that we should give different weight to different experiments. We perceive that only when they are all the same kind of experiments can this weight safely be put equal to the inverse of the variance. A fully documented paper should possibly be given more weight than one with little or no documentation.

There are various ways to interpret the ENDF/B files according to this theory. A most useful one to me is that they represent the summary of what we can tell rationally about the true values of the data on the basis of a certain class of facts. That is to say, we provide a conditional probability density function (pdf). Because

of the formulae we use, what we call the data files contain the expectation values of this joint pdf. The covariance files contain the second moment of this joint pdf. For many cross sections that we have known for a long time to play an important role in some applications, we have acquired a lot of data and by virtue of the central limit theorem the joint pdf is a joint normal one, at least not too far from the mean. For many other cross sections and data in the file this is far from being the case. This joint pdf, being a summary of what the class of facts considered tell us, is indeed application independent. The user must then make his own decision as to what to take as the true value for the data and this choice will be a function of his application and the joint pdf in the file.

The user may want first to modify this joint pdf to reflect observations which were not considered in the evaluation. This is what the so-called "adjustment" step is intended to do. It would be irrational for him not to consider all the information available to him. Whether to adjust or not is not the issue at all. We will never convince an engineer, who must make a decision where he perceives there is a risk to him, to ignore what he considers relevant information, unless we can prove to him that other information we used has made his information irrelevant. What should concern us as evaluator is to provide the user with the relevant material for him to determine if his information is redundant or not. We should also be interested in finding out if the user has information which is relevant to other potential users of our files. Because of our lack of confidence in how to deal today with what we call systematic errors and the confusion which seems to exist as to the exact relationship between what we place in the data files and what the user should rationally use in his application, we tend to believe that there are difficulties where the theory of logical inference tells us sometimes there is a difficulty but sometimes there is none. Today we can only react when using our common sense we perceive that a large mistake is being made, but we have difficulty in finding out how to correct it.

For the other data in the file where we do not provide covariance information, the user has little choice but to consider the number there as the true value, but he has no way of ascertaining the risks involved for him in doing so. Clearly, if his result or intended goal is only weakly dependent upon the data, he is not concerned, or should not be concerned. However, if his result is sensitive to these data and the risks to him are consequential, he has some difficulties. Of course the fact that in ENDF/B-V there are no covariance files for a particular data does not mean that the data are well known. This is a current difficulty with our version of ENDF/B-V, and users of the files should be aware of it.

ACKNOWLEDGEMENT

This research was sponsored by the Division of Basic Energy Sciences and the Division of Reactor Research and Technology, U.S. Department of Energy, under contract W-7405-eng-26 with the Union Carbide Corporation.

REFERENCES

1. F. G. Percy, "Introduction to Logical Inference and Application to Nuclear Data Uncertainty," to be published. The present paper is closely related to the introduction to the proposed treatise.

2. J. M. Keynes, A Treatise on Probability, MacMillan and Co., 1921.

3. E. T. Jaynes, Transactions on Systems Science and Cybernetics 4, 227 (1968).

4. T. Simpson, Royal Soc. of London Philosophical Transactions 49, 83 (1755).

5. Laplace, "Thèorie Analytique des Probabilités," Oeuvres Complete de Laplace, Vol. 7, Gauthies-Villars (1886), First Edition, 1812.

6. C. F. Gauss, C. F. Gauss Werbe, Vol. 4, p. 1, Royal Society of Göttingen (1880), First Edition, 1821.

7. F. G. Percy, "Lectures on Probability Theory," ORNL (1978).

8. F. G. Percy, Synthèse, to be published (1981).

9. H. Gruppelaar, contribution to this workshop.

Discussion

Block

You have described your 'new' theory, but you have given no examples. Can you provide us with some specific example, or examples, where this theory has given a new insight, a breakthrough, etc. on a practical experimental or evaluation problem?

Perey

In the short time available here I thought it would not be possible to give a detailed example. I have applied the theory to many problems and these will be reported elsewhere.

Poenitz

The suggestion that, given a number of facts (experimental results) which are mutually exclusive, only one of these can be correct, but we do not know which, appears to collide with the basic feature of the measuring process which is: to provide uncertain data. As a result of this feature we would expect that none of the facts is representing the true value existing in nature, though one may come by chance very close.

The selection of a value as true based upon consistency is again in conflict with measurement errors. Measured values may be consistent because systematic errors of these values are consistent. We have seen that again and again with nuclear data, a great deal of consistency may have been achieved but found to support a value later discovered to be unlikely.

Perey

When there are seemingly contradictory facts which are observed it must be that we are not observing related facts.

In the theory one does not select the true value based on consistency of the observations. Given the observations it is the probability density function which is assigned on the basis of consistency with the facts which cannot be mutually contradictory. If we claim there is an uncertainty it is because several values are possible for the true value. How one chooses in a particular application what value to use as if it were the true value depends upon what are the consequences to us if the value we choose does not turn out to be the true value. Given a set of observations the probability density function for the true value is unique, but several people in different applications may choose different values as the true one.

Moldauer

The ultimate aim is to relate one set of physical phenomenon to another set (e.g. to relate reactor performance characteristics to counts obtained in a cross section laboratory). We don't do this in one step but interpose the concept of "data." Does your theory throw light on the question of how our knowledge about the relationship between phenomena is affected by the two-step process experiment → data, data → application?

Perey

Yes. The relationship experiment → probability (density function) for the true value of the data is first made. Given a specific application and the consequences to us, what we choose as the true value is a function of the probability density function and of the consequences to us in the specific application. Given several different applications, what we choose to use as if it were the true value may be different.

Hale

What sort of implications does the "theory of logical inference" have for the usual techniques based on χ^2 minimization we are now using? In other words, is there still a "likelihood" parameter which, like the χ^2, needs to be minimized?

Perey

Not in the same way. The formula we often use which we derive by minimizing χ^2 can also be derived in this theory, but it is not obtained as the result of minimizing χ^2. In most instances that I am aware of, this formula results when we have, by virtue of the central limit theorem, a probability density function which is approximately joint normal and a likelihood function which is also normal and we apply Bayes' Theorem.

USE OF UNCERTAINTY DATA IN NEUTRON DOSIMETRY*

L. R. Greenwood

Argonne National Laboratory
Argonne, Illinois 60439

ABSTRACT

Uncertainty and covariance data are required for neutron activation cross sections and nuclear decay data used to adjust neutron flux spectra measured at accelerators and reactors. Covariances must be evaluated in order to assess errors in derived damage parameters, such as nuclear displacements. The primary sources of error are discussed along with needed improvements in presently available uncertainty data.

INTRODUCTION

The status of neutron dosimetry for materials effects irradiations was discussed in a recent review paper [1]. The term dosimetry in this case refers to the measurement of the neutron flux spectrum, as shown in Figure 1, and the use of such data to determine more fundamental damage parameters, such as nuclear displacements and transmutations. The passive, multiple-foil technique is used wherein materials are irradiated, activated or stable products are measured, integral reaction rates are determined, and, finally, a trial flux spectrum is adjusted to best fit the integral data. Detailed nuclear cross sections and decay data are required for such an analysis, and recent computer codes [2,3] accept a complete variance-covariance matrix for all input data.

The principal uncertainties encountered in neutron dosimetry are listed in Table I along with representative values. Integral measurements are quite accurate since most sources of error are well known and subject to rigorous analysis. Dosimetry cross sections and uncertainties are available in ENDF/B-V [4], although the files are by no means complete since they stop at 20 MeV, omit many useful reactions, and contain only limited covariance information. Uncertainties in the input flux spectrum are the most troublesome and typically are the largest source of error. Since

rigorous flux uncertainties are not generally available (e.g., from neutronics calculations), they tend to be rather subjective, based on previous experience or integral tests.

Damage production cross sections, as shown in Figure 2, are equally important with dosimetry cross sections since spectral-averaged nuclear displacements and transmutations are usually the final goal of neutron dosimetry for materials irradiations [5]. Unfortunately, the required nuclear data is very comprehensive, including all strong nuclear reactions and recoil distributions, and very poorly known, especially above 14 MeV. In fact, dosimetric uncertainties are typically equal to or less than intrinsic errors in the nuclear data. It is also important to note that a covariance matrix must be obtained for the final flux solution since covariance effects are typically very large and must be considered in the calculation of all spectral-averaged parameters.

UNCERTAINTIES IN INTEGRAL MEASUREMENTS

The most common uncertainties in the integral measurements are listed in Table II. Since most of terms can be measured experimentally, overall errors are typically less than ~2%, as confirmed by interlaboratory comparisons. Nevertheless, there are a number of special problems listed in Table II which have been found to cause larger than normal uncertainties. Furthermore, several of these problems concern nuclear data and should be of concern to this workshop.

Neutron self-shielding [6] with and without cadmium covers is presently included with the nuclear cross sections prior to spectral adjustment. Such effects are very important in mixed-spectrum reactors and can be as large as a factor of ten, as shown in Figure 3. Unfortunately, computer codes are not presently available for determining the uncertainty in these corrections, especially near large resonances; however, codes are under development for the new files in ENDF/B-V [7]. Scattering effects can also be important when the scattering cross section exceeds that for capture (e.g., in cobalt). Experimental measurements of self-shielding can be made; however, the spectrum is generally not well known. It is important to develop these uncertainties since data comparisons between thick and thin foils can, in principle, provide remarkably accurate flux measurements for neutrons in the thermal and resonance energy regions.

Burn-up corrections are needed for both the target and activation product at reactors having high thermal fluxes. For example, about half of the initial ^{59}Co atoms will be burned-up within six months for a dilute sample in the core of the High Flux Isotopes Reactor at Oak Ridge National Laboratory. Similar problems exist for the burn-up of ^{198}Au from capture in ^{197}Au at much lower thermal fluxes. Fast reactions can also be affected. For example, ^{58}Co is rapidly converted to ^{60}Co in a moderate thermal flux thereby necessitating corrections for both the $^{58}Ni(n,p)$

and $^{60}Ni(n,p)$ reactions (see Figure 4) as well as for the ^{59}Co $(n,2n)$ and (n,γ) reactions. In these latter cases neutron cross sections are very poorly known for ^{198}Au or ^{58}Co. Furthermore, all burn-up corrections are complicated by the need to know a spectrum prior to analysis. Hence, iterative techniques must be used to find self-consistent solutions. Uncertainties are consequently hard to quantify. Burn-up corrections will become increasingly important in the fusion program as fluences approach fusion reaction conditions.

Spatial flux and spectral gradients increase the relative errors between different integral measurements since corrections are needed to normalize all reaction rates to a common location. Be or Li(d,n) accelerator sources, such as the Fusion Materials Irradiation Test Facility now under construction at Hanford Engineering Development Laboratory, have especially steep gradients, as shown in Figure 5, and separate corrections are needed for each reaction due to changes in the spectra [8,9]. Fortunately, corrections can be measured experimentally by placing one material at several locations. Nevertheless, the errors could be reduced if more uncertainty data were available for neutronics calculations used to model the close-geometry neutron field in routine applications.

Temporal variations in flux and spectrum are important when half-lives are less than irradiation times since reaction rates may not represent the true average value. Flux variations are easily recorded and suitable corrections can be made. However, spectral changes due to reactor fuel changes or accelerator beam and target variations, are not well known. Hence, nuclear cross sections and uncertainties are needed for more long-lived or stable product (e.g., He) monitors to minimize this source of error. Very few dosimetry reactions with half-lives greater than one year are currently available.

DOSIMETRY CROSS SECTIONS

Dosimetry cross sections are evaluated in ENDF/B-V [4] below 20 MeV and many reactions have been extended to 44 MeV for fusion dosimetry [10]. Considerable effort has gone into integral testing of this data [8,9,11] and some results are summarized in Tables III and IV.

Many reactions are quite well known for reactor dosimetry, as demonstrated in Table III. However, many problems remain since (1) more reactions should be included in ENDF/B-V, (2) several discrepancies need to be resolved [e.g., $^{47}Ti(n,p)$, $^{60}Ni(n,p)$, $^{58}Ni(n,2n)$, and $^{237}Np(n,\gamma)$], (3) uncertainties are needed for resonance and self-shielding calculations, and (4) more reactions are needed with long-lived or stable (He) products. Resonance and self-shielding uncertainties are important since rather precise flux measurements are possible if reaction rates are compared for thick and dilute materials, with and without cadmium or gadolinium

covers [12]. Errors are difficult to quantify at present and some promising capture reactions are not included in ENDF/B-V (i.e., ^{55}Mn, ^{149}Sm, ^{176}Lu, and ^{186}W). The $^{64}Zn(n,\cdot)^{65}Zn$ reaction would be very useful in long irradiations due to long half-life and low thermal burn-up. The $^{93}Nb(n,n')$ reaction is also needed to improve reaction sensitivity below 500 keV.

Dosimetry cross sections are very poorly known above 28 MeV for accelerator neutron sources. The most important reactions are listed in Table V and total helium production cross sections are also needed for these elements. Although somewhat premature, uncertainties have also been estimated [10] for high-energy cross sections and must also be developed.

Competing reactions leading to the same activation product must also be considered. For example, very large contributions are listed in Table IV for the ^{46}Ti, ^{47}Ti, and ^{54}Fe (n,p) reactions from higher mass isotopes. Similar problems occur at higher neutron energies due to (n,xn) reactions on multi-isotopic elements (e.g., Ni, Zr, Ag, Lu, Tl). Total cross sections should be developed and uncertainties due to these effects must be considered.

Total helium production cross sections are also needed since (1) helium generation is critically important to damage production mechanisms in most materials and (2) helium accumulation fluence monitors [13] can be used for neutron dosimetry. Integral comparisons of radiometric and helium production cross sections are now in progress at reactors and accelerators [1]. Numerous discrepancies have been uncovered with the data in ENDF/B-IV, although better agreement is expected with the gas production files in ENDF/B-V. Uncertainty data is of course needed if the helium technique is to be routinely applied for neutron dosimetry purposes.

UNCERTAINTIES IN INPUT FLUX SPECTRA

The multiple-foil activation technique relies on some estimate of the flux spectrum prior to adjustment. At present this produces the largest source of uncertainty, as shown in Table I. At reactors, neutronics calculations are generally used, although error estimates are only rarely available. At accelerators, estimated spectra have been obtained from remote time-of-flight data averaged over the large solid angles used in close geometry irradiations. More accurate estimates could be obtained if thin target neutron yields and spectra were available. In all cases, one generally has to make an educated guess concerning spectral uncertainties. Integral testing [8,9,11] in well-known spectra can of course be used to evaluate and refine error estimates. However, no systematic procedure has been developed and sensitivity studies are needed to improve the technique. Furthermore, spectral adjustment is of course dependent on adequate foil

coverage or reaction sensitivity and does not work well in some energy regions, especially between 1 and 500 keV at reactors and below 1 MeV or above 30 MeV at accelerators.

It should also be mentioned that spectral adjustment codes are usually not reliable when very large discrepancies are found in the input spectrum. Unfortunately, this is often the case in some energy regions encountered in fusion dosimetry. For example, order of magnitude uncertainties are routine in estimates of the flux below 1 MeV at accelerators. If the flux estimate is much too low, then this region has a very low relative sensitivity and the proper solution may not be obtained or the shape may be distorted (e.g., non-Maxwellian thermal spectrum). Logarithmic adjustments can be used but it is difficult to adequately specify covariances. The problem is generally handled by trying various input spectra until a reasonable guess is obtained. More rigorous procedures are clearly desirable. However, it is usually true that such cases are not very important in terms of overall damage production. Systematic sensitivity studies might be used to improve the technique.

COVARIANCE DATA

The inclusion of covariance data in neutron dosimetry is partially due to new computer codes [2,3], but, more fundamentally, to significant improvements in the nuclear data base. ENDF/B-V [4] now includes some covariance data; however, all of the self- and cross-covariances needed for routine dosimetry are not available. Consequently, self-covariances have been assumed to have a Gaussian distribution wherein nearby flux and cross section groups are highly correlated and widely separated groups are uncorrelated. The width of the Gaussian for the flux spectrum is arbitrary and is often varied according to the number of foils and their response, similar to smoothing techniques in iterative, unfolding computer codes. Cross-correlations are generally ignored or assigned an arbitrarily small value.

Such uniform procedures for assigning covariances are simple and appear to work reasonably well in most instances. Nevertheless, problems can arise in that desired spectral shapes are not maintained, especially when large uncertainties are involved. For example, the final thermal spectrum may be non-Maxwellian or the fast spectrum may deviate from an assumed fission spectrum. Stronger, localized covariances might improve this situation; however, establishing such data is difficult and somewhat arbitrary. This is particularly true when the relative normalization and joining functions between various energy regions are unknown. As mentioned previously, the best procedure appears to involve changing the input spectrum by trial and error until a physically reasonable guess is obtained.

Clearly, a uniform, more objective approach to covariance data is needed. Hopefully data will improve in ENDF to the point

where a comprehensive dosimetry cross-section covariance data file can be generated for routine applications. Integral testing will then be required to assess the reliability of the data. Flux covariances can only be improved by including covariance data in neutronics calculations and by systematic sensitivity studies to develop physically reasonable data and techniques.

REFERENCES

1. L. R. Greenwood, Review of Source Characterization for Fusion Materials Irradiations, BNL-NCS-51245, May 1980.

2. F. G. Perey, Least Squares Dosimetry Unfolding: The Program STAYSL, ORNL/TM-6062 (1977).

3. F. Schmittroth, Nucl. Sci. Eng. 72, 19 (1979).

4. Evaluated Nuclear Data File B-V, National Neutron Cross Section Center, Brookhaven National Laboratory (1979).

5. Recommendations of IAEA Working Group on Reactor Radiation Measurements, Nucl. Eng. Des. 33, 92 (1975).

6. S. Pearlstein and E. V. Weinstock, Nucl. Sci. Eng. 29, 28 (1967).

7. Radiation Information Shielding Center, Oak Ridge National Laboratory (1980).

8. L. R. Greenwood, R. R. Heinrich, R. J. Kennerley, and R. Medrzychowski, Nucl. Technol. 41, 109 (1979).

9. L. R. Greenwood, R. R. Heinrich, M. J. Saltmarsh, and C. B. Fulmer, Nucl. Sci. Eng. 72, 175 (1979).

10. L. R. Greenwood, Extrapolated Neutron Activation Cross Sections for Dosimetry to 44 MeV, ANL-FPP/TM-115 (1979).

11. M. F. Vlasov, A. Fabry, W. N. McElroy, Status of Neutron Cross Sections for Reactor Dosimetry, IAEA, INDC(NDS)-84/L+M (1977).

12. L. Bozzi, F. Caporella, M. Cosimi, and M. Martini, Nucl. Inst. Meth. 119, 599 (1974).

13. D. W. Kneff, B. M. Oliver, M. M. Nakata, and H. Farrar IV, Helium Generation Cross Sections for Fast Neutrons, Symposium on Neutron Cross Sections from 10-50 MeV, BNL-NCS-51245, May 1980.

14. G. R. Odette and D. R. Doiron, Nucl. Technol. 29, 346 (1976).

15. C. Y. Fu and F. G. Perey, J. Nucl. Mater. 61, 153 (1976).

16. B. P. Bayhurst, J. S. Gilmore, R. J. Prestwood, J. B. Wilhelmy, N. Jarmie, B. H. Erkkila, and R. A. Hardekopf, Phys. Rev. C12, 451 (1975).

TABLE I.

Principal Sources of Error in Neutron Dosimetry.

Type of Error	Typical Value, %
Integral Measurements	<5
Neutron Cross Sections	5-30
Input Flux Spectra	30-100
Damage Parameter Cross Sections	10-100

TABLE II.

Principal Uncertainties in Integral Measurements.

Type of Error	Typical Value, %
Counting Statistics	<1
Detector Efficiency	<2
Nuclear Decay Data	<2
Coincidence Summing	<1
Gamma Self-Absorption	<1

Special Problems

Neutron Self-Shielding (Resonance)

Burn-up Corrections

Flux and Spectral Gradients

Temporal Variations in Flux or Spectra

TABLE III.

Typical Deviations between Measured and Calculated (ENDF/B) Activation Integrals on ORR (E7, 1 MW) after Spectral Adjustment (STAYSL). +Cd means cadmium covered (20 mil).

Reaction	Deviation, % (Measured-Calculated) IV	V
$^{197}Au(n,\gamma)^{198}Au$	-3	-1
+Cd	-1	+1
$^{45}Sc(n,\gamma)^{46}Sc$	-1	-9
+Cd	-2	+2
$^{59}Co(n,\gamma)^{60}Co$	-5	-7
+Cd	+2	+4
$^{58}Fe(n,\gamma)^{59}Fe$	+3	+3
+Cd	-1	+4
$^{238}U(n,\gamma)^{239}Np$	-4	-2
+Cd	0	+4
$^{237}Np(n,\gamma)^{238}Np$ (+Cd)	+15	+11
$^{235}U(n,f)$	+4	+1
+Cd	-3	-2
$^{237}Np(n,f)$ (+Cd)	-1	+1
$^{238}U(n,f)$ (+Cd)	+8	+2
$^{58}Ni(n,p)^{58}Co$	+6	+3
$^{60}Ni(n,p)^{60}Co$	-14	-13
$^{54}Fe(n,p)^{54}Mn$	+5	+3
$^{54}Fe(n,\alpha)^{51}Cr$	+11	+17
$^{46}Ti(n,p)^{46}Sc$	-3	+1
$^{47}Ti(n,p)^{47}Sc$	-18	-25
$^{48}Ti(n,p)^{48}Sc$	-8	+2
$^{197}Au(n,2n)^{196}Au$	+1	+1

TABLE IV.

Integral Cross Section Errors (ENDF/B) Deduced from Activation and Time-of-Flight Measurements in Be(d,n) Fields. Absolute errors are ±10%.

Reaction	E_D = 14-16 MeV IV	E_D = 14-16 MeV V	E_D = 40 MeV IV	E_D = 40 MeV V
$^{235}U(n,f)$	+7	+8	+1	+1
$^{238}U(n,f)$	+4	+4	-1	-1
$^{115}In(n,n')^{115m}In$	-1	-2	-3	-2
$Ti(n,p)^{46}Sc$	-7	-1	-89(+14)[a]	(+24)[a]
$Ti(n,p)^{47}Sc$	+2	+6	-798(+45)[a]	(-56)[a]
$^{48}Ti(n,p)^{48}Sc$	-7	-1	+2	+4
$Fe(n,p)^{54}Mn$	+6	-3	-88(+1)[a]	(+4)[a]
$^{56}Fe(n,p)^{56}Mn$	-2	-2	-4	-4
$^{59}Co(n,p)^{59}Fe$	-8	-4	+8	+5
$^{58}Ni(n,p)^{58}Co$	0	-3	+9	+3
$^{60}Ni(n,p)^{60}Co$	+14	-2	+3	+3
$^{27}Al(n,\alpha)^{24}Na$	+3	+6	0	-1
$^{54}Fe(n,\alpha)^{51}Cr$	-4	+1	-36	-20
$^{59}Co(n,\alpha)^{56}Mn$	-4	-2	-4	-5
$^{45}Sc(n,2n)^{44m}Sc$	-14	-15	-1	+3
$^{58}Ni(n,2n)^{57}Ni$	-11	+1	-30(+14)[b]	(+14)[b]
$^{59}Co(n,2n)^{58}Co$	+1	+6	-9	-3
$Zr(n,2n)^{89}Zr$	+13	+9	-4	-1
$^{93}Nb(n,2n)^{92m}Nb$	+7	+6	+6	+7
$^{169}Tm(n,2n)^{168}Tm$	--	--	+7	+10
$^{169}Tm(n,3n)^{167}Tm$	--	--	-9	-8
$^{197}Au(n,2n)^{196}Au$	-9	-8	-1	+1
$^{197}Au(n,3n)^{195}Au$	--	--	+8	+12
$^{197}Au(n,4n)^{194}Au$	--	--	+1	+1
$^{238}U(n,2n)^{237}U$	+4	+1	-11	-11

[a] Values in parenthesis include contributions from higher mass isotopes.

[b] Value in parenthesis modified according to Ref. 16.

TABLE V.

Threshold Activation Reactions Desired for Fusion Dosimetry Listed by Material in Order of Priority. Elements with multiple, long-lived products are favored. Many other reactions could also be used.

Reaction	Energy Range (MeV)	Reaction	Energy Range (MeV)
$^{59}Co(n,p)^{59}Fe$	4-28	$^{90}Zr(n,p)^{90}Y$	5-26
$(n,2n)^{58}Co$	10-30	$Zr(n,x)^{89}Zr$	12-36
$(n,3n)^{57}Co$	20-40	$(n,x)^{88}Zr$	18-45
$(n,4n)^{56}Co$	30-50	$^{8}{}^{9}Y(n,p)^{89}Sr$	4-25
$^{197}Au(n,2n)^{196}Au$	8-25	$(n,2n)^{88}Y$	12-34
$(n,3n)^{195}Au$	15-35	$(n,3n)^{87}Y$	22-50
$(n,4n)^{194}Au$	23-45	$(n,\alpha)^{86}Rb$	8-28
$Fe(n,x)^{54}Mn$	1-40	$^{169}Tm(n,2n)^{168}Tm$	9-28
$^{54}Fe(n,\alpha)^{51}Cr$	7-25	$(n,3n)^{167}Tm$	16-36
$^{54}Fe(n,t)^{52}Mn$	14-35	$(n,5n)^{165}Tm$	25-50
$^{58}Ni(n,p)^{58}Co$	2-25	$^{23}Na(n,2n)^{22}Na$	12-30
$(n,2n)^{57}Ni$	12-36	$^{107}Ag(n,2n)^{106m}Ag$	10-28
$(n,3n)^{56}Ni$	22-40	$(n,3n)^{105}U$	16-40
$^{60}Ni(n,p)^{60}Co$	3-30	$^{238}U(n,2n)^{237}Ag$	6-18
$^{93}Nb(n,n')^{93m}Nb$	0.1-10	$(n,f)f.p.$	1-50
$(n,2n)^{92m}Nb$	9-28	$^{55}Mn(n,2n)^{54}Mn$	11-28

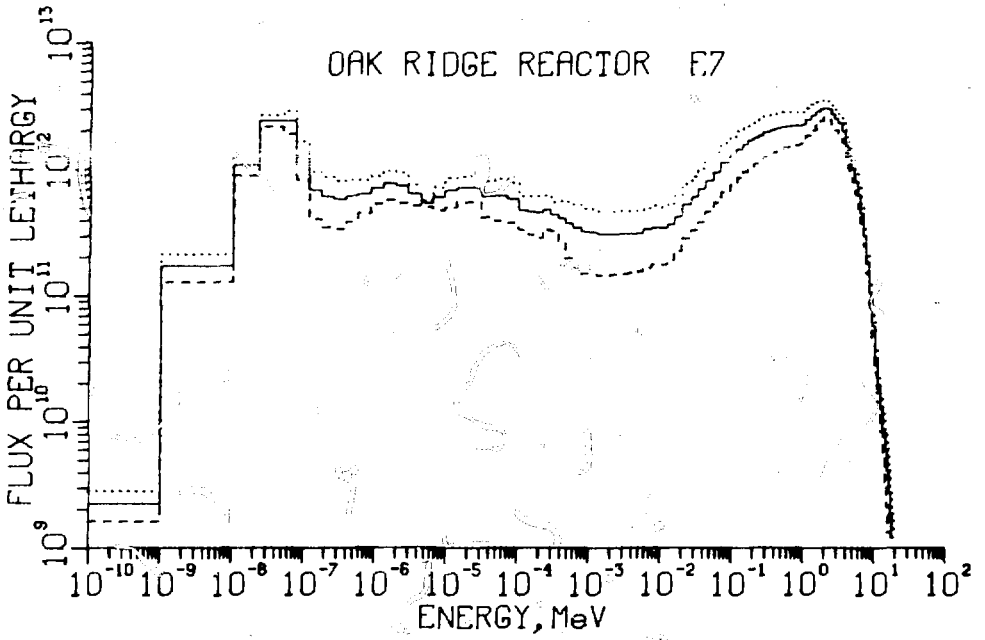

Fig. 1. Neutron flux spectrum for the Oak Ridge reactor (E7,1 MW) using the STAYSL computer code. The reactions are listed in Table III. The dotted and dashed lines represent one standard deviation error limit; however, covariances are very large.

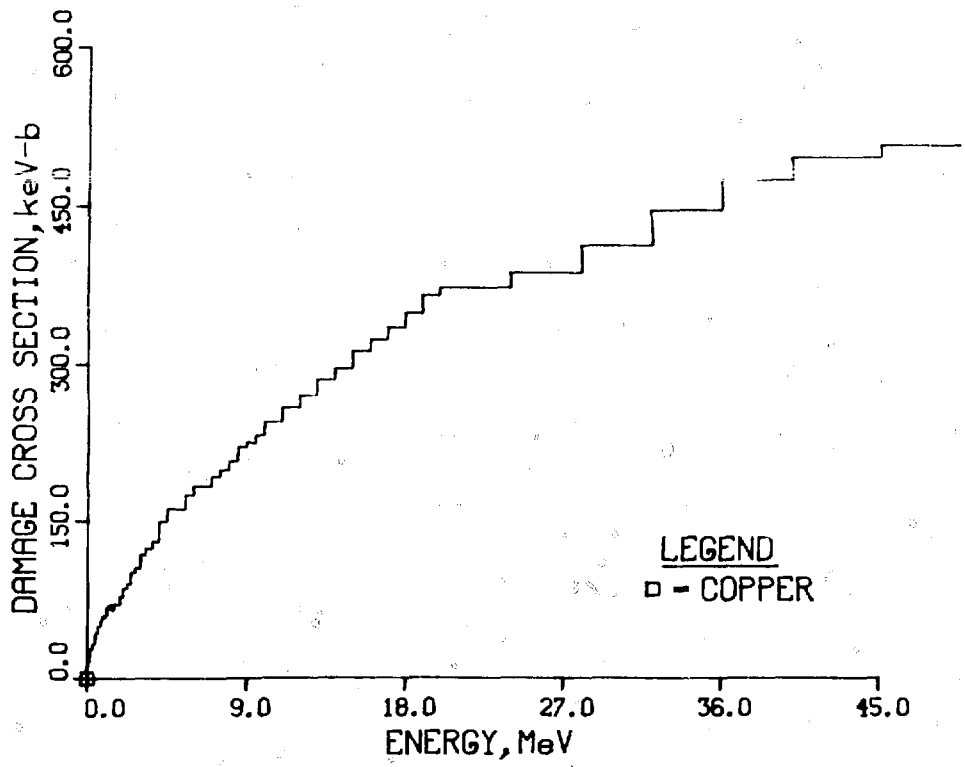

Fig. 2. Displacement damage cross section computed for copper using the DISCS [14] code and nuclear calculations of C. Y. Fu and F. G. Perey [15].

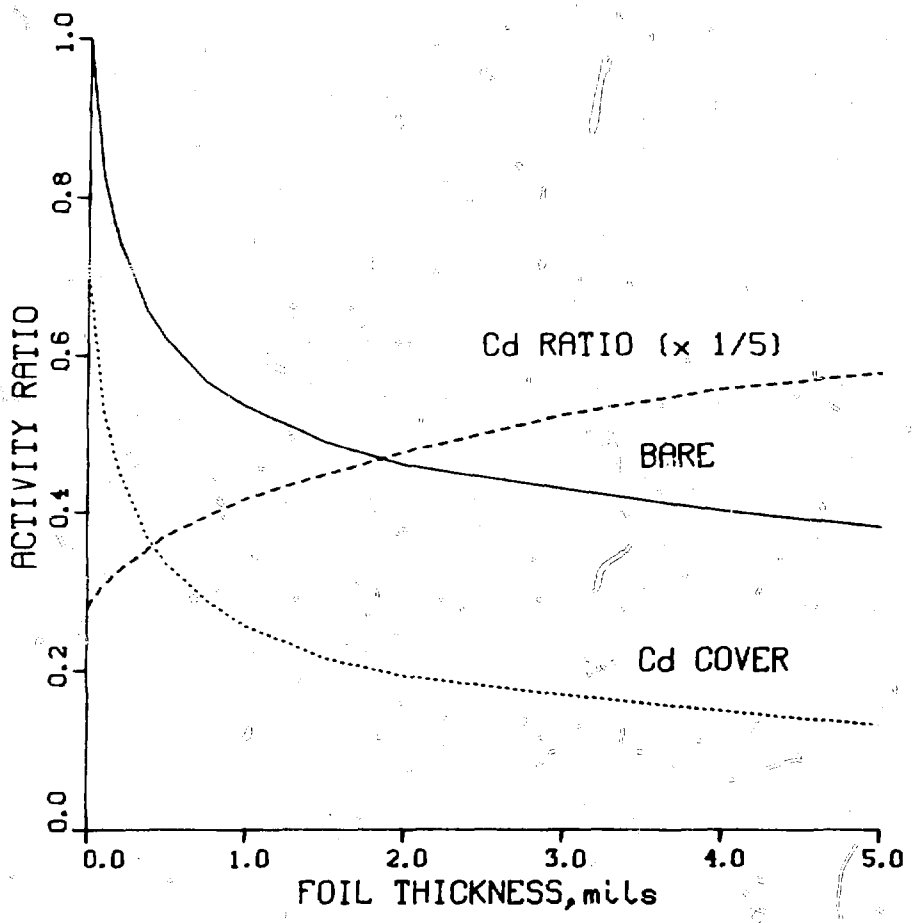

Fig. 3. Neutron self-shielding calculations for the $^{197}Au(n,\gamma)$ reaction, with and without a cadmium cover to suppress thermals. The ORR reactor spectrum is shown in Fig. 1. The cadmium ratio is also shown.

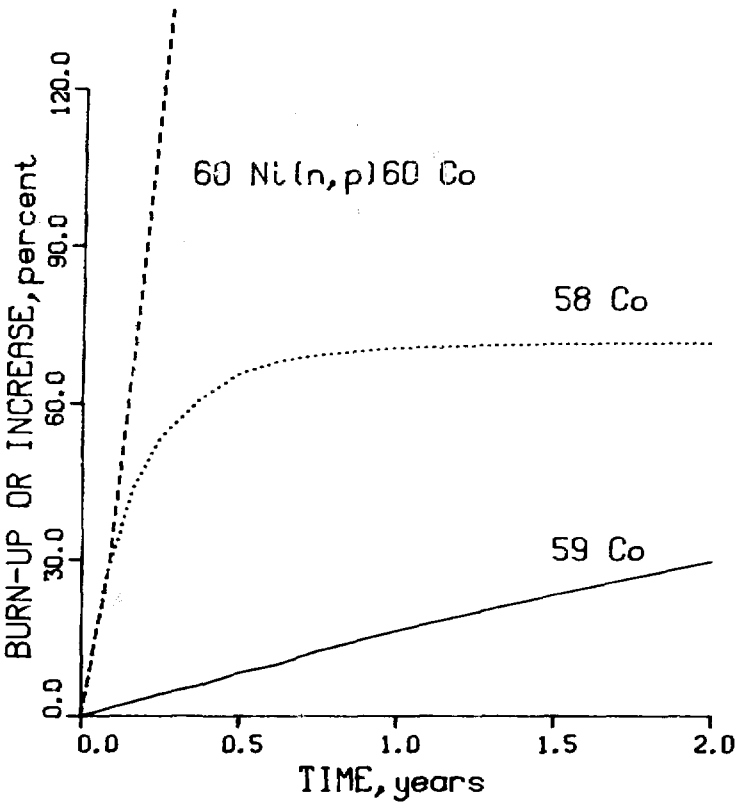

Fig. 4. Burnup effects calculated for nickel and cobalt reactions using the ORR reactor spectrum shown in Fig. 1. The curve labeled ^{59}Co shows the burn-up of a dilute cobalt target. The ^{58}Co curve represents the loss of activity for the $^{58}Ni(n,p)$ or $^{59}Co(n,2n)$ reactions. The $^{60}Ni(n,p)^{60}Co$ curve shows the increase in ^{60}Co activity due to production from the $^{58}Co(n,\gamma)^{59}Co(n,\gamma)$ process.

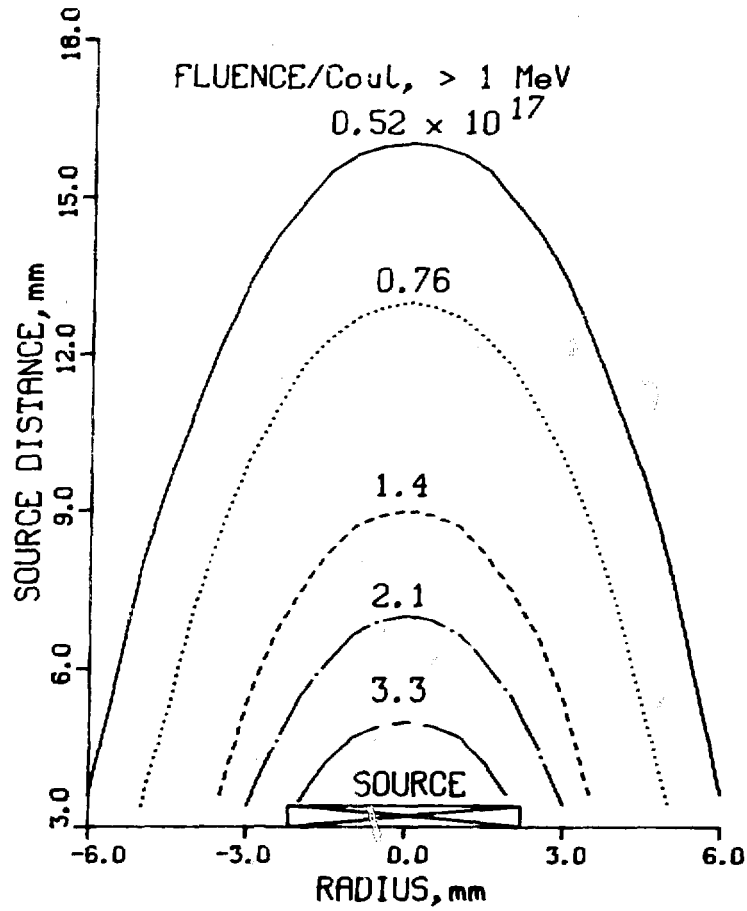

Fig. 5. Fluences measured by radiometric and helium dosimetry at the U. of C. Davis Cyclotron [Be(d,n), E_d = 30 MeV]. Note the very steep gradients, especially off-axis, and the very fine scale.

Discussion

Vonach

What kinds of correlations were considered in the Oak Ridge Reactor spectrum calculations? Correlations within each dosimetry reaction, or also correlations between cross sections for different reactions?

Greenwood

Correlations between reactions are presently ignored and are set equal to an arbitrarily small number. Self-correlations are assumed to be Gaussian, wherein nearby groups (flux and cross section) are completely correlated and widely separated groups are uncorrelated. Naturally, this is somewhat arbitrary and we would like to see an evaluated covariance file for dosimetry where all possible cross section covariances are included. Realistically, this effort may require many years of effort.

Schmidt

To what extent does the calculated neutron spectrum depend upon the choice of the input spectrum?

Greenwood

This strongly depends on the foil coverage or sensitivity (functions) of the reactions used and the neutron energy range being considered. In reactors, the input spectrum is very important, especially in the 1-500 keV energy range where reaction sensitivities are small. However, at high energy accelerators the sensitivity is very good and the input spectrum is not so important. Of course, one must be careful not to specify input errors and covariances that are too large. Sensitivity studies can be done to determine the importance of the input data for any given environment.

Smith

Why are integral reaction rates measured with uncertainties quoted to much better accuracies than often quoted in microscopic measurements?

Greenwood

There are two possible reasons for this: (1) systematic errors may be underestimated or (2) covariances between reaction rates may be ignored (e.g. when several assumed independent quantities are used to deduce a derived parameter). Of course, all errors and covariances must be considered for all integral and differential measurements.

SESSION III

USE OF INTEGRAL DATA
Chairman: F. Schmittroth HEDL

Lcp

CROSS-SECTION EVALUATION UTILIZING INTEGRAL REACTION-RATE MEASUREMENTS IN FAST NEUTRON FIELDS

R. A. Anderl

Idaho National Engineering Laboratory
EG&G Idaho, Inc.
Idaho Falls, Idaho 83415, U.S.A.

ABSTRACT

The role of integral reaction-rate data for cross-section evaluation is reviewed. The subset of integral data considered comprises integral reaction rates measured for dosimeter, fission-product and actinide type materials irradiated in reactor dosimetry fast neutron "benchmark" fields and in the EBR-II. Utilization of these integral data for integral testing, multigroup cross-section adjustment and point-wise cross section adjustment is treated in some detail. Examples are given which illustrate the importance of considering a priori uncertainty and correlation information for these analyses.

1. INTRODUCTION

Integral data have been used in a variety of ways in the evaluation of neutron cross sections. A convenient categorization of their use is as follows: (1) integral testing of evaluated cross sections, (2) cross-section normalization, (3) adjustment of nuclear model parameters, (4) adjustment of multigroup cross sections, and (5) adjustment of point-wise cross sections.

The first category, integral testing, is that which has been used historically in the evaluation of cross sections for the Evaluated Nuclear Data File (ENDF/B). According to this prescription integral data are used only to make "consistency checks" of cross sections which were evaluated on the basis of differential measurements and model calcuations. The "consistency check," or calculated/experimental (C/E) ratio for the integral quantity, then serves to point out the need for improvement of the differential data base for the specific cross section of interest. For the case of radiative capture or neutron-induced fission, the C/E

ratios are often indications of discrepancies in normalization for the evaluated cross section.

In the absence of differential data, integral data have been used to normalize cross-section curves obtained from model calculations. Integral data then have a direct impact on the generation of an evaluated cross section. This approach was used by Schenter [1] in the ENDF/B-IV evaluation of the capture cross sections for several fission-product class nuclides.

A third category of use has been the least-squares adjustment of important statistical model parameters (radiation widths, level spacings, strength functions) based on integral data [2]. According to this approach differential data and nuclear systematics are used to establish the a priori model parameters. The evaluated point-wise curve above the resolved resonance region is subsequently generated by the statistical model prescription with adjusted model parameters.

An applications-oriented approach to the use of integral data has been the generation of the French and Dutch adjusted multigroup cross-section libraries for fast reactors [3,4,5]. According to this approach, evaluated point-wise cross sections are based on differential measurements and nuclear model calculations. The point-wise cross section is expressed in a multigroup representation and group constants adjustments are made based on integral data measured in "benchmark" fast-neutron facilities. Adjusted multigroup libraries are then used for reactor physics calculations to predict the performance of similar fast-reactor systems.

A more controversial use of integral data is for adjustment of point-wise cross sections [2,6]. In this approach integral data and differential data are used simultaneously in a least-squares adjustment of the microscopic differential cross sections derived from earlier evaluations or nuclear model calculations. This approach has been used for some fission-product capture cross section evaluations for ENDF/B-V [7].

As is indicated by the title, this paper focuses on the use of a specific part of the integral data base for cross-section evaluation, namely, capture and fission reaction rates for samples of dosimetry, fission-product and actinide type materials irradiated in reasonably well-characterized fast neutron fields. These neutron fields include some reactor dosimetry "benchmark" fields [8] and the Experimental Breeder Reactor II (EBR-II) [9]. A brief development of these specific topics as they pertain to cross-section evaluation is given in section 2 of this paper.

Not included here is the role in cross-section evaluation of integral data obtained from the fast criticals (ZPR assemblies, GODIVA, JEZEBEL, etc.) located at Argonne National Laboratory (ANL) and Los Alamos Scientific Laboratory (LASL). This will be touched on elsewhere at this conference [10]. In addition, the role of integral data for cross-section evaluation in Europe will be covered by Gruppelaar and Dragt [11].

Rather than treat all five areas which categorize the use of integral data, this paper will be concerned with integral testing, multigroup cross-section adjustment and point-wise cross-section adjustment. The topic of integral testing is developed in section 3. Examples are given of conventional integral testing for dosimeter and fission-product cross sections and for the use of uncertainty and correlation information in the integral testing of the fission cross sections of ^{235}U, ^{238}U, and ^{239}Pu. The role of integral data for adjustment of multigroup cross sections is treated in section 4. General considerations for such use are outlined. Specific examples are given for such cross-section adjustment analyses as applied to relatively well-known dosimeter cross sections and to poorly-known fission-product cross sections. The emphasis of the examples is on the uncertainty and correlation information required for such analyses. In section 5, a discussion of the use of integral data for point-wise cross-section adjustment is given. An example is presented in which integral data, differential data and a point-wise curve from a nuclear model calculation are combined for a simultaneous evaluation of the capture cross section of ^{149}Sm. As a conclusion to this paper, section 6 includes an assessment of the use of integral data in the cross-section evaluation process along the areas developed here, namely, integral testing, multigroup cross-section adjustments and point-wise cross-section adjustments.

2. REACTION-RATE DATA BASE

The purpose of this section is not to detail the specific integral data but to give a general impression of the type, quality and quantity of the measured reaction-rate data. Details of the explicit neutron field characterization and the rate measurements are found in the quoted references. As stated earlier, the specific integral data base considered for this paper includes only integral reaction rates as defined by the following expression

$$R = \int \phi(E)\sigma(E)dE$$

where $\phi(E)$ represents the neutron flux spectrum and $\sigma(E)$ represents the reaction cross section. A multigroup formulation of this expression is generally used for the computation of reaction rates from the typical flux and cross-section multigroup representations. Often the integral data are reported as spectral-averaged cross sections, namely, the integral reaction rate divided by the integral flux.

Measured integral reaction rates, reaction-rate ratios, or integral cross sections have been determined from irradiations of well-characterized samples of dosimeter, fission-product and actinide class materials in various fast neutron fields. Typical reactions include (n,γ), (n,f), (n,p), (n,α), and (n,n') for

dosimeters, (n,γ) for fission products, and (n,γ) and (n,f) for actinides. Radiometric, mass-spectrometric, and fission-chamber techniques have been used in the determination of the reaction rates for the irradiated specimens. All three measurement approaches are, in principle, capable of producing very accurate measured reaction rates.

Nearly all of the dosimeter reaction rates suitable for data testing and cross-section evaluation have been measured or evaluated as part of the Inter-Laboratory Reaction Rate (ILRR) program [12] in the following benchmark neutron fields: ^{235}U fission-neutron spectrum [13], ^{252}Cf fission-neutron spectrum [13], Intermediate Energy Standard Neutron Field (ISNF) [14], BIG-10 [15], and Coupled Fast Reactivity Measurements Facility (CFRMF) [16]. A comparative summary description of these benchmark fields and others used for reactor dosimetry has been reported by Grundl and Eisenhauer [8]. A general report on the use of these benchmark fields for dosimetry applications and data testing has been given by Fabry et al. [17]. Fabry et al. [18] have also prepared a comprehensive compilation of integral cross sections for dosimeters irradiated in these "benchmark" fields. A summary of the radiometric measurements for dosimeters irradiated in CFRMF and BIG-10 has been reported by Greenwood et al. [19]. The results of back-to-back double fission chamber [20] measurements for actinide dosimeters in several benchmark fields have been summarized by Gilliam [21]. Nearly 100 dosimeter reaction rates for benchmark fields have been reported.

The U.S. integral data base for fission products and higher actinides has been established mainly from radiometric measurements for samples activated in the CFRMF [22,23,24]. Some integral capture rates have also been determined from mass spectrometric measurements for isotopically enriched rare-earth samples irradiated in FBR-.I [25]. There have been approximately 50 fission-product and approximately 5 higher actinide reaction rates measured from irradiations in the CFRMF. Nine fission-product reaction rates were obtained from the FBR-II experiment.

3. INTEGRAL TESTS

Conventional integral testing of cross sections requires both an accurate reaction-rate data base and, especially, an accurate characterization of the neutron energy spectrum for the irradiation field. Considerable effort has been made to characterize the benchmark neutron fields [12]. Methods employed have been based on neutronics calculations, active neutron spectral measurements, and passive neutron dosimetry. Of the benchmark neutron fields the fission-neutron spectra for ^{252}Cf and ^{235}U are most accurately characterized. Because of the simplicity of design, the ISNF and BIG-10 are also, in principle, easily characterized by neutronics calculations. Although it is a relatively complex facility when compared to other benchmark fields, the CFRMF has been studied in

detail, and a relatively accurate central neutron flux spectrum is available for data testing. Clearly, the neutron field characterization for locations in EBR-II is difficult and the least accurate.

The primary objective of a conventional integral test is to make a "consistency check" of an evaluated differential cross section by comparing the observed (measured) integral data to that computed using representations of the differential cross section and the neutron spectrum. Such integral tests have been used as indicators of the need for improved differential measurements. It should be noted that the integral test, as such, provides no information about detailed shapes (energy dependence) of cross sections. In fact, apparent consistency or inconsistency between differential and integral data can result if the shapes of the cross sections or neutron spectra are incorrect. For conventional integral tests to be meaningful it is essential, therefore, that shape characterization for the cross sections and neutron flux spectra be accurate. Integral tests are then useful in evaluating normalization discrepancies between differential data sets for a specific cross section.

Examples of integral tests for dosimeter and fission-product cross sections are given in Tables I and II. The integral data correspond to measurements made in the fast neutron field of the CFRMF. The neutron spectrum used in the calculation of both ENDF/B-IV and ENDF/B-V integral cross sections is based on a transport calculation using only ENDF/B-IV cross sections. With the exception of the measured ^{232}Th capture and fission integral cross sections [26], the data in Table I were taken from Maerker [27]. The first four dosimeter reactions are classified as broad response whereas the last four are classified as threshold. The data in Table II were taken from Barber and Anderl [23].

The integral tests for the dosimeter reactions indicate that changes made in the ENDF/B-V cross-section evaluation for all reactions except ^{232}Th(n,γ) and ^{27}Al(n,α) led to more consistency between measured and calculated integral data. It appears that changes in the cross-section evaluations for ^{232}Th(n,γ) and ^{27}Al(n,α) have led to a significant discrepancy between the measured and calculated integral data.

As is shown in Table II, integral testing for these fission-product cross sections points out large discrepancies between measured and calculated integral data both for ENDF/B-IV cross sections and for preliminary ENDF/B-V cross sections. These discrepancies generally indicate the lack of measured differential data available for the evaluation. Obviously there is need for improvement in the differential and integral data bases for these cross sections.

Most conventional data testing in the past did not include estimates of uncertainties in calculated quantities. As evaluated cross sections become better known, the interpretation of discrepancies between measured and calculated quantities becomes meaningful only if the contribution of uncertainty and correlation

information for both the irradiation field neutron spectrum and the sample neutron cross sections are considered for the calculated integral datum. Such an analysis was made by Broadhead and Wagschal [28] for fission-rate ratio measurements in the ISNF for $^{238}U(n,f)$ and $^{239}Pu(n,f)$ relative to $^{235}U(n,f)$. The principal results of this work are summarized in Table III. In this analysis the flux covariance matrix for the ISNF neutron spectrum was determined from a detailed sensitivity and uncertainty study [29] using the FORSS code system [30]. Covariances for the fission cross section were preliminary ENDF/B-V. With no uncertainties considered in the calculation of the reaction-rate ratio, the C/E "consistency checks" indicate a discrepancy outside the experimental error. However, when one considers uncertainties in the calculated ratios, the discrepancies are well within the combined experimental and calculation uncertainties. The conclusion is that, within the uncertainty of the integral test, the integral data and differential curve are consistent.

4. ADJUSTMENT OF MULTIGROUP CROSS SECTIONS

4.1 General Considerations

In principle it is possible to utilize integral data for samples irradiated in a variety of neutron fields in a least-squares adjustment analysis to obtain adjusted multigroup cross sections consistent with the body of integral data. Such a library could then be used for predicting the performance of reactor systems which are similar to or bracketed by the set of representative neutron fields. In general, such a task would entail a detailed treatment of uncertainties, correlations, and cross-correlations in the neutron differential cross sections, the irradiation field neutron spectra, the integral experiments, modeling, methods and, probably, many others. In practice, this appears to be a formidable task. However, there has been a significant effort in the Netherlands [4,5], in France [3], and in the U.S.A. [31] to produce adjusted cross-section libraries suitable for use in the fast-reactor programs.

It is not the purpose of this paper to review these efforts which will be touched on by Gruppelaar [11] and Marable [10] at this conference. However, I would like to present, by way of examples, how some integral reaction-rate data have been used to adjust multigroup dosimeter and fission-product cross sections. It is hoped that the presentation of these examples will illustrate how, in a practical sense, one can carry out such adjustment analyses for two very different categories of reactions, namely, "well-known" dosimetry type reactions and "poorly-known" fission-product type capture cross sections. The purpose of these examples is to show that adjustment of "well-known" cross sections demands an extensive and rigorous treatment of the uncertainties and correlations whereas the adjustment of poorly-known cross

sections can often yield meaningful results even if the a priori uncertainty and correlation treatment is quite approximate but conservative.

4.2 Adjustment of "Well-Known" Cross Sections

The example I will cite is that of the adjustment of multigroup fission cross sections for ^{235}U, ^{238}U and ^{239}Pu based on reaction-rate ratios measured in two benchmark neutron fields at the National Bureau of Standards (NBS), namely the ISNF and the ^{252}Cf field. These analyses have been done by Wagschal and collaborators [32] as part of their effort to apply least-squares methodology to Light Water Reactors Pressure Vessel damage dosimetry applications.

A detailed treatment of the uncertainties and correlations was made for the input data to the least-squares analysis. Modeling uncertainties in the flux spectra determination were minimized because of the geometrically simple neutron fields considered. The ^{252}Cf neutron spectrum was represented by a Maxwellian with a temperature of 1.42 MeV. A flux spectrum covariance matrix for this field was calculated using a 2% uncertainty in the temperature. The ISNF neutron spectrum arises from ^{235}U thermal fission modified by carbon reflection in the higher energy region and shaped at the lower end by absorption in a concentric spherical boron shell and should, in principle, be accurately determined by a neutronics calculation. A representation of the ISNF neutron spectrum was obtained from a transport calculation. The procedure for calculating the ISNF flux covariance matrix is detailed in Ref. 29. Fission cross-section covariance matrices for ^{235}U and ^{239}Pu were processed from ENDF/B-V and that for ^{238}U from ORNL internal files. Cross-element covariances were also considered. A very extensive analysis of the uncertainties and correlations for the integral measurements was made [33].

The least-squares module UNCOVER of the FORSS code system [30] was then used to obtain the "most likely" values of the fluxes, the fission integrals and the differential cross sections based on the uncertainties in the input data. New reduced uncertainties and correlations reflecting the input information were obtained. Changes in the flux and cross-section adjustments were observed in a comparison of an analysis in which all correlations were accounted for to analyses in which various correlations were neglected. Neglect of the correlations between the integral experiments did not impact the flux or cross-section adjustments significantly. However, for this analysis neglect of the cross-element covariances led to cross-section adjustments for ^{235}U which were opposite in sign to those for ^{238}U and ^{239}Pu. Such adjustments cannot be reconciled with what is expected for the highly-correlated differential cross sections which were derived from high accuracy ratio measurements. The conclusion is that for this level of analysis all correlations must be properly accounted for.

4.3 Adjustment of "Poorly-Known" Cross Sections

Many fission-product capture cross-section evaluations are based on model calculations and a rather limited set, if any, of measured differential data. Consequently, many of the differential cross sections are "poorly-known" with uncertainties > 25% in the keV to MeV region. Integral data have been used extensively to improve the knowledge of these cross sections [3,4,5].

To illustrate the role of integral data for adjustment of "poorly-known" cross sections an example is presented here in which capture cross sections for isotopes of Nd, Sm and Eu are adjusted based on integral reaction rates measured for samples irradiated in the EBR-II [25]. The emphasis of the presentation will be to highlight the uncertainty and correlation treatment. Specific results presented in this section and in section 5 for the case of ^{149}Sm demonstrate how adjusted multigroup cross sections can be used for evaluation purposes.

The integral experiment consisted of the following: (1) row 8-EBR-II irradiation of isotopically-enriched samples of Nd, Sm and Eu both at midplane and in the reflector, (2) simultaneous irradiation of passive dosimeters in the experiment capsules, (3) mass-spectrometric determination of the integral capture reaction rates for the rare-earth samples, (4) radiometric determination of the integral reaction rates for the dosimeters. The computer code FERRET [34] was then used for flux/cross-section adjustment analyses utilizing the measured integral reaction-rate data for the dosimeters and the rare-earth samples. The code is based on a log-normal extension of generalized least-squares methods [35] that allow complete covariance descriptions for the input data and the final adjusted data. Basically, these types of analyses were made with FERRET:

(1) neutron spectra characterization - neutron spectra in the experiment capsules were obtained by a simultaneous adjustment of the a priori fluxes identified for all capsules and dosimeter cross sections based on the measured dosimeter reaction rates and a priori uncertainties and correlations assumed for the input data,

(2) sequential fission-product cross-section adjustment - adjusted fission-product cross sections were generated from an analysis for which the input data included: (a) output adjusted fluxes and associated covariances from the spectrum unfolding analysis, (b) a priori fission-product cross sections and associated covariance matrices, (c) fission-product integral data and associated uncertainties,

(3) simultaneous adjustment of all cross sections and fluxes - input data for this least-squares analysis included (a) a priori fluxes and covariances, (b) a priori dosimeter cross sections and covariances, (c) a priori fission-product cross sections and

covariances, (d) integral data and associated uncertainties and correlations.

The *a priori* data base for these analyses included the following:

(1) multigroup representations of the neutron flux spectra at 2 midplane and 4 reflector locations, fluxes based on a neutronics calculation,
(2) multigroup representations of 10 dosimeter and 9 fission-product cross sections processed from ENDF/B-IV,
(3) flux and cross-section covariance matrices based on a parametric representation for the correlations between groupwise uncertainties,
(4) measured integral reaction-rate data for fission products (18 values) and dosimeters (58 values).

Elements of the *a priori* flux and cross-section covariance matrices were assumed to be composed of two components: an overall fractional normalization variance, C^2, and a second term $r_i \rho_{ij} r_j$ to describe any additional uncertainties and correlations. The correlation matrix ρ_{ij} was parametrized by

$$\rho_{ij} = (1-\theta)\delta_{ij} + \theta \exp\left(-\frac{(i-j)}{2\gamma^2}\right)$$

where θ denotes the strength of the short-range correlations and γ denotes their range. The values (r_i) are group-by-group fractional uncertainties.

A detailed treatment of the specific covariance parameters [25,36] is beyond the scope of this paper. However, important assumptions will be identified. In general, conservative assumptions were used to establish the *a priori* flux uncertainties and correlations. That is, relatively large flux normalization uncertainties and weak short-range correlations were assumed so that the final flux adjustments were dominated by the relatively accurate dosimeter reaction rates and cross sections in regions where their response is large. In addition, all cross correlations between *a priori* spectra for different spatial locations were set to zero.

At the time this work was initiated covariance information was not available from ENDF/B for the dosimeter cross sections. Covariance matrices for the dosimeter reactions were defined by an independent evaluation of Schmittroth [36].

Uncertainties and correlations were assigned to the *a priori* fission-product cross sections in a general way. A weakly-correlated covariance component of 20% was used for the resolved energy region. Above the resolved energy region a short-range correlated component was assigned that represented a 25% uncertainty at low energies which increased to 30% at 1 MeV and to 100% at 20 MeV. In addition, highly correlated components of 20% and 30% were included as additional normalization uncertainties for the unresolved and smooth energy ranges, respectively. These components reflect the uncertainties and correlations expected in

the cross sections as a consequence of the use of unresolved resonance parameters, model calculations and microscopic data to define the evaluated cross section in this region.

Partial results of the spectrum characterization analysis are presented in Fig. 1. The figure illustrates the adjustments made to the a priori fluxes for one of the midplane locations. Adjusted fluxes for the other locations were obtained from the same analysis. In the top plot in the figure, the a priori and adjusted multigroup fluxes are compared. The reduction in the fractional uncertainties for the flux, in the regions of response of the spectrum monitors, are shown in the bottom plot of the figure. Although the dosimeter cross sections are adjusted along with the neutron spectra, their adjustments are small and the flux characterization is very weakly dependent on cross-section adjustments.

An example of the adjustment of fission-product cross sections from the type (3) analysis (simultaneous adjustment of all cross sections and fluxes) is shown in Fig. 2. A comparison of the a priori and adjusted multigroup cross sections is shown in the top plot of the figure. Clearly the integral data have resulted in a significant upward adjustment in the cross section above the unresolved resonance region with some adjustment in the unresolved region itself. As shown in the lower part of Fig. 2, the least-squares analysis resulted in a reduction in cross-section uncertainty over the region of response.

The sequential problem analysis (2) yielded essentially the same result as the type (3) analysis. This result is significant because, in the sequential analysis, any cross correlations between spectral locations are not carried over to the second adjustment analysis. Such correlations are induced by the dosimetry integral data in the spectrum characterization analysis. The FERRET code [3,4] at the time of these analyses did not have the input capability of handling such cross-element correlations. Hence, for the level of analysis considered here (relatively large a priori uncertainties in the fluxes and fission-product cross sections) the treatment of a priori cross-element correlations is not of utmost importance to the adjustment analysis.

In principle, the cross-section evaluator could use the adjusted fluxes and covariances from the spectrum characterization analysis along with the measured fission-product reaction rates to integrally test his microscopic cross-section evaluation. On the other hand, he could also incorporate this same integral information directly in his evaluation process. A third approach is illustrated in section 5 in which an adjusted multigroup fission-product cross section and associated covariance matrix from the simultaneous analysis are utilized directly in a microscopic cross-section evaluation. The adjusted covariance matrix embodies all the related uncertainty and correlation information for the integral experiment and its use is essential in subsequent evaluation applications.

5. ADJUSTMENT OF POINT CROSS SECTIONS

Integral data have been used to a very limited extent for cross-section evaluation utilizing point cross-section adjustments. Although methods for doing so exist [2,37,38], such application has been made mainly for the evaluation of fission-product capture cross sections [7]. It is the purpose of this section to demonstrate, by way of example, how the results of an integral experiment can be utilized to improve a microscopic cross section.

As an example, a limited evaluation problem is presented for ^{149}Sm, in which integral data, microscopic data and a point-wise curve from a nuclear model calculation are combined into a simultaneous least-squares analysis with the FERRET code to generate an adjusted point-wise curve. The three sources of data for the evaluation, as shown in Fig. 3, include microscopic measurements by Shaw and collaborators [39,40], adjusted multigroup cross-section and covariance matrices from the EBR-II analysis (section 4.3), and an *a priori* point-wise curve taken from ENDF/B-IV. The point-wise curve, for all practical purposes, represents the nuclear model calculations on which it is based. The point-wise curve was assumed to have uncertainties of 10% below 100 eV and approximately 60% above 100 eV. The Shaw [39] values were assumed to have a relatively large normalization uncertainty (approximately 20%) but to be more precise in shape. Typical error bars for the microscopic data are indicated in the figure.

Two least-squares analyses were made. The first was an evaluation which combined only the microscopic data and the *a priori* curve. The second analysis combined the microscopic data, the *a priori* curve, and the adjusted multigroup cross section. The adjusted point-wise curve, for all practical purposes, was the same from both analyses and is given by the solid curve in Fig. 3. Adjusted uncertainties for the point-wise cross section ranged from approximately 20% to approximately 24% over the energy range 100 eV to 1 MeV for the analysis which did not include the integral data. When the integral data were included, these uncertainties were reduced to approximately 11% to 14% over these same energy ranges. The measured differential data have determined the shape of the adjusted curve. Incorporation of the integral data resulted in a reduction in the absolute normalization uncertainty for the adjusted curve.

The main point to be emphasized here and the reason for showing the ^{149}Sm example is to stress the importance of the output correlations that are a part of the EBR-II integrally-adjusted multigroup cross sections. These correlations are particularly important to a proper understanding of the sharp change in shape that is apparent in Fig. 3 (and in Fig. 2) for the EBR-II adjusted results just below 10 keV. Although a slight jog is also seen in the *a priori* curve (an evaluation anomaly), the main reason for the break in the multigroup curve stems from the choice of *a priori* correlations used to obtain it along with the response function for ^{149}Sm. In particular because the unresolved and

smooth energy regions (which join at 10 keV) were evaluated differently, they were assigned uncertainty components that were not correlated across 10 keV. Therefore, there was little a priori constraint to adjust values below and above 10 keV together. In hindsight, such a constraint could be added but might be hard to justify. However, the covariance matrix for the integrally adjusted cross section is very soft to independent renormalizations above and below 10 keV. Therefore, when the microscopic Shaw data were included in the evaluation, along with the adjusted multigroup data, the break disappeared as is clear in Fig. 3.

If one were to ignore the underlying covariances and compare the Shaw values and the multigroup result together, it would be easy to conclude that they were discrepant, a clearly incorrect conclusion. This example also illuminates the dangers in integrally adjusting the cross section and then discarding the covariance information as one might easily do in applications of benchmark adjusted dosimeter cross sections used in spectral unfolding.

Finally, an inconsistency in the present example must be pointed out. In this example, the ENDF/B-IV values are counted twice. They were used as a priori values in the original integral adjustment of the multigroup representation. They were used again as the a priori point-wise values in the final evaluation. This double counting is not likely to be a severe problem here as the associated uncertainties were relatively large to begin with. Nevertheless, it is wrong, and a proper evaluation should address the problem, e.g., by artificially increasing the assigned uncertainties. This example also highlights the care that must be exercised in this type of approach.

6. CONCLUDING REMARKS

In this paper an attempt was made to summarize the principal ways in which integral reaction-rate data have been used for cross-section evaluation. Explicit examples were given of the use of reaction-rate data for integral testing, multigroup cross-section adjustment and point-wise cross-section adjustment. The examples were developed in the context of the evaluation of dosimetry and fission-product cross sections. For each of the three types of applications of integral data, input data requirements were identified. An emphasis was placed on the inclusion of a priori uncertainties and correlations, especially for cross-section adjustment applications.

The use of integral data to make "consistency checks" of evaluated cross sections will probably continue to be the most acceptable application. In general in the past, no estimate of uncertainty in the calculated integral quantity was made as part of the consistency check. As was pointed out in the work of Broadhead et al. [28], it is desirable to estimate the calculated

uncertainty due to flux and cross-section uncertainties and correlations if a meaningful interpretation of apparent discrepancies is to be made. Such a consideration becomes especially important as the accuracy of the evaluated cross sections improves.

Direct utilization of integral data for the adjustment of cross sections has been done in a limited sense. Adjusted multigroup libraries which include adjusted group constants and covariances have been generated and used successfully for fast reactor applications [3,4,5]. In a very limited scope, integral data have been used directly for point cross-section adjustment in the evaluation process [7]. The questions of whether cross-section adjustments in this latter approach really result in an improvement of the basic cross section or whether they simply reflect modeling or other errors and are a parameterization of the integral data have been raised [6]. Marable addressed this question at this conference [10].

It is the viewpoint of this author that under certain conditions integral data can be used directly for point cross-section adjustments to improve an evaluated cross section. These conditions include: (1) integral experiments for single samples placed in well-characterized neutron fields, (2) identification and estimation of all significant errors and uncertainties for the integral experiment, (3) realistic estimates of the uncertainties and correlations in the fluxes and differential cross sections, (3) minimized model uncertainties, and (4) a valid formalism for doing the adjustment. Admittedly, this is a large task. However, as we mature in the development of realistic covariance files for ENDF/B and conduct careful experiments to build upon the existing data base, such application may prove useful.

ACKNOWLEDGEMENTS

This work was supported by the U. S. Department of Energy under DOE Contract No. DE-AC07-76ID01570. I appreciate several lengthy discussions with F. Schmittroth about the subject matter of this paper.

REFERENCES

1. R. E. SCHENTER, Hanford Engineering Development Laboratory, Private Communication (1975).

2. H. GRUPPELAAR and J. W. M. DEKKER, "Input of Integral Measurements on the Capture Cross-Section Evaluations of Individual Fission-Product Isotopes," in Proc. of the Second Advisory Group Meeting on Fission-Product Nuclear Data (FPND)-1977, Petten, Sept. 1977, IAEA-213, vol. 1, 219 (1978) and ECN-24 (1977).

3. J. P. CHAUDAT et al., "Data Adjustments for Fast Reactor Design," Trans. Am. Nucl. Soc. 27, 877 (1977).

4. J. W. M. DEKKER, "Tables and Figures of Adjusted and Unadjusted Capture Cross Sections Based on the RCN-2 Evaluation and Integral Measurements in STEK," vol. 1, ECN-14 (1977), vol. 2, ECN-30 (1977), and vol. 3, ECN-54 (1979).

5. J. W. M. DEKKER and H. CH. RIEFFE, "Adjusted Cross Sections of Fission-Product Nuclides from STEK Reactivity Worths and CFRMF Activation Data," vol. 1, ECN-28 (1977) and vol. 2, ECN-55 (1979).

6. S. PEARLSTEIN, "Interrelating Differential and Integral Nuclear Data," Nucl. Sci. Eng., 74, 215 (1980).

7. R. E. SCHENTER et al., "Evaluations of Fission-Product Capture Cross Sections for ENDF/B-V," USDOE Report HEDL-S/A-1907-FP, Hanford Engineering Development Laboratory (1979).

8. J. GRUNDL and C. EISENHAUER, "Benchmark Neutron Fields for Reactor Dosimetry," in Proc. of a Consultants Meeting on Integral Cross-Section Measurements in Standard Neutron Fields for Reactor Dosimetry, International Atomic Energy Agency, Vienna (1976), IAEA-208, vol. 1, 53 (1978).

9. L. J. KOCH, "EBR-II: An Experimental LMFBR Power Plant," Reactor Technology, 14, 286 (1971).

10. J. H. MARABLE, "The Adjustment of Cross Sections Based on Integral Experiments in Fast Critical Assemblies," this meeting.

11. H. GRUPPELAAR and J. B. DRAGT, "Cross-Section Adjustments Using Integral Data," this meeting.

12. W. N. McELROY and L. S. KELLOGG, "Fuels and Materials Reactor Dosimetry Data Development and Testing," Nuc. Tech. 25, 180 (1975).

13. H. H. KNITTER, "A Review on Standard Fission Neutron Spectra of ^{235}U and ^{252}Cf," in Proc. of a Consultants Meeting on Integral Cross-Section Measurements in Standard Neutron Fields for Reactor Dosimetry," International Atomic Energy Agency, Vienna (1976), IAEA-208, vol. 1, 183 (1978).

14. C. M. EISENHAUER et al., "Utilization of Standard and Reference Neutron Fields at NBS," in Proc. 2nd ASTM-EURATOM Symposium on Reactor Dosimetry, Palo Alto (1977), NUREG/CP-004, vol. 3, 1177 (1978).

15. E. J. DOWDY, E. J. LOZITO, and E. A. PLASSMAN, "The Central Neutron Spectrum of the Fast Critical Assembly BIG-TEN," Nucl. Tech. 25, 381 (1975).

16. J. W. ROGERS, D. A. MILLSAP and Y. D. HARKER, "CFRMF Neutron Field Flux Spectral Characterization," Nucl. Tech. 25, 330 (1975).

17. A. FABRY et al., "Status Report on Dosimetry Benchmark Neutron Field Development, Characterization and Application," in Proc. 2nd ASTM-EURATOM Symposium on Reactor Dosimetry, Palo Alto (1977), NUREG/CP-004, vol. 3, 1141 (1978).

18. A. FABRY et al., "Review of Microscopic Integral Cross-Section Data in Fundamental Reactor Dosimetry Benchmark Neutron Fields," in Proc. Consultants Meeting on Integral Cross-Section Measurements in Standard Neutron Fields for Reactor Dosimetry," International Atomic Energy Agency, Vienna (1976), IAEA-208, vol. 1, 233 (1976).

19. R. C. GREENWOOD et al., "Radiometric Reaction-Rate Measurements in CFRMF and BIG-10," in Proc. 2nd ASTM-EURATOM Symposium on Reactor Dosimetry, Palo Alto (1977), NUREG/CP-004, vol. 3, 1207 (1978).

20. J. A. GRUNDL et al., "Measurement of Absolute Fission Rates," Nuc. Tech. 25, 237 (1975).

21. D. M. GILLIAM, "Integral Measurement Results in Standard Fields," NBS Special Publication-493, 299 (1977).

22. Y. D. HARKER, J W ROGERS and D. A. MILLSAP, "Fission-Product and Reactor Dosimetry Studies at Coupled Fast Reactivity Measurements Facility," USDOE Report TREE-1259, Idaho National Engineering Laboratory (1978).

23. Y. D. HARKER and R. A. ANDERL, "Integral Cross-Section Measurements on Fission-Products in Fast Neutron Fields," in Proc. Specialists' Meeting on Neutron Cross Sections of Fission Product Nuclei, Bologna (1979), NEANDC(E)-209"L", 5 (1980).

24. Y. D. HARKER et al., "Integral Measurements for Higher Actinides in CFRMF," in Proc. International Conference on Nuclear Cross Sections for Technology, Knoxville (1979).

25. R. A. ANDERL, F. SCHMITTROTH, and Y. D. HARKER, Integral Capture Measurements and Cross Section Adjustments for Nd, Sm and Eu," USDOE Report EGG-PHYS-5182, Idaho National Engineering Laboratory (1980).

26. R. A. ANDERL and Y. D. HARKER, "Measurement of the Integral Capture and Fission Cross Sections for ^{232}Th in the CFRMF," in Proc. International Conference on Nuclear Cross Sections for Technology, Knoxville (1979).

27. B. A. MAGURNO, "Status of Data Testing of ENDF/B-V Reactor Dosimetry File," Proc. 3rd ASTM-EURATOM Symposium on Reactor Dosimetry, Ispra (1979).

28. B. L. BROADHEAD and J. J. WAGSCHAL, "The NBS Intermediate-Energy Standard Neutron Field (ISNF) Revisited," Trans. Am. Nucl. Soc., 33, 848 (1979).

29. B. L. BROADHEAD et al., "Calculation of the Flux Covariance Matrix for the National Bureau of Standards Intermediate-Energy Standard Neutron Field (NBS-ISNF)," Trans. Am. Nucl. Soc., 30, 590 (1978).

30. J. L. LUCIUS et al., "A Users Manual for the FORSS Sensitivity and Uncertainty Analysis Code System," USDOE Report ORNL-5316, Oak Ridge National Laboratory (1980).

31. J. J. WAGSCHAL et al., "ORACLE: An Adjusted Cross-Section and Covariance Library for Fast Reactor Analysis," in Proc. ANS Topical Meeting on Advances in Reactor Physics and Shielding, Sun Valley (1980).

32. J. J. WAGSCHAL, B. L. BROADHEAD and R. E. MAERKER, "Least-Squares Methodology Applied to LWR-PV Damage Dosimetry, Experience and Expectations," in Proc. International Conference on Nuclear Cross Sections for Technology, Knoxville (1979).

33. J. J. WAGSCHAL, R. E. MAERKER and D. M. GILLIAM, "Covariances of Fission-Integral Measurements at the NBS ^{252}Cf and ISNF Facilities and at the ORNL-PCA Facility," in Proc. 3rd ASTM-EURATOM Symposium on Reactor Dosimetry, Ispra (1979).

34. F. SCHMITTROTH, "FERRET Data Analysis Code," USDOE Report HEDL-TME 79-40, Hanford Engineering Development Laboratory (1979).

35. F. SCHMITTROTH, "A Method for Data Evaluations with Lognormal Distributions," Nucl. Sci. Eng. 72, 19 (1979).

36. F. SCHMITTROTH, "Covariances for Dosimeter Cross Sections," USDOE Report, HEDL-TC-1538, Hanford Engineering Development Laboratory (1979).

37. F. SCHMITTROTH, "Finite Element Basis in Data Adjustment," Nucl. Sci. Eng. 74, 168 (1980).

38. A. PAZY et al., "The Role of Integral Data in Neutron Cross-Section Evaluation," Nucl. Sci. Eng. 55, 280 (1979).

39. SHAW et al., Data in NEUDADA, NEA Data Bank.

40. R. W. HOCKENBURY et al., Bull. Am. Phys. Soc. 20, 560 (1975).

TABLE I

Integral Tests: CFRMF Dosimeter Data

Reaction	Measured Integral Cross Section (mb)	C/E[b]	
		IV[c]	V[d]
$^{115}In(n,\gamma)$	281.5(3.9)[a]	1.06	1.00
$^{197}Au(n,\gamma)$	424.(3.3)	0.98	1.00
$^{232}Th(n,\gamma)$	291.(3.1)	0.98	0.90
$^{235}U(n,f)$	1557.(3.4)	1.02	1.02
$^{27}Al(n,\alpha)$	0.161(3.1)	0.97	1.11
$^{58}Ni(n,p)$	24.0(3.4)	0.94	0.98
$^{115}In(n,n')$	51.0(5.9)	0.86	0.97
$^{232}Th(n,f)$	19.6(4.7)	0.82	0.95

[a]Percent uncertainty at the 1-sigma level.

[b]Ratio of "calculated" to "experimental" integral cross section.

[c]ENDF/B-IV cross section.

[d]Preliminary ENDF/B-V cross section.

TABLE II

Integral Tests: CFRMF Fission-Product Data

Reaction	Measured Integral Cross Section (mb)	C/E[b]	
		IV[c]	V[d]
$^{98}Mo(n,\gamma)$	54.4(6.4)[a]	1.23	1.09
$^{99}Tc(n,\gamma)$	267.(15)	1.04	1.26
$^{102}Ru(n,\gamma)$	88.9(6.6)	1.41	1.26
$^{109}Ag(n,\gamma)$	507.(9.7)	0.60	0.85

[a]Percent uncertainty at the 1-sigma level.

[b]Ratio of "calculated" to "experimental" integral cross section.

[c]ENDF/B-IV cross section.

[d]Preliminary ENDF/B-V cross section.

TABLE III

Integral Test: ISNF Experiments
Fission-Rate Ratios

Response	Measured Ratio	C/E[b]		Estimated Calculated Uncertainty	
		IV[c]	V[d]	Case 1[e]	Case 2[f]
$\frac{^{238}U(n,f)}{^{235}U(n,f)}$	0.920(0.6)[a]	0.962	0.972	4.2	2.1
$\frac{^{239}Pu(n,f)}{^{235}U(n,f)}$	1.155(1.1)	0.973	0.985	2.5	2.1

[a]Percent uncertainty at the 1-sigma level.

[b]Ratio of "calculated" to "experimental" response ratios.

[c]ENDF/B-IV cross sections.

[d]ENDF/B-V cross sections.

[e]Percent uncertainty including contributions from flux and cross section.

[f]Percent uncertainty including cross-section contributions only.

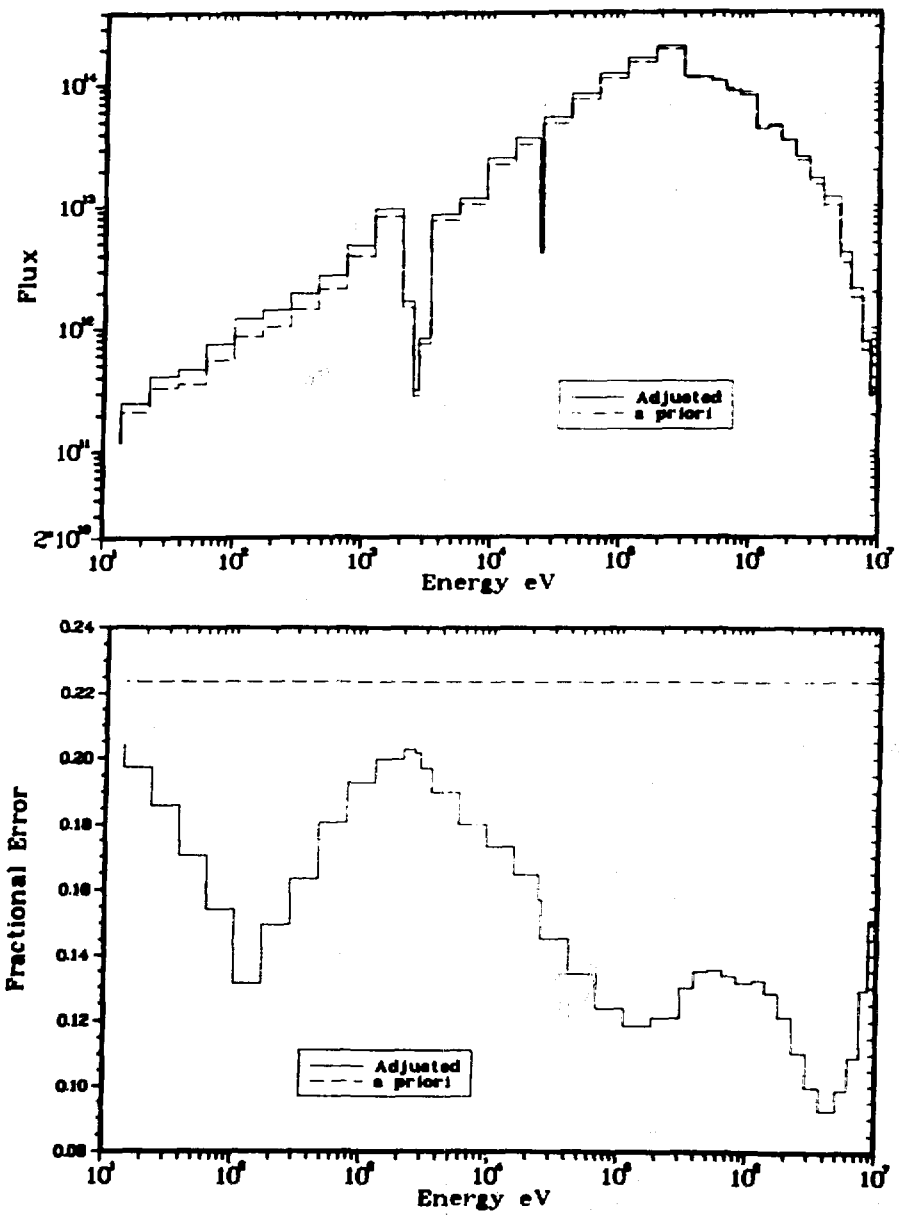

Fig. 1. Comparison of a priori and adjusted multigroup fluxes and fractional uncertainties for EBR-II midplane capsule location.

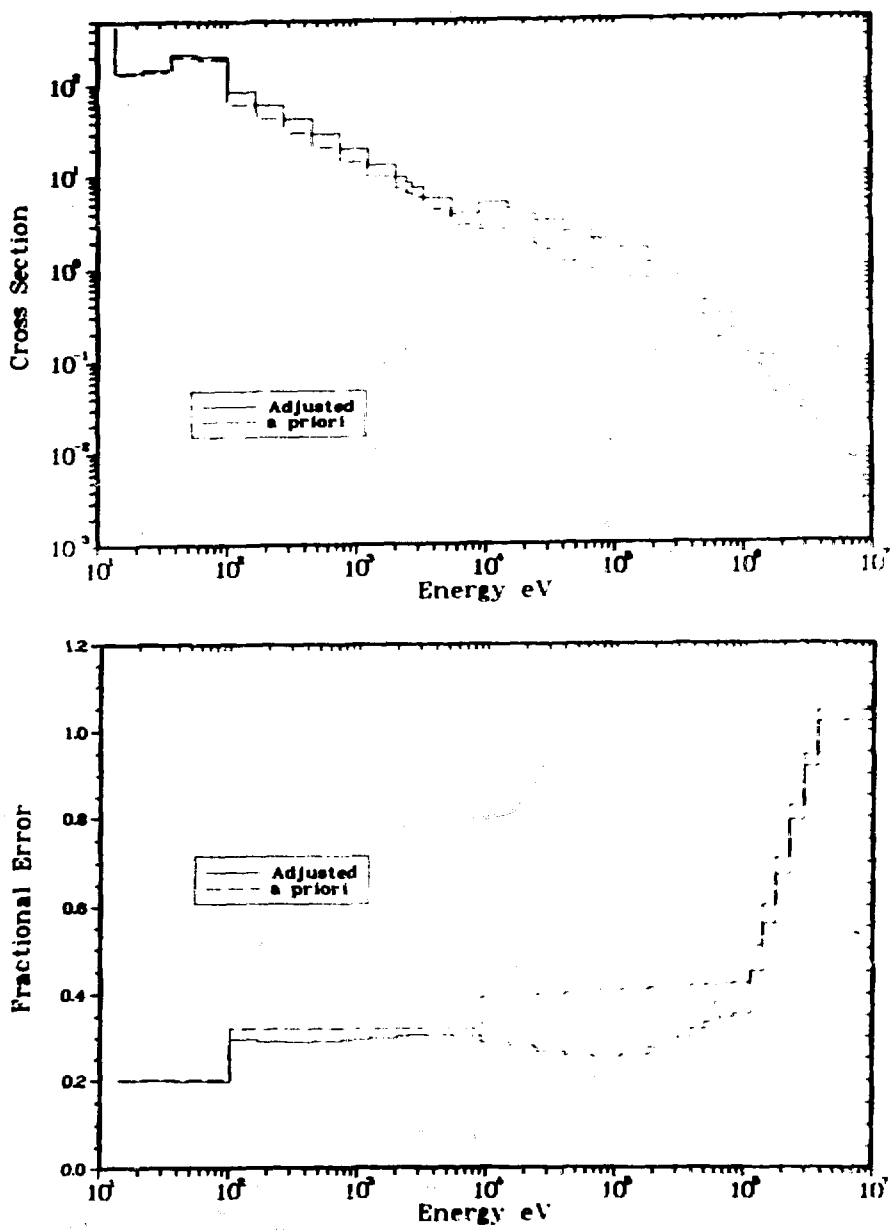

Fig. 2. Comparison of a priori and adjusted multigroup capture cross section and fractional uncertainties for ^{149}Sm.

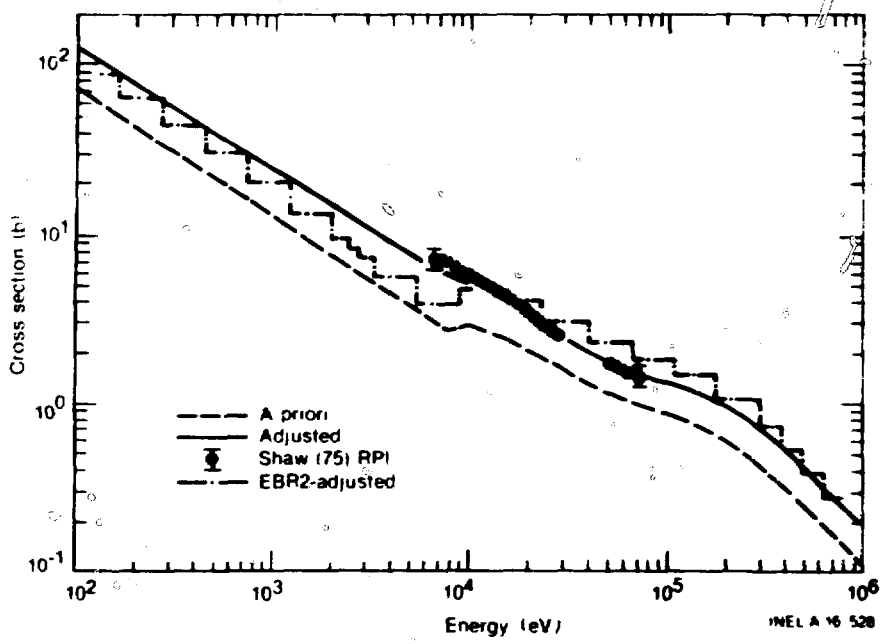

Fig. 3. ^{149}Sm capture cross-section evaluation example.

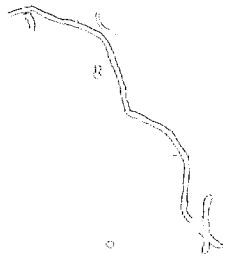

Discussion

Schmittroth

Earlier, some concern was expressed that small integral uncertainties may bias adjusted results in favor of the integral measurements. What are your experimental integral uncertainties, and do they bias the adjustments in favor of the integral measurements?

Anderl

The dosimeter reaction rates were determined by the radiometric method in which Ge(Li) detectors were used for gamma spectrometry. The saturated reaction rates were derived from measurements of the absolute gamma emission rates for "standard" gammas emitted from each irradiated dosimeter. Estimation of the reaction rate uncertainties for this analysis is straightforward. Total uncertainties for the dosimeter reaction rates for this experiment range from 2% to 12% and include the uncertainty in the spatial position of the dosimeters. Reaction rates for the isotopically enriched rare earth samples were derived, by and large, from mass spectrometric measurements of the capture product to parent nuclide isotope ratios. In principle isotopic ratio measurements can be made to ±0.5%, and reaction rates can be derived with low uncertainties. For this experiment, estimated rare earth reaction rate uncertainties ranged form 0.6% to 12%. I believe these uncertainty estimates are valid and do not bias the adjustments.

Peelle

In the last slide showing determination of a fission product cross section, was the form of the resulting cross section determined by some parameterizations?

Anderl

The form of the resulting cross section is essentially determined by the shape of the a priori cross section curve which was obtained from ENDF/B-IV. In the adjustment analysis based on integral data only a multigroup representation of this point wise curve was used. This adjusted multigroup cross section and associated covariance matrix were then used, along with the differential data, in a subsequent least squares analysis in which the ENDF/B-IV a priori cross section was represented by triangle functions (this representation is equivalent to a continuous piecewise linear parameterization). The shape of the adjusted

curve, dashed line, is then essentially determined by the differential data. The effect of utilizing the integral data is to reduce significantly the uncertainty in the normalization of the adjusted curve.

Young

How sensitive are your adjusted results to the assumed covariance data i.e., how well do covariances need to be known?

Anderl

Covariance sensitivities were not explicitly studied in this work.

Schmittroth (Comment)

I have done some covariance sensitivity studies. The adjustment of fission product cross sections reported here first required the unfolding of the neutron spectra based on integral dosimeter measurements. Thus, covariances were needed in three areas, dosimeter cross sections, a priori neutron spectra, and a priori fission product cross sections. The dosimeter cross section covariances are not particularly important as long as the dosimeter cross sections are relatively well known. The more uncertain neutron spectra are adjusted with the dosimeter cross sections held at relatively fixed values. On the other hand, the adjusted spectra (at least the uncertainties of the adjusted spectra) are sensitive to a priori correlations. With stronger initial correlations, the spectra are stiffer with respect to subsequent adjustments. The result is smaller final uncertainties. Similarly the adjusted fission product cross sections and their uncertainties are sensitive to a priori covariances. Since these covariance are often poorly known, it is important to assign conservative a priori correlations and uncertainties if the adjusted cross sections and their uncertainties are to be valid.

THE ADJUSTMENT OF GROUP CROSS SECTIONS BASED ON INTEGRAL EXPERIMENTS IN FAST BENCHMARK ASSEMBLIES

J. H. Marable

Oak Ridge National Laboratory
Oak Ridge, Tennessee 37830, U.S.A

ABSTRACT

Fundamental questions raised by Pearlstein concerning least-squares data adjustment are reviewed along with several examples. An approach is presented showing least-squares adjustment to be a logical tool for investigating the consistency of various data, calculational methods, and modeling procedures. Some results of the application of adjustment in the area of fast-reactor core physics are given.

INTRODUCTION

The purpose of this paper is to review several aspects, both practical and philosophical, of least-squares adjustment in the context of its application in the United States to fast reactors. Such adjustment work has been performed at Argonne National Laboratory [1] and at the Oak Ridge National Laboratory [2].

Fundamental questions concerning such data-adjustments were discussed in a recent note by S. Pearlstein [3]. These questions addressed two points, (1) whether data adjustments give improved estimates of nuclear data, and (2) possible limitations in the use of adjusted nuclear data due to the modification of the correlations brought about by incorporating integral experiment data.

In the following, Pearlstein's arguments and examples are reviewed. This author then expresses his own philosophy, which views adjustment as a vital confrontation of the various data and as an important test for consistency, over and above its possible use for decreasing the uncertainties of calculated integral parameters or of nuclear data. Some general and practical aspects of adjustment are then discussed. Finally, results of several applications of nuclear-data adjustment are presented.

Pearlstein's Analyses

As noted above, Pearlstein has raised questions which are most fundamental to data adjustment and its interpretation and use. In an attempt to find answers to these questions, Pearlstein applied linear least-squares adjustment to fourteen critical bare homogeneous cylinders containing aqueous solutions of 93% ^{235}U-enriched uranyl oxyfluoride. A simple calculational model was used based on the following equation

$$\exp(B^2\tau) = \nu\sigma_f/(\sigma_f + \sigma_c + \sigma_h (N_h/N_u)) \qquad (1)$$

wherein five parameters common to all fourteen experiments are specified as differential data. The five are the average number ν of neutrons released from fission, the neutron age τ, the ^{235}U fission cross section σ_f, the ^{235}U capture cross section σ_c, and the hydrogen capture cross section σ_h.

Parameters specific to each individual experiment were assumed to have no uncertainties. These parameters are the hydrogen-to-^{235}U atom ratio (N_h/N_u) and the geometric buckling B^2 given by

$$B^2 = (\pi/(H + 2d))^2 + (2.405/(R + d))^2 \qquad (2)$$

where H is the measured critical height, R is the radius, and d is the extrapolation distance with the assumed constant value of 2.3 cm.

Pearlstein finds the best least-squares fit assuming equal weighting of the fourteen experiments and complete uncertainty of the differential data. He then considers three least-squares adjustments based on three evaluations of the integral data, of the differential data, and of their uncertainties. Actually the evaluations differ only in the evaluations of the standard deviations of the fourteen integral experiments. For case 1, each of the fourteen integral experiments has a relative standard deviation evaluated at 10%; for case 2, 1%; and for case 3, 0.1%.

The three evaluations assume there are no systematic experimental errors or other source of correlation. Although the height considered as a response is a nonlinear function of the five differential data, it appears that Pearlstein restricts the analysis to a linear least-squares adjustment because this nonlinear aspect is not pertinent to the questions raised.

Pearlstein states that the example illustrates the following points:

1. The values of adjusted parameters optimizing the fit to integral data depend on the starting values and assigned uncertainties to differential and integral data.

2. Significant correlations that differ greatly from those assumed as input can be introduced among the fitted parameters by the adjustment process.

3. There is no restriction on the number of differential parameters or the number of integral measurements.

The use of "starting values" in point (1) above should be replaced by "experimental values" or rather "evaluated values" since, as will be shown later, the adjustment does not depend on the starting values (as defined below) but rather on the evaluated values as, of course, it should.

Values for chi-square per degree of freedom for case 1, 2, and 3 are 0.59, 25, and 3660, respectively. Pearlstein concludes that case 1 is the most acceptable. Many statisticians would go somewhat further and maintain that case 1 is the only acceptable one. For cases 2 and 3, which are characterized by large values of chi-square, he recommends the common practice of multiplying the standard deviations of the adjustment by the square root of chi-square per degree of freedom to arrive at reasonable uncertainty estimates. Pearlstein notes that significant correlations are introduced among the adjusted data, especially for cases 2 and 3; and he states that "correlations among differential and integral data are the most important result of data adjustment methodology." On the basis of these three cases he points out that adjustments may not in every case improve differential data, but the resulting parameterization can improve the agreement between calculated and experimental responses.

Pearlstein concludes the paper with the remarks that although data adjustment can improve estimates of integral data and provide reasonable estimates of their uncertainties, if the adjustment introduces new and different correlations, then the adjusted data should be regarded merely as a parameterization of the integral data since the data have been validated only when acting in specific combinations. However, this author fails to see the justification for this conclusion since ordinarily differential experiments themselves measure nuclear data when acting in specific combinations, which fact is expressed by correlations.

An Approach to Adjustment

The foregoing points highlighted in Pearlstein's paper indicate the difficulties one must face if one considers the possibility of applying adjustment to the improvement of nuclear data.

The fast-reactor physics group at Oak Ridge National Laboratory, in collaboration with other laboratories and reactor vendors, is interested in producing an adjusted library for application to fast-reactor design [4]. At the same time we are also interested in determining the extent to which nuclear data might be

improved, so that the adjusted library would be based on real physics and not mere mathematical parameterization. These hopes are based on the following arguments.

A group cross section adjustment incorporating integral experiments is relevant to associated nuclear data according to the degree that the variables faithfully represent real physical quantities. If at any stage a faithful representation of the physics is violated (such as, for example, the omission of a significant sensitivity, variance, or correlation), then the variables adjusted take on the character of a mathematical parameterization. On the other hand, if the physics is faithfully represented at all stages, then there is no a priori reason not to accept the results of an adjustment as being pertinent to nuclear data.

In order to successfully implement the foregoing as a principle, it is necessary to have means for determining if the physics has been violatd. Thus it is necessary to scrutinize all input data for accuracy, consistency, and completeness. However, the frequently quoted statement "garbage in, garbage out" is not necessarily appropriate. Analysis of adjustment results may very well lead to the conclusion that the input contains "garbage." But this conclusion arrived at through the analysis of adjustment is certainly valid. Further analysis of the adjustment may help to point out which among the input data is "garbage." Again, this conclusion of the adjustment is certainly valid and useful.

The output data of an adjustment must also be analyzed to understand what it is trying to tell us. Not only must the nuclear data changes and integral data changes be studied; the new standard deviations must be studied, and the various contributions to chi-quare must be understood. In particular, the chi-square test must be satisfactorily applied, and any adjustment which fails this test cannot be accepted since, almost certainly the mathematical representation of the physics has been violated.

If an adjustment passes the chi-square test, it must yet undergo further scrutiny. It is particularly important that the results of such a least-squares adjustment be communicated to evaluators and experimentalists acquainted with the original data in order to determine if the adjustment results are reasonable and what impact they may have. Interaction with designers is also important.

With the approach described above, adjustment is not a black box into which one feeds input data and blindly takes out adjusted mathematical parameters. On the contrary, with such an approach, adjustment is a logical tool for examining the consistency of the complex of nuclear data, integral data, analytic

methods, modeling procedures, numeric approximation, and group cross section processing. There is no logical, systematic way to combine integral and differential data other than through the least-squares adjustment procedure or one equivalent to it.

Adjustment Illustrated Graphically

For practical applications, it is important to have a strong and a correct intuition for adjustment. This is especially important for cross section adjustment which involves large amounts of data. Mathematically, the matrix equations, which may appear quite simple, are quite abstract. For these reasons a graphic illustration [5] of the concept of least-squares adjustment is particularly useful.

Figure 1 illustrates in two dimensions the adjustment process for a given calculational method represented by the curve M. Given infinitely-dilute group cross sections σ the method M determines the integral responses I. The evaluated responses and the infinitely-dilute group cross sections based on evaluated nuclear data are represented by the point x^e. One standard deviation is represented by the radius of a circle about x^e. The fact that a circle is shown instead of an ellipse is due to the choice by the person who drew the figure to make standard deviations of quantities along different axes correspond to the same length.

The result of calculation using method M and infinitely-dilute group cross sections σ leads to calculated integral values which with σ form the point x^c. The result of a least-squares adjustment (here nonlinear because M is curved) leads to the adjusted point x'. Note that the integral quantities are adjusted as well as the group cross sections.

The magnitude squared of the distance between x^e and x' measured in standard deviations is called chi-square (χ^2) and this provides a measure of the magnitude of the adjustment and is the basis for the chi-square test. Obviously, if χ^2 is rather large, the validity of the adjustment may be doubted. In such a case, a uniform increase in the standard deviations (and hence the radius of the circle about x^e) may help to pass the chi-square test; but this procedure does violence to the physics since the evaluated standard deviations are presumably based on physical considerations.

Similar considerations apply to the linear adjustment illustrated in Fig. 2. Here the method M is represented by a straight line corresponding to constant fixed sensitivities. The linearity allows the adjustment to proceed in a single step by simply projecting the vector $x^c - x^e$ on to the perpendicular to M. This projection is denoted by $P_\perp(x^c - x^e)$. Note that for any x^0 on

the plane, projecting $x^0 - x^e$ on to the normal to M leads to the same adjustment. This means that for the linear problem we can start with any set of cross sections values, calculate corresponding sensitivities and integral responses and project the vector $x^0 - x^e$ perpendicular to M to find the same $x' - x^e$. Hence the same set of adjusted cross section values and corresponding integral values are independent of the starting point, whether it be x^c or any other point x^0 on M.

The uncertainties of the adjusted responses and of the adjusted cross sections are represented by the darkened section of the plane about the adjusted point x'. Clearly, the adjustment produces adjusted cross sections and adjusted integral experiment which are correlated. These correlations are a result of the physics contained in the constraint imposed by the method M, i.e., the constraint imposed by the Boltzman equation, and this constraint contains valid physics as does the constraint which says a measured total cross section should equal the sum of the measured partial cross sections, which constraint also introduces correlations in cross section data.

Figure 3 illustrates a nonlinear adjustment, which may be performed by iteration of linear adjustments (provided the square distance $| x_i^c - x^e |^2$ converges to the global minimum χ^2). Starting with a rather arbitrary starting point X^c (which ordinarily would be x^c) a first linear adjustment would lead to x' as illustrated. Starting then with x^c (characterized by the same cross sections as x') a second adjustment would lead to x', which should be quite close to the desired point x'. If not, the procedure may be repeated.

Inclusion of Modeling and Calculational Uncertainties

In the foregoing discussion of Figs. 1 through 3, it has been assumed that method M for calculating responses from infinitely-dilute cross sections is exact, i.e., no errors are introduced by the calculational and modeling procedures. However, in reality there are errors inherent in modeling and calculational approximations. Figure 4 illustrates how a) method M can be modified to method M' by the introduction of a calculated-response corrector (or a calculational bias), b) uncertainties will be associated with such correctors independent of any uncertainty in nuclear data. A least-squares adjustment should take them into account as shown in Fig. 4. The adjusted point x is determined by minimizing the sum of the squares of the distance from M to M' (measured in units of corrector standard deviations) and of the distance from x to x^e (measured in units of evaluated integral experiment and group cross section standard deviations).

More generally, for a given integral quantity a chain of conceivable calculations is envisioned, all based on the same

nuclear data [6]. However, each calculation of the chain uses a simpler model or cruder calculational technique than the preceding calculation in the chain. Thus, in the chain

$$A \rightarrow B \rightarrow C \rightarrow \ldots \rightarrow Y \rightarrow Z \qquad (3)$$

A corresponds to the real integral experiment calculated with no approximations, and Z corresponds to the model actually calculated along with the accompanying approximating techniques. The other members of the chain B, C, ..., Y correspond to intermediate models and/or calculational techniques. Note that all calculations in the chain are based on the same evaluated nuclear data file. The response R_A corresponding to the real integral experiment A (and the given nuclear data base) is obtained from the response actually calculated R_Z by addition of the calculated-response correctors b_B, ... b_Z. Each corrector is just the difference between two calculated results corresponding to two consecutive members of the chain, i.e.,

$$\begin{aligned} b_B &= R_A - R_B \\ &\vdots \\ b_Z &= R_Y - R_Z \quad . \end{aligned} \qquad (4)$$

The calculated value A of the real integral experiment is given by

$$A = Z + b_B + \ldots b_Z$$

Calculated-response correctors are included in least-squares adjustment in exactly the same way as group cross sections. The sensitivities of the response to the correctors are either unity or zero according as the corrector applies to the response or not.

Applications Based on ENDF/B-IV

In the United States, data adjustment incorporating fast-reactor benchmark integral experiments has been performed at Argonne National Laboratory (ANL) and at Oak Ridge National Laboratory (ORNL). The ANL work was reported by Collins and Lineberry [1] at the Radiation Shielding Information Center's Sensitivity and Uncertainty Analysis Seminar-Workshop in Oak Ridge, August 22-24, 1978. Not only were standard deviations of integral experiments presented, but also correlations between reaction-rate ratios were calculated and presented for the first time. Table I shows these correlations according to a more recent version [1,4].

The Argonne adjustment work reported was based on fast benchmark assemblies ZPR-3/48, ZPR-6/6A, ZPR-6/7, ZPR-9/31 and

seven zero-leakage test zones of Zebra-8 series in the United Kingdom. Collins and Lineberry found good consistency between eigenvalue and 28c/49f comparisons. They conclude their paper with the observation that the data-adjustment method is a valuable means for studying the significance of integral parameters and that further study of reactivity worths and inclusion of more independently measured parameters were desirable.

ORNL adjustment work based on ENDF/B-IV nuclear data was reported in Reference [2]. Eleven fast-reactor benchmark integral experiment evaluations were supplied by the ANL group [1]. Two dosimetry integral experiments were evaluated by Wagschal, et al.[7]. The adjustment included a number of calculated-response correctors.

For the ORNL adjustment the chi-square per degree-of-freedom was 1.1, corresponding to a chi-square probability value of 0.33. This indicates that the adjustment should be acceptable as far as the chi-square test is concerned. The adjusted values of all integral experiments differed from the evaluation by less than one standard deviation.

The only nuclear data which underwent an adjustment greater than a standard deviation was the mean energy E of the ^{235}U fission spectrum, which value was adjusted upward 3.3%. This corresponds roughly to what actually occurred in going from ENDF/B-IV to ENDF/B-V.

The ORNL adjustment was applied to the calculation of the multiplication factor and the breeding ratio of a model of a large plutonium-oxide fueled liquid-metal fast-breeder reactor of conventional homogeneous design. The affect of the adjustment on these responses are shown in Table II. The breeding ratio reported in Table II was calculated for a reactor maintained at criticality by adjusting the fuel enrichment.

CONCLUSIONS

Although it is generally agreed that nuclear data adjustment incorporating integral experiment data leads to improved calculated values of integral quantities (at least within reasonable limits), there still remain doubts concerning its application to the improvement of nuclear data. In any case, the least-squares adjustment technique is a valuable tool for investigating the consistency of a large complex of nuclear data, integral data, the associated covariances, analytic methods, modeling procedures, numeric approximations, and group cross-section processing. In addition, it has been demonstrated that least-squares should be most useful for incorporating integral experiment data into design calculations. In this regard we here point out that the adjusted library ORACLE based on ENDF/B-V nuclear data and 29 fast benchmark integral experiments will be released soon.

ACKNOWLEDGMENTS

The author thanks C. R. Weisbin, R. W. Peelle, G. de Saussure, E. M. Oblow, F. G. Perey, J. J. Wagschal, and Y. Yeivin for many discussions and for their contributions to the formation of the author's ideas. My gratitude is offered to Ben Magurno for his excellent work and for his part in the organizing of this seminar. Finally, I thank Ann Houston for the typing of the manuscript. This work was performed under the auspices of the Department of Energy.

REFERENCES

1. P. J. Collins and M. J. Lineberry, "The Use of Cross Section Sensitivities in the Analysis of Fast Reactor Integral Parameters," Proc. RSIC Seminar and Workshop, "Theory and Application of Sensitivity and Uncertainty Analysis," Oak Ridge, Tennesse (August 1978). See also P. J. Collins et al., "Experimental Studies of 300 MWE heterogeneous Cores at ZPPR," International Symposium on Fast Reactor Physics Aix-en-Provence, IAEA-SM-244 (September 24-28, 1979).

2. J. H. Marable, C. R. Weisbin, and G. de Saussure, "Uncertainty in the Breeding Ratio of a Large Liquid-Metal Fast Breder Reactor: Theory and Results," Nucl. Sci. Eng. 75, 30 (1980).

3. S. Pearlstein, "Interrelating Differential and Integral Nuclear Data," Nucl. Sci. Eng. 74, 215 (1980).

4. C. R. Weisbin, J. H. Marable, P. Collins, C. Cowan, R. W. Peelle, and M. Salvatores, "Specifications for Adjusted Cross Sections and Covariance Libraries Based Upon CSEWG Fast Reactor and Dosimetry Benchmarks," Oak Ridge National Laboratory Report, ORNL-5517 (ENDF-276) (1979).

5. J. H. Marable, C. R. Weisbin, "Advances in Fast Reactor Sensitivity and Uncertainty Analysis," Proc. RSIC Seminar and Workshop, "Theory and Application of Sensitivity and Uncertainty Analysis," Oak Ridge, Tennessee (August 1978).

6. J. H. Marable, C. R. Weisbin, and G. de Saussure, "Combination of Differential Data and Integral Data," Chapter VI of Sensitivity and Uncertainty Analysis of Reactor Performance Parameters, to be published as Vol. 14 of Advances in Nuclear Science and Technology, J. Lewins and M. Becker, Editors.

7. J. J. Wagschal, R. E. Maerker, and D. M. Gilliam, "Detailed Error Analysis of Average Fission Cross Section Measurements in the NBS Standard Neutron Fields," Trans. Am. Nucl. Soc. 33, 823-825 (1979).

TABLE I

Correlation Matrix for ZPR Reaction Rate Ratios*

ZPR-3/48								
$^{28}c/^{25}f$	1	0.53	0.30	0.00	0.26	0.00	0.01	0.00	0.00	0.00
$^{49}f/^{25}f$		1	0.00	0.19	0.00	0.18	0.00	0.00	0.00	0.00
ZPR-6/6A										
$^{28}c/^{25}f$			1	0.26	0.36	0.00	-0.35	0.15	0.00	-0.15
$^{49}f/^{25}f$				1	0.00	0.48	-0.23	0.00	0.37	-0.26
ZPR-6/7										
$^{28}c/^{25}f$					1	0.24	0.40	0.21	0.12	0.19
$^{49}f/^{25}f$						1	0.34	0.04	0.57	0.24
$^{49}f/^{28}f$							1	0.05	0.24	0.53
PR-9/31										
$^{28}c/^{25}f$								1	0.17	0.19
$^{49}f/^{28}c$									1	0.46
$^{49}f/^{25}f$										1

*Column labelling is the same as for rows.
Data based on Reference[1].

TABLE II

The Effect of Incorporating Integral Experiments on Values and Uncertainties of Performance Parameters of a Large LMFBR*

Performance Parameter	Calculated Value and Standard Deviation	
	Based on Evaluated Data	Based on Adjusted Data
k_{eff}	1.000 +.031	1.014 +.005
Breeding Ratio (of critical reactor)	1.15 +.04	1.12 +.02

*Data taken from Reference[2].

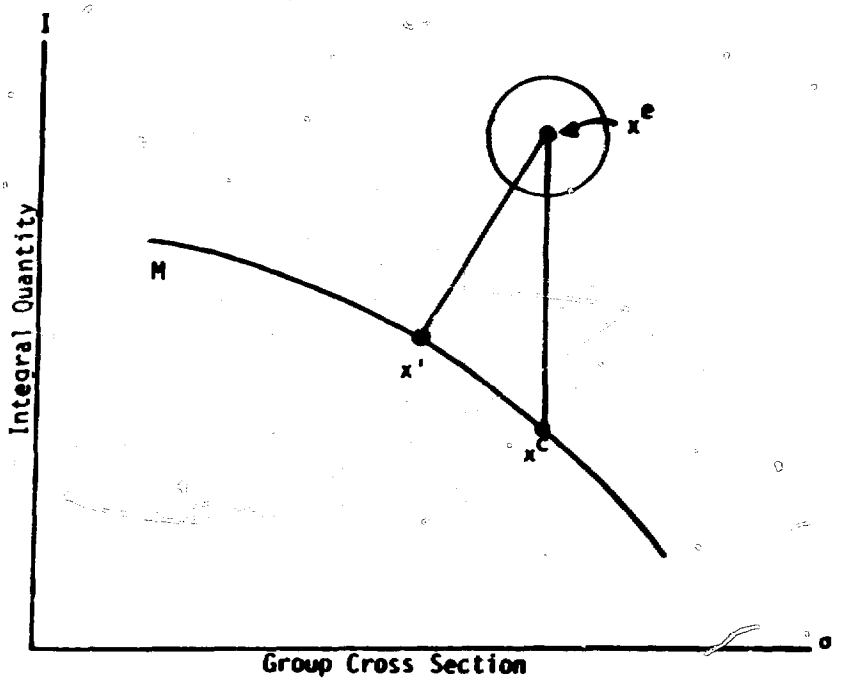

Figure 1. Graphic Illustration of Least-Squares Adjustment in Which the Integral Quantity I is Related to the Group Cross Section σ Through the Calculational Method M.

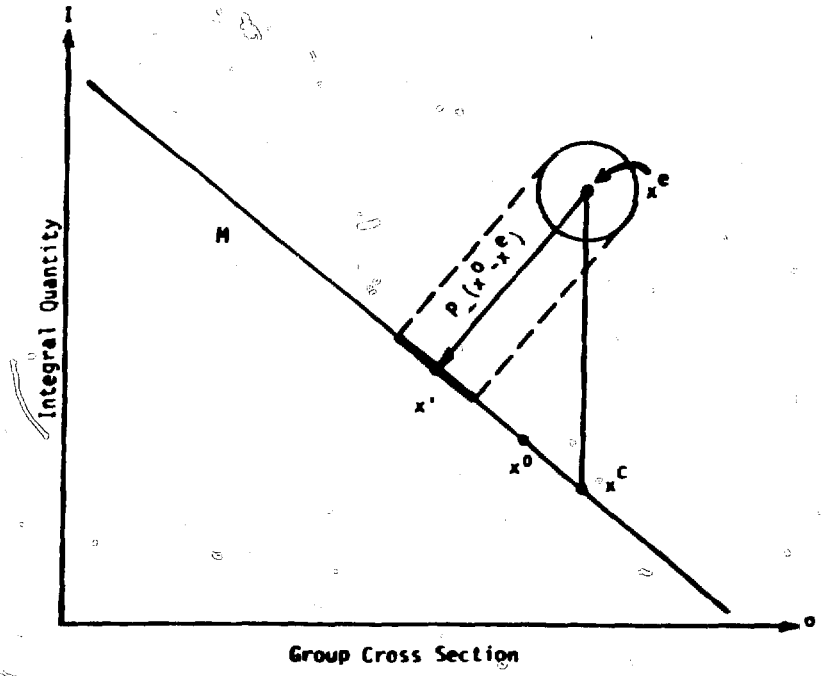

Figure 2. Graphic Illustration of Linear Least-Squares Adjustment in Which the Adjustment Vector $x'-x^e$ is Determined by Projecting x^c-x^e Perpendicular to M.

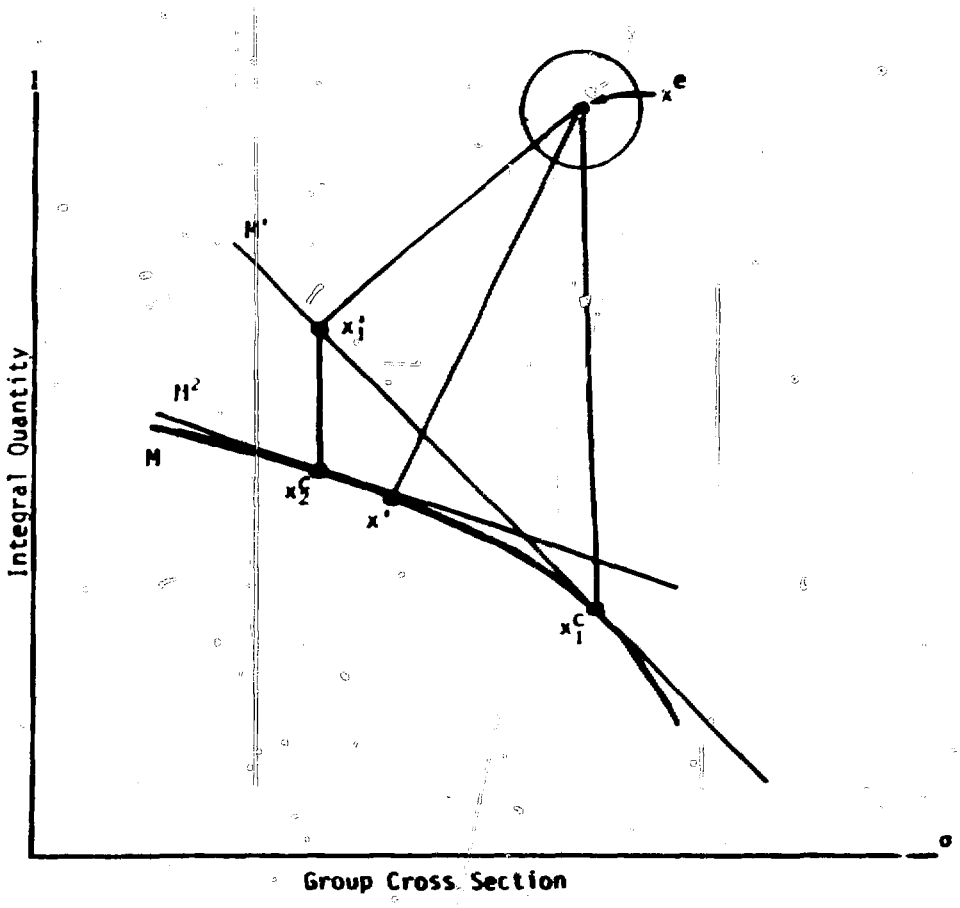

Figure 3. Nonlinear Least-Squares Adjustment Illustrated as a Sequence of Linear Adjustments.

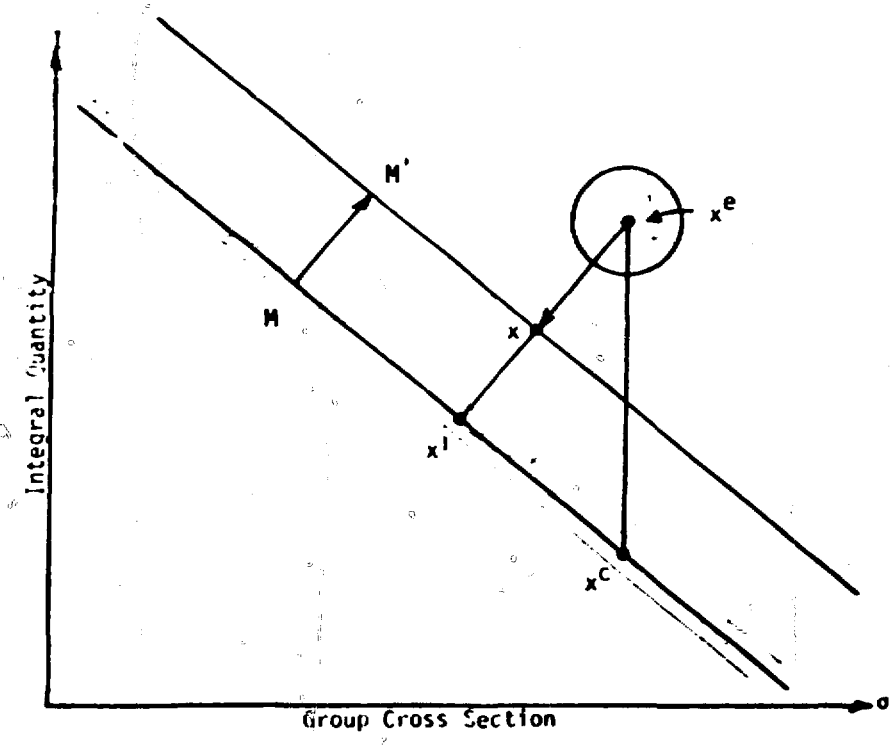

Figure 4. Uncertainty in Calculational Method M Leads to the Possibility of Adjusting the Method M to M'.

Discussion

Schmittroth

The adjusted cross section set ORACLE is the culmination of a large effort. What future areas do you see for needed work?

Marable

Existing covariances files are a weak area. One problem is the omission of covariances. If the omission is a diagonal element (i.e., a variance), one is assuming that the data are perfectly known. Perhaps even worse, if the omission is a correlation, one can have other serious problems e.g, if A is correlated to B and B is correlated to C, then C may have to be correlated to A. Thus, the neglect of correlations between A and C may very likely give a covariance matrix that is not positive definite. ENDF/B-V has a number of these serious and essential omissions. They should be sought out and filled up.

Schmidt

To what extent can you rely on the accuracy of the information going into the covariance files you use in your studies? How accurate are your covariance data?

Marable

Perhaps what we need is a sensitivity analysis for covariances, and I don't know that that has been done. I think the covariances are good enough for most purposes where they exist. Sol's work shows that it makes a difference whether you assume 10%, 1% or 0.1% uncertainties. But typically some people who evaluate covariances say they are known to about 50%. Other people say that uncertainties on uncertainties does not make sense. To me the 50% figure seems reasonable.

Poenitz

From a theoretical point of view I would agree with the suggestion that we derive our best knowledge by including all the experimental data in an evaluation, differential as well as integral. However, using integral data increases substantially the number of unknowns for which there may be few measurements, and we may actually decrease the degree to which the system is over determined. The result is a diffusion of our lack of knowledge.

One of your slides is for GODIVA, one of the simplest systems. But even there we might compensate $\sigma_{n,f}$ with $\bar{\nu}$.

However, there are strong indications that the cause of the discrepancies might be ^{235}U (n,n'), and it would be regretful if the former two were adjusted. More complex systems appear less able to pinpoint problems, and we merely distribute the blame.

Marable

I think you are correct in many ways. In particular the ^{235}U inelastic cross section has increased by 10-15% which I think is a prediction you made several years ago. But I don't think the inclusion of integral experiments diffuses our knowledge, it combines our knowledge. If the result doesn't make sense, it indicates something is wrong with the physics. For me adjustment is not a way to do new versions of ENDF/B, but it is a way to listen to what the integral measurements are saying.

Perey (Comment)

I am glad you emphasized the χ^2 - test. My experience with the theory of logical inference is that if you fail the χ^2 - test you are courting with disaster.

Stewart (Comment)

I would like to substantiate Wolfgang's (Poenitz) comments about the ^{235}U. The ^{235}U inelastic is perhaps incorrect in ENDF/B-V, not only in the total but also in the partials which reflect incorrect energy transfer which could then effect ratios like capture/fission. ^{239}Pu is probably in a similar condition since these data were evaluated at LASL in approximately 1966, and we now know much more about level structure, spins, parities, etc.

CROSS SECTION ADJUSTMENTS USING INTEGRAL DATA

H. Gruppelaar and J.B. Dragt

Netherlands Energy Research Foundation (ECN),
P.O. Box 1, 1755 ZG Petten, the Netherlands

ABSTRACT

Adjustment methods currently used in France, the Netherlands and the U.S.A. to adjust neutron capture cross sections in the fission-product mass range are reviewed. The methods include least-squares fitting of multi-group constants, multi-group cross section adjustment, model-parameter adjustment and direct point cross-section adjustment. Additional comments are given on logarithmic adjustment and on other recent approaches, which stress the inclusion of "method" uncertainties and the treatment of systematic ("negligence") errors. The evaluation of experimental data, a-priori cross sections and their covariance matrices is shortly discussed. Finally some conclusions and recommendations are summarized.

1. PREFACE

In this paper a review is given on the use of adjustment methods in neutron cross section evaluation. This review is mainly based upon the experience of the authors in the field of fission-product cross section adjustment and refer mostly to work performed at ECN [1-7], CEA-Cadarache [8,9] and HEDL [10-12]. At these laboratories adjusted fission-product data files have been obtained. Results of a first intercomparison between adjusted multi-group capture cross sections (RCN-2A and CARNAVAL-IV) were recently published [9]. The HEDL adjustment code [11] was used to obtain ENDF/B-V fission-product cross sections [12] which are partly based upon integral data obtained at ECN and Idaho. The integral data measured at EBR-II on fission products have also been analysed with the above-mentioned code [13]; the results will be reviewed by Anderl at this meeting [14]. Finally, extensive testing of JENDL-1 evaluated cross sections against integral data was reported by Iijima et al. [15]. These results will be incorporated in a future Japanese evaluation.

2. GENERAL LINEAR LEAST-SQUARES ADJUSTMENT TECHNIQUE

A quite general linear least-squares adjustment formalism can be derived from Bayes' theorem assuming Gaussian distributions for the measured and adjustable quantities [1]. Combining the measured quantities in a vector $\underline{R}^{exp}$ with covariance matrix $\underline{\underline{V}}$ and the a-priori known parameters in a vector $\underline{P}^{o}$ with covariance matrix $\underline{\underline{Q}}$ the "best" estimate of the parameters is found as the vector $\underline{P}'$ that minimizes[+]

$$q^2(\underline{P}) = (\underline{R} - \underline{R}^{exp})^T \, \underline{\underline{V}}^{-1} \, (\underline{R} - \underline{R}^{exp}) + (\underline{P} - \underline{P}^{o})^T \, \underline{\underline{Q}}^{-1} \, (\underline{P} - \underline{P}^{o}), \tag{1}$$

where

$$\underline{R} - \underline{R}^{o} = \underline{\underline{G}}(\underline{P} - \underline{P}^{o}). \tag{2}$$

In these equations $\underline{R}^{o}$ stands for quantities calculated from $\underline{P}^{o}$ and the "sensitivity"matrix* $\underline{\underline{G}}$ relates the variations $\underline{R} - \underline{R}^{o}$ and $\underline{P} - \underline{P}^{o}$. It is further assumed that $\underline{R}^{exp}$, $\underline{P}^{o}$ are statistically independent and that there are no uncertainties associated with $\underline{\underline{G}}$ (see Sect. 3).

Eqs. (1) and (2) can be considered as a standard least-squares fitting problem (rather than an "adjustment" problem) when the a-priori vector $\underline{P}^{o}$ is supposed to result from direct measurements. Then the "number of degrees of freedom" n equals the number of experimental data given in $\underline{R}^{exp}$.

The solution of the above-mentioned minimization problem can be denoted as follows [1]:

$$\underline{P}' - \underline{P}^{o} = \underline{\underline{A}} \, \underline{X}, \tag{3}$$

$$\underline{\underline{Q}}' - \underline{\underline{Q}} = -\underline{\underline{A}} \, \underline{\underline{W}}^{-1} \, \underline{\underline{A}}^T, \tag{4}$$

with

$$\underline{\underline{A}} = \underline{\underline{Q}} \, \underline{\underline{G}}^T, \tag{5}$$

$$\underline{X} = \underline{\underline{W}}^{-1} (\underline{R}^{exp} - \underline{R}^{o}),$$

where $\underline{\underline{W}}$ is the covariance matrix of the difference of experimental data ($\underline{\underline{V}}$) and a-priori data ($\underline{\underline{N}}$):

$$\underline{\underline{W}} = \underline{\underline{V}} + \underline{\underline{N}} = \underline{\underline{V}} + \underline{\underline{G}} \, \underline{\underline{Q}} \, \underline{\underline{G}}^T. \tag{7}$$

A *"goodness of fit"* parameter is obtained from a χ^2-test, which leads to the inner product:

[+] Superscript T indicates the transpose of a matrix.

* Also called "model matrix", "design matrix" or "method matrix".

$$\chi^2 = \underline{X}^T (\underline{R}^{exp} - \underline{R}^o). \qquad (8)$$

When χ^2 exceeds n it is advisable to increase the incertainties in the adjusted data by multiplying the adjusted covariance matrix with χ^2/n; see also Sect. 7.

If the second term in Eq. (1) is dropped no a-priori information is used and the system is only overdetermined when n exceeds the number of parameters p to be fitted to the experimental data. This fitting method was followed by the French [8], with the additional constraint that $\underline{P} - \underline{P}^o$ should not exceed twice the standard deviation of $\underline{P}^o$; otherwise the excessive parameters are fixed at the error limits. This means that the statistical distribution of $\underline{P}$ is assumed to be rectangular. Moreover, correlations between the parameters $\underline{P}^o$ are used in some way [8]. In this application the parameters $\underline{P}^o$ are group constants (4-6 groups) which have been collapsed to obtain the condition $n > p$. After adjustment the a-priori multi-group constants are used to translate the adjusted collapsed data into "adjusted" 25-group constants.

In solving Eqs. (1) and (2) one should take advantage of the statistical independence of various components of $\underline{R}^{exp}$ and $\underline{P}^o$ (*"partitioning"* [10]). When there are several independent subsets of $\underline{R}^{exp}$ it is easily demonstrated that one could reduce the adjustment problem to one subset first before adding new subsets sequentially. On the other hand, when $\underline{P}^o$ can be partitioned it is possible to reduce the problem to a number of separate adjustment problems. This could be useful in particular when one is only interested in a "partial adjustment" [1] of $\underline{P}$ (see Sect. 3). An interesting example of partitioning both $\underline{R}^{exp}$ and $\underline{P}^o$ is given by Schmittroth [10] in an application of neutron spectrum unfolding using integral dosimetry results ("elimination of subsidiary parameters").

Another way to reduce the size of the adjustment problem is to redefine the parameters to a vector of smaller size. Suppose that the old vector $\underline{K}$ can be calculated from the new vector $\underline{P}$. In that case the adjusted vector $\underline{P}'$ can be used to obtain $\underline{K}'$. When only the reverse relation $\underline{P} = \underline{S}\underline{K}$ is known, the calculation of $\underline{K}'$ is more involved. This situation occurs when $\underline{S}$ defines a multi-group collapsing scheme. The formal solution of this problem is given in Sect. 4, Eqs. (16-18). Approximative methods for this unfolding process could also be adopted. However, in many instances the collapsed group constants $\underline{P}'$ are useful for the required application. Schmittroth [10] notes that when $\underline{P}^o$ and $\underline{K}^o$ are a-priori known to be statistically independent sequential evaluation can be applied, $\underline{K}'$ playing the role of integral data.

3. METHOD UNCERTAINTY

Multi-Group Cross Section Adjustment

Eqs. (1) and (2) are quite general. In a simple application $\underline{R}^{exp}$ and $\underline{P}^{o}$ represent measured reaction rates and multi-group cross sections $\underline{\Sigma}^{o}$, respectively, $\underline{G}$ being a sensitivity matrix containing well-known group fluxes corresponding to the neutron fields in which the reaction rates were measured. Assuming that $\underline{G}$ has no "method" uncertainties, the solution of the adjustment problem is given by Eqs. (3-7).

Multi-Group Neutron Flux adjustment

Another possibility is to assume that $\underline{P}$ stands for multi-group fluxes $\underline{\psi}$ while the sensitivity matrix $\underline{G}$ is filled with well-known group cross sections. In this case the aim is to obtain adjusted flux spectra. Again no uncertainties are assumed in $\underline{G}$.

Adjustment of Cross Sections and Fluxes

Since both $\underline{\psi}$ and $\underline{\Sigma}$ usually contain uncertainties, a straightforward approach is to store them in one parameter vector

$$\underline{P} = \begin{pmatrix} \underline{P}_1 \\ \underline{P}_2 \end{pmatrix} = \begin{pmatrix} \underline{\psi} \\ \underline{\Sigma} \end{pmatrix}. \tag{9}$$

This approach was followed by Perey [16] in his dosimetry unfolding code STAY'SL. This code forces the user to introduce covariance matrices for cross sections and flux spectra (as well as possible correlations). It is assumed that the matrix $\underline{G}$ can be written as

$$\underline{\underline{G}} = (\underline{\underline{G}}_1 \; \underline{\underline{G}}_2) \tag{10}$$

with $\underline{\underline{G}}_1$ and $\underline{\underline{G}}_2$ expressed in terms of $\underline{\Sigma}^{o}$ and $\underline{\psi}^{o}$, respectively, i.e. without uncertainties. From straightforward application of Eqs. (3-7) adjusted parameters $\underline{\psi}'$ and $\underline{\Sigma}'$ and their covariances are obtained. However, it is not needed to follow this approach when $\underline{P}_1$ and $\underline{P}_2$ are statistically independent, i.e.

$$Q = \begin{pmatrix} \underline{\underline{Q}}_1 & \underline{\underline{0}} \\ \underline{\underline{0}} & \underline{\underline{Q}}_2 \end{pmatrix}, \tag{11}$$

and when one is only interested in adjustment of $\underline{P}_1$. In this case the scheme of Eqs. (3-6) can be followed for the quantities labeled with index 1, replacing Eq. (7) by

$$\underline{\underline{W}} = \underline{\underline{V}} + \underline{\underline{N}} + \underline{\underline{U}}, \tag{12}$$

where $\underline{\underline{U}}$ is the contribution of $\underline{P}_2$ to the uncertainty in the cal-

culated integral data: $\underline{\underline{U}} = \underline{\underline{G}}_2 \underline{\underline{Q}}_2 \underline{\underline{G}}_2^T$. This was called "partial adjustment" in Ref. [1], since the adjustments in $\underline{P}_2$ remain implicit. In recent litterature $\underline{\underline{U}}$ is called "method uncertainty" [21,23].

Definition of Method Error

In the above-mentioned example the matrix $\underline{\underline{U}}$ contains the "method error". A quite general definition of method error is obtained when we assume that $\underline{\underline{U}}$ accounts for *any error in the calculated integral data which is not already contained in* $\underline{\underline{V}}$. In this definition it is not required that the uncertainties in $\underline{\underline{G}}$ are explicitly known [16,23], in which case one could always add the elements of $\underline{\underline{G}}$ to the parameter vector $\underline{P}$ and reformulate the adjustment problem [16]. For instance, when there is an uncertainty in the calculational method used to generate integral data (e.g. because of a multi-group approximation) this uncertainty cannot easily be connected to elements of $\underline{\underline{G}}$. Another example provides the adjustment of model parameters, where "inherent" statistical model errors cannot be attached to parameters, although they constitute an essential uncertainty in the calculated integral data (see Sect. 4). In the last two examples one could assume that Eq. (2) is replaced by

$$(\underline{R} - \underline{R}^o) = \underline{\underline{G}}(\underline{P} - \underline{P}^o) + \underline{\Delta} - \underline{\Delta}^o \qquad (13)$$

where $\underline{\Delta}$ is a "noise" vector ($\underline{\Delta}^o = \underline{0}$) with covariance matrix $\underline{\underline{U}}$. When Eq. (13) is denoted as

$$(\underline{R} - \underline{R}^o) = (\underline{\underline{G}}\ \underline{\underline{1}}) \begin{pmatrix} \underline{P} - \underline{P}^o \\ \underline{\Delta} - \underline{\Delta}^o \end{pmatrix} \qquad (14)$$

it is easily seen that we have reduced our problem to Eqs. (1,2) by adding a noise vector $\underline{\Delta}$ to the adjustable parameters. Thus, it is always possible to reduce the adjustment problem to Eqs. (1,2).

The parameter vector $\underline{\Delta}$ was introduced in this section as a "noise" vector. In Refs. [23,24] relation (13) is also adopted, where the vector $-\underline{\Delta}$ is interpreted as a "bias" of which the a-priori value $-\underline{\Delta}^o$ is known from previous comparisons between integral data and cross sections.

Correlations Between A-Priori Data and Method

In the previous subsection we did not assume correlations between a-priori data and method, but these could easily be included when the elements of $\underline{\underline{G}}$ are added to $\underline{P}$. A quite general formulation of the problem was given by Marable and Weisbin [23], which in our notation can be written as

$$q^2 = \begin{pmatrix} \underline{R} - \underline{R}^{exp} \\ \underline{P} - \underline{P}^{o} \\ \underline{\tilde{G}} - \underline{\tilde{G}}^{o} \\ \underline{\Delta} - \underline{\Delta}^{o} \end{pmatrix}^{T} \underline{C}^{-1} \begin{pmatrix} \underline{R} - \underline{R}^{exp} \\ \underline{P} - \underline{P}^{o} \\ \underline{\tilde{G}} - \underline{\tilde{G}}^{o} \\ \underline{\Delta} - \underline{\Delta}^{o} \end{pmatrix}, \qquad (15)$$

with the constraint of Eq. (13). In Eq. (15) a tilde means that matrix elements are written as a vector. The covariance matrix $\underline{C}$ is supposed to contain no correlations between $\underline{R}^{exp}$ and the a-priori data. It is noted that Marable and Weisbin [23] follow an alternative geometric approach to solve the adjustment problem.

In this subsection we give an example of a correlated a-priori vector (neutron spectra) and method matrix (cross sections). This was the case in the adjustment of STEK flux and adjoint fluxes [17] of which the a-priori values were obtained from a core calculation using multi-group cross sections of the reactor materials (e.g. ^{235}U). The integral data used for the adjustment included reactivity worths of B, ^{235}U and various fission rate ratios. Obviously there are strong correlations between the neutron spectra and ^{235}U cross sections $\underline{\Sigma}_u$, indicating that Perey's scheme [16] should be followed, i.e. a combination of spectra and cross sections in one parameter vector. However, since the spectra are a function of heavy metal cross sections (mainly ^{235}U) it is possible to express $\underline{\psi}$ in terms of $\underline{\Sigma}_u$, such that a new parameter vector can be defined with only group cross sections which are statistically independent for each sample. Thus, partial adjustment can be applied on this new vector, leading to an adjusted vector $\underline{\Sigma}_u'$, the adjustments in the other dosimetry cross sections remaining implicit. From the vector $\underline{\Sigma}_u'$ "adjusted" STEK neutron spectra were calculated [17]. This example shows that a careful selection of a set of independent parameters and application of partial adjustment can be very advantageous in adjustment calculations.

Unwanted Implicit Adjustments

Once the neutron spectrum has been determined with corresponding covariance matrices it can be used as a "reference" spectrum for the analysis of a large class of integral cross section measurements. For instance, the STEK spectra [17] were used in an extensive series of fission-product cross section adjustments [3,4]. From the previous discussion it is evident that in each cross section adjustment calculation the neutron spectra will be re-adjusted. Although normally this adjustment is small it is an unwanted implicit adjustment, since one usually prefers to use very accurate cross section data for this purpose. Therefore, in the case of analysis of STEK data the vector $\underline{\psi}$ was constrained to the reference value, although the corresponding method uncertainty was included in the calculation of the covariance matrix of $\underline{\Sigma}$.

4. MODEL PARAMETER ADJUSTMENT

Eqs. (1) and (2) are not restricted to the adjustment of multigroup constants. Gandini and Salvatores [18] and Dragt et al. [1] have suggested to adjust the model parameters of the cross sections, from which adjusted point cross sections could be calculated ("consistent method" [18]). In this application the vector $\underline{P}^o$ contains these model parameters and $\underline{Q}$ is their co-variance matrix. It is advisable to adopt a set of statistically independent parameters (or independent subsets of parameters) as far as possible.

The above-mentioned method is particularly useful when the evaluation is entirely based upon nuclear-model calculations and when the uncertainties in the parameters can be easily derived. This could be the case in capture cross section calculations [1,2, 6] utilizing a statistical model, of which the main model parameters are deduced from "external" sources (see also Sect. 8). In practice, these parameters are often "tuned" to fit differential measurements and it becomes more difficult to estimate the uncertainties and correlations of the "tuned" parameters. Apart from this difficulty model parameter adjustment is attractive to the evaluator, because before recalculating the cross sections with adjusted parameters he may interfere, avoiding unphysical adjustments. Another possibility is to improve the systematics of important parameters such as the mean level spacing, average capture width [6] or the γ-ray strength function.

In model parameter adjustment a notable "method error" (Sect. 3) is encountered. This error arises from inherent statistical-model uncertainties caused by fluctuations in the neutron widths or in the number of levels per energy interval [2]. These uncertainties allow for so-called "non-statistical effects", which often reflect the uncertainty in the statistical-model estimate. A disadvantage of parameter adjustment with respect to multigroup cross section adjustment is that these method errors may lead to implicit adjustments, which are not noted by the evaluator. A mixed approach is possible, however (see below).

Another drawback of parameter adjustment is that it is not easy to apply it in the resolved resonance range, where the number of parameters can be quite large. In our application of parameter adjustment [6] we have assumed a number of *important parameters* only. By performing a normal multi-group cross section adjustment calculation the adjusted model parameters $\underline{K}'$ and their covariance matrix $\underline{L}'$ are obtained *a-posteriori* from the relations [1]:

$$\underline{K}' - \underline{K}^o = \underline{B}\,\underline{X}\,, \tag{16}$$

$$\underline{L}' - \underline{L}^o = -\underline{B}\,\underline{W}^{-1}\,\underline{B}^T \tag{17}$$

with

$$\underline{B} = \underline{L}\,\underline{S}^T\underline{G}^T. \tag{18}$$

In Eq. (18) $\underline{\underline{S}}$ is the sensitivity matrix for parameter variations. The adjustment of the parameters corresponds with an amount $\underline{\Sigma}'_p = \underline{\underline{S}}(\underline{K}' - \underline{K}^o)$, expressed in multi-group constants. The residual adjustment $\underline{\Delta\Sigma}' = \underline{\Sigma}' - \underline{\Sigma}'_p$ accounts mainly for adjustments in the resolved resonance range. Also adjustments in the range where there are large inherent statistical model errors are included in $\underline{\Delta\Sigma}'$. The parameters $\underline{P}'$ are used to re-evaluate point cross sections, the remaining problem being the inclusion of residual adjustments in the evaluation.

In the forthcoming RCN-3 evaluation [25], which has been completed now for 30 materials, the above-mentioned procedure was followed starting from the unadjusted RCN-2 evaluation [26]. The adjustments were made to fit integral STEK and CFRMF data, reviewed in Ref. [5]. In addition some revisions were applied (e.g. for Mo [7]), based upon recent differential data. For most materials the multi-group cross section adjustments [4] in the resolved resonance range were small, so that no revisions were needed in the corresponding point cross sections which are stored in KEDAK format. In the case of ^{133}Cs a correction was applied in the highest part of the resolved resonance range by multiplying the capture cross section with an exponentially increasing smooth correction factor, which was obtained from a "rough fit" through the relative group cross section adjustments, see Fig. 1. In general the evaluator should be conservative in applying corrections in this energy range, but in the case of ^{133}Cs there are other indications for missed strength in the highest part of the resolved resonance range, e.g. the argument that the statistical model predicts higher average capture cross sections than those calculated from resolved resonance parameters [27], see also Fig. 2. In Figs. 3 and 4 portions of the unadjusted and adjusted group cross sections [4] and corresponding point sections are shown, together with available experimental data measured at laboratories indicated in the legend (see CINDA literature index [28]). The adopted RCN-3 curve [25] is slightly different from the adjusted one. This was due to the fact that a revision was made in the calculation of the total cross section. This also affected the capture cross section since the same optical model was used to obtain the neutron transmission coefficients in the capture cross section calculation.

Instead of adopting a physical model parametrization one could also use a *mathematical parametrization*. This approach was followed at HEDL, using the following "finite-element" representation [11]:

$$\sigma(E) = \sum_i h_i(E)\sigma_i \,, \qquad (19)$$

where $h_i(E)$ is a triangle or "roof" function with triangle coordinates $(\log E_{i-1},0)$, $(\log E_i,1)$ and $(\log E_{i+1},0)$. In this representation additional end points have to be defined. Since the coefficients are just the point cross sections σ_i at neutron energies E_i their treatment is discussed in the next section.

5. DIRECT POINT CROSS SECTION ADJUSTMENT

Instead of multi-group cross sections the vector $\underline{P}$ in Eqs. (1, 2) could also contain point cross sections $\underline{\sigma}$ of which the elements σ_i, energies E_i and an appropriate interpolation scheme (e.g. Eq. (19)) define the cross section at each energy. The main advantage of this approach is that differential experimental data could easily be included in $\underline{R}$.

The sensitivity matrix relating differential cross sections and $\underline{\sigma}$ is given by Eq. (19); for the relation with integral data a similar expression is used [11]:

$$R = \sum_i H_i \sigma_i \tag{20}$$

with

$$H_i = \int h_i(E)\phi(E)dE . \tag{21}$$

Adjustment calculations of cross sections in an extended resolved resonance region become very tedious in this scheme. Therefore, average cross sections are introduced [12] in this region, e.g. by introducing multi-group cross sections in $\underline{\sigma}$. In the thermal range the cross section is usually smooth and Eq. (19) can be used. The histogram part of the cross section could be parametrized by means of block functions or, approximatively, with triangle functions. In the last-mentioned case adjustments do not conserve the block shape of the histograms, as was the case in the application of adjustment of ENDF/B fission-product cross sections [12].

The above-mentioned scheme is very convenient to obtain adjusted point cross sections fitted to both integral data and differential data. As in the previous section, adjustments in the resolved resonance range are difficult to include in practice. A drawback of the method is that still the number of parameters can be quite large. Morecver, the evaluator does not gain insight in the adjustments of underlying physical model parameters.

Another approach to direct point cross section adjustment has been followed by Pazy et al. [19] who have formulated the adjustment problem in terms of continuous functions. In their discription the a-priori cross section $\sigma^o(E)$ is a continuous function of energy and the integral data r are functionals of $\sigma(E)$ and may also be a continuous function of another parameter E'. Their minimization problem can be denoted as:

$$q^2(\sigma) = \int \left[\frac{\sigma(E)-\sigma^o(E)}{\Delta\sigma^o(E)}\right]^2 w_\sigma(E)dE + \int \left[\frac{r(E',\sigma(E))-r^o(E')}{\Delta r^o(E')}\right]^2 w_r(E')dE', \tag{22}$$

where $\Delta\sigma^o$ and Δr^o are standard deviations and w_σ and w_r are density functions which reflect the number of measurements per energy

interval on which the a-priori quantities are based. In this picture correlations are not included, although in applications w could be interpreted as a constant over a wide energy interval. This incomplete uncertainty treatment limits the applicability of the above-mentioned method.

6. LOGARITHMIC ADJUSTMENT

A possible drawback of the methods discussed before is due to the assumed Gaussian distribution of $\underline{P}$, which may lead to unrealistic adjustments, such as negative values for cross sections. This could be avoided by considering lognormal distributions [1,10,11] or constraining the vector $\underline{P}$ within prescribed error limits [8], which could be asymmetric.

It is most appropriate to assume the logarithms of the cross-sections $\underline{P}$ to be normally distributed. In the minimization of Eq. (1) the second term is then to be replaced by

$$(\underline{Z} - \underline{Z}^{o})^{T} \, Q_{z}^{-1} \, (\underline{Z} - \underline{Z}^{o}) \tag{23}$$

with

$$\begin{aligned} \underline{Z} &= \ln \underline{P}, \\ \underline{Z}^{o} &= \ln \underline{P}^{o} \end{aligned} \tag{24}$$

The first term is not changed: integral data are still assumed to be normally distributed. Several approximations with regard to the dependence of $\underline{R}$ on $\underline{Z}$ (or $\underline{P}$) are possible, e.g.:

(a) Assume $\underline{R}$ to be linear in $\underline{Z}$ (i.e. variations in $\underline{R}$ proportional to relative variations in $\underline{P}$). Then the whole adjustment procedure remains the same as before, with $\underline{P}$ replaced by $\underline{Z}$ in the equations. The a-posteriori distribution for $\underline{Z}'$ is normal again, i.e. the adjusted cross sections follow a logarithmic normal distribution. This idea was followed in Ref. [1].

(b) Assume – as before – that $\underline{R}$ is linear in $\underline{P}$ (or can be linearized). Then the a-posteriori distribution for $\underline{P}'$ is no longer logarithmic normal. The most probable value for $\underline{P}'$ cannot be found from a closed expression, but must be computed by iteration. This approach has been worked out in much detail by Schmittroth [10].

It seems to be reasonable to assume a lognormal distribution for most a-priori cross sections, particularly in case of large uncertainties. The distribution is especially appropriate if the a-priori data originate from a measurement that contains certain relative errors and short-range correlations, together with a relative normalization error from an independent normalization measurement (see Sect. 8). The product of the two lognormal quantities is again lognormal.

The best choice for the dependency of $\underline{R}$ on $\underline{Z}$ or $\underline{P}$ depends on the

character of the integral data. In case of reaction rates the linear dependency on $\underline{P}$ (case b) seems to be most realistic: variations in reaction rates are proportional to absolute cross section variations rather than relative ones. So case b seems to be preferable in this application, in spite of the mathematical and statistical complexity.

It is very important to note that in these approaches the *most probable values* are used as estimates for the cross sections (both a-priori and a-posteriori), and *not* the mean (or expectation) values. For lognormal distributions (i.e. the prior distribution in both cases and the posterior distribution in case a) the following relation exists:

$$\langle P_k \rangle = P_k \exp \tfrac{1}{2}(Q_z)_{kk} , \qquad (25)$$

where P_k is the $k^{\underline{th}}$ element of the most probable vector $\underline{P}$ used in Eq. (24). Such a simple relation does not exist for the posterior distribution in case b.

Likewise some care is needed to translate an error matrix of $\underline{P}$ into the corresponding error matrix of $\underline{Z}$ or vice versa. In case of the lognormal distribution this relation is [10]

$$(Q_z)_{kl} = \langle P_k \rangle \langle P_l \rangle (\exp Q_{kl} - 1). \qquad (26)$$

The relation can be used to obtain the error matrix of the prior data in the minimization expression (23), and the reverse relation produces adjusted cross section errors in case a. The formula does not hold for adjusted data in case b. It has been shown in Ref. [10] that the linear approximation

$$(Q_z)_{kl} = \langle P_k \rangle \langle P_l \rangle Q_{kl} \qquad (27)$$

is always reasonable in practice. This simple linear relation was used throughout in Ref. [1].

7. SYSTEMATIC ERRORS

It is basically true that Eqs. (3-7) should only be applied when there is statistical consistency between integral data and a-priori information. In the formulation of Sect. 2 this means that χ^2/n should be close to 1. The confidence interval of this quantity follows from the χ^2-distribution for n degrees of freedom. When χ^2/n exceeds unity it is "common practice" to multiply the initial or final covariance matrices with χ^2/n to "force" consistency.

However, it should be stressed that before doing so the evaluator should try to find the origin of the discrepancy. In some cases one could a-priori assume that (most of) the discrepancy is due to systematic errors in either the integral data or the a-priori cross sections. The French [8] implicitly assume that systematic errors in the integral data are small by adopting a rectangular uncertainty distribution of the a-priori data with wide error limits. In this way the a-priori information is almost not used. When, for instance, the shape of the a-priori cross sections is well-known from differential data and the main uncertainty is the normalization, it might be better

to estimate this normalization from a comparison between integral and a-priori data.

Recently, Chao [20,21] has investigated the situation of significant discrepancies between integral data and a-priori information in much detail. He introduced the concept of "negligence" to deal with neglected systematic errors. A simple estimate of this negligence $\underline{E}$ and its covariance matrix $\underline{\underline{F}}$ can be expressed in terms of integral data by [21,22]

$$\underline{E}^o = \underline{R}^{exp} - \underline{R}^o = \underline{R}^{exp} - \underline{\underline{G}}\underline{P}^o, \tag{28}$$

$$\underline{\underline{F}}^o = \underline{\underline{V}} + \underline{\underline{N}} . \tag{29}$$

The transformation of the negligence in terms of a-priori parameters $\underline{P}^o$ is much more involved [21,22]. The "best" estimates of $\underline{E}$ and $\underline{\underline{F}}$ are obtained from

$$\underline{E} = \frac{1}{1+\lambda}\,\underline{E}^o, \tag{30}$$

$$\underline{\underline{F}} = \frac{1}{1+\lambda}\,\underline{\underline{F}}^o, \tag{31}$$

where λ is related to χ^2/n by

$$\frac{\chi^2}{n} = \frac{\lambda+1}{\lambda} , \tag{32}$$

assuming that χ^2/n exceeds 1. These quantities could be used to *correct* either the integral data or the a-priori data[+] (Chao calls this "adjustment", departing from the usual definition) before combining them in the adjustment proces like discussed in Sect. 2.

Also when it is not a-priori known which quantity should be corrected, Chao [22] gives estimates for the corrections. These estimates are as follows:

negligence in integral data:

$$\underline{E}_R = \frac{1}{1+\lambda}\,\underline{\underline{V}}(\underline{\underline{N}}+\underline{\underline{V}})^{-1}\,\underline{E}^o , \tag{33}$$

negligence in a-priori data (in terms of integral data):

$$\underline{E}_p = \frac{-1}{1+\lambda}\,\underline{\underline{N}}(\underline{\underline{N}}+\underline{\underline{V}})^{-1}\,\underline{E}^o . \tag{34}$$

Thus, the total negligence is still given by the previous Eq. (30).

We like to note that Chao needed an assumption in order to arrive at a division between the two negligences Eqs. (33,34). His "model" was to weight the negligence components in the probability distributions by the error matrices of initial experimental and a-priori integral data, $\underline{\underline{V}}$ and $\underline{\underline{N}}$, respectively. This leads immediately to the proportionalities with $\underline{\underline{V}}$ and $\underline{\underline{N}}$ in Eqs. (33,34). This assumption leads to nice symmetrical results. It

---

[+] Or, more generally, to correct only the suspected parts of $\underline{R}^{exp}$ or $\underline{P}^o$.

should be noted, however, that there is no physical reason whatsoever for systematic errors to be related to the corresponding experimental uncertainties. So the mathematically logical assumption of Chao is physically completely arbitrary, and may even be misleading. One should use Chao's formulas with some care; they present a convenient statistical tool to be used if inconsistencies arise to gain quantitative understanding of the discrepancies, but they can never be a substitute for the real task of the physicist, namely to find the physical source of the discrepancy.

Using the corrections given in Eqs. (33,34) the results of the adjustment of corrected integral data and a-priori values leads exactly to the results of Sect. 2, provided that the posterior covariance matrices are multiplied with χ^2/n. This gives a foundation to the practice of scaling-up covariance matrices with the factor χ^2/n when this quantity exceeds 1.

In Ref. [22] Chao has also included model uncertainties, which leads to differences compared to the above treatment, provided that $\chi^2 \gg 1$. His final expression for adjusted integral data in the presence of method uncertainties can be denoted as:

$$\underline{R}' - \underline{R}^{exp} = -\underline{\underline{V}}(\underline{\underline{N}} + \underline{\underline{V}} + \frac{\cdot}{2+\cdot}\,\underline{\underline{U}})^{-1}\,\underline{E}^{o}, \qquad (35)$$

which differs from the usual solution by a scaling factor $(\cdot+2)/\cdot$ of matrices $\underline{\underline{V}}$ and $\underline{\underline{N}}$. The corresponding covariance matrix is much more complicated [24]. It is remarkable to note the asymmetry in this equation. This is due to the fact that $\cdot$ is determined by imposing a χ^2-test on [22]

$$n = \underline{E}^{oT}\,[(1+\cdot)(\underline{\underline{N}} + \underline{\underline{V}}) + \underline{\underline{U}}]^{-1}\,\underline{E}^{o}\ . \qquad (36)$$

Evidently, no "method negligence" is included, i.e. it is assumed that $\underline{\underline{U}}$ has the character of statistical "noise" (Sect. 3). If a "negligence" is included in the method as well, reformulation of the adjustment problem as discussed in Sect. 3 reduces the problem to the previous situation, i.e. a solution given by Eqs. (3-7), with covariance matrices multiplied with χ^2/n.

8. DATA EVALUATION AND UNCERTAINTY ASSESSMENT

Prior to any adjustment procedure all data, sensitivity matrices and covariance matrices need to be evaluated. A few comments on the determination of neutron spectra have already been given (Sect. 3). Some other remarks on the data evaluation problems follow below.

Experimental data; self shielding

As an example of the evaluation of integral data we mention here the analysis of the STEK integral data which are small-sample reactivity worths in five reactor cores [5]. Most STEK samples were chemical and isotopic mixtures, subjected to self-shielding.

Another complication was that part of the reactivity worth is caused by scattering rather than capture. When these effects are small, corrections could be applied to obtain "clean" data, referring to the capture reactivity effect of a pure isotope measured in infinite dilution. In our application [1-5] we have corrected only for chemical admixtures and scattering effects. In the adjustment a number of isotopic mixtures having various degress of self-shielding were considered. This approach avoids iterative procedures which would be needed otherwise. On the other hand, the size of the matrices involved in the adjustment process became quite large and strong correlations were introduced in the a-priori cross sections belonging to the various samples. By extending the a-priori cross section vector with isotopic cross sections in infinite dilution the required adjusted data were obtained ("indirect adjustment" [1]). The covariance matrix $\underline{V}$ of the (corrected) experimental data was obtained by including uncorrelated statistical experimental errors, errors due to uncertainties in sample composition, normalization errors and errors due to the scattering correction [1,5]. Another - quite different - example of integral data evaluation is reported in Ref. [29]. See also Refs. [13-15].

A-priori cross sections

The assessment of uncertainties to the a-priori cross sections should be made during the evaluation process. In the resolved resonance range a straightforward way to obtain uncertainties in multi-group constants is to use the uncertainties of the resolved resonance parameters and to apply the error propagation law [1]. Complications arise because of self shielding and correlations between various resonance parameters [1]. At higher energies three evaluation procedures could be distinguished, which are based on:

(a) nuclear model calculations with parameters from external sources (i.e. no differential cross section measurements available),
(b) selection, averaging, smoothing, interpolation and extrapolation of differential data,
(c) model calculations with parameters "tuned" to available differential data.

In the first approach [1,2] the parameters could come from averaged resolved resonances (e.g. mean level spacing, average capture width, neutron strength function), level scheme data, Q-values, differential data from related cross sections (e.g. optical-model parameters from total cross section data), systematics or theory. These "external" sources can be used to assign parameters and their uncertainties (with possible correlations). From these parameters the covariance matrix of (group) cross sections can be calculated [1,2]. Additional uncertainties in multi-group cross sections dealing with the validity of the model cannot be attached to parameters, but need to be included also. Here we refer to Ref. [2] for a discussion of these statistical-model errors. An advantage of this approach is that both "short-range" and "long-range" correlations are introduced in quite a natural way.

In the second approach [19] mentioned above the main task of the evaluator is to review the various differential data and to trace

back the uncertainties and correlations. Usually the evaluator can only indicate for each measurement the statistical uncertainties and a common normalization error, expressing the measured points by

$$\sigma_i = \eta f_i \,, \tag{37}$$

where η is the normalization constant. For lognormal distributed quantities the relative covariance can be expressed as [11]

$$\frac{Q_{ij}}{\langle\sigma_i\rangle\langle\sigma_j\rangle} = (1+c^2)(1+r_i r_j \rho_{ij}) - 1 \,, \tag{38}$$

where c and r_i are the fractional uncertainties in η and f_i and ρ_{ij} is the (unknown) correlation coefficient of f_i and f_j. Assuming that ρ_{ij} is a short-range correlation it could be parametrized as [11]

$$\rho_{ij} = (1-\Theta)\,\delta_{ij} + \Theta \exp\left[-\frac{(i-j)^2}{2\gamma^2}\right] . \tag{39}$$

It is the task of the evaluator to assume reasonable values for Θ and γ which refer to the fraction of short-range correlation and its range, respectively. This information should follow from the experimental method (resolution). From Eqs. (37-39) or similar representations the co-variance matrix of the (group) cross sections can be calculated.

In the last-mentioned approach, which is probably closest to common evaluation practice, the parameters are modified (mostly within their uncertainties) to improve the agreement with differential data. This may lead to smaller uncertainties in the parameters. However, these uncertainties are difficult to estimate when the parameters are "tuned" by means of "trial and error" methods. Therefore, it seems better to introduce the differential data in an adjustment process, like described in Sect. 5. Integral data could be included, if needed, at the same time. Thus we advocate to base the a-priori data and their uncertainties upon nuclear model calculations and to adjust the calculated data to differential and/or integral data.

9. CONCLUSIONS

Most cross section adjustment problems can be formulated by Eqs. (1,2) with the solution [1] given by Eqs. (3-7), assuming no uncertainties in $\underline{G}$ [Eq. (2)] and no correlations between experimental data and a-priori data. Important simplifications may be obtained by taking advantage of the statistical independence of the various components (partitioning, partial adjustment) or a transformation of the parameters [1,10].

If the relation between a-priori integral data and parameters is not rigid, "method" errors $\underline{U}$ need to be included in the covariance matrix of the difference of experimental and calculated integral data [Eq. (12)]. This is easily shown by extending the adjustable vector

with elements of $\underline{G}$ [1,10,16,23] and/or a "noise" term $\underline{\Delta}$ to account for those statistical uncertainties which are not included in the elements of $\underline{G}$ (Sect. 3). In this reformulated adjustment problem the adjustments in $\underline{G}$ and $\underline{\Delta}$ are obtained explicitly from the usual solution Eqs. (3-7).

Instead of adjusting multi-group cross sections one could also adjust the underlying physical model parameters [1,18] when their number is not too large. In a practical application [6,25] a selection of important statistical-model parameters has been adjusted by applying Eqs. (16-18) [1] after completing the multi-group cross section adjustment. The parameters were used to obtain "adjusted" point cross sections [25]. Adjustments in the resolved resonance range are much more difficult to transfer to point cross sections (Sect. 4).

"Direct" point cross-section adjustment has been applied at HEDL [10-12]. This method is also problematic in the resolved resonance range, but it has the important advantage that differential experimental data could be easily used together with the integral data [12].

In principle it is also possible to formulate the adjustment problem for continuous functions [19], but it seems rather difficult to include correlations in a proper way (Sect. 5).

Logarithmic adjustment [1,10,11], i.e. assuming lognormal distributed adjustable quantities, has to be recommended for most cross sections, to ensure positivity and to cope with asymmetric error limits. The problem can be reduced to Eqs. (1,2) when the relation between integral data and the logarithm of cross sections is assumed to be linear [1]. In that case the distribution of the adjusted cross sections is again lognormal [1]. Otherwise, iterations may be needed and the statistical distribution of adjusted parameters is more complicated [10]. Furthermore, interpretation problems may arise due to the difference between the expectation and most probable values (Sect. 6).

The statistical χ^2-test (Eq. 8) is a useful tool to detect inconsistencies, of which the source should be investigated by means of a re-analysis of all data involved. When this source cannot be detected, but it is a-priori known that systematic errors are absent (or small) in either the experimental or a-priori data still a correction should be applied to the suspected data. A statistical estimate of this "negligence" [21] follows from Eqs. (30,31). If the origin of the inconsistency is completely unknown a possible - but arbitrary - approach follows from a distribution of the negligence over both experimental and a-priori data in a ratio according to their respective uncertainties [22]. The result of this approach leads to the usual solution Eqs. (3-7), except that the covariance matrix of the adjusted data should be multiplied with the value of χ^2 per degree of freedom. Inclusion of model parameters complicates this picture. However, reformulation of the adjustment problem as discussed in Sect. 3 reduces the problem to the previous situation (Sect. 7). Chao [22] treats the special case that it is a-priori known that the negligence is not due to the method, assuming method errors with a statistical ("noise") character.

In practice a large effort is needed to evaluate experimental

data, a-priori data, sensitivity matrices and covariance matrices. Usually the a-priori data are evaluated cross sections based upon model calculations and differential data. A recommended approach is to consider model parameters (based upon "external" sources) as a-priori data. The calculated point cross sections could then be adjusted to experimental data as described in Sect. 5 [11]. In such a procedure the three independent data sources, i.e. model parameters, differential cross section data and integral data are used in a consistent way, provided that the covariance matrix of the calculated cross sections is derived from the parameter covariance matrix [1,2,18]. Other information used in this process is contained in the theoretical relations and their method uncertainties.

10. REFERENCES

1. J.B. Dragt et al., Methods of adjustment and error evaluation of neutron capture cross sections; application to fission product nuclides, Nucl. Sc. and Eng. 62 (1977) 117.

2. H. Gruppelaar, Uncertainty estimates of statistical theory calculations of neutron capture cross sections of fission products, Proc. of a Consultants Meeting on the use of Nuclear theory in neutron nuclear data evaluation, Trieste, Dec. 1975, IAEA-190, vol. 2 (1976) 61, IAEA, Vienna.

3. J.W.M. Dekker, Tables and figures of adjusted and unadjusted capture group cross sections based on the RCN-2 evaluation and integral measurements in STEK, vol. 1, ECN-14 (1977), vol. 2, ECN-30 (1977) and vol. 3, ECN-54 (1979).

4. J.W.M. Dekker and H.Ch. Rieffe, Adjusted cross sections of fission product nuclides from STEK reactivity worths and CFRMF activation data, vol. 1, ECN-28 (1977) and vol. 2, ECN-55 (1979).

5. M. Bustraan et al., Integral determination of fission product neutron cross sections for application in fast reactors, Proc. of the second advisory group meeting on Fission product nuclear data (FPND) - 1977, Petten, Sept. 1977, AEA-213, vol. 1 (1978) 627 and ECN-27 (1977).

6. H. Gruppelaar and J.W.M. Dekker, Impact of integral measurements on the capture cross section evaluations of individual fission product isotopes, Proc. of the second Advisory Group Meeting on Fission product nuclear data (FPND) - 1977, Petten, Sept. 1977, IAEA-213, vol. 1 (1978) 219 and ECN-24 (1977).

7. H. Gruppelaar and J.W.M. Dekker, Evaluation and adjustment of radiative capture cross sections of natural Mo and the stable Mo isotopes, Proc. Specialists' Meeting on Neutron data of structural materials for fast reactors, Geel, Dec. 1977, p. 213 (1979) Pergamon Press; extended report ECN-40 (1978).

8. J. Chaudat, J. Barré and A. Khairallah, Improvements of the predicted characteristics for fast power reactors from integral experiments: Cadarache version III multigroup cross section set, Proc. Int. Symp. on Physics of fast reactors, Tokyo, Oct. 1973, p. 1207 (1973).

9. H. Gruppelaar, P. Hammer and L. Martin-Deidier, Intercomparison of adjusted data sets for capture cross sections of fission products, Proc. Specialists' Meeting on Neutron cross sections of fission product nuclei, Bologna, Dec. 1979, NEANDC(E) 209 "L" (1980) p. 299.

10. F. Schmittroth, A method for data evaluation with lognormal distributions, Nucl. Sc. and Eng. 72 (1979) 19.

11. F. Schmittroth, FERRET data analysis code, HEDL-TME 79-40 (1979) and private communication (1980).

12. R.E. Schenter et al., Evaluations of fission product capture cross sections for ENDF/B-V, Proc. Int. Conf. on Nuclear cross sections and Technology, Knoxville, Oct. 1979.

13. R.A. Anderl et al., Neodymium, Samarium and Europium capture cross-section adjustment based on EBR-II integral measurements, Proc. Specialists' Meeting on Neutron cross sections of fission product nuclei, Bologna, Dec. 1979, NEANDC(E) 209, "L" (1980) p. 363.

14. R.A. Anderl, Cross section evaluation utilizing integral reaction-rate measurements in fast neutron fields, this meeting.

15. S. Iijima et al., Fission product neutron cross section evaluations for JENDL and the integral tests, Proc. Specialists' Meeting on Neutron cross sections of fission product nuclei, Bologna, Dec. 1979, NEANCD(E) 209, "L" (1980) p. 317.
Note: The problems of calculating self-shielding of STEK samples mentioned in this reference are due to the circumstance that no perturbed spectra ϕ^* have been used to calculate integral data, i.e. $\underline{\Sigma}.\underline{\phi}$ instead of $\underline{\Sigma}.\underline{\phi}^*$. In Refs. [1-5] the elements of $\underline{\Sigma}$ were multiplied by the ratio ϕ_i^*/ϕ_i.

16. F.G. Perey, Least-squares dosimetry unfolding: The program STAY'SL, ORNL/TM-6062 (1977).

17. J.W.M. Dekker et al., Adjusted neutron spectra of STEK cores for reactivity calculations, ECN-35 (1978).

18. A. Gandini and M. Salvatores, Nuclear data and integral measurements correlation for fast reactors. Part 3: The consistent method, RT/FI (74) 3, 1974.

19. A. Pazy et al., The role of integral data in neutron cross section evaluation, Nucl. Sc. and Eng. 55 (1974) 280.

20. Y.A. Chao, A new approach to the adjustment of group cross sections fitting integral measurements, Proc. of a seminar-workshop on Theory and application of sensitivity and uncertainty analysis, Oak Ridge, Aug. 1978, ORNL/RSIC-42 (1979) 281.

21. Y.A. Chao, New approach to the adjustment of group cross sections fitting integral measurements, Nucl. Sc. and Eng. 72 (1979) 1.

22. Y.A. Chao, A new approach to the adjustment of group cross sections fitting integral measurements, Nucl. Sc. and Eng. 75 (1980) 60.

23. J.H. Marable and C.R. Weisbin, Advances in fast reactor sensitivity and uncertainty analysis, Proc. of a seminar-workshop on Theory and application of sensitivity and uncertainty analysis, Oak Ridge, Aug. 1978, ORNL/RSIC-42 (1979) 25.

24. C.R. Weisbin et al., Application of sensitivity and uncertainty methodology to fast reactor integral experiment analysis, Nucl. Sci. and Eng. 66 (1978) 307.

25. H. Gruppelaar, Documentation of the adjusted RCN-3 evaluation of neutron cross sections in the fission-product mass range, to be published.

26. H. Gruppelaar, Tables and figures of RCN-2 fission-product cross section evaluation, vol. 1, ECN-13 (1977), vol. 2, ECN-33 (1977) and vol. 3, ECN-65 (1979).

27. P. Ribon et al., Evaluation des sections efficaces de capture et de diffusion inélastique de 26 produits de fission, Note CEA-N-1832 (1975).

28. CINDA, An index to the literature on microscopic neutron data, IAEA, Vienna, 1980. Most experimental data were obtained from the NEA Data Bank at Saclay.

29. L. Martin-Deidier, Mesure intégrale de la capture des produits de fission dans les réacteurs à neutrons rapides, Rapport CEA-R-5023 (1979).

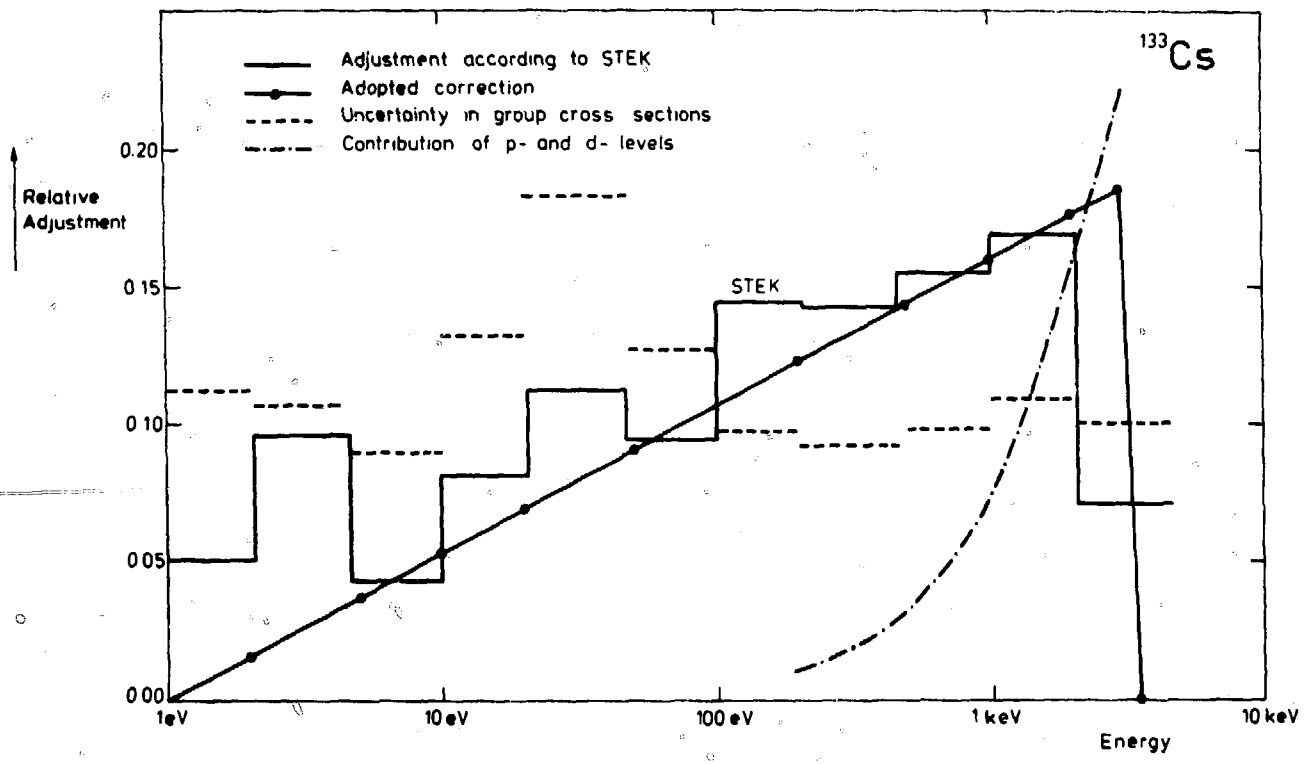

Fig. 1. Adopted [25] smooth correction factor for the capture cross section of ^{133}Cs in the resolved resonance range (up to 3.5 keV) compared with relative multi-group cross section adjustments [4], mainly based upon STEK integral data.

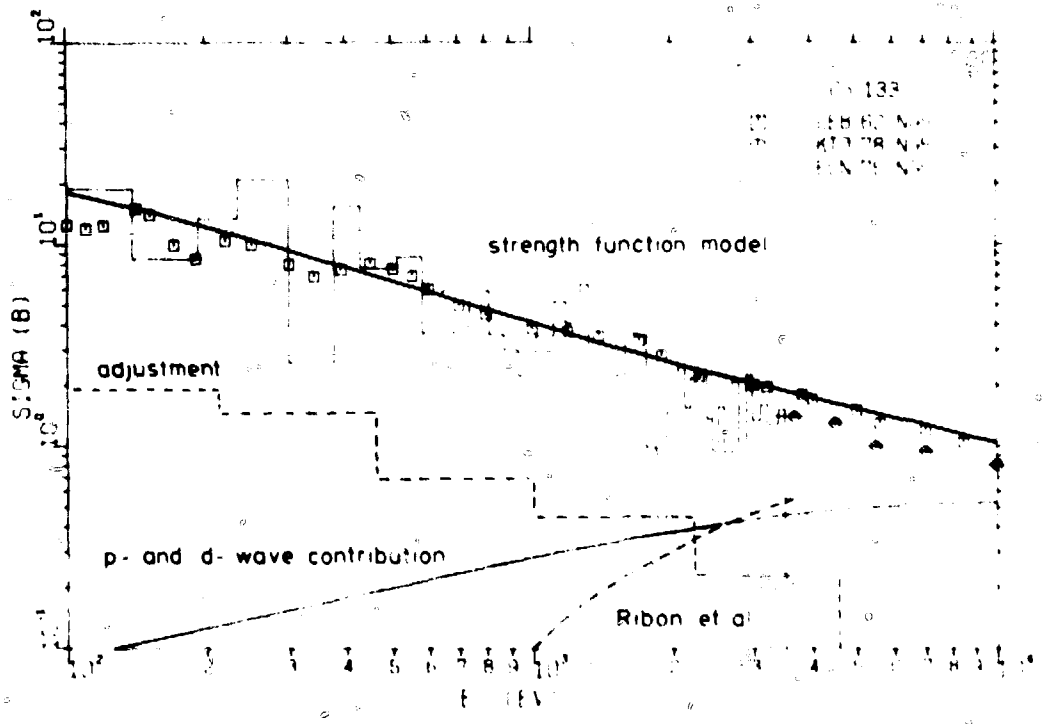

Fig. 2. Comparison of ^{133}Cs capture cross section calculated from resolved resonance parameters [26] (full-line histogram) with statistical-model prediction and broad-resolution data [28]. Also shown are adjustments based upon STEK [4], the p- and d-wave contribution and the additive correction applied by Ribon et al. [27].

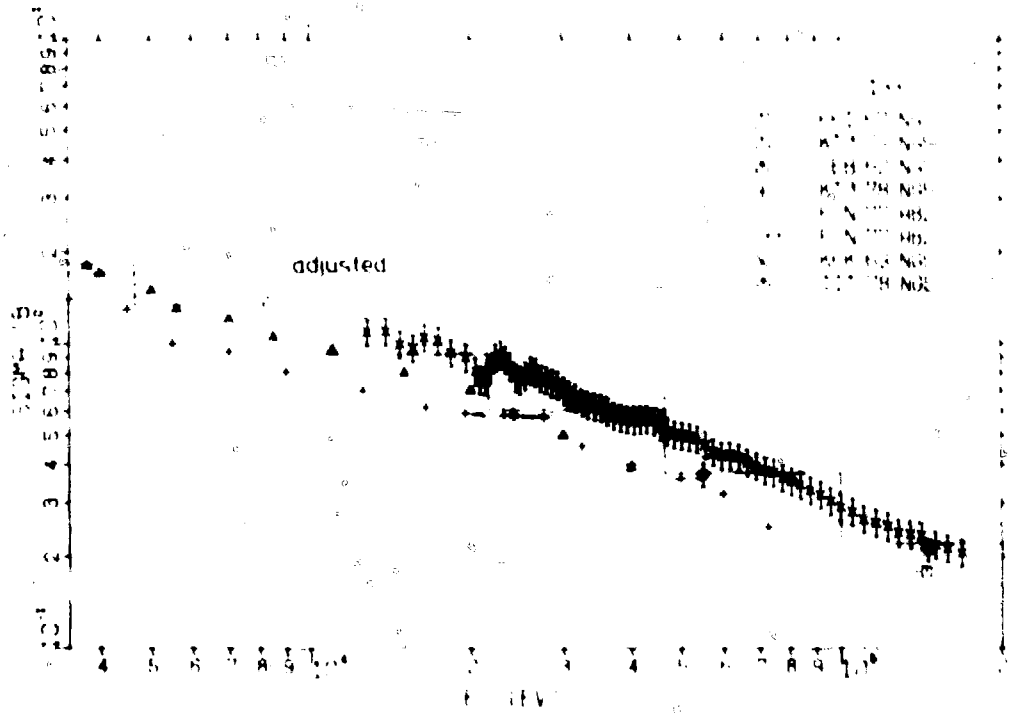

Fig. 3. Unadjusted and adjusted multi-group capture cross sections of ^{133}Cs based upon STEK and CFRMF integral data [4] compared with experimental data [28] at 3.5 to 200 keV.

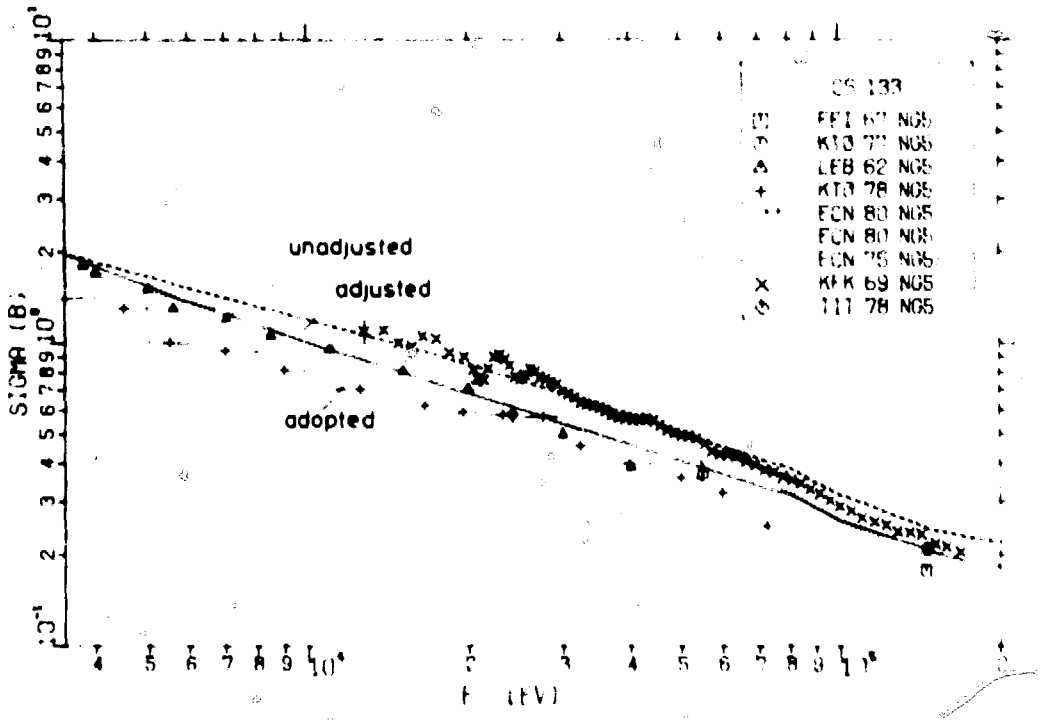

Fig. 4. Unadjusted [26], adjusted and adopted [25] evaluated curves for the ^{133}Cs capture cross section compared with experimental data [28] at 3.5 to 200 keV.

Discussion

Peelle

For all speakers, what do you see as any desirable difference in the use of simple integral experiments involving perhaps a single reaction rate in a "clean" spectrum, and complex benchmarks like critical experiments.

Rowlands (Comment)

I consider that it would be appropriate to take certain "simple" types of integral measurement into account explicitly when producing ENDF/B libraries. These are measurements of reaction rates in well-defined spectra and measurements for single substances. For example, useful information could be obtained from spectrum measurements in the iron block experiment on details of cross section structure (such as minima), and this is best taken into account in ENDF/B rather than an applications library. However, more general integral data are best taken into account by adjusting an applications library.

I also have a question. You assume that fission product cross sections have a lognormal distribution. Does this introduce a bias into the average cross section for the sum of all fission products present in a reactor? I suspect that if the uncertainties are distributed in this way, the sum overestimates the average cross section.

Gruppelaar

With regard to the possible effect of the lognormal assumption on the summed fission-product cross section, I would like to reply that this is certainly a point that needs to be further investigated. It is true that uncertainties in these pseudo fission-product cross sections are mainly of systematic nature, and the effect you mentioned could be one of the possible contributions.

Rowlands (Comment)

As well as representing methods uncertainties "explicitly," it is possible to represent integral measurement uncertainties in terms of separate systematic error uncertainties (or bias), and, the effects of composition uncertainties in the same way. It is not necessary to introduce these additional variables because all that is required is the covariance matrix for (C-E). However, it is interesting to obtain these systematic error estimates (or bias estimates) explicitly. The different ways of treating these effects does not affect the adjustments.

Gruppelaar

I fully agree with your last point. The advantage of an explicit formulation is that one is forced to think of all kinds of possible uncertainties. It seems advisable to formulate an adjustments problem first in its most explicit form before it is decided which parameters one would like to obtain from the adjustment calculation, introducing method errors for the remaining (implicit) parameters. I would like to note that certain uncertainties cannot easily be attached to explicit parameters, for instance the uncertainties introduced by neutron width fluctuations of the calculated (statistical-model) cross sections. These error sources are easily overlooked, but they may be very important because they allow for local variations in the cross sections just above the resolved resonance range.

Pearlstein (Comment)

The influence of integral data on ENDF/B can be exaggerated. Recent adjustments of fission product cross sections based on integral data is not typical of the general case. The ENDF/B ^{235}U fission cross section is based on what will be a good measurement standard and not on what will necessarily give good answers in criticals. The systematic errors associated with integral data still require caution in its use (integral data) to adjust differential data. Some small risks are taken to ensure that ENDF/B will be useful for applications because it is believed that this is necessary to continue ENDF/B development.

The conditions for using integral data to improve differential data have still not been addressed. Differential data can be used in the forward direction to calculate integral data because the laws of physics are assumed to be understood. This is all right provided the physicist has thought of everything. But there are generally too many degrees of freedom to improve differential data working backward from integral data. Consistency between integral data and differential data does not necessarily imply understanding. In my analysis of 14 bare homogeneous criticals I used five parameters (cross sections), but actually it is only a two independent variable problem. The critical height can be observed to depend only on volume (buckling) and the ratio of hydrogen to uranium. This information is sufficient to predict heights for intermediate cases. It is not obvious that the use of a five parameter theory to represent a two parameter problem will necessarily improve our understanding of differential data.

Perey

I like very much your presentation. I do not share, however, your enthusiasm for the log normal distribution in most applications you seem to use it. I think you use it mostly to treat relative data, and in general it would take a very special situation to lead to a lognormal distribution.

Gruppelaar

The lognormal distribution was adopted at our laboratory mostly for practical reasons, to avoid negative values of the adjusted capture cross sections at high energies, where the uncertainties are quite large and must be asymmetric. Assuming lognormal distributed cross sections is a convenient way to cope with these problems.

Menapace

In connection with the method of adjusting model parameters and from discussions with one of the authors Gandini, it was realized that special care should be taken to properly account for correlations among the parameters (e.g., average Γ_γ and mean level spacing). In addition, the adjusted parameters should be considered only as an indication by evaluators who have to consider their physical compatibility and then utilize this information in a further evaluation.

Gruppelaar

I think that what you are saying about Γ_γ and D_{obs} is that these two parameters are certainly correlated. And after adjustment they are even more correlated. But these correlations could be introduced. Of course, you must be very careful in the interpretation of any adjusted parameter.

SESSION IV

RADIOACTIVITY DATA
Chairman: C.W. Reich EG&G

EVALUATION PROCEDURES FOR EXPERIMENTAL DECAY DATA

R. L. Bunting and C. W. Reich

Idaho National Engineering Laboratory
EG&G Idaho, Inc.
Idaho Falls, Idaho 83415, U.S.A.

ABSTRACT

The file of radioactive-nuclide decay data included in ENDF/B is intended to provide a commonly available base of evaluated decay data relevant to reactor research and technology and to nuclear-power applications. Consequently, the types of data it contains have been carefully chosen to permit their application to a wide variety of reactor-related problems while still retaining a relatively compact size. In this paper, we briefly review the history and purpose of the decay-data evaluations for ENDF/B, together with the sources and types of experimental data considered. The importance of the generic relationships of the radiations emitted following nuclear decay is discussed and their treatment in ENDF/B is illustrated. For purposes of illustration, an example of an experimental decay-data evaluation is presented. The procedures for accounting for the various atomic processes associated with nuclear decay are presented. The increasing availability of data from the study of the complex decay schemes of nuclides with large decay energies (e.g., short-lived fission products) presents a special challenge for reactor-related decay-data evaluations. The unique problems posed by inherent limitations in these data are pointed out. The need for new data types and experimental techniques specially tailored to produce the information required for reactor-technology applications is indicated. The potential relevance of existing beta-strength-function measurements as one means of addressing these problems is discussed.

I. INTRODUCTION

Seven years ago, the nuclear-data content of the Evaluated Nuclear Data File (ENDF/B) was expanded to permit the inclusion

of detailed information from radioactive-nuclide decay. The impetus for this expansion was provided by the recognized need for a common, reliable base of evaluated data for use in summation-code calculations of the fission-product decay-heat source term. To address this need an ad-hoc working group, the Decay-Heat Task Force, was organized. The data base produced by this group appeared in 1974 as the Fission-Product File in Version IV of ENDF/B. The INEL participation in the work of the Task Force centered in two areas: (i) deciding on the types of decay data to be included and their organization; and (ii) preparing evaluations of these data for a number of "important" fission-product isotopes. A detailed discussion of the categories of decay data incorporated into ENDF/B-IV and their organization, together with a listing of those nuclides for which decay-data evaluations were carried out, is given in Refs. 1 and 2.

With the completion of this initial phase of the decay-data evaluation effort, as evidenced by the incorporation of the results into ENDF/B-IV, the emphasis of this work was directed toward future versions of ENDF/B. The decay data included in Version V of ENDF/B differ in two respects from those in Version IV. First, the nuclide coverage has been considerably expanded. Version IV contained INEL-evaluated decay data for 198 nuclides (and isomeric states), 180 for the Fission-Product File and 18 for the General Purpose File [1]. For ENDF/B-V, decay-data evaluations have been done for nuclides in three separate files: the Fission-Product File; the Actinide File and the Activation File. In the Fission-Product File, experimental decay-data evaluations now exist for 318 isotopes (including isomeric states). In the Actinide and Activation Files, such evaluations are included for 60 nuclides and 71 nuclides, respectively. [In addition, a MOD for the Actinide File is presently being prepared. This will include evaluations for 42 more nuclides. This MOD, together with the Actinide File, will provide coverage of all the isotopes in the major actinide decay chains.]

The second respect in which the decay data in ENDF/B-V differ from those in Version IV lies primarily in the treatment of several processes not explicitly considered in the Version-IV file. Generally these changes do not represent major modifications in the structure of the file but rather closer definitions of some of the previously defined quantities. This permits the Version-V data, for example, to provide an improved description of the temporal relationships in delayed-particle emission, the radiation spectra associated with internal-conversion and the "continuous" radiation spectra associated with such processes as internal bremsstrahlung and delayed-neutron emission. Our experience to date with this expanded data format has been such that we do not foresee major changes in it in future versions of ENDF/B. Consequently, it seems appropriate at this point to present a brief overview of the types of decay-scheme data that are presently being incorporated into ENDF/B and the evaluation procedures that are involved in generating this information.

II. DECAY-DATA EVALUATION FOR ENDF/B

A. General Considerations

The primary function of the decay data in ENDF/B is to provide a description of the energy emitted in radioactive decay, both the form in which it appears and the time at which it is produced. In this respect, the ENDF/B decay-data file is not intended to replace such broadly oriented data compilations as the Nuclear Data Sheets [3] or the Table of Isotopes [4] but rather to present an evaluated subset of those data, tailored to the identified needs of the nuclear-power program.

The types of decay data included in ENDF/B can be broken down into two general categories: level properties and radiation spectra. Data in the former category are provided only for ground states and isomeric states. [Isomers, which by convention in the file are excited states with half-lives $\geq$0.1 s, are treated on an equal footing with ground states: each isomeric state has its own set of evaluated data, separate from those of its associated ground state.] The level information includes half-life, spin and parity, decay modes and, for each decay mode, the total energy available to it (Q-value) and the fraction of decays of the state which proceed via that mode. In the schematic decay scheme shown in Fig. 1, for example, the isomeric state $^{A}Z^{*}$ decays via β^{-}, β^{+} + e.c., delayed-neutron emission and via γ emission (isomeric-transition decay) to the ground state; thus, information on four decay modes must be provided. If isomers exist in the daughter nuclei and are populated in the parent-state decay, the energy associated with their decay will exhibit a time dependence different from that of the parent. [This can be a significant effect in some applications, such as, for example, decay heat.] The ENDF/B decay-data file takes this into account by treating the feeding of a daughter-nucleus isomeric state as being a separate decay mode, distinct from that feeding the ground state (even though, of course, the same type of radiation from the parent is involved in both cases). In this case, the radiation emitted following the isomeric-state decay is included in the data set for that isomer and not in that for the parent nucleus. In Fig. 1, for example, since it feeds both a daughter-nucleus isomeric state and ground state (in the e.c. + β^{+} decay), the parent isomeric state will have five listed decay modes in ENDF/B, even though only four radiation types are actually emitted in its decay. Furthermore, the transition γ^{*} will be found in the data set of the daughter-nucleus isomer, $^{A}(Z-1)^{*}$, and not in that of the parent state, $^{A}Z^{*}$. A good example of how this situation is treated in ENDF/B is provided by the well-known case of ^{137}Cs. The characteristic 661.6-keV γ ray associated with ^{137}Cs actually arises from the decay of 2.55-min ^{137m}Ba. Even though the ground state of ^{137}Cs decays only via β^{-} emission, its ENDF/B data set lists two decay modes and no γ radiation; the 661.6-keV γ ray is listed in the data set of ^{137m}Ba.

Data in the second category, that involving radiation spectra, include energy and intensity information for the various individual transitions, as well as computed average-energy values. Radiation types for which such spectral data are presently included are β^-, β^+, α, γ, conversion-electron, x-ray, annihilation radiation and internal bremsstrahlung. Delayed-neutron spectra, as well as those of spontaneous-fission neutrons, protons, etc. can readily be treated as well; but no such data have been included in ENDF/B at the present time. Other information, unique to different radiation types and which are useful in deriving important quantities from them, is also given. Examples of these are the γ-ray multipolarities, used to derive conversion-electron and x-ray spectral information (see Sect. III.E below) and the forbiddenness character of the $\beta^\pm$ transitions, which is needed to compute average β energies (see Sect. III.A below).

Since the focus of the present discussion is on the details of the evaluation of decay data for ENDF/B rather than on the structure and organization of the data within the file, we will not emphasize this latter information here. Discussions together with specific examples of this file format, at least as it is organized prior to its translation into the standard ENDF/B format, are given in Refs. 5 and 6.

B. A Sample Experimental Decay-Data Evaluation

In order to more fully illustrate the decay-data evaluation process and the relationships of the adjacent members of a decay chain, a sample evaluation for some members of the A=88 decay chain is given here. The data discussed in this section and given in the referenced figures are taken from Ref. 7.

Fig. 2 illustrates one of the simplest types of decay schemes which must be treated by the evaluator, one in which the intensity of the decay branch to the daughter-nucleus ground state is known to be zero. At the time this evaluation for ^{88}Y was completed, no single set of published γ-ray data was conclusive enough to completely describe all the details of the decay scheme. To determine the absolute γ-ray emission rate (cf. Fig. 2), the total γ-ray transition intensity to the ground state was first determined using a set of γ-ray relative-intensity values. This set of evaluated relative intensities was chosen such that the intensity values from a number of studies could be referenced to a common ground-state γ-ray transition, namely that of γ_4. This choice of data provided a common link for the various references used in the evaluation. Based on all the available data and the adopted conversion and pair-production coefficients, the absolute γ-ray intensities were determined by requiring that the total γ-related feeding of the ground state was 100%. The above procedure is also often referred to as an intensity normalization. (For clarity, the uncertainties for the measured and deduced values have been omitted here. The calculation of the uncertainties for the deduced quantities is straightforward and the details are contained

in Ref. 7.) Finally, the electron-capture (e.c.) decay intensities were determined from the γ-ray transition-intensity balances at each level. Additionally, the atomic vacancies produced in the e.c.-decay and internal-conversion processes can be used to calculate the conversion- and Auger-electron spectra; and the annihilation radiation intensity can be deduced from the pair-production coefficient, $\alpha\pi$, and the β^+ intensity. References to $\sim$30 published journal articles were used in the ^{88}Y evaluation. The large number of references used in this evaluation correctly indicates that this is a well-studied decay. However, the numerous publications actually report selected measurements for only a few of the quantities (i.e., γ-ray intensities) observed in the decay. The procedure illustrated here shows our method for arriving at a common set of values for all of these quantities, consistent with this extensive, but only partially overlapping, set of results.

The second example, the decay of ^{88}Rb, is given in Fig. 3. As in the previous example, this decay populates levels in the daughter nucleus, ^{88}Sr. Some of the γ rays observed in the ^{88}Y and ^{88}Rb decays will depopulate the same ^{88}Sr levels. Hence, the measured γ-ray energy values in one decay may be improved if more precise energy measurements have been made for the other. Here, ^{88}Y is a γ-ray energy calibration standard and was used as such in the experimental determination of the ^{88}Rb γ-ray energies. For the ^{88}Rb decay there have been three relatively good measurements of the intensity of the ground-state β^- transition, β_0. This is rather unusual, since the measurements of the intensities of ground-state β transitions are seldom done as part of a "routine" decay-scheme study: they are generally difficult to carry out and much of the nuclear-structure information sought in these works can be deduced without a precise knowledge of this quantity. The point to be made here is that, even with a precise value for β_0, the propagation of errors may lead to an undesirably large uncertainty in the absolute γ-ray intensity determination (or intensity normalization). This lack of precision will also affect the reported intensities of the γ-ray and β spectra and, through them, the average energies of the various decay modes. Groups located at several laboratories are addressing this problem of absolute γ-ray intensity determinations, but the available data encompass only a few of the radionuclides for which otherwise good decay-scheme data are available.

In some instances it may be possible to deduce the intensities of an unknown ground-state beta branch from a careful analysis of a decay chain containing at least one nuclide which has a well-known ground-state branch. This procedure is illustrated in Fig. 4. Note that the tabular data given in Fig. 4 correspond to those given in Fig. 3. A carefully measured ratio, R, relating the γ-ray intensity in the ^{88}Rb decay to that in the ^{88}Kr decay for the transient equilibrium condition given here, is required. The value R usually represents a time-integrated quantity and it is calculated at some time after the isolation of the ^{88}Kr parent activity. A calculated activity ratio, A, can be obtained by integrating the

parent-daughter decay curves. Using these data, along with the known intensity of the ^{88}Rb ground-state beta branch, β_0(Rb) from Fig. 3, one can calculate the ^{88}Kr ground-state beta branch, β_0(Kr). The values calculated for these results also illustrate the error propogation for such calculations. The procedure described here was used to determine the value (13±7)% for β_0(Kr). Before the A=88 evaluation was completed, the results of a direct measurement of β_0(Kr) were published. This measurement reported a value of (13±5)% for β_0(Kr). The excellent agreement of these two values supports the validity of the evaluation techniques described above for cases where unknown ground-state beta transitions must be deduced from other considerations. The A=88 evaluation quotes (13±5)%, the measured value, as the adopted value for β_0(Kr).

III. COMPUTATION OF AVERAGE-ENERGY VALUES FROM EVALUATED DECAY DATA

One of the important categories of decay data included in ENDF/B is the average energy (per decay) for the various emitted radiation types. Provision in the ENDF/B format structure is made for the inclusion of an average-energy value for each of the spectrum types treated. Some of the possible spectrum types are:

(a) β^-
(b) e.c.+β^+ (e.c.=electron capture)
(c) α
(d) n, p
(e) γ-ray
(f) e^- (conversion and Auger)
(g) x-ray, internal bremsstrahlung and annihilation radiation (i.e., photons not resulting from a transition between two nuclear levels).

(At the present time no spectral information for protons or neutrons is included in the file.) The average-energy data for these radiation types are further grouped into three general categories: electrons; photons; and heavy particles. The electron category contains β^-, β^+, conversion electrons and Auger electrons. The photon group includes contributions from γ rays and the radiations in (g) above, while the remaining contributions are included under the heading of heavy particles.

The average energy and atomic-spectra calculations to be discussed here are performed using the computer code PCDE [8], which has been developed at INEL. PCDE also carries out the necessary file-editing steps to incorporate the calculated results into the final evaluated decay-data files.

A. The $\beta^\pm$ Spectra

The $\beta^\pm$ endpoint energy, $E_{\beta i}$, and intensity, $I_{\beta i}$, for the individual $\beta^\pm$ transitions are generally determined from the

analysis of the decay scheme. The β spectrum of an individual transition is, of course, continuous and the shape of this spectrum is different for β^+ and β^- as well as for the different angular momentum transfers in the decay. The two distinct spectral shapes treated in the ENDF/B evaluations are those of the allowed and first-forbidden unique beta transitions. The first-forbidden nonunique and second-forbidden nonunique spectral shapes cannot generally be calculated and must be measured. Few measurements of these spectra exist, however, and the allowed spectral shape is assumed for these transitions for the purpose of calculating the average energy, $\langle E_\beta \rangle$, in ENDF/B. All other transitions are assumed to have the shape of a first-forbidden, unique spectrum. The average energy for a $\beta^\pm$ transition is related to the β endpoint energy, E_{β_i}, by the expression

$$\langle E_{\beta_i} \rangle = f_\beta \, (Z, E_\beta, \text{Shape}) \times E_{\beta_i} \quad .$$

In the above expression for $\langle E_{\beta_i} \rangle$, f_β is a function of the β-spectral shape, the daughter nuclide Z-value and the β-endpoint energy. The calculated values for $f_\beta(Z,E_\beta)$, or $\langle E_{\beta_i} \rangle / E_{\beta_i}$, used in PCØDE to determine the average energy for a β transition were obtained using the computer code LØGFT [9,10] supplied by the Nuclear Data Project at ORNL. LØGFT is also the general code utilized by the U.S. Nuclear Data Network for calculating the β^--decay and $(\beta^+ + \text{e.c.})$-decay properties. Four tables of f_β are used in PCØDE. These tables include the allowed and first-forbidden unique values for both β^- and β^+ transitions. Each table consists of 160 values, 16 energy values from 10 keV to 10 MeV for each of 10 Z-values from Z=10 to Z=100. A double cubic-spline interpolation procedure is used to first define $f_\beta(Z,E)|_{E_i}$ for each energy for the specified daughter-nucleus Z-value and then compute $f_\beta(Z,E_i)|_Z$ for each β-endpoint energy. A plot of f_β for the allowed β^- transitions is shown in Fig. 5. The smooth curves were generated from the cubic-splines interpolation procedure in PCØDE using a 100-point energy mesh. The overall average β energy for the decay, $\langle E_\beta \rangle$, is determined using the expression

$$\langle E_\beta \rangle = \sum_i f_{\beta_i}(Z,E,\text{Shape}) \times E_{\beta_i} \times I_{\beta_i} \quad ,$$

where the sum is over all the individual β transitions and I_{β_i} is the intensity (in β's per decay) of the i-th β transition.

1. Uncertainty in the average β-decay energy - $\sigma\langle E_\beta \rangle$

Special consideration has been given to the calculation of the uncertainty in the average β-decay energy. First we note that the uncertainty in the endpoint energy, $\sigma\langle E_{\beta_i} \rangle$, of each transition is as a general rule, equal to the uncertainty in the Q-value for the decay. Second, the sum of th tal β-decay

intensity is constrained to be equal to the β-decay fraction. Because of this imposed constraint, a simple error propogation based on the uncertainties in the β intensities alone does not provide an accurate estimate of the uncertainty in $\langle E_\beta \rangle$. (It significantl overestimates this uncertainty.) That portion of $\sigma\langle E_\beta \rangle$ which is due to the uncertainty in the β intensities, $\sigma'\langle E_\beta \rangle$, can be shown [11] to be given by the expression

$$\sigma'^2 \langle E_\beta \rangle = \sum_i [\langle E_{\beta_i} \rangle \sigma(I_{\beta_i})]^2 - \frac{[\sum \langle E_{\beta_i} \rangle \sigma^2(I_{\beta_i})]^2}{\sum \sigma^2(I_{\beta_i})} \quad . \qquad (1)$$

The first term of Eq. (1) is the usual expression of the variance for the unconstrained problem, while the second term gives the reduction in $\sigma'\langle E_\beta \rangle$ as a consequence of the constraint. To complete the calculation of $\sigma\langle E_\beta \rangle$, the uncertainties in the overall β-intensity normalization and the Q-value are combined in quadrature with $\sigma'\langle E_\beta \rangle$.

B. Electron-Capture (e.c.) + Positron Decay

In the case of e.c. + β^+ decay, additional contributions to the total average energy other than the β^+ treatment described above exist and must be taken into account. Each positron gives rise to two annihilation quanta ($E = m_0c^2 = 511$ keV). The total β^+ intensity, then, can be used to calculate the contribution of the annihilation radiation to the photon spectrum. Also electron-capture is always present when β^+ decay is possible. This process gives rise to the production of x-rays (and neutrinos as well, but these latter radiations are not included in the data file). To calculate the x-ray intensities, the atomic vacancies produced in the electron-capture process must be computed. The probability, $P_K(P_L)$ of producing an atomic vacancy in the K(L)-atomic shell is defined as the number of K(L) vacancies per e.c. decay. These probabilities are determined from calculations based on LØGFT [9,12]. These probabilities depend on the energy available to the electron-capture transition, Z and the different angular momentum transfers in the decay. The electron binding energies used in PCØDE for the K through N_I shells are taken from Ref. 13. The total number of K-shell vacancies, V_K, in the e.c.-decay process is given below as a function of the calculated probabilities, P_K, and the electron capture intensity per decay, $Ie.c._i$,

$$V_K = \sum_i I_{e.c._i} P_K(Z,E_i) \quad .$$

A similar expression can be written for the L-shell vacancies. The calculation of the x-ray and Auger-electron spectra resulting from the filling of these vacancies is discussed in section III.G below.

C. The α-Decay Contribution to the Average Energy

The energy values listed for the individual α transitions in the ENDF/B files are the observed α-transition energies. These differ somewhat from the decay energy available to these transitions. The difference between the available energy and the observed energy is carried by the recoiling nucleus. In calculating the average α-decay energy given in ENDF/B, this recoil energy is included. This is done by multiplying the observed α energy by the factor A/(A-4), where A is the mass of the decaying nuclide (and 4 is the α-particle mass). Since the sum of the α intensities is constrained to be equal to the α-branching fraction of the parent nuclide, the calculation of the uncertainty in $\langle E_\alpha \rangle$ is carried out in a manner similar to that for β^- and β^+ radiations [see Eq. (1)].

D. The Treatment of Neutron and Proton Energy Spectra

Provisions exist for incorporating both continuous and discrete neutron and proton spectra in ENDF/B. However, there are no current examples of these spectral types in the file and since the procedures for treating these data are straightforward, we have chosen not to discuss them here.

E. The Gamma-Ray Spectrum

The treatment of the γ-ray spectrum is straightforward. The average energy per decay, $\langle E_\gamma \rangle$, is given as the sum of the products $E_{\gamma_i} I_{\gamma_i}$ for each γ ray, i, in the spectrum. The intensity values, I_{γ_i}, in this case represent the number of photons emitted per decay. Since the γ-ray intensities are not "constrained" in the same sense as are those of the primary radiations (e.g., β^-, α), the uncertainty in $\langle E_\gamma \rangle$ can be calculated using a standard error propagation expression, viz.

$$\sigma^2 \langle E_\gamma \rangle = \sum_i \left[(\sigma(E_{\gamma_i}) \cdot I_{\gamma_i})^2 + (\sigma(I_{\gamma_i}) \cdot E_{\gamma_i})^2 \right].$$

The internal-conversion process, generally associated with γ-ray processes, is considered in somewhat more detail in ENDF/B-V than it was in the Version-IV File. The known γ-ray multipolarities and/or measured internal-conversion coefficients, which are included in the file, are used to calculate the conversion-electron spectrum and associated electron-shell vacancies. The use of γ-ray multipolarities to calculate the conversion-electron information is preferred over the use of measured internal-conversion coefficients, since the multipolarity is generally derived from a much broader range of experimental data. The use of the γ-ray multipolarities for these calculations is also preferred since the theoretical internal-conversion coefficients

derived from them are generally more precise than the measured values. In a number of well-documented situations, the measured internal-conversion coefficients differ significantly from the theoretical values. Examples of this are provided by the L_I- and L_{II}-shell conversion coefficients for some highly retarded E1 transitions in the actinide region and measured penetration effects for certain M1 transitions. In such cases, the evaluators generally choose to use the measured values, rather than the theoretically predicted ones based on the γ-ray multipolarity, to compute the conversion-electron and x-ray spectra.

F. The Conversion-Electron Spectra

The ENDF/B conversion electron spectrum is generated from known γ-ray energies and intensities, using their associated internal-conversion coefficients or γ-ray multipolarities. (See section III.E above.) Up to six electron lines (K, L_I, L_{II}, L_{III}, M and N+) are calculated for each γ-ray transition. The M+ (or N+) notation signifies the M (N) plus higher shells.) The energy of the conversion-electron ejected from the j-th atomic (sub)shell is calculated from the relation

$$CE(j) = E_\gamma - BE(j) \quad ,$$

where BE(j) represents the atomic electron binding energy for the j-th (sub)shell and E_γ is the γ-ray energy. The corresponding conversion-electron intensity is calculated from the relation

$$CI(j) = I_\gamma \alpha_j \quad ,$$

where I_γ is the γ-ray intensity (in photons per decay) and α_j is the j-th (sub)shell internal-conversion coefficient. The number of electron vacancies generated in the K- and L-shells from this process is given by the relation,

$$V_K = I_\gamma \alpha_K \qquad \text{and}$$

$$V_L = I_\gamma (\alpha_{L_I} + \alpha_{L_{II}} + \alpha_{L_{III}}),$$

respectively.

If a γ-ray entry has associated with it a multipolarity, PCODE calculates a set of theoretical internal conversion coefficients for the K, L_I, L_{II}, L_{III}, M_I, . . ., M_V, and N+ atomic shells using the theoretical values in Refs. 14, 15, 16, 17. The electron spectrum resulting from the internal conversion of this transition is calculated as indicated above. The five M-subshell lines are contracted into a single M-shell entry by summing the electron intensities and calculating a single intensity-weighted energy value. All non-zero conversion data for the K, L_I, L_{II}, L_{III}, M and N+ shells are entered into the spectrum.

The calculated α_K, α_L, α_{M+} and α_{TOTAL} values are also recorded with the appropriate γ-ray record in the final ENDF/B file.

Uncertainties in the conversion-electron intensities are calculated from the uncertainties specified in I_γ and α_j. The uncertainties in α_j are determined using either the quoted uncertainties in the mixing ratio of the transition or an assumed 3% uncertainty in the theoretically calculated α_j values, whichever is larger.

A similar procedure is used to calculate the conversion-electron contribution from the γ rays for which the K-, L- and M-conversion coefficients are specified. The electron energy associated with these shells is given as CE(K), CE(L_{II}) and CE(M_{III}), respectively. The uncertainty in the electron intensities is defined as above, using the stated uncertainty in the α_j's.

Because the conversion-electron list can become quite extensive, only those entries are retained in the ENDF/B file contents whose intensities are either greater than 1% of the most intense line or whose contribution to the average conversion-electron energy is at least 1%. All of the computed conversion-electron lines are used in the calculation of the average energy, even though not all lines are listed in the ENDF/B electron spectrum.

G. The X-Ray Spectrum

The x-ray spectra contained in ENDF/B are calculated from the number of K- and L-shell atomic vacancies generated in electron-capture decay and conversion-electron emission. Other data required for these calculations include values for relative x-ray emission rates and fluorescence yield data.

For each spectrum, the number of K-x-ray lines included depends on the Z-value for the final nucleus according to the following:

$Z < 6$	no x-ray calculations are performed
$6 \leq Z < 20$	K_α, K_β
$20 \leq Z < 36$	K_{α_1}, K_{α_2}, K_β
$36 \leq Z \leq 100$	K_{α_1}, K_{α_2}, $K_{\beta_1'}$, $K_{\beta_2'}$.

(The notation used here is the standard Siegbahn notation [18].) The $K_{\beta_1'}$ component includes the $K_{\beta_1} + K_{\beta_3} + K_{\beta_5}$ lines and the $K_{\beta_2'}$ component includes the $K_{\beta_2} + K_{\beta_4}$ lines. The expressions used to calculate the K-x-ray intensities and energies in ENDF/B are conventional expressions based on the values for the relative x-ray emission rates, K_α/K_β, $K_{\alpha_2}/K_{\alpha_1}$ and $K_{\beta_2'}/K_{\alpha_1}$, and electron binding energies. The values for the relative x-ray emission rates are taken from Ref. 18. Values for ω_K and $\bar{\omega}_L$, the K-shell and average

fluorescence yields; and n_{KL}, the number of L-shell vacancies created in filling a K-shell vacancy, are obtained from Ref. 19. It should be noted that the relative intensities of the various components of the K-x-ray peak structure can be reliably calculated using these expressions and give good agreement with those observed experimentally.

In contrast with the situation for the K x-rays, the relative intensities of the L-x-ray spectrum cannot be reliably calculated. The total L-x-ray intensity, however, is related to the total number of K- and L-shell vacancies, and this quantity can be calculated rather simply and with some confidence. Consequently, for ENDF/B, the total L-x-ray intensity has generally been collected into a single line. The energy of this L-line has been chosen to be that of $L\beta_1$. This choice appears to provide a reasonable average of the L-x-ray spectra for a number of measured cases in the actinide nuclei.

In a number of cases in the actinide nuclei, measurements of the L-x-ray spectra have been reported. In these cases the experimental data are given in ENDF/B for the four prominent peaks in the spectrum (namely, $L\ell$, $L\alpha$, $L\beta$ and $L\gamma$).

Two additional data types which are included in the ENDF/B x-ray listings are: (i) the annihilation radiation produced in β^+ decay and in pair-production processes involving higher-energy ($>2m_0c^2$) photons; and (ii) the continuous-energy photon distributions, such as those produced in internal bremsstrahlung. These data contribute to the overall photon spectrum but do not arise from direct transitions between nuclear levels.

IV. THE CHALLENGE OF COMPLEX DECAY SCHEMES

The increasing use of the techniques of on-line isotope separation and fast radiochemical separation in nuclear spectroscopy is producing a large amount of new decay-scheme data on short-lived nuclides. These data have provided a wealth of new and interesting nuclear-structure information. However, they present potentially difficult problems for an evaluator interested in incorporating them into an energy-oriented data file, such as ENDF/B. These difficulties result from the fact that such nuclides generally have large Q-values (greater than, say, 5 MeV). For the medium-heavy and heavier nuclei ($A \geq 100$), these decays populate regions of rather high level density in the excitation spectrum of the daughter nucleus. In such cases, which in many respects resemble the situations encountered in neutron-capture gamma-ray spectroscopy, an appreciable fraction of the gamma-ray strength may be unobserved. Consequently, achieving a realistic intensity (and hence energy) balance within these complex decay schemes becomes difficult, if not impossible.

Attention has been called to this problem by Hardy et al. [20]. Using statistical arguments in the context of a specific case, namely the electron-capture decay of ^{146}Gd (Qe.c. = 5 MeV), they demonstrated that much of the γ-ray intensity could remain unobserved under normal experimental conditions. They suggested that this (unexpected) nonobservation of a significant fraction of the γ-ray intensity called into question the validity of many complex decay schemes determined from conventional nuclear-spectroscopic methods.

This possibility has significant implications for the evaluation of decay data for ENDF/B, in particular for the short-lived fission products. A knowledge of their decay data is important for the calculation of the decay-heat source term, especially at short cooling times. It also calls into question the utility of the conventional nuclear-spectroscopic studies as a means of producing realistic values for those quantities important for decay heat. [Note that this problem is independent of the usual, and well-recognized, problems of unassigned or misassigned γ-ray transitions and inadequate counting statistics.] Thus, for complex decay schemes, the conventional evaluation methods, using the measured γ-ray intensity information to deduce β intensities and compute average-energy values may lead to a systematic (and unrealized) bias in these quantities.

To produce accurate values for these average energies, it appears that specialized experimental techniques, designed specifically to measure them, may be required. Total-absorption β- and γ-ray spectroscopy seems to be a promising method to do this. In fact, examples of the use of such information to provide "experimental" $\langle E_\beta \rangle$ and $\langle E_\gamma \rangle$ values already exist in the ENDF/B-V Fission-Product File. The measurement of β-strength-function data for a number of short-lived fission products [21] employed a total-absorption technique. It has been pointed out [6,22] that this β-strength-function information could be used, at least in principle, to infer $\langle E_\beta \rangle$ and $\langle E_\gamma \rangle$ values for the fission-product isotopes studied. Since no other measured data had been reported for the radiations emitted in the decay of 38 of these isotopes, these deduced average-energy values were included in the ENDF/B-V Fission Product File. The initial motivation for this was primarily to increase the number of nuclides in the file for which "experimental" average-energy data were listed.

It should be pointed out that the β-strength-function data of Ref. 21 were not measured with the specific objective of producing average-energy values, and the accuracy required to determine these values may not be inherent in the data. Consequently, our use of these data for this purpose, while "in principle" justified, may in practice be open to question. However, for those nuclides which have both measured β-strength data and conventionally measured decay-scheme data, the agreement in the two sets of average-energy values appears reasonably good [6,22]. It seems likely that, for future versions of ENDF, the "data of choice" for average-energy values of short-lived fission products will result,

not from the conventional nuclear-spectroscopic studies, but from new experiments, specially designed for this purpose.

REFERENCES

1. C. W. REICH, R. G. HELMER and M. H. PUTNAM, "Radioactive-Nuclide Decay Data for ENDF/B," USAEC Rep. ANCR-1157 (ENDF-210) Idaho National Engineering Laboratory (1974).

2. C. W. REICH and R. G. HELMER, "Radioactive-Nuclide Decay Data in Science and Technology," in Proc. Conf. on Nuclear Cross Sections and Technology, Washington, D.C. (1975), NBS Special Publication 425, Vol. 1, p. 14-20.

3. Nuclear Data Sheets, Academic Press, New York and London.

4. C. M. LEDERER and V. S. SHIRLEY, editors, Table of Isotopes, Seventh Edition, John Wiley and Sons, New York (1978).

5. C. W. REICH, "Status of Beta- and Gamma-Decay and Spontaneous-Fission Data From Transactinium Isotopes," in Proc. IAEA Advisory Group Meeting on Transactinium Isotope Nuclear Data, Karlsruhe (1975), REPORT IAEA-186, Vol. III, p. 265-308 (1976).

6. C. W. REICH, "Applications of Fission-Product Decay Data," in Proceeding of the Isotope Separator On-Line Workshop, Brookhaven National Laboratory, (1977), USDOE REPORT BNL-50847, p. 109-148 (1978).

7. R. L. BUNTING and J.J. KRAUSHAAR, "Nuclear Data Sheets for A=88," Nucl. Data Sheets, 18, 87 (1976).

8. R. L. BUNTING, "PCØDE-A Computer Code for Generating Atomic Spectra and Average Nuclear Decay Energies using the INEL Decay Data Master File," Idaho National Engineering Laboratory, Unpublished (1979).

9. W. B. EWBANK, "LOGFT-A Computer Code for Calculating $\beta^{\pm}$ - and Electron-Capture-Decay Properties," Oak Ridge National Laboratory - Nuclear Data Project, Private Communication (1977).

10. N. B. GOVE and M. J. MARTIN, "LOG-f Tables for Beta Decay," Nucl. Data Tables, 10, 206 (1971).

11. F. W. SPRAKTES, Idaho National Engineering Laboratory, Private Communication (1976).

12. M. J. MARTIN and P. H. BLICHERT-TOFT, "Radioactive Atoms. Auger-Electron, α-, β-, γ-, and x-ray Data," Nucl. Data Tables, 8, 1 (1970).

13. J. A. BEARDEN and A. F. BURR, "Reevaulation of X-Ray Atomic Energy Levels," Rev. Mod Phys., 39, 125 (1967).

14. R. S. HAGER and E. C. SELTZER, "Internal Conversion Tables. K-, L-, M-Shell Conversion Coefficients for Z=30 to Z=103," Nucl. Data Tables, A4, 1 (1968).

15. O. DRAGOUN, H. C. PAULI and F. SCHMUTZER, "Tables of Internal Conversion Coefficients for N-Shell Electrons," Nucl. Data Tables, A6, 235 (1969).

16. I. M. BAND, M. B. TRZHASKOVSKAYA and M. A. LISTENGARTEN, "Internal Conversion Coefficients for Atomic Numbers Z=30," At. Data and Nucl. Data Tables, 18, 433 (1976).

17. W. B. EWBANK, Oak Ridge National Laboratory - Nuclear Data Project, Private Communication (1976) Data values from Refs. 14, 15, 16 on magnetic tape.

18. S. I. SALEM, S. L. PANOSSIAN and R. A. KRAUSE, "Experimental K and L Relative X-Ray Emission Rates," At. Data and Nucl. Data Tables, 14, 91 (1974).

19. M. J. MARTIN, Oak Ridge National Laboratory - Nuclear Data Project, Private Communication (1976).

20. J. C. HARDY et al., "The Essential Decay of Pandemonium: A Demonstration of Errors in Complex Decay Schemes," Phys. Letters 71B, 307 (1977).

21. K. ALEKLETT, G. NYMAN and G. RUDSTAM, "Beta-Decay Properties of Strongly Neutron-Rich Nuclei," Nucl. Phys. A246, 425 (1975).

22. C. W. REICH and R. L. BUNTING, "The Use of Data from β-Strength Function Experiments to Calculate Average β- and γ-Decay Energies," Contributed paper to the Second IAEA Advisory Group Meeting on Fission-Product Nuclear Data, Petten, the Netherlands (1977).

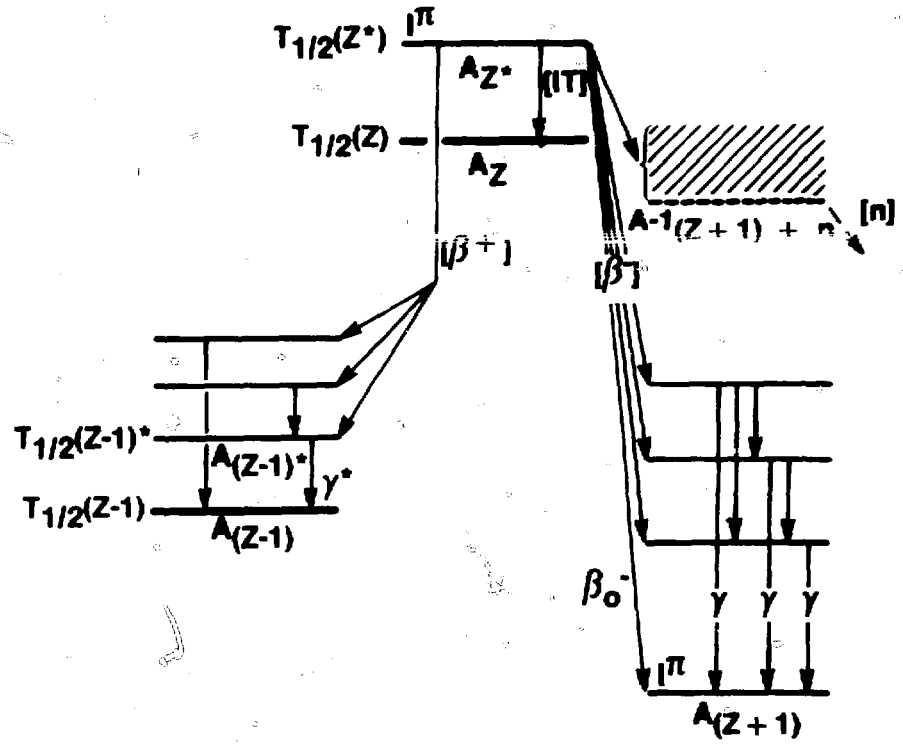

Fig. 1) A schematic decay scheme illustrating possible decay modes for a hypothetical state $^{A}Z^{*}$. Four distinct radiation types depopulating $^{A}Z^{*}$ are denoted by the square brackets. However, since an isomeric state in the daughter nucleus is also fed in the β^{+} decay, five decay modes (two for $[\beta^{+}]$) are necessary to represent the $^{A}Z^{*}$ decay in ENDF/B.

γ-ray intensity ratios from the results of many measurements

$\gamma_4/\gamma_2 = 1.064$
$\gamma_5/\gamma_4 = 6.0 \times 10^{-3}$
$\gamma_6/\gamma_4 = 9.5 \times 10^{-5}$
$\alpha_k(\gamma_4) = 1.4 \times 10^{-4}$
$\alpha_{\pi}\ (\gamma_4) = 2.3 \times 10^{-4}$

No g.s. β^+ feeding, hence Σ (I_γ's to g.s.) = 100
Result: $I_{\gamma_4} = 99.36$

ε-branching deduced from γ-ray intensity balances at each level

$(\beta^+ + \varepsilon)_0 = 0$
$(\beta^+ + \varepsilon)_1 = 5.36$
$(\beta^+ + \varepsilon)_2 = 94.55$
$(\beta^+ + \varepsilon)_3 = 0.03$
$(\beta^+ + \varepsilon)_4 = 0.068$

Decay Scheme - Schematic

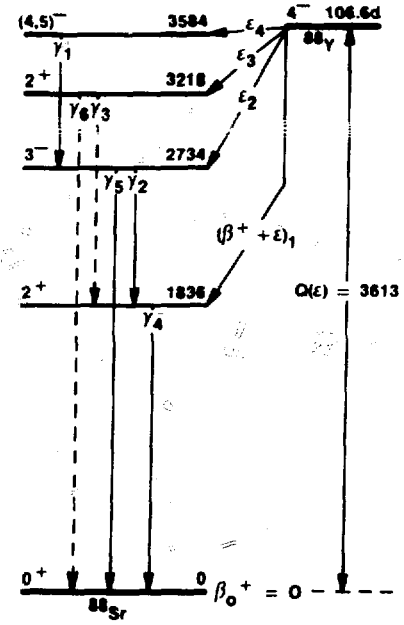

Fig. 2) A sample ENDF/B decay-data evaluation (for ^{88}Y) illustrating the use of an evaluated set of γ-ray intensities to deduce the (β^+ + electron capture) intensities.

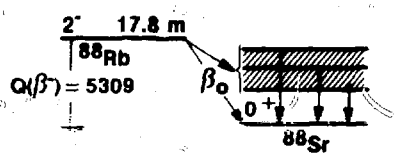

Case	β_0	Technique
1	76.2% ± 4.0	$2\pi\beta$
2	75.4% ± 2.5	$\pi\sqrt{2}\beta$
3	77.4% ± 1.4	$4\pi\beta$
4	76.9% ± 1.2	Weighted Average

Σ (γ-transitions to g.s.) = 1023[11] in γ-ray relative intensity units

$N \cdot \Sigma(\gamma\text{'s to g.s.}) = 100 - \beta_0(\text{Rb})$

Case	N	σ(%)	I(1836γ)%
1	0.0233[39]	∼17	23.3 ± 3.9
2	0.0241[25]	∼10	24.1 ± 2.5
3	0.0221[14]	∼6	22.1 ± 1.4
4	0.0226[12]	∼5	22.6 ± 1.2

Fig. 3) The absolute γ-ray intensity normalization for the ^{88}Rb decay as determined from four values of the intensity of the ^{88}Rb ground-state β^- decay transition. The effects of the error propagation are shown in the final values deduced from the normalization procedure.

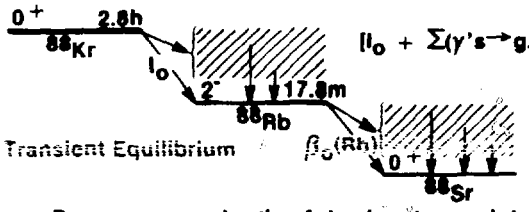

$$[I_o + \Sigma(\gamma\text{'s} \rightarrow \text{g.s.})]_{Rb} = [\Sigma(\gamma\text{'s} \rightarrow \text{g.s.})]_{Sr} \cdot R \cdot A \cdot 1/F$$

R = measured ratio of dominant γ-ray intensities in two spectra at equilibrium (= 0.715[36])

A = ratio of $^{88}Kr/^{88}Rb$ decay rates at time of R (= 0.894)

F = $|100-\beta_o(Rb)|/100$

Case	F	$I_o(\gamma)$	$\beta_o(Kr)\%$
1	0.238	288	10.5^{178}
2	0.246	198	7.4^{114}
3	0.226	434	15.0^{81}
4	0.231	371	13.1^{74}

$\beta_o(Kr)$ From recent direct measurement 13% ± 5

Fig. 4) The use of a decay chain to determine the values of an unknown ground-state β^- decay intensity. The intensity of the unknown branch, $[\beta_0(Kr)]$, can be expressed in terms of a known value, $[\beta_0(Rb)]$, and the relative γ-ray intensities for the two decays at equilibrium.

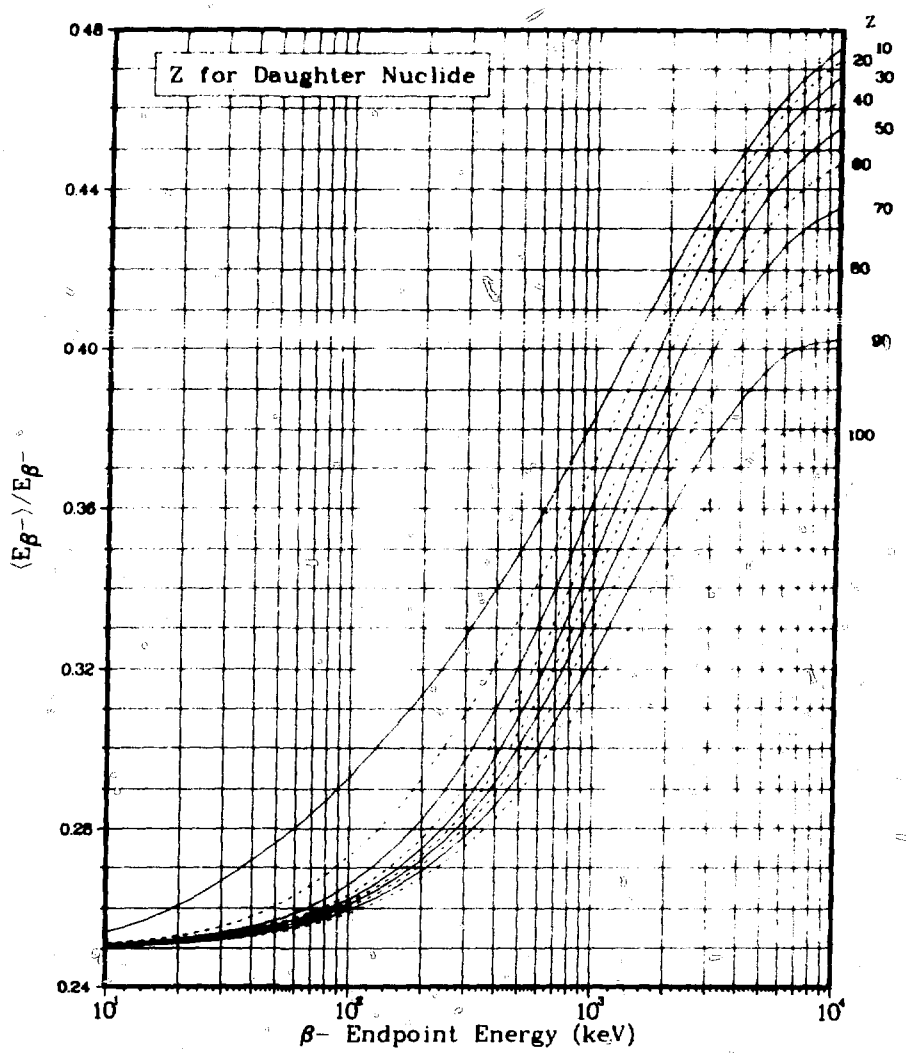

Fig. 5) Values for $f_\beta = \langle E_\beta \rangle / E_\beta$ for allowed β^- transitions.

Discussion

Smith

Is the decay file consistent with internationally accepted intensity and energy standards?

Bunting

For the nuclides on the Activation File there is some overlap of the evaluated decay data and what can be termed as primary or secondary reference standards for energies and intensities. In these cases an attempt has been made to incorporate the reference data into the file. The Fission-Product File is a different story. Because of the usually short fission-product half-lives, there are only a very few of the 318 fission-product nuclides that can be related to reference standards. These few cases arise from situations similar to that indicated for the ^{88}Rb and ^{88}Y decays. For this case, the γ-ray energies for the A=88 decay chain were deduced by the experimenter and evaluators using the accepted ^{88}Sr γ-ray energies. There is little that can be done by the evaluator for most of the nuclides other than to accept the author's published list of γ-ray energies and intensities. A true adjustment procedure would require detailed knowledge about the individual experimental calibration procedures for energies and intensities. These details are rarely given in the published results. The evaluator's major task for these files usually involves verifying that the reported transitions are indeed properly assigned to their parent activity rather than attempting to adjust the γ-ray energies and intensities

Reich

Also in reference to your question, we are aware of certain commonly accepted evaluations, such as, for example, the Rytz tables of alpha energies and intensities. There is also at present a coordinated research program with the IAEA to produce standard absolute-intensity values for the γ-rays from certain important actinide isotopes. In situations of this sort we attempt, of course, to incorporate this information into the file. The purpose of the file is not to produce yet another set of evaluated data; and where possible, where we think it is realistic, we try to include the results of what are commonly referred to as accepted standards for intensities and energies.

Smith

Should the experimenter use this file as a reference standard?

Reich

In that regard, the present file is of "uneven" quality. We hope that, for Version VI, the file contents can be used for this purpose.

Dup

THEORETICAL ESTIMATES OF DECAY INFORMATION FOR "NON-EXPERIMENTAL" NUCLIDES.

F. Schmittroth

Hanford Engineering Development Laboratory
Richland, Washington 99352, U.S.A.

ABSTRACT

Methods of estimating nuclear decay data for short-lived neutron rich nuclides are reviewed. The emphasis is on average decay energies. The connection with other data such as half-lives, delayed neutrons, and anti-neutrino spectra is noted within the context of the beta strength function. Integral data tests are made by comparisons of calculated and measured decay heat for ^{235}U.

INTRODUCTION

In decay heat summation calculations, about one-third of the computed decay heat immediately following a reactor scram arises from short-lived theoretical nuclides [1]. The term "theoretical" is used to indicate that the experimental decay data for these nuclides is too meagre to estimate their average decay energies (and sometimes half-lives). Although the fractional contribution of these nuclides decreases rapidly with increasing shutdown time, they still contribute nearly 10% at 100s cooling time, a time important to reactor Loss-of-Coolant-Accidents (LOCA). Moreover, since any estimates of their decay energies have relatively large uncertainties, they contribute disproportionately to the uncertainty in decay heat summation calculations.

This paper reviews ways that decay data can be theoretically estimated for very short-lived nuclides. The emphasis is on decay energies; however some consideration is given to half-lives, delayed neutron calculations, and even antineutrino studies. Much of the discussion is in the context of beta strength functions although other simple models are noted. Practical applications of these methods are discussed and carried through to data testing.

CONNECTION WITH BETA STRENGTH FUNCTIONS

The total number of beta decays to an electron energy range ΔE_β and a range of final state energies ΔE_f in the daughter nucleus is

$$\Delta N = T^{(-)} \rho_N(E_f) \Delta E_\beta \Delta E_f , \qquad (1)$$

where $T^{(-)}$ is the beta-decay transition operator and $\rho_N(E_f)$ gives the density of states in the final nucleus (a δ-function for discrete transitions). Another convenient quantity is the relative beta feed to levels near E_f:

$$b(E_f) = \frac{1}{\lambda} \int_0^{Q_\beta - E_f} dE_\beta \left\{ T^{(-)} \right\} \rho_N , \qquad (2)$$

where the normalizing integral is the decay constant

$$\lambda = \frac{\ln(2)}{T_{1/2}} = \int_0^{Q_\beta} dE_f \int_0^{Q_\beta - E_f} dE_\beta \left\{ T^{(-)} \right\} \rho_N . \qquad (3)$$

The integrals in Eq. (2) can be evaluated in the customary way to give

$$b(E_f) = \left[\frac{\rho_N(E_f) \; |M|^2_{av}}{d} \right] f^{(-)}(Z, Q_\beta - E_f) \; T_{1/2} \qquad (4)$$

where $f^{(-)}$ is the statistical rate function and d = 6270 s. Eq. (4) provides a natural definition for the beta strength function which is identified with the term in brackets and contains the nuclear structure information in the reduced matrix element $|M|^2_{av}$:

$$S_\beta(E_f) = \frac{1}{d} \rho_N(E_f) \; |M|^2_{av} . \qquad (5)$$

Average beta and gamma energies are given by

$$\langle E_\beta \rangle = \int E_\beta \; dN , \qquad (6)$$

and

$$\langle E_\gamma \rangle = \int E_\gamma \; dN . \qquad (7)$$

One other item of interest is the relative beta feed to levels above the pairing energy

$$\alpha' = \int_P^{Q_\beta} b(E_f)\, dE_f \quad . \tag{8}$$

Next, following England [2], we use his approximation for allowed spectra,

$$\frac{dP}{dE_\beta} \; F(-Z,E_\beta) \propto \frac{p^2}{W_\beta} \quad , \tag{9}$$

where W_β is the total relativistic energy and the other symbols have their usual meaning, to further evaluate Eqs.(6-8). The results are

$$\frac{\langle E_\beta \rangle}{m_e c^2} = \frac{1}{2\eta} \int_o^{Q_\beta} S_\beta(E_f) \left[X^4(X^2 + 4X + 5) \right] dE_f \quad , \tag{10}$$

$$\frac{\langle E_\gamma \rangle}{m_e c^2} = \frac{1}{\eta} \int_o^{Q_\beta} S_\beta(E_f) \left[X^4(X^2 + 5X + 10) \right] dE_f \quad , \tag{11}$$

and

$$\alpha' = \frac{1}{\eta} \int_P^{Q_\beta} S_\beta(E_f) \left[X^3(X^2 + 5X + 10) \right] dE_f \quad , \tag{12}$$

where

$$\eta = \int_o^{Q_\beta} S_\beta(E_f) \left[X^3(X^2 + 5X + 10) \right] dE_f \quad , \tag{13}$$

and

$$X = \frac{Q_\beta - E_f}{m_e c^2} \quad . \tag{14}$$

Given the uncertainties in $S_\beta(E_f)$, the allowed approximation is of little concern here.

One striking feature of these integrals is the large powers of X in the integrand. As a consequence, transitions to low lying states (small E_f) are strongly emphasized. These transitions are governed by beta decay selection rules so that the prediction of average decay energies is complicated, and the usefulness of

strength functions is curtailed. The need for a proper treatment of these low-lying transitions was emphasized by Yoshida [3]. Nevertheless, in some applications such as reactor decay heat calculations where numerous short-lived nuclides can contribute together, the calculation of average decay energies with a slowly varying strength function still makes sense.

Delayed neutron yields and half-life systematics are also directly obtainable from these equations but are not pursued in detail here. Delayed neutron yields are given by the beta feed above the neutron separation energy with a correction for gamma competition [4], and half-lives are obtainable from Eq.(3).

Another closely related area of recent interest is the calculation of anti-neutrino spectra from fission reactors. These spectra are crucial to the interpretation of recent weak-interaction experiments designed to shed light on the fundamental properties of the neutrino [5]. Once the beta-strength function is known, the beta feed for fission-product nuclides with unknown branching can be determined. The desired reactor anti-neutrino spectrum is then obtained by folding in a spectrum for discrete transitions and summing over all fission products [5].

BETA STRENGTH FUNCTIONS

Both theoretical and experimental approaches have been used to obtain beta strength functions (see Hansen [6] for a comprehensive review). A major theoretical effort was initiated by Takahashi and Yamada [7] in their gross theory of beta decay. In their work, a smoothly varying strength function is obtained on the basis of assumed collective Fermi and Gamow-Teller excitations. Yoshida [3] has implemented their approach to obtain estimates of decay energies for a number of short-lived fission products important to decay heat.

On the experimental side, a large number of strength functions have been measured for short-lived neutron-rich nuclides at the OSIRIS facility by Aleklett, Nyman, and Rudstam [8]. They summarize their results by noting that the reduced matrix element $|M|^2_{av}$ in Eq.(4) is roughly constant with respect to the excitation energy E_f for energies above the pairing energy. This behavior is equivalent to a strength function proportional to the nuclear level density. Davis et al [5] have exploited this trend to calculate anti-neutrino spectra from fission reactors. As with the average decay energies, the transitions to low lying states must be treated separately. In the approach by Davis et al, systematics were developed for α' the relative beta feed above the pairing energy. The residual branching $1-\alpha'$ was then distributed among three hypothetical states at 0, P/3, and 2P/3 (P = pairing energy).

In the work based on the gross theory of beta decay, Yoshida [3] has used a slightly different method to account for transitions to low-lying states. Based on the gross theory, all the

branching below a hypothetical state in the daughter nucleus at an energy Q_{oo} was collapsed to this state. Systematic values for Q_{oo} were then obtained by adjusting Q_{oo} to obtain the experimentally measured average decay energies ^{oo} for 19 nuclides. Values of Q_{oo} of 0 to 2.5 MeV were obtained with an adopted value of ~ 1 ^{oo} MeV. It was also found that adjustments of Q_{oo} to half-life data improved the prediction of average decay energies.

THEORETICAL ESTIMATES OF DECAY DATA

In spite of the rough approximations inherent in the beta-strength function approach, Eqs.(10 & 11) are quite constraining and in general predict that $\langle E_\beta \rangle$ and $\langle E_\gamma \rangle$ are roughly proportional to Q_β. In fact, the simple prescription $\langle E_\beta \rangle = \langle E_\gamma \rangle = \frac{1}{3} Q_\beta$ used by Tobias [9] and by Blachot and Fiche [10] works quite well.

A more elaborate parameterization was used for ENDF/B-IV [11]. About 150 nuclides with experimental decay energies were used to obtain the following equations:

$$\langle E_\beta \rangle / Q_\beta = 0.474 + 0.0177P + 0.00406(N-Z) - 0.00252A, \quad (15)$$

$$\langle E_\gamma \rangle / Q_\beta = 0.0399 - 0.0110\ P + 0.0100(N-Z) + 0.000191A. \quad (16)$$

For example, for ^{87}Br these formulas give $\langle E_\beta \rangle / Q_\beta = 0.344$ and $\langle E_\gamma \rangle / Q_\beta = 0.214$ with $Q_\beta = 6.6$ MeV, values quite close to the $1/3\ Q_\beta$ prescription. It is interesting to note the significant $(N-Z)$ term for $\langle E_\gamma \rangle$. As one moves toward neutron rich nuclei, the trend is for a greater proportion of gamma energy. A similar trend was noted by Spinrad's group at Oregon State University.

For ENDF/B-V, a beta-strength function approach was used similar to the work of Davis et al [5] in estimating antineutrino spectra. A constant reduced nuclear matrix element was assumed, or equivalently a strength function proportional to the nuclear level density ρ_N. There are large uncertainties in the strength functions and, accordingly, a simple constant temperature formula for ρ_N was chosen. Because of the importance of beta transitions to low-lying states, one additional parameter Θ was introduced which describes the relative normalization of an assumed constant nuclear density below the pairing energy:

$$\rho_N(E_f) = \begin{cases} \Theta & E_f < P \\ (1-\Theta)\ e^{E_f/T} & E_f \geq P \end{cases} \quad (17)$$

The nuclear temperature was parameterized by a single vari-

able C_T:

$$T = C_T \, T_{GC} \quad , \tag{18}$$

where T_{GC} is the nuclear temperature determined by Gilbert and Cameron [12]. The normalization Θ was allowed to have a very simple A-dependence by introducing two parameters Θ_1 and Θ_2 for the light and heavy fission product mass peaks respectively. The three parameters Θ_1, Θ_2, and C_T were then determined by fitting to the decay energies for 276 nuclides evaluated by Reich for ENDF/B-V [11]. Additionally, measured α values for 67 nuclides reported by Aleklett et al, were included in the fit. The results obtained are $\Theta_1 = \Theta_2 = 0.5$ and $C_T = 3$. The least-squares residuals were not sensitive to very small changes in these parameters and rounded values were selected for convenience. This parameterization was then used to generate average beta and gamma energies for all ENDF/B-V fission products where experimental values were unavailable. For a few nuclides, decay energies were estimated by Reich and Bunting by the direct use of measured strength functions [13].

Many more short-lived fission products have experimental half-lives than have experimental decay energies, and the estimation of theoretical half-lives is of less practical concern. These estimates can be obtained the same as for decay energies; however simple parameterizations suffice. In general these descriptions are close to the well known rule [14]

$$T_{1/2} \propto Q_\beta^{-5} \quad . \tag{19}$$

DATA TESTING

This section gives a very short review of the effect of these theoretical estimates in decay heat summation calculations. Figure 1 shows a breakdown of the relative contributions of three categories of fission-product nuclides to the decay heat following a fission pulse of ^{235}U (thermal):

(1) 276 experimental nuclides evaluated by Reich [11],
(2) 38 nuclides evaluated by Reich [13] on the basis of measured strength functions, and
(3) 430 nuclides with theoretical decay energies,

all from ENDF/B-V [11]. For decay times beyond 100 s, the contribution of the theoretical nuclides rapidly becomes negligible. For a more realistic finite reactor operating history, their contribution is further diminished.

Decay heat calculations based on three different evaluations of decay data are compared in Figure 2. Graphs are shown separately for the total decay heat and the beta and gamma components. Each graph displays the fractional deviation of the calculation

from a recent comprehensive decay heat evaluation for ^{235}U [15]. ENDF/B-IV yields [11] were used in all cases. The dotted curve labeled ENDF-IV represents the use of the complete ENDF/B-IV fission product data file. The ENDF-V (prelim) dashed curve uses theoretical decay energies based on the same parameterization Eqs. (15 & 16) used for ENDF/B-IV but with updated Q_β values. The substantial changes seen are mostly due to revised decay data (half-lives and decay energies) for the experimental nuclides. Also, many nuclides that were classed as theoretical in version IV have been changed to experimental in version V of ENDF/B. Finally, the solid curves, labeled ENDF-V (revised), represent the use of decay energies based on the strength function parameterization described above. The small differences seen between the use of the different decay energy parameterizations reflect their relative consistency and the dominant effect of the experimental nuclides.

The lack of improvement in the decay heat calculations based on the latest theoretical decay energies, especially for the gamma component, is disappointing. Unless the experimental decay heat evaluations are seriously in error, the calculated gamma component is about 20% low for decay times less than 100 s. Since this component is low even at 200 s where the experimental nuclides contribute over 90% of the total gamma energy, there is an indication of a systematic error in the experimental evaluations for the short-lived nuclides. Such an error would also affect the theoretical estimates since they are based in part on the experimental values. As a practical matter, one must continue to depend strongly on experimental decay heat assessments for the short cooling times. Improvement in the calculated values is still highly desirable, however, because of the flexibility such calculations afford and because once their general validity is established, they can be confidently applied in areas where direct measurements are unavailable.

The assessment of uncertainties in model estimates of decay energies is difficult, especially where one is extrapolating beyond the measured values. Some general comments can still be made however. The standard deviations obtained from the variance between the theoretical values and the experimental values were 0.37 MeV for $\langle E_\beta \rangle$ and 0.82 MeV for $\langle E_\gamma \rangle$. The larger value for $\langle E_\gamma \rangle$ reflects the larger dispersion of experimental values for $\langle E_\gamma \rangle$. Beta Q-values are typically known for experimental nuclides. However many [16] of the Q-values for the theoretical nuclides are estimated from semi-empirical mass formulas. This source of uncertainty contributes, very roughly, an additional 25% uncertainty [16]. Because this source of uncertainty is expected to be strongly correlated over the different nuclides, it is an important component of the total uncertainty in decay heat calculations at very short (<100 s) cooling times.

Not too long ago, decay heat summation calculations were thought to be very unreliable at very short times because of the lack of data for the short-lived nuclides. This situation has been dramatically improved. Nevertheless there is still room for substantial improvement, especially for the separate beta and gamma components.

REFERENCES

1. F. Schmittroth, Nucl. Sci. Eng. 59, 117 (1976).

2. T.R.England, "An Investigation of Fission Product Behavior and Decay Heating in Nuclear Reactors," Ph.D. thesis, Univ. of Wisconsin (1969).

3. T. Yoshida, Nucl. Sci. Eng. 63, 376 (1977).

4. O.K.Gjotterud, P.Hoff, and A.C.Pappas, Nucl. Phys. A303, 281 (1978).

5. B.R.Davis, P Vogel, F.M.Mann, and R.E.Schenter, Phys. Rev. C19, 2259, (1979).

6. P.G.Hansen, "The Beta Strength Function," in Advances in Nuclear Physics, Vol. 7, edited by M. Baranger and E. Vogt (1973 Plenum Press).

7. K.Takahashi and M.Yamada, Prog. Theor. Phys. 41, 1490 (1969).

8. K.Aleklett, G.Nyman, and G.Rudstam, Nucl. Phys. A246, 425 (1975).

9. A.Tobias, "Data for the Calculation of Gamma Radiation Spectra and Beta Heating from Fission Products," (Revision 3), CEGB Report RD/B/M2669, (1973).

10. J.Blachot and C.Fiche, "Bibliotheques de donnes nucleaires non neutroniques des isotopes radioactifs produits de fission et noyeaux lourds," in Intl. Conf. on Neutron Physics and Nuclear Data for Reactors, Harwell (1978).

11. The Evaluated Nuclear Data File (ENDF/B) is maintained at the National Nuclear Data Center (NNDC) at Brookhaven National Laboratory.

12. A.Gilbert and A.G.W.Cameron, Can. J. Phys. 43, 1446 (1965).

13. C.W.Reich and R.L.Bunting, "The Use of Data from β-Strength Function Experiments to Calculate Average β- and γ- Decay Energies," a contribution to Review Paper 12 in 2nd IAEA Advisory Group Meeting on Fission Product Nuclear Data, Petten, Netherlands (Sept. 1977).

14. K.Way and E.P.Wigner, Phys. Rev. 73, 1318, (1948).

15. G.K.Schenter and F.Schmittroth, "Beta and Gamma Decay Heat Evaluation for the Thermal Fission of ^{235}U," International Conf. on Nuclear Cross Sections for Technology (Oct. 1979) Knoxville, Tennessee.

16. F.Schmittroth and R.E.Schenter, Nucl. Sci. Eng., 63, 276 (1977).

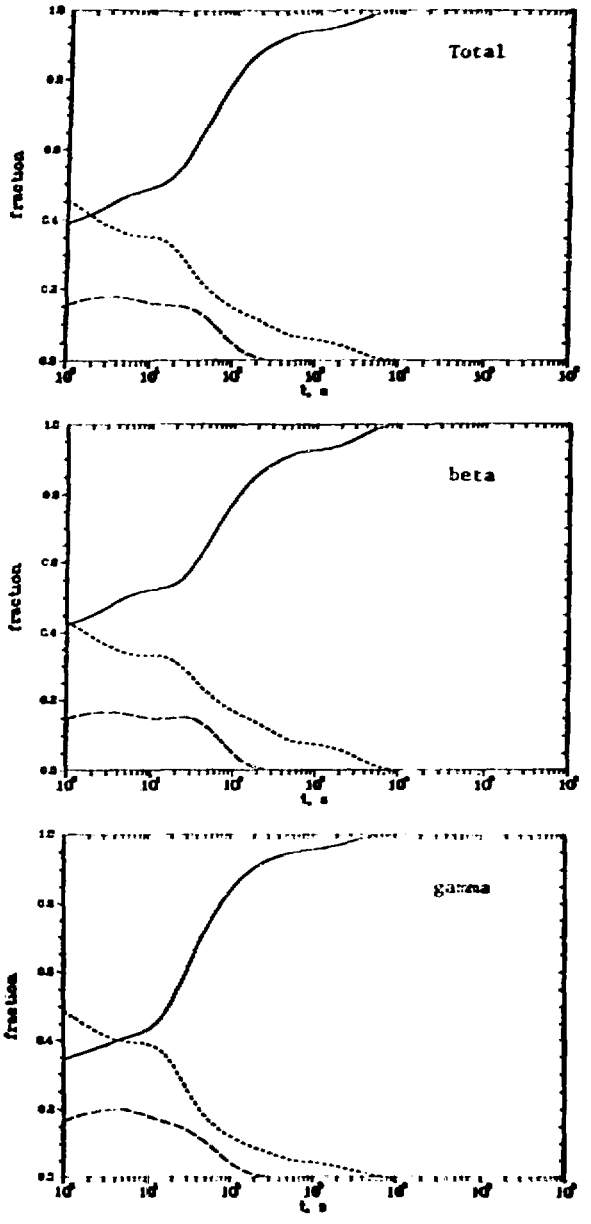

Figure 1. Fractional Contributions to Calculated Decay Heat for a Pulse Fission of ^{235}U (thermal). ——— denotes experimental nuclides by Reich [11]; --- denotes measured strength functions [13]; .... denotes theoretical.

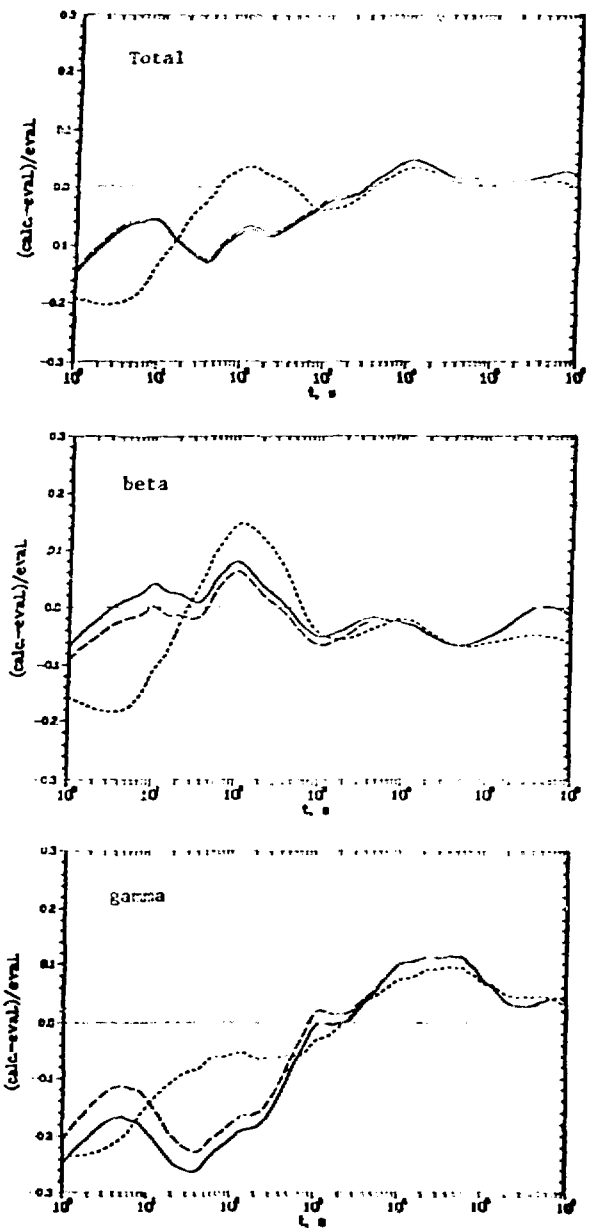

Figure 2. Comparison of Calculated and Evaluated Decay Heat for a Pulse Fission of ^{235}U (thermal). ——— denotes ENDF-V (revised); ---- denotes ENDF-V (prelim); .... denotes ENDF-IV.

Discussion

Lone

What model do you use to calculate gamma energies (spectra) from the decay?

Schmittroth

The decay scheme is governed by the beta-strength function; and then it is assumed that , once the beta decay takes place, all the energy from that level then goes into gamma energy. We are not computing the gamma spectra as such. We are just computing the average decay energy.

Lone

In this case there is no competition between the particle emission and the gamma emission or is the whole solely going into gamma energy?

Schmittroth

We have considered it. There would be some competition from the delayed neutrons, but we have totally ignored that.

Lone

Recently, a lot of work has been done at Chalk River on the unstable nuclei looking at the total lifetimes and also the gamma and neutron emission. The model which fits the gamma spectra fairly reasonably is the same we use for the stable nuclei, which is the Brink-Axel model. The high energy transitions are more pronounced and that consequently gives you more yield in the gamma channel, even when the neutron and other channels are available. So, that may be one other reason that your gamma energy is low.

Schmittroth

It would be worth looking into.

Reeder

This may be more of a comment. The Studsvik group, and Rudstam in particular, have done similar calculations using their own data base. In particular, they calculated the antineutrino spectrum and decay heat. As I recall. their agreement with the experimental values in both cases was somewhat better than what ENDF if giving. Is that still the case?

Schmittroth

I am really not sure. I might say that sometimes these comparisons aren't all that obvious. The comparison we made was with an evaluation that we made. Many of the comparisons you see are with some particular experiment, the Oak Ridge experiment for example. These measurements for short times are a little bit discrepant among themselves.

Rowlands

As I understand it, there is an inconsistency between calculation and measurement for ^{235}U and for ^{239}Pu total decay heat. Do the new data bring more consistency into this situation?

Schmittroth

I don't think so. The only difference between the Pu and U when you make the calculation is in the fission-product yields. Bob Schenter has done some calculations where he has used the ENDF/B-V yields as opposed to the ENDF/B-IV yields. The differences you see in decay-heat calculations are small, like 1%, 2%. They really are a different order of magnitude than the differences we see here.

Dup

STATUS OF AND OUTSTANDING PROBLEMS IN DELAYED NEUTRON DATA, P_n VALUES AND ENERGY SPECTRA*

P. L. Reeder

Pacific Northwest Laboratory
Richland, Washington 99352, U.S.A.

ABSTRACT

This review gives an experimentalist's view of the current status of delayed neutron data for individual precursors. The emphasis is on precursors among the fission products although some new results on precursors outside the fission product region are discussed briefly. Delayed neutron emission probabilities (P_n) reported since the 1979 Vienna Workshop are presented along with world average P_n values and uncertainties. A comparison is made between delayed neutron energy spectra measured by ^{3}He spectrometers at three different laboratories. Comparisons are drawn between spectra measured by ^{3}He spectrometers and spectra measured by proton recoil spectrometers. The uncertainty analyses used by several researchers measuring spectra are presented to illustrate the diversity of approaches presently in use. Average neutron energies obtained from spectra are compared to average energies obtained by an independent ring ratio technique. Discrepancies for spectra with low average energies are noted. From the fission yields and data on individual precursors, one can calculate "group" properties for a specific fissioning system. Comparisons of calculated group properties (i.e. yields, average energies, energy spectra) to experimental group properties are made.

INTRODUCTION

This survey will cover from an experimentalists viewpoint the current status of research on properties of individual delayed neutron precursors. The justification for much of this research

*This paper is based on work sponsored by the Division of Nuclear Sciences of the Department of Energy and performed under DOE Contract No. DE-AC06-76RLO-1830.

is the importance of delayed neutrons in reactor kinetics, so some emphasis will be given to how weighted corbinations of data on individual precursors compare to delayed neutron measurements on unseparated fission products.

Most of the known delayed neutron precursors are among the fission products, but the process is possible for neutron rich nuclides throughout the nuclidic chart. For example, energy spectra for delayed neutrons from ^{11}Li $^{27-31}$Na, and $^{42-51}$K have recently been measured [1,2,3]. Very recently, the process of beta-delayed two neutron emission has been observed in ^{11}Li and ^{30,31,32}Na [1,4]. However, most of this talk will be concerned with precursors in the mass region $79 < A < 142$ which are produced by fission.

For reactor purposes, the data of primary interest are the half-life of the precursor, the neutron emission probability, the energy spectrum of the neutrons, and the fission yield of the precursor. The fission yields are very important when combining data on individual precursors, but it is a separate topic which will not be considered in this talk. If the energy spectrum is known, it is a simple matter to calculate the average energy of the spectrum. The average energy can also be measured directly as will be discussed later.

For nuclear physics purposes there are many other properties of interest such as the beta decay energy (Q_β), the neutron binding energy (B_n), the competition between neutron and gamma emission, and the population of excited states in the final nuclide (i.e., the $\beta n\gamma$ process). Detailed neutron and gamma spectroscopy including n-γ coincidence measurement provide information on the density of excited states and the beta strength function. These nuclear physics topics are currently of great interest to experimentalists and theoreticians, but will be omitted from further discussion here.

For many years, the study of individual precursors was difficult so that reactor physicists developed techniques for lumping the precursors into six groups based on half-life. Experimentally there were measurements of group half-lives and group abundances for several fissioning systems as illustrated by the data of Keepin [5]. Low resolution energy spectra for four of the half-life groups were available from the work of Batchelor and Hyder[6].In recent years, the use of on-line isotope separators has made possible detailed studies on individual precursors. We can now calculate group half-lives, group abundances and group energy spectra for any fissioning system by use of the data for individual precursors and the appropriate fission yields. Furthermore the delayed neutron properties for unseparated fission products under equilibrium conditions can be calculated as a function of fissioning system and excitation energy from individual precursor data and fission yields.

The accuracy of these group and equilibrium calculations depends on the accuracy of the input data, so in the following sections we discuss the experimental problems in obtaining the data on individual precursors.

INDIVIDUAL PRECURSORS

Half-lives

At the 1977 Petten conference, Rudstam compiled average half-lives for 67 precursors [7]. Table I lists these values with slight revisions and additions based on some recent publications [8,9,10]. Half-lives from different laboratories generally are in good agreement except for a few cases near the limits of known nuclides. Half-life measurements have been made by beta, gamma, or neutron counting techniques. Neutron counting gives much simpler decay curves than beta counting so half-lives based on neutron counting are usually preferred. Some typical results from beta and neutron counting are shown in Table II [11].

Emission Probabilities - P_n

Delayed neutron emission probabilities have recently been reviewed by Rudstam for the 1979 consultants' meeting in Vienna [12]. Some 65 precursors including a few isomers were evaluated. Since that meeting, the Studsvik group has published some new Br and I values [10] and slightly revised some of their data [9] included in the 1979 review.

The uncertainties quoted on many of the P_n measurements range from 2 to 10% - yet the values reported often range over much larger factors. Thus there has been a serious problem of systematic uncertainties in measurements from different laboratories. As an example, our own measurements on Br, Rb, I, and Cs precursors published in 1977 [11] were about 25% higher than the world average P_n values. Our technique was to determine the number of precursor atoms in the sample by direct ion counting with an electron multiplier whereas most other measurements determined the number of precursor atoms by beta counting and decay curve analysis. We therefore performed a new set of P_n measurements on Rb and Cs precursors using both the ion counting and beta counting techniques to look for systematic differences. The two techniques gave similar results, but we did find some systematic effects which caused our earlier results to be too high. The 25% discrepancy was a combination of several effects. A 10-15% reduction in ion counting efficiency was discovered due to ions striking the first dynode of the electron multiplier giving no secondary electrons and thus zero pulse height. Another significant correction was due to asymmetry in the emission of neutrons from the ^{252}Cf source which was used to calibrate photoneutron sources used in determining the efficiency

of the neutron counter as a function of energy. The P_n values we now obtain [13,14] agree within the assigned uncertainties (≈10%) with the values measured by the Studsvik group.

In the past, a number of P_n measurements were performed by an indirect method in which the delayed neutron yield was measured and the number of precursor atoms was determined from measured or estimated fission yields. Because of the uncertainties in fission yield values, this indirect method is inferior to the direct methods possible at on-line isotope separator facilities.

Another problem in P_n measurements was insufficient knowledge of the energy dependence of the neutron counter efficiency. We now know that the average energy for a particular delayed neutron energy spectrum can range from 200 to 600 keV. Except for the Studsvik and our own work, experimenters have usually measured the neutron counter efficiency at one energy and have assumed an efficiency which was independent of energy. This could lead to errors of the order of 7% in our own counter for example.

In view of the revisions in our own data and the new publications from Studsvik, I have recalculated some of the world average P_n values and have listed them in Table I. The changes from Rudstam's 1979 list are relatively small, but the uncertainties have been reduced in a number of cases. However, we do have a difference of opinion as to how to estimate the uncertainty on the weighted average P_n values.

In Ref. 12, Rudstam calculated two uncertainties for each set of P_n measurements. One uncertainty was based on the weighting factors and is given in Eq. (1)

$$\sigma_{\bar{x}} = 1/\sqrt{\Sigma W_i} \qquad (1)$$

where $W_i = 1/\sigma_i^2$ and σ_i is the uncertainty assigned to a particular measured value. The other uncertainty was based on the standard deviation of the distribution as given in Eq. (2).

$$S_{\bar{x}} = \left(\frac{\Sigma W_i (x_i - \bar{x})^2}{(n-1)\Sigma W_i} \right)^{1/2} \qquad (2)$$

The adopted error was the larger of $\sigma_{\bar{x}}$ or $S_{\bar{x}}$.

However, because of the concern over the large spread in experimental values outside the uncertainty estimates, Rudstam made an additional correction to the error based on the value of chi-squared per degree of freedom (χ^2_ν). If the square root of χ^2_ν was greater than 1.0, the adopted error was multiplied by $(\chi^2_\nu)^{1/2}$ - otherwise the adopted error was unchanged. In our opinion, the additional correction $(\chi^2_\nu)^{1/2}$ is not needed, so the uncertainties with the P_n values given in Table I are the larger of the two values, $\sigma_{\bar{x}}$ or $S_{\bar{x}}$.

As a final comment on the P_n data, the $^{97,98}Y$, $^{147,148}Ba$, and ^{147}La values listed in Table I are unpublished values from

G. Engler [15] and are rather large compared to predictions based on energy systematics [16,17,18].

Delayed Neutron Spectra

Delayed neutron spectra for individual precursors have been measured at three laboratories by use of ^{3}He ionization chamber spectrometers [19,20,21]. In addition, the spectrum for ^{87}Br has been measured using a proton recoil detector [22]. A mixed spectrum of $^{87,88}Br$ has been measured by the time-of-flight technique [23]. Other time-of-flight measurements have been performed on Rb precursors but have not been published [24]. Other time-of-flight experiments are in progress [25] or are being set up [26]. The most extensive work has been done with ^{3}He spectrometers so the following discussion will focus on the results, problems, and error analysis of the ^{3}He spectrometer technique.

To illustrate the extremes in delayed neutron spectra, we show in Fig. 1 the spectrum for ^{27}Na, measured by Ziegert, et. al. [2], which is a light mass precursor not found among the usual fission products. The spectrum contains one intense peak with possibly some other peaks of much lower intensity. In this light mass nuclide, the density of states in the emitter nuclide, ^{27}Mg, is relatively low and the neutron peak is clearly the result of a transition from a single level. A more typical spectrum is that shown in Fig. 2 for ^{93}Rb, again taken from the Mainz group [19]. This nuclide is an odd Z, even N precursor decaying to an even Z, odd N emitter which gives a final nuclide with even Z, even N. The density of states in the emitter nuclide is quite high but neutron emission goes only to the ground state of the final nuclide. The resulting spectrum appears to have many overlapping peaks but it is not clear whether each peak is due to a single transition from an isolated level. A further example is the spectrum for ^{94}Rb shown in Fig. 3 [19]. In this case the density of states in the emitter nuclide is high and neutron emission goes to many excited states in the even Z, odd N final nuclide. By neutron-gamma coincidence experiments it has been shown that this spectrum is the superposition of complicated spectra to the ground and at least 3 of the excited states in ^{93}Sr [27].

The spectra shown so far have all come from the Mainz group. Their spectra are characterized by good resolution (≈ 12 keV on the thermal neutron peak = 1.6% resolution FWHM) and by good statistical accuracy in comparison with spectra from other laboratories. However in view of the large corrections for detector response, efficiency, etc., it is useful to compare the spectra from other laboratories directly. Spectra for $^{93,94,95}Rb$ and ^{143}Cs are available from the Studsvik group [20] and the SOLAR group [21] as well as the Mainz group. These spectra are compared in Figs. 4-7. The spectra first published by the Studsvik group

were cut off below about 100 keV. The spectra shown here are the result of a revised analysis which extended the spectra down to about 50-75 keV and reduced the relative intensity at energies below 200 keV [28]. One concludes from the comparison plots that the general shape of the spectra are reproduced by all three laboratories and the peak structures are also reproduced. However, the peak intensities show some variations particularly below 200 keV. For example the strong peak at 13.7 keV in the Mainz spectrum for ^{95}Rb has an intensity which is 10% of the intensity between the limits of 100 to 1000 keV. In the SOLAR spectrum, this peak corresponds to 4% of the intensity between 100-1000 keV. The conversion of the raw pulse height spectrum to the neutron emission spectrum is very sensitive to how the conversion process is done - especially at the low energy end of the spectrum. As another example of this problem, the Mainz group analyzed their spectrum for ^{137}I to obtain beta strength functions in a paper published in 1979 [29]. However, a new analysis published in 1980 gave a neutron intensity below 300 keV which was 40% lower than that in the earlier analysis [30].

The measurement of delayed neutron spectra is difficult for many reasons. First of all, the ^{3}He spectrometer has a low efficiency (≈.01%) which means that experiments require long running times (several days). The detector is sensitive to acoustical noise and vibrations so that great care must be taken to achieve good resolution over long time periods. Background corrections are usually quite important. Low counting rates means that the statistical accuracy is significant particularly for the Studsvik and SOLAR data. At low energies the subtraction of the large peak due to thermalized neutrons is important. Neutron scattering is an important problem so the shielding and other material in the vicinity of the source and the detector must be minimized. The calibration of the detector response to monoenergetic neutrons is a complete problem by itself and care must be taken to ensure that the calibration and measurement conditions are identical. A complete response function analysis of the experimental data requires a complicated computer analysis and not all researchers have done this. Corrections must also be made to the data for gamma pile-up pulses which produce high energy tails on the peaks. Finally the detector efficiency as a function of neutron energy must be carefully measured.

If one considers the proton-recoil technique new calibration and analysis problems are involved. A direct comparison of the ^{87}Br delayed neutron spectrum measured by both the ^{3}He spectrometer technique and the proton-recoil technique is shown in Fig.8. Note that the energies of the peaks are reproduced well but the intensities of the peaks are quite different. In the proton-recoil experiment massive lead shielding was used to reduce gamma-ray effects rather than pulse-shape analysis. Part of the discrepancy in intensity might be due to the experimental environment. However, the lower average energy obtained from the spectrum by proton-recoil is supported by an independent measure of the average

energy discussed below.

The analysis of the uncertainties associated with the delayed neutron spectra has only recently been given serious attention. Many of the spectra have been published without error estimates on the final spectra. In our own work [21] (SOLAR) we have estimated the uncertainties for each of the corrections independently and have made no attempt to look for correlation effects. A response function analysis was not used - instead the ratio of valley height to peak area was determined from calibration spectra. Following the procedure of Evans and Krick, [31] we used a subtraction process, beginning at the high energy end of the spectrum, to correct the number of counts in a given channel for the counts due to higher energy neutrons by use of the valley height to peak ratio. The uncertainty on this continuum correction was rather arbitrarily assumed to be 20% of the correction to account for the non-uniformity of the tail region. This uncertainty was a major contributor to the overall uncertainty for the energy region below about 400 kev. Above 400 kev, the major uncertainty was due to the statistical accuracy of the pulse-height data and the background subtraction. The combined uncertainties were equal to the observed data for some of our spectra above 1 MeV. However as shown in Fig. 9 for ^{93}Rb, the uncertainties were of the order of 10-15% at the most intense part of the spectrum (250 keV). The uncertainties that Rudstam assigned to the spectra from Studsvik [28] were about the same as those from SOLAR except that to achieve comparable statistical accuracy, the Studsvik spectra were lumped into larger energy bins as shown in Fig. 10.

The Studsvik group has always analyzed their data by use of response functions. This procedure has now been adopted by the Mainz group and by the Birmingham group.

The general procedure is to fit the experimental pulse height response curves, such as shown in Fig. 11 for monoenergetic neutrons at 961 keV, with an expression with six or more parameters. The expression used by the Birmingham group [32] for example is given in Eq. (3).

$$Y(E)=P(1)\left\{\exp\left(-\tfrac{1}{2}\left(\frac{E-E_n}{P(2)}\right)^2\right)+P(3)\exp\left(-\tfrac{1}{2}\left(\frac{E-(E_n-P(4))}{P(5)}\right)^2\right)+P(6)\omega(E)\right\}$$

where

$Y(E)$ is the magnitude of the pulse height distribution at the energy E

E_n is the energy of the incident neutrons

$\omega(E)$ is the wall effect prediction (taken from Ref. 33)
P(1) is a normalizing factor
P(2) - P(6) are the parameters obtained by a least square fit

The parameters P(2) - P(6) as a function of incident neutron energy are fit by polynomial expressions of up to fourth order. The spectrometer response to neutrons of any given energy can then be obtained by interpolating values of the parameters P(2) - P(6) from the polynomial expressions and calculating the response from Eq. (3).

Various procedures have been employed for unfolding the neutron spectrum from the pulse-height spectrum. The iterative procedure used by the Birmingham group is as follows.

The measured pulse-height distribution A(I) is related to the true neutron spectrum C(J) by the response function matrix R(I,J) where R(I,J) is the probability that a neutron in the Jth channel will give a pulse in the Ith channel.

$$A(I) = \sum_J R(I,J)C(J) \qquad (4)$$

The response matrix is normalized to the efficiency of detecting a neutron of energy J, i.e. EFF(J)

$$\sum_I R(I,J) = EFF(J) \qquad (5)$$

R(I,J) can then be replaced by Z(I,J) EFF(J) where Z(I,J) is the response matrix normalized to unity. Eq. (4) then becomes

$$A(I) = \sum_J Z(I,J)EFF(J)C(J) \qquad (6)$$

The iteration process begins with an approximation to C(J) designated as $C_0(J)$ determined by dividing the measured pulse height spectrum A(I) by the efficiency EFF(J). Eq. (6) is then used to calculate an approximate pulse-height spectrum designated as $A_0(I)$. An improved estimate to C(J) is then obtained from the following expression:

$$C_1(J) = C_0(J) + \frac{A(I) - A_0(I)}{EFF(J)} \qquad (7)$$

The process of calculating $A_k(I)$ is repeated until suitable agreement is obtained with A(I) as determined by a chi-squared test.

Because the unfolded spectrum is obtained from the matrix relationship of Eq. (4) a complete error analysis should take into account both the uncertainties in the pulse height data A(I) and the response matrix R(I,J). All the covariance information should also be included. This is currently being attempted by the Birmingham group.

Rudstam orignally used an iterative procedure, but recently has gone to a modified deconvolution scheme [34]. The uncertainties in the response function parameters are treated as systematic uncertainties and are combined quadratically with the uncertainties in the counting statistics. The response function uncertain-

ties are obtained by variation of a parameter by 20% and determining the effect on the resulting spectrum.

The Mainz group has been able to obtain a large number of delayed neutron spectra with good counting statistics. With 12 keV resolution on the thermal peak, the spectrum analysis has been done down to about 10 keV. With such good energy resolution, much of the effort at Mainz has gone into detailed analysis of the peak structure with the emphasis on the nuclear physics information to be obtained. Peak fitting routines such as SAMPO and NEUTRN have been used to obtain centroids and peak areas. With high resolution detectors, the fraction of pulses in the tail region was thought to be small (≈10%). However, when the complete response function correction was applied to the ^{137}I spectrum, the intensity below 300 keV was reduced 40% as mentioned above. It is not clear whether similar changes are necessary in other spectra from the Mainz group.

To summarize the present status of delayed neutron spectra, measurements have been performed on 32 different precursors. The quality of the spectra in terms of statistical accuracy and resolution varies greatly depending on the technique and the laboratory doing the work. There are substantial uncertainties in the intensities of the spectra below 200 keV although overall shapes and peak structures have been reproduced at different laboratories. There is a need for measurements done by techniques other than the ^{3}He spectrometer, such as time-of-flight and proton recoil. It is particularly desirable to develop new detectors with higher efficiency and better resolution.

Average Energies

If the energy spectrum from a given precursor is known, the average energy can easily be calculated. Estimating the uncertainty on that average energy is more difficult because of possible systematic uncertainties in the spectrum unfolding procedures.

We have therefore developed an experimental procedure to measure the average energies directly [35, 13]. The technique is based on the ratio of counts in rings of counter tubes embedded in different thicknesses of polyethylene moderator. The technique can be applied to precursors with very low neutron emission probabilities or to precursors with low fission yield because of the high efficiency of the neutron counter. Average energies measured by this technique can be compared to average energies calculated from the spectra to check the data analysis procedures used to obtain the spectra. In Fig. 12 is shown a comparison of average energies obtained by the ring ratio technique to average energies calculated from the spectra obtained by the Mainz group [19]. Above 350 keV, there is reasonable agreement. However, below 350 keV the ring ratio technique gives lower average energies than those calculated from the spectra. One advantage of the ring ratio technique is that it has no cutoffs at high or low energies. Both techniques are sensitive to the background

subtraction used. In fact, the average energy for the ^{97}Rb spectrum measured at the OSTIS facility at low counting rates was 754 keV [36]. The same spectrum measured at ISOLDE at higher counting rates had an average energy of 533 keV [19]. The cause of this discrepancy is not known which suggests that the experimental environment may have unknown effects on the observed spectrum.

Aside from checking the validity of spectrum measurements, the average energy might be used as a simple parameter to approximate the delayed neutron spectrum. The prompt neutron spectrum from fission has often been described by a Maxwellian distribution with the general form

$$N(E) = A\sqrt{E}\exp(-E/T) \qquad (8)$$

where A is a normalization constant and T is a parameter related to the average energy by the expression.

$$\bar{E} = \frac{3}{2}T \qquad (9)$$

We are currently calculating delayed neutron spectra from Eq. (8) using $\bar{E}$ values for particular precursors and comparing them with the actual spectra. Such a comparison is shown in Fig. 13 for ^{94}Rb. A one parameter formula obviously cannot reproduce the peak structure seen in many delayed neutron spectra. However, it might be a suitable approximation for reactor kinetics calculation.

GROUP DATA

Half-life and Abundance Data

As more information becomes available on the individual precursors, there is less justification for lumping the precursors into six half-life groups. In agreement with Rudstam's comments in 1977, [7] the six group classification should be abandoned whenever possible.

From the experimental viewpoint, there is little change in the group half-life and abundance data since the review articles by Amiel in 1973,[37] Tuttle in 1975,[38] and Rudstam in 1977 [7]. The calculations of group parameters from P_n data and fission yields for individual precursors has been done by many authors with the most recent calculation for ^{235}U published by Alexander and Peng [39]. The total delayed neutron yield was in excellent agreement with the experimental value from Keepin. However, the three longer lived groups had lower calculated yields than the experimental yields and the three shorter-lived groups had higher calculated yields than the experimental values by roughly 10% each way. The authors suggested that the P_n values might be at fault. An alternative explanation might be that the fission yields of the short-lived precursors are too high relative to the fission

yields of the long-lived precursors.

Group Average Energies and Spectra

Experimental delayed neutron spectra separated into half-life groups are available from the work of Batchelor [6] and from Fieg [40]. The delayed neutron spectra in the current ENDF/B-V file can be weighted by the appropriate fission yields and summed to calculate group spectra and average energies for the groups. An alternative procedure is to take the average energies for individual precursors measured by the ring ratio technique, weight them by the fission yields, and calculate group average energies. The results of such a calculation are shown in Table III and compared with the experimental values. Note that none of the experimental spectra extended below 100 keV.

EQUILIBRIUM DATA

Total Delayed Neutron Yield

The dependence of the total delayed neutron yield ($\bar{\nu}_d$) as a function of fissioning system and excitation energy was covered in the review articles by Tuttle [30,41]. Recent calculations of $\bar{\nu}_d$ using the ENDF/B-V fission yields have been reported by England, et al. [42]. They report that 15 out of 20 calculated $\bar{\nu}_d$ values agree within the uncertainties with evaluated measurements.

Equilibrium Spectra

Experimental spectra of delayed neutrons from unseparated fission products have been measured by Fieg [40], Sloan and Woodruff [43], Eccleston and Woodruff [44], and Grant and Woodruff [45] by means of proton-recoil detectors. Similar experiments have been done by Evans and Krick [31] and Weaver et al. [46] by use of the ^{3}He spectrometers. The spectra measured by Woodruff and co-workers have more intensity at energies below 200 keV than the spectra reported by others. This discrepancy is still unexplained.

In the same manner as for the group spectra, it is possible to use fission yield data and spectra for individual precursors to calculate the equilibrium spectrum for any fissioning system. This has been done by England [47] using the ENDF/B-V yields and a set of 24 spectra supplied by Rudstam. Comparisons of the calculated spectrum and the measured spectrum for fast fission of ^{235}U are shown in Figs. 14 and 15. An interesting conclusion from the current calculations is that the shape of the spectrum is the same for thermal, fast, and 14 MeV neutron induced fission in spite of large changes in the fission yields and total delayed neutron yields.

BETA-DELAYED TWO NEUTRON EMISSION

For nuclides which are extremely neutron-rich, it may be energetically possible for beta decay to go to excited states which are above the binding energy for a pair of neutrons. For example, the beta decay energy for ^{11}Li is 20.7 MeV, the binding energy for a single neutron in the daughter nuclide ^{11}Be is 0.503 MeV, and the binding energy for two neutrons is 7.315 MeV. A recent publication from the ISOLDE group [1] gives the P_n value for single neutron emission as 43 ± 9% and the P_{2n} value for two neutron emission as 9 ± 3%. Additional examples of 2n emission have recently been discovered at ISOLDE [4]. The measured P_{2n} values for $^{30-32}$Na are 1.2, 0.7, and 5.7 respectively.

From energy systematics, one can calculate the beta decay energies (Q_β) and two neutron binding energies (B_{2n}) for precursors in the fission product region [48]. The predicted two neutron precursors all have very low fission yields and consequently would have little influence in reactor physics. However, predicted two neutron precursors such as ^{84}Ga, ^{92}Br, ^{98}Rb, ^{142}I, and ^{148}Cs are all accessible by present on-line isotope separator techniques. The beta-delayed two neutron emission is interesting to nuclear physicists because of the possibility of studying n-n correlation effects.

CONCLUSIONS

There have been great improvements in the last ten years in the quantity and quality of data on individual delayed neutron precursors as evidenced by the data given in Table I. Discrepancies and uncertainties in P_n values have been reduced for the major precursors of concern to reactor physics to the point where uncertainties of 5 - 10% can be assigned. Delayed neutron spectra of individual precursors are available. However, data analysis procedures have not become standardized. Particularly at energies below 200 keV, there are notable discrepancies between spectra measured by the same technique at different laboratories and between spectra measured by different techniques.

REFERENCES

1. R. E. Azuma, L. C. Carraz, P. G. Hansen, B. Jonson, K.-L. Kratz, S. Mattsson, G. Nyman, H. Ohm, H. L. Ravn, A. Schröder, and W. Ziegert, Phys. Rev. Lett. 43, 1652 (1979).
2. W. Ziegert, A. Schröder, H. Ohm, K.-L. Kratz, G. Nyman and the ISOLDE Collaboration, Institut für Kernchemie der Universität Mainz - Jahresbericht 1978, p. 20.
3. W. Ziegert, H. Ohm, A. Schröder, K.-L. Kratz, G. Nyman, L. C. Carraz, P. G. Hansen, B. Jonson, H. L. Ravn, and the ISOLDE Collaboration Institut für Kernchemie der Universität Mainz - Jahresbericht 1978, p. 23.
4. H. Ravn, ISOLDE-CERN, private communication, March 1980.
5. G. R. Keepin, Physics of Nuclear Kinetics, Addison - Wesley Publishing Co., Reading, Massachusetts (1956).
6. R. Batchelor and H. R. McK.Hyder, J. Nucl. Energy 3, 7 (1956).
7. G. Rudstam, Proceedings of the Second Advisory Group Meeting on Fission Product Nuclear Data, Petten 5 - 9 Sept. 1977, IAEA-213 (IAEA, Vienna, 1978) p. 567.
8. P. Peuser, H. Otto, M. Weis, G. Nyman, E. Roeckl, J. Bonn, L. von Reisky, and C. Spath, Z. Physik A289, 219 (1979).
9. E. Lund, P. Hoff, K. Aleklett, O. Glomset, and G. Rudstam, Z. Physik A294, 233 (1980).
10. K. Aleklett, P. Hoff, E. Lund, and G. Rudstam, Z. Physik A295,331 (1980).
11. P. L. Reeder, J. F. Wright, and L. J. Alquist, Phys. Rev. C 15, 2108 (1977).
12. G. Rudstam, Proceedings of the Consultants' Meeting on Delayed Neutron Properties, Vienna, 26-30 March, 1979. INDC (NDS) - 107/G + Special (IAEA, Vienna, 1979) p. 69.

13. P. L. Reeder and R. A. Warner, Pacific Northwest Laboratory Report - PNL-SA-7536-Rev., July 1980.
(submitted to Nucl. Instrum. Methods)

14. P. L. Reeder and R. A. Warner, Pacific Northwest Laboratory Report - PNL-SA-8766, July 1980.
(To be submitted to Phys. Rev. C)

15. G. Engler, Soreq, private communication to G. Rudstam, March 1979.

16. W. Rudolph and K.-L. Kratz, Z. Physik A281, 269 (1977).

17. K.-L. Kratz and G. Herrmann, Z. Physik 263, 435 (1973).

18. Y. Nir-El and S. Amiel, Proceedings from the Cargèse 3rd International Conference on Nuclei far from Stability, Cargèse 19-26 May 1976, CERN Report 76-13 (1976) p. 322.

19. K.-L. Kratz, Proceedings of the Consultants' Meeting on Delayed Neutron Properties, Vienna, 26-30 March, 1979.
INDC(NDS) - 107/G + Special (IAEA, Vienna, 1979) p. 103.

20. S. Shalev and G. Rudstam, Phys. Rev. Lett. 28, 687 (1972).
S. Shalev and G. Rudstam, Nucl. Phys. A230, 153 (1974)
G. Rudstam and S. Shalev, Nucl. Phys. A235, 397 (1974)
S. Shalev and G. Rudstam, Nucl. Phys. A275, 76 (1977).
G. Rudstam, J. Radioanal. Chem. 36, 591 (1977).

21. P. L. Reeder, L. J. Alquist, R. L. Kiefer, F. H. Ruddy, and R. A. Warner, Nucl. Sci. Eng. 75, 140 (1980).

22. P. K. Ray and E. S. Kenney, Nucl. Instrum. Methods 134, 559 (1976).

23. N. G. Chrysochoides, J. N. Anoussis, C. A. Mitsonias, and D. C. Perricos, J. Nucl. Energy 25, 551 (1971).

24. G. I. Crawford, U. of Glasgow, private communication to K.-L. Kratz, see Ref. 19.

25. M. Shaanau, IKP, KFA Jülich, private communication, 1980.

26. D. Clark, Cornell U., private communication, 1980.

27. A. Schröder, H. Ohm, W. Rudolph, K. Sümmerer, K.-L. Kratz, K. D. Wünsch, G. Jung, J. Crancon, and C. Ristori, Phys. Lett. 90 B, 57 (1980).

28. G. Rudstam, Studsvik, private communication, Aug. 1979.

29. K.-L. Kratz, W. Rudolph, H. Ohm, H. Franz, M. Zendel, G. Herrmann, S. G. Prussin, F. M. Nuh, A. A. Shihab-Eldin, D. R. Slaughter, W. Halverson, H. V. Klapdor, Nucl. Phys. A317, 335 (1979).

30. H. Ohm, M. Zendel, S. G. Prussin, W. Rudolph, A. Schröder, K.-L. Kratz, C. Ristori, J. A. Pinston, E. Monnand, F. Schussler, and J. P. Zirnheld, Z. Physik A296, 23 (1980).

31. A. E. Evans and M. S. Krick, Nucl. Sci. and Eng. 62, 652 (1977).

32. D. Weaver, U. of Birmingham, private communication, Aug. 1980.

33. R.Batchelor, R.Aves and T.H.R.Skyrme, Rev.Sci.Instrum.26,1037 (1955)

34. G. Rudstam, The Uncertainty of Neutron Energy Spectra Deduced from Measured Pulse Spectra in a ^{3}He Spectrometer, Studsvik Science Research Laboratory Report, 1980.

35. P. L. Reeder, J. F. Wright, and L. J. Alquist, Phys. Rev. C 15, 2098 (1977).

36. K.-L. Kratz, Contributed paper to RP 13 of the 2nd Advisory Group Meeting on Fission Product Nuclear Data, Petten 5-9 Sept. 1977, IAEA-213 (IAEA, Vienna, 1978).

37. S. Amiel, Proceedings of a Panel on Fission Product Nuclear Data, Bologna, 26-30 Nov. 1973, CONF-731133 Vol. 2, p. 33 International Atomic Energy Agency (1973).

38. R. J. Tuttle, Nucl. Sci. Eng. 56, 37 (1975).

39. D. R. Alexander and Y. K. Peng, Nucl. Sci. Eng. 70, 184 (1979).

40. G. Fieg, J. Nucl. Energy 26, 585 (1972).

41. R. J. Tuttle, Proceedings of the Consultants' Meeting on Delayed Neutron Properties, Vienna, 26-30 March, 1979. INDC(NDS) - 107/G + Special (IAEA, Vienna, 1979) p. 29.

42. T. R. England, R. E. Schenter, and F. Schmittroth, International Conference on Nuclear Cross Sections for Technology, Knoxville, Oct. 22-26, 1979, Los Alamos Scientific Lab., Report LA-UR 79-2890.

43. W. R. Sloan and G. L. Woodruff, Nucl. Sci. Eng. 55, 28 (1974).

44. G. W. Eccleston and G. L. Woodruff, Nucl. Sci. Eng. 62, 636 (1977).

45. P. J. Grant and G. L. Woodruff, submitted to Nucl. Sci. Eng. Oct. 1979.

46. D. R. Weaver, J. G. Owen, and J. Walker, Proceedings of the Consultants' Meeting on Delayed Neutron Properties, Vienna 26-30 March 1979. INDC(NDS) - 107/G + Special (IAEA, Vienna, 1979) p. 207.

47. T. England, Los Alamos, private communication, Aug. 1980.

48. P. Haustein, Brookhaven, private communication, April, 1980.

TABLE I. Delayed neutron precursors, half-lives, emission probabilities and mean energies.

Precursor	Half-life (sec)	P_n (%)	$\bar{E}$ (keV)
79 Ga	3.00 ± .09	.098± .010	360±70
80 Ga	1.66 ± .02	.84 ± .06	370±70
81 Ga	1.23 ± .01	12.0 ± .9	370±70
82 Ga	.60 ± .01	21.4 ± 2.2	
83 Ga	.31 ± .01	43.0 ± 7.0	
83 Ge	1.9 ± 0.4		
84 Ge	1.2 ± 0.3		
84 As	5.6 ± .3	.061± .026	
85 As	2.03 ± .01	53. ±18.	730±150
86 As	0.9 ± 0.2	12. ± 3.	
87 As	.73 ± .06	44. ±14.	
87 Se	5.60 ± .16	.19 ± .03	
88 Se	1.52 ± .06	.6 ± .3	
89 Se	.41 ± .04	5.0 ± 1.5	
91 Se	.27 ± .08	21. ± 8.	
87 Br	55.6 ± .1	2.48 ± .11	180±40
88 Br	16.0 ± .2	6.55 ± .28	220±30
89 Br	4.38 ± .03	13.0 ± .8	460±20
90 Br	1.92 ± .02	22.5 ± 1.4	500±100
91 Br	.542± .008	15.6 ± 2.6	880±180
92 Br	.362± .012	22. ± 6.	
92 Kr	1.85 ± .01	.033± .003	
93 Kr	1.29 ± .01	1.96 ± .14	340±70
94 Kr	.208± .009	5.7 ± 2.2	
92 Rb	4.50 ± .02	.0108± .0007	160±40
93 Rb	5.85 ± .04	1.31 ± .06	390±20
94 Rb	2.76 ± .02	9.92 ± .28	410±30
95 Rb	.384± .005	8.45 ± .25	450±30
96 Rb	.197± .003	13.3 ± .5	460±20
97 Rb	.170± .002	25.1 ±1.3	540±30
98 Rb	.116± .005	15.1 ±1.2	480±100
99 Rb	.066± .008	14. ±3.	
100 Rb	.051± .017		
97 Sr	.43 ± .03	.27 ± .09	
98 Sr	.80 ± .10	.36 ± .11	
99 Sr	.6 ± .2	3.4 ±2.4	
97m Y	1.13 ± .04	.06 ± .02	
98 Y	.60 ± .05	3.44 ± .95	
99 Y	1.4 ± .2	1.2 ± .8	

TABLE I. Delayed neutron precursors, half-lives, emission probabilities and mean energies. (Continued)

Precursor	Half-life (sec)	P_n (%)	$\bar{E}$ (keV)
123 Ag	.39 ±.03		
127 In	3.76 ±.03	.68 ± .06	
127m In	1.12 ±.02	.04 ± .04	
128 In	.84 ±.06	.059± .008	
129 In	1.26 ±.02	2.5 ± .5	550±110
129m In	.59 ±.02	.25 ± .05	
130 In	.58 ±.01	1.40 ± .09	510±100
131 In	.28 ±.01	1.72 ± .23	
132 In	.155±.04	4.2 ± .9	
133 Sn	1.47 ±.03		
134 Sn	1.04 ±.02	17. ±7.	530±110
134 Sb	10.4 ±.1	.112± .009	
135 Sb	1.71 ±.02	15.5 ±1.4	860±180
136 Sb	.82 ±.02	23. ±8.	
136 Te	17.5 ±.2	.9 ± .4	300± 20
137 Te	2.8 ±.7	2.5 ± .5	
138 Te	1.4 ±.4	6.3 ±2.1	
137 I	24.5 ±.1	6.49 ± .31	550± 30
138 I	6.53 ±.08	5.32 ± .36	420± 40
139 I	2.31 ±.03	9.3 ± .4	410± 80
140 I	.60 ±.01	8.8 ±1.1	400± 80
141 I	.44 ±.01	26. ±3.	270± 50
141 Xe	1.73 ±.01	.044± .005	
142 Xe	1.24 ±.03	.42 ± .03	
143 Xe	.30 ±.03		
141 Cs	24.9 ±.2	.037± .007	190± 30
142 Cs	1.71 ±.01	.093± .006	210± 40
143 Cs	1.78 ±.01	1.61 ± .08	270± 30
144 Cs	1.002±.005	3.06 ± .25	270± 40
145 Cs	.585±.008	13.6 ±1.0	320± 20
146 Cs	.335±.007	13.3 ± .6	400± 20
147 Cs	.21 ±.03	25.4 ±3.2	510±100
147 Ba	2.23 ±.20	5.21 ± .50	
148 Ba	.50 ±.05	23.9 ±2.1	
147 La	10.0 ±1.0	.50 ± .17	

TABLE II. Half-lives (sec) of Rb and Cs precursors[a]

Mass	Beta Counting	Neutron Counting
92	4.54 ±.02	
93	6.12 ±.08	5.82 ±.03
94	2.83 ±.03	2.73 ±.01
95	.377 ±.004	.369 ±.005
96	.205 ±.004	.197 ±.002
97	.182 ±.007	.167 ±.002
142	1.70 ±.02	1.70 ±.09
143	1.79 ±.02	1.79 ±.04
144	1.00 ±.04	.99 ±.02
145	.65 ±.03	.577 ±.006
146		.28 ±.03

[a] Ref. 11

TABLE III. Comparisons of calculated group $\bar{E}$ and experimental group $\bar{E}$ for various fissioning systems.[a]

Group	Fraction [b]	Calc. $\bar{E}$ [c]	Fieg $\bar{E}$ [d]	Batchelor $\bar{E}$ [e]
		^{235}U + Thermal Neutrons		
1	1.00 ± .00	.18 ± .04	.28 ± .03	.25 ± .02
2	1.00 ± .00	.42 ± .04	.48 ± .05	.46 ± .01
3	.98 ± .01	.44 ± .02	.45 ± .05	.41 ± .02
4	.92 ± .04	.49 ± .05	.43 ± .04	.45 ± .02
5	.56 ± .09	.53 ± .08		
6	.81 ± .12	.47 ± .02		
Total	.88 ± .02	.46 ± .02	.43 ± .04	
		^{235}U + 14 MeV Neutrons		
1	1.00 ± .00	.18 ± .04	.29 ± .03	
2	1.00 ± .00	.34 ± .03	.46 ± .05	
3	.97 ± .01	.44 ± .02	.43 ± .04	
4	.95 ± .03	.49 ± .05	.48 ± .05	
5	.53 ± .10	.52 ± .07		
6	.89 ± .08	.45 ± .02		
Total	.92 ± .02	.44 ± .02	.45 ± .05	
		^{238}U + 14 MeV Neutrons		
1	1.00 ± .00	.18 ± .04	.28 ± .03	
2	1.00 ± .00	.44 ± .05	.47 ± .05	
3	.96 ± .02	.44 ± .02	.44 ± .04	
4	.91 ± .04	.52 ± .06	.43 ± .04	
5	.62 ± .09	.50 ± .06	.38 ± .04	
6	.89 ± .07	.44 ± .03		
Total	.87 ± .03	.48 ± .03	.45 ± .04	

TABLE III. Comparisons of calculated group $\bar{E}$ and experimental group $\bar{E}$ for various fissioning systems.[a] (Continued)

Group	Fraction [b]	Calc. $\bar{E}$ [c]	Fieg $\bar{E}$ [d]	Batchelor $\bar{E}$ [e]
		^{239}Pu + 14 MeV Neutrons		
1	1.00 ± .00	.18 ± .04	.30 ± .03	
2	1.00 ± .00	.35 ± .03	.48 ± .05	
3	.96 ± .01	.44 ± .02	.41 ± .04	
4	.92 ± .07	.50 ± .07	.43 ± .04	
5	.33 ± .15	.48 ± .05		
6	.92 ± .05	.46 ± .02		
Total	.86 ± .05	.42 ± .03	.43 ± .04	

[a] All energies in MeV

[b] Fraction = fraction of delayed neutron group yield for which average energy data are available

[c] This work. Fission yields from B. Rider, NEDO-12154-2E

[d] Ref. 40

[e] Ref. 6

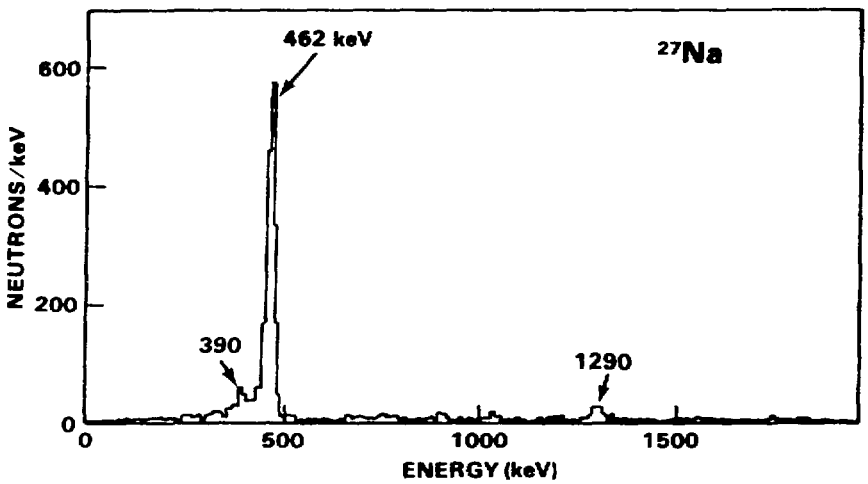

Fig. 1. Delayed neutron spectrum of ^{27}Na.
Data from Mainz, Ref. 2

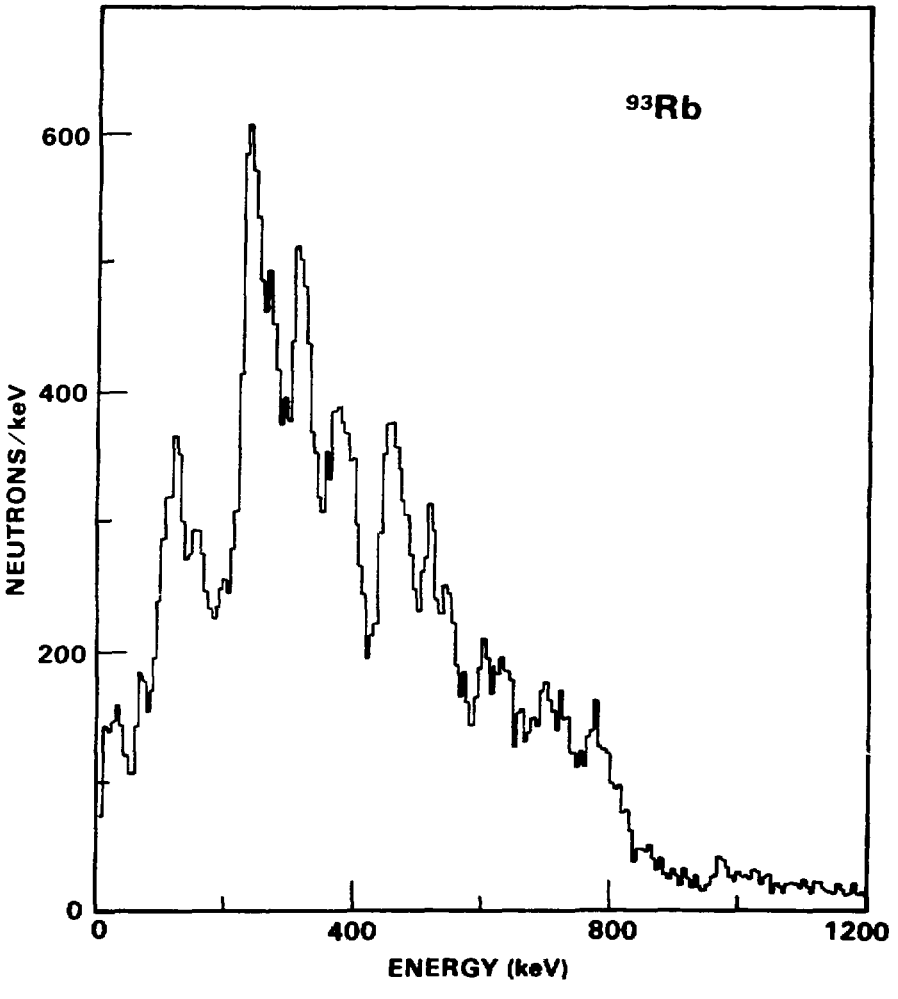

Fig. 2. Delayed neutron spectrum of ^{93}Rb.
Data from Mainz, Ref. 19

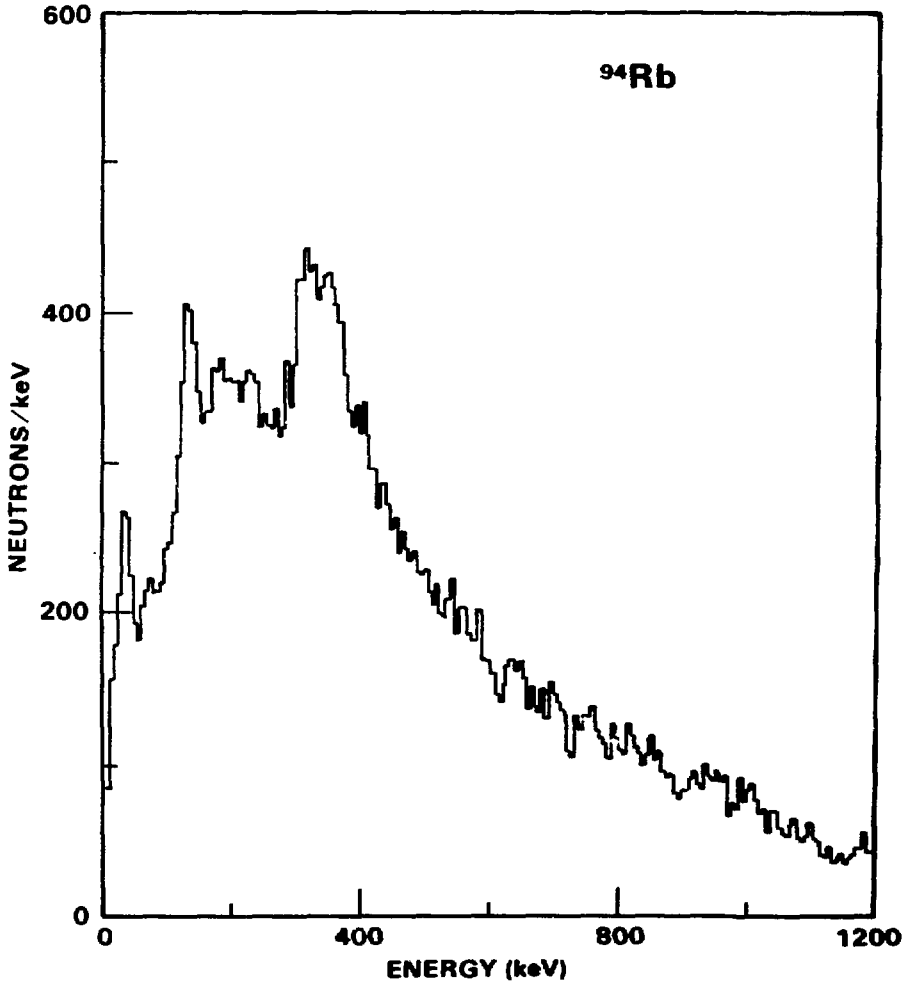

Fig. 3. Delayed neutron spectrum of ^{94}Rb.
Data from Mainz, Ref. 19

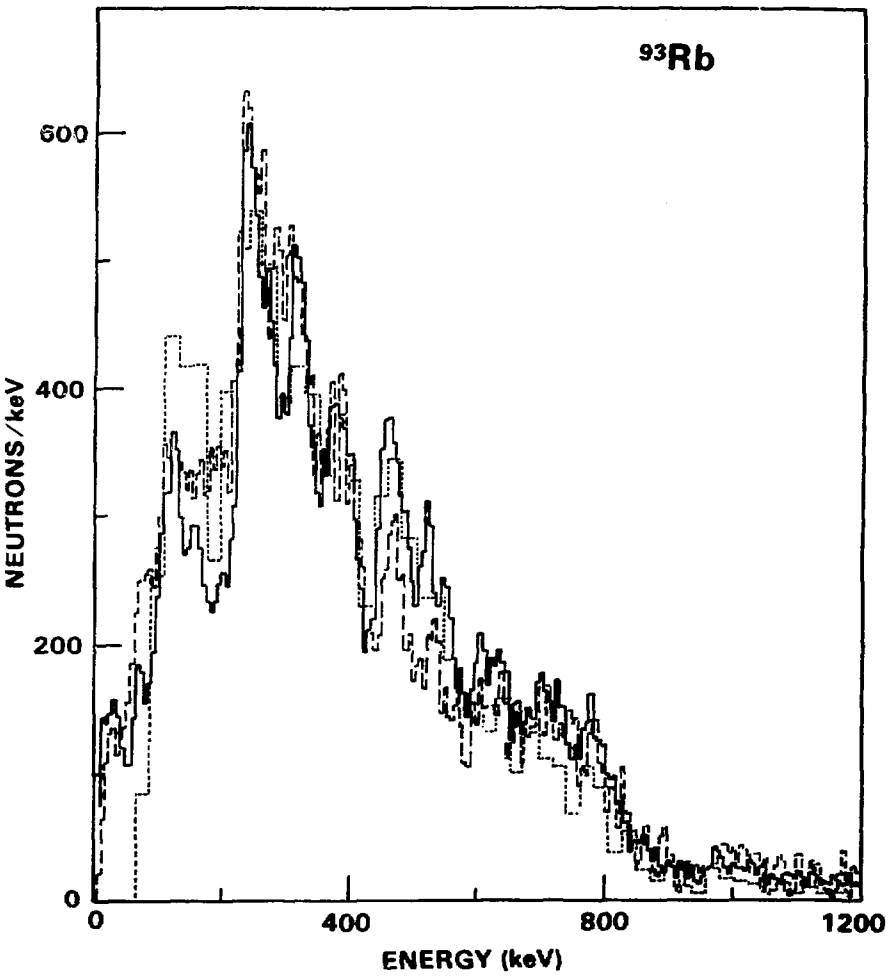

Fig. 4. Delayed neutron spectrum of ^{93}Rb.
Solid curve = data from Mainz, Ref. 19
Dashed curve = data from PNL, Ref. 21
Dotted curve = data from Studsvik, Ref. 28

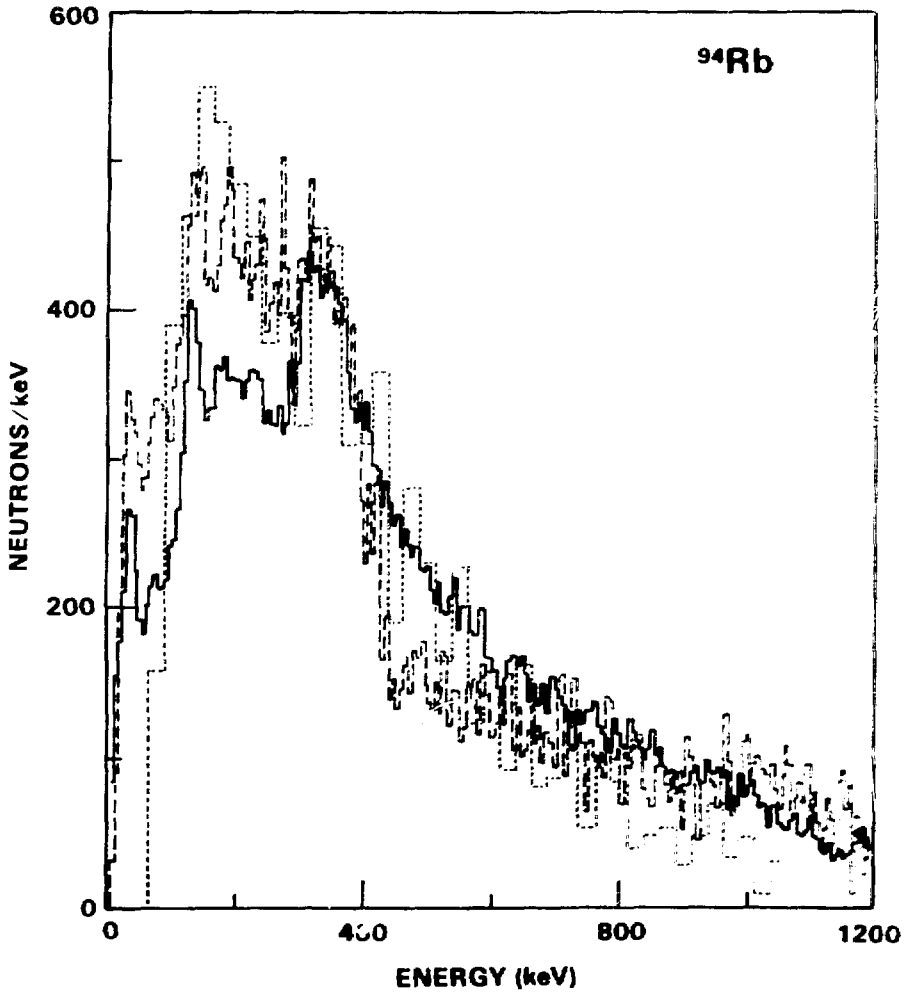

Fig. 5. Delayed neutron spectrum of ^{94}Rb.
Solid curve = data from Mainz, Ref.19
Dashed curve = data from PNL, Ref. 21
Dotted curve = data from Studsvik, Ref. 28

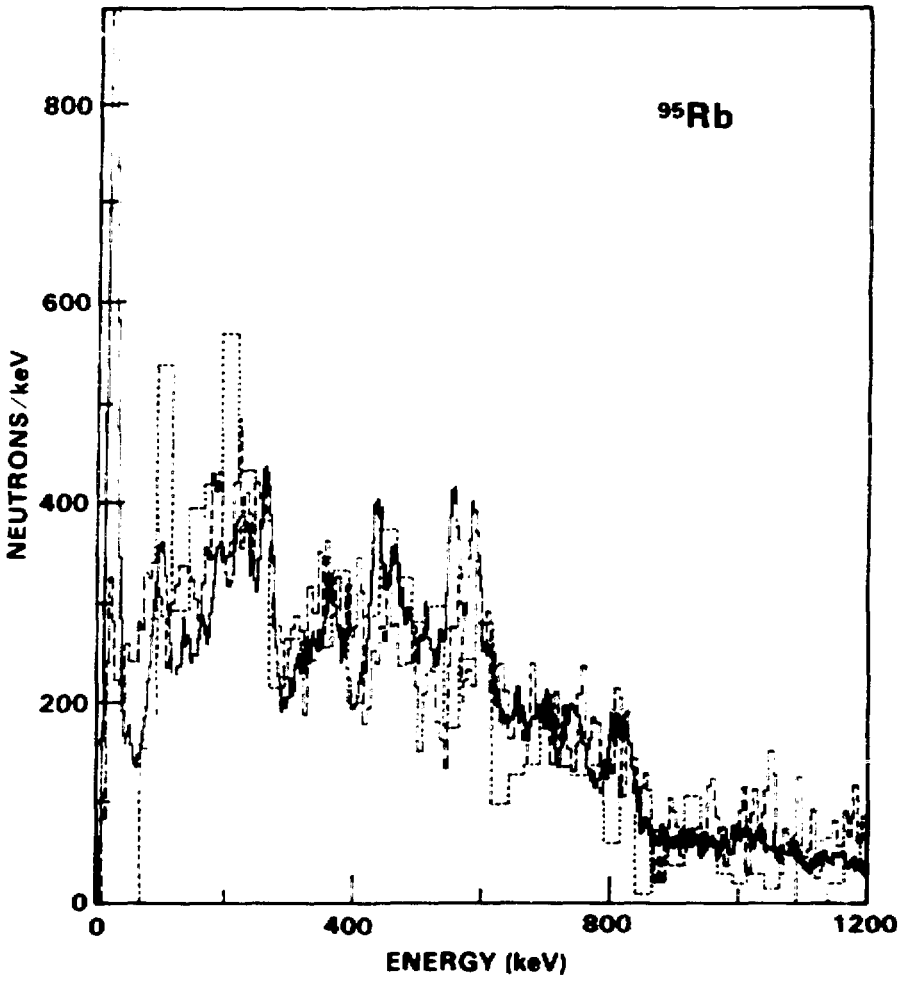

Fig. 6. Delayed neutron spectrum of ^{95}Rb.
Solid curve = data from Mainz, Ref. 19
Dashed curve = data from PNL, Ref. 21
Dotted curve = data from Studsvik, Ref. 28

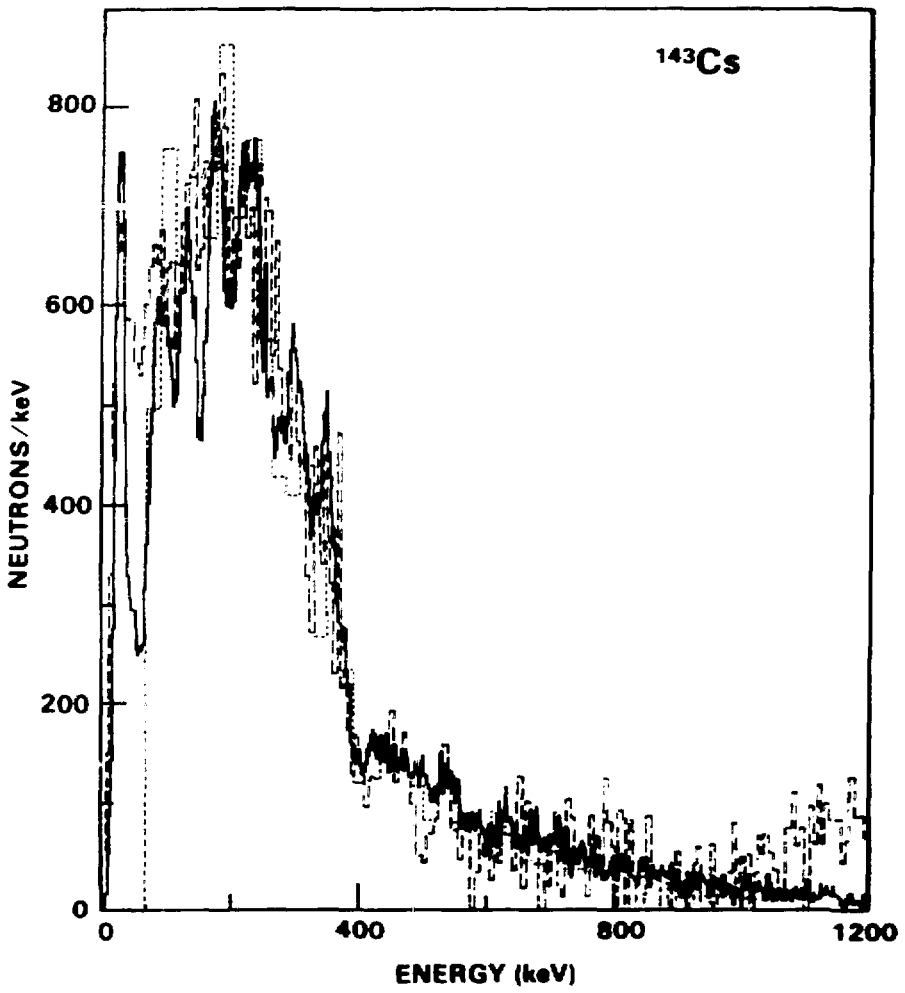

Fig. 7. Delayed neutron spectrum of ^{143}Cs.
Solid curve = data from Mainz, Ref. 19
Dashed curve = data from PNL, Ref. 21
Dotted curve = data from Studsvik, Ref. 28

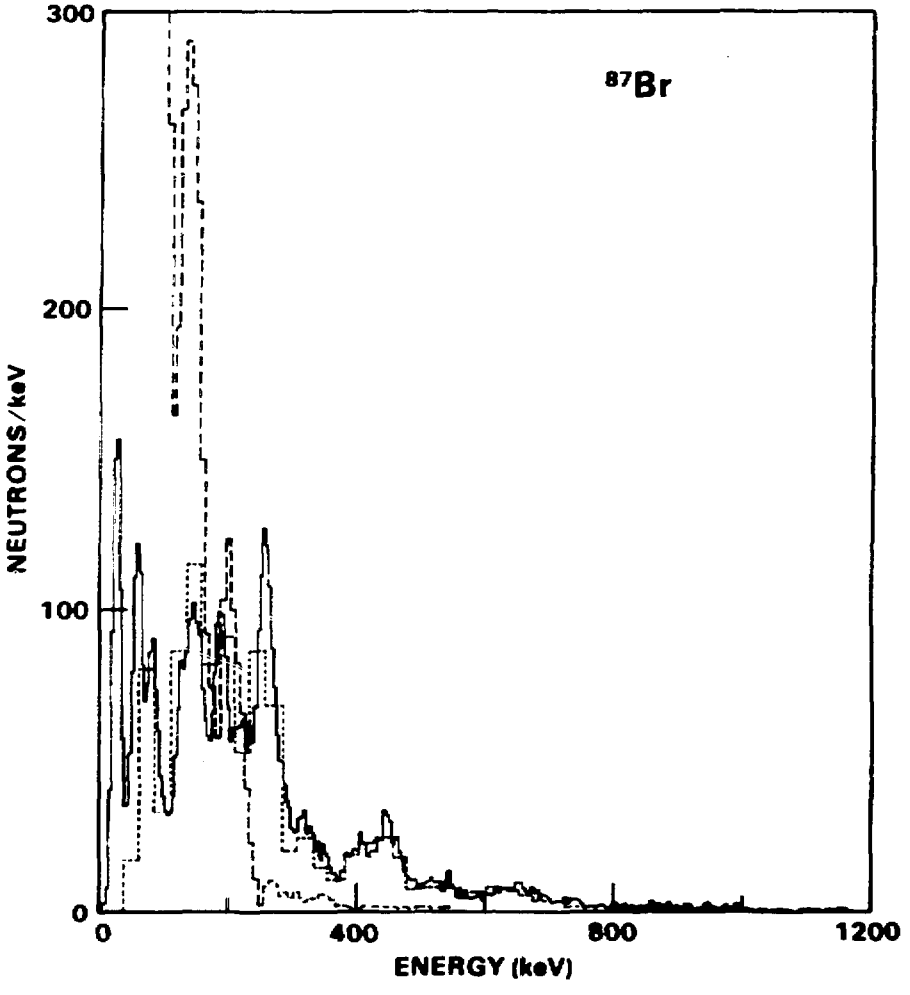

Fig. 8. Delayed neutron spectrum of ^{87}Br.
Solid curve = data from Mainz, Ref. 19
Dashed curve = data from Penn State, Ref. 22
Dotted curve = data from Studsvik, Ref. 28

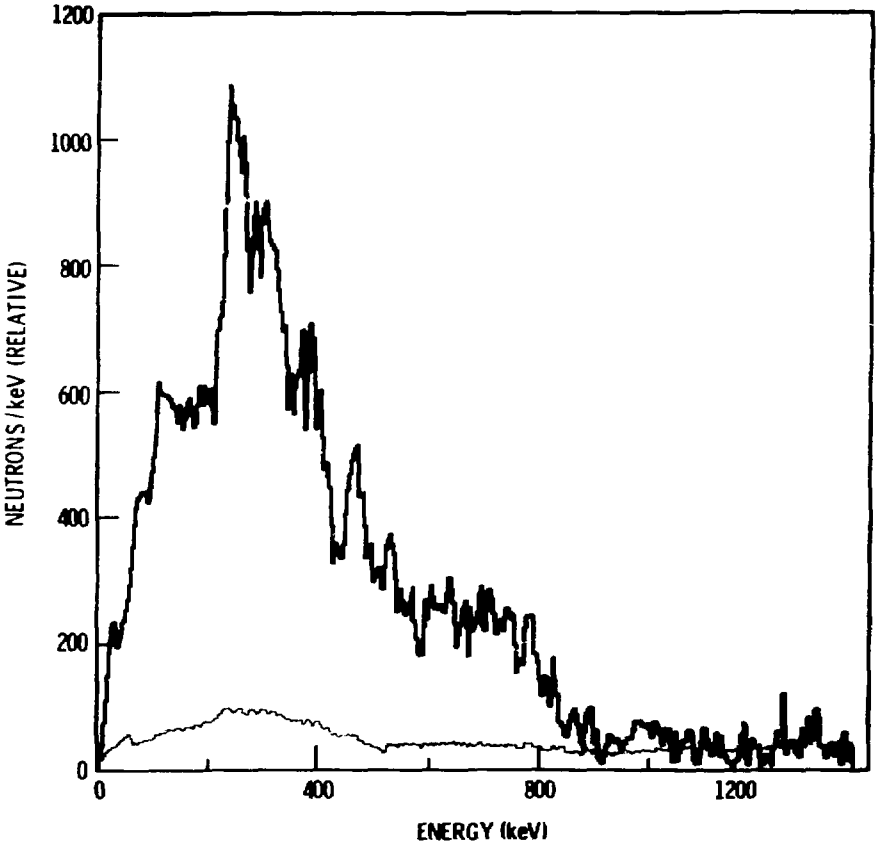

Fig. 9. Delayed neutron spectrum of ^{93}Rb.
Data from PNL, Ref. 21
Lower curve shows absolute value of combined uncertainties.

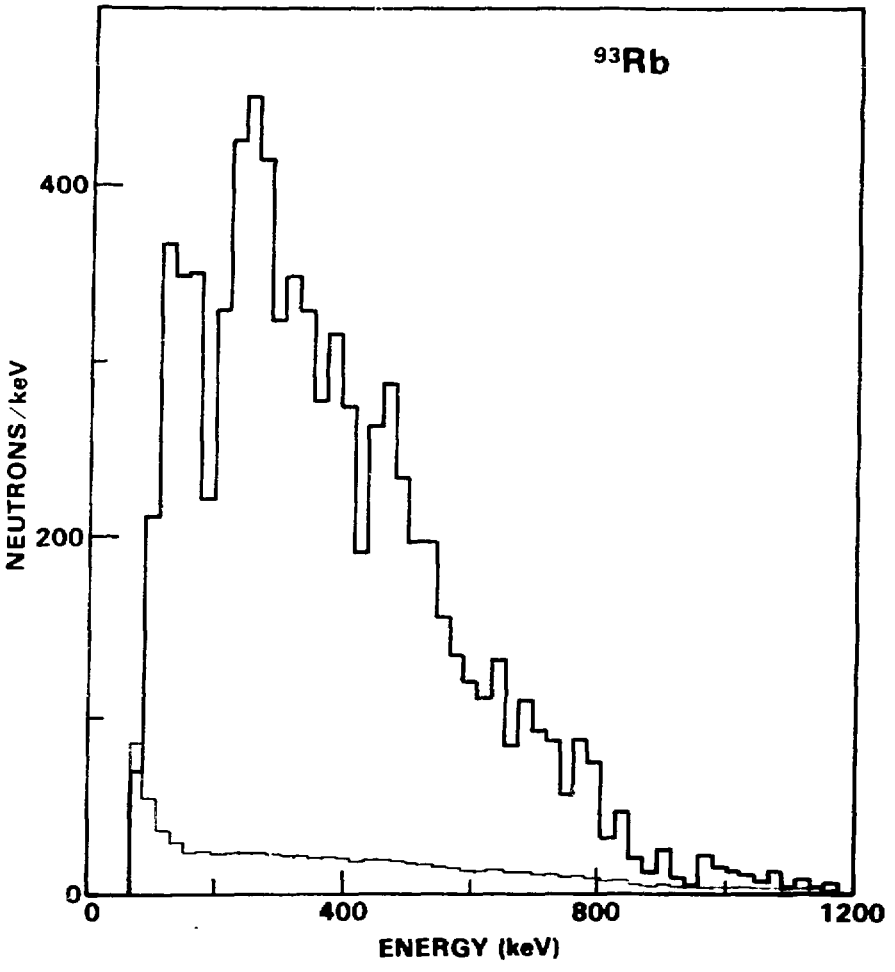

Fig. 10. Delayed neutron spectrum of ^{93}Rb.
Data from Studsvik, Ref. 28
Lower curve shows absolute value of combined uncertainties.

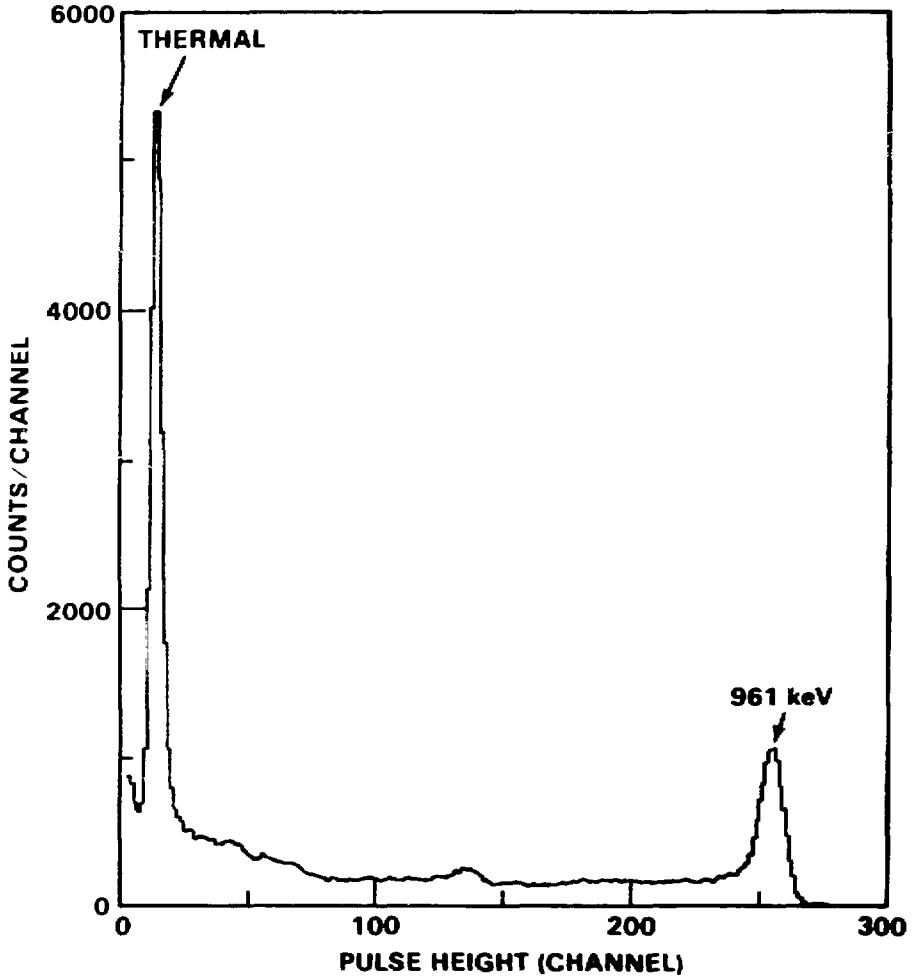

Fig. 11. Pulse height spectrum from ^{3}He spectrometer for 961 keV monoenergetic neutrons. Data from PNL.

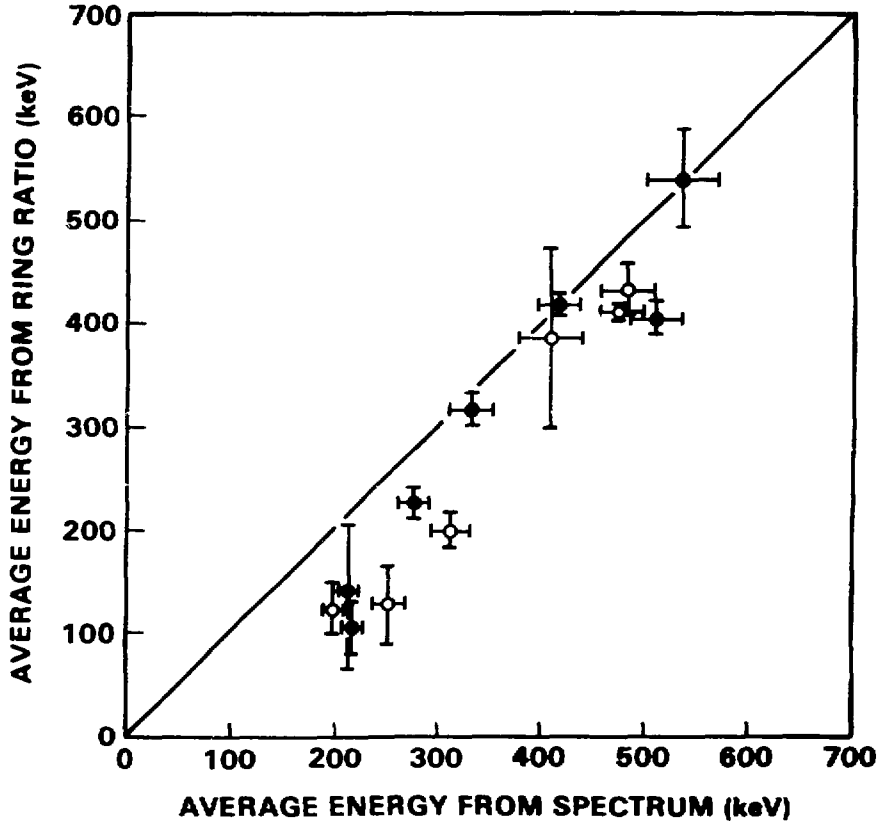

Fig. 12. Comparison of average energies determined by ring ratio technique with average energies calculated from delayed neutron spectra.
Ring ratio data from PNL, Ref. 13
Spectral data from Mainz, Ref. 19

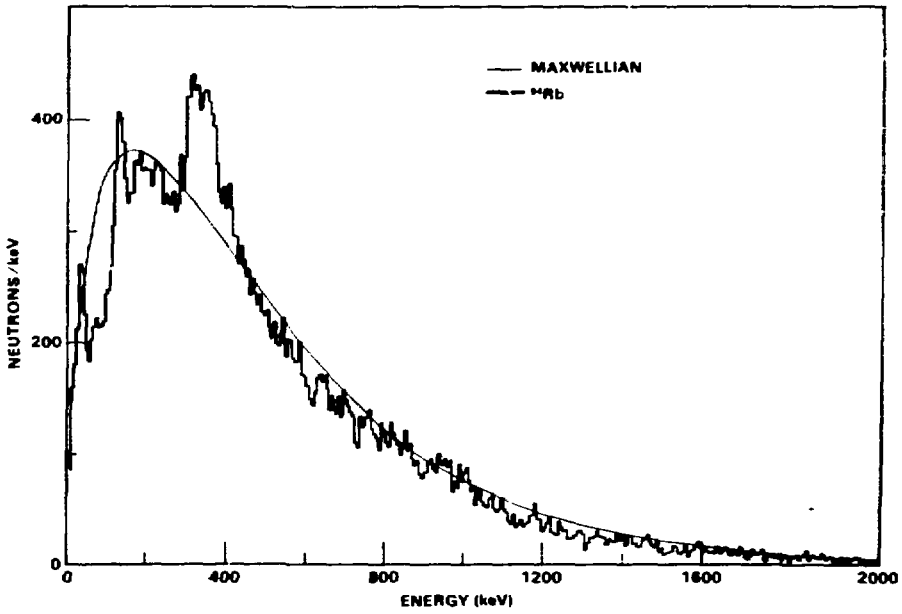

Fig. 13. Comparison of Maxwellian energy distribution with $\bar{E}$ = 500 keV to ^{94}Rb delayed neutron spectrum ($\bar{E}$ = 474 ± 20). Delayed neutron data from Mainz, Ref. 19. The spectra have been normalized to give equal areas in the energy range from 100 to 1000 keV.

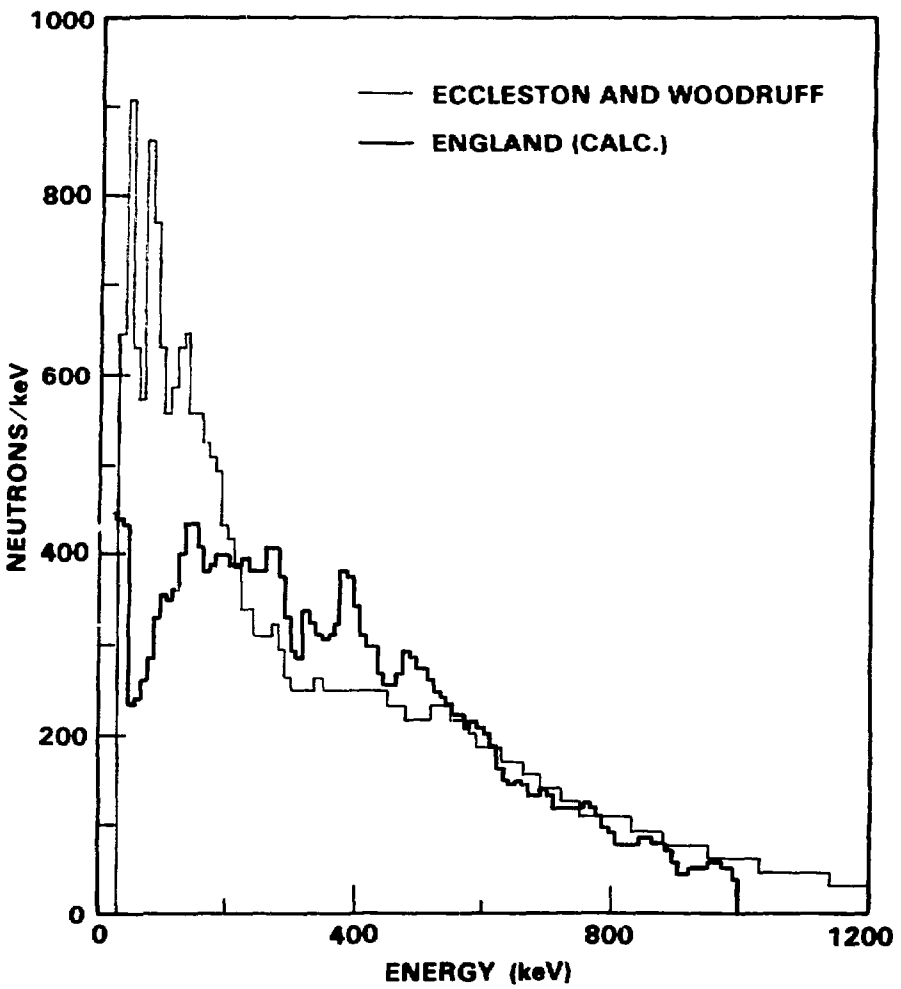

Fig. 14. Comparison of delayed neutron equilibrium spectrum calculated from ENDF/B-V yields with experimental spectrum obtained by Eccleston and Woodruff, Ref. 43 Fissioning system is fast neutrons on ^{235}U.

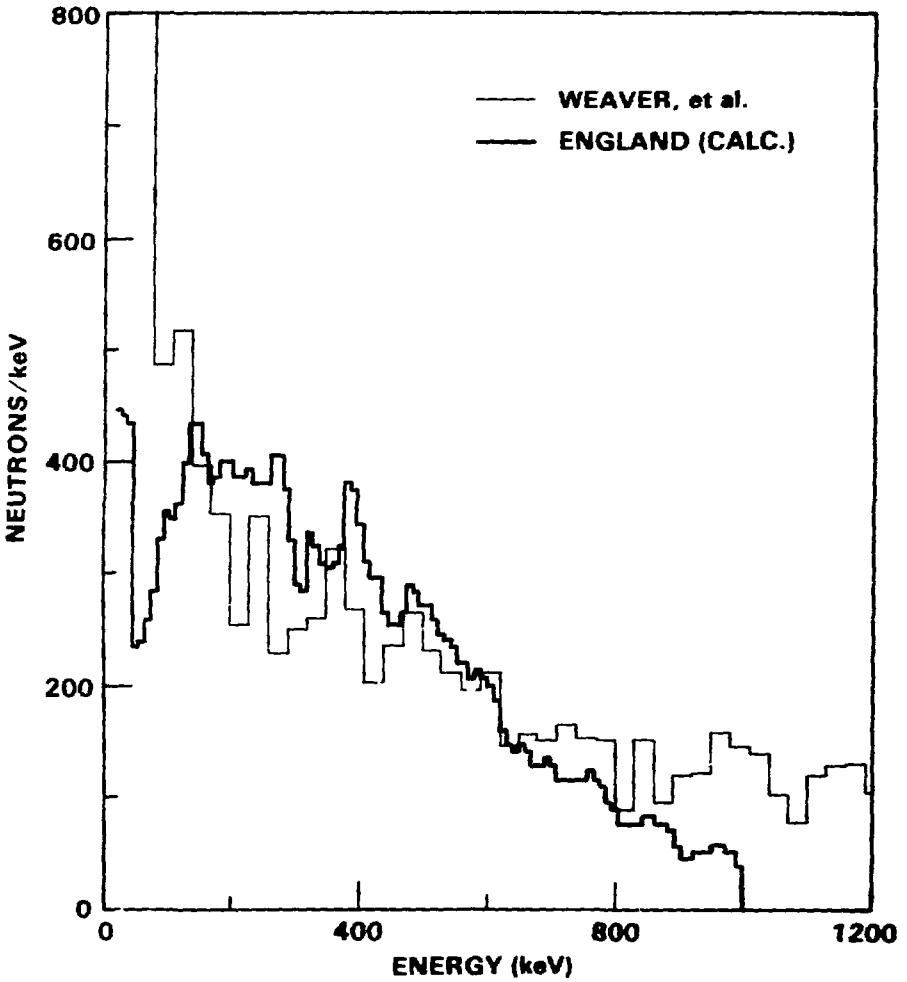

Fig. 15. Comparison of delayed neutron equilibrium spectrum calculated from ENDF/B-V yields with experimental spectrum obtained by Weaver, et al., Ref. 46. Fissioning system is fast neutrons on ^{235}U.

Discussion

Poenitz

Leona Stewart pointed out that these spectra are not represented in the ENDF/B file right now and that it made some quite important differences. What actually is used and has anybody looked into what kind of effects would be the result of using these much softer spectra?

Reeder

I am glad you asked that question because I have two more slides that I didn't have time to show which show a comparison that Tal England made. Rudstam sent the Los Alamos group a set of 28 or so spectra that he had which were then weighted by the fission yields and combined into an equilibrium delayed neutron spectrum. We can go to the last two slides. The solid curve (see Fig. 14) here is the LASL calculated equilibrium spectrum for fast neutron fission of ^{235}U. An interesting result of the calculation is this peak at low energy which was not present in the previous versions of ENDF. They had assumed that the delayed neutron spectrum just went down to zero because there were no data available. Now with the spectra that Rudstam has supplied, a peak is seen at this low energy region and I emphasized when I showed ^{95}Rb that there is a very strong peak at 14 keV, which is one of the contributors to this peak. If we compare the Eccleston-Woodruff experimental data for the same system (this is a delayed neutron spectrum taken by a proton recoil detector) they end up with a lot more intensity in the region below ~200 keV. That is very disturbing. We have the same comparison of the calculated values (see Fig. 15), this time the experimental data were obtained by Weaver, the Birmingham group, using a ^{3}He spectrometer. Again they end up with a lot more intensity at the low energies and in this case they end up with excess intensity at high energies relative to these spectra which are calculated from fission yields and the individual precursor spectra. You gave me an opportunity to give the last half of my talk. Did I answer your question?

Poenitz

Is there any knowledge about what the effects on reactor parameters would be?

Reeder

I would refer you to the Workshop on Delayed Neutron Data at the Vienna Conference. There is a paper by Philip Hammer. He

discussed the effect of delayed neutron spectra on reactor power calculations, k_{eff} and I think he would be satisfied with something like 15% uncertainties on the delayed neutron spectra. That would still give him 1% uncertainties on k_{eff}.

Stewart

One of the problems, I think, is that many of the measurements are relative, correct? The spectral measurements are not absolute.

Reeder

They are not absolute. They are normalized by way of the fission yields and P_n value.

Stewart

Secondly, you may be missing some of the neutrons from some of the precursors because you don't have all of them.

Reeder

The set available right now is a limited set, but it does include 85% to 90% of the intensity.

Stewart

I realize that. I am just trying to make the point. I think that one of the things that perhaps Wolfgang (Poenitz) was mentioning is the difference in what is in File 5 which is, quite often, what the reactor physicist uses. That is a six-group set and that comparison, I think, is one that he was asking about, I'm not sure.

Reeder

I am sorry, I am not equipped to handle that.

GENERAL REVIEW AND DISCUSSION (SESSIONS I-IV)

J.J. Schmidt, IAEA

SUMMARY REVIEW FIRST DAY (22 September)

(Processing Needs, Uncertainties, Integral Data, Radioactivity Data)

J.J. Schmidt

Nuclear Data Section
International Atomic Energy Agency
Vienna, Austria

I do not know whether I should thank the organizers of this workshop for the mammoth task they entrusted to me, i.e. to summarize the high lights of each day of this Workshop. However, after having listened to all the very interesting and inspiring talks and discussions today, I consider it a real privilege to be with you in this meeting. I shall try my best to summarize today's major results and outlooks while being conscious of the fourth alternative of a discussion speaker, pointed out this morning by our Workshop Chairman, that afterwards I will remember what I should have said. While I apologize for not being in a position to give detailed credit to each paper and each speaker, I hope to bring out the major stimuli and concerns expressed in today's sessions. After having finished my summary remarks, I would like to ask the Chairmen of the individual sessions to correct and add to my remarks so as to complete the picture of today's achievements.

Let me start by recalling to you the situation as it was in about 1960. This is illustrated in Figure 1. At that time the nuclear data users were essentially thermal and (increasingly) fast reactor physicists. They had certain ideas of the nuclear data they would need and asked other physicists, henceforth called evaluators, to provide the data. These evaluators tried for the first time, to consolidate the rather sparse data information then available into the first rather embryonic evaluated data files. These files were then converted into rather crude multigroup cross section libraries for use in still fairly simple neutronics calculations for reactor design.

Today's lectures have exemplified how much more complex this situation has become over the past 20 years. The present situation in 1980 is visualized in Figure 2. Starting with the bottom of the figure, we have many more application fields and much more sophisticated data uses than in 1960. They comprise not only various types of thermal and fast breeder reactors and the fuel cycles associated with them, but also safeguards, safety, radiation damage and associated dosimetry, shielding of reactors and accelerators, fusion research and technology, medical therapy and radioisotope production, to mention only the more important fields. In order to meet modern design, operation and safety criteria, the required data detail and accuracies for the most of these applications have become much more stringent over the past two decades.

The data requirements are apparently strongly application-dependent. In thermal reactors the thermal neutron reaction rates and hence, the thermal cross sections are most important; in fast reactors the keV and MeV cross sections. Fusion data needs center in the MeV range up to about 16 MeV. Shielding physicists are particularly concerned with the neutron windows caused by the deep cross section minima of iron and other shielding materials. Much sophisticated experimental work has gone into the accurate determination of the cross sections in these minima. Medical therapy and radioisotope production need neutron and charged particle data to 50 MeV and higher. Going to these higher energies implies adding a new degree of complexity to evaluated data files due to the increased number of reaction exit channels and increased complexity of reaction products. Neutron dosimetry applications for the determination of fission and fusion reactor radiation damage need a limited number of activation reactions with high accuracy to about 50 MeV.

As you can see from Figure 2, originally, evaluated nuclear data libraries were planned to be application-independent. However, with the increased diversity of applications there is a growing tendency for separating specialized evaluated nuclear data files, e.g. fission product nuclear data, dosimetry data and others, from the larger bulk of general purpose files. Once the size of evaluated data files to be processed becomes unwieldy, one might think of creating application-oriented special preprocessed evaluated data libraries as an interim step between the big application-independent files and multigroup data processing, as was pointed out this morning by MacFarlane. I shall come back to this problem later.

Let me now start with a systematic consideration of Figure 2 starting at the top. We have apparently reached a stage which was typical in Greek antiquity,that all science starts with philosophy and eventually ends up in application. I trust Francis Perey will agree, that unlike the Greeks who sometimes produced a philosophy without going to an application, he will eventually turn his theory of logical inference to practical applications. I should stress that his theory has the strong merit of being directed towards the nightmare of every evaluator, i.e., the treatment of systematic errors, and promises to provide a mathematical tool for dealing with those probabilities which cannot be expressed in frequencies like statistical probabilities.

The problem of systematic errors, the major hindrance in every evaluation (to arrive at scientifically reliable values) must certainly be given the greatest possible attention. Another (though small) difficulty occurring in all cross section evaluations has to do with the fact that continuous functions have to be described by sequences of discrete points which have to be interpolated. Nothing can be done about this except using, where possible, formula descriptions of the data in order to reduce the magnitude of the data storage and handling problem.

Until about two years ago, evaluated nuclear data libraries contained only point cross section data, parameters and formulae. Since then, with the ENDF library taking the lead, there is an increased user demand for associating uncertainties, or more generally variance-covariance information with the evaluated data. The data adjustment session today gave a vivid illustration of the work needed to arrive at meaningful covariance data and how to store, use and process them. A really good job in this area demands a much larger effort than previous data evaluation without uncertainty specification and has to be very well justified in each case on the basis of user needs. In this context one should remember a point which was not clearly brought out in today's discussions; that the usefulness of covariance matrices is intimately connected with the truthfulness of the information that goes into them. With limited or insufficient information in hand, a good thumb-rule estimate of an evaluated data uncertainty will be easier, cheaper, and more efficient than deriving a complex covariance matrix.

On the other side let me remind you that Francis Perey emphasized on previous occasions that in principle one has to take covariances into account. One cannot deal for example with one cross section of one nuclide independent of cross sections of other nuclides if they have all been measured by the same method or against the same standard. Taking into account those and other correlations will improve the description of evaluated data uncertainties.

Such an improvement has already taken place e.g., in the field of reactor dosimetry cross sections. In the first step, dosimetry data files now contain covariances accounting for correlations between different energies for one and the same nuclide and reaction. What will be needed in a next step are covariances between different reactions and nuclides. Again to be practical, this is a small field with a limited number of reactions, and to put all the covariances together for these reactions and process them by neutron spectrum unfolding for radiation damage estimates is still a manageable job. However, what about deriving complete correlation matrices for all reactions for one full nuclide in ENDF/B, say ^{238}U? Talking about ^{238}U, one has to immediately consider ^{235}U etc, and there is virtually no end to all the correlations which would have to be considered. I can only confront you with this question, without knowing the answer. This is not a question of principle, but a question of practicality. With more experience in correlations we will gain more insight and come closer to an answer to this question.

Let me now discuss the three major inputs into contemporary evaluation. The classical and most important input continues to be the measured data. However, applied nuclear theory, nuclear models, and systematics have undergone significant progress in recent years and inter-and extrapolation and "local" (data in a $A \pm \Delta A$ range) fitting and prediction, represent an important

addition and consistency check to experimental data. However, since all theory is based on parameters derived from experimental evidence, it cannot replace an accurate experiment for an important reaction.

The third input comes from adjustment of microscopic data to what one may roughly subdivide into simple and complex integral data. With John Rowlands I would call one reaction for one nuclide in a well-defined neutron spectrum a simple integral datum. An example would be an infinite dilute capture resonance integral or an average fission cross section measured in the ^{252}Cf prompt fission neutron spectrum.

I trust everyone will agree with me that there is no harm in a physically carefully conceived adjustment of a small limited portion of an evaluated data file to such simple integral data. The unique feedback to evaluated microscopic data becomes difficult and ambiguous as the integral data becomes more complex. Here, I am thinking of measurements in more complex benchmarks such as ZPR facilities or in reactors. Complex integral data are subject to so many influences from many materials, many reactions, and heterogeneities in material composition etc., that one has to make sure that what one changes in an evaluated data library is consistent with all possible cases of integral data: for example, a range of reaction rate ratios, k_{eff} values etc., for a range of critical assemblies. One should also bear in mind that integral data, whether simple or complex, are not necessarily more accurate than differential data since the use of a fission chamber in a differential or integral fission measurement should not really make a difference in the uncertainties associated with such measurements. Considerable progress has been made over the past years in data adjustment. The three talks which we heard today during the data adjustment session illustrated considerable improvements in the mathematical as well as physical sophistication which goes into today's adjustment procedures. However, I would still continue to foresee a major role for complex integral data adjustment in pinpointing possible inconsistencies in microscopic data and enforcing their reevaluation or re-measurement.

Now let me turn to the right side of Figure 2. Present-day evaluated data libraries contain a large, ever increasing volume of point data, supplemented by parameters and formula, (this is true particularly of ENDF/B) and uncertainty information. In this morning's panel discussion Carter drew attention to the large increase in data points from Version IV to Version V of ENDF/B. Evaluated data libraries risk becoming so large that they may present serious data handling problems.

The panelists, in particular MacFarlane, pointed out that one should and could make more use of parametric data representation and in this way reduce the volume of data to be stored. Extensive pointwise tabulations of well-defined resolved resonance cross sections for a number of fission reactor materials can be replaced by lists of resolved resonance parameters and the appropriate

formulae which describe the cross sections . The lists can then be used directly as input to multigroup cross section codes. Another example is the parametric description of neutron elastic scattering angular distribution data. At high energies say above 15 MeV, they resemble a rather simple diffraction pattern. Instead of using 30 or 40 Legendre polynomial coefficients they could be described by fairly simple functions thus allowing a more compact representation and easier multigroup data processing afterwards.

The detail to which the data are needed, often depends strongly upon the specific application of the data. The deep minima in several structural material resonances are of paramount interest in shielding design, but of no interest in reactor design. On the other hand, present day facilities such as ORELA can measure neutron cross sections often to a much greater detail than may be needed or realistically be handled by the data user. One example for this, which in fact illustrates an immense scientific achievement, is the detailed set of ORELA measurements of the change in neutron elastic scattering angular distributions over many iron resonances.

These facts and considerations unavoidably lead to the principal question which Alan Smith brought forward and which will certainly become even more stringent in the future; do the data users, reactor and shielding designers and other users, really need data to such a detail? The effort, i.e. money and manpower, spent in generating data must be in balance with the user's realistic data requirements. There is a continuing need for various classes of users to specify the practical detail to which they require nuclear data.

New applications such as FMIT or biomedical applications, will increase the upper energy limit of evaluated neutron data libraries from the current 15-20 MeV to about 100 MeV and thus lead to a size increase of such libraries. To ease the concurrently increasing data handling problems in these and other special applications (where different user classes would need data in non-overlapping energy ranges or in different detail, or a limited number of nuclear reactions and isotopes) pre-processing or further split up of the general-purpose evaluated data libraries should be contemplated.

The more complex and voluminous evaluated data libraries become, the more serious become the problems connected with the testing and updating of these libraries. I sympathize with the points brought forward by MacFarlane and Ozer during the panel discussion this morning i.e., one should not easily give up what has been achieved in the last version of an evaluated data library and changes should be introduced only if they are absolutely sure to achieve a definite improvement in all pertinent applications. The size of the effort put into a re-evaluation and an assessment of data uncertainties should be in proportion to the importance of the data in question.

So far, when I spoke about evaluated data uncertainties, I meant uncertainties directly connected with the data. Additional uncertainties arise or may arise through the stages of pre-processing and multigroup processing of the evaluated data and their eventual application in nuclear calculations. With Henryson, one may therefore question the need for an accurate evaluation if afterwards in the application, this accuracy may risk being diminished or even lost.

This brings me to the final question: how long will nuclear data evaluation be needed. Poenitz gave one straight-forward answer to this question, i.e., since the data required for current nuclear technology applications are still not met, more evaluations (and certainly more experiments) are still needed. The new upcoming application fields will need additional evaluation effort, and in a way the field is open-ended.

Having said all this I almost feel that evaluation is not only an art, but at least very close to a science, but maybe I am overimpressed by today's challenging talks and will change my mind by tomorrow. I will certainly not change my conviction that evaluation is an art.

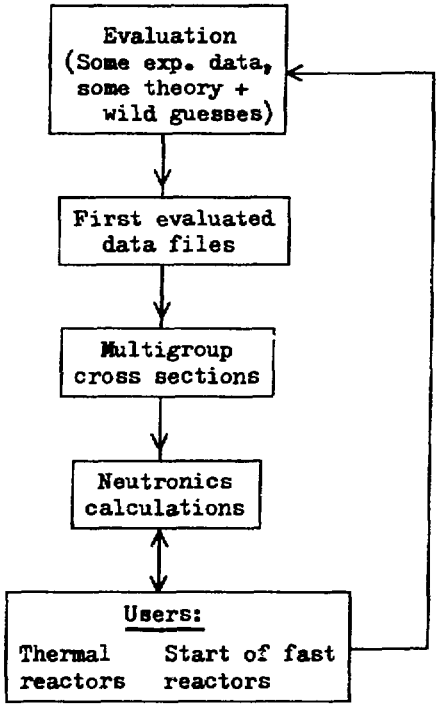

Figure 1. "Zero-phase" situation around 1960

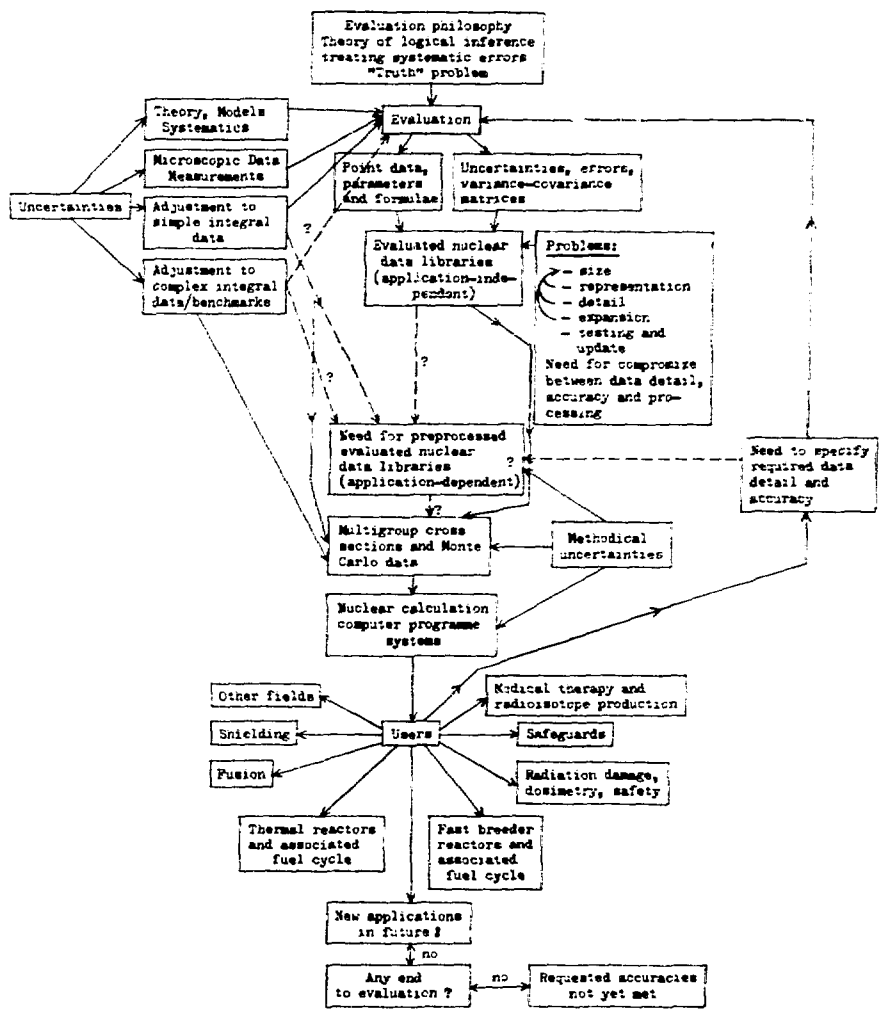

Figure 2. Situation in 1980

SESSION V

STANDARDS AND OTHER PRECISION DATA EVALUATIONS
Chairman: P. Young LANL

DATA INTERPRETATION, OBJECTIVE EVALUATION PROCEDURES AND MATHEMATICAL TECHNIQUES FOR THE EVALUATION OF ENERGY-DEPENDENT RATIO, SHAPE AND CROSS SECTION DATA*

W. P. Poenitz

Applied Physics Division
Argonne National Laboratory
9700 South Cass Avenue
Argonne, Illinois 60439 USA.

ABSTRACT

The evaluation of several energy-dependent cross sections which are of importance for practical applications is considered. The evaluation process is defined as the procedure which is used to derive the best knowledge of these cross sections based on the available direct experimental data information, and, using theoretical models, on the auxiliary data base. The experimental data base represents a multiple overdetermination of the unknown cross sections with various correlations between the measured values. Obtaining the least-squares estimator is considered as the standard mathematical procedure to derive a consistent set of evaluated cross section values. Various approximations made in order to avoid the monstrous system of normal equations are considered and the feasibility of the exact solution is demonstrated. The variance - covariance of the result, its reliability and the improvements obtained in iterative steps are discussed. Finally, the inclusion of auxiliary, supplementary information is considered.

I. INTRODUCTION

The subject of the present considerations and review is the evaluation of neutron cross sections which are of specific importance and thus have to be known with lesser uncertainties than others. This involves cross sections used in practical applications such as $^{235}U(n,f)$, $^{238}U(n,\gamma)$ as well as the standard cross

*This work performed under the auspices of the U.S. Department of Energy.

sections (H(n,n), ^{6}Li(n,α), ^{10}B(n,α), ^{10}B(n,αγ), Au(n,γ)). For reasons which will become clear later on, some other cross sections are involved as well (^{6}Li(n,n), ^{10}B(n,n)). Following the intent of this meeting, we not only consider the state of the evaluations of these data but the evaluation process as well.

It should be clear from the outset that an evaluator is not expected to derive his opinion of the subject of the evaluation but the best knowledge of it. Nuclear data evaluations can be divided in historic terms into an

'Age of Archaic Evaluations',

where unjustifiable and subjective evaluation methods were used, an

'Age of Enlightenment',

where it was recognized that the archaic evaluation techniques had severe drawbacks, and an

'Age of Renaissance',

where it was discovered that exact solutions techniques were developed some 180 years ago. As in other areas of history, these periods cannot be sharply divided. But clearly, about 10 years ago, evaluation procedures for nuclear data were still in the 'Dark Ages' where archaic techniques were well entrenched, and appropriate methods were used only infrequently. Wild lines were drawn through data points and subjective opinion carried the day. It has been recognized in the last few years that appropriate techniqeus were well developed and applied in other disciplines of science and engineering and should be employed as well in the evaluation of nuclear data. Increasingly, improved techniques were used, but unfortunately, the archaic age is slow in dying: e.g., it would be easy to point out a number of evaluated cross sections in ENDF/B-V which were based upon one data set where many were available. Because of this staying power of unscientific, archaic methods, techniques and argumentation, it will be hard to avoid to point out fallacies which will be obviously recognized as such by many.

As we desire to derive the best knowledge of some quantities existing in nature, we have to consider what this knowledge consists of.

I.1. The Best Knowledge

The philosophy or theory of knowledge, developed by many important men, and culminating with Kant's 'Critique of Pure Reason' [1], tells us that knowledge has two sources: 'a priori', which is knowledge developed from reasoning along, and

'a posteriori', which is knowledge after the fact, e.g., after performing an experiment. As we are not in the area of logic or mathematics, where knowledge may be derived purely 'a priori', we have to be concerned whether our knowledge is purely 'a posteriori' or, to some extent, can be derived 'a priori'. Certainly, laws of nature have been found in physics, but the area applying to nuclear cross sections is still in a state of modeling and our knowledge is empirical, thus it is derived 'a posteriori'. A good example are cross sections which may be derived from the optical model. The optical model was not conceived 'a priori' but 'a posteriori' following the pioneering measurements of total neutron cross sections by Barshall [2] which showed systematic structure as a function of energy and nuclear mass. It was possible to predict other cross sections with this model. But, as measurements for such predicted cross sections became available, the model predictions were found in conflict with these experimental results. The conflicts lead to refinements of the model, in successive steps, changing the shape of the potential, adding a surface absorption potential, spin-orbit coupling, introducing non-local potentials, etc., always in response to disagreement with new measurement results. As of now, the optical model is still a model, of great value, but dependent on numerous parameters derived from fitting experimental data. It obviously follows that predictions with the optical model cannot be better than the quality of the whole of the experimental data base. This does not mean that optical model predicitons cannot be better, in some instances, than a singular experimental data set. A case in point is the total cross section of ^{233}U. The ENDF/B-IV evaluation used a line through the available experimental data. An optical model fit of these data would have provided a more physical shape but still erroneous values. It was appropriately recognized by evaluators for ENDF/B-V [3] that the experimental data for ^{233}U in the energy range below 1 MeV were in conflict with data for neighboring nuclei. A prediction based on a parameterization with data for other nuclei was utilized instead. However, then a new data set became available and the evaluation was changed to match this data set. Experimental data are uncertain, thus, the best knowledge of the ^{233}U total neutron cross section would be obtained by a simultaneous fit of the transactinides with the optical model, accounting for uncertainties of the data and the model. Such simultaneous optical model fitting is now being done, for example, by Madland and Young [4] and Poenitz [5].

The best knowledge of the quantities to be evaluated is derived by including all the direct and indirect information available. The primary source is the experimental data base, differential and integral, as our knowledge is 'a posteriori'. nuclear models and integral systems models provide the link between the data. Figure 1 shows a schematic of the maximum information leading to our evaluated (or best knowledge) cross section. This maximum information has been used, for example,

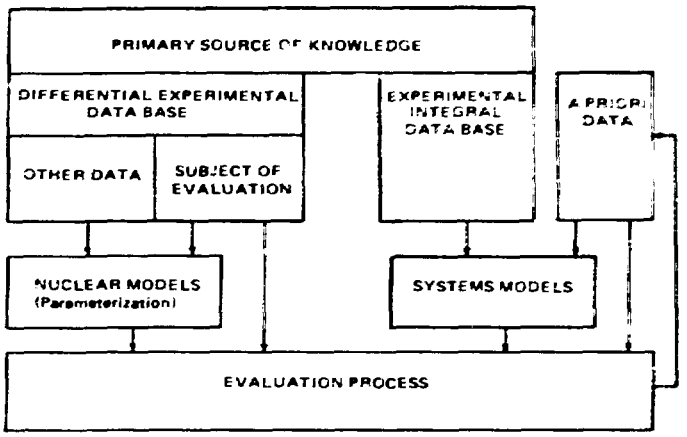

Fig. 1. Information Available for Cross Section Evaluations.

by Schenter's group [6] for the evaluation of fission product nuclei. The result of such evaluation (which includes the integral data) is often called an adjusted cross section set. An adjusted, best knowledge cross section set is justified and desirable, specifically in cases of sparce differential information, as in the case of fission product nuclear data.

One may require, however, another approach, based on the intended use of the evaluated data. A separate evaluation of the differential data with utilization of the nuclear models provides for a "testing" of the integral systems modeling of experimental integral values. The large number of parameters involved in an integral system causes a diffusion of the lack of knowledge for some parameters (discrepancies) by distributing the blame between all of the parameters (cross sections). The French library data on the components of stainless steel provide an example. Though this library predicted available integral data very well, it was due to compensation and a design calculation for a different compositon of stainless steel would have resulted in erroneous predicitons [7].

Thus, in the following we restrict our considerations to the evaluation of differential data of the primary data base and the utilization of auxiliary information provided by the nuclear models.

I.2. Outline of an Objective Evaluation Process

One of several features of an objective evaluation process is not to select data based upon subjective judgment. However, the fitting of the available experimental nuclear data with nuclear models involves non-linear fitting of such monstrous

proportions that it is obviously beyond the range of present technology. This suggests to divide the evaluation process into steps as shown schematically in Fig. 2. The first major step consists of assembling the available experimental data, extraction of actually measured quantities, and the application of corrections to the reported values and their errors if such can be proven to be required. Updating constants ($T_{1/2}$) etc., used in the calculation of these values, recalculation of corrections with improved techniques (Monte Carlo) and data used in their calculations are acceptable. However, reintroduction of subjective methods (for example unjustified re-assignments of uncertainties) must be rejected.

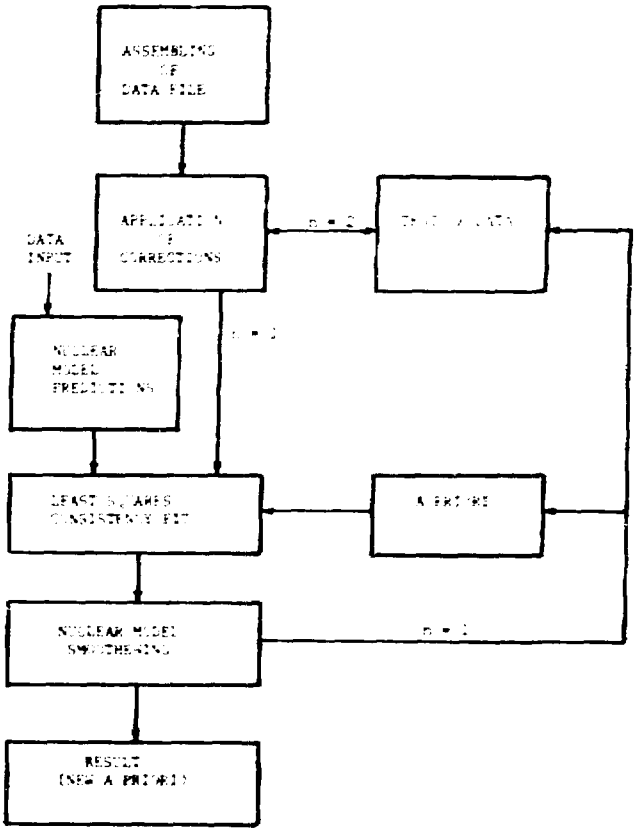

Fig. 2. Schematic of the Evaluation Procedure.

The second step is the evaluation of the experimental data in a simultaneous least-squares fit as discussed below which yields a consistent set of values which represent the

best knowledge from the experiments. The third step is the utilization of nuclear models which permit to use auxillary data information. The process is then repeated in iterative steps in order to obtain further improvements.

II. THE MEASUREMENT PROCESS AND INTERPRETATION OF THE EXPERIMENTAL DATA BASE

It is obvious that the evaluation process should be considered in context with the subject of the evaluation, the data base. An understanding of the measurement-process and the quantities derived appears required. Mathematical procedures can lead their own independent life, but the answer will surely be misleading if they are based upon a misconception of its elements. This may well be a danger we are facing now, as more and more evaluators become enchanted with powerful tools provided by statistical analysis, but do not understand the data base and thus "take off into a dream world".

II.1. Types of Measurements, Originally Measured Quantities

It must be realized that experimenters in the area of cross section measurements rarely present what they have measured. A measurement of the shape of the ratio of two cross sections, say $\sigma_{n,f}(^{235}U)/\sigma_{n,n}(^{1}H)$, will surely be presented as a measurement of the $^{235}U(n,f)$ cross section after using some reference for the $H(n,n)$ cross section and normalization to some other absolutely measured or more or less arbitrarily choosen value. Comparison with other measurements are then made, differences pointed out and possible explanations given. All of which is an exercise in futility because the quantities measured were not the values discussed. This does not mean that the measurement was meaningless, in the contrary, it may have been an very important input for the quantity, for example a cross section shape, which was actually measured.

The first task for the evaluator, who wants to derive the best knowledge of one or several unknowns, is to rediscover the actually measured quantities, thus to reduce the given information to the truly new information obtained in the specific experiment. An example for the problems resulting from ignoring the originally measured quantities is the common procedure to evaluate a specific cross section for which N measurements are available without differentiating between K measurements which were made relative to the same reference cross secton and N-K absolute and independent measurements. Such procedure is identical to forming the average between 3 and 4 by calculating (3 + 3 + 4 + 4 + 4 + 4)/7 (assuming N=7 and K=5). Such fallacies may not be very obvious if correct and sophisticated techniques are used for the derivation of the evaluated cross section.

A measurement may have been presented as a cross section measurement over an energy range (E_k,E_i) but in reality the shape may have been measured in two segments, (E_k, E_ℓ), (E_j,E_i), (with $E_j < E_\ell$) and a normalization point obtained at E_n (with $E_k \leq E_n \leq E_i$). The true information obtained from these measurements which should be used as input for the evaluation are three sets of data: 1. the absolute value at E_n, 2. the segment in (E_ℓ, E_k), and 3. the segment in (E_j,E_i). The composite cross section should not be used, it will bias the evaluation as will be seen later on.

The types of measurements used to derive the data under present consideration are transmission experiments which yield total cross sections, reaction cross section or ratio measurements, shape measurements of cross sections or ratios which leave the normalization of the data undetermined, and absorption cross section measurements. Total cross sections are derived from the expression

$$\sigma_{tot}(E) = \frac{1}{a} \ln \frac{C_o(E) - b_o - \sum_i b_{oi}(E)}{C(E) - b - \sum_i b_i(E)} \cdot \prod_j f_j(E) \quad , \qquad (1)$$

where a is the sample constant, b is a constant background and $b_i(E)$ an energy dependent background. The $f_j(E)$'s are correction factors, for example for deadtime, resonance self-shielding, etc. The $C_o(E)$ and $C(E)$ are the detector counts without and with the sample. Reaction cross sections are derived from

$$\sigma_x(E) = \frac{C_x(E) - b_x - \sum_i b_{xi}(E)}{C_n(E) - b_n - \sum_i b_{ni}(E)} \cdot \prod_i a_i \cdot \prod_j f_j(E) \quad , \qquad (2)$$

where $C_x(E)$ and $C_n(E)$ are the count rates for the observed reaction and the neutron detector, respectively. The a_i are independent on energy and stand for sample masses, efficiency calibrations etc. The $f_j(E)$ are energy dependent corrections and the energy dependence of the counting efficiencies. The same expression [2] applies for ratio measurements with $C_n(E) \rightarrow C_y(E)$ and $\sigma_x(E) \rightarrow R_{xy}(E) = \sigma_x(E)/\sigma_y(E)$. In a shape measurement (cross section or ratio), the product $\prod_i a_i$ remains undetermined and only the energy dependence of the cross section is obtained: $S(E) = C \cdot \sigma(E)$ with $C = \prod_i a_i$ an unknown factor. The central expressions in (1) and (2) can be restated as

$$\frac{C_x(E)\left(1 - \frac{b_x}{C_x(E)} - \frac{\sum b_{xi}(E)}{C_x(E)}\right)}{C_n(E)\left(1 - \frac{b_n}{C_n(E)} - \frac{\sum b_{ni}(E)}{C_n(E)}\right)} \quad , \tag{3}$$

which shows that background corrections are energy dependent correction factors. Equations (1), (2) and (3), obvious to the experimenter, were recounted here in order to show that i) no additive terms occurs, and ii) the shape measurement is a measurement of the energy dependence of the cross section with an undetermined factor and not an undetermined bias. An evaluator who uses polynomials in fitting experimental data will not find support for an interpretation of the a_0-term of the polynomial as a background of the measured values. In addition, the constant background which enters as an energy dependent background-to-foreground ratio is usually small and well determined, thus of negligible error and not adjustable.

II.2. Overdetermination of the Data Base

If several measurements exist for the same unknown quantity, it is well recognized that an overdetermination exists and it is well accepted, that the best estimator for the quantity is obtained as a weighted average of the measured values. This is the least-squares-estimator, if it is based on the minimization of the sums of the squares of the deviations between the measured values and the average value.

Another form of overdetermination exists if a value was measured for one quantity, another value for a second quantity, and a third measurement was made, for example for the ratio or sum of the two quantities. Obviously, three values were measured for only two unknown quantities.

These two types of overdetermination are dealt with mathematically identical. However, we note here that an important difference may exist which makes the second type more valuable for obtaining an unbiased estimator: Measurements of the same quantity may be subject to similar errors, specifically the psychological error explained below, and thus result in an biased evaluated value. Measurements of different quantities are more likely to be subject to different errors and therefore more probably provide a data base with overall random errors.

Absolute measurements of several cross sections are of equal value (assuming equal accuracy) and our best knowledge of any one of these cross sections is determined by all of the measurements if ratio measurements between them are available. Because of the equivalence of any absolute measurement, a real justification for declaring some cross sections "standards" or even "primary standards" and "secondary standards" does not

exist. However, defining some cross sections as "standards" because their physical behavior provides for convenient detection schemes has resulted in a concentration of absolute measurements on these cross sections. This permits us to limit our considerations to these "standards" and some cross sections which are important for applications and for which therefore also absolute measurements were carried out.

Removal of the second type of overdetermination is sometimes referred to as a consistency fit or a simultaneous evaluation of several cross sections. Such simultaneous evaluations were carried out, for example, for the thermal parameters [8], and for standard, fission and capture cross sections [9,10].

II.3. Errors, Uncertainties, and Correlations

It is assumed that the experimental values have been reported in terms of the following parameters.

E	The average energy at which a value was measured,
ΔE	The uncertainty of this energy,
R_{es}	The energy resolution or energy spread,
σ, R	The measured cross section or ratio,
$\Delta\sigma$	The total uncertainty of the measured value,
$\Delta\sigma_{st}$	The statistical uncertainty of the measured value

It is a basic feature of the measuring process to result in uncertain values. The true uncertainty is composed of several components, which may be subdivided as follows [9, 11, 12]:

$\Delta\sigma_R$	The normalization uncertainty, which is the uncertainty of a, $\prod_i a_i$ in Eqs. (1) and (2). This is an energy independent systematic uncertainty and thus totally correlated for all measured values $\sigma(E_i)$. It contains the uncertainties of the sample masses, calibration etc.
$\Delta\sigma_s$	The energy dependent systematic uncertainties which were estimated or calculated from the uncertainties of models and parameters used to calculate corrections, background subtraction, energy dependence of efficiencies, etc. Because of the energy dependence of these uncertainties, these errors correlate the measured values only par-

tially, often causing larger correlations for values at adjacent energies than between values measured at substantially different energies.

$\Delta\sigma_{st}$ The statistical uncertainty caused by the limited number of events counted for the primary reaction rates as well as for the background. Note that the statistical error may become a totally correlated systematic error if a shape measurement is normalized to an absolute value or if two segments are normalized to one another in the overlap range.

$\Delta\sigma_{a}$ The accidental error which may be revealed by repeating the identical experiment (i.e. reproducibility),

$\Delta\sigma_{u}$ The unknown error, which is systematic in nature and caused by not recognizing necessary corrections or underestimating uncertainties,

$\Delta\sigma_{ps}$ The psychological error which is caused by satisfaction with agreement obtained with values reported by others, thus neglecting the search for additional effects in the measuring process or equipment which would require corrections, or, the opposite, that is the dissatisfaction with a disagreement with prior reported values and the subsequent search for one-directional corrections.

The last three error sources affect the evaluation in a similar way, that is, as an unkonwn error. However, their differences help to understand some effects, for example historical trends in reported cross sections as shown in Ref. 9.

We may differentiate between two types of correlations in considering the interdependence between different measured values caused by correlated errors:

i) Measurements of a cross section or ratio at different energies in one experiment are usually made with the same sample and detectors, thus all values are partially correlated.

ii) Measurements of different cross sections may be based upon the same neutron detection technique and thus causes these measurements to be correlated. Correlations between different measurements of the same cross section may be caused because the same sample or the same detector was used.

Figure 3 shows schematically how the different types of errors will influence an evaluation and what the correlation matrix for the energy-dependent measurement will look like. We assume for this demonstration an absolute measurement of a cross section as a function of energy and one additional independent measurement obtained only at one energy.

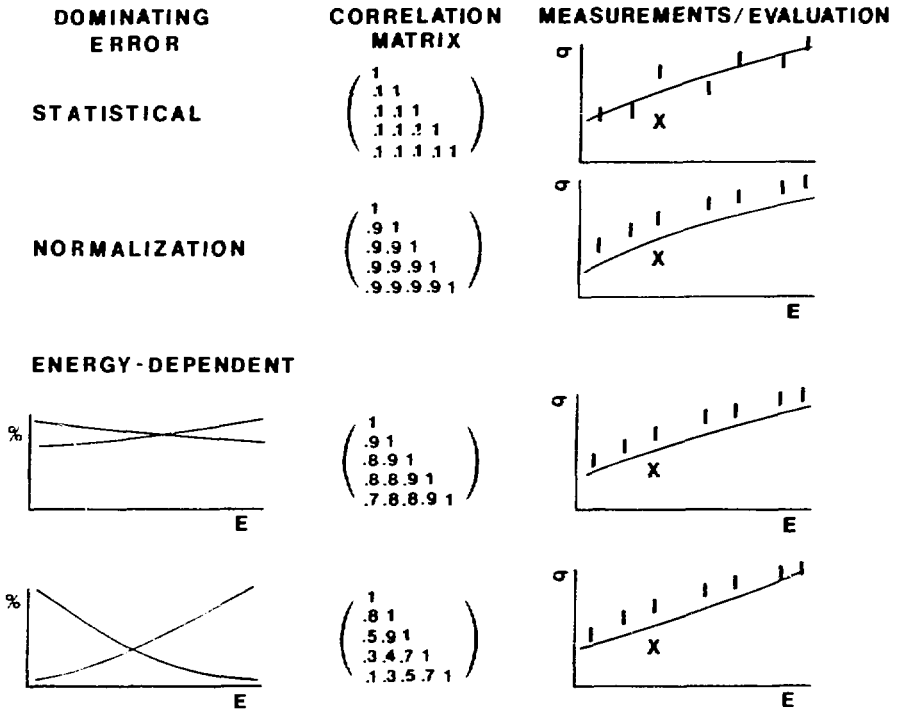

Fig. 3. The Effect of Dominating Errors on an Evaluation. The Correlation Matrix is Shown for the Energy-Dependent Measurement.

Our knowledge is improved only at the energy where the additional measured value was obtained if the dominating error is statistical. However, our knowledge is improved over the whole

energy range by the additional independent measurement if the dominating error is due to the normalization. The effect on the evaluation result for dominant energy dependent errors is similar as for the case of dominant normalization errors if the energy dependence of the systematic errors is weak. Strongly energy dependent systematic errors cause a "flexibility" of the shape measured in the one experiment.

An additional cross section uncertainty is caused by the energy dependence of the cross section and the energy uncertainty, ΔE. This can be derived approximately from

$$\Delta\sigma_E^2 = \left(\frac{\partial\sigma}{\partial E}\right)^2 \Delta E^2 + \sum_i \left(\frac{\partial\sigma}{\partial f_i}\right)^2 \left(\frac{\partial f_i}{\partial E}\right)^2 \Delta E^2 + 2 \sum_{i,k} \frac{\partial\sigma}{\partial f_i} \frac{\partial f_i}{\partial E} \frac{\partial\sigma}{\partial f_k} \frac{\partial f_k}{\partial E} \Delta E^2 \quad , \tag{4}$$

where the first term is the cross section uncertainty caused by the energy dependence of the cross section and the second term is that caused by the energy dependence of efficiencies and corrections. The third term is a pairwise sum which causes a reduction if two of the factors have the opposite energy dependence. The first term usually suffices because of the second-order nature of corrections and the choice of flat-efficiency detectors. The same expression [4] applies for ratio measurements with $\sigma \to R$. However, the cross section uncertainty of a cross section measured relative to another cross section and used as such in the evaluation is given by

$$\Delta\sigma_E^2 = \left(\frac{\partial\sigma}{\partial E}\right)^2 \Delta E^2 + \left(\frac{\partial\sigma_R}{\partial E}\right)^2 \Delta E^2 - 2 \frac{\partial\sigma}{\partial E} \frac{\partial\sigma_R}{\partial E} \Delta E^2 \quad , \tag{5}$$

A measured value differs from the true cross section by the true errors:

$$\sigma_i = \sigma_o + \sum_{k=1}^{m} p_{ik} \frac{\partial\sigma_i}{\partial f_{ik}} \Delta f_i + v_i \quad , \tag{6}$$

where σ_i is the measured value, σ_o is the true cross section $\partial\sigma_i/\partial f_{ik}$ is the sensitivity of the cross section to the k.th factor used to derive the measured value, and Δf_{ik} is the estimated uncertainty for this factor. The p_i have some distribution (normal if the uncertainty is statistical) but are unknown. Also unknown is the additional unknown error v_i. It is not possible to determine the true errors (along with the true value σ_o) because the system of equations obtained with repeated measurements remains hopelessly underdetermined.

II.4. Energy Range, Average Cross Sections, Fluctuations

The energy range choosen for an evaluation which has the aim of obtaining the best knowledge must be selected based on regions of available absolute data information. A limited energy range may be of interest for particular applications, for example fast reactor design calculations. The best knowledge of the cross sections in this range is not only determined by measurements within this range but by well known absolute thermal and 14 MeV cross sections as well. Energy dependent absolute and shape measurements provide the link between the range of interest and such particular sources of information as values at .0253 eV and 14 MeV.

We are interested here in the evaluation of average cross sections. At thermal energy this is simply the value at 0.0253 eV. In the resolved resonance range bin average values would be used. Above the resolved resonance range the cross section values at specific energies, averaged over fluctuations which exist for some of the cross sections in the unresolved energy range, are the subject of the evaluation.

Experimental values measured in a range of fluctuating cross sections depend on the resolution of the measurement and require a correction in order to obtain average cross section values. Such corrections can be obtained from high resolution measurements which are available for Au(n,γ), ^{238}U(n,γ) and ^{235}U(n,f). Where such measurements are not available (e.g. above 100 keV) an error may be estimated by extrapolation from the high resolution data available at lower energies [15, 16, 17].

For many evaluations an energy grid is established for which cross section values are obtained [9, 12, 13, 14, 17]. The energy grid density should be choosen to present the gross structure of the cross section. Somewhat different techniques are used to obtain "experimental values" at these grid points. The method used here and at previous occasions [12] is demonstrated in Fig. 4. Experimental values from one data set which are within the range given by the centers between neighboring energy grid points are extrapolated to the grid point by using the shape obtained from (in sequence of preference)

i) an analytical a priori representation of the cross section (for example available for the H(n,n) cross section)

ii) a polynomial fit through neighboring points of an a priori cross section.

The weighted average value is then obtained at the grid energy point. The error of this point consists of the minimum systematic error of the contributing data values and a reduced statistical error.

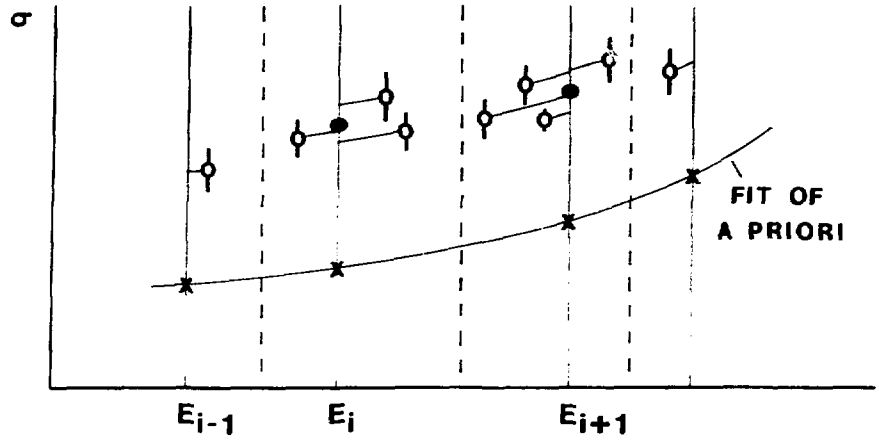

Fig. 4. Energy Grid and Procedure to Obtain "Experimental" Values at a Grid Energy.

Another approach is used by Schmittroth and Schenter [14], who introduce triangle or "roof" functions centered around the grid point. This procedure corresponds to the above, using linear extrapolation. Bhat [13] uses a polynomial fit of the difference between the experimental values and an a priori cross section. The latter procedure requires that grid values are only picked where data are in the vicinity of the grid energy. Tagesen et al. [27] form the average of data points adjacent to the grid point (correcting for the energy dependence of the cross section) and assign as an error the average error which appears to be an overestimate.

III. THE EVALUATION OF THE EXPERIMENTAL DATA

III.1. The Least-Squares-Estimator

The method of least-squares-evaluation of overdetermined data was devised by Gauss [18] (in prep school) and independently by Legendre [19] about 180 years ago. Though Legendre's publication on the subject actually preceded that by Gauss, the latter appears to be most frequently credited with this method in the literature, presumably because it has been generally accepted that he used the technique for some 10-15 years prior to its publication in all his calculations, and because he provided a foundation for the theory of least-squares-estimation (actually three successive explanations, the second basing on maximum likelihood estimation, previously derived by Bernoulli, and the third, the most general, based on the requirement of an unbiased estimator of minimum variance).

The unknown quantities in our consideration are the cross sections $\sigma_\ell(E_i)$, where ℓ refers to a specific reaction and E_i to the energy grid values. The energy grid must be identical for all cross sections; however, not all cross sections need to be included at all grid points. Additional unkonwn quantities are the normalization factors, a_k, of the cross section shape and ratio shape measurements. We denote the unknowns in consecutive order with σ_1, σ_2 ... σ_j, a_1, a_2 ... a_ℓ, where σ_1, σ_2 ... σ_i are the cross sections at consecutive energy grid points for one of the cross sections, σ_{i+1}, σ_{i+2} .... σ_k those for another, etc.

The values obtained from the experimental data at the grid points with the procedure described above provide the n measured values

$$m_i = f(\sigma_1, \sigma_2 \ldots \sigma_j; a_1, a_2 \ldots a_\ell) \qquad i = 1 \ldots n \tag{7}$$

which overdetermine the system of $j + \ell$ unknown quantities with $n - j - \ell$ degrees of freedom. The least-squares-procedure to remove the overdetermination is to make adjustments, v_i, on the measured values, m_i, in order to obtain a consistent set of values

$$m'_i = m_i + v_i \quad . \tag{8}$$

Making such adjustments, v_i, is justified because the measured values have errors, ε_i, and we may set $v_i = \varepsilon_i$. We minimize the adjustments such that

$$F = \sum_i v_i^2 = \text{Min} \quad . \tag{9}$$

In order to obtain a linear relationship between the measured values, errors, and variables, σ_i, a_k, we make a Taylor-series expansion of f around prior estimated values of σ, a, which we denote ϑ, $\hat{a}$

$$f(\sigma_1, \sigma_2 \ldots \sigma_j; a_1, a_2 \ldots a_\ell) = f(\vartheta_1, \vartheta_2 \ldots \vartheta_j; \hat{a}_1, \hat{a}_2 \ldots \hat{a}_\ell)$$

$$+ (\sigma_1 - \vartheta_1) \left.\frac{\partial f}{\partial \sigma_1}\right|_{\vartheta,\hat{a}} + (\sigma_2 - \vartheta_2) \left.\frac{\partial f}{\partial \sigma_2}\right|_{\vartheta,\hat{a}} + \ldots$$

$$\ldots + (a_1 - \hat{a}_1) \left.\frac{\partial f}{\partial a_1}\right|_{\vartheta,\hat{a}} + \ldots \tag{10}$$

and neglect the higher order terms. In addition, we substitute

$$\delta_i = \frac{\sigma_i - \hat{\sigma}_i}{\hat{\sigma}_i} \quad , \qquad \rho_k = \frac{a_k - \hat{a}_k}{\hat{a}_k} \tag{11}$$

and make a transformation of the measured values

$$M_i = \frac{m_i - f(\hat{\sigma}_1, \hat{\sigma}_2, \ldots \hat{\sigma}_j; \hat{a}_1, \hat{a}_2 \ldots \hat{a}_\ell)}{\Delta m_i} \tag{12}$$

where Δm_i is the squareroot of the variance of the measured value, m_i, i.e. the standard deviation. The set of linear equations which we obtain is

$$M = \frac{\hat{\sigma}_i}{\Delta m} \delta_i + \varepsilon \qquad \text{for cross section measurements} \tag{13a}$$

$$M = \frac{\hat{\sigma}_i/\hat{\sigma}_k}{\Delta m} \delta_i - \frac{\hat{\sigma}_i/\hat{\sigma}_k}{\Delta m} \delta_k + \varepsilon \quad \text{for ratio measurements} \tag{13b}$$

$$M = \frac{\hat{\sigma}_i}{\Delta m} \delta_i + \frac{\hat{\sigma}_k}{\Delta m} \delta_k + \ldots + \varepsilon \quad \text{for total cross section measurements} \tag{13c}$$

$$M = \frac{\hat{a}_\ell \hat{\sigma}_i}{\Delta m} \delta_i + \frac{\hat{a}_\ell \hat{\sigma}_i}{\Delta m} \rho_\ell + \varepsilon \quad \text{for cross section shape measurements} \tag{13d}$$

$$M = \frac{\hat{a}_\ell \hat{\sigma}_i/\hat{\sigma}_k}{\Delta m} \delta_i - \frac{\hat{a}_\ell \hat{\sigma}_i/\hat{\sigma}_k}{\Delta m} \delta_r + \frac{\hat{a}_\ell \hat{\sigma}_i/\hat{\sigma}_k}{\Delta m} \rho_\ell + \varepsilon$$

for a ratio shape measurement, and (13e)

$$M = c_i \delta_i + c_{i+1} \delta_{i+1} + \ldots \ldots + \varepsilon \tag{13f}$$

$$C_i = \frac{\phi_i \Delta E_i}{\sum \phi_k \Delta E_k} \cdot \frac{\hat{\sigma}_i}{\Delta m} \qquad \text{for an average cross section measurement.}$$

Equations (13a-f) give the expressions obtained for the different types of measurements considered here. Expressions for other quantities can be obtained as easily.

These equations can be written as a matrix equation

$$M = A\,\delta + \varepsilon \tag{14}$$

where M is the measurement vector, A is the coefficient matrix, δ is the vector of the unknowns (actually containing ρ as well), and ε is the error vector. We obtain the least-squares estimator for δ by minimization of the scalar

$$F = \varepsilon^T C_M^{-1} \varepsilon = (M - A\delta)^T C_M^{-1} (M - A\delta) \tag{15}$$

where C_M is the variance - covariance matrix of M, and T denotes the transpose. We assume that the variance - covariance matrix, C_m, of the measurements, m_i, is known and obtain the variance - covariance matrix, C_M, from

$$C_M = Q\, C_m\, Q^T \tag{16}$$

where for a linear transformation, as above,

$$Q = \begin{pmatrix} \frac{\partial M_1}{\partial m_1} & \frac{\partial M_2}{\partial m_1} & \cdots \\ \frac{\partial M_1}{\partial m_2} & \frac{\partial M_2}{\partial m_2} & \cdots \\ \vdots & \vdots & \\ \vdots & \vdots & \\ \vdots & \vdots & \end{pmatrix} \tag{17}$$

Choosing the transformation Eq. (12) results in the correlation matrix of the originally measured values

$$\text{VAR-COVAR (M)} = C_M = \text{COR (m)} \quad . \tag{18}$$

According to the Gauss-Markov-theorem, extended to correlated measurements by Aitken, the least-squares-estimator is an unbiased estimator with minimum variance. Minimization of F is achieved with

$$\frac{\partial F}{\partial \delta_i} = 0 \tag{19}$$

which yields the normal equations for δ,

$$\delta = (A^T C_M^{-1} A)^{-1}\, A^T C_M^{-1} M \tag{20}$$

and following from error propagation

$$C_\delta = (A^T C_M^{-1} A)^{-1} \tag{21}$$

as the variance - covariance matrix of the least-squares-estimator δ. The results for the σ's are derived from the δ's and the variance - covariance matrix, as above, from C_δ

$$\sigma = (1 + \delta) \cdot \hat{\sigma} \quad , \; a = (1 + \rho) \cdot \hat{a} \quad , \; C_\sigma = Q\, C_\delta\, Q^T \; , \tag{22}$$

Q, of course, derived from the different transformation.

Using, as an approximation, the assumption of uncorrelated data yields

$$C_M = I \quad ,$$

the identity matrix, and therefore

$$\delta = (A^T A)^{-1} A^T M \quad , \tag{23}$$

with

$$C_\delta = (A^T A)^{-1} \quad . \tag{24}$$

We note that $A^T C^{-1} A$ and $A^T C^{-1} M$ in Eq. 20 have the same structure and we can include M as an additional column vector in A. Instead of inverting C we could then resolve the linear equation system $A = CB$, where $B = A^T C^{-1} A_{r+1}$, which is computationally faster and more accurate. Likewise, the solution, δ, can be obtained from the resolution of the linear equation system $(A^T B_r)\delta = A^T B_{r+1}$, if we are not interested in the variance - covariance of the solution, δ.

The formalism summarized above is represented in textbooks too many to reference here, some of the more handy for applications are given in Ref. 20. In some of these FORTRAN programs ready to use for obtaining the solution, $\delta = (A^T C^{-1} A)^{-1} (A^T C^{-1} M)$, are given, but usually only usable for small n. Software packages for matrix inversions and the resolution of linear equation systems are readily available. At Argonne, a software package, LINPAC, is available which was developed at Argonne in cooperation with other laboratories and universities and is extremely efficient [21].

The coefficient matrix, A, is of size N(=n) x R(=j+ℓ). Its structure is shown in Fig. 5. The elements, a_{ik}, are the coefficients from the Taylor series expansions (Eqs. 13a-f). Usually no more than three elements in a row are nonzero. However, for total cross section values, each partial cross section has a nonzero entry. For average cross section data as many entries as there are unknowns for this cross section are nonzero. Columns are similarly nearly empty. But for shape data there are as many entries as experimental values in the set. The coefficient matrix consists of submatrices given by the experimental data sets as indicated in Fig. 5.

The correlation matrix, C_M, is of size N x N and its structure is shown in Fig. 6. It consists of submatrices around the diagonal which correspond to the correlation matrices of particular data sets, and nonzero off-diagonal blocks which contain the correlation coefficients between different experiments.

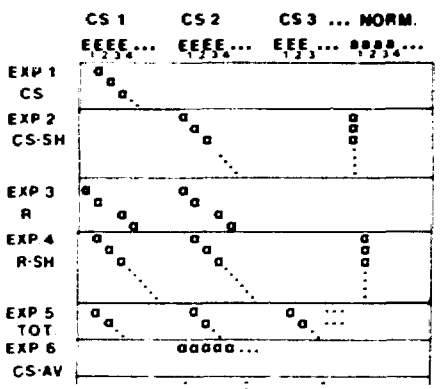

Fig. 5. The Entries into the Coefficient Matrix, A.

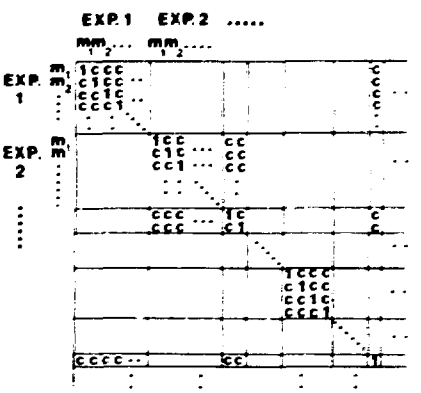

Fig. 6. Schematic of the Correlation Matrix, C.

A consistency least-squares-fit of measured values for two activation cross sections of ^{115}In, a ratio between them, and an absorption cross section at thermal energy [22] may serve as a very simple example for the application of the above formalism to nuclear data. Four experimental values were available for only two unknowns and a least-squares-fit provided a consistent set of values. The same procedure was used to obtain consistent data for several energy-dependent cross sections by employing Eq. 23 [9]. The formalism has been applied more recently for the evaluation of single cross sections as a function of energy using Eq. 20 [42, 14].

The size of the presently considered system is not quite that simple. We are concerned about the simultaneous evaluation of ~10 cross sections, an energy grid of ~100 points appears desirable, and about 10 measurements are available per cross section (less for some, more for others; also ratio and total cross section measurements would have to be counted). Thus, we estimate that $N \sim 10^4$. We find that the correlation matrix, C, alone exceeds computer core memory by several orders of magnitude. Since we recognized that many elements of the coefficient matrix, A, and the correlation matrix, C, are zero, sparce matrix storage and handling might be used (a sparce matrix software package, for example is available at the Harwell Software Library). Inversion of the correlation matrix as well as the subsequent matrix multiplication would take days and appears cost-prohibitive.

III.2. Approximations Used to Avoid the Monstrous System of Normal Equations and Their Shortcomings

The easiest way out of the seemingly huge system of normal equations (Eq. 20) would be to find approximations which are well justified. Before considering such approximations, let us first consider a procedure which is commonly used (probably without realization that it is an approximation to the correct least-squares procedure) and yields a biased estimator which is not of minimum variance.

It is common practice to normalize cross sections, most often obtained relative to another cross section, at thermal energies. Evaluators use such data by updating to the most recent reference cross sections and thermal cross section value. Then they obtain an (hopefully weighted) average values at all energies higher than thermal. Subsequently the possible agreements or discrepancies are pointed out and commended or lamented. The procedure appears to be logical as the thermal value is the preferable absolute value available for these measurements. However, this procedure represents a separation of the general least-squares problem into two steps, each of which may have been handled by the least-squares method. The separation introduces an approximation and results in a biased estimator which does not have minimum variance. The difference between the "logical" use of the available information and the least-squares procedure is shown in Fig. 7. The answer is, of course, different. The difference (the bias) can be easily estimated. It will be $\lesssim 0.3\%$ if the shape values differed by ~10%, thus it is small compared with the data difference. However, the difference for the variance may be much larger, depending on its derivation for the "logical" procedure.

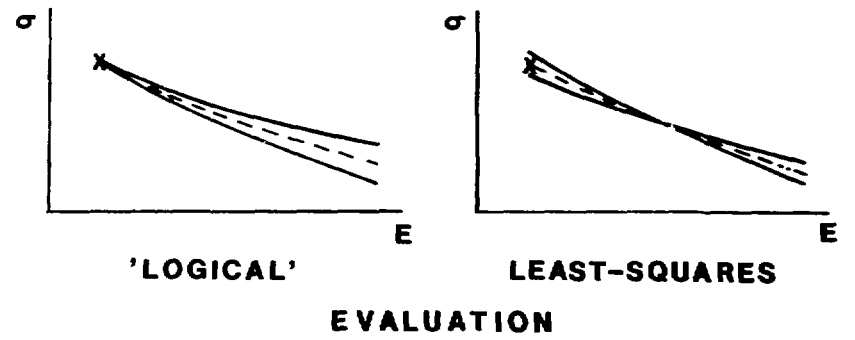

Fig. 7. Comparison of a "Logical" and the Least-Squares Evaluation.

Next, we consider approximations intentionally made to avoid the size of the system given with Eq. 20. The major problem appears to be the correlations which require Eq. 20 to be used instead of Eq. 23. Correlations between experimental data sets can be easily removed. Three different cross sections measured by the same experimentalists using the same neutron flux detection technique or the same calibrated neutron detector provide information for one of these cross sections, say $\sigma_1(E)$, and the ratio between the other two, $R_{23}(E) = \sigma_2(E)/\sigma_3(E)$. Measurements of a cross section with the same sample as used in another measurement of the same cross section can be used as a shape data set. The correlations are removed in each of these examples without loosing much information. Most other sources for correlations between different data sets were already removed by using the originally measured quantities, e.g. ratios, for the evaluation.

The major source of correlations between values of one data set seems to be due to the normalization (mass, efficiency, etc.). To give an example: The recent absolute measurements of the ratio between the cross sections $^{235}U(n,f)$ and $H(n,n)$ by Kari [23] have a total uncertainty of ~3% of which ~2.5% are due to the normalization and ~1% due to statistics. Other measurements, mostly for the shape of a cross section or ratio, have small systematic and thus negligible correlated errors. For example, the measurements of the shape of $\sigma_{n,f}(^{235}U)/\sigma_{n,n}(H)$ by Carlson and Patrick [24] have an uncertainty of ~2-3% but only a 0.5% systematic uncertainty.

This suggests to separate the evaluation of the shape from the evaluation of the normalization. The data would be treated as totally uncorrelated for the shape evaluation and as totally correlated for the evaluation of the normalization. We immediately recognize that we obtain a biased estimator as a consequence of separating the evaluation into two steps as shown above. However, because the bias appears to be very small, this will be acceptable. This procedure was used in various evaluations [9, 12, 25].

The evaluation of the shape can be carried out in several ways:

i) The energy dependent absolute data and the shape data are normalized to an 'a priori' cross section and then a least-squares estimator is obtained [9]. The discontinuity of the available data information may result in a dependence on the a priori cross section which might not be removed in iterative steps.

ii) The unknown normalization contained in the equations [13] can be removed by Gaussian elimination. This corresponds to forming the ratio of the measured shape data (or absolute data) to a value at any energy, $R_{ik} = a\cdot\sigma(E_i)/a\cdot\sigma(E_k)$. The evaluation of the ratios, R_{ik}, by least-squares methods then defines the shape of the cross section [25].

iii) Another method recently devised to avoid the small bias introduced by separating the shape evaluation from the normalization evaluation consists of shifting the shape "up or down" parallel to the σ - axis. This corresponds to adding or subtracting a constant to the measured values which appears to be in contradiction to the way the experimental data are derived (see Eqs. 1-3, the normalization is a factor, thus "shifting" would be only permissible on a logarithmical scale). The problems this procedure creates can be easily demonstrated if the shape measurements change over a large range. For example, suppose two measurements of $^{235}U(n,f)$ were quoted at thermal energy with 587b and 585b and at 30 keV with 2b and 1.9b, respectively, and they were shifted to a new normalization value of 583b at thermal. The result at 30 keV would be -1.05b.

III.3. The Solution of the Least-Squares Problem

We realize that Gauss and his contemporaries must have faced a similar problem (as we do today) with the large number of the normal equations. Of course, their data base was small compared to ours, maybe 100-200 values where we have 10^4. However, they did not have a computer. And indeed, Gauss points out in his supplement on the theory of least-squares [26] that, if a new data value becomes available, the calculation does not have to be repeated but the new value can be easily combined with the prior result. Gauss proceeds to provide proof for this and draws the obvious conclusion that reduced calculational effort will result by subdividing a large data base and to obtain subset-estimators which are to be combined in a subsequent step.

Using this suggestion, we first rearrange the sequence of the experimental data sets in such a way, that those which are correlated appear in one block. This results in a correlation matrix shown in Fig. 8. A convenient feature of a number-matrix of this type is that its inverse has the same structure and consists of the inverses of the submatrices. The subdivision of the matrix is given by the correlated and uncorrelated data sets. The simple rules of matrix multiplications immediately lead to the conclusion that $C^{-1}A$ has again a subdivision by data blocks, as shown also in Fig. 8. Multiplication with the transpose of the coefficient matrix, A^T, however, does not retain this separation. But we realize that the resulting matrix $B = A^TC^{-1}A$ has elements, β_{ik}, which are additive contributions from the different data blocks. The triple products which contribute to the element, β_{ik}, can be arranged in a similar geometric structure as the structure of the matrix, C. The result of the above is that we do not need to store the huge correlation matrix, C, we do not need to invert it, which reduces the problem of computer

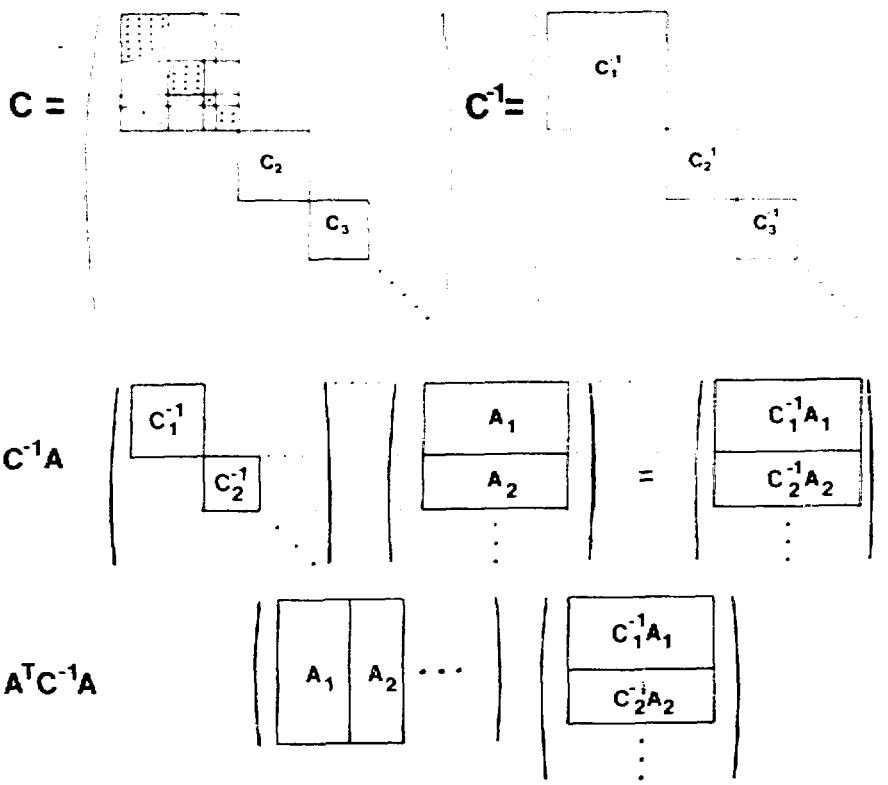

Fig. 8. The Reordered Correlation Matrix, C, and the Separation of Experimental Data Blocks in $A^T C A$.

time and storage space by several orders of magnitude. The contributions of the matrix product $A^T C^{-1} A$ to the elements β_{ik} can be obtained by handling one correlated or uncorrelated data block at the time. Sparce matrix storage and handling can be employed for the A matrix which further reduces the size of the required DO - loops.

The addition of a new data set, once a solution has been obtained, becomes as straightforward as shown by Gauss [26] and has been extended to correlated data as well [28]. The solution after evaluating i experimental data blocks and obtaining a new, (i + 1)th block which is uncorrelated with the previous data is obtained from

$$\delta_{i+1} = C_{\delta_{i+1}} A_{i+1}^T C_{i+1}^{-1} M_{i+1} \qquad (25)$$

$$C^{-1}_{\delta_{i+1}} = C^{-1}_{\delta_i} + A^T_{i+1}\ C^{-1}_{i+1}\ A_{i+1} \qquad (26)$$

It has been shown by Schmittroth [45] that the inversion of the matrix in Eq. (26) which is required for use in Eq. (25) can be avoided.

It appears that the simplest procedure to add new information would be to do this directly by addition to the matrix elements, β_{ik}. A new measurement which is correlated with a data set previously included in the evaluation would require to first subtract the contribution from this set, combine it with the new data and then to add the new correlated block. Use of iterative steps in the evaluation appears also more straightforward by working directly with the β_{ik}'s.

III.4. The Variance - Covariance of the Result

Using the evaluation method outlined above provides the variance - covariance matrix of the result, $(A^TC^{-1}A)^{-1}$ for correlated data, and $(A^TA)^{-1}$ for uncorrelated data. We note that off-diagonal nonzero correlation coefficients occur even if the original data were (or were assumed to be) uncorrelated. The source for these correlations of the result are the ratio and total cross section measurements. It seems to be an obvious advantage to obtain the variance - covariance matrix as integral part of the evaluation process. In contrast, subsequent derivation of the uncertainty information appears to lead to many problems. For example, if the evaluation was biased, the subsequent derivation of the uncertainty will be unsymmetric.

The large amount of data contained in the correlation matrix usually causes it to be given in a reduced form. Care must be taken not to improperly extrapolate such information. The evaluated results still have a random error contribution. Thus extrapolation should not be to the diagonal 1.0 but to a lower value (see Fig. 9). However, if the evaluation result of the experimental data was subsequently fitted with a nuclear model, correlation increases for adjacent energies and a shape of the correlation matrix indicated by the dashed line in Fig. 9 can be expected.

The variance - covariance matrix in the above formalism is derived from error propagation, based on the assumption of random errors. Thus the variance of the estimator of a set of values, σ_i, with weights, w_i, is given by

$$V = \frac{\sum w_i\ (\sigma_i - \sigma)^2}{(n-1)\ \ w_i} \quad . \qquad (27)$$

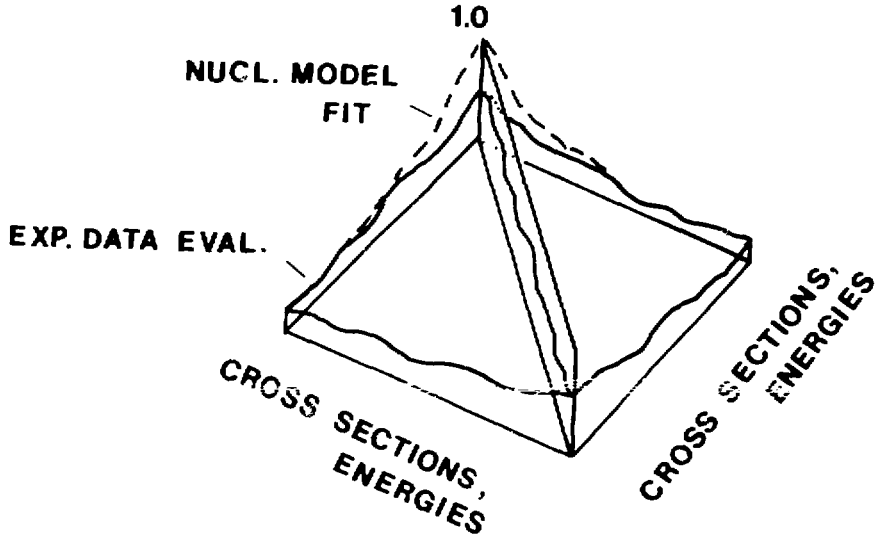

Fig. 9. Graphical Representation of the Correlation Matrix of the Result.

This probably will underestimate the true uncertainty of the result as the errors are not truely random. The problem has been often discussed but no unique answer exists. Grigoryan et al. [29] adjust the variance based upon differences between the external and internal errors by various combinations thereof, based upon prior work by Birge [30]. Tagesen et al. [27] select the larger of the external or internal error. Peelle [31] used a χ^2 test and suggests to increase the uncertainties by $\sqrt{\chi^2}$.

III.5. The Use of the Solution and its Variance - Covariance in Iterative Steps and Additional Analysis.

There are several reasons for using iterative steps, e.g. repeating the evaluation after a result was obtained. A rather trivial reason is that the Taylor-series expansions, Eqs. (13a-f), result in some cases in non-zero higher order terms. Of greater concern must be the influence of discrepant data on the result, specifically if such data are quoted with small (internal) errors. Usachev [32] points out that the evaluator obtains an improved knowledge of the quantity and thus has a means to find possible unknown errors of individual measurements. The problem is widely discussed in the literature [33] but procedures differ and have some subjective character. These methods range from rejection (Chauvenet's criterion) to error adjustment. It appears in the

area of nuclear data more often than once that a new measurement resulted in values which were in disagreement with prior reported data sets of good consistency but were later proven to be correct or at least in the "right direction". Thus, the rejection of data, employed for example by Tagesen et al. [27] is not to be recommended. Introduction of weights based on the evaluators judgment [10] appears to introduce subjective elements. The best procedure seems to be to add an unknown error to the discrepant measurement based upon a criterion for the probability that the measurement result represents the true values. A lesser than 2.3% (2 standard deviations) probability seems to be sufficiently cautious.

A more detailed analysis may be carried out and error reassignment refined. A χ^2-test of the shape of a data set would reveal whether statistical errors were appropriately accounted for, or accidental errors occurred. It can be tested whether the unknown error was due to the normalization or energy dependent systematic effects. The reassigned error can then be accounted for as totally or partially correlated.

IV. THE USE OF AUXILIARY INFORMATION

The result obtained from the evaluation of the experimental data can be further improved by utilizing nuclear models. The first obvious benefit comes from a fit of the evaluated data with a nuclear model. The evaluated experimental data will show local fluctuations which are caused by statistical (uncorrelated) errors, data inconsistencies and an insufficient number of input data at some energy grid points. A nuclear model fit will remove these fluctuations and provide a result which is highly correlated for adjacent energies. This is shown for the capture cross section of ^{238}U in Fig. 10.

The nuclear model may also be used to obtain cross section information which is independent on the evaluated experimental cross sections, if other experimental data are available to determine the model parameters. In case of the capture cross section of ^{238}U, the major parameters are

V The real optical potential strength,

V_E The energy-dependence of V,

R_R The radius of the real potential,

A_R The diffusness of the real potential,

W The imaginary optical potential strength,

W_E The energy-dependence of W,

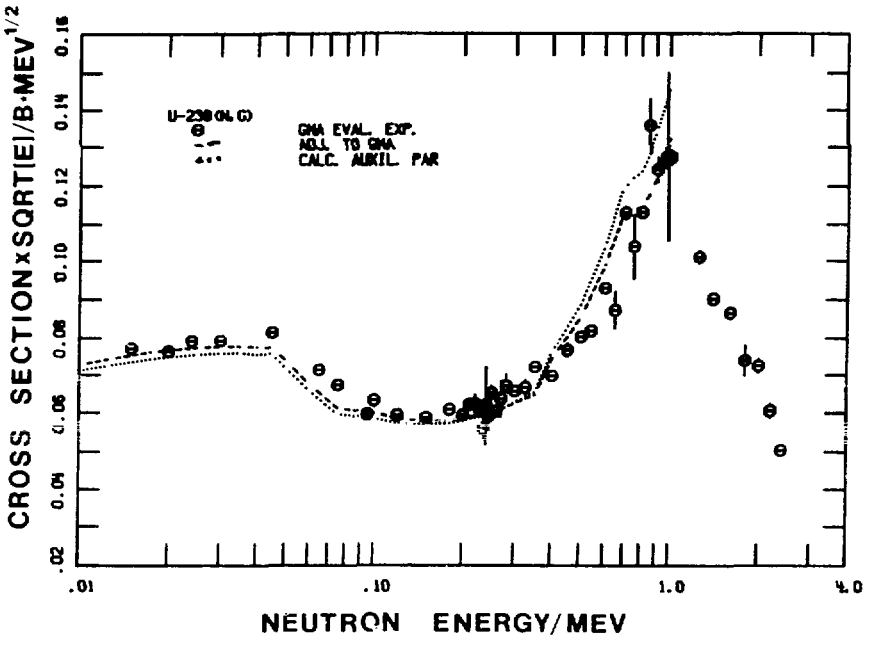

Fig. 10. Theoretical Model Calculations for $^{238}U(n,\gamma)$.

R_I	The radius of the imaginary potential,
A_I	The diffusness of the imaginary potential,
V_{SO}	The spin-orbit potential strength,
a	The level density parameter related to nuclear temperature,
σ	The spin-cut-off parameter of the level density,
E_G	The energy of the giant dipole resonance,
Γ_G	The width of the giant dipole resonance,
E_i, J_i, π_i	Parameters of low lying levels of the target nucleus,
Γ_γ/D	The gamma width over the average level spacing near the binding energy.

More refined models require the introduction of more parameters. The optical model parameters, V through V_{SO}, can be determined with total and scattering cross section measurements. Values for the level density parameters are known from a variety of sources. Γ_γ/D may be calculated from the level density formula and the giant dipole resonance, however, the resulting values are in substantial discrepancies with measured values. Thus, one prefers to use Γ_γ/D as determined experimentally close to the neutron binding energy.

In order to combine the cross section obtained from the nuclear model calculation with the directly evaluated data, its uncertainty has to be known. It consists of several components:

i) The data uncertainties used to derive the model parameters cause uncertainties of these parameters

ii) The model approximations cause uncertainties of the predictions.

The former can be quantitatively determined, however, the latter are much more difficult to assess. The next step is the determination of the sensitivity of the calculated cross section to the model parameters and to obtain its uncertainty.

The cross sections obtained from the fit of the evaluated experimental data can now be combined with the cross section obtained from the nuclear model calculation which is based upon other auxiliary data information by obtaining a weighted average. This is shown in Fig. 10 using again $^{238}U(n,\gamma)$ as an example. Another approach would be to include the model prediciton with its uncertainty in the original least-squares fit as an input set.

V. COMPARISON OF VARIOUS EVALUATIONS

The least-squares fitting program used in 1970 [9] which based on Eq. 23 was modified in order to include correctly correlations according to Eq. 20. This program is called GMA (for Gauss-Markov-Aitken) and follows the outline given in Sections III.1 and III.3. Results obtained with this program may be compared with other evaluations for which approximations were used. A first run was made using as input only data for $^{235}U(n,f)$ and ratios to H(n,n) above 100 keV. This permits to compare the GMA result with the evaluations by Konshin et al. [34], Poenitz [12], and Bhat [35]. The data base used by Konshin et al. was somewhat different from the one used by Poenitz and by Bhat. Konshin et al [34] included correlations in the determination of weights for the experimental data. Their procedure differs from the commonly used method which was summarized in Section III.1, however, should be expected to lead to similar results. Poenitz [12] used approximations

to handle correlations as outlined in Section III.2. Bhat [35] employed a technique of data fitting which was developed by Forsythe [36], neglecting correlations. Fission spectrum average cross sections were used by Poenitz but not by Konshin et al. nor Bhat. The results from these evaluations are compared in Fig. 11 with the result from GMA. Interative steps (see Section III.5) and nuclear model smoothening were not yet applied in GMA.

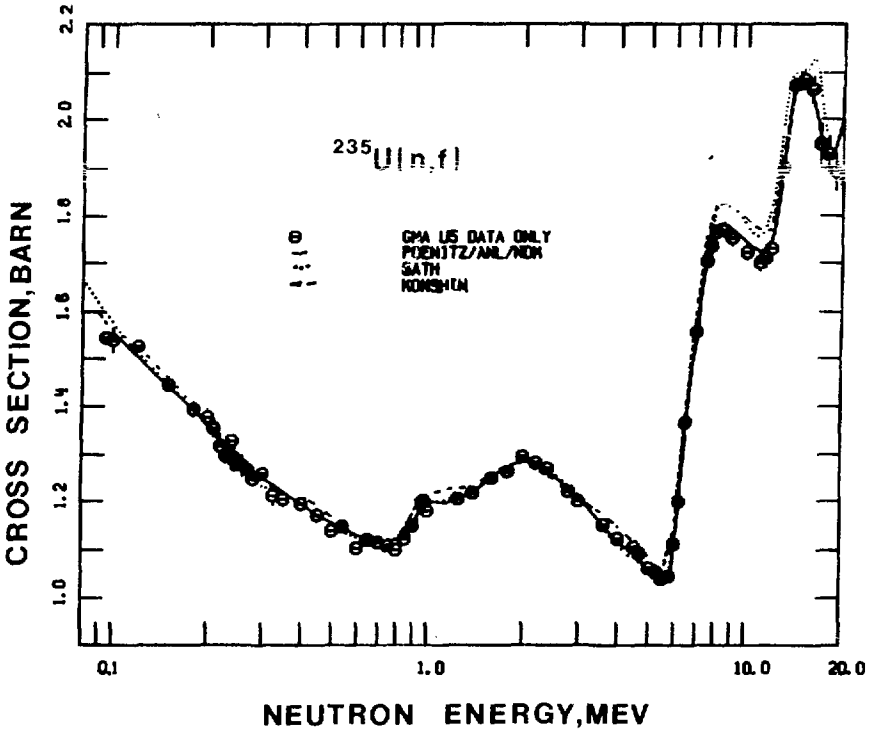

Fig. 11. Comparison of Several ^{235}U(n,f) Evaluations.

The agreement between the evaluations by Poenitz [12] and by Bhat [35] is very good in the energy range from 100 keV to 6 MeV and confirmed by the present GMA result. The evaluation by Konshin et al. [34] differs by 2-3% in the energy ranges 0.8-1.5 MeV and 3.5-6 MeV. The difference appears to be due to several factors: i) one particular data set has an excessively high weight between 1 and 6 MeV, ii) the cross section uncertainties due to energy uncertainties were not taken into account, and iii) the data base was lacking some of the newer sets included by Poenitz [12] and by Bhat [35].

Konshin et al. [34] obtained between 8 and 12 MeV ~2.5% higher values as a consequence of their higher values between 3.5 and 6 MeV, this means that they agree in shape with the evaluation by Poenitz [12], a result also confirmed by GMA. The evaluation by Bhat [35] differs above 8 MeV by ~2.5% and more than 4% at 16 MeV. This appears to be the consequence of not taking into account the correlated errors.

A more direct comparison can be made by consideration of the ratio between values in the 8.0-8.5 MeV range vs. the 5.0-5.5 MeV range:

Experimental values	
Kari [37]	1.687 ± .028
Czirr and Sidhu [39]	1.688 ± .019
Poenitz [40]	1.745 ± .061
Smith et al. [41]	1.625 ± .036
Average	1.681 ± .015
Ratios from Evaluations	
Konshin et al. [34]	1.703 ± .029
Poenitz [12]	1.710
Bhat [35]	1.736
GMA (present)	1.680 ± .016

Correlated errors were taken into account in the calculation of the experimental ratio values.

The least-squares consistency fit of data for $^{235}U(n,f)$, $^{197}Au(n,\gamma)$, $^{238}U(n,\gamma)$ and $^{6}Li(n,\alpha)$ resulted 10 years ago in substantially lower $^{235}U(n,f)$ cross section values than the direct measurements would have indicated (Poenitz [9]). This difference appears to be much less for the present data base, e.g. the consistency of the experimental data has greatly improved. Figure 12 shows the difference between the GMA result for $^{235}U(n,f)$, using $^{235}U(n,f)$ data alone and using data on $^{235}U(n,f)$, $^{238}U(n,\gamma)$, $^{197}Au(n,\gamma)$, $H(n,n)$, $^{6}Li(n,\alpha)$, $^{6}Li(n,n)$, $^{10}B(n,\alpha)$, $^{10}B(n,\alpha\gamma)$, and $^{10}B(n,n)$, and ratios as well as total cross sections for these reactions. This result may somewhat change as all data were not yet included in the fit.

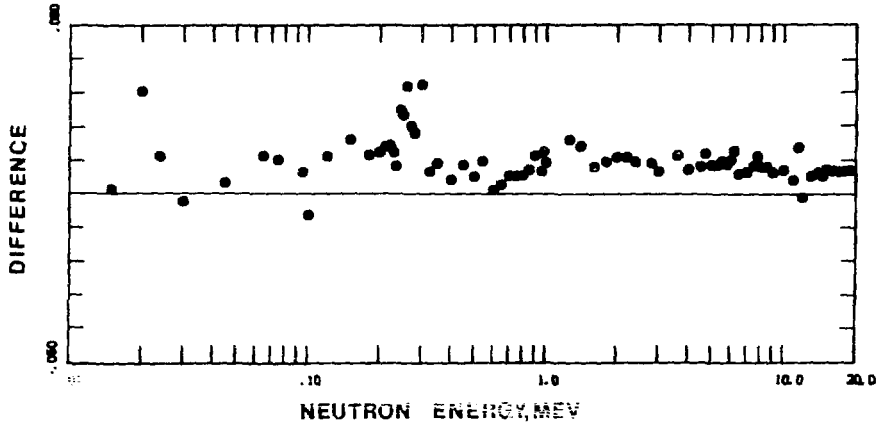

Fig. 12. The Difference for $^{235}U(n,f)$ between an Evaluation of $^{235}U(n,f)$ Data and a Simultaneous Evaluation of Several Cross Sections.

The thermal cross section of $^{235}U(n,f)$ evaluated by Leonard [37] (583.54 ± 2.92 b) was used as input for the fit. The fitting result is 588.6 ± 2.5 b, in better agreement with a value which would be obtained from a consistency fit of the 2200m sec data (Lemmel [39]). The thermal cross section for $^{6}Li(n,\alpha)$ obtained from the GMA fit is 942.4 ± 2.4 b in contrast with 935.9 B presently used on ENDF/B-V. Antoher "oddity" appears to be that the GMA evaluated value for $^{235}U(n,f)$ at ~14 MeV is lower than any of the measured values (by ~1.5%).

An interesting consideration is the H(n,n) cross section. It is sometimes pointed out that cross sections measured relative to the H(n,n) cross section should be preferred (or heavier weighted) in an evaluation because the H(n,n) cross section is so well known. This appears to be a pseudological or incomplete logical argument because the uncertainty of a cross section measurements does not depend on the uncertainty of the reference cross section alone, but on its implementation as well (besides other factors). The H(n,n) cross section is well known because it is identical to the total cross section (above thermal energies), but in cross section ratio measurements it is used as a reaction cross section and the problems associated with the determination of the reaction rate seem to have caused discrepancies up to ~30%. The present fit indicates somewhat lower cross sections for $\sigma_{n,n}(H)$ at higher energies (>3 MeV). This may be a consequence of $^{235}U(n,f)$ absolute data which are lower than those measured relative to H(n,n).

VI. CONCLUSIONS AND RECOMMENDATIONS

VI.1. Evaluation Procedures

It was shown that the simultaneous evaluation of the most important cross sections (standards and $^{238}U(n,\gamma)$, probably $^{239}Pu(n,f)$ to be added) is feasible. It is therefore recommended that these cross sections should be obtained from such evaluation for ENDF/B-VI. The merit of "randomizing" the systematic errors by involving several cross sections in a simultaneous evaluation can be seen in Fig. 13. The average differences of two evaluations in the 25 keV - 1 MeV energy range relative to the present GMA result (average standard deviations are shown by dashed lines) are shown. In three out of four cases the prediciton from the objective evaluation technique using a least-squares consistency fit proved better than other evaluations at that time [43] and even fall within the (somewhat optimistic) standard deviations of the GMA result. The fourth case is a standoff.

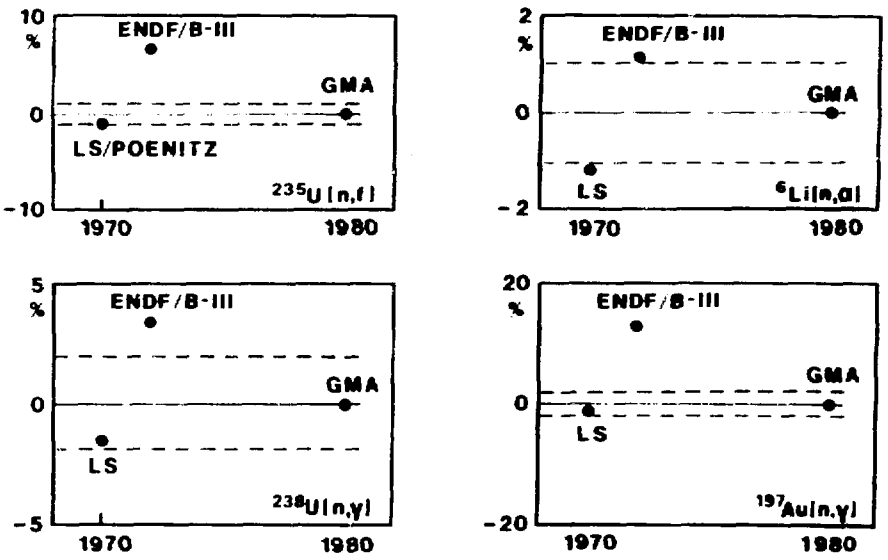

Fig. 13. Comparison of ENDF/B-III and a Least-Squares Evaluation with Present GMA Results. The Average Differences are Shown in Chronological Order.

Subjective evaluation might be very tempting, specifically if the data base is very poor. An example is shown in Fig. 14. Available data for the $^{23}Na(n,2n)$ cross section are discrepant and some evaluators choose one data set above all the others. The evaluation shown in the graph was based upon all available data (Adamski et al. [44]). Which evaluated result will prove

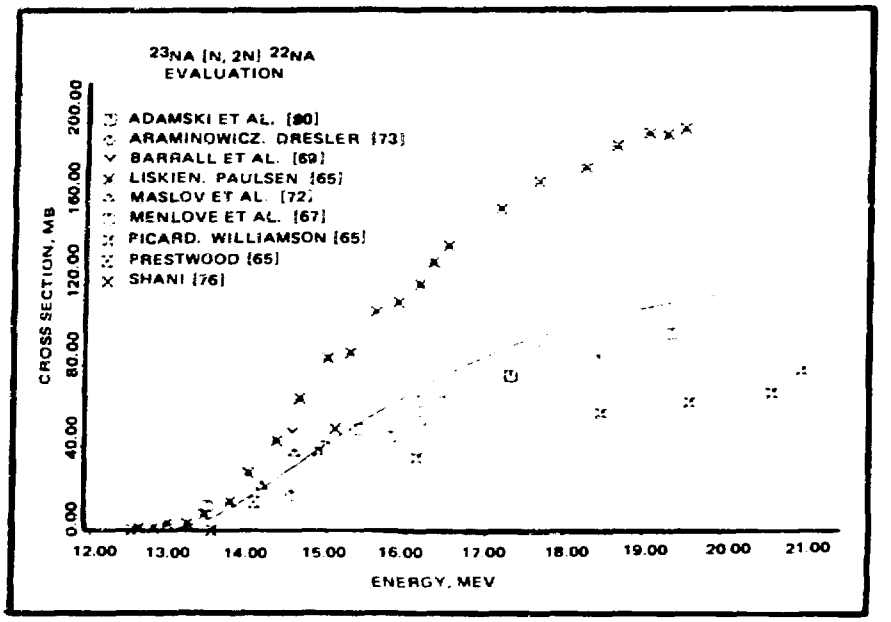

Fig. 14. $^{23}Na(n,2n)$. A Sore Data Base and an Objective Evaluation.

correct remains to be seen, but for now it may be noted that the evaluation which used all the available data appears to agree better with a prediction by Pearlstein's method for calculating these cross sections.

VI.2. Data Reporting and Data Files

Past data reporting has been insufficient, specifically when larger amounts of data were involved. The information needed from the experimenter is, besides the values E, ΔE, Res, $\Delta\sigma$, $\Delta\sigma_{st}$ (see Section III.3), the error components for each data point. This could be stored in a standard format on a data file, for example

$\Delta\sigma_R$ (normalization uncertainty, in percent)

$(E,\ V,\ \Delta E/E,\ Res/E,\ \Delta V_{tot}/V,\ \Delta V_{st}/V,\ \Delta_i,\ i = 1 \ldots k)_\ell,$

$\ell = 1 \ldots n$

for example in 2E10.4, 15F4.1. Here E is the energy, V the measured quantity, $\Delta E/E$ the energy uncertainty, Res/E the resolution, $\Delta V_{tot}/V$ the total error, $\Delta V_{st}/V$ the statistical error, and Δ_i the 11 most important energy-dependent error components; all but E and V in percent. The most important point is that the experimenter gives this information for the actually measured quantity and all the subsets obtained in the experiment. It seems not required that the experimenter derives the variance - covariance matrix for his data, it certainly would be undesirable if that is given instead of the information requested above. The variance - covariance matrix reduces the detailed information and besides requires more storage space.

VI.3. Improvement of Knowledge

Our knowledge of the cross sections important for practical applications is determined by the experimental data base. In order to improve our knowledge we have two options:

i) to reanalyze the data base at hand

ii) to add to this data base improved information.

A decision which choice to make will depend on the cost-efficiency much more than anything else. A recent study of past measurements of $\bar{\nu}$ of ^{252}Cf cost about one man year [45]. Ten measured values are in that data base of which four were re-analyzed. We have to deal with $\sim 10^4$-10^5 data values in several hundred data sets. This suggests an expenditure of ~100 man years and we suggest that this will not be cost-effective. Past data give us a standard deviation of ~1% for the evaluated cross section of $^{235}U(n,f)$ and ~2-3% for $^{238}U(n,\gamma)$. Working these data over which have at best 2-3% uncertainties and differ by up to 10% for $^{235}U(n,f)$, and have uncertainties of ~3-5% and differ up to 20% for $^{238}U(n,\gamma)$ will not improve our knowledge significantly. It is suggested that instead of reshuffling the same old data, a new generation of measurements should be made. These new measurements must be usable to test the significance of our prior kowledge. For $^{235}U(n,f)$ and $^{238}U(n,\gamma)$ this means that only measurements with $\lesssim$1% and $\lesssim$2%, respectively, will have any significance.

Another important question which should be ask is whether it will be cost-effective to attempt to recover all the detailed error information of past experiments. An answer can be obtained by assuming the extreme cases for these unknown errors (see Fig. 3). If the results are not significantly different, it will not be cost-effective to expend the resources on the task of improving our knowledge of the detailed errors. A test of this kind was made with GMA and showed that for the presently considered cross sections and their data base the results are not significantly different.

ACKNOWLEDGMENT

The author appreciated helpful discussions with R. Peelle, F. Perey and A. Smith.

Note: The intent of this paper was to discuss evaluation procedures, not to present evaluation results. GMA results quoted or shown may change with improved input and should not be used or quoted as an evaluation result.

REFERENCES

1. E. KANT, "Critique of Pure Reason," McMillan, Toronto.
2. H. H. BARSHALL, Phys. Rev., 86, 431 (1952).
3. D. G. MADLAND, LASL, private communication (1978).
4. D. G. MADLAND and P. G. YOUNG, Proc. Conf. Neutr. Phys. and Nucl. Data, Harwell, p. 349 (978).
5. W. P. POENITZ et al., Proc. Conf. Nuclear Data and Technology, Knoxville (1979), to be published.
6. R. E. SCHENTER and T. R. ENGLAND, Proc. Specialists Meeting on Neutron Cross Sect. of Fiss. Prod. Nuclei, Bologna, p. 253 (1979).
7. T. Y. BARRE, Proc. Specialists Meeting on Neutron Capture of Structural Materials, Karlsruhe, KFK 2046, p. 258 (1975).
8. O. H. WESTCOTT et al., At. Energy Rev. 3, 3 (1965).
9. W. P. POENITZ, Proc. Symposium Neutron Standards and Flux Normalization, Argonne, AEC Symposium Series 23, 331 (1970).
10. M. G. SOWERBY and B. H. PATRICK, Proc. 2nd Intl. Conf. Nuclear Data for Reactors, Helsinki, Vol. 2, 703 (1970).
11. L. N. USACHEV, Intl. Nucl. Data Committee Report, INDC (CCP)-45/L (1974).
12. W. P. POENITZ, Argonne National Laboratory Report, Nucl. Data and Measurement Series, ANL/NDM-45 (1979).
13. M. BHAT, Brookhaven National Laboratory, private communication (1980).

14. F. SCHMITTROTH and R. E. SCHENTER, Nucl. Sci. Eng., 74, 168 (1980).
15. C. D. BOWMAN et al., Proc. Specialists Meeting on Neutron Fission Cross Sections, Argonne, ANL-76-90 (1976).
16. W. P. POENITZ, Proc. Conf. Nuclear Data and Technology, Knoxville (1979), to be published.
17. H. LISKIN and H. WEIGMANN, Intl. Nucl. Data Committee Report, INDC(EUR)-11/G.
18. C. F. GAUSS, "Theoria Motus Corpum Coelestium", Goettingen, 1909.
19. A. M. LEGENDRE, "Nouvelles methodes pour la détermination des orbites des comètes," Paris 1906.
20. S. L. MEYER, "Data Analysis for Scientists and Engineers," John Wiley and Sons, Inc., (1975), also S. BRANDT, "Statistical and Computational Methods in Data Analysis," North-Holland Publ. Comp. (1970), also W. T. EADIE et al., "Statistical Methods in Experimental Physics," North-Holland/American Elsevier (1971).
21. J. J. DONGARRA et al., "LINPACK" Users' Guide, SIAM, Philadelphia (1979).
22. K. H. BECKURTS et al., Nucl. Sci. Eng., 17, 329 (1963).
23. K. KARI, Nuclear Research Center Karlsruhe Report, KfK 2673 (1978).
24. A. D. CARLSON and B. H. PATRICK, Conf. Neutr. Physics and Nuclear Data, Harwell, p. 880 (1978).
25. W. P. POENITZ and P. T. GUENTHER, Proc. Spec. Meeting on Fast Neutron Fission Cross Sections, Argonne, ANL-76-90 (1976).
26. C. F. GAUSS, "Methode der kleinsten Quadrate," Berlin, 1887 (Stankiewicz).
27. S. TAGESEN et al., Physics Data, ISSN 0344-8401 (1979).
28. RAIFFA and SCHLAIFER, "Applied Statistical Decision Theory," MIT Press (1961).
29. YU. I. GRIGORYAN et al, Intl. Nucl. Data Committee Report, INDC(CCP9-75/LN) (1976).
30. R. T. BIRGE, Phys. Rev., 40, 207 (1932).
31. R. W. PEELLE, Proc. Spec. Meeting on Fast Neutron Fission Cross Sections, ARgonne, ANL-76-90 (1976).
32. L. N. USACHEV, Intl. Nuclear Data Committee Report, INDC (CCP)-45/L (1979).
33. E. M. PUGH and G. H. WINSLOW, "The Analysis of Physical Measurements," Addison-Wesley (1966), (also see Ref. 20).
34. V. A. KON'SHIN et al., Intl. Nuclear Data Committee Report, INDC(CCP)-132/LV (1979).
35. M. BHAT, private communication to CSEWG Committee, (1980).
36. F. E. FORSYTHE, J. Soc. Ind. Appl. Math., 5, 74 (1957).
37. B. R. LEONARD et al., Electric Power Research Inst. Report, EPRI-NP-167 (1976).
38. H. D. LEMMEL, Proc. Symp. Neutr. Standards and Applications, NBS Special Publication 493, 170 (1977).
39. W. P. POENITZ, Nucl. Sci. Eng., 64, 894 (1977).

40. R. K. SMITH et al., Bull. Am. Phys. Soc., 2, 196 (K4), (5704).
41. C. FU and F. PEREY, Nuclear Data Tables (1979).
42. M. K. DRAKE, ENDF/B-III Cross Section Measurement Standards, BNL 17188 and BNL 17007 (1972).
43. L. ADAMSKI et al., submitted to Nucl. Sci. Eng., (1980).
44. J. R. SMITH, private communication (1980).
45. F. SCHMITTROTH, Hanford Engineering Development Laboratory Report, HEDL-TME 77-51, UC-79d (1978).

Discussion

Perey

As I understood your talk, I think I agree with all of the formulas that you have given. As I pointed out in my talk, all of these formulae are valid, at least under some conditions, and have been used for literally centuries. There is one point that I would like clarified. I think you used a so-called a priori curve for interpolating the data. Do you include uncertainties and correlations on that curve? That is, you find it convenient (but it is not necessary) to bring all of the experiments to a common grid before you average them for the evaluations. This procedure can lead to problems, and you could improve your technique by putting an uncertainty on that curve with correlations, and these could then be propagated in your calculations, even though you do not really have to bring everything to the same point.

Poenitz

I do include such an uncertainty. For every step in the process, I add an uncertainty for doing that step. I believe, however, that it is totally unimportant because normally you have experimental data on both sides and interpolation errors tend to average out or cancel.

Perey

This is particularly true, as you point out, if you take into account the energy uncertainties and especially the systematic errors, which most people forget. There is a code, which is being rewritten by Pete Fu and Dave Hettrich at Oak Ridge, that does these things and is nearly finished. It includes the procedure you have described including the breakdown of the sets and the correlated sets in ENDF format. That is, the code produces the data with the ENDF interpolation scheme that you specify i.e., linear-log, log-log, etc., and produces and uses the covariance matrices for the data as well as the output directly in ENDF format.

Poenitz

All of these features are, of course, in the code I described, except the ENDF format is not used.

Rowlands

I wonder if you could clarify the output covariance data. Do I understand correctly that you produce covariance matrices for the 100 reference energy points? You also mentioned that you allowed for uncertainties on the interpolation curve. Do you produce information that relates also to the interpolation curve?

Poenitz

The output is, of course, the cross sections that are derived from your estimator, and the output is also called the variance-covariance matrix of the result. Because it evaluates several cross sections at the same time, the analysis includes the variance-covariance matrices for the first reaction, the second reactin, etc. We then obtain the diagonal plots from the side variance-covariance matrix, which gives us more information for each specific cross section. We also get the off-diagonal plots that are the correlation coefficients between one cross section and another. This also answers a question Joe Schmidt had yesterday as to how we get the correlation between different cross sections. We evaluate several at the same time.

Rowlands

How is this output information represented in ENDF/B-V? If by energy block data, is useful information about the uncertainties in energy gradients being lost?

Poentiz

The output is collapsed into energy groups. Regarding energy gradients, you can get this information from interpolation providing you know how it was collapsed. In collapsing, one probably should not reduce the statistical part of the uncertainties, which in principle would happen. Rather, one should keep the statistical information in a form that can be directly interpolated.

Rowlands

My second question is similar to one asked by Al Smith yesterday concerning the number of points needed to represent cross sections in ENDF/B. You use polynomial representations between your reference energies, and this prompts me to ask whether it would be possible to use in ENDF/B fitting methods other than log-log or linear-linear that would allow cross sections to be represented with fewer energy points. For example, cubic spline fitting

routines are generally available and fast to use. I do not think it would be too great a task to rewrite the integration routines in the ENDF/B codes to use such an interpolation method. Do you have any comments?

Poenitz

In my analysis code, I have a choice of interpolation methods. I can use an analytical expression as, for example, I used for the the H(n,n) cross section, or I can use a polynomial fit or a power series for interpolations. As regards ENDF/V interpolation schemes, the CSEWG Formats Subcommittee, which is a very conservative group, oversees interpolation matters, and I would not like to intrude into that area.

Howerton

I would like to respond briefly to John's question about more flexible interpolation schemes in ENDF. All it takes is money and time to extend the processing codes and to revise and perform new evaluations.

Pearlstein

I would also like to respond to John Rowlands' questions as to why more general interpolation schemes such as cubic splines are not used in ENDF formats. The next step in using ENDF often requires integration of cross sections over energy. The presence of extremely narrow resonances necessitates use of a very closely spaced energy grid, and additional points must be added to prevent numerical integration errors. More compact files are possible, but practical use often requires them to be expanded again.

Peelle

I would like to make what I think is a very uncontroversial comment. Your development, and corresponding developments by others, now makes possible the joint evaluation of the many interlocking energy-dependent neutron cross sections. The problem for the evaluators now remains the proper characterization of the experimental data (uncertainties, correlations, resolutions, etc.). Since most papers do not highlights all the required information, this task will be a substantial one. This demonstrated capability to handle the standards evaluation problem, when much experimental data exist, is a signal event that should lead to a qualitative leap in the validity of our evalutions of these cross sections. I believe it must also affect how the work for evaluators will be organized.

Poenitz

I had intended some remarks on this topic, but because of the time limitation, I could not make them during the paper. The whole problem is, of course, a file problem. In the past we have not filed our experimental data in a proper way. The data are in all kinds of formats and all kinds of quantities are given, but frequently they are not the originally measured quantities. And the errors are mostly not quoted in the file. If we had a file on which all this information from the experiments were stored, the evaluation could be done in less than a minute. That is, it costs about $10 to invert our matrix that occupies the whole core of a modern computer.

EVALUATION METHODS FOR NEUTRON CROSS SECTION STANDARDS*

M.R. Bhat

Brookhaven National Laboratory
Upton, New York 11973

ABSTRACT

Methods used to evaluate the neutron cross section standards are reviewed and their relative merits assessed. These include phase shift analysis, R-matrix fit and a number of other methods by Poenitz, Bhat, Kon'shin and the Bayesian or generalized least-squares procedures. The problems involved in adopting these methods for future cross section standards evaluations are considered and the prospects for their use discussed.

INTRODUCTION

Methods used to evaluate the neutron cross section standards are discussed in this review and their relative merits assessed. The commonly accepted neutron reactions and the useful energy ranges as standards as given in ENDF/B-V are: $^{1}H(n,n)^{1}H$ (scattering cross section 1 keV-20 MeV; MAT = 1301), $^{6}Li(n,t)^{4}He$ (thermal to 100 keV; MAT = 1303), $^{10}B(n,\alpha_0)^{7}Li$, $^{10}B(n,\alpha_1)^{7}Li^*$ (thermal to 100 keV; MAT = 1305), C(n,n) (carbon elastic scattering angular distribution up to 1.8 MeV; MAT = 1306), $^{3}He(n,p)t$ (thermal to 50 keV; MAT = 1146), $^{197}Au(n,\gamma)$ (200 keV - 3.5 MeV; MAT = 1379) and $^{235}U(n,f)$ (at thermal energy and from 100 keV-20 MeV; MAT = 1395) [1]. The different evaluation procedures used with these may be divided into three broad categories. They are: (A) phase shift analysis for $^{1}H(n,n)^{1}H$; (B) R-matrix fit for $^{6}Li(n,t)^{4}He$, $^{10}B(n,\alpha_0)^{7}Li$, $^{10}B(n,\alpha_1)^{7}Li^*$ and C(n,n): and (C) a miscellany of methods used with $^{3}He(n,p)t$, $^{197}Au(n,\gamma)$ and $^{235}U(n,f)$. A discussion of these methods may be further subdivided into:

*This work was performed under the auspices of the U.S. Department of Energy.

(i) The physical model used,
(ii) types of data,
(iii) statistical model and evaluation procedure and,
(iv) comments and problems.

Use of a physical model to fit a set of data is preferred as opposed to an arbitrary functional or polynomial fit. Apart from providing a physical insight into the nuclear reaction under consideration, a physical model makes credible interpolation or extrapolation of the evaluation to energy regions where there are no data. The physical model, because of its unitarity and other constraints, could also help in identifying discrepant data sets. It can point out inconsistencies in the results of an evaluation such as for example the negative value of ϵ_1, the $^3S_1 - {}^3D_1$, mixing parameter in $^1H(n,n)^1H$ scattering. This inconsistency is ascribed to lack of completeness of input data and further studies using sensitivity analysis point out new types of measurments which could clear up these problems. If the evaluation process is thought of as a type of data reduction, in which a large amount of data are expressed more succinctly in terms of a fewer number of parameters, a physical model is helpful in identifying the parameters to be determined from the data as opposed to energy, mass and other variations governed by the physics of the reaction. Further studies of the systematics of these parameters could lead to greater understanding of the reaction under study. An example of this is the determination of the resolved resonance parameters and the strengtn function and other systematics derived from it. However, it should be noted that the physical model chosen must be flexible with enough adjustable parameters so that a good fit to the measured data may be obtained consistent with their assigned errors.

Since this review is mainly concerned with evaluation methods, different data sets for the standards and any of the problems associated with them will not be discussed. Instead, broad categories of data will be mentioned with an indication as to the physical parameters they help to determine.

The statistical model (which has nothing to do with nuclear reaction theories with the same name) and the evaluation procedure are the particular concern of this Workshop and will be discussed in detail with particiuar emphasis on the methods used for the ENDF/B-V standards [1]. Possible shortcomings in these methods and any suggestions for improvements will also be mentioned. As stated earlier, if the evaluation is thought of as a data reduction process, it should be carried out with a minimum loss of information contained in the original data. This information pertains to the data as well as their statistical and systematic errors and any correlations amongst them. Hence, the need for the use of a full variance-covariance matrix of the input data as has been emphasized by Perey [2], Peelle [3,4] and others.

A discussion of the evaluation methods is followed by mention of the problems of neutron cross section standards evaluation and the future outlook for this activity. The problems of implementing some of the recent improvements in the evaluation techniques are also mentioned ending with a brief summary of this review.

Some aspects of the standards evaluation not discussed here deal with (1) evaluation of thermal data and (2) numerical procedures. Because of their high precision, thermal data are used to normalize cross sections in the higher energy region and form an integral part of the analysis. These methods will be discussed by Mughabghab [5] in this Workshop. Numerical procedures enable one to implement the various evaluation methods and deal with different problems such as having to work with a computer with a finite word size, ill conditioned matrices and using numerically stable algorithms. A number of recent advances made in this field are given in Ref. 6-9 and will not be discussed here.

EVALUATION METHODS

A. Phase Shift Analysis

In the energy region from 1 keV-20 MeV the neutron scattering cross section of hydrogen is smooth, large and without any structure-essential qualities needed in a cross section standard. The evaluation in ENDF/B-V is by L. Stewart et al. [10,11] and is based on the work of Hopkins and Breit [12] derived from the Yale phase shift analyses. The variance-covariance files for this evaluation were generated by Foster and Young [13] and give uncertainty information for total, scattering and capture cross sections. In implementing neutron scattering from hydrogen as a standard, it is essential to know the elastic differential scattering for use in recoil telescope detectors [14].

(1) Physical Model

The physical model used for the evaluation is to make a phenomenological phase shift analysis of the different types of data needed to determine the (n,p) scattering matrix. Details of such analysis have been given by Wilson [15], Arndt and MacGregor [16] and Breit and Haracz [17] and a number of other papers. In this analysis, conservation of the total angular momentum J, parity, the isospin T and time-reversal invariance are assumed. With the assumption of charge independence, both the p-p scattering data corresponding to T=1 and the n-p scattering data with T=0, 1 are used in the analysis. Further, because of the tensor force between nucleons, there is a mixing of L states which differ by two units of angular momentum. The nucleon-nucleon scattering phases are denoted by $\delta(^{2S+1}L_J)$ where S is the total spin, J the total angular momentum and L stands for S,P,D,F,G,H corresponding to L=0,1,2,3,4,5 in the usual spectroscopic notation. The mixing parameters which mix states with L=J+1 for the same total J are denoted by ε_J. The relationship between the phase shifts and the measured quantities such as the angular distribution and the different polarization parameters have been given by Stapp [18]. The evaluation consists in forming a χ^2 using experimental observables,

errors and their theoretical expressions in terms of phase shifts and determining the unknown parameters by minimization. In this procedure, it is difficult to make a clear-cut separation between the physical model and the details of the evaluation procedure as the behaviour of the parameters are determined by an appeal to theory. Thus, in this particular case there is much greater intrusion of theory in the evaluation method and this will be made clear wherever possible.

(2) Types of Data

The input data used in the evaluation fall into two broad groups viz., the low energy data usually of high precision and the scattering and polarization data at higher energies. They are listed in Table I together with their estimated precision. Their current best values are not shown as they vary from one compilation to another.

The binding energy of the deuteron B=2.224628±0.00003 MeV is taken from Wapstra and Bos [19]. The uncertainty estimates of the remaining low energy data in Table I are from Koester [20], Lomon and Wilson [21], and Sher et al. [22] for the p-p scattering parameters a_{pp} and r_{opp}. These are supposed to give the order of magnitude of the data uncertainties and vary from one compilation to another. The deuteron radius R is derived from the binding energy B [15]. The free atom n-p scattering cross sections at low energies have been carefully measured by Houk [23], Dilg [24] and others. This cross section σ_0 depends on the weighted sum of the squares of the triplet and singlet scattering lengths a_t and a_s. To determine a_t and a_s, additional data on the coherent scattering length f are used as it depends linearly on a_t and a_s. The coherent scattering length f is most accuractely determined at present using the gravity spectrometer as described by Koester [20]. The low energy n-p scattering phase shift δ is expressed in terms of the scattering length a, the effective range r_0 and the wave number k in the shape independent approximation as [25].

$$k \cot \delta = -\frac{1}{a} + \frac{1}{2} k^2 r_0 \qquad (1)$$

From a_t and the deuteron binding energy, the triplet effective range r_{ot} is calculated. Similarly, from low energy scattering data and a_s one may extract the singlet effective range r_{os}. Proton-proton scattering data below 30 MeV were analyzed by Sher et al. [22] and after applying corrections to the observed data corresponding to a number of physical effects they arrived at the singlet scattering length and effective range for proton-proton scattering. It is found that in doing phase shift analysis, by adding the requirement that S-wave phases extrapolate to the scattering length and the effective range expansion at low energies, excellent fits could be obtained to low energy data [26-29].

Since nucleon-nucleon interaction is spin dependent, a

complete specification of the scattering matrix requires a number of experiments. These have been discussed by Wilson [15] and Moravcsik [30] who list some five different types of experimental data which should be measured over 0^0-90^0 scattering angles for p-p and 0^0-180^0 for (n,p) scattering to specify the scattering matrix for each isospin state. These experiments include angular distributions, polarization, polarization transfer and spin correlation experiments for (n,p) and (p,p) scattering. For (n,p) interaction, one can measure in addition, the total cross section. The available data for (p,p) and (n,p) scattering and their uncertainties have been listed in a number of papers [27,28,29,31,32] and vary from about one percent to several percent depending on the difficulty of the data measurement. In general, the data on (p,p) scattering are much more complete than the (n-p) data. Because of this fact, (p,p) scattering is analyzed to determine the T=1 scattering phase shifts first and assuming charge independence, they are used along with the (n,p) data to extract the T=0 phase shifts. As is seen later on, large uncertainties in the evaluated parameters, multiple solutions and in some cases problems with the sign of the final value are caused by this less than complete data base and of course the experimental errors.

The (p-p) and (n-p) data have been measured over a number of years at different laboratories using experimental techniques of different degrees of sophistication. In addition, to the known and estimated errors, the data are bound to have unknown systematic errors. Hence, if at all possible, some kind of unbiased data selection should be made provided the discrepant data sets could be identified. This process as carried out by the Livermore group [27] may be described as follows. The purpose of this selection is to find out whether or not a particular experiment can be considered to be compatible with other data. One obvious procedure in comparing two identical experiments is to see whether the error bars overlap or not. However, the (p-p) and (n-p) scattering data are of such varied nature differing in type, energy and angle that such direct comparison can be made very rarely. Therefore, as a general criterion of compatibility, it is demanded that they be described by the same phase-shift representation. This procedure is carried out as follows. A subset D of data self-consistent and complete enough to give a set of parameters by χ^2 minimization is chosen; and let the minimum χ^2 be devoted by χ^2_D. If now an experiment E (not included ir D) with N_E experimental points is added to this set, and a minimum χ^2_{D+E} is obtained, the change in the χ^2 minimum per additional degree of freedom is defined as

$$f_c = (\chi^2_{D+E} - \chi^2_D)/N_E \qquad (2)$$

This f_c includes not only the χ^2 minimum increase due to the additional points N_E but also their influence on the fit as determined by their compatibility or lack of it with the set D. For a set E compatible with D, it is demanded that f_c be of the order of unity.

As has been emphasized [27] it is important to recognize that f_c is a measure of the compability between the data sets D and E only within the constraints of the model used for the fit. The details of this selection procedure are given in Ref. 27 and 16.

(3) Statistical Model and Evaluation Procedure

The p-p and n-p scattering data have been most extensively analyzed by the Livermore group [16,26-29,31,32,] and the Yale group [17,33,34] for many years. In addition, such analyses have also been done at a number of other institutions. In the case of every group, the evaluation procedures have evolved over a number of years and to do full justice to them, the original papers should be consulted. Though the details of analyses vary from group to group, they have some common features which will be discussed in this review. These are summarized here by discussing the procedures adopted by the Livermore group.

The basic idea of the fitting procedure is to use χ^2 minimization to find the set of parameters which best describe the data. The χ^2 is defined as [16,35]

$$\chi^2 = \sum_{i=1}^{N_D} \left[(\alpha^n \theta^i(p) - \theta^i_{exp})/\Delta\theta^i_{exp} \right]^2 + \sum_{j=1}^{N_\alpha} \left[(\alpha^j - 1)/\Delta\alpha^j_{exp} \right]^2 \quad (3)$$

where $\theta^i(p)$ are the observables predicted by the set of parameters p, θ^i_{exp} are the experimental values of these observables and $\Delta\theta^i_{exp}$ their experimental errors (one standard deviation), i is the index which varies from 1 to N_D where N_D is the number of data points; α^n are the normalization parameters N_α in number, p stands for the set of parameters specifying the phase shifts (N_p in number). The normalization parameters are introduced for sets of data points where the entire set has a correlated uncertainty in the measured values. The minimum is found by varying the parameters and normalization constants (p_j, α^n). There are a number of techniques used to find the minimum of such a χ^2 function and they are described by Arndt and MacGregor [16]. They also discuss the problem of estimating the errors and their correlations for the evaluated parameters and the goodness-of-fit.

One of the problems noted in the earliest computer based phase shift analysis of 310 MeV p-p scattering data by Stapp et al. [18] was the multiplicity of solutions viz. eight that were obtained. Out of these, some three were rejected as their χ^2_{min} values lay between 34.6 and 52.3 for 22 degrees of freedom and it was estimated that the probability of χ^2_{min} >34 was about 5%. For the remaining solutions, χ^2_{min} varied from 17.9 to 34.2 and a clear cut choice other than that determined by χ^2_{min} could not be made to choose amongst these. The mulitplicity of solutions was attributed to data errors and the incomplete data base in the sense that though the data were made up of five types of

experiments they did not extend over the whole angular range. Also, in the phase shift analysis, partial waves up to $\ell_{max}=5$ were used with the phase shifts corresponding to the higher partial waves being set equal to zero. It was suggested [36] that an improvement in the phase shift analysis could be made by setting the higher -ℓ phases equal to the one-pion exchange contribution. This reduced the number of solution to two and made a significant improvement in the analysis [37]. This feature of using one-pion exchange potential and other theoretical calculations as adjuncts to the nucleon-nucleon scattering analysis has continued since then.

The phase shift analysis is done using experimental data confined to a narrow range of energies (energy independent analysis) or with data spanning a wider range of a few hundred MeV (energy dependent analysis). In the case of energy independent analysis, the low angular momentum phases are treated as free parameters to be determined by fitting the data and the high angular momentum phases are represented by their one-pion exchange contributions. For the energy dependent analyses, the Livermore group uses the following expression for phase shifts [27]

$$\delta_{\ell}^{(S,J)}(E) = \delta_{\ell o}^{(S,J)}(E) + \sum_{i=1}^{N} \alpha_i^{(S,J)} F_{\ell i}(E) \qquad (4)$$

where ℓ is the orbital angular momentum, J and S are total momentum and spin and E is the laboratory kinetic energy. For $\ell=0$, the phase has at its asymptotic lower limit the appropriate effective range expansion [27,29] and for $\ell\neq 0$, $\delta_{\ell o}^{(S,J)}$ are set equal to the one-pion exchange values. The functions $F_{\ell i}(E)$ are derived from theory and the $\alpha_i^{(S,J)}$ are treated as free parameters to be determined from the fit. The energy-dependent form of the phase shifts are chosen with guidance from theory and with enough free parameters to fit the data. Results of energy-independent analyses at a few energies are compared with those of energy-dependent analyses and if they agree, this is taken as an indication that the energy-dependent fits are not form-limited.

As mentioned earlier, the p-p scattering data base is in general more complete than the n-p scattering data. Because of the incomplete data base and the data uncertainties, the evaluated parameters are not determined uniquely especially at low neutron energies. One of the vexing problems of (n-p) scattering phase shift analysis has been the negative value of ε_1, the $^3S_1$-$^3D_1$ mixing parameter. Because the electric guadruple moment of deuteron is experimentally measured to be positive, it is expected that ε_1 should be positive at very low energies [38]. According to theoretical calculations ε_1 is also expected to be positive at low energies [39]. Also, the phase $\delta(^1P_1)$ as determined from the phase shift analysis, though it has a negative value as given by theory, is found to have a smaller magnitude as compared to theoretical estimates [29]. To get around these problems, the

Livermore group constrained their fit to pass exactly through the Wisconsin data [40] which measured the ratio $\sigma(164^{o})/\sigma(89^{o})$ = 1.134+.016 for (n-p) scattering at 24 MeV. This constrained solution was found to give ε_1 and $\delta(^1P_1)$ values that were in reasonable agreement with those expected from theory. Though the Yale solutions are not constrained by experimental data, as has been pointed out by MacGregor et al. [28] (pages 1294-1299), the reason the Yale solutions do not have the type of problems which the Livermore solutions have and they follow a one-pion exchange contribution type of behaviour at low energies is because they are constrained to do so. These experimental or theoretical constraints are necessary because the low energy (n,p) data are not yet adequate to give a unique solution to the problem.

The ENDF/B-V (n,p) scattering evaluation is based on the Hopkins and Breit analysis [12] which is mainly based on the results obtained by the Yale N-N Interaction group [33,34]. A brief discussion of the Yale and Livermore [29] phase-shift analyses is given in Ref. 12. These authors conclude that the results of these two analyses are in essential agreement; and the differences between the cross sections or polarizations as calculated from the Yale or Livermore phase shifts are less than the uncertainties associated with the experimental data. The Hopkins and Briet evaluation has been confirmed by some measurements done after the evaluation. These are the Davis and Barschall total cross section data from 1.5-27.5 MeV [41], the Masterson differential data at 24 MeV [42], the Burrows data [43] at 24.0 and 27.2 MeV and the Cookson et al. data [44] at 27.3 MeV.

Since the phase shifts are extracted from the experimental data by least-squares minimization, the errors in the evaluated parameters and their correlations are determined from the error matrix. The details may be found in the article by Arndt and MacGregor [16], or other papers [26,35]. The variance -covariance files for the ENDF/B-V evaluation were derived by Foster and Young as described in Ref. 13. These are given for total, scattering and capture cross sections. However, the variance-covariance files, could be obtained from the error matrix originating as part of the evaluation process. As has been emphasized by Stewart and Young [45] use of hydrogen as a cross section standard is limited only by the accuracy with which one measures and knows the differential elastic scattering. Hence, a variance-covariance matrix dealing with the uncertainties in this quantity appears to be more pertinent in the evaluated data files and is not available at present.

(4) Comments and Problems

In this section, a few brief comments on the statistical model used and the problems of the (n-p) data base will be made. First, from the form of the χ^2 used in Eq. (3), it is assumed that the individual data points in the whole data base are independent. This assumption neglects any correlations in the data uncertainties

of quantities measured in the same experiment. There are usually such non-zero correlations. Second, since "the normalization parameters are introduced for sets of data points where the entire set has a correlated uncertainty in the measured values" [16] is considered as a solution to the first problem, normalization parameters cannot allow for energy dependent systematic errors. In addition to assuming that the systematic errors are constant, this also implies that the statistical errors are small compared to the systematic errors — an assumption which may not be true. Though these simplifying assumptions are made in practice, one should carefully examine the data bases to see whether they do indeed hold true for the particular data under consideration. Of course, the correct procedure is to work out the full variance-covariance matrix for the input data and use it in the analysis.

The status of the hydrogen scattering cross section and the problems of data discrepancies has recently been reviewed by Stewart and Young [45] and Uttley [46]. One of the phase shift analyses of p-p and n-p scattering data was done by Arndt et al. after the Hopkins and Breit work and dealt with the data near 50 MeV [47]. They found that the allowed range of values for ε_1 (the $^3S_1$-$^3D_1$ mixing parameter) varied from about -10^0 to $+3^0$, though theoretical calculations predicted about $+2.78^0$. The χ^2 vs ε_1 plot indicated that the χ^2 surface was essentially flat between -10^0 and $+3^0$. To obtain a unique solution, even when ε_1 was constrained to $+2.78^0$, $\delta(^1P_1) = -3.52+1.04^0$, was obtained which was estimated to be 4.5 standard deviations above the predictions of theoretical models. As a result of this study, one of the conclusions reached by these authors was that existing n-p data on total, differential elastic and polarization cross sections could not remove this ambiguity in ε_1 as these data were not sensitive to changes in ε_1. In order to understand these problems with ε_1 and $\delta(^1P_1)$ better, Binstock and Bryan [48] carried out a detailed sensitivity analysis of the various n-p scattering ob-observables to the phase parameters near 50 MeV. This confirmed their earlier conclusion that ε_1 was not sensitive to the σ_{tot}, $d\sigma/d\Omega$ or polarization data; however, they observed that it was sensitive to a number of polarization transfer or spin correlation parameters. These in order of decreasing sensitivity are A_{zz}, C_{pp}, A'_t, C_{kk}, A_t, D_t, C_{nn} and A_{xx}. Further they observed that the differential cross section is sensitive to $\delta(^1P_1)$ at backward angles and to the triplet-D parameters at both forward and backward angles. Inaccurate $d\sigma/d\Omega$ data, therefore, could vitiate the $\delta(^1P_1)$ evaluation by giving wrong triplet-D phases from the forward data and then giving incorrect contribution at the backward angles. Therefore, these authors emphasize the need for good absolute $d\sigma/d\Omega$ data at both near 0^0 and 180^0. There have been some recent measurements by the UC Davis group of the n-p spin correlation parameter A_{yy} at 50 MeV [49], the (n-p) differential cross section data at 25.8 and 50.0 MeV [50], polarization at 50 MeV [51,52], differential scattering cross section at 63.1 MeV [53] and a remeasurement of $A_{yy}(\theta)$ at 50.0 MeV [54] with several

improvements in the experimental technique. They were able to considerably reduce the normalization uncertainty in A_{yy}. These new data with the other Davis data [51,50,53,55,49] and the data of Langsford et al. [56] were used for a phase shift analysis at 50 MeV and Fitzgerald et al. obtain $\varepsilon_1 = 3.6^0 \pm 1.0^0$ and $\delta(^1P_1) = -6.4^0 \pm 1.1^0$ [54]. These values are said to be in much better agreement with model-dependent calculations. From the above discussion, it appears that further studies and measurments are needed to get better (n-p) scattering phase shift parameters. It would be interesting to carry out the type of Binstock-Bryan sensitivity analysis at a lower energy of say 25 MeV to identify the data needed to determine ε_1 and $\delta(^1P_1)$. Maybe, they will be the same data singled out at 50 MeV. More measurements of these quantities viz. absolute $d\sigma/d\Omega$ at forward and backward angles and the various polarization transfer and spin correlation parameters are also needed. In addition, a statistical model using the full variance-covariance matrix could be used in the analysis to obtain better phase-shift parameters.

B. R-Matrix Analysis

R-matrix analysis was used to evaluate $^6Li(n,t)^4He$, $^{10}B(n,\alpha_0)^7Li$, and $^{10}B(n,\alpha_1)^7Li^*$ and C(n,n) as standards for ENDF/B-V. The first three reactions were evaluated by G.M. Hale and co-workers [57,58] and he will discuss these at this Workshop [59]. The Carbon scattering was analyzed by Fu and Perey [60]. There will also be a discussion of R-matrix methods by Froehner in this Workshop. Therefore, this discussion of C scattering will be very brief with only a few comments on the (MAT = 1306, ENDF/B-V) evaluation. Fu and Perey have assembled the variance-covariance files for total, scattering, non-elastic, total inelastic, inelastic scattering to discrete states and the continuum, capture, (n,p), (n,d) and (n,α) reactions [1,60] as part of the evaluation process. An earlier evaluation of this reaction by Reynolds et al [61,62] done for ENDF/B-III (MAT = 1165) used coupled-channel analysis and a few comments will be made comparing these two procedures.

(1) The Physical Model

R-matrix theory has been discussed in detail in a number of review articles [63,64] and a few of the characteristics of this physical model will be mentioned.

In R-matrix theory, the configuration space of all the interacting nucleons is divided into an internal region which corresponds to all the interacting nucleons being close together in physical space. This internal region is separated from an external region where the nucleon forces between nucleons do not act. Corresponding to this surface of separation there are channel radii a_c for different reaction channels or interacting particles. Usually, a_c is set equal to the sum of the radii of the interacting particles. Thus, R-matrix theory deals usually with two-body breakup reactions, with three-body breakup being considered as a succession of two-body

reactions [63]. Usually, since data corresponding to only a limited energy region are analyzed in an R-matrix fit, provision should be made to represent the tails of resonances that lie outside the region of fit. Bound levels are represented by a few resonances whose parameters are determined to be consistent with low energy data and the contributions of positive energy resonances at higher energies.

(2) Types of Data Used

In R-matrix analysis, where levels corresponding to a particular compound system are investigated, data for all the reaction channels producing the same compound nuclear system are used. As has been pointed out by Hale [57], experimental data corresponding to all the reaction channels influence the R-matrix parameters through unitarity and other general physical constraints and discrepant experiments may be identified and separated from the main body of data. Thus, a comprehensive multilevel, mulitchannel R-matrix analysis is expected to give a good representation of the data consistent with their errors.

^{13}C occurs in natural carbon with an abundance of 1.11%. Though the measured data are for natural carbon, the evaluations are for ^{12}C [65,66,60]. This problem has been discussed [65,66] and the data indicate that the cross sections for ^{13}C are very close to the corresponding ones for ^{12}C except in the vicinity of the 0.153, 1.751 MeV resonaces of ^{13}C which lie in the standards region of up to 1.8 MeV. Hence, it is felt [66] that the vitiating influence of this isotope, especially in elastic scattering, would not distort the elemental results beyond the current experimental errors except at the ^{13}C resonances. However, an evaluation of the ^{13}C data and its inclusion in the evaluated data file is recommended [65,67].

The data used in the evaluation [60] are for total, differential scattering and for differential polarization cross sections. The total cross section data were smoothed and averaged using the full variance-covariance matrices and a procedure based on Bayes' theorem as described by Fu and Perey [60].

(3) Statistical Model and Evaluation Procedure

As mentioned earlier, a study of natural carbon data involves ^{12}C as the major isotope. Since ^{12}C has zero spin, only one channel spin s=1/2 is involved and for neutron energies below the inelastic threshold at about 4.81 MeV, only elastic scattering is possible. Capture cross section is also negligible below ~2 MeV. Thus, in effect, there is only one open channel below 4.8 MeV and the R-matrix reduces to an R-function. Fu and Perey [60] used the R-function

$$R_{\ell J}(E) = \sum_{\lambda} \left[\frac{\gamma^2_{\lambda}}{E_{\lambda} - E} \right]_{\ell J} + R^{\infty}_{\ell J}(E) \qquad (5)$$

where γ_λ^2 and E_λ are the reduced width and the characteristic energy respectively of the λ-th state of given J^π, and $R^\infty_{\ell J}(E)$ is the corresponding background term given by

$$R^\infty_{\ell J}(E) = R_0 + R_1 E + R_2 E^2 \qquad (6)$$

where E is the laboratory energy of the incident neutron in MeV. The corresponding phase shift is

$$\delta_{\ell J}(E) = \tan^{-1}\left[\frac{P_\ell(\rho)\, R_{\ell J}(E)}{1 - \left[S_\ell(\rho) - b_{\ell J}\right] R_{\ell J}(E)}\right] - \phi_\ell(\rho) \qquad (7)$$

where $\rho = ka$, k being the wave number of the incident neutron and a the interaction radius. The interaction radius was set equal to 3.72 fm, a value recommended by Lane et al., [68]. In the above expression, $P_\ell(\rho)$ is the penetration factor, $(S_\ell - b_{\ell J})$ the shift factor for boundary value $b_{\ell J}$ and $\phi_\ell(\rho)$ is the hard sphere phase. The boundary values $b_{\ell J}$ were chosen such that the E_λ fall near the observed resonance energies. All other parameters were determined by fitting the data without any constraints.

The evaluation procedure consists in forming χ^2 corresponding to each of the measured quantities and minimizing them using an interactive graphics program. Only diagonal elements of the data variance-covariance matrices were used in the minimazation [69]. The variance-covariance matrices of the fit were evaluated as part of the evaluation.

(4) Comments and Problems

Since, the evaluation is the result of a χ^2 minimization, the data uncertainty files may be derived from the error matrix as part of the evalution. However, the error estimates and their correlation would be more representative of the true state of affairs if the full variance-covariance matrices for data are used in the evaluation. In addition, it would be useful to have the data uncertainty information for elastic differential scattering in the evaluated data files as it is the standard. Some of these error estimates are given in the evaluation report [60]. As has been mentioned earlier, an independent evaluation of ^{13}C data, if available, could allow for the 1.11% impurity of ^{13}C in natural carbon data.

An alternate physical model was used for carbon to obtain an evaluation for ENDF/B-III (MAT = 1165) [61,62]. The reasons for adopting this procedure are given [61] and include having to vary from one energy region to another reduced widths (considered energy-independent) and the energy of at least one resonance. These authors found the usual description of the background cross section in terms of hard-sphere phase shifts inadequate and had to use potential-well phase shifts in their place. These potential-well parameters had to be changed from one energy region to another. Because of these

reasons and as a means of understanding the underlying physics better, these workers used the coupled channel analysis. However, coupled channel analysis seems to have its own peculiar problems [61,62]. For example, the coupling parameter β which fits the data was very small compared to the experimental value obtained in Coulomb excitation. In addition, the potential well parameters had to be changed so that the different shell model states agreed with experimental data. Though they were able to fit the available data on total, differential and polarization experiments satisfactorily, the coupled channel analysis approach appears to involve much more work than an R-function fit. There appears to be a much greater involvement of theoretical models, some ad hoc procedures and no fewer number of parameters to be adjusted. With a greater intrusion of theoretical models the error estimates of the final results is not simple. The R-function fit for this reaction appears to be the simpler procedure.

C. Other Evaluation Methods

The cross section standards discussed here are $^{3}He(n,p)t$ (from thermal to 50 KeV), $^{197}Au(n,\gamma)$ (200 keV-3.5 MeV) and $^{235}U(n,f)$ (at thermal energy and 100 keV-20 MeV). One interesting feature of these reactions in the standards region is that they cannot be expressed explicity in a functional form (except for $^{3}He(n,p)t$ in the $1/v$ region) with an energy dependence determined by the physics of the reaction as for example in the Breit-Wigner formula for resonances. If such a functional form was known, it would be a simple matter to write an expression for χ^2, minimize it with respect to the unknown parameters and determine them. Since this is not the case, a number of other evaluation techniques have to be used to arrive at a best representation of the data. These are: (a) Empirical Evaluation, (b) Poenitz, (c) Bhat, (d) Kon'shin, and the (e) Bayesian Methods.

a. Empirical Evaluation Method

$^{3}He(n,p)t$ reactions in ENDF/B-V was evaluated by L. Stewart for ENDF/B-III, used in Versions IV and V without any changes [11,70]. This evaluation continues to be a valid representation of data base as it stands now [71]. There are no variance-covariance files for this evaluation. This and other evaluations of light elements will be further discussed by Stewart at this Workshop [72]. The final evaluated curve is not the result of a χ^2 minimization statistical procedure. Also, explicit use of the variance-covariance information of the input data is not made. However, it should be appreciated that this evaluation uses a number of adjunct data such as inverse and charge-conjugate reactions, elastic scattering of charged particles and other information in arriving at the best representation of the data. Thus, the final evaluation was based on experimental data, quite a bit of auxilary information and the evaluator's experience. It is proposed to call such a procedure — Empirical Evaluation Method (a name suggested by my colleague A. Prince) — to distinguish it from an eyeguide drawn through the experimental points. Empirical as used here means "originating in or based

on observation or experience" [73]. As mentioned before, uncertainty files for the evaluation are not readily obtained as part of the evaluation procedure. However, it may be possible to assemble them using the SUR program approach described by Peelle [4] where the scatter of the input data about the evaluated curve are considered to provide a guide to the uncertainties of the evaluation.

The $^{197}Au(n,\gamma)$ cross section was evaluated by S.F. Mughabghab [74] using the empirical evaluation procedure. The gold capture data were renormalized to the other ENDF/B-V standards and evaluated. Explicit use of the data variance-covariance matrices is not made. The evaluated data uncertainty files give only the diagonal elements as error estimates.

b. Poenitz Method

The thermal energy evaluation of $^{235}U(n,f)$ for ENDF/B-V is by Leonard et al. [75]. The fission cross section from 100 keV-20 MeV was evaluated by Poenitz [76]. His evaluation method is described in this reference [76] with a bibliography of earlier discussions. Changes and improvements made since then have been discussed at this Workshop [77]. Poenitz carried out an evaluation of $^{235}U(n,f)$ using his method and the available data in October 1978 [78]. This evaluation was renormalized upward by multiplying by 1.009 on the recommendation of the Normalization and Standards Subcommittee of the Cross Section Evaluation Working Group (CSWEG) [78] and forms the evaluation in ENDF/B-V. The evaluation method as it was used to derive the ENDF/B-V cross section, did not explicity use the full variance-covariance matrices of input data and it did not produce the uncertainty files for the evaluation. These were generated by Peelle [79]. Subsequent to this work, Poenitz reevaluated $^{235}U(n,f)$ with an updated data base and published it along with discussion of the evaluation [76]: In general, the ENDF/B-V evaluation is 0.1-1.9% higher than the 1979 evaluation.

c. Bhat or Ratio Method

The evaluation procedure developed by the author of the review [80] may be described as follows. It recognizes the fact that the physics of fission does not enable one to give a functional form for the $^{235}U(n,f)$ cross section for 100 keV-20 MeV and that it cannot be readily parameterized uniquely. Use is also made of the fact that the experimental data lie in a rather narrow band about a mean. Therefore, a curve may be drawn to lie evenly amongst the data points and the values of this reference curve read off. The procedure is to work with the ratios of experimental data and their errors divided by the corresponding values read off this curve. This is found to have the following advantages.

(1) It linearizes the $^{235}U(n,f)$ fitting problem since the energy dependence of the cross section is divided out.
(2) Since the experimental data lie within a few percent about a mean; the ratios of the experimental data divided by the

reference curve should lie within a few percent of the straight line y=1.0. Thus, any method of fitting the ratios can make use of the fact that the final curve is anchored about the line y=1.0 with deviations characteristic of an individual data set being of the order of a few percent.

(3) It enables us to obtain a least-squares fit to the experimental data and a best fit corresponding to a minimum of χ^2 defined in the usual way. Also, the variance-covariance matrix for the fit can be calculated.

(4) After having obtained a best fit for all the data, one could analyze each data set by forming ratios. A decomposition of these ratios into orthogonal polynomials having energy dependence corresponding to different powers of the neutron energy can give us useful information on the systematic errors in each data set, thus providing clues to possible corrections to eliminate them.

Details of the Ratio Method

The absolute fission data used (Table II) are plotted on a graph paper and a smooth curve lying evenly amongst the data points is drawn. The values of this reference curve are read off and assembled in the ENDF/B Tab. 1 format with a linear interpolation code. The procedure calls for determing the shape information contained in the relative and absolute data sets and incorporating this shape information into the reference curve. The shape information is obtained by analyzing one data set at a time to preserve the intra-data-set correlations. The next step is to use only the absolute data and renormalize the reference curve with the shape information to include magnitude as well as the inter-data-set shape information contained in them. A code URAN [80] has been developed and tested to carry out this procedure.

Some 17 data sets were used for this purpose and are given in Table III. One starts from a reference curve drawn as mentioned earlier and goes through the following steps (1)-(4) for each data set.

(1) Determine $r(E_i) = \sigma_{exp}(E_i)/\sigma_R(E_i)$; $\Delta r(E_i) = \Delta\sigma_{exp}(E_i)/\sigma_R(E_i)$

for the experimental data $\sigma_{exp}(E_i)$ and their total error $\Delta\sigma_{exp}(E_i)$ at neutron energies E_i using values $\sigma_R(E_i)$ read off from the reference curve.

(2) Fit the ratios $r(E_i)$ with errors $\Delta r(E_i)$ in terms of orthogonal polynomials and using the F-test (see Appendix) and the χ^2_{min}/degrees of freedom determine the maximum degree of polynomial fit. Use of orthogonal polynomials gets around the problem of having to invert an ill-conditioned matrix usually encountered in a polynomial fit of degree of about six or greater.

(3) The fitted curve is interpolated on to a denser energy grid formed by the union of the energy grid of the reference curve and the experimental data points. This energy grid is further thinned by rejecting energy points in the grid which lie less than .5% from one another. The thinning is done only on the energy grid; no

experimental points are thrown out. In interpolating the fitted curve, its value as well as the error of the fit are calculated at the grid points.

(4) The fitted curve for each data set is then shifted along the y-axis (i.e., the curve is moved parallel to itself keeping the x-axis and the same shape) and a weighted average of the shapes of all the data sets is determined.

(5) This weighted average is fitted with orthogonal polynomials (or smoothed) and a smooth curve representing the average shape curve (for the ratios of experimental data to the reference curve) $\ell(E_i)$ and its weights $\omega(E_i)$ are determined.

(6) This curve is shifted along the y axis such that $\sum_i \ell(E_i)\omega(E_i)=1.0$. This is done to make sure that only the shape of the reference curve and not its magnitude is changed when it is multiplied by $\ell(E_i)$.

(7) The reference curve $\sigma_R(E_i)$ is multiplied by $\ell(E_i)$ to obtain the new reference curve. At this stage, the new reference curve may be plotted, χ^2/degrees of freedom calculated to check the fit. One may then go to step (1) and go through the whole process until it is felt that the reference curve has all the shape information in it and further iterations do not produce any change.

At this stage, the intra-data-set shape information in both the relative and absolute data sets have been built into the reference curve. In addition, by going through steps (8)-(10) inter-data-set shape information or the shape information contained in the relative positioning of the absolute data sets is incorporated into the evaluation.

(8) The 13 absolute data sets (Table II) were merged and energy sorted assuming that the different sets are statistically consistent. The reference curve from step (7) is used and ratios $r(E_i) = \sigma_{exp}(E_i)/\sigma_R(E_i)$ and their errors $\Delta r(E_i) = \Delta\sigma_{exp}(E_i)/\sigma_R(E_i)$ are formed.

(9) These ratios with their errors are fitted using orthogonal polynomials as before. The χ^2/degrees of freedom and the F-test are used to determine the maximum degree of the polynomial fit (see Appendix).

(10) The fitted curve then multiplies the reference curve to give the new reference curve and χ^2/degree of freedom etc., are calculated.

In practice, it is found that a best fit corresponding to a minimum in the χ^2 is found in one iteration and further iterations confirm that one has indeed reached a minimum.

Further tests such as fission spectrum average of the evaluated cross section may be carried out but they have not yet been coded into URAN.

The result of such a fit (solid line) is shown in Figs. 1-4. For comparison are shown the Poenitz evaluation [76] (dashed curve) and the ENDF/B-V evaluation (Δ). The curve obtained from this procedure agrees with the Poenitz evaluation from 100 keV-8 MeV to within ∿1.8% or less. Above 8 MeV, it follows the Kari [81] data and is about 1.0-4.9% higher than the Poenitz evaluation.

In Fig. 5 are shown the ENDF/B-IV and V evaluations with some of the recent experimental data between 0.6-6.6 MeV. It is noted that the trend of the Barton data [82] between 2-6 MeV shows a "tilt" with respect to the ENDF/B-V evaluation. The Poenitz [83] and the Carlson and Patrick data [84] on the other hand show a "concave" shape with respect to the Version V evaluation in the same energy region. If ratios of these data sets are formed with respect to the best representation of all data or the evaluation, and are fitted by orthogonal functions, one can expect to calculate the "tilt" and the "bow" or "concave" shape terms as the coefficients of the second ($\sim x$) and the third degree ($\sim x^2$) orthogonal polynomials (see Appendix). This could provide clues to systematic errors in data due to effects which vary as the first and second powers in energy. Such analyses could provide useful clues in pinpointing and correcting for systematic errors in data.

A number of improvements in this procedure are possible. As it stands now, the method does not use the full variance-covariance matrices of input data. Further, the energy grid of the average shape curve is less than ideal. It is planned to rectify these defects in the near future. It should, however, be pointed out that this method does lead to a least-squares fit to the data and can be applied to any case where the form of the data or cross section as a function of energy is not known.

d. Kon'shin Method

Recently, two reports [85,86] describing a method proposed by Kon'shin et al. to evaluate fission cross section and alpha data have been published. The authors claim to have developed a method of evaluating data and the errors in them with allowance for correlations between partial errors of different experiments. This method has been applied to evaluate σ_f and α for ^{235}U and ^{239}Pu.

The authors point out the importance of allowing for correlations in errors in experimental data which are used in an evaluation and the correlations in errors of the final result. As an example, in the case of $^{235}U(n,f)$ data, some 12 types of experimental errors are considered followed by a detailed discussion of these errors and their correlations. Such a discussion is useful and should form part of any evaluation effort. The subsequent evaluation procedure, however, is new. An expression is written for the difference between the evaluated values σ_{ev} and σ_0 (the unknown true value of the quantity being measured) squared and averaged over the statistical distribution in terms of the weights a_i^2 and their correlations and partial errors. This expression is minimized with respect to the weights a_i^2 and the corresponding values of these weights are determined. In the words of the authors,

> "..the algorithm described here was used in a computer program which employs the partial errors and the correlations between them as a basis for determining by the iteration method, the "weights" of the experimental data which will minimize the error in the evaluated

value, the errors in the evaluated values at different points and the coefficients of correlation between them" [85].

Thus, it appears as though, having decided on an evaluation, (which is presumably drawn through a set of points, the details are not given), the weights of the data are changed to make the evaluation "look good." The usual procedure is to keep the weights as determined from the precision of the data unchanged and vary the "evaluation" subject to proper statistical criteria. The weights are seldom set to be other than those given by the data measurer and that too for reasons that can be defended and justified. A little reflection shows that one obvious result of this procedure would be to give high weights to those data points which happen to lie close to the evaluation and low weights to others. This is exactly what seems to happen in Table 2.1[85] of one of the reports. In this Table, the column K=0 corresponds to no correlations assumed and the weights = $\frac{1}{\sigma_i^2}$ = inversly as the variance of data (the usual procedure) and K and K=1 are for ascribed correlations and full correlation. From this Table, in the 2nd and 3rd column (K≠0) non-zero weights are obtained for only a few data sets as a result of minimization procedure described above. Such a procedure which assigns zero weights to more than half the input data sets must be treated with caution. This evaluation procedure is curious and the exact purpose of this interesting exercise is not clear.

e. Bayesian Methods

Use of Bayes' theorem [87] in data evaluation is relatively new and the methods based on it form an interesting group. The essential idea is to use Bayes' theorem to incorporate new knowledge obtained from measurement (likelihood) into the prior knowledge (from previous measurements usually or conjecture sometimes) to obtain updated information or knowledge a posteriori. There are many ways of stating Bayes' theorem; however, for our purpose it is written as:

$$\text{posterior distribution} \propto \text{prior distribution} \times \text{likelihood} \qquad (8)$$

where the prior distribution expresses the state of knowledge of a physical parameter in terms of a distribution, and the above equation states how it gets changed by the knowledge of the same quantity obtained from a new measurement and represented by the likelihood. This equation may be put in more concrete terms if we assume that the prior and likelihood are given by: $N(\mu_0,\sigma_0^2)$ and $N(\mu_1,\sigma_1^2)$ respectively where $N(\mu,\sigma^2)$ stands for a normal distribution with mean μ and variance σ^2. It can be shown that using the above equation (8) one obtains [87] a posterior distribution $N(\mu_2,\sigma_2^2)$ where

$$\frac{1}{\sigma_0^2} + \frac{1}{\sigma_1^2} = \frac{1}{\sigma_2^2} \qquad (9)$$

$$\frac{\mu_0}{\sigma_0^2} + \frac{\mu_1}{\sigma_1^2} = \frac{\mu_2}{\sigma_2^2} \qquad (10)$$

The above expressions are the same as those used in obtaining weighted average of two quantitites μ_0 and μ_1 with variances σ_0^2 and σ_1^2 and whose weights w_i are inversely proportional to the variances. The above results may also be obtained by minimizing the expression

$$q^2 = \frac{(\mu-\mu_0)^2}{\sigma_0^2} + \frac{(\mu-\mu_1)^2}{\sigma_1^2} \qquad (11)$$

with respect to μ. From Equations (9) and (10) it is evident that the new measurement can make a significant improvement in our knowledge of the mean provided its variance σ_1^2 is significantly smaller than σ_0^2. Otherwise, the prior knowledge given by $N(\mu_0,\sigma_0^2)$ which could have been obtained from previous experiments or a conjecture would remain essentially unchanged. Hence, new data have to be significantly more precise to influence old data.

Extension of these ideas to data adjustment using integral experiments was made by Dragt [88,89]. Dragt showed that if integral experiments are considered to represent new knowledge their effect on differential data may be derived using Bayes' theorem with the assumption of multivariate normal distributions for these quantities or by minimizing an expression corresponding to Equation (11) in the general case. This is also called a generalized least-squares method in that it denotes an extension of the usual least-squares method in using full variance-covariance matrices for input data and the evaluation and also prior information [90]. Let the vector T denote a set of n_t nuclear data with a covariance matrix M of order $(n_t \times n_t)$ and having a Gaussian distribution. Let the new knowledge be represented by n_r measured integral quantities written as vector R with a covariance matrix V of order $(n_r \times n_r)$. The same integral quantities calculated from T are denoted by $\bar{R}$. Their dependence on T is expressed by the sensitivity matrix $G(n_r \times n_t)$ containing partial derivatives of $\bar{R}$ with respect to T so that

$$\bar{R} = G\,T \qquad (12)$$

Dragt has shown that by minimizing an expression analogous to (11) viz:

$$q^2 = (T'-T)^t M^{-1}(T'-T) + (\bar{R}'-R)^t V^{-1}(\bar{R}'-R') \qquad (13)$$

where T' the adjusted quantities are found by minimizing equation (13) and $\bar{R}'$ are the new values for the integral quantitites belonging to T' and

$$\bar{R}' = \bar{R} + G(T'-T) \tag{14}$$

Here t denotes transpose of the matrices. One obtains T' and the new covariance matrix M' as solutions of

$$(M^{-1} + G^t V^{-1} G)(T'-T) = G^t V^{-1}(R-\bar{R}) \tag{15}$$

$$M' = (M^{-1} + G^t V^{-1} G)^{-1} \tag{16}$$

Procedures for sloving these equations have been discussed [89] and this method has been applied by Perey [91,92] to dosimetry problems. Schmittroth has also discussed the generalized least-squares method [90,93] and written a code FERRET [94] to implement it. He has also proposed a finite element representation of cross section data given by a continuous function and illustrated the procedure in the case of ^{54}Fe(n,p) cross section from threshold to 20 MeV [95]. Hetrick and Fu have written a code GLUCS [96] which is a generalized least-squares program and used it to evaluate ^{32}S(n,p), ^{56}Fe(n,p) and ^{65}Cu(n,2n) using previous evaluations of these reactions and the new ratio data [97]. As has been mentioned earlier, one important feature of these evaluation methods based on Bayes' theorem or generalized least-squares is that they use the full variance-covariance information for input data and generate such matrices for the evaluation. In addition, they could use prior information in the form of a previous evaluation or a nuclear model calculation. Though these methods have not yet been used for any of the cross section standards, there is no reason why they cannot be. The prior information could also be in the form of a curve drawn through experimental points with a rough uncertainty estimate. This initial estimate could then be refined using this procedure. Schmittroth's finite element representation ensures that smooth prior curves transform into smooth posterior curves. The GLUCS code does not as yet have any specific method to do this and relies on the fact that the experimental data points are densely distributed and hope no unphysical wiggles would appear in the final curve [98]. If there are any problems, some smoothing procedures could be built into it.

As a further aid in understanding the above Equations (15) and (16), it is instructive to establish a one-to-one correspondence between them and the Equations (9) and (10) for the simple one dimensional case. They can be rewritten as:

$$\frac{1}{\sigma'^2} + \frac{1}{\sigma^2} = \frac{1}{\sigma^2} \tag{17a}$$

$$M^{-1} + G^t V^{-1} G = M'^{-1} \tag{17b}$$

and

$$\frac{\mu_0}{\sigma_0^2} + \frac{\mu_1}{\sigma_1^2} = \frac{\mu_2}{\sigma_2^2} \tag{18a}$$

$$M^{-1} T + G^t V^{-1} G \left(T+G^{-1}(R-\bar{R})\right) = (M^{-1} + G^t V^{-1} G)T' = M'^{-1} T' \tag{18b}$$

From these equations, one notices that the correspondence between $\frac{1}{\sigma_0^2}$ the inverse of variance of μ_0 and M^{-1} the inverse of the variance matrix of the prior data T; $\frac{1}{\sigma_1^2}$ of the new data corresponds to $G^t V^{-1} G$ (the sensitivity matrix occurs here because the new data are integral data R rather than data of the same type as T) and $\frac{1}{\sigma_2^2}$ corresponds to M'^{-1} the inverse of the variance matrix for the posterior distribution. The same correspondence is in Equation (18) where the $(R-\bar{R})$ has an extra factor G^{-1} which converts the difference between the measured values R and the values $\bar{R}$ calculated from T into a correction ΔT to T to give the value of T which corresponds to the integral measurements R.

In addition to this correspondence, these equations may also be interpreted in terms of Fisher's definition of "information" [99]. There are many definitions of "information" in statistics and communication theory and Fisher's definition is one of them. In proposing this definition, Fisher required that [99]

(1) the information in a set of observations should increase with the number of observations,
(2) it should be conditional on what one wants to learn from the experiment, that is, data which are irrelevant to the parameters of interest should contain no information, and
(3) information should be related to precision; the better the precision of the experiment, the greater the information.

With these ideas in mind, Fisher proposed a definition of information which may be written as:

$$\left[I_{\underline{x}}(\underline{\theta})\right]_{ij} = -E\left[\frac{\partial^2}{\partial\theta_i \partial\theta_j} \ln L(\underline{x}|\underline{\theta})\right] \tag{19}$$

where $I_{\underline{x}}(\underline{\theta})$ is an expression for the amount of information given by

an observation $\underline{x}$ about the parameter θ and L is the likelihood function considered as a function of both $\underline{x}$ and $\underline{\theta}$. Thus, if x is normally distributed with variance σ^2 and unknown mean μ, then the information about μ from a single observation is

$$I_1(\mu) = \frac{1}{\sigma^2} \tag{20}$$

and from N independent observations

$$I_N(\mu) = \frac{N}{\sigma^2} \tag{21}$$

From the definition (19) it follows that in the general case of the mulitvariate distribution the information matrix for the vector T is

$$I_T(T) = \frac{1}{M} \tag{22}$$

and similarly

$$I_R(T) = G^t V^{-1} G \text{ provided} \tag{23}$$

$$E\left[G^t V^{-1} G\right] \simeq G^t V^{-1} G \tag{24}$$

In the expression in (23) it should be noticed that we are asking for the information about T from the observed multivariate normal distribution of R. This explains the reason for the presence of the sensitivity matrix G. If the new data are of the same type as T one would get only V^{-1}. The condition (24) may or may not hold; if not, G should be replaced by some mean <G> corresponding to an average over the distribution of R.

With this interpretation in mind, Equation (17a) corresponds to the information about the prior mean $(1/\sigma_0^2)$ being added to the information about the mean of the new data $(1/\sigma_1^2)$ to give the information about the mean of the posterior distribution $(1/\sigma_2^2)$. The same interpretation holds for Equation (17b) were we have information matrices. Equation (18) shows how the means are weighted by the corresponding "information" to give the posterior mean weighted by its information.

From the above expressions the following observations may be made:

(1) the transfer of information about the mean of a quantity is full and faithful only when the new data are of the same type as the prior data i.e., G=1.0

(2) the amount of information transferred to the prior is $G^t V^{-1} G$ and depends on where G is evaluated i.e., T or the prior mean and its energy dependence.

From the above equations it is also noticed that in one iteration, the amount of information contained in the new data has been transferred to the prior. Hence, iterations using the same data over again are not justified. Hence, so long as the above equations based on linear approximation are valid, one should not iterate though the values obtained will depend on T or where G's are calculated. This supports a statement made by Perey [91] justifying only one iteration in this method.

PROBLEMS AND PROSPECTS

From the above discussion of evaluation methods, it is apparent that future evaluations will have to make explicit use of the full variance-covariance information about the input data. Unfortunately, this information is not available in most cases. Hence, the first task of the evaluator or any specialized committees convened to coordinate an evaluation would be to sift through the available information and construct the covariance matrices. Perey [91] and Peelle [3,4] have discussed this problem and endorsed it as an extremely useful endeavor worthy of being published. Of course, the ideal thing would be for the measurer to come up with the covariance information. If such data uncertainty information becomes available it should be stored in the neutron data files like CSISRS (Cross Section Information Storage and Retrieval System) to facilitate data exchange. If in a measurement involving ratios with respect to a standard, the standard evaluation used to convert these ratios into cross sections and the covariance files will have to be stored in the data files. All these extra data will involve format changes and additional effort on the part of the Data Centers. Perhaps the changes should be tried out with a few of the cross section stanards and then extended to dosimetry and other reactions where the data usage and analysis have become sophisticated enough to make use of this additional information.

One of the favorite complaints professional statisticians have against physicists is that the statisticians are consulted after an experiment is done and not before. While it is true that the physics experiments need not be "designed" with the same care as in the life sciences because of greater control over the experimental conditions, there is some virtue in thinking through the possible systematic and statistical errors and their correlations before doing an experiment. Such an in depth error analysis in the planning phase of an experiment could reveal unexpected correlations and dependence of the new data on other measurements. This would also be helpful in working out the covariance data for the experiment after it is done.

Future data evaluations, at least for standards, are expected to use

(1) full covariance information for input data,
(2) objective evaluation procedure based on a well-defined statistical model,
(3) produce variance-covariance information for the evaluation and have,
(4) full and complete documentation of the evaluation procedure and the data base used.

A consistent evaluation of the neutron cross section standards has been advocated by Poenitz [100] and others for a number of years. This is because the standards are related by a number of ratio data and any correlations brought about by the process of measurement.

After each of the standards has been analyzed to understand its problems and discrepancies, a consistent analysis of all of them by an objective procedure and full error information would be a worthwhile objective.

SUMMARY

Evaluation methods used with the neutron cross section standards have been reviewed in this article. In addition to the methods used for those reactions where the functional form of the cross sections are known, a number of new procedures have been proposed for cases where this is not so. Hence, it is now possible to use objective evaluation methods for all the standards reactions. The need to use the full covariance information of the input data has been stressed. It is hoped that the data measurers would cooperate to provide this information for their data. It is also obligatory to obtain full uncertainty files for the evaluations as part of the evaluation process. A consistent evaluation of the primary cross section standards should also be carried out.

ACKNOWLEDGEMENTS

It gives me great pleasure to thank my colleagues at the National Nuclear Data Center for many discussions I had with them and especially Tom Burrows, M. Divadeenam and Sol Pearlstein who read the manuscript and offered many useful suggestions and comments. My grateful thanks are also due to Prof. R.A. Arndt of the Virginia Polytechnic Institute and State University, Blacksburg, Virginia for some useful conversations and sending me the reprints of his papers.

APPENDIX

Orthogonal Polynomials and the F-test

The method used to generate the orthogonal polynomials follows closely the work of Forsythe [101], with modifications suggested by Martin [102].

If there are n data points $y_1 \ldots\ldots y_n$ with errors $\Delta y_1 \ldots\ldots \Delta y_n$ measured at $x_1 \ldots\ldots x_n$; the weight matrix is assumed to be diagonal with elements,

$$W_j = \frac{1}{(\Delta y_j)^2} \tag{A.1}$$

and the orthogonal polynomials ϕ_k are defined to be orthogonal if

$$\sum_{j=1}^{n} W_j \, \phi_k(x_j)\phi_\ell(x_j) = 0 \quad \text{for } k \neq \ell \tag{A.2}$$

To construct the polynomials of high orders with a computer with a finite word size, the x_j are normalized to lie within the interval [-1,+1] and the three term recurrence relations used are as follows:

$$\phi_1(x) = 1/2$$

$$\phi_2(x) = (2x+\beta_1)\phi_1(x)$$

and for $k \geq 2$

$$\phi_{k+1}(x) = (2x+\beta_k)\phi_k(x) + \gamma_{k-1}\,\phi_{k-1}(x) \tag{A.3}$$

where

$$\beta_k = -2\sum_{j=1}^{n} W_j x_j \phi_k^{\,2}(x_j) \Big/ \sum_{j=1}^{n} W_j \phi_k^{\,2}(x_j) \tag{A.4}$$

$$k = 1,2,3\ldots.$$

and

$$\gamma_{k-1} = -\sum_{j=1}^{n} W_j \phi_k^2(x_j) / \sum_{j=1}^{n} W_j \phi_{k-1}^2(x_j)$$

$$k=2,3,4.... \qquad (A.5)$$

If the observations y_j are fitted by a number of p parameters as

$$f_j = \sum_{k=1}^{p} \theta_k \phi_k(x_j) \qquad (A.6)$$

the least-squares estimates of the parameters are:

$$\theta_k = \sum_{j=1}^{n} W_j y_j \phi_k(x_j) / \sum_{j=1}^{n} W_j \phi_k^2(x_j)$$

$$k=1,2....p. \qquad (A.7)$$

From the three-term recurrence relationship (A.3, A.4) it is noticed that the orthogonal polynomials

$$\phi_k(x) \sim x^{k-1} \qquad (A.8)$$

hence, the various coefficients have the following simple interpretation. Because $\phi_1(x) = 1/2$; $\theta_1/2$, gives a normalization for the curve as a whole; $\theta_2 \sim x$ a tilt term and $\theta_3 \sim x^2$ a "bow" term and so on. This simple visualization is helpful in understanding how the function obtained by fitting the ratios of experimental data to the reference curve affects the reference curve when it is multiplied by it to obtain a new reference curve.

If one uses p orthogonal polynomials to obtain a least squares fit, the sum of squared residuals at the minimum is given as

$$S_p = \sum_{j=1}^{n} W_j \left[y_j^2 - \sum_{k=1}^{p} \theta_k^2 \phi_k^2(x_j) \right] \qquad (A.9)$$

To test whether the p-th coefficient is statistically significant one calculates [103],

$$\frac{\left(S_{p-1} - S_p\right)(n-p)}{S_p} \qquad (A.10)$$

and if this is greater than F(1,(n-p)) at the 1% confidence level, the coefficient θ_p is considered to be non-zero. In addition, one should also look at the $\chi^2/(n-p)$ for the p-coefficient fit and in running the program in addition to the F-test, the number of parameters was chosen such that $\chi^2/(n-p)$ was between 2.0 and 0.2. Another criterion to use would be to look at a visual display of the fit on a screen for various values of p. This has not been implemented yet.

REFERENCES

1. R. Kinsey, "ENDF/B Summary Documentation, ENDF-201," (BNL-NCS-17541, 3rd Edition, 1979).

2. F.G.J. Perey, "Formats and Procedures for ENDF/B Error Files," (May 1973) and other documents,(Private Communication).

3. R.W. Peelle, "Requirements on Experiment Reporting To Meet Evaluation Needs," p. 421 in "Proc. of the NEANDC/NEACRP Specialists Meeting on Fast Neutron Fission Cross Sections of U-233, U-235, U-238 and Pu-239," ANL-76-90 (1976).

4. R.W. Peelle, "Uncertainty in the Nuclear Data Used for Reactor Calculations," Chapter II of "Sensitivity and Uncertainty Analysis of Reactor Performance Parameters," by C.R. Weisbin, R.W. Peelle, J.H. Marable, P. Collins, E. Kujawski, E. Greenspan and G. de Saussure (1980). To be published in Advances in Nuclear Science and Engineering, Plenum Press.

5. S.F. Mughabghab, "New Aspects in the Evaluation of Thermal Cross Sections." Proc. of this Workshop.

6. G.E. Forsythe, M.A. Malcolm and C.B. Moler, "Computer Methods for Mathematical Computations," Prentice-Hall, Inc. (1977).

7. C.L. Lawson and R.J. Hanson, "Solving Least-Squares Problems," Prentice-Hall, Inc. (1974).

8. G.W. Stewart, "Introduction to Matrix Computations," Academic Press (1973).

9. J.J. Dongarra, C.B. Moler, J.R. Bunch, G.W. Stewart, "LINPACK User's Guide," Society for Industrial and Applied Mathematics, Philadelphia (1979).

10. L. Stewart, R.J. LaBauve and P.G. Young, "Evaluated Nuclear Data for Hydrogen in the ENDF/B-II Format," LA-4574 (ENDF-141) (1971).

11. G.M. Hale, L. Stewart and P.G. Young, "Light Element Standard Cross Sections for ENDF/B Version IV," LA-6518-MS (ENDF-244) (1976).

12. J.C. Hopkins and G. Breit, "The $^{1}H(n,n)^{1}H$ Scattering Observables Required for High-Precision Fast Neutron Measurements," Nuclear Data Tables A9, 137 (1971).

13. P.G. Young "Summary Documentation of LASL Nuclear Data Evaluations for ENDF/B-V," LA-7663-MS (1979) Appendix B.

14. C.H. Johnson, "Recoil Telescope Detectors," Chapter II.C in "Fast Neutron Physics," Part I. J.B. Marion and J.L. Fowler (Eds), John Wiley and Sons, Inc. (1960).

15. Richard Wilson, "The Nucleon-Nucleon Interaction," John Wiley and Sons, Inc. (1963).

16. Richard A. Arndt and Malcolm H. MacGregor, "Nucleon-Nucleon Phase Shift Analyses by Chi-Squared Minimization," p. 253 in "Methods in Computational Physics," Vol. 6, Nuclear Physics, B. Adler, S. Fernbach and M. Rotenberg (Eds). Academic Press (1966).

17. G. Breit and R.D. Haracz, "Nucleon-Nucleon Scattering," p. 21 in "High Energy Physics," Vol. I, E.H.S. Burhop (Ed.) Academic Press (1967).

18. H.P. Stapp, T.J. Ypsilantis and N. Metropolis, "Phase-Shift Analysis of 310 MeV Proton-Proton Scattering Experiments," Phys. Rev. 105, 302 (1957).

19. A.W. Wapstra and K. Bos, "The 1977 Atomic Mass Evaluation," Atomic Data and Nuclear Data Tables 19, 175 (1977).

20. L. Koester, "Neutron Scattering Lengths and Fundamental Neutron Interactions, Springer Tracts in Modern Physics 80, pp. 1-55, Springer-Verlag (1977).

21. E. Lomon and R. Wilson, "Neutron-Proton Scattering at a Few MeV," Phys. Rev. C9, 1329 (1974).

22. M.S. Sher, P. Signell and L. Heller, "Characteristics of the Proton-Proton Interaction Deduced from the Data Below 30 MeV," Annals of Physics 58, 1 (1970).

23. T.L. Houk, "Neutron-Proton Scattering Cross Section at a Few Electron Volts and Charge Independence," Phys. Rev. C3, 1886 (1971).

24. W. Dilg, "Measurement of the Neutron-Proton Total Cross Section at 132 eV, "Phys. Rev. C11, 103 (1975).

25. H.A. Bethe, "Theory of the Effective Range in Nuclear Scattering," Phys. Rev. 76, 38 (1949).

26. R.A. Arndt and M.H. MacGregor, "Determination of the Nucleon-Nucleon Elastic-Scattering Matrix.V New Results at 25 MeV," Phys. Rev. 154, 1549 (1967).

27. M.H. MacGregor, R.A. Arndt and R.M. Wright, "Determination of the Nucleon-Nucleon Scattering Matrix.VII (p,p) Analysis from 0 to 400 MeV," Phys. Rev. 169, 1128 (1968).

28. M.H. MacGregor, R.A. Arndt and R.M. Wright, "Determination of the Nucleon-Nucleon Scattering Matrix.IX (n,p) Analysis from 7 to 750 MeV," Phys. Rev. 173, 1272 (1968).

29. M.H. MacGregor, R.A. Arndt and R.M. Wright, "Determination of the Nucleon-Nucleon Scattering Matrix.X (p,p) and (n,p) Analysis from 1 to 450 MeV," Phys. Rev. 182, 1714 (1969).

30. M.J. Moravcsik, "The Two-Nucleon Interaction," Clarendon Press, Oxford (1963).

31. R.A. Arndt, R.H. Hackman and L.D. Roper, "Nucleon-Nucleon Scattering Analyses, I. Proton-Proton Scattering from 1 to 500 MeV," Phys. Rev. C9, 555 (1974).

32. R.A. Arndt, R.H. Hackman and L.D. Roper, "Nucleon-Nucleon Scattering Analyses, II. Neutron-Proton Scattering from 0 to 425 MeV and Proton-Proton Scattering from 1 to 500 MeV," Phys. Rev. C15, 1002 (1977).

33. R.E. Seamon, K.A. Friedman, G. Breit, R.D. Haracz, J.M. Holt and A. Prakash, "Phenomenological Phase-Parameters Fits to N-N Data up to 350 MeV," Phys. Rev. 165, 1579 (1968).

34. G. Breit, J. Lucas and M. Tischler, "Concerning the n-p Scattering Cross Sections at 24 MeV," Phys. Rev. 184, 1668 (1969).

35. R.A. Arndt and M.H. MacGregor, "Determination of the Nucleon-Nucleon Elastic-Scattering Matrix IV. Comparison of Energy-dependent and Energy-independent Phase-Shift Analyses," Phys. Rev. 141, 873 (1966).

36. P. Cziffra, M.H. MacGregor, M.J. Moravcsik and H.P. Stapp, "Modified Analysis of Nucleon-Nucleon Scattering I. Theory and p-p Scattering at 310 MeV," Phys. Rev. 114, 880(1959).

37. M.H. MacGregor, M.J. Moravcsik and H.P. Stapp, "Modified Analysis of Nucleon-Nucleon Scattering II. Completed Analysis of p-p Scattering at 310 MeV," Phys. Rev. 116, 1248 (1959).

38. See Reference 17, footnote 15, pp. 127-128.

39. D.Y. Wong, "One-Meson Contribution to the Deuteron Quadrupole Moment," Phys. Rev. Letters 2, 406 (1959).

40. L.N. Rothenberg, "Neutron-Proton Angular Distribution at 24 MeV," Phys. Rev. C1, 1226 (1970).

41. J.C. Davis and H.H. Barschall, "Fast-Neutron Total Cross Section of Deuterium," Phys. Rev. C3, 1708 (1971) and J.C. Davis, K.A. Weaver, D. Hilscher, H.H. Barschall and A.B. Smith, "Total Cross Section of Protons for 2.5 MeV Neutrons," Phys. Rev. C4, 1061 (1971).

42. T.G. Masterson, "Differential Cross Sections for Small Angle Scattering of 24 MeV Neutrons by Protons," Phys. Rev. C6, 690 (1972).

43. T.W. Burrows, "Angular Distribution of 24.0 and 27.2 MeV Neutrons Scattered by Protons," Phys. Rev. C7, 1306 (1973).

44. J.A. Cookson, J.L. Fowler, M. Hussain, R.B. Schwartz and C.A. Uttley," The Angular Distribution of Neutron Scattering From Hydrogen at 27.3 MeV," Nuc. Phys. A299, 365 (1978).

45. L. Stewart and P.G. Young, "Hydrogen Scattering Cross Section, $^{1}H(n,n)^{1}H$" in "Standard Reference and Other Important Nuclear Data" ENDF-300 (BNL-NCS-51123) (1979).

46. C.A. Uttley, "The H(n,n)H Cross Section" in INDC/NEANDC Nuclear Standard File, 1978 Version, INDC-30/L+Sp (March 1980).

47. R.A. Arndt, J. Binstock and R. Bryan, "Nucleon-Nucleon Scattering Near 50 MeV. I. Phase-Shift Analysis of the Data," Phys. Rev. D8, 1397 (1973).

48. J. Binstock and R. Bryan, "Nucleon-Nucleon Scattering Near 50 Mev. II. Sensitivity of Various n-p Observables to the Phase Parameters," Phys. Rev. D9, 2528 (1974).

49. S.W. Johnsen, F.P. Brady, N.S.P. King, M.W. McNaughton and P. Signell, "Measurement of the n-p Spin Correlation Parameter A_{yy} at 50 MeV," Phys. Rev. Letters 38, 1123 (1977).

50. T.C. Montgomery, B.E. Bonner, F.P. Brady, W.B. Broste and M.W. McNaughton, "Neutron-Proton Differential Cross Section Measurements at 25.8 and 50.0 MeV," Phys. Rev. C16, 499 (1977).

51. J.L. Romero, M.W. McNaughton, F.P. Brady, N.S.P. King, T.S. Subramanian and J.L. Ullman, "Neutron-Proton Polarization at 50 MeV," Phys. Rev. C17, 468 (1978).

52. R. Garrett, J.W. Watson, F.P. Brady, D.H. Fitzgerald, J.L. Romero, J.L. Ullmann and C. Zanelli, "Neutron-proton Analyzing Power at 50 MeV," Phys. Rev. C21, 1149 (1980).

53. N.S.P. King, J.D. Reber, J.L. Romero, D.H. Fitzgerald, J.L. Ullmann, T.S. Subramanian and F.P. Brady, "Neutron-proton Scattering I. Differential Cross Section at 63.1 MeV," Phys. Rev. C21, 1185 (1980).

54. D.H. Fitzgerald, F.P. Brady, R. Garrett, S.W. Johnsen, J.L. Romero, T.S. Subramanian, J.L. Ullmann and J.W. Watson, "Neutron-proton Scattering II. Spin Correlation Parameters $A_{yy}(-)$ at 50 MeV," Phys. Rev. C21, 1190 (1980)

55. F.P. Brady, W.J. Knox, J.A. Jungerman, M.R. McGee and R.L. Walraven, "Precise Measurement of Neutron-Proton Total Cross Section from 25 to 60 MeV," Phys. Rev. Letters 25, 1628 (1970).

56. A. Langsford, P.H. Bowen, G.C. Cox, G.B. Huxtable and R.A.J. Riddle, "A Measurement of Polarization in Neutron-Proton Scattering in the Energy Range 20-120 MeV," Nuc. Phys. 74, 241 (1965).

57. G.M. Hale, "R-matrix Analysis of the ^{7}Li System," in "Neutron Standards and Applications," Proc. of a Symposium, NBS Special Pub. 493, p. 30 (1977) and p. 3-6-1 in Ref. 1 (1979).

58. G.M. Hale, L. Stewart and P.G. Young, "Summary Documentation for ^{10}B," p. 5-10-1 in Ref. 1 (1979).

59. G.M. Hale, "Use of R-matrix Methods for Light Element Evaluations," Proceedings of this Workshop.

60. C.Y. Fu and F.G. Perey, "Neutron Scattering Cross Sections of Carbon Below 2 MeV Recommended from R-matrix Fits to Data," Atomic Data and Nuclear Data Tables, 22, 249 (1978).

61. J.T. Reynolds, C.J. Slavik, C.R. Lubitz and N.C. Francis, "Coupled-Channel Calculation of ^{12}C-Neutron Scattering," Phys. Rev. 176, 1213 (1968).

62. N.C. Francis, C.R. Lubitz, J.T. Reynolds, C.J. Slavik and R.G. Stieglitz, "Carbon as a Cross Section Standard Between 0 and 2 MeV," p. 166 in "Neutron Standards and Flux Normalization," Proc. of a Symposium held at Argonne National Lab. AEC. Symposium Series 23 (1977).

63. A.M. Lane and R.G. Thomas, "R-matrix Theory of Nuclear Reactions," Rev. Mod. Phys. 30, 257 (1958).

64. H. B. Willard, L.C. Biedenharn, P. Huber and E. Baumgartner, "Resonance Processes with Fast Neutrons," Part II, P. 1217 in "Fast Neutron Physics," J.B. Marion and J.L. Fowler (Eds), John Wiley and Sons (1963).

65. J.C. Lachkar, "Evaluation and Use of Carbon as a Standard," Neutron Standards and Applications, Proc. of a Symposium NBS. Sp. Publication 493, p. 93 (1977).

66. A. Smith, R. Holt and J. Whalen, "Neutron Scattering from ^{nat}C in the Few MeV Region," ANL/NDM-43 (1978).

67. W.P Poenitz and A.B. Smith, "The Fast Neutron Cross Section of ^{nat}C,"Standard Reference and Other Important Nuclear Data, ENDF-300 (BNL-NCS-51123) (1979).

68. R.O. Lane, R.D. Koshel and J.E. Monahan, "Polarization and Differential Cross Section for Neutrons Scattered from ^{nat}C," Phys. Rev. 188, 1618 (1969).

69. C.Y. Fu, Private Communication (1980).

70. L. Stewart, "The ^{3}He(n,p)T, ^{6}Li(n,α)T and ^{10}B(n,α) Standard Cross Sections," in Neutron Standard Reference Data, Proc. of A Panel, Vienna, 20-24 Nov. 1972, p. 149, IAEA Vienna (1974).

71. L. Stewart, Private Communication (1980).

72. L. Stewart, "Methods Used in Evaluating Data for the Interaction of Neutrons With Light Elements (A<19)," Proceedings of this Workshop.

73. Webster's Seventh New Collegiate Dictionary. G & C. Merriam Company, Springfield, MA (1969).

74. S.F. Mughabghab, "Evaluation of the Capture Cross Section of ^{197}Au," BNL-NCS-21774 (1976).

75. B.R. Leonard Jr., D.A. Kottwitz, J.K. Thompson, "Evaluation of the Neutron Cross Sections of ^{235}U in the Thermal Energy Region," EPRI NP-167 (1976).

76. W.P. Poenitz, "Evaluation of ^{235}U(n,f) Between 100 keV and 20 MeV," ANL/NDM-45 (1979).

77. W.P. Poenitz, "Data Interpretation, Objective Evaluation Procedures and Mathematical Techniques for the Evaluation of Energy-Dependent Ratio, Shape and Cross Section Data," Proceedings of this Workshop.

78. W.P. Poenitz, Private Communication (1978).

79. P.W. Peelle, "Uncertainty Files for ^{235}U Cross Sections," Appendix B of EPRI-NP-346 (1977).

80. M.R. Bhat, "A New Procedure to Obtain A Least-Squares Fit to ^{235}U(n,f) from 0.05-20.5 MeV, preliminary draft of a document circulated amongst members of N&S Subcommittee of CSEWG (May 1980).

81. K. Kari, "Messung Der Spaltquerschnitte Von ^{239}Pu und ^{241}Pu Relativ Zum Spaltquerschnitt Von ^{235}U Und Streuquerschnitt H(n,p) In Dem Neutronenenergiebereich Zwischen 0.5-20 MeV," KFK-2673 (1978).

82. D.M. Barton, B.C. Diven, G.E. Hansen, G.A. Jarvis, P.G. Koontz and R.K. Smith, "Measurement of the U-235 Fission Cross Sections Over the Neutron Energy Range 1 to 6 MeV," Nuc. Sci. Eng. 60, 369 (1976).

83. W.P. Poenitz, "Additional Measurements of the ^{235}U(n,f) Cross Section in the 0.2-3.2 MeV Range," Nuc. Sci. Eng. 64, 894 (1977). Data as given in Ref. 76.

84. A.D. Carlson and B.H. Patrick, "Measurements of the ^{235}U Fission Cross Section in the MeV Energy Region," Neutron Physics and Nuclear Data for Reactors, Proc. of an International Conf., Harwell (1978), p. 980, Preliminary data as given in Ref. 76.

85. V.A. Kon'shin, E. Sh. Sukhovitskij and V.F. Zharkov, "Determination of the Errors in Evaluated Data with Allowance for Correlations. Evaluation of $\sigma_f(^{235}U)$, $\alpha(^{235}U)$, $\alpha(^{239}Pu)$ and $\sigma_f(^{239}Pu)$ for the Evaluated Nuclear Data Library BOYaD-3," INDC(CCP)-132/LV, IAEA, Vienna (1979).

86. V.A. Kon'shin, V.F. Zharkov and E. Sh. Sukhovitskij, "Evaluation of the ^{235}U Fission Cross-Section in the Energy Range 0.1 keV-20 MeV," INDC(CCP)-148/L, IAEA, Vienna (1980).

87. G.E.P. Box and G.C. Tiao, "Bayesian Inference in Statistical Analysis," Addison-Wesley Publishing Co., Reading, MA (1973).

88. J.B. Dragt, "Statistical Considerations on Techniques for Adjustment of Differential Cross Sections with Measured Integral Parameters," p. 85, RCN-122, Reactor Centrum Nederland (1970).

89. J.B. Dragt, J.W.M. Dekker, H. Gruppelaar and A.J. Janssen, "Methods of Adjustment and Error Evaluation of Neutron Capture Cross Sections; Application to Fission Product Nuclides," Nuc. Sci. and Eng. 62, 117 (1977).

90. F. Schmittroth, "Varied Applications of a New Maximum-Likelihood Code with Complete Covariance Capability," CRNL/RSIC-42, Oak Ridge National Lab. (1979).

91. F.G. Perey, "Contributions to Few-Channel Spectrum Unfolding," ORNL/TM-6267 (ENDF-259) (1978).

92. F.G. Perey, "Least-Squares Dosimetry Unfolding: The Program STAY'SL," ORNL/TM-6062 (ENDF-254) (1977).

93. F. Schmittroth, "Generalized Least-Squares for Data Analysis," HEDL-TME 77-51 (UC-79d), Hanford Engineering Development Lab. (1978).

94. F. Schmittroth, "FERRET Data Analysis Code," HEDL-TME 79-40 (UC-79,79d), Hanford Engineering Development Lab. (1979).

95. F. Schmittroth and R.E. Schenter, "Finite Element Basis in Data Adjustment," Nuc. Sci. and Eng. 74, 168 (1980).

96. D.M. Hetrick and C.Y. Fu, "GLUCS: A Generalized Least-Squares Program for Updating Cross Section Evaluations with Correlated Data Sets," ORNL/TM-7341 (ENDF-303) (1980).

97. C.Y. Fu, D.M. Hetrick and F.G. Perey, "Simultaneous Evaluation of ^{32}S(n,p), ^{56}Fe(n,p), ^{65}Cu(n,2n) Cross Sections," Proc. Conf. Nuclear Data for Technology, Knoxville, 1979 (to be published).

98. C.Y. Fu, Private Communication (1980).

99. W.T. Eadie, D. Dryard, F.E. James, M. Roos and B. Sadoulet, "Statistical Method in Experimental Physics," North-Holland Publishing Co. (1971).

100. W. P. Poenitz, "Interpretation and Intercomparison of Standard Cross Sections," p. 331 of "Neutron Standards and Flux Nomalization," Proc. of a Symposium, Oct. 21-23, 1970, Argonne National Laboratory, AEC Symposium Series 23 (1971).

101. G.E. Forsythe, "Generation and Use of Orthogonal Polynomials for Data-Fitting with a Digital Computer," J. Soc. Indust. Appl. Math, 5, 74 (1957).

102. B.R. Martin, "Statistics for Physicsts," Academic Press, Inc. (1971) p. 153.

103. See p. 238 of Ref. 99.

104. W.P. Poenitz, "Relative and Absolute Measurements of the Fast-Neutron Fission Cross Section of Uranium-235," Nuc. Sci. Eng. 53, 370 (1974).

105. M. Cance and G. Grenier, "Absolute Neutron Fission Cross Sections of ^{235}U, ^{238}U and ^{239}Pu at 13.9 and 14.6 MeV," Nuc. Sci. Eng. 68, 197 (1978).

106. P.H. White, "Measurements of the ^{235}U Neutron Fission Cross Section in the Energy Range 0.04-14 MeV," Jour. Nuc. Energy A/B19, 325 (1965).

107. O.A. Wasson, Private Communication (1978).

108. I. Szabo and J.P Marquette, "Measurement of the Neutron Induced Fission Cross Sections of Uranium 235 and Plutonium 239 in the MeV Energy Range," Proc. of the NEANDC/NEACRP Specialists Meeting on Fast Neutron Cross Section of U-233, U-235, U-238 and Pu-239, Argonne National Laboratory, ANL-76-90, p. 208 (1976).

109. M.C. Davis, G.F. Knoll, J.C. Robertson and D.M. Gilliam, "Absolute Measurements of ^{235}U and ^{239}Pu Fission Cross-Sections with Photoneutron Sources," Annals of Nuc. Energy 5, 569 (1978).

110. O.A. Wasson, "The ^{235}U Neutron Fission Cross Section Measurement at the NBS Linac," Proc. of the NEANDC/NEACRP Specialists Meeting on Fast Neutron Cross Sections of U-233, U-235, U-238 and Pu-239, Argonne National Laboratory, ANL-76-90, p. 183 (1976).

111. R. Arlt et al., International Nuclear Data Comm. Report, INDC/GDR-7.16, 10 (1978).

112. J.B. Czirr and G.S. Sidhu, "Fission Cross Section of Uranium-235 from 3 to 20 MeV," Nuc. Sci. Eng. 57, 18 (1975) and "Fission Cross Section of Uranium-235 from 0.8 to 4 MeV," Nuc. Sci. Eng. 58, 371 (1975).

113. R.K. Smith. R.L. Henkel and R.A. Nobles data as communicated to the author by Gordon E. Hansen (LASL) in a letter dated Feb. 14, 1980.

114. D.B. Gayther, "Measurement of the ^{239}Pu Fission Cross Section and its Ratio to the ^{235}U Fission Cross Section in the Energy Range from 1 keV to 1 MeV," Proc. of Conf. on Nuclear Cross Sections and Technology, NBS. Sp. Pub. 425, Vol. II, p. 564 (1975).

115. F. Kaeppeler, KFK-1772 (1973).

TABLE I

Types of Data Used in $^{1}H(n,n)^{1}H$ Phase Shift Analysis

Data Type	Approximate Precision
Deuteron Binding Energy B	0.001%
Deuteron Radius R (from B)	0.002%
Epithermal Scattering Cross Section σ_o	0.07%
Coherent Scattering Length f	0.03%
a_t (from σ_o and f)	0.06%
a_s (from σ_o and f)	0.03%
r_{ot} (from a_t and B)	0.3%
r_{os} (from a_s and low energy scattering)	2%
a_{pp}	0.05%
r_{opp}	0.6%
Total, differential elastic scattering, polarization, spin transfer and spin correlation (n,p) data	1-several %
Differential elastic scattering, polarization spin transfer and spin correlation (p,p) data	1-several %

TABLE II

Absolute $^{235}U(n,f)$ Data Used in Shape/Magnitude Fit

No.	Author	Ref.	Energy Range (keV)	AN/SAN	Comments
1	Barton, et al.	82	3.0+3	10000/1	
2	Poenitz	83	1.93+2 - 8.275+3	45000/71	Black Det.
3	Poenitz	104	3.99+2 - 3.5+3	13000/2	Black Det.
4	Poenitz	104	4.98+2	40000/2	VSO_4 Bath
5	Poenitz	104	4.48+2 - 6.44+2	40000/2	Assoc. Activ.
6	Kari	81	1.0+3 - 2.031+4	45000/4	
7	Cancé & Grenier	105	1.39+4 , 1.46+4	40000/2	
8	White	106	6.7+1 - 1.41+4	18000/1	
9	Wasson & Meier	107	2.54+2 - 1.217+3	31000/1	Preliminary
10	Szabo, et al.	108	5.1+1 - 5.53+3	17000/1	non-White Counter
11	Davis, et al.	109	1.4+2 - 9.64+2	36000/1	
12	Wasson	110	5.5+1 - 7.5+2	45000/10	
13	Arlt	111	1.47+4	40000/2	

TABLE III

$^{235}U(n,f)$ Data Sets Used in Shape Fit

No.	Author	Ref.	Energy Range (keV)	AN/SAN	Comments
1	Barton et al.	82	1.0+3 - 6.0+3	10000/1	
2	Czirr & Sidhu	112	7.54+2 - 2.01+4	11000/1	
3	Poenitz	104	6.8+1 - 3.5+3	13000/1	grey det. data
4	Poentiz	104	3.99+2 - 3.5+3	13000/2	black det. data
5	Smith, et al.	113	2.22+3 - 2.05+4	16000/1	
6	Szabo, et al	108	5.1+1 - 5.53+3	17000/1	non-white counter
7	White	106	6.7+1 - 1.41+4	18000/1	
8	Kari	81	1.0+3 - 2.031+4	45000/4	
9	Poenitz	83	1.93+2 - 8.275+3	45000/71	black det. data
10	Carlson & Patick	84	1.171+3 - 6.203+3	45000/151	Preliminary
11	Szabo, et al.	108	5.5+1 - 2.1+3	30000/1	White counter
12	Wasson & Meier	107	2.54+2 - 1.217+3	31000/1	Preliminary
13	Davis, et al.	109	1.4+2 - 9.64+2	36000/1	
14	Gayther	114	5.5+1 - 9.5+2	45000/8	
15	Wasson	110	5.5+1 - 7.5+2	45000/10	
16	Kaeppeler	115	5.46+2 - 1.175+3	45000/111	
17	Kaeppeler	115	5.13+2 - 1.164+3	45000/112	

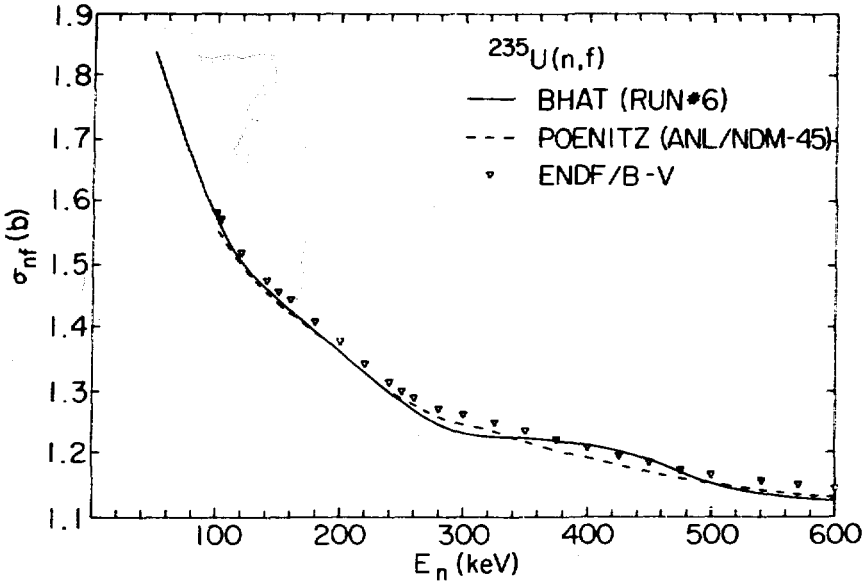

Fig. 1. Comparison of ENDF/B-V, Poenitz and Bhat Evaluations of ^{235}U(n,f) From 100-600 keV.

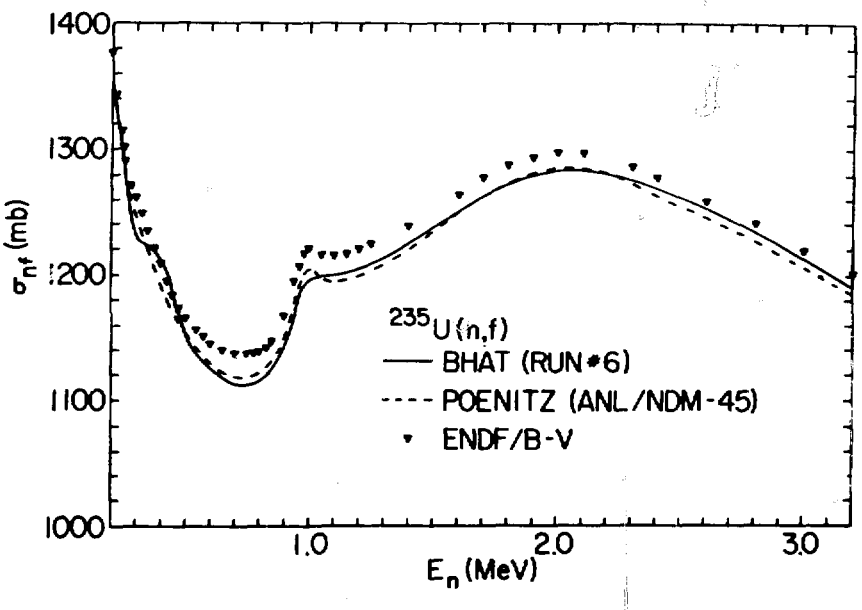

Fig. 2. Comparison of ENDF/B-V, Poenitz and Bhat Evaluations of ^{235}U(n,f) From 0.2-3.2 MeV.

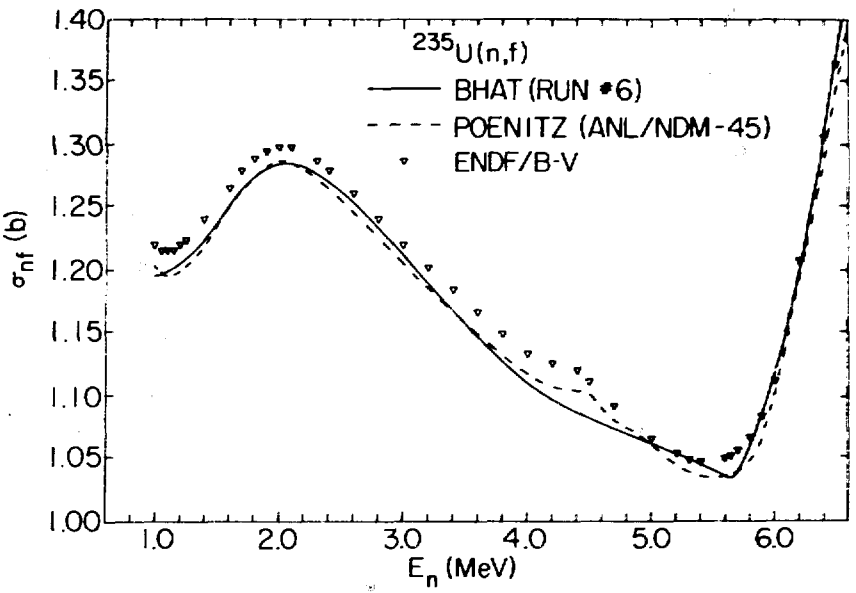

Fig. 3. Comparison of ENDF/B-V, Poenitz and Bhat Evaluations of ^{235}U(n,f) From 1.0-6.6 MeV.

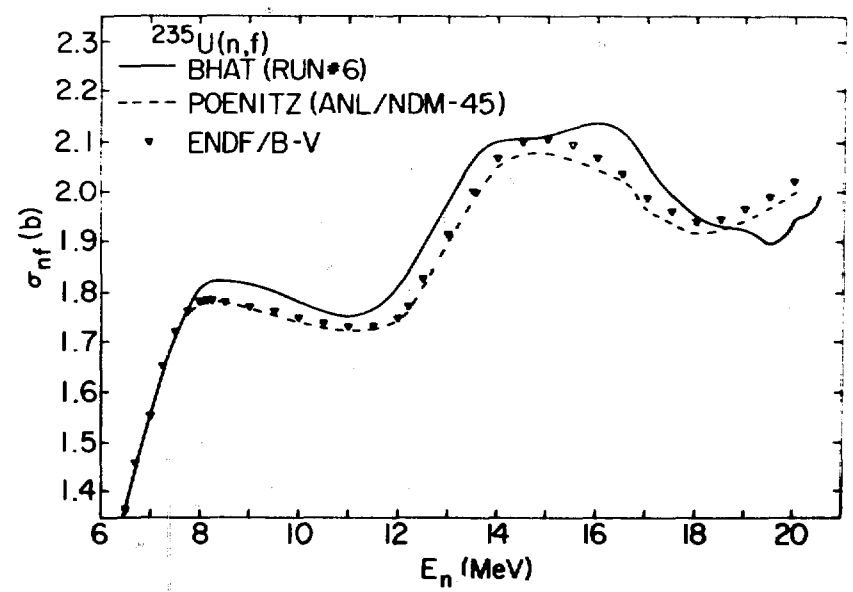

Fig. 4. Comparison of ENDF/B-V, Poenitz and Bhat Evaluations of ^{235}U(n,f) From 6-20 MeV.

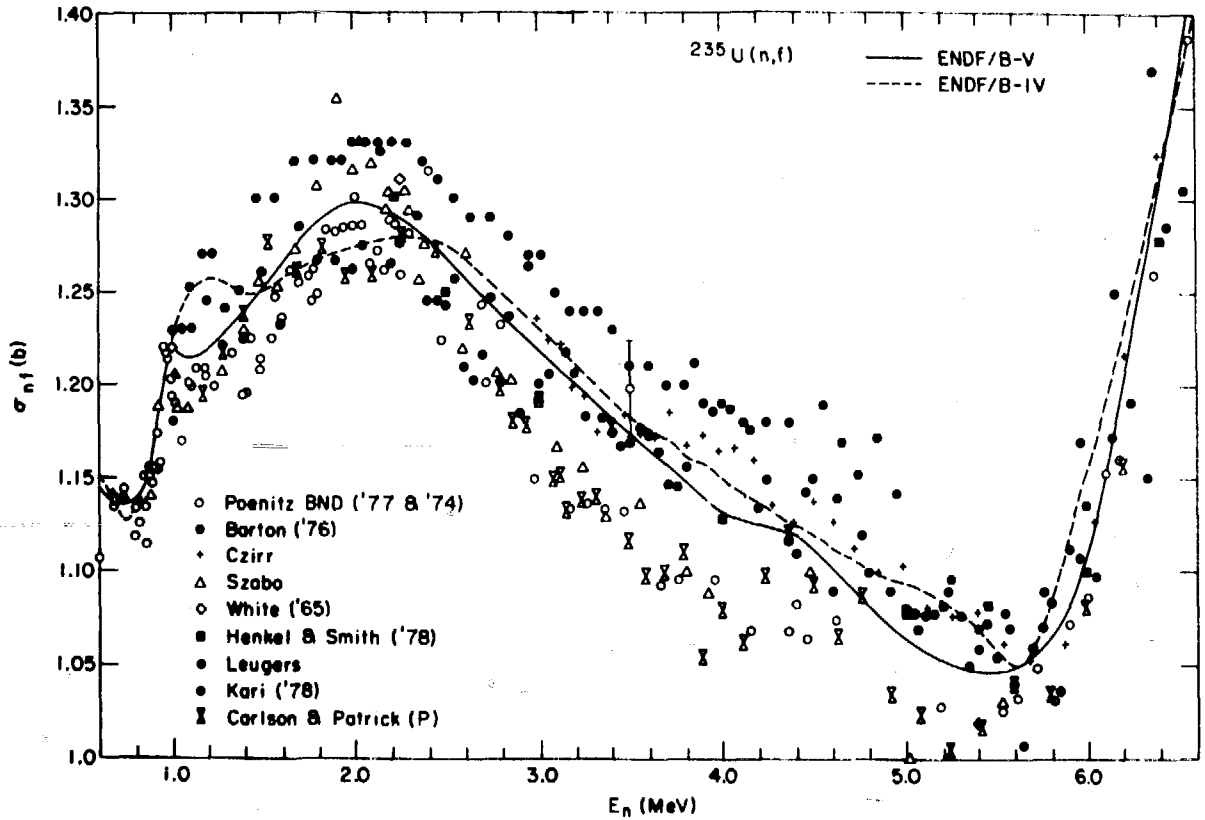

Fig. 5. Experimental ^{235}U(n,f) Data From 0.6-6.6 MeV With ENDF/B-IV, V Evaluations.

Discussion

Poenitz

In your talk, you requested that experimentalists report the variance-covariance matarix of their results. Actually, I think what we really want from the experimenter is his error components. The evaluator can easily derive the variance-covariance matrix from the components. It would not be good if the experimenter provided the full matrix because some information would be lost, that is, the variance-covariance matrix has already collapsed some information. In addition, keeping just the error components requires much less data storage.

Bhat

I did not go into details in the talk, but the proposed method for storing this information in our data files is exactly as you describe. That is, it requests experimenters to divide error information into components and the component errors are stored.

Perey

I concur strongly with Wolfgang on that matter. Being an advocate of variance-covariance matrices, people think I advocate publishing those matrices. I think it is very important not to publish necessarily the variance-covariance matrices, and I strongly support Wolfgang's statement that instead you should provide the error components. One very simple reason for this is the sacrosanct attitude that data from an experiment is sacred. I regard it as our duty as evaluators to look at the data and apply any corrections that may be justified. At the time the experimenter generated his uncertainty components, he may have had a very good reason for not making certain assumptions or for assuming certain things that we no longer believe. So we have to update the information. It is not a question of challenging the experimentalist but rather of updating our state of knowledge. Therefore, we need to have the error components to be able to do this.

One additional point, which is very important, is that essentially we have been doing this in our experimental papers. It is long tradition to provide a detailed explanation of what we call the error components. What we have failed to do in most instances is to provide the explicit formula on how you use these components to generate the covariance matrix and this is really the accession point that is missing from our papers today. We have difficulty analyzing an experimental paper when we do not understand the procedure whereby the observables and the uncertainty have been combined to generate the quantity of interest (the ratio or the relative value). It is this formula on how to combine the different components that is missing and should

be provided in experimental papers. It is a great handicap in using past experiments when this information is absent. Having made this comment, I strongly support Wolfgang. In your tabulation and exchange of international data, these are the components that have to be obtained, and somehow you will also have to provide for this formula in your tabulations.

I wanted to make one other comment having to do with your information measure. The subject of what is the information content of a probability density function has a long history. It was discovered and was a major contribution of Shannon in his famous 1948 papers that the unique and only measure of information content was $\sum_i p_i \log p_i$.

Bhat

There is some question about that , i.e., whether it is unique and the only measure of information content. But please go on.

Perey

The point that information content can be derived is a unique one for discrete distributions only. It is not true for continuous distributions and, in fact, the work of Jaynes, which I referred to and which culminated in his 1968 paper, came from a realization that one needed to introduce a measure to cause the information to be invariant under the representation that was used. This particular measure, which had to introduced, turned out to be exactly the irreducible representation of the transformation group. And this is how the whole invariance theory came into being. So I think your definition of information measure as M to the power minus one is greatly challenged by many people today.

Bhat

You see, there are different definitions of information. There is Shannon's definition, there is Kullback's definition, there is Weiner's definition--there are definitions and definitions. I did not have time to go into all of them and some are of interest only to the mathematical statistican. Fisher's definition is the one that seems to be appropriate for the interpretation of these data adjustment equations. Besides, I did not want to introduce Shannon's definition of the idea of entropy because sometimes I think this tends to cloud the issue rather than clear it.

Perey

I beg to differ; it is a question of opinion here. The whole success of quantum mechanics and statistical mechanics indeed owes very much to the grand canonical ensemble and to the formulation of entropy which is directly related to that information measure and, in fact, to the uniqueness of the information measure.

Rowlands

Concerning your discussion of the measure of the information content of integral measurements used when evaluating differential cross sections, I think that the main reason for producing evaluated data libraries is to predict integral properties. I wonder, therefore, whether one should consider the information content of the integral measurements relative to the application. Also, I do not understand why you say that one should not iterate when fitting data. Provided that the adjustment is taken into account as a bias in the next stages of fitting, I think this is the right way to proceed.

Bhat

I think I qualified my statement about not iterating to include the provision that the linear approximations are correct. Now, in the case of iterating, I think one of the things you have to keep in mind is that you should not change your prior, because that usually comes from experimental data. I think Bob Peelle stressed this point earlier.

As regards the information content of integral experiments, all I wanted to say was that this is where sensitivity coefficients come in (because the integral data are a function of the differential data and you want to get information about the mean of the differential data from the distribution of integral data). If you take a small enough energy range so that is is essentially constant, then there are no problems. But if your energy range is large, then the energy dependence gets factored in.

Smith

I must make a few remarks. I am involved in some complex multi-parameter experiments. I think they have many similarities with the landing of a supersonic aircraft on an aircraft carrier deck. It is always a crash. The problem is to control it. And I guess what I am really worried about is that I hear Wolfgang and Mulki, in their excellent talks, asking me to quantify that crash in all its pristine virgin glory, and I really am struck dumb with that prospect. It is awesome.

One of the proponents of information theory (over many beers last night) agreed with me, I think, that there are some noble old artisans that practice this art (and in many ways it is an art and not a science) and that their judgements are made from witchcrafts much as if they were in a florentine workshop. The names that were kicked about were Larry Cranberg, whose inelastic scattering cross-section measurements for U-238 appeared in 1953 and 1954 papers. I would throw the data away, but his judgment was marvelous and I think it is difficult to quantify that sort of thing. Also, there are people like Tom Bonner who created things

that are still widely and successfully used. I do not know how Tom Bonner did it, but he did it right. At least time seems to indicate this.

Getting down to the more realistic things of life, one of the key things that was cited in the lectures yesterday, I believe by Mr. Gohar, was the breeding yield for Li-7 in a fusion device. If you look at that evaluation, you will find that it has some real problems. Now I wonder, do we want to commit our time to trying to massage that same old set of numbers or do we want to get some new numbers? Personally, I prefer the new number approach. I think given the amount of fixed resources (at best fixed, maybe dwindling), you have got to ask yourselves if you want to load your experimenter with the much more burdensome chore of reanalyzing old experiments or do you want him to resolve the Li-7 problem by a new measurement? (And not by a bunch of statistical numbers on the same old data). Wolfgang, I think, had an example of it there on U-235. Ten years later he is now back to about the same number that he had long ago. My question is, should I worry about doing another experiment with 2% accuracy on the U-235 fission cross section and quantify all its glorious uncertainties if I can, or should I struggle for a factor of five improvement in accuracy that I think will really make an impact? Maybe I will not know that accuracy better than 25 or even 50%, but perhaps that is the way to go. I would like an answer to that question.

I will make one final remark. Last Friday there was a lecture in one experimental group in this country and a supervisor got kind of nasty. The point of the lecture was to urge experimentalists in the group to publish the experimental data that they hade accumulated over the past two years. Now, if I ask people, who I cannot now get to publish results, to add all these extra error assignments which are really unknown in some cases, then instead of having perhaps ten total cross sections in the fission product region, you will maybe have half of one. So, you have to decide whether you want ten measurements that are not fully specified or do you want the half of one. This is the judgment you have to make . There are only so many resources, and I think you have to face up to these things

Bhat

One of the complaints you hear from experimentalists about evaluators is that "they do not understand my data," or "look at what he has done with my wonderful data."To get around this complaint, at least in the case of standards measurements, I think it is the duty of the experimenter if he wants his errors treated correctly (statistical errors, systematic errors, correlated errors, etc.), to write the information down in his publication.

It is true that it is more work, but the standards measurements form a class by themselves. For a standards measurement where you are worried about 2,3 or even 1% uncertainties, perhaps it is part of the game that you have to take the trouble to put down all the error information in black and white.

SESSION VI

SUBRESONANCE AND THERMAL REGION
Chairman: S.F. Mughabghab BNL

NEW ASPECTS IN THE EVALUATION OF THERMAL NEUTRON CROSS SECTIONS*

S. F. Mughabghab

Brookhaven National Laboratory
Upton, N. Y. 11973, U.S.A.

ABSTRACT

Because of recent advances in experimental techniques, which improved the accuracies of thermal capture and scattering cross sections by an order of magnitude, a more stringent approach in the evaluation of the thermal constants is developed. In the present approach, the following aspects are introduced: (1) a consistency between thermal cross sections, coherent and incoherent scattering lengths, and neutron resonance parameters is achieved; (2) a consistency between the isotopic and element cross sections is sought; in addition, for each isotope, the requirement that the partial cross sections add up to the total is fulfilled; (3) where possible, charged particle data particularly derived from (d,p) reactions on light and medium weight istopes are used in locating the positions and strengths of bound levels. Such a procedure is useful in the evaluation of the shape of the cross sections in the thermal region; and (4) the Lane-Lynn theory of direct capture is called upon to calculate thermal cross sections and check for consistencies for certain isotopes.

Extensive examples to illustrate these procedures are presented.

---

*This work was performed under the auspices of the U.S. Department of Energy.

I. INTRODUCTION

I would like to start this review by asking a question: Why study and evaluate thermal neutron cross sections?

The answer to this is that the neutron has a "charm" and the neutron interaction at thermal energies is fundamental and important for several reasons:

1. Thermal cross sections are fundamental in testing high energy theories. Examples which can be cited are the pion exchange[1-2] and the quark models[3]. The pion exchange model was called upon by Riska and Brown[1] to explain a 10% discrepancy between the measured cross section of H and previous calculations and by Hadjimichael[2] to calculate the radiative neutron-deuteron capture cross section (520 ± 50 μb). The quark model was applied by Carlitz et al.[3] to achieve consistency between measured and calculated neutron-electron interaction scattering length. The latter calculation gives an indication of the structure and charge properties of the neutron.

2. Thermal cross sections are important ingredients in low energy nuclear theory:

a. Accurate knowledge of the singlet and triplet scattering lengths of H is basic for theoretical models dealing with the (n,p) interaction.

b. Scattering lengths of the four nucleon systems, n-^{3}H and n-^{3}He, can also shed light on the nucleon-nucleon interaction.[4] Experimental values of the thermal neutron scattering lengths of ^{3}H and ^{3}He favor the Yukawa over the exponential form factors.

c. Spin dependent scattering lengths (and subsequently incoherent scattering lengths) of light and medium weight nuclides can test the accuracy of shell model calculations.[5]

3. Thermal total and partial capture cross sections provide experimental tests of the validity of the Lane-Lynn theory of direct capture. Verification of this theory will be presented. This will be followed by a discussion of the applicability and limitations of the theory.

4. For light and medium weight nuclides, thermal cross sections can compliment charged particle data in predicting spins and (d,p) spectroscopic factors of final states.

5. Thermal cross sections can check the completeness of resonance parameters, and can be used to derive the potential scattering radius R which is important in optical model calculations.

6. Thermal cross sections are important in determining the absolute neutron capture γ-ray intensities which in turn are used as a tool in the identification of elements and impurities in samples.

7. Improved knowledge of the thermal cross sections are required for reactor cycle and burn-up calulations. This would result in improved design of thermal reactors.

8. Thermal cross sections are used as standards. Examples are the capture cross sections of ^{197}Au, ^{59}Co, ^{55}Mn, the scattering cross sections of H, C, Si, V, Ni, and the fission cross sections of ^{235}U, ^{239}Pu.

II. PROCEDURE IN THE EVALUATION

We briefly outline in this section the various steps involved in the evaluation of thermal cross sections.

1. The first step in any evaluation is compilation of the experimental data. A complete and correct documented data base must be available. The CSISRS Library can be used for that purpose with a supplementation of the most recent data which may not be yet in the computerized files.

2. This is followed by a reduction of the data to a standard form. The following steps are required:

a. The reported cross sections are normalized to the standard cross sections of ^{55}Mn, ^{59}Co, ^{197}Au, (capture), C, Si, V, Ni (scattering), ^{235}U, ^{239}Pu, ^{252}Cf (fission), and to the most recent recommend half lives and abundances.

b. Corrections for reactor neutron spectrum and isotopic impurities, if possible, are made. This can be achieved with the aid of catalogues of strong γ-ray intensities and resonances, provided that the authors reported the required information.

c. A correction due to the shape of the cross section is made. This is possible if the locations of positive energy resonances and bound levels are known.

3. Weighted averages of the normalized data are produced and internal and external errors are calculated.

4. The last step requires consistency checks.

a. A consistency between thermal capture cross sections, coherent and incoherent scattering lengths, and neutron resonance parameters is achieved.

b. A consistency between the isotopic and element cross sections is sought; in addition, for each isotope, the requirement that the partial cross sections add up to the total is fulfilled.

c. The Lane-Lynn theory of direct capture is called upon to calculate thermal cross sections and check for consistencies between thermal capture cross sections and scattering lengths for certain isotopes.

d. For light nuclides, one can utilize the principle of charge symmetry to calculate, for example, scattering cross sections. An excellent example is provided by the analysis of Hale and Dodder[6] for the reaction $p+^{3}He \Longleftrightarrow n+T$. These authors predicted the singlet and triplet scattering lengths $a_+=3.32$ fm, $a_-=4.45$ fm and consequently $a=3.6$ fm.

5. In the actinide region, one can achieve additional consistency between σ_γ, σ_f, σ_a, σ_s, α,n,$\bar{\nu}$ by the least squares method.

Since this method is adequately described by Leonard[7] and Lemmel[8] I will forego its discussion.

III. THEORETICAL CONSIDERATIONS

At this stage, it is important to review some of the theoretical relations which will be used extensively in the discussion.

A. Coherent Scattering Amplitudes

The spin dependent scattering amplitudes a_+ and a_- associated with s-wave resonances of spins $I + 1/2$ and $I - 1/2$ (where I is the spin of a target nucleus) can be written in terms of the resonance parameters as

$$a_{\pm} = R' + \sum_j \frac{\lambda_j \Gamma_{nj}}{2(E-E_j)-i\Gamma_j} \qquad (1)$$

where the summation is carried out over resonances with the same spin. The total coherent scattering amplitude is then the sum of the partial amplitudes weighted by their spin statistical factors g_+ and g_-,

$$a = g_+ a_+ + g_- a_-$$

$$g_+ = \frac{I+1}{2I+1} \qquad g_- = \frac{I}{2I+1} \qquad (2)$$

The coherent scattering amplitude for each spin state Eq. (1) can be separated into real and imaginary parts:

$$a_{coh} = R' + \sum_j \frac{\lambda_j \Gamma_{nj}(E-E_j)}{4(E-E_j)^2+\Gamma_j^2} + i \sum_j \frac{\lambda_j \Gamma_{nj}\Gamma_j}{4(E-E_j)^2+\Gamma_j^2} \qquad (3)$$

$$= a_r + i a_i$$

where a_r and a_i are the real and imaginary components, respectively. It is interesting to note that the imaginary part can be related to the absorption cross, σ_a by:

$$a_i = \frac{k\,\sigma_a}{4\pi} \qquad (4)$$

where k is the wave number.

With the exception of few nuclides, neutron resonances are located far away from thermal energies. Under these conditions and for $E_j \gg \Gamma_j$ the coherent scattering amplitude takes the simple form

$$a = R' - 2.277 \times 10^3 \frac{\Gamma^0_{nj}}{E_{oj}} \quad . \qquad (5)$$

Another important relation which is required in the analysis of experimental data is the one between the free, a, and bound, b, coherent scattering amplitudes

$$b = \left(\frac{A + 1.0087}{A}\right) a + Z\, b_{ne} \qquad (6)$$

where b_{ne} is the neutron-electron interaction length. Its most accurate value was determined recently by Koester et al.[9]

$$b_{ne} = -\left(1.38 \pm 0.03\right) \times 10^{-3} \text{ fm} \quad .$$

The coherent and spin-incoherent free scattering cross sections can be described in terms of the coherent scattering amplitudes by:

$$\sigma_{coh} = 4\pi \left(g_+ a_+ + g_- a_-\right)^2$$

$$\sigma_{inc\ (spin)} = 4\pi\, g_+ g_- \left(a_+ - a_-\right)^2 \qquad (7)$$

For an element with several isotopes, an additional incoherent scattering cross section arises due to differences in the coherent scattering amplitudes of the various isotopes.

$$\sigma_{inc\ (isotopic)} = 4\pi \sum_m \sum_n \frac{1}{2}\, f_m f_n \left(a_m - a_n\right)^2 \qquad (8)$$

where f_n and a_n are respectively the abundance and the scattering amplitude of the n-th isotope.

In recent years, specialized techniques based on the wave properties of the neutron (interference, refraction, reflection, and diffraction) have been developed which resulted in highly improved knowledge of the coherent scattering amplitudes of the various isotopes and elements. These methods, as well as the Christiansen filter method, are described in the excellent review article by Koester.[10]

These relations provide the link between the thermal neutron cross sections and resonance parameters and can serve to check the consistency of the resonance parameters. A knowledge of the magnitude of the potential scattering radius R′ at low neutron energies and its variation with mass number is required. This is derived from an analysis in the resonance region supplemented by theoretical calculations.[11] The variation of the potential scattering radius with mass number and its comparison with optical model calculations[11] is shown in Fig. 1.

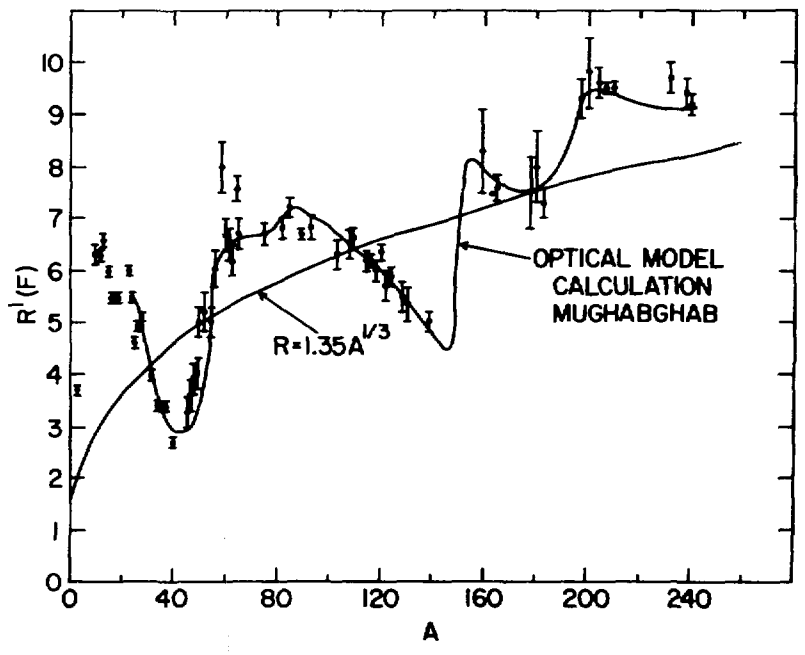

Fig. 1 A plot of the potential scattering radius with mass number, A.

B. Relationship Between S_{dp} and Γ_n^0

In this section, we present a useful relationship between the reduced neutron width Γ_n^0 and the (d,p) spectroscopic factor and determine the normalizing factor. In particular, the single particle dimensionless bound reduced neutron width for s-wave resonances is determined by a comparison of the experimental (d,p) and (n,n) data.

The (d,p) spectroscopic factor can be defined as the square of a ratio of dimensionless reduced neutron widths,

$$S_{dp} = \frac{\theta_n^2}{\theta_{sp}^2} \tag{9}$$

where θ_n^2 is expressed by:

$$\theta_n^2 = \frac{\gamma_n^2}{\frac{\hbar^2}{MR^2}} \tag{10}$$

and the reduced neutron width γ_n^2 for s-wave neutrons is defined as

$$\gamma_n^2 = \frac{\Gamma_n}{2kR} \tag{11}$$

where k is the wave number and R is the nuclear radius.

Substituting Eqs. (10) and (11) into (9), and using an interaction radius $R=1.35\ A^{1/3}$ fm, one gets

$$S_{dp} = 7.40\times10^{-5}\ A^{1/3}\ \frac{\Gamma_n^0}{\theta_{sp}^2} \tag{12}$$

where Γ_n^0 is expressed in eV units.

Note that θ_{sp}^2 is model dependent. For example the use of harmonic oscillator wave functions[12] gives $\theta_{sp}^2 = 0.036$. Instead of relying upon model calculations, we apply Eq. (12) to the $^{12}C+n$ system to derive θ_{sp}^2.

Meadows and Whalen[13] carried out a precise measurement of the total cross section of natural carbon (98.89% ^{12}C) in the energy region 100-1500 keV. Within the framework of single level R-matrix analysis, the authors obtained an excellent fit of the total cross section throughout the whole energy region. The derived reduced neutron width of the bound level at -2020 keV is γ_n^2 = 540 keV for an interaction radius of 4.80 fm. This bound level was studied by Darden et al.[14] by the (d,p) stripping reaction, for which a spectroscopic factor S_{dp} = 1.1 is obtained. Substituting these values in Eq. (12), one derives

$$\theta_{sp}^2 = 0.175$$

and hence,

$$S_{dp} = 4.21 \times 10^{-4} A^{1/3} \Gamma_n^0 \qquad (13)$$

This relation is used extensively in converting the (d,p) spectroscopic factors to reduced neutron widths.

C. The Lane-Lynn Theory of Direct Capture

Before recalling the essential relationships required in the analysis of partial and total capture cross sections, it is instructive to describe briefly the historical development of the experimental investigations dealing with this exciting field. Finally, the first quantitative verification of the Lane-Lynn[15] theory is presented.

1. Historical Pespective

a. In 1958, Groshev and his collaborators[16] observed a correspondence between γ- ray intensities and (d,p) spectroscopic factors for final states characterized by l_n=1 for the even-even target nuclides ^{24}Mg, ^{28}Si, ^{32}S, ^{40}Ca as well as odd even isotopes ^{23}Na, ^{27}Al, and ^{31}P. The suggestion was put forth[16] that a direct capture mechanism plays an important role in these nuclides.

b. Two years later, Lane and Lynn[15] formulated within the framework of R-Matrix theory a detailed theory of direct capture by subdividing phase space into internal and external regions. The partial capture cross sections for El transitions were explicitly calculated in terms of an algebraic expression. The essential feature of the theory is the dependence of the partial capture cross section on the (d,p) spectroscopic strength and on the gamma-ray energy.

c. The capture theory of Lane-Lynn motivated experimentalists[17] to search for a correlation between reduced γ-ray strengths, I_γ/E_γ^3, and stripping strengths, $(2J_f+1)\ S_{dp}$, where J_f is the spin of the final state populated by the γ-ray. For a quantitative study of the correspondence between (n,γ) and (d,p) data, Hughes, Kennett, and Prestwich[18] introduced the correlation coefficient:

$$\rho = \frac{\sum_i \left(\Gamma^0_{\gamma i} - \overline{\Gamma}^0_\gamma\right)\left(S_i - \overline{S}\right)}{\left[\sum_i \left(\Gamma^0_{\gamma i} - \overline{\Gamma}^0_\gamma\right)^2 \sum_i \left(S_i - \overline{S}\right)^2\right]^{1/2}} \qquad (14)$$

where $\overline{\Gamma}^0_\gamma$ and $\overline{S}$ are the average values and the summation is carried out over i=n final states. For the reaction $^{55}Mn(n,\gamma)\ ^{56}Mn$ a correlation coefficient ρ=0.84 for eight final states was found.[18] Similar studies were carried out for the Ca isotopes,[19-21] Ba, $^{138,142}Ce$, ^{142}Nd[22] which revealed in some nuclides high correlation coefficients approaching unity.

d. A significant development was the $^{37}Cl\ (n,\gamma)\ ^{38}Cl$ investigations of Spits and Akkermans[23] who reported at the Budapest Conference that the correlation coefficient was substantially improved when an E_γ instead of an E_γ energy dependence was considered. Other nuclides in the same mass region ^{27}Al, ^{31}P, ^{32}S, ^{40}Ar, and the Ca isotopes, exhibited the same trends.

e. Since such E_γ-dependence was not yet understood,[24] Kopecky, Lane, and Spits[25] pointed out that this behavior is predicted by the Lane-Lynn theory and arises because of the energy dependence of the radial dipole matrix element.

f. The observation[26] that high correlation coefficients were reported for those nuclides whose potential scattering radii, R', differ significantly from the interaction radius $R=1.35A^{1/3}$ indicated the presence of a (R-R') term in the direct capture cross section.

g. The previous observation motivated Mughabghab[27] to carry out the calculations in the framework of the Lane-Lynn theory and its verification for ^{136}Xe as well as ^{138}Ba, ^{144}Sm, and ^{29}Si was presented.[27]

2. The Direct Capture Cross Section for E1 Transitions. In this subsection, we present the expression for the direct capture cross section as derived by Lane and Lynn[15]:

$$\sigma_{\gamma f,\mu}^{(\text{pot})} = \frac{0.082}{R\sqrt{E}}\left(\frac{Z}{A}\right)^2 \theta_{I_t}^2 \sum_{J} \frac{(2J_f+1)}{6(2i_p+1)} \frac{1}{|1-\rho' R_{cl}|^2} \times \left[y^2\left(\frac{y+3}{y+1}\right)^2 + 2\mathcal{M}_c \frac{y^2(y+2)(y+3)^2}{(y+1)^4} + (\mathcal{M}_c+\mathcal{B}_c)^2 y^4\left(\frac{y+2}{y+1}\right)^2\right] \quad (15)$$

The reader is referred to the original article[15] for the nomenclature. In most cases, it can be shown that B_s, which is related to the neutron capture cross section, is very small and as a result could be ignored in the relationship. For nonzero spin target nuclides ($I \neq 0$), s-wave capture results in channel spins I+1/2 and I-1/2. For equal capture in these components (i.e., A_s is the same for the two channel spins) the above expression can be simplified to the following form:

$$\sigma_{\gamma f}(\text{potential}) = \sigma_{\gamma f}(\text{hard sphere})\left[1 + \frac{R-a_s}{R}\, y_f \frac{y_f+2}{y_f+3}\right]^2$$

$$\text{where } \sigma_{\gamma f}(\text{hard sphere}) = \frac{0.062}{R\sqrt{E_n}}\left(\frac{Z}{A}\right)^2 \mu \frac{2J_f+1}{6(2I_t+1)} S_{dp}\left(\frac{y_f+3}{y_f+1}\right)^2 y_f^2 \quad (16)$$

$$y_f^2 = R^2\, 2m E_\gamma / \hbar^2$$

and a_s is the coherent scattering amplitude.

The variable μ takes into account the multiplicity due to the incident-neutron channel spin. For $I_t = 0$, $\mu = 1$. However, for a target nucleus with nonzero spin, I_t:

$$\mu = 1 \quad \text{for } J_f = I_t \pm 3/2$$

$$\mu = 2 \quad \text{for } J_f = I_t \pm 1/2$$

It is interesting to note that the second term within the brackets of Eq. (16) represents the resonance channel contribution and it has a large effect in those nuclides where R is much

different from R; i.e., in the neighborhood of A=35 and 138 (Fig. 1).

We emphasize that Eq. (16) holds under the following conditions:

a. even-even nuclides,

b. for nuclides with $I \neq 0$ and a_s is the same for $I+1/2$ and $I-1/2$,

c. if a_s is not the same for $I+1/2$ and $I-1/2$, Eq. (16) is still applicable for transitions to final states with $J_f = I \pm 3/2$; otherwise, Eq. (16) needs modifications requiring the $P_{1/2}$ and $P_{3/2}$ components of S_{dp} as well as spin statistical factors.

3. Verification of the Lane-Lynn Theory. The experimental test of the Lane-Lynn theory of direct capture of slow s-wave neutrons was provided by the reaction ^{136}Xe (n,γ) ^{137}Xe. Three facts[27] presented signatures that direct capture plays a dominant role in the reaction mechanism of this isotope. These are: (1) nearby s-wave neutron resonances are not known in ^{136}Xe, (2) the neutron capture cross section is small,[28] and (3) the correlation coefficient between γ-ray and (d,p) strengths is maximized to a value of 0.984 for an $E_\gamma^{1.2}$ dependence of the partial capture cross sections.

On the left-hand side of Fig. 2 is demonstrated the variation of the correlation coefficient with the power, n, of the gamma-ray energy. On the right-hand side is represented the

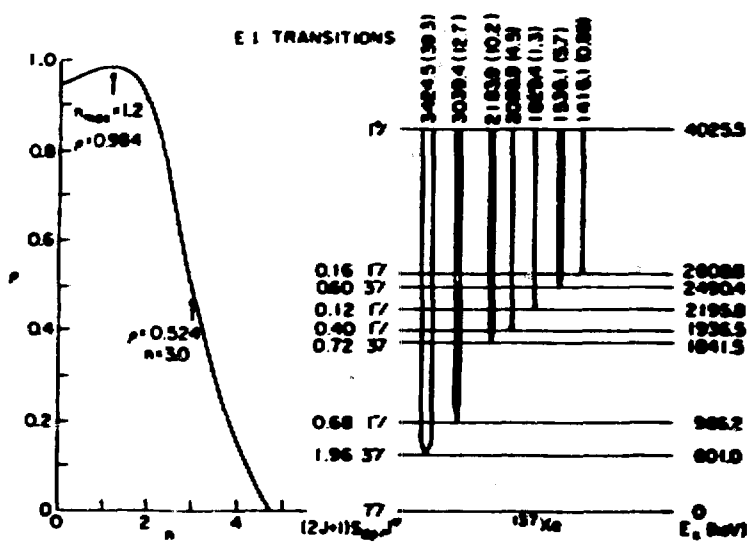

Fig. 2 Study of the variation of the correlation coefficient with the reduction factor n for the reaction ^{136}Xe$(n,\gamma)^{137}$Xe. Note that ρ approaches unity for n=1.2 which is a signature for direct capture. The right-hand side of the figure shows the measured primary E1 transitions populating the low lying states of ^{137}Xe.

pertinent El transitions feeding final states with large (d,p) strengths. The relative γ-ray intensities[29] are normalized to absolute values by two methods[27] which yield results accurate to within 10%. These are displayed in the second column of Table 1. The final states, their spins, and spectroscopic strengths are shown in columns 3, 4, 5, respectively. The partial capture cross sections are calculated with the aid of Eq. (16) based on the parameters of Table 1 and an interaction radius of $1.35\ A^{1/3}$ fm. The last column gives the experimental partial capture cross sections obtained by $\sigma_{\gamma f} = I_{\gamma f}\sigma_{\gamma}$ where $\sigma_{\gamma} = 260 \pm 20$mb. As shown, the agreement between the theoretical and experimental values is remarkable. Additional impressive examples are presented in Section IV.

Table 1

$^{136}Xe\ (n,\gamma)\ ^{137}Xe$

E_γ(keV)	$I_{\gamma f}$(%)	E_x(keV)	J_f	$(2J_{f+1})S_{dp}$	$\sigma_{\gamma f}$ (mb) Theo	$\sigma_{\gamma f}$ (mb) Exp.
3424.55	39.3±3.9	601	$^3/_2$	1.96	104	102
3039.37	12.7±1.7	986	$^1/_2$	0.68	30.6	33.3
2183.88	10.2±0.9	1841	$^3/_2$	0.72	23.9	26.5
2088.93	4.5±0.5	1936	$^1/_2$	0.40	12.7	11.7
1829.44	1.3±0.1	2106	$^1/_2$	0.12	3.3	3.4
1535.09	5.7±0.6	2490	$^3/_2$	0.60	14.1	14.8
1415.91	0.85±.09	3609	$^1/_2$	0.16	3.5	2.2
SUM	74.55			4.64	192.1	193.9

IV. APPLICATIONS

In this section, we present several interesting and remarkable examples illustrating the ideas and principles developed in the previous sections.

A. The Capture Cross Section and Absolute γ-ray Intensities of $^{12}C\ (n,\gamma)\ ^{13}C$.

The pertinent El transitions in the reaction $^{12}C\ (n,\gamma)\ ^{13}C$ are the ground state transition $s_{1/2} \longrightarrow p_{1/2}$ and the transition feeding the second excited state $s_{1/2} \longrightarrow p_{3/2}$. With the aid of

the (d,p) spectroscopic factors measured by Darden et al.[14] (H D optical model parameters) and an interaction radius $1.35A^{1/3}$ (3.09 fm), the partial capture cross sections are calculated by Mughabghab[31] for the first time and are presented in Fig. 3. A total capture cross section of 3.39 mb is then obtained, which is in good agreement with a recommended[28] value of 3.4±0.3 mb and with the most recent accurate value[32] 3.53±0.07 mb.

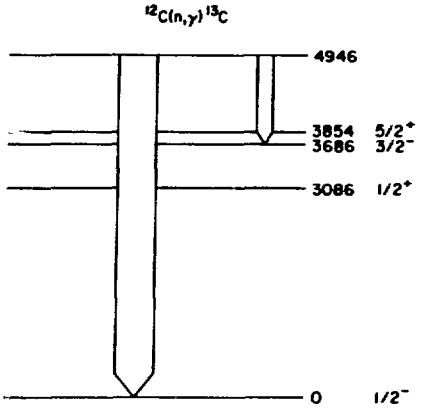

E_γ(keV)	(2J+1)S	I_γ(%) THEORY	I_γ(%) EXP.	σ_γ(mb) THEORY
4946	2.2	67.3	67.47±.92	2.28
1260	0.4	32.7	32.14±.64	1.11
				3.39

Fig. 3 Comparison between theoretical and measured partial capture cross sections as well as gamma-ray intensities for the reaction ^{12}C (n,γ) ^{13}C.

Included also in Fig. 3 are the measured[33] and calculated values of the two gamma-ray intensities. As indicated, the agreement between the two sets is indeed surprisingly remarkable in view of the fact that the spectroscopic factors are known to an accuracy of 10-15%. The other surprise which emerged from this study is the fact that the use of an interaction radius of $1.35\ A^{1/3}$ for a nucleus as light as ^{12}C described well the data. It is emphasized here that the same relationship for the interaction radius was used in the calculations of the radiative capture of neutrons by ^{136}Xe.

B. The Capture Cross Section of ^{13}C and the (d,p) Spectroscopic Factors

This nuclide provides us with an interesting example of interference phenomena between hard sphere and potential capture. As will be demonstrated shortly, a precise knowledge of the coherent scattering amplitude for channel spin I+1/2 is required. Since the spin of the target nucleus is 1/2, s-wave capture by ^{12}C results in spins of 1 and 0. The $p_{1/2}$ ground state and the second excited $p_{1/2}$ state at 6589 keV both have spins and parity 0^+ and therefore can be reached only by electric dipole radiation from capturing state 1^-. Therefore, the coherent scattering amplitude a_+ as well as the (d,p) spectroscopic factors must be known to a high degree of accuracy. At the start, let us check the consistency of the bound incoherent scattering amplitude, $b_+ - b_-$ with the (d,p) spectroscopic factors for s-wave states. Glattli et al.[34] employed the method of pseudomagnetism for measuring the spin dependent scattering amplitudes of slow neutrons for various isotopes. A value of $b_+ - b_- = -1.2 \pm 0.2$ fm was obtained.[34] Employing the Christiansen filter method, Koester et al.[35] obtained for ^{13}C, $b = 6.19 \pm 0.09$ fm. Combining these two measurements, one obtains:

$$a_+ = 5.47 \pm 0.09 \text{ fm}$$

$$a_- = 6.59 \pm 0.36 \text{ fm}$$

Table 2
Spectroscopic Information of ^{14}C

E_x (MeV)	E_n (MeV)	J^π	ℓ	S_{dp} (a)	S_{dp} (b)	Γ_n (keV) (c)	S_{dp} (c)
0		0^+	1	2.61 2.09	0.067		
6.094	-2.083	1^-	0	0.87, 0.78	0.20	0.791	0.78
6.589		0^+	1		0.20		
6.903	-1.275	0^-	0	1.03	0.24	0.949	0.94

(a) Ref. 37 (b) ref. 36 (c) Present analysis

It is interesting to point out here that Normand[5] calculated within the framework of the shell model an incoherent scattering length $b_+ - b_- = -0.95$ fm for a value of b=6.19 fm. This is in good agreement with a measured value of -1.2±0.2 fm. Using

this latter value, the information[36] that the reduced neutron width of the state at 6.903 MeV is 1.2 times larger than that at 6.094 MeV, the contribution of positive energy resonances, and Eq. (5), one obtains reduced neutron widths 0.791 and 0.949 keV, respectively, for the 6.0944 and 6.903 MeV states of ^{14}C. These values correspond to spectroscopic factors Eq. (13) 0.78 and 0.94, respectively, and are included in Table 2. Note that the spectroscopic factor for the first excited state derived in this analysis is in excellent agreement with the value extracted by Datta[37] for the case where distorted wave Born calculations using optical model parameters of Watson[39] are applied. Because of this fact, a value of S_{dp}=2.09 instead of 2.61 for the ground state of ^{14}C is chosen in the calculation of the partial capture cross section feeding the ground state. The theoretical value for the ground state transition is found to be $\sigma_{\gamma 0}=1.19^{+0.80}_{-0.60}$ mb. The large errors on this value are a reflection of the uncertainty in a_+(1.65%)! We emphasize that such large uncertainties in the calculated values are in general unusual. They are the exceptions rather than the rule. The ^{13}C nucleus represents a unique case of strong destructive interference between potential and hard sphere capture Eq.(16). This arises because of the comparatively large value of the γ-ray energy populating the ground state and the large negative difference between R and a_+, i.e., $R-a_+=-2.30$ fm. Because of this interesting situation, the variation of $\sigma_{\gamma 0}$ with a_+ is investigated and the results are described in Fig. 4. Of interest is the parabolically rapid change of $\sigma_{\gamma 0}$ with a_+. A minimum value occurs at about 5.2 fm and at 6.0 fm $\sigma_{\gamma 0}$ takes a value of 9 mb.

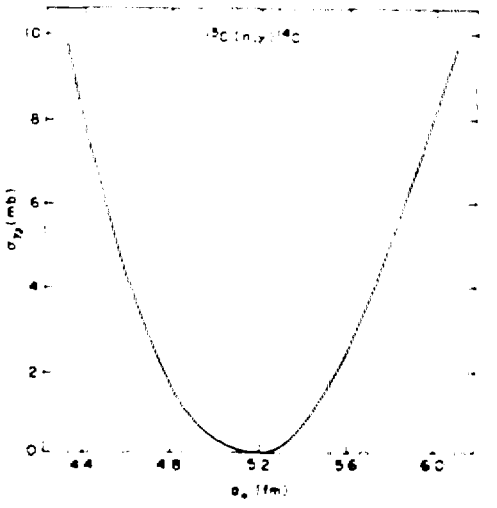

Fig. 4 Variation of the partial capture cross section populating the ground state of ^{14}C with the scattering length, a_+.

Comparison of the present calculations can be made with the very recent measurement of Lone[33] who determined the ^{14}C absolute gamma-ray intensities feeding the ground state and the second excited state at 6.589 MeV. These are (84.0±2.3)% and (8.5±0.5)%, respectively. In addition, the ratio of the capture cross sections of ^{13}C and ^{12}C was found to be:

$$\frac{\sigma_\gamma(^{13}C)}{\sigma_\gamma(^{12}C)} = 0.388 \pm 0.010 \quad .$$

Adopting a capture cross section[32] 3.53±0.07 mb for ^{12}C, one obtains σ_γ (^{13}C) =1.37±0.04 mb and a partial capture cross section 1.15±0.04 mb for the ground state transition. This value is in excellent agreement with the theoretical value 1.19 mb!

Since the spectroscopic factor for the 6.589 MeV state of ^{14}C is not yet determined, we apply Eq. (14) to obtain S_{dp}=0.058±0.004 for this state. It will be of interest to measure this value. A summary of the present results and measurement[33] is presented in Table 3.

Table 3
Comparison of Theoretical and Measured Partial Capture Cross Section for ^{13}C

E_γ (keV)	I_γ(%)	E_x(keV)	J^π	ℓ	S_{dp}	σ_γ(mb) (b)	σ_γ(mb) (c)
8174	84.0±2.3	0	0^+	1	2.09[a]	1.10	1.15±0.4
1586	8.5±0.5	6589	0^+	1	0.058±0.004 (b)		0.12± .01

(a) Ref. 37. Value corresponding to a Watson Potential
(b) Present Results
(c) Ref. 33

C. The Coherent Scattering Amplitudes of B, ^{10,11}B and the Capture Cross Section of ^{11}B

Because of interest by solid state physicists in the coherent and incoherent scattering amplitudes of natural boron and its stable isotopes, ^{10,11}, we present in some detail an evaluation of these quantities and consequently apply the Lane-Lynn theory to obtain a better estimate of the capture cross section of ^{11}B. In addition, ^{11}B provides an interesting example of illustrating the requirement of modifying Eq. (16) in order to take into account the unequal contributions of the two channel spins of the initial state. At first, let us consider the coherent scattering amplitude of ^{11}B. Two discrepant values, one by Koester et al.[40] (b=6.66±0.02 fm) and the other by Craven and Sabine[41] (b=6.1±0.1 fm) are at present available. Recourse to the known positive[42] and negative[43] energy s-wave neutron resonances indicates that the resonance parameters, combined with a potential scattering radius of R =4.98 fm, are in agreement with b=6.66 fm. The former value is in excellent agreement with a potential scattering radius of $R = R(1+R^{\infty}) = 4.95$ fm derived from the data of White et al.[42] Furthermore, the resonance parameters provide information on the free spin-dependent scattering lengths:

$$a_+ = 5.27 \text{ fm}$$
$$a_- = 7.53 \text{ fm}$$

which yield an incoherent scattering amplitude $a_+ - a_- = -2.26$ fm and hence an incoherent scattering cross section of 0.150 b. We note here that, since the spin dependent scattering lengths have not yet been measured independently, it will be informative to determine them by the method of pseudomagnetism.[34] This is essential because of the important role of these quantities in the Lane-Lynn theory.

We draw attention to the point that a coherent scattering amplitude 6.66±0.02 fm for ^{11}B implies a vanishingly small value for the real part of the coherent scattering amplitude of ^{10}B (0.00±0.22 fm). This conclusion is based on b=5.34±0.04 fm for natural baron.[28] The imaginary component of ^{10}B coherent scattering amplitude can be determined with the aid of Eq. (4) and its value is 1.067±0.003 fm. A summary of the present analysis is shown in Table 4.

At this stage, let us turn our attention to the study of the ^{11}B capture cross section. Since the recommended[28] value, 5.5±3.3 mb, has such a large uncertainty, it is instructive to evaluate it in terms of the Lane-Lynn theory. However, because the scattering amplitudes for the two spin states of ^{11}B are quite different, the capture cross sections for the two channel spins $I \pm 1/2 = 2,1$ are different. As pointed out previously, the Lane-Lynn expression requires a modification to take into account the spin factors and the $p_{1/2}$ and $p_{3/2}$ amplitudes of the (d,p)

Table 4
Scattering Parameters of B and Its Isotopes

Abundance	B	^{10}B 19.8%	^{11}B 80.2%
b_r(fm)	5.34±0.04	0.00±0.22	6.66±0.02
b_i(fm)	0.2113±0.06	(1.067±.003)	
a_+(fm)		-3.21	5.27
a_-(fm)		4.03	7.53
R'(fm)		4.1	4.98
σ_s(b)	4.27±0.07	2.23±0.06	4.84±0.04
σ_{inc}(b)	1.26±0.03	2.11±0.08	0.15±0.03

spectroscopic factors of the final states.[44] Denote the $p_{1/2}$ and $p_{3/2}$ amplitudes of S_{dp} by $S_{3/2}$ and $S_{1/2}$ so that $S_{dp}=S^2_{3/2}+S^2_{1/2}$. A comparison of the (d,p) and (n,γ) strengths for a target nucleus with spin I=3/2 (i.e. ^{11}B) is shown in Table 5. Note that for final spin states I±3/2 (i.e. J_f=3,0) the (n,γ) strengths are still correlated with the (d,p) strengths. Also note that for equal contributions from the two channel spins, 2 and 1, the interference terms between $S_{3/2}$ and $S_{1/2}$ cancel out, and as a result the (n,γ) and (d,p) strengths are still correlated. However, for unequal contribution from channel spins 2 and 1, it is obvious that the (n,γ) strength is no longer necessarily correlated with the (d,p) spectroscopic factors. Consequently, the Lane-Lynn relationship requires correction factors which are derived[31] and are described in Table 5.

In order to be able to carry out the calculations, the relative strengths of the $p_{1/2}$ and $p_{3/2}$ amplitudes need to be known. In principle, such information can be derived from (d,p) experiments carried out with vector-polarized deuterons. However, this knowledge is scanty, and therefore, as an alternative, one has to resort to some guidance from theoretical investigations similar to that of Cohen and Kurath.[45]

The pertinent electric dipole transitions in ^{12}B are those populating the ground state (1^+), the first, and fourth excited states at 953 keV (2^+) and 2724 keV (0^+), respectively. It is assumed that the M1 transition feeding the 1674 keV state (2^-) is weak. In the (d,p) study of Monahan et al.,[43] it is suggested that the ground and the first excited states are characterized by pure $p_{1/2}$ orbitals while the state at 2724 keV is a pure $p_{3/2}$

state. These are to be compared with the predictions of Cohen and Kurath[45] who described the ground state as possessing 14% $p_{3/2}$ component while the first and fourth excited states are pure $p_{1/2}$

Table 5
Comparison Between (d,p) and (n,γ) Strengths For
Electric Dipole Radiation of Target Nucleus with Spin I=3/2

(d,p) Strength	J_f	(n,γ) Strength Channel Spin 2	Channel Spin 1
$7\,S^2_{3/2}$	3	$7\,S^2_{3/2}$	0
$5(S^2_{3/2} + S^2_{1/2})$	2	$\frac{5}{2}(-S_{3/2} + S_{1/2})^2$	$\frac{5}{2}(S_{3/2} + S_{1/2})^2$
$3(S^2_{3/2} + S^2_{1/2})$	1	$\frac{1}{2}(S_{3/2} - \sqrt{5}\,S_{1/2})^2$	$\frac{1}{2}(\sqrt{5}\,S_{3/2} + S_{1/2})^2$
$S^2_{3/2}$	0		$S^2_{3/2}$

and $p_{3/2}$ states respectively. Accordingly, the calculations of partial capture cross sections and γ-ray intensities are calculated on the basis of both of these conclusions regarding the components of the ground state. The results which are displayed in Table 6 show the calculated total as well as partial capture cross sections which are in good agreement with the experimental value, 5.5±3.5 mb. Also shown are the predictions of the absolute γ-ray intensities which have not yet been measured. In order to test these theoretical results, it will be of great interest to measure the total capture cross section with better accuracy as well as the gamma-ray spectra due to capture in ^{11}B.

Table 6
Theoretical Values of the Total, Partial Capture Cross Sections, and Absolute Gamma-Ray Intensities of ^{11}B

E_γ(MeV)	E_x(MeV)	J	S_{dp}[a]	σ_γ(mb)[b]	I_γ(%)[b]	σ_γ(mb)[c]	I_γ(%)[c]
3.370	0	1^+	0.69	3.77	58.9	3.54	57.4
2.417	0.953	2^+	0.55	2.56	40.0	2.56	41.5
0.646	2.724	0^+	0.21	0.07	1.1	0.07	1.1
Total				6.40	100	6.17	100

(a) Ref. 43
(b) Present results on basis of a pure $p_{1/2}$ ground state
(c) Present results on basis that the ground state contains 14% $p_{3/2}$ component.

D. Neutron and Nuclear Spectroscopy of ^{19}F

So far, we have dealt with the evaluation of thermal cross sections. Now, we present an example illustrating the inverse process whereby the thermal constants can be used as a powerful tool in the evaluation of the s-wave resonance parameters and the deduction of properties of bound p-states. This can best be appreciated by examining the $^{19}F(n,\gamma)^{20}F$ and $^{19}F(n,n)^{19}F$ reactions at thermal energies. Fluorine is especially important in view of its possible use in the design of the breeder blanket for fusion reactors.

The total neutron cross section of ^{19}F ($I^\pi = 1/2^+$) reveals[46] an unresolved doublet at 270 keV, one component of which is an s-wave resonance whose parameters are naturally not well determined[28] (Γ = 25±10 keV, Γ_γ = 4.2±1.8 eV). The negative sign of the incoherent scattering amplitude[47] ($b_+ - b_-$ = -0.19±0.02 fm) can be accounted for in terms of either a bound s-wave resonance with zero spin or alternatively a positive resonance with spin 1. The polarization data of Gul'ko et al.,[48] which indicate that 42% to 70% of the capture of thermal neutrons is formed in channel spin 1, is the arbitrator, thus confirming a spin assignment of 1 for the 270 keV resonance. In fact, it will be shown shortly that 75% of thermal capture takes place in channel spin 1. Attributing the difference in the

coherent scattering amplitudes, b_+ and b_-, to the s-wave 270 keV resonance, and applying Eq. (5), one derives a value, $\Gamma_n = 11 \pm 1$ keV. The error is attributed to the uncertainty of the incoherent scattering amplitude. The present value of the neutron scattering width is in reasonable agreement with the previous estimate.[28]

To determine the radiative width of the 270 keV resonance, the direct capture cross section have to be determined. This is achieved by describing the two transitions populating the $\ell_n = 1$ final states to a direct capture mechanism. On the basis of this assumption, which will be subsequently verified, a value of 4.7 mb is obtained on the basis of a total capture cross, 9.6±0.5 mb, and the known E1 gamma-ray intensities.[49]

The difference between these values, (9.6-4.7=4.9 mb) is attributed to internal resonance capture arising from the s-wave resonance at 270 keV. With the aid of the Breit-Wigner relationship, one obtains then a radiative width of 4.9±0.7 eV for the 270 keV resonance.

Because the coherent scattering amplitudes of the two channel spins are practically the same, it follows then that the direct capture components of the corresponding channel spins are equal. Therefore, the total capture cross section in channel spin 1 is equal to 7.25 mb (4.9+4.7x1/2). Consequently, 75% of the capture is formed in channel spin 1. This is in conformity with the upper limit reported by Gul'ko et al.[48]

The (d,p) spectroscopic factors and spins of the ^{20}F states at E_x=5937 keV and 6019 keV can be determined by applying Eq. (16) and the information[50] that the (d,p) cross section of the 6019 keV state is about 1.5 times that of the 5937 keV state. The absolute intensities of the gamma rays feeding these two states were adopted from the investigations of Spilling et al.[49] because of the use of a filtered thermal beam to remove the contribution of fast neutrons. The results of the present analysis are displayed and are compared with those of Mosley and Fortune.[51] As shown, the agreement in the values of the spectroscopic factors is indeed very good. However, there is a marked discrepancy with regard to the spin assignment of the 6019 keV state. The present study indicates that $\mu=2$ and hence $J=1$ for this state. One plausible explanation of the discrepancy is the postulation that the 6019 keV state is a closely spaced doublet, one component of which is characterized by $\ell_n=3$, $J=2^-$.

On the other hand, combining the present results with those of Ajzenberg-Selove,[52] ($J^\pi=1^-,2^-$) one arrives at a spin assignment of $J^\pi=2^-$ for the 5937 keV state.

Table 7
Nuclear Spectroscopy of ^{20}F P-States

E_γ (keV)	(a) I_γ (%)	μ	(b) σ_γ (mb)	E_x (keV)	(c) S_{dp}	(d) S_{dp}	(c) J^π	(d) J^π
665.5	15.4	1	1.46	5937	0.588	0.43	$2^-, 0^-$	
583.5	34.0	2	3.23	6019	0.714	0.68	1^-	2^-

(a) Ref. 50
(b) Experimental partial capture cross sections
(c) Present study
(d) Ref. 51

E. The Direct Capture Components of $^{20,22}Ne$, ^{26}Mg, and ^{34}S

For many of the light to medium weight nuclides, the number of final states which are characterized by a neutron orbital angular momentum, $\ell_n=1$, is limited. As a consequence, this aspect renders the study of the reaction mechanism with the aid of correlation analysis limited.(53) This difficulty now is resolved, thanks to the ^{136}Xe (n,γ) ^{137}Xe reaction,(27) by carrying out the quantitative calculations, Eq. (16), and subsequently making a comparison with the experimental data. In this section, we present $^{20,22}Ne$, ^{26}Mg, and ^{34}S as representative examples illustrating this situation. The absolute gamma-ray intensities and (d,p) spectroscopic factors are surveyed and collected from the literature and compilations.(54) The calculations of partial capture cross sections are carried out by the author adopting the procedures described previously. The results are displayed in Table 8. As is readily evident by inspection of the last two columns, there is a general good agreement between the theoretical and experimental values. It seems that the theory can predict the strong transitions to an accuracy ranging from 6% to 15% as opposed to 30% for the weaker ones. This trend can be attributed to the uncertainty in both the spectroscopic factors and the γ-ray intensities. However, there is a marked discrepancy for the 2083 keV gamma line of ^{35}S. As noted in Table 8, the calculated value is 25.9 mb compared to a measured value of 41.4 mb. An internal resonance capture component of 1.9 mb, which is interfering constructively with the direct capture component and is due to the s-wave resonances at

301 and 357 keV, can resolve this discrepancy. This is achieved if a radiative width of about 2 eV is attributed to these resonances.

Table 8
Theoretical and Experimental Partial Capture Cross Sections of $^{20,22}Ne$, ^{26}Mg, ^{34}S

Isotope	E_γ (MeV)	I_γ %	$(2J_f+1)S_{dp}$	σ_γ (mb) (a)	σ_γ (mb) (b)
^{20}Ne	2.536	80.7	2.4	29.9	29.8
^{20}Ne	1.070	13.6	0.48	5.0	4.4
^{22}Ne	1.980	75.0	1.2	26.2	22.5
^{22}Ne	1.364	12.5	0.22	4.5	3.0
^{26}Mg	2.882	62.0	1.6	23.7	21.1
^{26}Mg	1.615	11.7	0.62	4.5	6.5
^{34}S	4.638	56 ± 6	2.1	128.8	120
"	3.184	7.0 ± 0.9	0.4	16.1	15.2
"	2.797	6.1 ± 0.8	0.3	14.0	11.0
"	2.083	18 ± 1.5	0.96	41.4	25.9
"	2.023	12 ± 1.5	0.76	27.6	21.0

(a) Experimental Values
(b) Present Study

F. The Thermal Constants of the Ca Isotopes

As was pointed out previously, the Ca isotopes were among the first to reveal large correlation coefficients between reduced gamma-ray intensities and (d,p) spectroscopic strengths, [19-20]

thus suggesting that direct capture plays an important role in the reaction mechanism. Because of historical reasons as indicated earlier, it is instructive to carry out the numerical calculations of the capture cross sections for the purpose of comparing the results with the corresponding measurements. In addition, as was stressed previously in the many examples we explored, this procedure allows the determination of the coherent scattering lengths as well as the evaluation of the thermal cross sections. However, an apriori knowledge that direct capture dominates is required. Because of space limitations, the results are briefly described for each isotope.

1. $^{40}Ca\ (n,\gamma)\ ^{41}Ca$:

Although ^{40}Ca is a doubly magic nucleus with the expectation that the direct capture mechanism is totally dominant, a comparison between the theoretical and experimental partial capture cross sections indicates a lack of good general agreement. This is attributed to internal resonance capture (compound processes) resulting from capture in the tail of a nearby bound s-wave level. However, we note that the transition populating the excited state 1943 keV (S_{dp}=1.25) shows reasonable agreement, whereby the computed value is 119 mb as compared to an experimental value of 152 mb.

2. $^{42}Ca(n,\gamma)\ ^{43}Ca$:

This isotope exhibits a large correlation coefficient, 0.91, between reduced gamma-ray intensities and (d,p) strengths. However, since the coherent scattering length is not experimentally determined, the calculations cannot be carried out readily. Alternatively, we applied the measured partial capture cross section feeding the excited state at 2046 keV (E_γ=5886 keV) to arrive at a coherent scattering length of 3.15±0.20 fm for ^{42}Ca. Subsequently, it is shown that the total capture cross section, 680±70 mb, is totally due to direct capture.

3. $^{44}Ca(n,\gamma)\ ^{43}Ca$

Since the coherent scattering amplitude for ^{44}Ca is well determined,[28] b=1.8±0.1 fm, one fortunately can carry out the calculations readily without resort to the use of any adjustable parameters. A total direct capture cross section of 867 mb is then derived which is in excellent agreement with a measured value, 880±50 mb. A comparison between the theoretical and measured partial capture cross sections is described in Fig. 5 and detailed in Table 9. The (d,p) spectroscopic factors are adopted from Ref. 55. Note the remarkable agreement between theory and experiment, particularly for the two gamma-ray transitions feeding the excited states at 1435 and 1900 keV.

4. $^{46}Ca(n,\gamma)\ ^{47}Ca$:

A coherent scattering amplitude, b=2.55±0.25 fm, is derived for this nucleus.

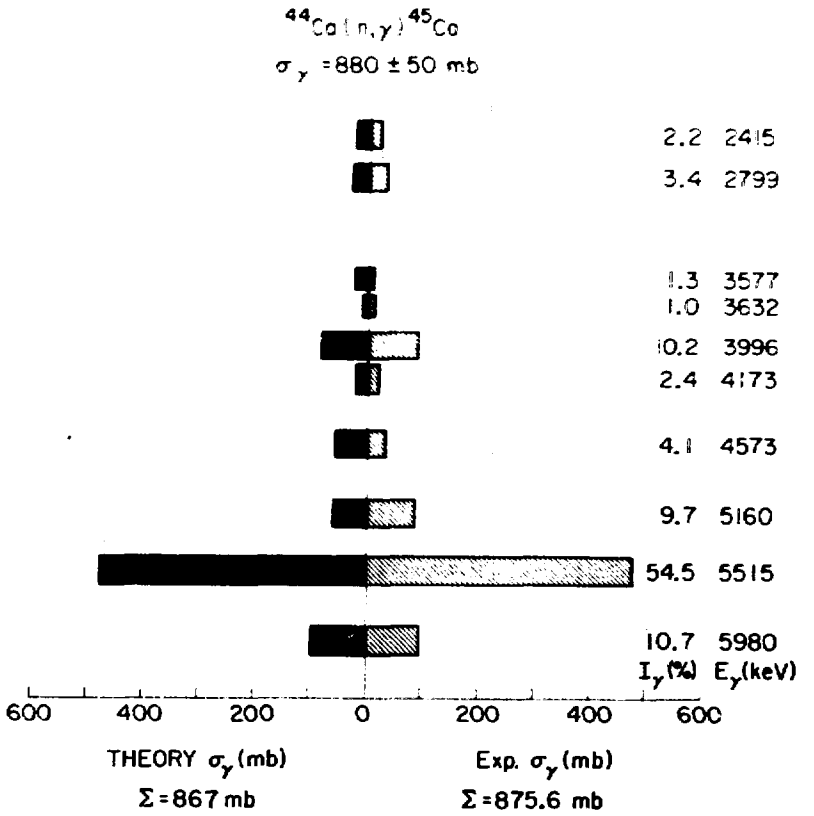

Fig. 5 Comparison of predicted and measured partial capture cross sections for the reaction $^{44}Ca(n,\gamma)\ ^{45}Ca$. The two columns on the right-hand side represent the absolute gamma-ray intensities and the corresponding γ-ray energies. A total capture cross section of 867 mb is predicted, which is in very good agreement with the experimental value, 880 ± 50 mb, thus demonstrating that direct capture dominates in this case.

Table 9
Theoretical and Experimental Comparisons
of Partial Radiative Widths for $^{44}Ca(n,\gamma)\ ^{45}Ca$

E_f (keV)	E_x (keV)	$(2J_f+1)\ S_{dp}$ [a]	I_γ (%) [b]	Γ_γ (mb) [c]	Γ_γ (mb) [d]
5980.3	1435	0.40	10.7	94	96
5515.1	1900	2.20	54.5	480	475
5165.5	2249	0.30	9.7	85	59
4572.5	2842	0.34	4.1	36	57
4173.0	3242	0.14	2.4	21	21
3996.0	3419	0.49	10.2	90	69
3631.5	3783	0.08	1.0	9	10
3576.8	3838	0.19	1.3	11	23
2799.3	4616	0.34	3.4	30	30
2415.4	4999	0.36	2.2	19	27
SUM			99.5	875	867

a) Ref. 20
b) Ref. 55
c) Experimental values
d) Present tneoretical calculations

5. $^{48}Ca(n,\gamma)\ ^{49}Ca$:

Similarly, a coherent scattering amplitude, b=1.5±0.2 fm is calculated for ^{48}Ca. We point out here that, since this is significantly smaller than R'=3.1 fm for A=48 (Fig. 1), this value suggests the presence of a positive energy s-wave resonance. It is interesting to search for this resonance by carrying out total cross section measurements below 30 keV, an as yet unexplored energy region.

G. Estimates of Capture Cross Sections of Fission Products

Finally, we note here that the procedures outlined previously can be applied to the estimations of capture cross sections of fission products. For example, in WRENDA 76/77 two requests for the thermal capture cross sections $^{132}Te(n,\gamma)\ ^{133}Te$ and ^{126}Sn $(n,\gamma)\ ^{127}Sn$ are noted for the purpose of calculations of fission product poisons.

Since both of these nuclides are radioactive with comparatively short half lives, it is experimentally difficult, as yet, to determine the cross sections easily. This can be circumvented by carrying out the calculations in the framework of the Lane-Lynn theory on the simple assumption that the single particle (d,p) strengths in ^{126}Sn and ^{132}Te are the same as those in the corresponding stable isotopes, ^{124}Sn and ^{130}Te, for which $(2J_f+1)S_{dp}$ values are available. The results of these calculations[55] are:

$$^{126}Sn\ (n,\gamma)^{127}Sn \qquad \sigma_\gamma = 0.120b$$

$$^{132}Te\ (n,\gamma)^{133}Te \qquad \sigma_\gamma = 0.135b$$

We stress that if low-lying resonances are located close to thermal energies, which is most unlikely, then these values are considered as lower limits.

V. CONCLUSION

To summarize, we outlined briefly the various interesting reasons for the study of thermal cross sections, described a procedure in the evaluation, discussed the relations employed in the analysis, and placed emphasis on the Lane and Lynn theory of direct capture. In the third section, we explored the application of the Lane-Lynn theory to the light and medium weight isotopes and discovered remarkable agreement between theory and experiment, particularly for $^{12,13}C$ and ^{20}F, and some of the Ca isotopes. In additions, we were able to derive (d,p) spectroscopic factors, spins of final states, and scattering lengths. In some cases, we pointed out some fruitful ideas for future investigations.

Finally we emphasize that these methods and procedures are applied in the evaluation of the thermal cross sections and

resonance parameters which will appear in the forthcoming edition of BNL 325, Vol. 1.

Finally, I hope I was able to convey to you some of the excitement which can be derived in the study and evaluation of thermal cross sections.

ACKNOWLEDGMENT

The author is greatly indebted to Dr. M. A. Lone for sending his $^{12,13}C$ data prior to publication and to Professor L. Koester for a stimulating correspondence regarding the coherent scattering amplitudes of B and its isotopes.

REFERENCES

1. D. O. Riska and G. E. Brown, Phys. Letters B38, 193 (1972).
2. E. Hadjimichael, Phys. Rev. Letters 31, 183 (1973).
3. R. D. Carlitz, S. D. Ellis, and R. Savit, Phys. Letter B 68, 443 (1977).
4. V. F. Kharchenko and V. P. Levashev, Nucl. Phys. A243, 249 (1980).
5. J. M. Normand, Nucl. Phys. A291, 126 (1977).
6. G. M. Hale and D. C. Dodder, LA-UR 80-1399 (1980) and Private Communication.
7. B. R. Leonard, Nuclear Cross Sections and Technology. NBS Special Publication 425, Vol. 1, 281 (1975).
8. H. D. Lemmel, ibid, Vol.1, 286 (1975).
9. L. Koester, W. Nistler, and W. Waschkowski, Phys. Rev. Letters 36, 1021 (1976).
10. L. Koester, In Springer Tracts in Modern Phys., Vol. 80, 1 (1977).
11. S. F. Mughabghab, The Third Neutron Cross Sections and Technology Conference Vol. 1, 386 (March 15-17, 1971).
12. A. M. Lane, Rev. Mod. Phys. 32 519 (1960).
13. J. W. Meadows and J. F. Whalen, Nucl. Sci. and Eng. 41 351 (1970).
14. S. E. Darden, et al., Nucl. Phys. A208, 77 (1973).
15. A. M. Lane and J. E. Lynn, Nucl. Phys. 17, 563, 586 (1961).
16. L. V. Groshev et al. Second Geneva Conf. of the Peaceful Uses of Atomic Energy, Vol. 15, 138 (1958).
17. O. A. Wasson, K. J. Wetzel, and C. K. Bockleman, Phys. Rev. 136B, 1640, (1964).
18. L. B. Hughes, T. J. Kennett, and W. V. Prestwich, Nucl. Phys. 80, 131 (1966).
19. H. Gruppelaar, A. M. F. Den Kamp, and A. M. J. Spits, Nucl. Phys. A131 180 (1969).
20. H, Gruppe ar, P. Spilling, A. M. J. Spits Nucl. Phys. 114A, 463 (19?
21. S. E. Ar: ll, R. Hardell, O. Skeppstedt, and E.Wallander, Neutron ' pture Gamma Ray Spectroscopy, Studsvik, August 1969, p. il.
22. M. A. J. Mariscotti, J. A. Moragus, W. Gelletly, and W. R. Kane, Phys. Rev. Letters 22, 303 (1969).
23. A. M. J. Spits and J. A. Akkermans, Nucl. Structure Study with Neutrons, Budapest 1972. See also Nucl. Phys. 215A, 250 (1973).
24. L. M. Bollinger, Photonuclear Reactions and Applications, edited by B. Berman, Vol. 2, p. 783, March 26-30, 1973.
25. J. Kopecky, A. M. J. Spits and A. M. Lane, Phys. Letters 49B, 323 (1974).
26. S. F. Mughabghab, III School on Neutron Physics, Alushta, U.S.S.R., April 19-30 1978, p. 328.

27. S. F. Mughabghab, Phys. Letters 81B, 93 (1979). See also S. F. Mughabghab and R. E. Chrien, Neutron Capture Gamma Ray Spectroscopy edited by R. E. Chrien and W. R. Kane p. 265, Plenum Press New York and London 1979.
28. S. F. Mughabghab and D. I. Garber, BNL Report 325, Vol. I, Neutron Cross Sections.
29. S. G. Prussin et al., Phys. Rev. C16, 1991 (1977).
30. B. Fogelberg and W. Mampe, Z. Phys. A281, 89 (1977).
31. S. F. Mughabghab, Colloquium, Chalk River Nuclear Laboratory, Canada, August 21, 1980.
32. E. Jurney, Private Communication (1980).
33. M. A. Lone, Private Communication (1980).
34. H. Glattli et al., Le Journal De Physique 40, (1979) and references therein.
35. L. Koester, K. Knopf, and W. Waschowski, Z. Phys. A292, 95 (1979).
36. R. N. Glover and A. D. W. Jones, Nucl. Phys. 84, 673 (1966).
37. S. K. Datta, G. P. A. Berg, and P. A. Quin, Nucl. Phys. A 132, 1 (1978).
38. R. O. Lane, H. D. Knox, P. Hoffmann-Pinther, R. M. White, and G. F. Auchampaugh to be published Nucl. Phys.
39. B. A. Watson, P. P. Singh, and R. E. Segel, Phys. Rev. 182, 977 (1969).
40. L. Koester and K. Knopf, NEANDC(E)182U, Vol. 5, 78 (1978) and Private Communication (1980).
41. B. M. Craven and T. M. Sabine, Acta Cryst. 20, 214 (1966).
42. R. M. White, R. O. Lane, H. D. Knox, and J. M. Cox, and Nucl. Phys. A340, 13 (1980).
43. J. E. Monahan, H. T. Fortune, and C. M. Vincent, Phys. Rev. 3C, 2192 (1971).
44. Hans-Ulrich Gersch, Fortschritte der Physik, 17, 313 (1969).
45. S. Cohen and D. Kurath, Nucl. Phys. A101, 1 (1967).
46. C. H. Johnson, J. A. Harvey, D. C. Larson, and N. W. Hill, ORNL 5025 116 (1975).
47. A. Abragam et al., Phys. Rev. Letters 28, 805 (1972). See also Ref. 34.
48. A. D. Gul'ko, S. S. Trostin, and A. Hudoklin, Yad. Fiz. 6, 657 (1967).
49. P. Spilling, H. Gruppelaar, H. F. Devries, and A. M. J. Spits, Nucl. Phys. A111, 395 (1968).
50. A. A. Rollefson, P. F. Jones, and R. J. Shea, Phys. Rev. 1C, 1761 (1970).
51. C. A. Moseley and H. T. Fortune, Phys. Rev. 16C, 1697 (1977).
52. F. Ajzenberg-Selove, Nucl. Phys. A190, 1 (1972).
53. S. F. Mughabghab, Neutron Capture Gamma Ray Spectroscopy, Petten, the Netherlands, Sept. 2-6, 1974, p. 53.
54. P. M. Endt and C. Van der Leun, Nucl. Phys. A130, 1 (1978).
55. G. Brown, A. Denning, and J. G. B. Haigh, Nucl. Phys. A225, 267 (1974).

56. S. F. Mughabghab, Proceedings of the Specialists' Meeting on Neutron Cross Sections of Fission Product Nuclei, Bologna, Dec. 12-14 1979, NEANDC(E)209 "L", p. 1979.

Discussion

Smith

Do you attempt to maintain consistency with the ENDF files e.g. R-matrix parameters of ^{12}C .

Mughabghab

Because of the time lag between the two publications, which results in two different data basis, it is difficult to maintain consistency between the BNL-325 and ENDF parameters. To illustrate the point by an example, there is now available a set of recent resonance parameter data by Cierjacks and collaborators (Nucl. Inst. Methods 169, 185, 1980) which will be incorporated in BNL-325 evaluation and which I believe is not in the ENDF file.

Lone

Because of the importance of the valence contribution in some mass regions, should one separate this component before evaluating the average total radiative width?

Mughabghab

Absolutely yes. In some mass regions, (the 2P, 3S, 3P giant resonances) the valence component is significant. Since this component is correlated with the reduced neutron width of the resonances, it may result in large fluctuations. Therefore, in obtaining an average value, it is important to subtract out this valence component.

Lone

I would like to make a comment. The contribution of chemical impurities to thermal neutron capture cross sections could be quite high in elements with low capture cross neutrons. It is important that the experimentalist investigate the impurity contents and mention these in the publication.

Mughabghab

Such a procedure will be most useful to the evaluators. We strongly recommend that experimentalists, report this information in publications.

Block

In Bob Little's measurement of the capture and total cross section of ^{232}Th in the energy region 0.01-20 eV, it was noted that the total and capture cross sections could not be fit with only multilevel resonance parameters. An extra 1/V capture term had to be added to produce the fit to both cross sections. Can you comment on the nature of this rather 1/V capture term which is not derived from negative and positive energy levels? For example, is this direct capture?

Mughabghab

I suspect that the (d,p) spectroscopic factors of the final low lying states of ^{233}Th are not large. Since the direct capture component is proportional to these factors, correspondingly it follows that the direct capture is small. It will be of interest to calculate the direct capture component for ^{232}Th in the framework of the Lane-Lynn theory.

Note added in proof

Two p-states at excitation energies 539.5 and 583.5 keV with spectroscopic factors 0.032 and 0.027 respectively are known. The direct capture component for both of these states is only 0.57 mb.

SESSION VII

RESOLVED RESONANCE REGION

Chairman: S.F. Mughabghab BNL

NEW TECHNIQUES FOR MULTI-LEVEL CROSS SECTION CALCULATION AND FITTING

F. H. Fröhner

Institut für Neutronenphysik und Reaktortechnik
Kernforschungszentrum Karlsruhe
Postfach 3640, 7500 Karlsruhe 1
Federal Republic of Germany

ABSTRACT

A number of recent developments in multi-level cross section work are described. A new iteration scheme for the conversion of Reich-Moore resonance parameters to Kapur-Peierls parameters allows application of Turing's method for Gaussian broadening of meromorphic functions directly to multi-level cross section expressions, without recourse to the Voigt profiles ψ and χ. This makes calculation of Doppler-broadened Reich-Moore and MLBW cross sections practically as fast as SLBW and Adler-Adler cross section calculations involving the Voigt profiles. A convenient distant-level treatment utilizing average resonance parameters is presented. Apart from effectively dealing with edge effects in resonance fitting work it also leads to a simple prescription for the determination of bound levels which reproduce the thermal cross sections correctly. A brief discussion of improved resonance shape fitting techniques is included, with emphasis on the importance of correlated errors and proper use of prior information by application of Bayes' theorem.

1. INTRODUCTION

Modern techniques for resonance cross section calculations were reviewed in [1] and in G. Hale's contribution to this conference [2]. Important new developments since the publication of [1] concerning (1) Doppler-broadening of Reich-Moore and multi-level Breit-Wigner (MLBW) cross sections, (2) treatment of distant levels, (3) treatment of bound levels, (4) improvement of conventional least-squares shape analysis by inclusion of correlated errors and prior information via Bayes' theorem are presented in what

follows.

2. WIGNER-EISENBUD AND KAPUR-PEIERLS PARAMETERS

Resonance theory gives the well known relation between the partial cross sections $\sigma_{cc'}$ and the collision matrix (S-matrix) elements $U_{cc'}$ (see [1])

$$\sigma_{cc'} = \pi\lambda\!\!\!^{-2}_{c} g_c |\delta_{cc'} - U_{cc'}|^2 \qquad (1)$$

where the subscripts c,c' denote entrance and exit channel, respectively, and g_c is the spin factor. The collision matrix is symmetric because the nuclear hamiltonian is invariant under time reversal, and unitary because the probabilities for transitions into the various exit channels must add up to unity. Utilizing the unitarity of U one can express the total cross section σ_c as a linear function of $U_{cc'}$,

$$\sigma_c = \sum_{c'} \sigma_{cc'} = 2\pi\lambda\!\!\!^{-2}_{c} g_c (1 - \mathrm{Re}\ U_{cc}). \qquad (2)$$

Therefore the simplest expressions are always obtained for the total cross section whereas the expressions for the elastic-scattering cross section σ_{cc} are always most complicated due to the Kronecker symbol $\delta_{cc'}$ in Eq. (1). It is therefore often more convenient to calculate σ_{cc} as the difference between σ_c and the other partial cross sections than from Eq. (1). Wigner and Eisenbud [3] showed that for nuclear reactions with two collision partners in each channel the collision matrix can be expressed in terms of the resonance parameter matrix R,

$$U_{cc'} = e^{-i(\phi_c+\phi_{c'})} \left\{ \delta_{cc'} + iP_c^{1/2} \left[(1-RL^o)^{-1} R \right]_{cc'} P_{c'}^{1/2} \right\}, \qquad (3)$$

$$R_{cc'} = \sum_{\lambda} \frac{\gamma_{\lambda c}\gamma_{\lambda c'}}{E_\lambda - E}. \qquad (4)$$

Alternatively one can write U in terms of the level matrix A [4],

$$U_{cc'} = e^{-i(\phi_c+\phi_{c'})} \left(\delta_{cc'} + i \sum_{\lambda,\mu} \Gamma_{\lambda c}^{1/2} A_{\lambda\mu} \Gamma_{\mu c'}^{1/2} \right), \qquad (5)$$

$$(A^{-1})_{\lambda\mu} = (E_\lambda - E)\delta_{\lambda\mu} - \sum_c \gamma_{\lambda c} L_c^o \gamma_{\mu c}, \qquad (6)$$

where $L^o_{cc'} = (I_c - B_c) f_{cc'} = (S_c - B_c + iP_c) f_{cc'}$; $\gamma_c^{1/2} = \omega_{cc'} \sqrt{2P_c}$. (7)(8)

The boundary parameters B_c are arbitrary. They are prescribed values of the logarithmic derivatives of radial eigenfunctions at the channel radius a_c. For $r_c > a_c$ the nuclear interaction must be negligible, i.e. a_c must be large enough but otherwise it is arbitrary. Both a_c and B_c occur in boundary conditions which, together with the Schrödinger equation, define the radial eigenfunctions for $r_c \leq a_c$ and the eigenvalues E_λ. The width amplitudes $\gamma_{\lambda c}$ are essentially the values of these eigenfunctions at $r_c = a_c$. The E_λ and $\gamma_{\lambda c}$ can be calculated only for simple models such as the shell model or the optical model (cf. e.g. [1]) but normally they are just fit parameters, available for parametrization of the cross sections. The hard-sphere phase shifts ϕ_c and the logarithmic derivatives L_c, on the other hand, can be calculated from the known outgoing wave functions $O_c(r_c)$ for the external region ($r_c \geq a_c$),

$$L_c = a_c \frac{O_c'(a_c)}{O_c(a_c)} , \tag{9}$$

$$\phi_c = \arg O_c(a_c) = \arctan \frac{\mathrm{Im}\, O_c(a_c)}{\mathrm{Re}\, O_c(a_c)} . \tag{10}$$

For neutral projectiles the O_c are proportional to the Hankel functions $h_\ell^{(2)}$ of the second kind,

$$O_c(r_c) = ik_c r_c h_\ell^{(2)}(k_c r_c)$$

$$\left\{ \approx i^{-\ell} e^{ik_c r_c} \quad \text{for} \quad k_c r_c \gg \sqrt{\ell(\ell+1)} \right\} , \tag{11}$$

where $k_c = 1/\lambda\!\!\!^{-}_c$. The properties of the Hankel functions yield

$$L_o = ik_c a_c = iP_o , \qquad L_\ell = -\ell - \frac{(k_c a_c)^2}{L_{\ell-1} - \ell} , \tag{12}$$

$$\phi_o = k_c a_c , \qquad \phi_\ell = \phi_{\ell-1} - \arg(L_{\ell-1} - \ell). \tag{13}$$

The energy dependence of L_c^o for photon and fission channels can usually be neglected. The two main versions of the R-matrix formalism differ only by the choice of B_c: The Wigner-Eisenbud version [3] is obtained if B_c is chosen as real and constant. The resonance parameters E_λ, $\gamma_{\lambda c}$ are then also real and constant, and all energy dependences (of $R_{cc'}$, L_c^o, ϕ_c) can be calculated explicitly. The simplest expressions are obtained with the choice $B_c = S_c$ for the photon and fission channels and $B_c = -\ell$ for elastic and inelastic scattering channels. If a_c is taken as small as

possible, i.e. just outside the nuclear interaction sphere, the eigenvalues E_λ coincide essentially with the cross section peaks. The explicitly known energy dependences make the Wigner-Eisenbud version very convenient for most purposes. A certain problem, however, is the required inversion of either a channel matrix, $(1-RL^o)^{-1}$, or a level matrix, A^{-1}, both of which have very high (strictly speaking infinitely high) rank.

The Kapur-Peierls version [5] is obtained if one puts $B_c=L_c$. This eliminates the matrix inversion problem, since $1-RL^o = 1$, but causes the boundary conditions to be energy dependent so that one has different eigenvalues and -functions for each energy. In other words the eigenfunctions and eigenvalues depend on energy and this energy dependence is specified only indirectly via the boundary conditions. Nevertheless formulae of the Kapur-Peierls type are useful in narrow energy ranges, i.e. for Doppler broadening calculations. We shall write the complex, E-dependent Kapur-Peierls resonance parameters as $\mathcal{E}_\lambda$, $g_{\lambda c}$ in order to distinguish them from the real, constant Wigner-Eisenbud parameters E_λ, $\gamma_{\lambda c}$. The Kapur-Peierls collision matrix,

$$U_{cc'} = e^{-i(\phi_c+\phi_{c'})} \left(\delta_{cc'} + i \sum_\lambda \frac{G_{\lambda c}^{1/2} G_{\lambda c'}^{1/2}}{\mathcal{E}_\lambda - E} \right) , \qquad (14)$$

contains, in contrast to Eqs. (3) and (5), a simple sum over levels, with complex partial width amplitudes $G_{\lambda c}^{1/2}$ defined by

$$G_{\lambda c} = g_{\lambda c}\sqrt{2P_c} \qquad (15)$$

(compare Eq. (8)).

3. THE PRACTICALLY IMPORTANT MULTI-LEVEL APPROXIMATIONS

For parametrization and evaluation of nuclear resonance cross sections three approximations are available,

- the multi-level Breit-Wigner (MLBW) approximation,
- the Adler-Adler approximation,
- the Reich-Moore approximation.

The MLBW approximation is the least, the Reich-Moore approximation the most accurate of these. A convenient starting point for their discussion is the inverse level matrix, Eq. (6), with real and constant (Wigner-Eisenbud) E_λ and $\gamma_{\lambda c}$.

3.1 The Reich-Moore Approximation

Usually many photon channels contribute to the sum in Eq. (6). Their $\gamma_{\lambda c}$ have practically random signs, therefore the off-diago-

nal sums ($\lambda \neq \mu$) tend to be much smaller than the diagonal sums ($\lambda = \mu$). Their omission causes thus only little error. Following Reich and Moore [6] we can therefore write

$$\sum_{c\in\gamma} \gamma_{\lambda c} L_c^o \gamma_{\mu c} \approx \delta_{\lambda\mu} \sum_{c\in\gamma} \gamma_{\lambda c}^2 L_c^o \equiv \delta_{\lambda\mu}(-\Delta_{\lambda\gamma} + i\Gamma_{\lambda\gamma}/2). \tag{16}$$

Choosing $B_c = S_c$ for photon channels (= const as mentioned before) one gets

$$(A^{-1})_{\lambda\mu} = (E_\lambda - E - i\Gamma_{\lambda\gamma}/2)\delta_{\lambda\mu} - \sum_{c\notin\gamma} \gamma_{\lambda c} L_c^o \gamma_{\mu c} \tag{17}$$

This inverse level matrix can be considered as derived from a "reduced" R-matrix with the photon channels eliminated and E_λ replaced by $E_\lambda - i\Gamma_{\lambda\gamma}/2$,

$$R_{cc'} = \sum_\lambda \frac{\gamma_{\lambda c}\gamma_{\lambda c'}}{E_\lambda - E - i\Gamma_{\lambda\gamma}/2} \qquad (c,c' \in \gamma). \tag{18}$$

All partial cross sections except that for radiative capture can then be calculated from Eqs. (1) and (3) with the reduced R-matrix instead of the full R-matrix (4). Matrix inversion is no longer a problem for the overwhelming majority of practically important cases: The reduced R-matrix is of rank 1 (an R-function) for all non-fissile nuclei below the lowest inelastic-scattering threshold, and of low rank if few inelastic-scattering or fission channels are open.

This Reich-Moore approximation is exact in the limit of one level or one photon channel (or none) and otherwise it is very accurate. Its non-reduced collision matrix can be considered unitary, and the cross section for radiative capture can either be calculated as the difference

$$\sigma_{c\gamma} = \sigma_c - \sum_{c'\in\gamma} \sigma_{cc'} \tag{19}$$

or from the non-reduced collision matrix with the approximation (16) as

$$\sigma_{c\gamma} = \pi\lambda_c^2 g_c \sum_\lambda \Gamma_{\lambda\gamma} \left| \frac{\sum_{c'\in\gamma} \left[P^{1/2}(1-RL^o)^{-1}P^{-1/2}\right]_{cc'} \Gamma_{\lambda c'}^{1/2}}{E_\lambda - E - i\Gamma_{\lambda\gamma}/2} \right|^2 \tag{20}$$

Eq. (20) is the generalization of an expression given for s-wave capture by Harris [7]. The Reich-Moore approximation is very flexible in the sense that a few photon channels, for instance

those with untypically large transition strengths, can be retained and treated explicitly together with the non-photonic channels while the other photon channels are eliminated (cf. [8]). Finally it should be noted that light nuclei are usually treated with phase shift or R-function formulae which can be considered as Reich-Moore formulae for zero radiation width [1].

In spite of these attractive features Reich-Moore parameters were banned from ENDF. One reason may have been the rather obscure description of the Reich-Moore formalism in [9] which makes it look very complicated to the uninitiated. The main reason, however, were the difficulties encountered when Reich-Moore cross sections have to be Doppler broadened. These difficulties no longer exist as explained below.

3.2 The MLBW Approximation

If the off-diagonal elements of the inverse level matrix are neglected altogether (and not just their photon channel components as in the Reich-Moore approximation),

$$\sum_c \gamma_{\lambda c} L_c^o \gamma_{\lambda' c} = A_{\lambda\lambda'} \sum_c \gamma_{\lambda c}^2 L_c^o = A_{\lambda\lambda'} (-E_\lambda + i\Gamma_\lambda/2), \tag{21}$$

inversion of A^{-1} becomes trivial. One obtains the MLBW approximation, with

$$U_{cc'} = e^{-i(\phi_c+\phi_{c'})} \left(S_{cc'} + i \sum_\lambda \frac{\Gamma_{\lambda c}^{1/2} \Gamma_{\lambda c'}^{1/2}}{E_\lambda - E - i\Gamma_\lambda/2} \right) \tag{22}$$

This collision matrix is not unitary except in the special case of a single level (single-level Breit-Wigner approximation, SLBW). It therefore tends to yield non-physical cross sections ($\sigma_c > 4\pi\lambda_c^2 g_c$) wherever levels overlap strongly (see Fig. 1). For mild level overlap the MLBW approximation is quite acceptable, however. In any case it is much better than the popular but often very bad approximation, sometimes termed "many-level Breit-Wigner" approximation, which results if cross sections are calculated simply as sums of SLBW terms (plus potential scattering terms in σ_c and σ_{cc}).

In the ENDF format the MLBW approximation is admitted only for elastic scattering. All other partial cross sections are taken as sums over SLBW terms, and the total cross section is the sum of these and the elastic-scattering cross section. Although this prescription ensures that all cross sections are positive it does not prevent wildly unphysical values near the peaks of strongly overlapping resonances. For light and medium-weight nuclei this approximation is therefore often unsatisfactory. Difficulties have also been encountered in the interference minima (windows) of the

total cross sections of structural materials and other light nuclei (Figs. 1a, 1d).

3.3 The Adler-Adler Approximation

The Adler-Adler approximation is obtained if one neglects in Eq. (6) the energy dependence of all L_c^0, not just that for photon and fission channels. Generalizing the s-wave formulae of Adler and Adler [10] to arbitrary ℓ one can do this in a symmetrical way by taking

$$\sum_c \gamma_{\lambda c} L_c^0(E) \gamma_{\mu c} = \sum_c \gamma_{\lambda c} \frac{L_c^0(E_\lambda) + L_c^0(E_\mu)}{2} \gamma_{\mu c} \quad . \tag{23}$$

Diagonalization of the inverse level matrix yields then the collision matrix in the form of a pole expansion,

$$U_{cc'} = e^{-i(\phi_c+\phi_{c'})} \left\{ \delta_{cc'} + i \sum_\lambda \frac{G_{\lambda c}^{1/2} G_{\lambda c'}^{1/2}}{\epsilon_\lambda - E} \right\} \tag{24}$$

where $G_{\lambda c} \equiv 2P_c g_{\lambda c}$. In contrast to the Kapur-Peierls parameters of Eqs. (14), (15) the complex Adler-Adler parameters $\epsilon_\lambda, g_{\lambda c}$ do not depend on energy. The approximation (25) means essentially that the energy dependence of level shifts and total widths in the resonance denominators is neglected. Therefore the Adler-Adler approximation works very well for fissile nuclei, where $\Gamma_\lambda = \Gamma_{\lambda\gamma} + \Gamma_{\lambda f} = \text{const}$, but not so well for light or medium-mass nuclei for which $\Gamma_\lambda = \Gamma_{\lambda n} = 2P_\lambda(E)\gamma_{\lambda n}^2$ (cf. Fig. 1). Nevertheless it is much better than the MLBW approximation.

A severe test for the accuracy of the various approximations, especially with respect to unitarity, is the calculation of capture cross sections as the difference (19) between total and scattering. For relatively light nuclei this is a small difference between two large numbers so that small violations of unitarity produce very big errors. Calculations for nuclei such as Na or structural materials showed that the Reich-Moore approximation gave results in excellent agreement with Eq. (20) whereas the MLBW and Adler-Adler results were quite useless.

4. DOPPLER BROADENING OF MULTI-LEVEL CROSS SECTIONS

The Kapur-Peierls collision matrix (14) yields cross section expressions which can be written in the concise form

$$\sigma_c = 4\pi\lambda^2 g_c \left\{ \sin^2\phi_c + \mathrm{Re}\left[e^{-2i\phi_c} \sum_\lambda \frac{G_{\lambda c}}{G_\lambda} (\psi_\lambda + i\chi_\lambda) \right] \right\} , \tag{25}$$

$$\sigma_{cc'} = \sigma_c\delta_{cc'} - 4\pi\lambda\!\!\!^{-2}g_c \mathrm{Re}\Big[\sum_\lambda \frac{G_{\lambda c}^{1/2} G_{\lambda c'}^{1/2}}{G_\lambda} W_{cc'}(\mathcal{E}_\lambda^*)^*(\psi_\lambda + i\chi_\lambda)\Big] , \quad (26)$$

where
$$W_{cc'}(\mathcal{E}_\lambda^*) = \delta_{cc'} + i \sum_\mu \frac{G_{\mu c}^{1/2} G_{\mu c'}^{1/2}}{\mathcal{E}_\mu - \mathcal{E}_\lambda^*} , \quad (27)$$

$$\psi_\lambda + i\chi_\lambda = \frac{iG_\lambda/2}{E-\mathcal{E}_\lambda} = \frac{G_\lambda^2/4}{(E-E_\lambda')^2+G_\lambda^2/4} + \frac{i(E-E_\lambda')G_\lambda/2}{(E-E_\lambda')^2+G_\lambda^2/4} , \quad (28)$$

with
$$G_\lambda \equiv -2\mathrm{Im}\mathcal{E}_\lambda , \qquad E_\lambda' \equiv \mathrm{Re}\mathcal{E}_\lambda . \quad (29)$$

The functions ψ_λ, χ_λ are the symmetric and asymmetric Breit-Wigner line shapes. They contain the main (resonance-type) energy dependence, all other quantities vary slowly with energy. Therefore Doppler broadening with the usual Gaussian kernel requires simply that ψ_λ and χ_λ be taken as the Voigt profiles

$$\psi_\lambda = \frac{1}{\Delta\sqrt{\pi}} \int_{-\infty}^{\infty} dE' e^{-(E'-E)^2/\Delta^2} \frac{G_\lambda^2/4}{(E'-E_\lambda')^2+G_\lambda^2/4} , \quad (30)$$

$$\chi_\lambda = \frac{1}{\Delta\sqrt{\pi}} \int_{-\infty}^{\infty} dE' e^{-(E'-E)^2/\Delta^2} \frac{(E'-E_\lambda')G_\lambda/2}{(E'-E_\lambda')^2+G_\lambda^2/4} , \quad (31)$$

where $\Delta = \sqrt{4EkT/A}$ is the Doppler-width (kT: Lamb-corrected temperature in energy units, A: target/projectile mass ratio), cf. [1]. If we consider neutron cross sections for specific reactions (total, (n,n),(n,f),(n,γ),...) rather than for specific channels (c,c') we can write, in the notation of Adler and Adler [10],

$$\sigma_t \equiv \sum_{c\in n} \sigma_c = \sigma_p + \frac{1}{\sqrt{E}} \sum_\lambda \frac{1}{\nu_\lambda} \left(G_\lambda^{(t)}\psi_\lambda - H^{(t)}\chi_\lambda\right) , \quad (32)$$

$$\sigma_x \equiv \sum_{c\in n} \sum_{c'\in x} \sigma_{cc'} = \frac{1}{\sqrt{E}} \sum_\lambda \frac{1}{\nu_\lambda} \left(G_\lambda^{(x)}\psi_\lambda - H^{(x)}\chi_\lambda\right), \quad (x=n,\gamma,f) \quad (33)$$

where σ_p is the potential-scattering cross section, $G_\lambda^{(x)}/(\sqrt{E}\nu_\lambda)$ and $H_\lambda^{(x)}/(\sqrt{E}\nu_\lambda)$ are sums over all coefficients of ψ_λ and χ_λ in Eqs. (25) and (26), with $\nu_\lambda \equiv G_\lambda/2$ and $\sqrt{E}$ coming from $\lambda\!\!\!^{-2}P_c$. The

level sums run over all contributing levels irrespective of JΠ, the spin factors g_c being absorbed in the Adler-Adler coefficients $G_\lambda^{(x)}$, $H_\lambda^{(x)}$.

Eqs. (32), (33) show that Doppler-broadened multi-level cross sections can be calculated most conveniently with the Voigt profiles if the Adler-Adler parameters $\mathcal{E}_\lambda=\mu_\lambda+i\nu_\lambda$, $G_\lambda^{(x)}$, $H_\lambda^{(x)}$ are available. In MLBW approximation one must use Eqs. (25) and (26), with $G_{\lambda c}=\Gamma_{\lambda c}$, $G_\lambda=\Gamma_\lambda$ (compare Eqs. (14) and (22)). This, however, is time-consuming if many levels are to be included, because double sums over levels must be calculated for $\sigma_{cc'}$ (over λ in Eq. (26), over μ in Eq. (27)). The Voigt profiles cannot be used directly with the Reich-Moore approximation. Of course, it is always possible to convert a set of Reich-Moore parameters to Kapur-Peierls parameters at a given energy. For $\ell=0$ this can be done e.g. with the POLLA code [11]. More generally Wigner-Eisenbud parameters can be converted to Kapur-Peierls parameters as follows [12]. The collision matrix must be invariant under the corresponding change of boundary parameters (e.g. from $B_c=-\ell$ to $B_c'=L_c$). This means $(1-RL^o)^{-1}R=R'$, if R' denotes the Kapur-Peierls R-matrix corresponding to B_c'. With the abbreviations

$$K \equiv L^{o1/2}RL^{o1/2}\,, \qquad K' = L^{o1/2}R'L^{o1/2} \tag{34}$$

one has

$$(1-K)^{-1} = 1+K'\,. \tag{35}$$

The Kapur-Peierls resonance energies are the complex poles $\mathcal{E}_\lambda$ of R' and K', i.e. the solutions of

$$\det\left[1-K(\mathcal{E}_\lambda)\right] = 0\,. \tag{36}$$

The residues of R' at the pole $\mathcal{E}_\lambda$ are

$$g_{\lambda c}g_{\lambda c'} = \frac{1}{\sqrt{L^o_c L^o_{c'}}}\;\frac{\operatorname{cof}\left[1-K(\mathcal{E}_\lambda)\right]_{cc'}}{\sum\limits_{c,c'}\dot{K}(\mathcal{E}_\lambda)_{cc'}\operatorname{cof}\left[1-K(\mathcal{E}_\lambda)\right]_{cc'}} \tag{37}$$

where cof denotes the cofactor matrix ($\operatorname{cof}X = X^{-1}\det X$ for non-singular X), and

$$\dot{K}(E)_{cc'} \equiv \left[L^{o1/2}\,\frac{\partial R}{\partial E}\,L^{o1/2}\right]_{cc'} = \sqrt{L^o_c L^o_{c'}}\sum_\lambda \frac{\gamma_{\lambda c}\gamma_{\lambda c'}}{(E_\lambda-E)^2}\,. \tag{38}$$

Eqs. (37), (38) follow from Eq. (35) in the limit $E\to\mathcal{E}_\lambda$, where L^o is considered as unaffected by the limiting process. Eq. (36)

can be solved by iteration. Denoting the trace of a matrix by tr we write

$$\det(1-K) = 1-\mathrm{tr}K+F \ , \tag{39}$$

where $-\mathrm{tr}K+F$ is the sum of $\det(-K)$ and all principal minors of $\det(-K)$ (see e.g. [13]),

$F = 0$	for 1 (elastic) channel
$F = \det(-K)$	for 2 channels
$F = \det(-K)+\mathrm{tr}\ \mathrm{cof}(-K)$	for 3 channels
etc.	

Next we write, in Wigner-Eisenbud representation,

$$-\mathrm{tr}K(\mathcal{E}_\lambda) = -\sum_\mu \frac{1}{E_\mu-\mathcal{E}_\lambda}\sum_c L_c^o\gamma_{\mu c}^2 = \sum_{\mu\neq\lambda}\frac{\Delta_\mu-i\Gamma_\mu/2}{E_\mu-\mathcal{E}_\lambda}+\frac{\Delta_\lambda-i\Gamma_\lambda/2}{E_\lambda-\mathcal{E}_\lambda} \ , \tag{40}$$

where the definition (21) is used. Insertion of (39) with (40) in (36) yields

$$\mathcal{E}_\lambda = E_\lambda + \frac{\Delta_\lambda-i\Gamma_\lambda/2}{1+\sum_{\mu\neq\lambda}\frac{\Delta_\mu-i\Gamma_\mu/2}{E_\mu-\mathcal{E}_\lambda}+F(\mathcal{E}_\lambda)} \ . \tag{41}$$

This equation is readily solved by iteration, starting with the rather plausible initial approximation $\mathcal{E}_\lambda = E_\lambda+\Delta_\lambda-i\Gamma_\lambda/2$. In Reich-Moore approximation E_μ must be replaced by $E_\mu-i\Gamma_{\mu\gamma}/2$, Γ_μ by $\Gamma_\mu-\Gamma_{\mu\gamma}$ everywhere. Once $\mathcal{E}_\lambda$ is known with sufficient accuracy one can calculate the residues with Eq. (37). Fig. 2 shows natural cross sections calculated from Reich-Moore parameters directly and from the Kapur-Peierls cross section expressions (25) - (29) after conversion of the Reich-Moore parameters according to Eqs. 37 - 41. The relative differences were of order 10^{-4} for σ_γ and of order 10^{-5} for all other cross sections. One can use this prescription to establish, at each energy of a suitably chosen grid, the Kapur-Peierls parameters and then calculate Doppler-broadened cross sections with the Kapur-Peierls expressions (25) - (29) involving the Voigt profiles. This requires the same time as is needed for a similar MLBW calculation plus the time needed for parameter conversion at each energy. Test calculations showed that about three times as much computer time is needed for Reich-Moore cross sections as for MLBW cross sections [12]. Fortunately one can reduce the time requirements for both Reich-Moore and MLBW cross sections drastically (in fact to about those for SLBW calculation) if one does not insist on using the Voigt profiles. It turns out that a method available for fast calculations of ψ and χ can be applied directly to multi-level cross sections.

5. TURING'S METHOD FOR GAUSSIAN BROADENING OF MEROMORPHIC FUNCTIONS

Bhat and Lee-Whiting [14] showed that the Voigt profiles can be calculated very fast with a method developed by Turing for Gaussian broadening of meromorphic functions (functions with given poles). It so happens that the combination $\psi + i\chi$ represents the simplest case of such a function, one single pole:

$$\psi+i\chi = \frac{1}{\Delta\sqrt{\pi}} \int_{-\infty}^{\infty} dE' e^{-(E'-E)^2/\Delta^2} \frac{i\Gamma/2}{E'-E_o+i\Gamma/2}$$

$$= \frac{iy_o}{\sqrt{\pi}} \int_{-\infty}^{\infty} dx \frac{e^{-x^2}}{x-z_o} \qquad (42)$$

with $$x \equiv \frac{E'-E}{\Delta} \quad , \qquad z_o = x_o+iy_o \equiv -\frac{E-E_o+i\Gamma/2}{\Delta} \qquad (43)$$

To calculate the integral in (42) Turing [15] considered the contour integral (see Fig. 3)

$$\int_C dz \frac{e^{-z^2}}{z-z_o} \frac{1}{1-e^{2\pi iz/h}} = 2\pi i \left(\sum_{n=-\infty}^{\infty} \frac{e^{-n^2h^2}}{nh-z_o} \frac{h}{-2\pi i} + \frac{e^{-z_o^2}}{1-e^{2-iz_o/h}} P \right)$$

$$= \int_{\infty+i\pi/h}^{-\infty+i\pi/h} dz \frac{e^{-z^2}}{z-z_o} + \int_{\infty+i\pi/h}^{-\infty+i\pi/h} dz \frac{e^{-z^2}}{z-z_o} \frac{e^{2\pi iz/h}}{1-e^{2\pi iz/h}}$$

$$+ \int_{-\infty-i\pi/h}^{\infty-i\pi/h} dz \frac{e^{-z^2}}{z-z_o} \frac{1}{1-e^{2\pi iz/h}} \qquad (44)$$

where $P = \begin{cases} 0 \\ 1/2 \\ 1 \end{cases}$ for $y_o \begin{cases} > \\ = \\ < \end{cases} \pi/h$.

For $y_o < 0$ the path of integration for the first integral in the last line can be shifted to the real axis. Furthermore, an upper limit can be established for the absolute square of the last two integrals (cf. [14]). The result is

$$\psi+i\chi = \frac{1}{\Delta\sqrt{\pi}} \sum_{n=-\infty}^{\infty} \delta E\, e^{-(E_n-E)^2/\Delta^2} \frac{i\Gamma/2}{E_n-E_o+i\Gamma/2} +$$

$$+ \sqrt{\pi}\,\frac{\Gamma}{\Delta} \frac{e^{-(E-E_o+i\Gamma/2)^2/\Delta^2}}{1-e^{-2\pi i(E-E_o+i\Gamma/2)/\delta E}} P + F \qquad (45)$$

where $\delta E = h\cdot\Delta$, $E_n = E+n\delta E$, (46)

$$P = \left\{ \begin{matrix} 0 \\ 1/2 \\ 1 \end{matrix} \right\} \text{ for } \frac{\Gamma/2}{\Delta} \left\{ \begin{matrix} > \\ = \\ < \end{matrix} \right\} \frac{\Delta}{\delta E}\,, \qquad (47)$$

$$F \le \frac{2}{\sqrt{\pi}} \left[1+\left(\frac{E-E_o}{\Gamma/2}\right)^2\right]^{1/2} \left|1-\left(\frac{2\pi\Delta}{\Gamma\delta E}\right)^2\right|^{-1} \frac{e^{-(\pi\Delta/\delta E)^2}}{1-e^{-2(\pi\Delta/\delta E)^2}} \qquad (48)$$

The factor $\exp\left[-(\pi\Delta/\delta E)^2\right]$ is extremely small for $\delta E < \frac{\Delta}{2}$. Neglecting F, Bhat and Lee-Whiting obtained accuracies of 10^{-7} or better for ψ and χ with $\delta E/\Delta = 0.7$. Eq. (45) shows then that Turing's approximation is essentially a simple sum approximation to the integral (sum term) plus a correction term which appears only if the pole is narrow compared to the grid of the sum term ($P > 0$ only if $\Gamma/2 \le \pi\Delta^2/\delta E$). The grid in turn is to be taken as somewhat smaller than the Doppler width. Moreover, even for relatively narrow poles the pole term can be neglected if the pole is not close to E because of its proportionality to $\exp\left[-(E-E_o)^2\right]$. For essentially the same reason one needs only sum terms with $-5 \lesssim n \lesssim 5$. Many group constant and resonance analysis codes calculate the Voigt profiles with this fast technique.

If one applies Turing's method to each term in the Kapur-Peierls cross section expressions (25), (26) one gets again a sum approximation to the integral plus correction terms for narrow, nearby poles, e.g.

$$\sqrt{E}\,\bar{\sigma}_c(E) = \frac{1}{\Delta\sqrt{\pi}} \sum_{n=-N}^{N} \delta E\, e^{-(E_n-E)^2/\Delta^2} \sqrt{E_n}\,\sigma_c(E_n)$$

$$+ \sqrt{E} \sum_{\lambda} C_\lambda G_\lambda \frac{e^{-(E-\mathcal{E}_\lambda)^2/\Delta^2}}{1-e^{-2\pi i(E-\mathcal{E}_\lambda)/\delta E}} P_\lambda \qquad (49)$$

where C_λ is the coefficient of $\psi_\lambda+i\chi_\lambda$ in Eq. 25. Now the unbroadened cross section $\sigma_c(E_n)$ can be calculated directly with Eqs. 2, 3 and 18 from the unconverted Reich-Moore parameters. Since no double sums are needed this calculation is about as fast as an

SLBW calculation. The pole term, on the other hand, requires the Kapur-Peierls parameters $\mathcal{E}_\lambda$, G_λ, but because of the factor P_λ (cf. Eq. (47)) only for relatively narrow resonances, and only near their peaks. In these narrow energy ranges one can neglect the energy dependence of C_λ, G_λ and $\mathcal{E}_\lambda$. It is therefore sufficient to convert parameters and to calculate the coefficients C_λ at only very few energies, namely at the formal resonance energies of the narrow resonances, $E_\lambda = \mathrm{Re}\,\mathcal{E}_\lambda$ (Eq. (29)). The time for calculation of the sum terms and pole terms is essentially the same as in SLBW calculations. The only additional time required is that for conversion to Kapur-Peierls parameters at few energies. For large numbers of levels this is only a small fraction of the total time. The Doppler width appearing as the natural mesh size in Turing's method makes it very convenient for resonance shape fitting.

The same technique can be used for MLBW cross sections. In this case the Kapur-Peierls parameters are simply $\mathcal{E}_\lambda = E_\lambda + \Delta_\lambda - i\Gamma_\lambda/2$, $g_{\lambda c} = \gamma_{\lambda c}$, and no conversion is needed at all. Thus the calculation is practically as fast as an SLBW calculation, the time required increasing linearly with the number of levels, whereas the time required for a $\sigma_{cc'}$ calculation with the Voigt profiles increases quadratically with the number of levels because of the double sum in Eq. (26).

The Gaussian broadening in Eqs. (30) and (31) is not quite exact. For the free-gas model the exact kernel was given by Solbrig [16]. Formally it is identical to the Watt spectrum used to describe fission neutron spectra [17], i.e. to a Galileo-transformed Maxwellian spectrum. In terms of speeds one can write

$$v^2\bar{\sigma}_{cc'}(v) = \frac{1}{v_T\sqrt{\pi}}\Big[\int_{-\infty}^{\infty} dv' e^{-(v'-v)^2/v_T^2}\, v'^2\sigma_{cc'}(v') - 2\int_{0}^{\infty} dv' e^{-(v'+v)^2/v_T^2}\, v'^2\sigma_{cc'}(v')\Big] \qquad (50)$$

where $E = mv^2/2$, $kT = Mv_T^2/2$ (m: neutron mass, M: target-nuclear mass). The second integral is negligible for $E \gtrsim 4kT/A$, so that above a few meV this is again a Gaussian convolution of $\delta_{cc'} - U_{cc'}$ for $\sigma_{cc'}$ (and of $1 - \mathrm{Re}U_{cc}$ for σ_c) which can be calculated with Turing's method, the poles being located at $v_\lambda = \pm\sqrt{2\mathcal{E}_\lambda/m}$. This approach is implemented in the newly developed Doppler-broadening code DOBRO. Fig. 4 shows an example where a 3-channel Reich-Moore calculation, with 35 levels included explicitly, yielded a complete set of cross sections in 3.7 seconds.

6. LEVEL-STATISTICAL TREATMENT OF DISTANT LEVELS

Modern evaluated files contain parameters for hundreds of levels. Such large numbers suggest a level-statistical treatment of the more distant levels as an additional means to speed up the calculations. The easiest and most direct way to do this is to split the R-matrix into a local and a distant-level term,

$$R_{cc'} = R^{o}_{cc'} + \sum_{\lambda=1}^{\lambda_c} \frac{\gamma_{\lambda c}\gamma_{\lambda c'}}{E_\lambda - E - i\Gamma_{\lambda\gamma}/2} \quad , \tag{51}$$

and to replace the sums in $R^{o}_{cc'}$ by integrals,

$$R^{o}_{cc'} = \left(\sum_{\lambda=-\nu}^{\infty} - \sum_{\lambda=1}^{\lambda_c} \right) \frac{\gamma_{\lambda c}\gamma_{\lambda c'}}{E_\lambda - E - i\Gamma_{\lambda\gamma}/2}$$

$$\approx \left(\int_{-\infty}^{\infty} - \int_{\bar{E}-I/2}^{\bar{E}+I/2} \right) \frac{dE'}{D_c} \frac{E'-E+i\bar{\Gamma}_\gamma/2}{(E'-E)^2+\bar{\Gamma}_\gamma^2/4} \left\langle \gamma_c \gamma_{c'} \right\rangle \quad . \tag{52}$$

Here $\bar{E}$ and I are midpoint and length of the interval containing the ν local levels, D_c is the average level spacing and $\bar{\Gamma}_\gamma$ the average radiation width. Since $(E'-E)^2 \gg \bar{\Gamma}_\gamma^2/4$ for the distant levels we can neglect $\bar{\Gamma}_\gamma^2/4$ in the last expression. Moreover we can neglect the off-diagonal elements of $\langle \gamma_c \gamma_{c'} \rangle$ because of the random signs of the γ_c. Finally we can introduce the usual definitions of the pole strength s_c and the distant-level function R^{∞},

$$s_c = \frac{\langle \gamma_c^2 \rangle}{D_c} \quad , \qquad R^{\infty}_c = \oint_{-\infty}^{\infty} dE' \frac{s_c(E')}{E'-E} \tag{53) (54}$$

where $\oint$ denotes Cauchy's principal value. With all this we obtain the final expression

$$R_{cc'} = \sum_{\lambda=1}^{\lambda_c} \frac{\gamma_{\lambda c}\gamma_{\lambda c'}}{E_\lambda - E - i\Gamma_{\lambda\gamma}/2}$$

$$+ \delta_{cc'} R^{\infty}_c + 2 s_c \operatorname{artanh} \frac{E-\bar{E}}{I/2} + \frac{i\bar{\Gamma}_\gamma I/4}{I^2/4-(E-\bar{E})^2} \delta_{cc'} \quad . \tag{55}$$

In many cases R^{∞}_c and s_c vary little between $\bar{E}-I/2$ and $\bar{E}+I/2$ so that one can treat them as adjustable constants which can be

determined simultaneously with the E_λ and $\gamma_{\lambda c}$ in a shape fit to resonance data in this interval. On the other hand they can be obtained from an optical-model calculation. Thus resonance fits can provide a check on differing optical-model calculations. For a large number of structural-material isotopes effective radii, $R'_c = (1-R^\infty_c)a_c$, were obtained from fits to transmission data. Fig. 5 shows one of the fits. The effective radii thus obtained are consistent with a coupled-channel calculation but not with a spherical optical model as shown in Fig. 6.

Johnson and Winters [18] went even further. They actually determined optical-model potentials for s- and p-wave neutrons interacting with ^{32}S from detailed shape analysis of transmission data. Subtracting the local resonance terms from R_{cc} they obtained the distant-level R-functions shown in Fig. 7. The artanh behavior (cf. Eq. (55)) is clearly seen.

This level-statistical description of the distant-level part of the R-matrix is more convenient than the use of dummy levels outside the range $\bar{E}-I/2 \ldots \bar{E}+I/2$ or of expansions of the type $R^0 = A(E-\bar{E}) + B(E-\bar{E})^2 + \ldots$ It utilizes only two parameters with a clear meaning, R^∞_c and s_c, both of which can be obtained from an optical model and then refined in a shape fit. Furthermore, the potential-scattering parameters R^∞_c and s_c are quite insensitive to extensions of the range of parametrization (inclusion of more resonances), in contrast to dummy levels. Nevertheless, since the purely statistical treatment of distant levels may be inadequate if untypically weak or strong levels are located just outside the interval $\bar{E}-I/2 \ldots \bar{E}+I/2$, it is good practice to include such "nearby" levels explicitly in the sum in Eq. (55) whenever possible.

7. DISCRETE BOUND LEVELS

An example of the nearby levels just mentioned are levels just below the elastic threshold ($E_\lambda < 0$). In most cases one bound level per spin state is enough for a good description of low-energy, e.g. thermal, cross sections, provided the level-statistical term of Eq. (55) is employed for all more distant bound (and distant unbound) levels. At sufficiently low energies cross sections with $\ell \geq 1$ are negligible. For $\ell = 0$ one has

$$U_{cc} = e^{-2ik_c a_c} \frac{1+ik_c a_c R_{cc}}{1-ik_c a_c R_{cc}} \qquad (c\phi\gamma) \ , \qquad (56)$$

with R_{cc} given by Eq. (55), if only elastic scattering and radiative capture are energetically possible. Assuming that one bound level suffices one can solve Eq. (56) for the corresponding sum term in R_{cc}. With $k_c a_c \gamma^2_{\lambda c} = \Gamma_{\lambda n}/2$, $a_c R^\infty_c = a - R'_c$ and $2k_c a_c s_c = s_0\sqrt{E/1eV}$ one gets for ℓ discrete unbound levels and 1 bound level with parameters E_o, Γ_n, Γ_γ

$$\frac{i\Gamma_n/2}{E_o-E-i\Gamma_\gamma/2} = -\sum_\lambda \frac{i\Gamma_{\lambda n}/2}{E_\lambda-E-i\Gamma_{\lambda\gamma}/2}$$

$$- i\left[k_c(a-R'_o)+S_o\right]\sqrt{\frac{E}{1eV}}\ \mathrm{artanh}\ \frac{E-\bar{E}}{I/2}+\frac{i\bar{\Gamma}_\gamma/I}{1-\left(\frac{E-\bar{E}}{I/2}\right)^2}\ \Bigg]$$

$$+\frac{U_{cc}e^{2ik_ca_{c-1}}}{U_{cc}e^{2ik_ca_{c+1}}}\quad(\equiv \Delta_{cc})\ . \tag{57}$$

Assuming all E_λ, $\Gamma_{\lambda n}$, $\Gamma_{\lambda\gamma}$ as well as R'_c, S_o and $\bar{\Gamma}_\gamma$ to be known and calculating U_{cc} from the cross sections σ_c and $\sigma_{cc} = \sigma_c-\sigma_{c\gamma}$ at some low energy E (e.g. 0.0253 eV), via

$$\mathrm{Re}\ U_{cc} = 1 - \frac{\sigma_c}{2\pi\lambda_c^2 g_c}\ , \tag{58}$$

$$\mathrm{Im}\ U_{cc} = \pm\sqrt{\frac{\sigma_{cc}}{\pi\lambda_c^2 g_c} - \left(\frac{\sigma_c}{2\pi\lambda_c^2 g_c}\right)^2} \tag{59}$$

(cf. Eqs. (1) and (2)) one can evaluate the right-hand side of Eq. (57). Equating the result, Δ_{cc} say, to the left-hand side and separating real and imaginary parts one finds eventually

$$-E_o = -E + \frac{\mathrm{Im}\ \Delta_{cc}}{\mathrm{Re}\ \Delta_{cc}}\frac{\Gamma_\gamma}{2}\ , \tag{60}$$

$$\frac{\Gamma_n}{2} = -\frac{|\Delta_{cc}|^2}{\mathrm{Re}\ \Delta_{cc}}\frac{\Gamma_\gamma}{2}\ . \tag{61}$$

With only two equations for the three unknowns E_o, Γ_n, Γ_γ we can choose one of them arbitrarily and then calculate the others. The approximate constancy of the radiation widths from level to level suggests to take Γ_γ as the mean radiation width $\bar{\Gamma}_\gamma$ obtained from the Λ discrete unbound levels. The sign ambiguity in Eq. (59) is due to the fact that the cross sections depend on Re U_{cc} and $|U_{cc}|^2$. Usually the positive sign can be discarded immediately because it yields $E_o > 0$ contrary to the assumption of a bound level. Note that in Eqs. (57) and (61) all neutron widths are to be calculated at the energy E by

$$\Gamma_{\lambda n}(E) = \Gamma_{\lambda n}(|E_\lambda|)\sqrt{E/|E_\lambda|} = \Gamma^o_{\lambda n}\sqrt{E} \tag{62}$$

(including that for the bound level, $\lambda = 0$).

Eqs. (60) and (61) are a good approximation also for thermally fissile nuclei for which one finds an additional approximate equation for the fission width of the bound level,

$$\frac{\Gamma_f}{2} = -\frac{|\Delta_{cf}|^2}{\mathrm{Re}\,\Delta_{cc}}\frac{\Gamma_\gamma}{2} \tag{63}$$

$$\text{with}\quad |\Delta_{cf}|^2 \equiv \frac{\sigma_{cf}}{\pi\lambda\!\!\!^{-2} g_c} - \sum_{\lambda=1}^{\infty}\frac{\Gamma_{\lambda n}\Gamma_{\lambda f}/4}{(E_\lambda - E)^2 + \Gamma_\lambda^2/4} - S_o\sqrt{\frac{E}{1eV}}\,\frac{\bar{\Gamma}_f/I}{1-\left(\frac{E-\bar{E}}{I/2}\right)^2}\,, \tag{64}$$

and σ_{cf} being the fission cross section for entrance channel c at energy E.

If, for target nuclei with nonzero spin, the level spins are unknown, and only $g\Gamma_n$ is known for unbound levels instead of g and Γ_n separately, one obtains the prescription

$$-E_o = -E + \frac{\mathrm{Im}\,\Delta_{nn}}{\mathrm{Re}\,\Delta_{nn}}\frac{\Gamma_\gamma}{2}\,, \tag{65}$$

$$\frac{g\Gamma_n}{2} = -\frac{|\Delta_{nn}|^2}{\mathrm{Re}\,\Delta_{nn}}\frac{\Gamma_\gamma}{2}\,, \tag{66}$$

$$\frac{g\Gamma_f}{2} = -\frac{|\Delta_{nf}|^2}{\mathrm{Re}\,\Delta_{nn}}\frac{\Gamma_\gamma}{2}\,, \tag{67}$$

with

$$\Delta_{nn} = \frac{W_{nn}-1}{W_{nn}+1} - \sum_{\lambda=1}^{\infty}\frac{ig_\lambda\Gamma_{\lambda n}/2}{E_\lambda - E - i\Gamma_\gamma/2} - ik(a-R')$$

$$- iS_o\sqrt{\frac{E}{1eV}}\,\mathrm{artanh}\,\frac{E-\bar{E}}{I/2} + S_o\sqrt{\frac{E}{1eV}}\,\frac{\bar{\Gamma}_\gamma/I}{1-\left(\frac{E-\bar{E}}{I/2}\right)^2}\,, \tag{68}$$

$$\Delta_{nf} = \frac{\sigma_f}{\pi\lambda\!\!\!^{-2}} - \sum_{\lambda=1}^{\infty}\frac{g_\lambda\Gamma_{\lambda n}\Gamma_{\lambda f}/4}{(E_\lambda - E)^2 + \Gamma_\lambda^2/4} - S_o\sqrt{\frac{E}{1eV}}\,\frac{\bar{\Gamma}_f/I}{1-\left(\frac{E-\bar{E}}{I/2}\right)^2}\,, \tag{69}$$

and

$$W_{nn} = e^{2ika}\left[1 - \frac{\sigma}{2\pi\lambda\!\!\!^{-2}} - i\sqrt{(2ka_{coh})^2 - \left(\frac{\sigma}{2\pi\lambda\!\!\!^{-2}}\right)^2}\right]. \tag{70}$$

The directly observable total and fission cross sections at energy E are weighted sums over the two s-wave spins, $\sigma = \Sigma_c g_c \sigma_c$, $\sigma_f = \Sigma_c g_c \sigma_{cf}$. The total widths are to be approximated by $\Gamma_\lambda = \Gamma_{\lambda f} + \Gamma_{\lambda\gamma} + 2g_j\Gamma_{\lambda n}$. The same effective radii R' and strength functions S_0 were assumed for both spin states, as in Eq. (57), and the channel subscript c was dropped for ℓ_c and k_c. Furthermore we used the relationship between the coherent scattering length a_{coh} and the elastic cross sections for each spin state, $a_{coh} = \Sigma_c g_c \sigma_{cc}/4\pi$. Specialization to one spin state ($I = 0$ or $g_c = g_c$) or to nonfissile nuclei ($\sigma_f = 0$, $\Gamma_{\lambda f} = \Gamma_f = 0$) leads to the prescriptions given above.

It is found that the bound-level parameters found with this prescription are usually quite adequate to reproduce all measured partial cross sections not only at the chosen (e.g. thermal) energy but over the whole low-energy range. The lower limit of the range of explicitly given resonances can be taken e.g. as two mean level spacings below the lowest unbound level, $E-I/2 = E_1-2D$, or one level spacing below the neutron threshold, $E-I/2 = -D$. Sometimes it is necessary to shift it towards lower energies to get consistent results ($E-I/2 < E_0 < 0$) but in general the calculated cross sections are not sensitive to the exact choice. Figs. 8 and 9 show low-energy cross sections obtained with this method for ^{241}Am with one bound level. The fit to the measured data is quite comparable to that in [18] where no less than 5 bound levels were used.

8. MODERN PROCEDURES IN RESONANCE ANALYSIS

This last section is devoted to the more general problem of non-linear parameter estimation as encountered in resonance analysis of neutron data. As more and better shape analysis codes become operational (see [1] and [2]) area analysis methods are phased out. It is not true that shape analysis fails and must be replaced by area analysis if instrumental resolution is bad, as is often stated. Actually shape analysis is always more convenient because it can deal with many resonances simultaneously, and with a reasonable description of the resolution function its results are not inferior but most of the time superior to area analysis results. It is just the case of only partially resolved multiplets where shape analysis, treating all components simultaneously, gives better results more rapidly than area analysis, where difficult wing corrections must be applied to each component and often several iterations are required to get the final results for the whole multiplet.

So far shape analysis codes employed what may be called primitive least-squares techniques: (1) correlations among data points, due e.g. to common background subtraction or normalization, are neglected, (2) prior knowledge about the cross section parameters is used at best in a very limited way, namely to fix first guesses for the iteration procedure which in general is re-

quired because of the nonlinearity of the mathematical model (R-matrix theory). Parameter estimation was thus based essentially on the data in hand and the resulting parameters had to be combined with the prior knowledge after the fit by some kind of weighted averaging.

A more rigorous and convenient approach consists in (1) using the full uncertainty information including correlated errors and (2) in combining prior information with the new information contained in the data to be fitted by means of Bayes' theorem and and then to search for the most probable parameters. Consider

- observables y_i, $i = 1, 2, \ldots I$ (e.g. transmissions)
- parameters x_μ, $\mu = 1, 2, \ldots M$ (cross section parameters)
- a model $y = y(x)$ (R-matrix theory)

where $y = (y_1, y_2, \ldots y_I)$, $x = (x_1, x_2, \ldots x_M)$ are vectors in the data and parameter spaces, respectively, and $I > M$. Suppose

(a) that even before the data y_i became available one had some prior knowledge about the parameters x_μ, namely estimates ξ_μ and correlated errors $M_{\mu\nu}$ (or at least variances $M_{\mu\mu}$), so that the probability for x to be the true value, given ξ, can be taken as

$$p(x|\xi) \propto \exp\left[-\frac{1}{2}(x-\xi)^+ M^{-1}(x-\xi)\right] \qquad (71)$$

where $^+$ denotes the transpose;

(b) that a new measurement yielded values η_i and correlated errors V_{ik} for the observables y_i, so that the likelihood to obtain these values provided the true parameter vector is x, be taken as

$$p(\eta|y) \propto \exp\left[-\frac{1}{2}(\eta-y(x))^+ V^{-1}(\eta-y(x))\right] . \qquad (72)$$

The assumption of multi-variate Gaussians in (71) and (72) is an approximation which may fail for large distances $|x-\xi|$ and $|\eta-y(x)|$ but for small distances it is expected to be reasonable and in any case sufficient for parameter estimation purposes.

One can now combine the prior probability (71) and the likelihood (72) by means of Bayes' theorem to get the probability density function for x, given the data η and the prior estimates ξ,

$$p(x|\xi\eta) \propto p(\eta|x)p(x|\xi)$$

$$\propto \exp\left[-\frac{1}{2}(x-\xi)^+ M^{-1}(x-\xi) - \frac{1}{2}(\eta-y(x))^+ V^{-1}(\eta-y(x))\right] . \qquad (73)$$

The most probable vector x is the one that minimizes the exponent,

$$(x-\xi)^{+}M^{-1}(x-\xi)+(\eta-y(x))^{+}V^{-1}(\eta-y(x)) \equiv \chi^2 = \min . \qquad (74)$$

We shall consider this particular parameter vector as the improved estimate and call it ξ'. Note that without prior knowledge M^{-1}, and thus the first term, vanishes. Neglecting then also the off-diagonal elements of V^{-1} one gets the starting condition for primitive least-squares fitting as used in conventional shape analysis of nuclear resonance data.

The condition (74) is equivalent to

$$M^{-1}(x-\xi)-\dot{y}(x)^{+}V^{-1}(\eta-y(x)) = 0 \qquad (75)$$

where $\dot{y}$ is the rectangular matrix of sensitivity coefficients,

$$\dot{y}_{i\mu} = \frac{\partial y_i}{\partial x_\mu} . \qquad (76)$$

Eq. (75) is easily solved for x if y is a linear function of x. In nuclear resonance work, however, y(x) is nonlinear and one must iterate, for instance with the Newton-Raphson method (in M dimensions). Starting with the prior most probable values, $x_0 = \xi$, one finds after n steps

$$x_{n+1} = \xi+\left[M^{-1}+\dot{y}(x_n)^{+}V^{-1}\dot{y}(x_n)\right]^{-1}\dot{y}(x_n)^{+}V^{-1}\left[\eta-y(x_n)-\dot{y}(x_n)(\xi-x_n)\right]$$

and finally the new estimate

$$\xi' = \xi+\left[M^{-1}+\dot{y}(x_\infty)^{+}V^{-1}\dot{y}(x_\infty)\right]^{-1}\dot{y}(x_\infty)^{+}V^{-1}\left[\eta-y(x_\infty)-\dot{y}(x_\infty)(\xi-x_\infty)\right] . \qquad (77)$$

The new correlated errors are obtained as follows. We consider a small domain around $x = x_\infty = \xi'$ where y(x) can be considered to be linear. Then the right-hand side of (73) reduces to a product of two multivariate Gaussians which is equivalent to another multivariate Gaussian with the most probable value $x = \xi'$ and correlated errors given by

$$M'^{-1} = M^{-1}+\dot{y}(x_\infty)^{+}V^{-1}\dot{y}(x_\infty) . \qquad (78)$$

In practice, of course, one does not need infinitely many iterative steps as the notation x_∞ implies. Usually half a dozen steps or less are quite enough.

Sometimes it is better to write everything in terms of the covariance matrices M and V instead of their inverses. For instance, a common (systematic) background uncertainty in the data, $\delta\eta_i = b$, leads to $V_{ik} = \delta\eta_i\delta\eta_k = b^2$. The matrix V is then singular and V^{-1} is undefined. It can be shown that Eqs. (77) and (78) are equivalent to

$$\xi' = \xi + M\dot{y}(x_\infty)^+\left[V+\dot{y}(x_\infty)M\dot{y}(x_\infty)^+\right]^{-1}\left[\eta-y(x_\infty)-\dot{y}(x_\infty)(\xi-x_\infty)\right] , \quad (79)$$

$$M' = M-M\dot{y}(x_\infty)^+\left[V+\dot{y}(x_\infty)M\dot{y}(x_\infty)^+\right]^{-1}\dot{y}(x_\infty)M , \quad (80)$$

The pairs of equations (77), (78) and (79), (80) show explicitly how the prior estimates and uncertainties ξ, M are updated by new data η,V so that the new (posterior) estimates and uncertainties are ξ',M'. The minus sign in Eq. (80) corresponds to the reduction of the uncertainties by the new data. The change of the estimates and the reduction of the uncertainties is seen to be small if the sensitivity coefficients $\dot{y}_{i\mu}$ are small and vice versa.

This iterative least-squares approach with full account of parameter and data correlations and of prior information is implemented in the shape analysis code SAMMY that is being developed at ORNL by F. Perey and Nancy Larson. So far the code, which uses the Reich-Moore formalism, works for transmission data. An extension to capture data is under development. Even in its present state the code has clearly shown the advantage of including the prior probability (71). This allows mathematically straightforward incorporation of prior knowledge in the fit procedure and at the same time constrains the parameter search to a reasonable domain in a smooth way, avoiding the problems of sharp limits typical for linear programming. Moreover, uncorrelated portions of the data can be analyzed successively in separate runs, proper transfer of the accumulated information from one run to the next being ensured.

9. CONCLUSIONS

A short characterization of the practically available multilevel formalisms was given. The fact that the Reich-Moore formalism can be considered as automatically ensuring unitarity of the collision matrix makes it universally applicable to light and heavy nuclei, with weakly or strongly overlapping levels, near thresholds, transmission windows and resonance peaks. Actually most modern shape fitting codes use variants of the Reich-Moore formalism. The Adler-Adler representation does not automatically guarantee unitarity unless obtained by conversion from Reich-Moore parameters. As it neglects the energy dependence of total widths it leads to errors for light and medium-weight nuclei, especially

near thresholds. The MLBW approximation is definitely non-unitary and in case of strong level overlap, near cross section peaks and minima often necessitates large corrections. In the ENDF file these are given as a "smooth" cross section component which, however, is often not smooth at all.

Doppler broadening can be calculated by means of the Voigt profiles. This is very fast with Adler-Adler parameters (time proportional to number of resonances), slow with MLBW and Reich-Moore parameters (time proportional to squared number of resonances, with additional time needed for conversion to Kapur-Peierls form at each energy in case of Reich-Moore parameters). A new prescription, however, yields Doppler-broadened Reich-Moore and MLBW cross sections about equally fast as Adler-Adler cross sections. The trick is to apply Turing's method for Gaussian broadening to the multi-level cross section expressions directly rather than to the zero-temperature Voigt profiles. The necessity to convert Reich-Moore parameters to Kapur-Peierls parameters is then reduced to the resonance energies of narrow levels instead of all energies. In view of these developments it appears appropriate to reconsider the question whether Reich-Moore parameters should not be readmitted to the ENDF/B file.

Further recent developments in resonance cross section work concern the representation of distant levels. It is found that a level-statistical treatment of the distant-level part of the R-matrix, involving strength functions and effective radii either as fit parameters or as quantities obtained from optical-model calculations, is the most rigorous and convenient way to deal with edge effects in resonance fits. This approach can also be used to determine the parameters of representative bound levels from those of discrete unbound and distant bound and unbound levels and from the thermal cross sections.

Finally attention was drawn to the possibility to improve existing shape analysis codes by allowing for correlated data errors and by formalized inclusion of prior information by means of Bayes' theorem.

REFERENCES

1. F. H. FRÖHNER, "Applied Neutron Resonance Theory," in Nuclear Theory for Applications, IAEA, Vienna, 1980; also available as report KfK 2669 (1978).

2. G. M. HALE, "Use of R-matrix Methods for Light Element Evaluations," Workshop on Evaluation Methods and Procedures, these proceedings.

3. E. P. WIGNER and L. EISENBUD, Phys. Rev. 72 (1947) 29, E. P. WIGNER, J. Am. Phys. Soc. 17 (1949) 99.

4. A. M. LANE and R. G. THOMAS, Rev. Mod. Phys. 30 (1958) 257.

5. P. L. KAPUR and R. E. PEIERLS, Proc. Roy. Soc. (London) A166 (1938) 277; R. E. PEIERLS, Proc. Cambridge Phil. Soc. 44 (1947) 242.

6. C. W. REICH and M. S. MOORE, Phys. Rev. 111 (1958) 929.

7. D. R. HARRIS, Neutron Cross Sections and Technology, Washington D.C., 1966 (CONF 660303), p. 833.

8. B. J. ALLEN, A. R. DE L. MUSGROVE and W. K. BERTRAM, Neutron Data of Structural Materials for Fast Reactors, Oxford etc., 1979, p. 497.

9. M. K. DRAKE (ed.), "Data Formats and Procedures for the ENDF Neutron Cross Section Library," report ENDF 102, (1970).

10. F. T. ADLER and D. B. ADLER, Nucl. Data for Reactors, IAEA, Vienna, 1970.

11. G. DE SAUSSURE and R. B. PEREZ, report ORNL-TM-2599 (1969).

12. F. H. FRÖHNER, Neutron Physics and Nuclear Data, Harwell, 1978, p. 306.

13. G. A. KORN and T. M. KORN, Mathematical Handbook for Scientists and Engineers, New York etc., 1961, p. 367.

14. M. R. BHAT and G. E. LEE-WHITING, Nucl. Instr. Meth. 47 (1967) 277.

15. A. M. TURING, Proc. London Math. Soc., Ser. 2, 48 (1943) 180.

16. A. W. SOLBRIG, JR., Nucl. Sci. Eng. 10 (1961) 167, see also Ref. [1] p. 69.

17. B. E. WATT, Phys. Rev. 87 (1952) 1037, see also D. G. MADLAND, "Prompt Fission Neutron Spectra and ν_p," these proceedings.

18. J. E. LYNN, B. H. PATRICK, M. G. SOWERBY and E. M. BOWEY, Report AERE-R 8528 (1979).

19. C.H. Johnson and R.R. Winters, Phys. Rev. C21(1980)2190

20. SWEDISH NUCLEAR DATA COMMITTEE, "Compilation of Actinide Neutron Nuclear Data", Report KDK-35 (1979)

21. H. Beer and R.R. Spencer, "keV Neutron Radiative Capture and Total Cross Sections", Report KfK 2063(1974)

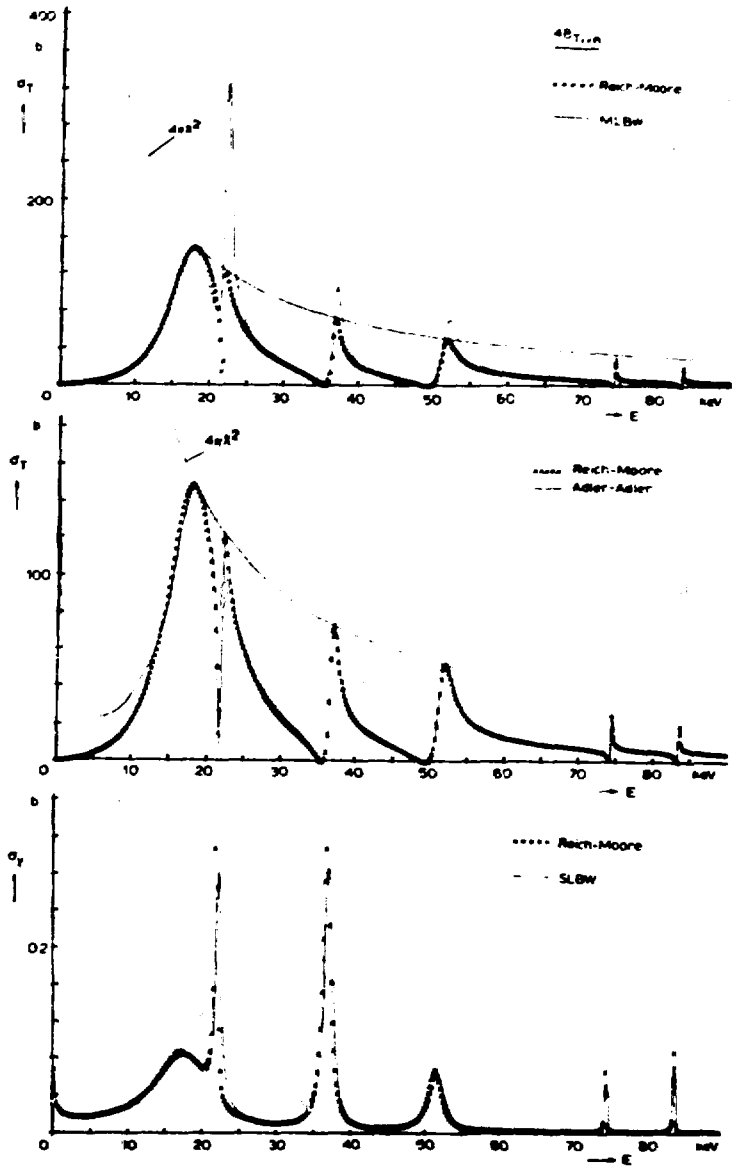

Fig. 1 a-c Illustration of inadequacy of approximations admitted by ENDF/B conventions for medium-mass nuclei. Reich-Moore values are exact. The unitarity limit $\sigma_T < 4\pi\lambda^2$ is seriously violated by MLBW, less by Adler-Adler. The latter fails at low energies [12].

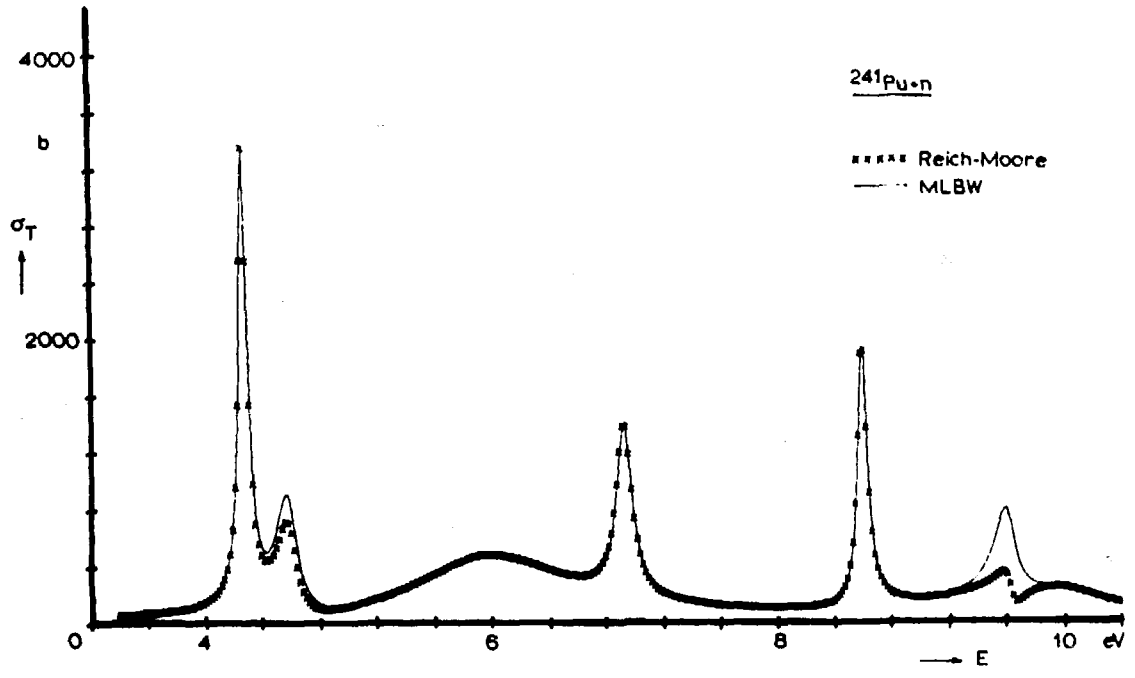

Fig. 1 d **Example for failure of MLBW approximation to reproduce strongly interfering doublets in the total cross section of a heavy nuclide. Reich-Moore values are exact, calculated with two open fission channels.**

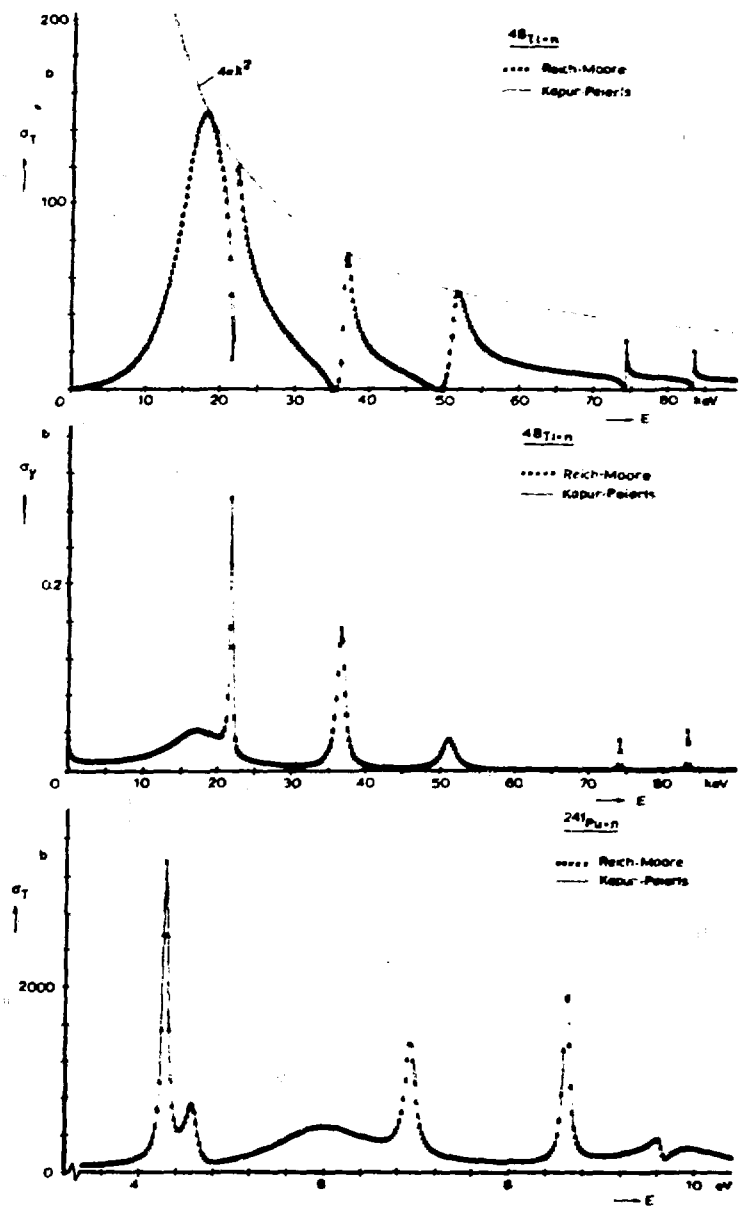

Fig. 2 Verification of Reich-Moore/Kapur-Peierls conversion prescription, Eqs. 41 and 37, for a light and a heavy, fissile nuclide. Reich-Moore values were calculated directly from unconverted, Kapur-Peierls curves from converted resonance parameters [12].

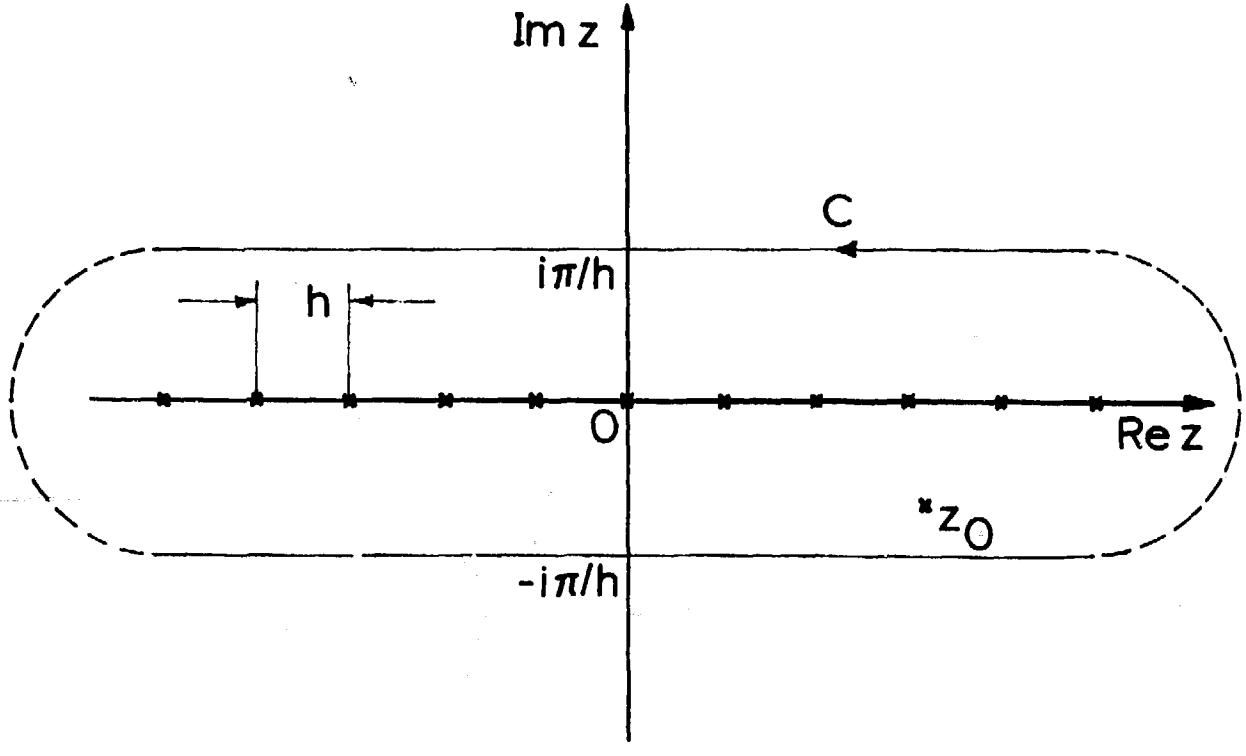

Fig. 3 The contour (C) and the poles (x) for Turing's integral, Eq. 44.

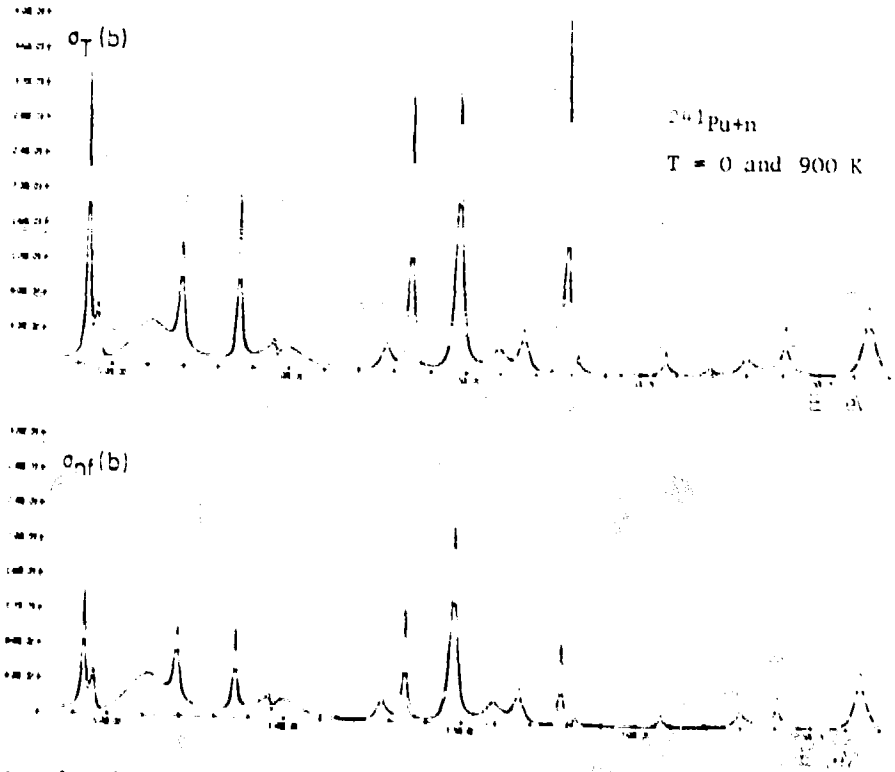

Fig. 4 a-b Natural and Doppler-broadened total and fission cross sections of ^{241}Pu+n, calculated with a 3-channel Reich-Moore formalism and direct application of Turing's method to the multi-level cross section expressions (i.e. without Voigt profiles).

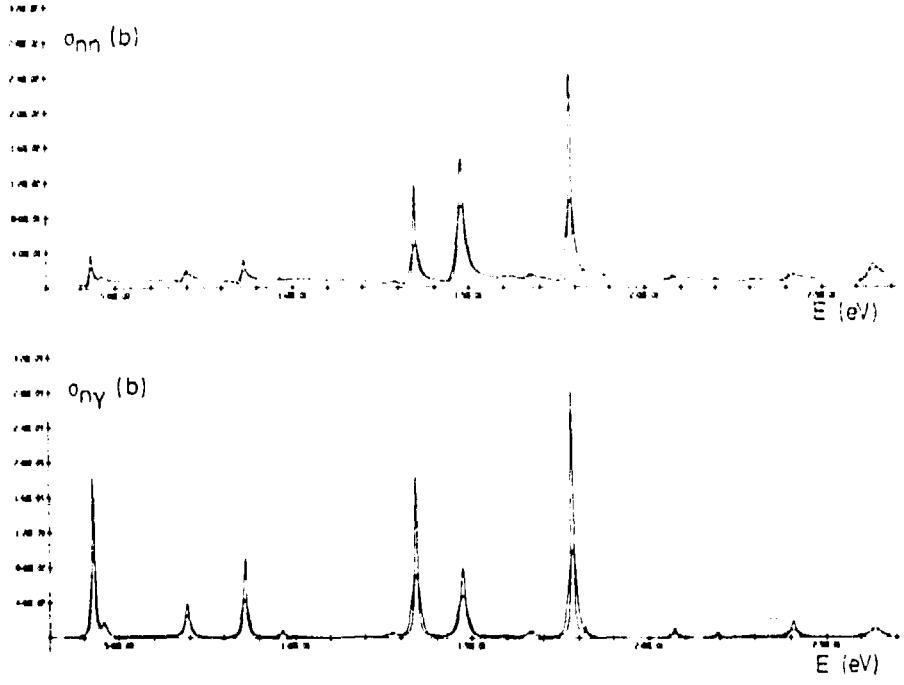

Fig. 4 c-d Natural and Doppler-broadened scattering and capture cross sections of ^{241}Pu+n, calculated with 3-channel Reich-Moore formulae and direct application of Turing's method (i.e. without Voigt profiles). The complete set of cross sections between 4.5 and 27 eV shown in Figs. 4 a-d, involving 35 resonances and 760 energies, was generated within 3.7 s on an IBM/370-168 computer.

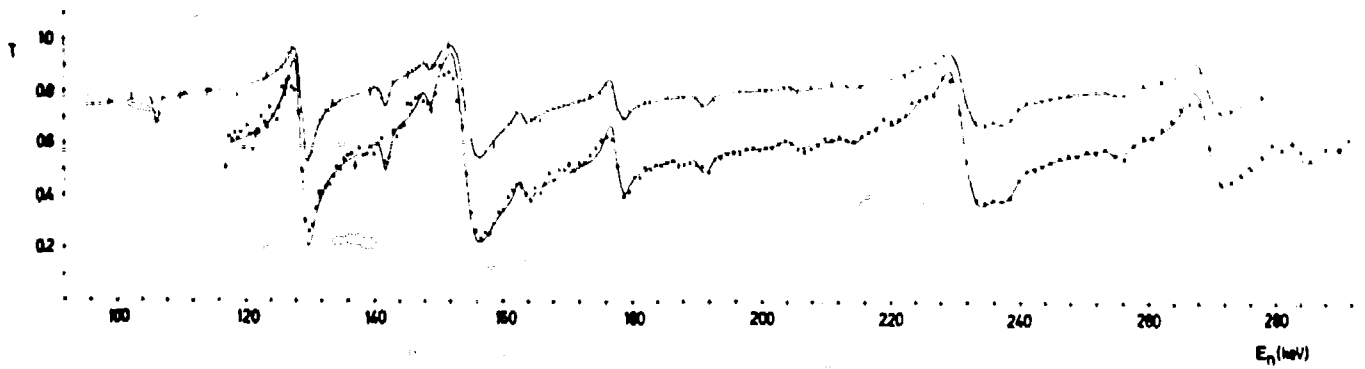

Fig. 5 Shape fits to two sets of transmission data simultaneously with the level-statistical treatment of distant levels, Eq. 55. Note the consistently good fit even near the limits of the range of the fit (from [21]).

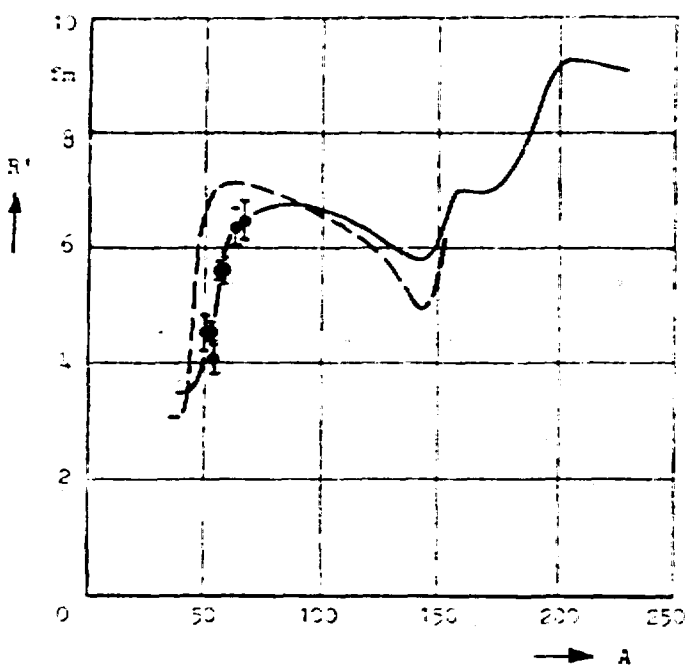

Fig. 6 Effective nuclear radii obtained for Cr, Fe and Ni isotopes by shape fits to transmission data below 300 keV with the level-statistical treatment of distant levels, Eq. 55. The broken curve was calculated with a spherical, the solid line with a deformed optical potential (see [1] for further references).

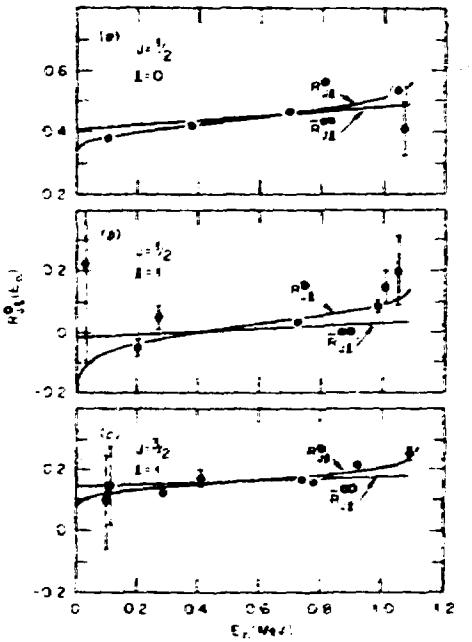

Fig. 7 Distant-level R-functions obtained by Johnson and Winters from transmission shape fits [19]. Solid circles: total R-function minus local-level sum, curve: optical-model calculation. The ar$_\infty$tanh behavior (cf. Eq. 55) is clearly seen. R^∞ is taken not as a constant as in Eq. 55 but as a linear function of energy.

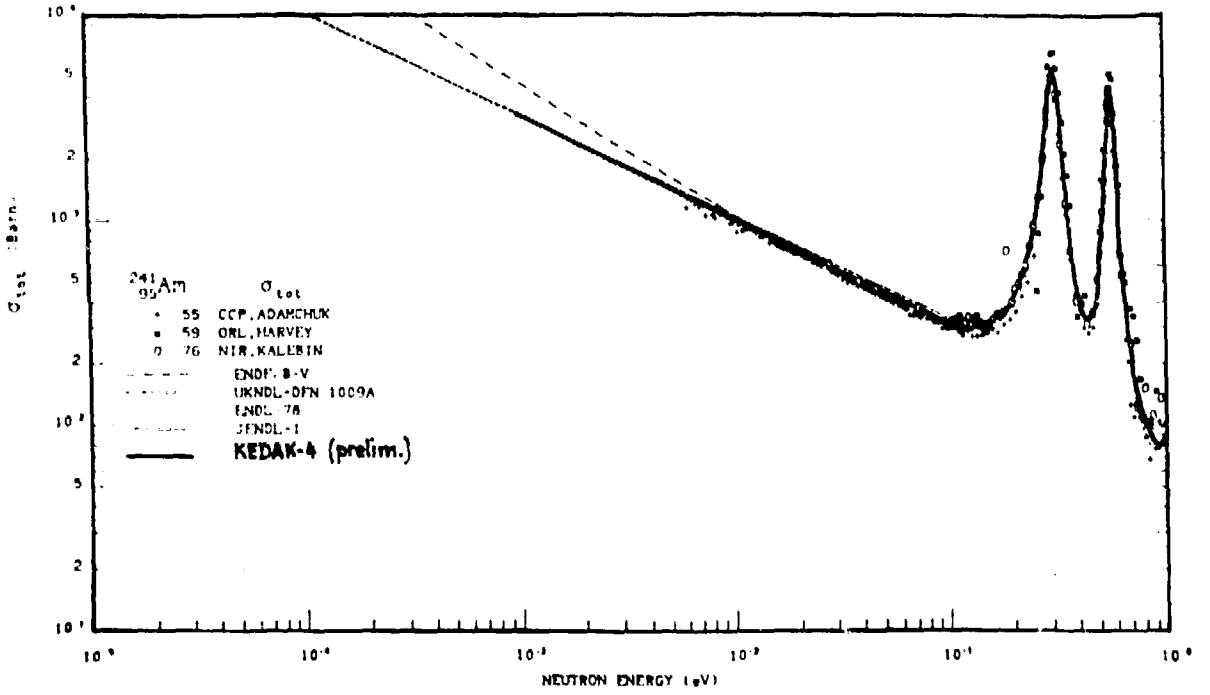

Fig. 8 Comparison between measured and evaluated total cross sections of ^{241}Am+n [20]. The KEDAK-4 curve was calculated with distant-level terms according to Eq. 57 and one bound level adjusted so as to reproduce the 2200 m/s cross sections.

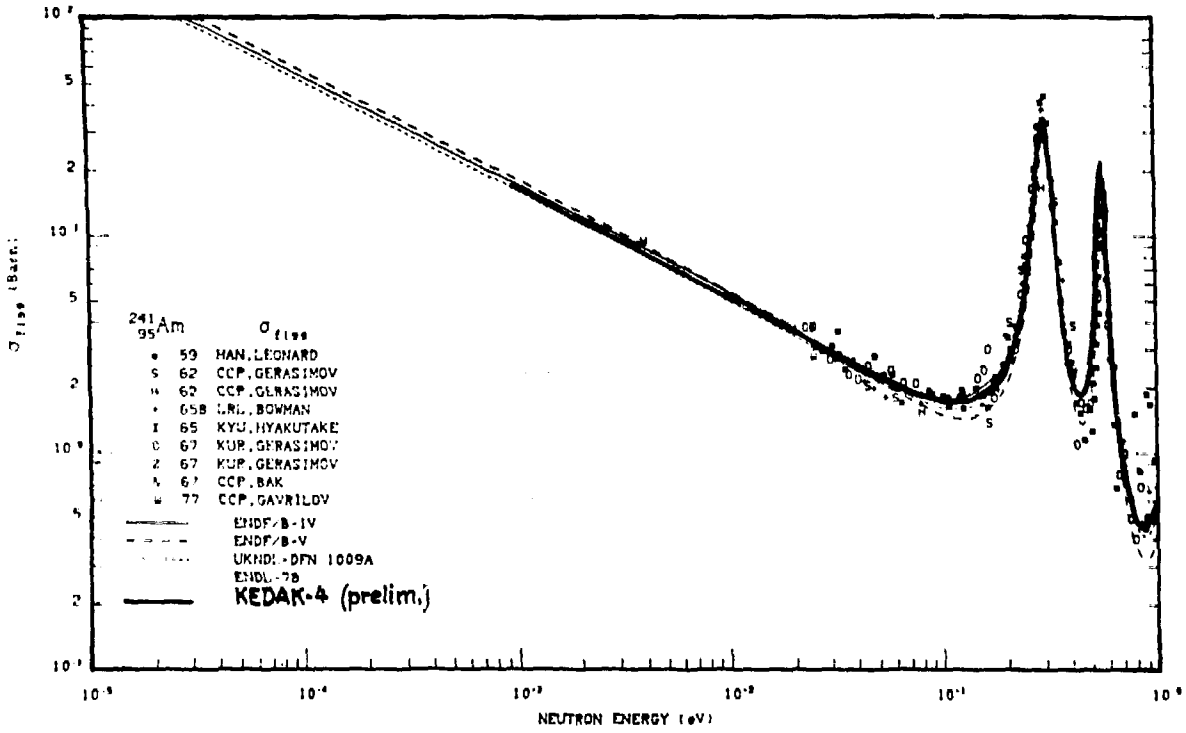

Fig. 9 Comparison between measured and evaluated fission cross sections of ^{241}Am+n [20]. The KEDAK curve was calculated with distant-level-terms according to Eqs. 68-70 and one bound level adjusted so as to reproduce the 2200 m/s cross sections.

Discussion

Mughabghab

I would like to make the following general comment. If additional information, such as the spin dependent scattering lengths, is available, one can get a better handle on fitting the thermal region. In some cases additional fitting constraints, such as the minimum in the total cross section of Sc at 2 keV, are imposed. In general, two bound levels are required to achieve a good fit to the shape of the cross section in the thermal region.

Schmidt

In principle, the thermal cross sections must be calculated from all positive and all negative resonances. How can you get such a good description of thermal energy dependent cross sections as you demonstrated for several actinides by taking only one bound level per spin state into account.

Froehner

Because all the other levels are taken into account by the distant level terms involving the parameters R^{∞}, S, and $\bar{\Gamma}_{\gamma}$.

Patrick

When assigning parameters to bound levels, it sometimes turns out that if one level is included, the required parameters are non-physical (e.g. the reduced neutron width may be 10 times the average of the resolved resonances). Are there any circumstances in which this matters? It was to maintain physically acceptable values that we included five bound levels in our ^{241}Am evaluation rather than just one.

Froehner

Very large widths can occur if the bound level has to yield the distant level contribution for a very large energy interval below the neutron threshold. If this interval is chosen of the order of 1 average spacing the widths of the bound level are usually quite reasonable, but even very large widths would not bother me as long as the thermal region is described correctly.

Mughabghab

Except for light nuclides where one can obtain guidance from the (d,p) data, the parameters of bound levels are not unique. They are to be considered as a tool of describing the behavior of the cross section in the thermal region.

Block

We observed for ^{238}U that we could not calculate the capture cross section between the low energy resonances to better than ~20% because we do not know the signs of the partial radiation widths. Is this also a problem for the structural materials?

Froehner

The signs of the partial radiation width amplitudes are not needed in the Reich-Moore approximations. We had no problem with the capture cross sections between resonances, neither for heavy elements nor for structural materials, mainly because the statistical errors of the data between resonances are larger than the capture cross sections expected with or without channel capture.

EVALUATION OF TRANSMISSION MEASUREMENTS

Robert C. Block

Gaerttner Linac Laboratory
Department of Nuclear Engineering
Rensselaer Polytechnic Institute
Troy, New York 12181 USA

ABSTRACT

The evaluation of transmission data requires a working knowledge of both the corrections applied to the experimental data and the detailed analyses employed to deduce the neutron total cross section or the resonance parameters from the transmission data. Corrections typically applied to transmission data are reviewed, and several examples of data obtained from transmission measurements are presented to illustrate common problems that must be taken into account during evaluation.

INTRODUCTION

A neutron transmission measurement is performed either to obtain directly the neutron total cross section or to obtain parameters, such as resonance parameters, from which the total cross section can be deduced. The problem facing the evaluator is to choose wisely amongst the data from several transmission measurements and arrive at the 'best overall' total cross section or parameters such that violence is done neither to the experimental data nor to the application for which the evaluated data are required. Unfortunately, the evaluator is frequently faced with several mutually conflicting sets of experimental data, each with an imprimator of stated accuracy and each the result of many detailed and complex corrections with which usually only the measurer is intimately knowledgeable. To complicate further the evaluator's task, experimental data typically span many years and analyses and corrections applied to more recent measurements have not been applied uniformly to all the data. It is thus crucial that the evaluator be knowledgeable about the nuances of experimental transmissions measurements, the effects of background, resolution, systematics, etc. in order that he carry out his job properly.

This paper attempts to describe from an experimentalist's point of view some of the problems typically encountered in neutron time-of-flight (TOF) transmission measurements. TOF measurements have been selected, both from the personal experience and bias of the author and from the fact that most neutron transmission measurements today use the TOF technique. TOF transmission measurements span the energy range from less than ten millielectron volts to tens of MeV, a range over which the total cross section varies greatly both in magnitude and in complexity and for which the transmission measurement technique and the sample thicknesses must be matched to the cross section dependence. Several examples of transmission measurements in different energy regions will be presented to illustrate both common and energy-region-dependent problems.

NEUTRON TRANSMISSION MEASUREMENT: "ONE OF THE EASIEST MEASUREMENTS TO MAKE!"

Many years ago this author looked upon transmission measurements as one of the easiest measurements to perform. After all, all one has to do is cycle a sample in and out of a collimated neutron beam and take the ratio of the sample in and sample out counting rate recorded by a detector at the end of the flight path. The neutron total cross section is then determined from the familiar expression

$$\sigma_t = -1/N \ln T$$

where N is the sample thickness (in b^{-1}) and T is the measured transmission corrected for deadtime losses and background. Unfortunately, however, the interpretation of transmission data is far more complex, and it is important to remind ourselves just what is actually measured in a transmission experiment.

The transmission experiment basically consists of cycling a sample in and out of the neutron beam, so it is useful to look at the detected counting rate for each sample position. The sample 'out' position detector counting rate O(E) is given approximately by

$$O(E) \simeq \int_0^\infty n(E,E')\, e_n(E')\, dE' + \left\{ \int_0^\infty n(E,E'' \rightarrow E''')e_n(E''')dE''' \right.$$

$$+ \int_0^\infty [\, g(E,E_g) + g(E,E'''' \rightarrow E_g)]\, e_g(E_g)\, dE_g$$

$$+ SB_b + SB_a \Big\}$$

$$\simeq \int_0^\infty n(E,E')\, e_n(E')\, dE' + OB(E) \qquad (1)$$

where higher order background terms have been neglected. The nominal neutron energy E is typically taken at the peak of the neutron distribution arriving at the detector, n(E,E') is the intensity of neutrons (in neutrons per second) per unit energy which are distributed in energy E' and which arrive at the detector with no collision after passing through the sample position, $e_n(E')$ is the neutron detector efficiency, $n(E,E'' \rightarrow E''')$ is the intensity of neutrons per unit energy which pass through the sample position with energy E'' but are scattered into the detector with energy E''', $g(E,E_g)$ is the intensity of gamma rays per unit gamma ray energy which pass through the sample positions and arrive with no collision at the detector with energy E_g, $g(E,E'''' \rightarrow E_g)$ is the intensity of gamma rays per unit energy arriving at the detector with energy E_g which were the result of a neutron of energy E'''' passing through the sample position and subsequently producing the gamma ray, SB_b is a beam-dependent steady-state background in the detector, and SB_a is the ambient steady-state background, which is independent of the sample position. The first term on the right of Eq. (1) is the counting rate from the primary collimated beam of neutrons which pass through the sample position and arrive at the detector with no collision. The other terms represent background counting rates; these terms are represented in Eq. (1) by OB(E), the 'out' background. As can be seen, the background is quite complex, being composed of both neutron and gamma ray components. Even the steady-state beam-dependent background SB_b is complex; an example is the iodine neutron activation that occurs in NaI crystals and which has a troublesome 25-minute halflife.

The corresponding sample 'in' counting rate is given by

$$I(E) \simeq \int_0^\infty e^{-N\sigma_t(E')}\, n(E,E')\, e_n'(E')\, dE' + \Big\{ \int_0^\infty e^{-N\sigma_t(E'')}$$

$$\cdot\, n\,(E,E'' \rightarrow E''')\, e_n'(E''')\, dE''$$

$$+ \int_0^\infty \Big[e^{-N\sigma_g(E_g)}\, g(E,E_g) + e^{-N\sigma_t(E'''')}\, g(E,E'''' \rightarrow E_g) \Big]$$

$$\cdot\, e_g(E_g)\, dE_g + SB_b' + SB_a \Big\}$$

$$\simeq \int_0^\infty e^{-N\sigma_t(E')}\, n(E,E')\, e_n'(E')\, dE' + IB(E) \quad . \qquad (2)$$

The first two terms on the right of Eq. (2) account for the transmission of neutrons passing through the sample of thickness N (in units of b^{-1}) with neutron total cross section σ_t. The neutron detector efficiency has changed to e_n' to account for possible sample-dependent effects in the detector; e.g., deadtime losses or gamma-flash-induced shifts in detector efficiency that are affected when the transmission sample partially shields the detector from the target. The third term accounts for the transmission of gammas and neutrons through the sample which ultimately arrive at the detector with gamma ray energy E_g; σ_g represents the total gamma cross section. The beam-dependent steady state background, SB_b', is now changed by the presence of the sample in the beam. The four background terms are grouped together and represented by IB(E) in Eq. (1).

As just described, the background terms in Eq. (1) and Eq.(2) are very complicated functions of both gamma rays and neutrons, and determination of these background terms is one of the most difficult tasks of a transmission measurement. Various experimental techniques are used, such as the insertion of black resonance absorbers or scatterers into the beam and observing the background, but unfortunately almost all transmission experiments rely upon the extrapolation of a background measured either at a different energy or with a different sample in the beam to the background that exists in the energy region or sample position of interest. Undetermined systematic effects are usually present in the estimation of these backgrounds, and the evaluation of transmission data must estimate how well the background corrections have been understood and applied.

To determine the neutron transmission from the measured detector counting rates, deadtime and efficiency change corrections are applied to the data such that I(E), IB(E), O(E) and OB(E) are replaced by I'(E), IB'(E), O'(E) and OB'(E) and e_n and e_n' are

replaced by the corrected efficiency e_n^c . The experimental transmission $T_m(E)$ is then

$$T_m(E) = \frac{I'(E) - IB'(E)}{O'(E) - OB'(E)} = \frac{\int_0^\infty e^{-N\sigma t(E')}\, n(E,E')\, e_n^c(E')\, dE'}{\int_0^\infty n(E,E')\, e_n^c(E')\, dE'} \quad (3)$$

The neutron total cross section or the resonance parameters are determined from Eq. (3). If the experimental resolution is either very good or the cross section varies very slowly with energy, $\sigma_t(E')$ can be replaced by $\sigma_t(E)$ and Eq. (3) reduces to the familiar relation $T_m(E) = e^{-N\sigma_t(E)}$, from which is obtained $\sigma_t(E) = -1/N \ln T_m(E)$. In many measurements, especially in the resonance region, the resolution is not good enough to assume a constant total cross section over the range of energies for which $n(E,E')$ is significant and the data must be analyzed further. In the resolved resonance region both area and shape analyses are applied to $T_m(E)$ to determine the resonance parameters. However, older measurements typically used a single-level formalism, while several more recent measurements have used a multi-level formalism. Care must then be exercised by the evaluator in comparing single-level and multi-level resonance parameters, especially the effects of resolution and how distant levels have been treated in the multi-level analysis.

In the unresolved resonance region Eq. (3) typically represents a local average over the transmission through the sample. Some measurements report an effective average total cross section: $\overline{\sigma_t^{eff}}(E) = -1/N \ln T_m(E)$. However, this effective average cross section is smaller than the average total cross section because of self-shielding effects, and thus the effective average cross section is both sample thickness and temperature dependent. The data are usually analyzed in terms of either ladders of pseudo resonances or probability tables.

In the very low energy region Bragg Scattering can introduce significant structure into the transmission. Here the data must be analyzed in terms of both the chemical and physical structure of the sample, properties which are frequently poorly known.

Thus, considering all of the background, resolution, sample, electronic, etc. corrections that must be applied to interpret transmission measurements, even if a transmission measurement is one of the easiest to make, it is still not an easy measurement.

SELECTED EXAMPLES OF TRANSMISSION MEASUREMENTS

The author apologizes for the biased selection of transmission measurements that will now be discussed. It is convenient to discuss work one is most familiar with, and unfortunately this leads to a larger emphasis of experiments that the author has been involved with. However, as many problems are common to the interpretation and evaluation of transmission data, this biased selection should still serve to illustrate these features.

^{232}Th Transmission Measurement at Low Energies

Three recent transmission measurements of ^{232}Th have been reported in the energy range from 0.006 meV to $\gtrsim$20 eV [1,2,3]. The measurements by Little et al. [1] were carried out by TOF at the RPI Gaerttner Linac Laboratory using metallic thorium samples which were between 0.5 and 3 mean free paths thick. The counting data were obtained with a ^{6}Li-glass neutron detector. Sample thickness uncertainties were $\sim$0.3%. The major experimental correction to the data was the determination of background, and black filters of Co, W, Au, In and Cd were used to evaluate the background at 132, 18.8, 4.9, 1.44 and below 0.3 eV, respectively; the thorium transmission samples determined the background at the 21.8- and 23.5-eV resonances for the sample in data. The major uncertainty in the background correction was the determination of the time-dependent background component. This was deduced from the black filter measurement with and without the thorium sample in the beam, and the deduced shape was assumed to vary smoothly between the blacked-out energies. It was also assumed that this shape was the same for both the sample in and out conditions. The support for these assumptions was the experience that this type of background dependence was common for many of the TOF measurements at RPI and elsewhere.

The total cross section, determined from $-1/N \ln T_m(E)$, is shown in Fig. 1 along with the evaluated data ENDF/B-IV [4] and ENDF/B-V [5], and also in Fig. 2 with a multilevel fit to the data above 0.1 eV. The measured total cross section is in agreement with the fast-chopper measurement of Chrien et al. [2] to within a few percent and with the recent linac measurements of Olsen et al. [3] to within 0.5 percent. Above 0.1 eV, the transmission data serve to raise the thorium total cross section from the low value in ENDF/B-IV, although the ENDF/B-V data overpredicts this measured cross section by several percent. In Fig. 2, the data were fitted with a multilevel formalism with the program MLEVL [6], and here it was noted that the addition of a picket fence of negative-energy levels plus a strong level just below the binding energy were needed to balance out the effect of the positive-energy levels and to fit the thermal capture cross section.

Below 0.1 eV, the situation is very interesting. The effect of Bragg Scattering in the transmission samples is very evident, and this effect is not included in the evaluated data sets. The multilevel fit in Fig. 2 also did not account for Bragg Scattering. The net effect of the Bragg Scattering is to introduce significant structure into the total cross section, and the measured cross section falls considerably below the evaluated data in this energy range. The experimental scattering cross section, formed by subtracting the capture from the total cross section, is compared in Fig. 3 with the calculated scattering cross section. The calculation determined the effect of Bragg Scattering from the known lattice structure in metallic thorium. It can be seen in Fig. 3 that the experimental data show the same Bragg peaks as the calculated cross section, although the experimental resolution did broaden the observed structure. In Fig. 3(a), a 1/v-dependent capture cross section was subtracted from the measured total cross section, while in Fig. 3(b), the measured capture cross section was subtracted. However, since capture cross section is a topic separate from the thrust of this talk, the reader is referred to reference [1] for a discussion of the capture cross section.

^{238}U Transmission Measurements in the Resonance Region

A recent example of an extensive set of transmission measurements in the resolved resonance region is the ORNL transmission measurements of ^{238}U from 0.52 to 4000 eV [7], and from 0.88 to 100 keV [8]. A total of seven sample thicknesses were used in these measurements, and measurements were carried out with a 42-m and a 150-m flight path. Black resonance filters of Co, Al, Mn and In were used in the lower energy measurements to determine the shape and magnitude of the background; while Na, Al and Mn were used in the higher energy measurements. The shape of the time-dependent background was assumed to be the same for all sample thicknesses, and this assumption was supported by the general consistency of the results. The authors took into account the gamma-ray component in their high-energy background caused by hydrogen capture in the moderator, and they also estimated the uncertainty in their time-dependent background shape caused by the well-known effect that the background measured by a black filter depends upon the width of the blacked-out region.

A least-squares multilevel shape-analysis program SIOB [9] was used to fit several sets of transmission data simultaneously with the multilevel Breit Wigner formula. In order that there not be an imbalance in the number of levels taken into account, Olsen et al. included all levels within an equal energy span above and below the region being analyzed plus a picket fence of levels extending to infinity above and below the energy span selected. For the low-energy data, a gaussian resolution function was used, but an asymmetric resolution function was required at higher energies. The excellent fits which were obtained are illustrated in Fig. 4

for the energy range from 0.52 to 55.5 eV and in Fig. 5 from 2469 to 2731 eV.

In analyzing their low-energy data, Olsen et al. observed that the resonance parameters and effective radius are correlated, so it becomes rather difficult for the evaluator in choosing amongst many data sets. The effective radius at low energy depends strongly upon the strength of the levels just below the binding energy. Strong anticorrelations were observed between the neutron and radiation widths when the resonance-potential interference was small. When the interference was large, this anticorrelation decreased, but in turn a strong correlation was then observed between the neutron width and the effective radius. In analyzing their high-energy data, Olsen et al. required an asymmetric resolution function to get consistent results, as well as to fit the shape of very narrow resonances, and this asymmetric resolution function resulted in the largest neutron widths determined for the high-energy ^{238}U resonances. Thus, any evaluation of the high-energy ^{238}U resonance data from several laboratories should examine the effect of an asymmetric resolution function.

The task facing the evaluator is to re-examine the older measurements to see if the effects observed in the more recent measurements will lead to revised resonance parameters or errors, and to re-evaluate the revised data.

Unresolved Resonance Region

Transmission measurements in the unresolved resonance region are interpreted in terms of average resonance parameters and fluctuations about the average. Measurements by Bryan et al. [10] emphasized both the sample thickness and temperature dependence of ^{238}U and Ta transmission in the unresolved resonance region below 100 keV. Metallic samples were used which were at room temperature, cooled to liquid nitrogen temperature or heated to 1000°K. The largest correction applied to the data was for the time-dependent background, and black filters of S, Al, Mn and Co were used to span the energy range from 0.1 to 100 keV. The effect of sample contraction or expansion with temperature was determined at low energies between resonances where the change in transmission was attributed to the change in sample thickness.

The measured transmissions for five samples of ^{238}U at 295°K and for two each at 770K and 973°K are shown in Fig. 6. The data have been averaged over 10-percent-wide energy bins to obtain a local energy average over a large number of ^{238}U resonances. These data have been analyzed in terms of the s- and p-wave strength functions, the effective scattering radius, the average s- and p-wave level spacings, and the average s- and p-wave radiation widths. Both analytical and stochastic analyses have been used.

The results provide a correlated set of average parameters which can be compared to the resolved resonance parameters extrapolated into this energy range. Thus this type of measurement can serve as a semi-integral test of the extrapolated microscopic data and can be used by the evaluator in trying to resolve conflicting results from resolved resonance region measurements.

Filtered Beam Transmission Measurements

Recently the use of thick resonance-potential-interference filters have been used with pulsed neutron sources to obtain bands of neutrons which are well separated from each other in TOF. These filtered neutrons have a very low background of gamma rays and off-energy neutrons, and the background is accurately determined during the measurements by observing the counting rate in the blacked-out regions on either side of the filtered band. This technique has proved extremely useful in determining deep minima in the total cross section by using the same material in the filter and the transmission sample. Cross section minima in Fe [11,12, 13,14], Na [15], Sc[16], Si[13], and ^{56}Fe[17] have been measured by this method. An example of this type of measurement is shown in Fig. 7 for the 24.37-keV minimum in ^{56}Fe, where the ≈10 mb total cross section minimum can readily be accounted for by the ^{56}Fe resonance parameters and a 5.67-fm effective scattering radius.

In addition to providing a direct measurement of the total cross section in deep minima, the filtered-beam method can also provide an accurate measurement of the total (or partial) cross section at one or more bands of energy that correspond to one or more minima in the filter. Transmission measurements have been made at the 24.3-keV Fe-filtered band for Be, O and C [19] and H [20] with a 30-cm-thick Fe filter and with an accuracy of a few tenths of a percent. This type of 'single energy' measurement can provide an accurate total cross section measurement and can also serve as a benchmark to which high-resolution TOF measurements can be compared. Since the filtered beam transmission measurement is not plagued with the large time-dependent background typically observed in unfiltered TOF measurements, the combination of the unfiltered and filtered beam measurements can serve to normalize the unfiltered beam results at these discrete filter energies.

SUMMARY

The transmission measurement is simple in principle but can be quite complex in actual practice. The problems of background determination, resolution broadening and analytical formalism can all introduce systematic biases in the interpretation of the results. The evaluator is thus forced to understand and to estimate the magnitude of these effects in determining an evaluated cross

section which combines all experimental results on an equal basis.

REFERENCES

[1] R. C. LITTLE, D. R. HARRIS AND R. C. BLOCK, "The Neutron Total Cross Section of ^{232}Th from 0.1 to 18 eV," Trans. Am. Nucl. Soc., 32, 748 (1979). R. C. LITTLE, R. C. BLOCK, D. R. HARRIS, R. E. SLOVACEK AND O. N. CARLSON, "Neutron Capture and Total Cross Section Measurements of ^{232}Th from 0.006 eV to 18 eV"(to be published).

[2] R. E. CHRIEN, H. I. LIOU, M. J. KENNY AND M. L. STELTS, "Neutron Cross Sections of Th-232," Nucl. Sci. Eng., 72, 202 (1979).

[3] D. K. OLSEN, R. W. INGLE AND J. L. PORTNEY, "Precise Transmission and Analysis of Neutron Transmission Through ^{232}Th" (to be presented at the 1980 ANS Topical Meeting, Sun Valley, Idaho).

[4] Evaluated Neutron Data File B, Version IV, National Nuclear Data Center, Brookhaven National Laboratory.

[5] Evaluated Neutron Data File B, Version V, National Nuclear Data Center, Brookhaven National Laboratory.

[6] R. C. BLOCK, D. R. HARRIS, S. H. KIM AND K. KOBAYASHI, "^{238}U Resonance Self-Indication Capture Measurements and Analysis," NP-996 (1979), Electric Power Research Institute.

[7] D. K. OLSEN, G. de SAUSSURE, R. B. PEREZ, E. G. SILVER, F. C. DIFILIPPO, R. W. INGLE AND H. WEAVER, "Precise Measurement and Analysis of Neutron Transmission Through Uranium-238," Nucl. Sci. Eng., 62, 479 (1977).

[8] D. K. OLSEN, G. de SAUSSURE, R. B. PEREZ, F. C. DIFILIPPO, R. W. INGLE AND H. WEAVER, "Measurement and Resonance Analysis of Neutron Transmission Through Uranium-238," Nucl. Sci. Eng., 69, 202 (1979).

[9] G. de SAUSSURE, D. K. OLSEN AND R. B. PEREZ, "SIOB: A Fortran Code for Least-Squares Shape Fitting Several Neutron Transmission Measurements Using the Breit-Wigner Multilevel Formula," ORNL/TM-6286, Oak Ridge National Laboratory (1978).

[10] T. Y. BYOUN, R. C. BLOCK AND T. SEMLER, in Proc. of National Topical Meeting on New Developments in Reactor Physics and Shielding, Kiamesha Lake, New York, Book 2, 1115, CONF72091 (1972).

[11] F. RAHN, H. CARMADA, G. HACKEN, W. W. HAVENS, JR., H. LIOU, J. RAINWATER, M. SLAGOWITZ AND S. WYNCHANK, Nucl. Sci. Eng., 47, 372 (1972).

[12] J. A. HARVEY, in Proc. of New Developments in Reactor Physics and Shielding, Kiamesha Lake, New York, 1075, CONF720901 (1972).

[13] K. A. ALFIERI, R. C. BLOCK AND P. J. TURINSKY, Nucl. Sci. Eng., 51, 25 (1973).

[14] K. KOBAYASHI, Y. FUJITA AND Y. OGAWA, Annals of Nucl. Sci., 4, 449 (1977)

[15] P. H. BROWN , B. L. QUAN, J. J. WEISS AND R. C. BLOCK, Trans. Am. Nucl. Soc., 21, 505 (1975).

[16] H. I. LIOU, R. E. CHRIEN, R. C. BLOCK AND K. KOBAYASHI, Nucl. Sci. Eng., 67, 326 (1979).

[17] H. I. LIOU, R. E. CHRIEN, R. C. BLOCK AND U.N. SINGH, Nucl. Sci. Eng.,70, 150 (1979).

[18] R. C. BLOCK, Y. FUJITA, K. KOBAYASHI AND T. OOSAKI, J. of Nucl. Sci. and Tech., 12, 1 (1974).

[19] Y. FUJITA, K. KOBAYASHI, T. OOSAKI AND R. C. BLOCK, Nucl. Physics A258, 1 (1976).

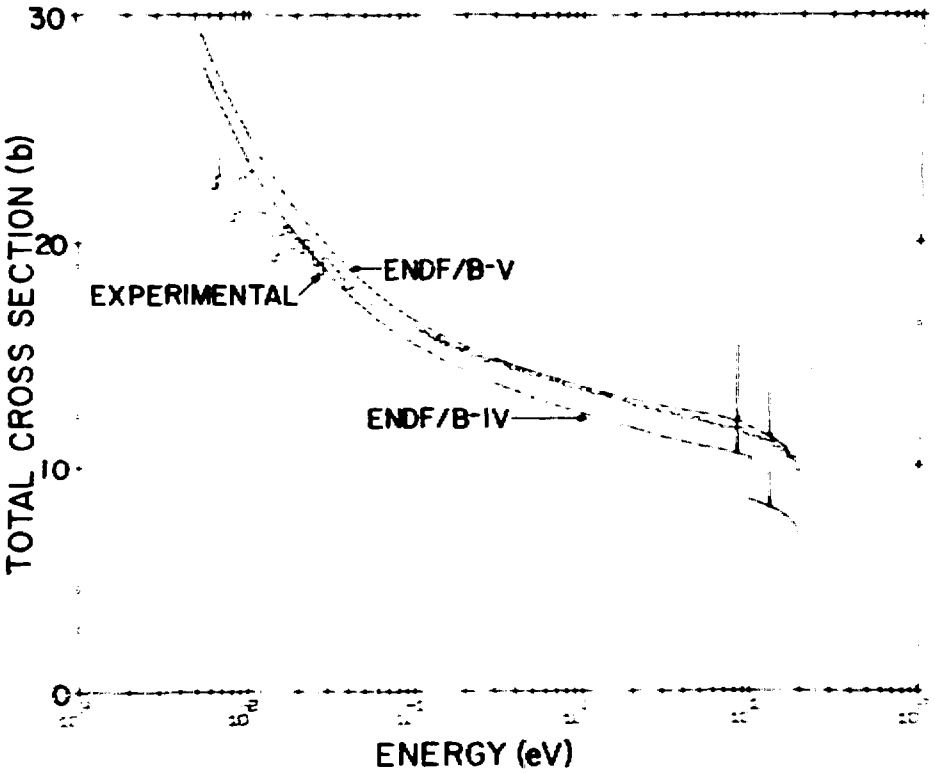

Fig. 1 The ^{232}Th measured neutron total cross section [1] compared with ENDF/B-IV and ENDF/B-V.

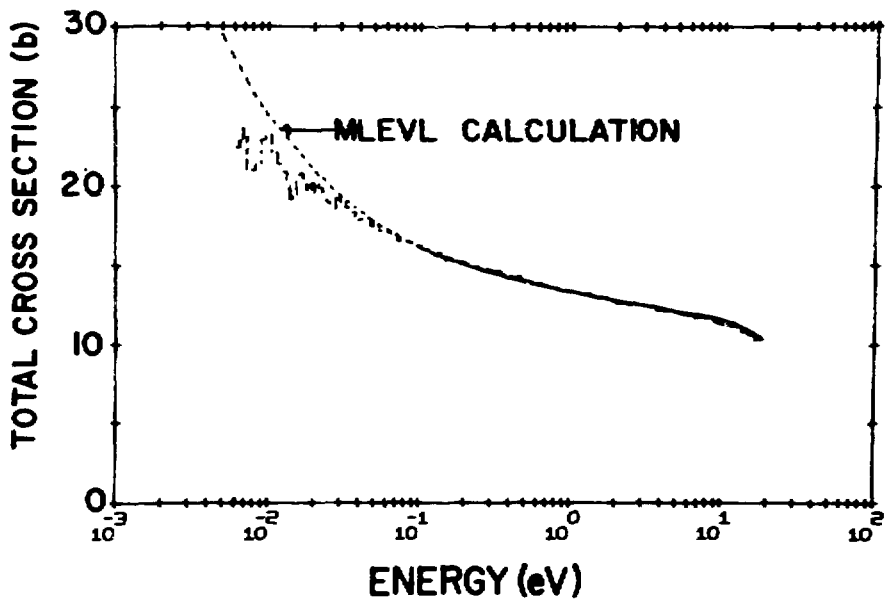

Fig. 2 The ^{232}Th measured neutron cross section fitted by the multilevel program MLEVL [1].

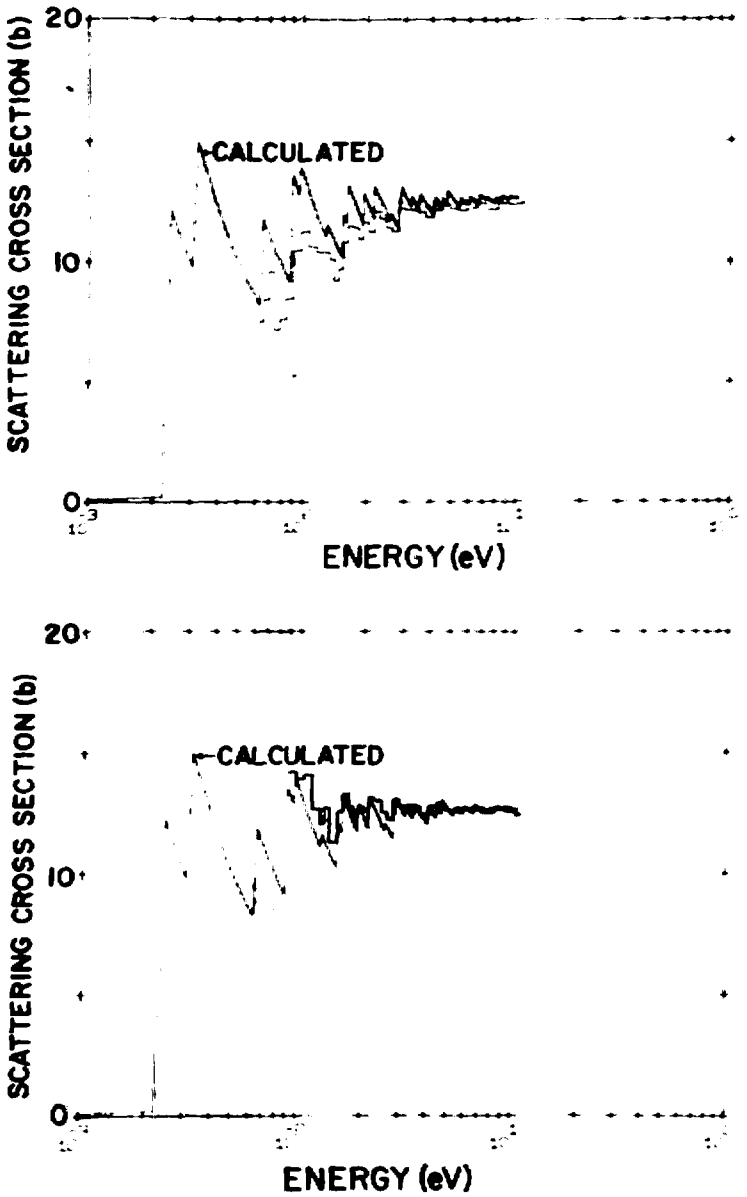

Fig. 3 The calculated scattering cross section, including Bragg Scattering, compared to (a) the measured total cross section minus a 1/v capture cross section (upper figure), and (b) the measured total cross section minus the measured capture cross section (lower figure) [1].

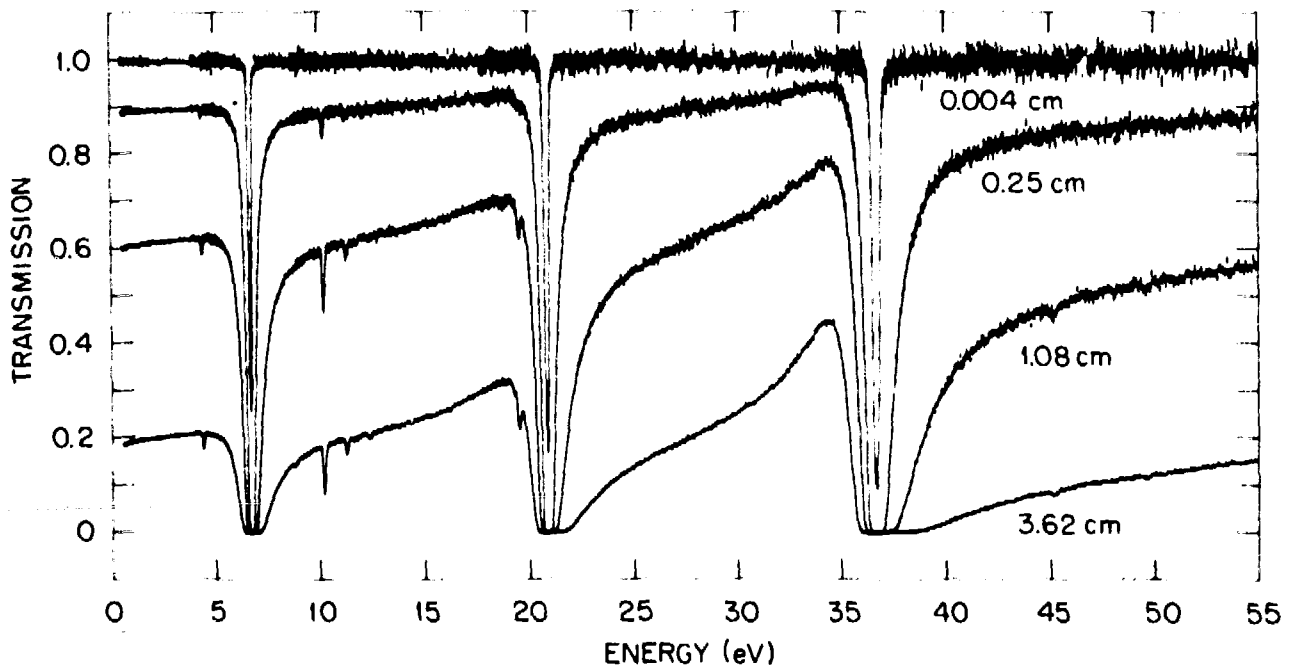

Fig. 4 Simultaneous least-squares fit to neutron transmissions from 0.52 to 55.0 eV through seven samples of ^{238}U. For clarity, only the fit to the 0.0036-, 0.254, 1.08- and 3.62-cm-thick samples is shown [7].

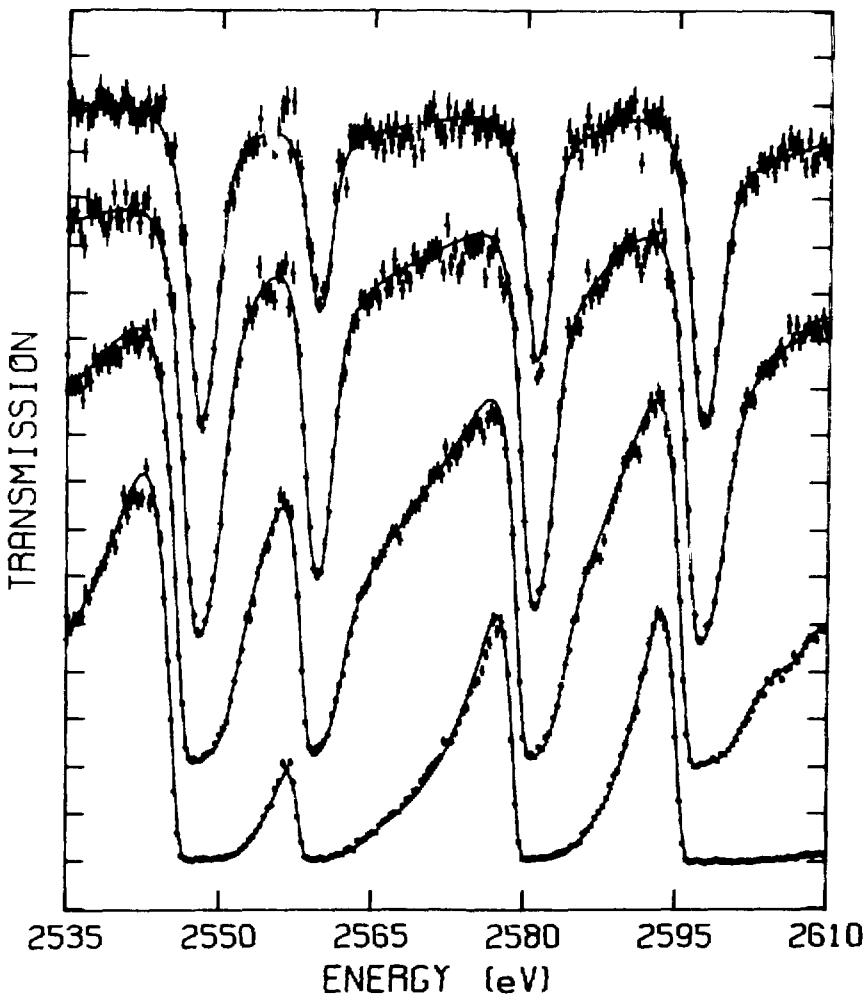

Fig. 5 Least-squares fit to (from top to bottom) 0.076-, 0.254-, 1.080- and 3.620-cm-thick ^{238}U sample transmissions from a four-sample simultaneous search in the energy region from 2469 to 2731 eV [8].

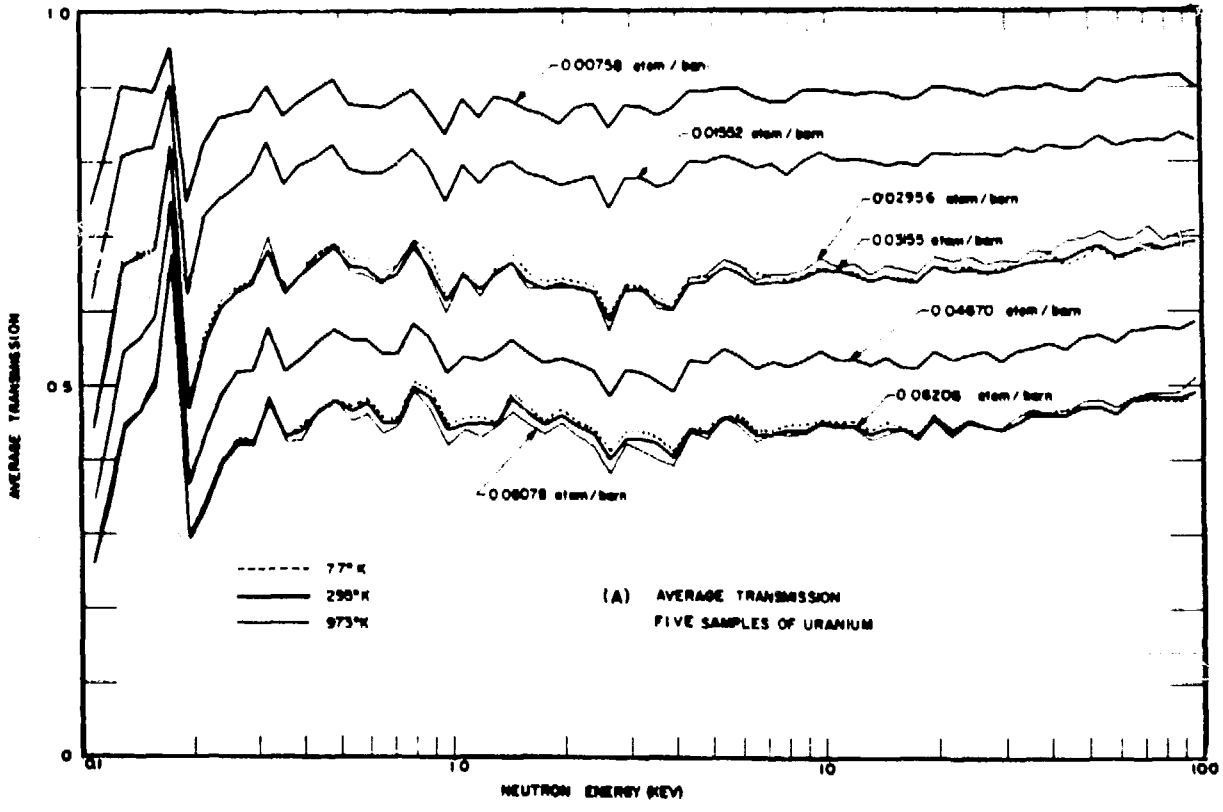

Fig. 6 The transmission of depleted uranium for different sample thicknesses and temperature [10].

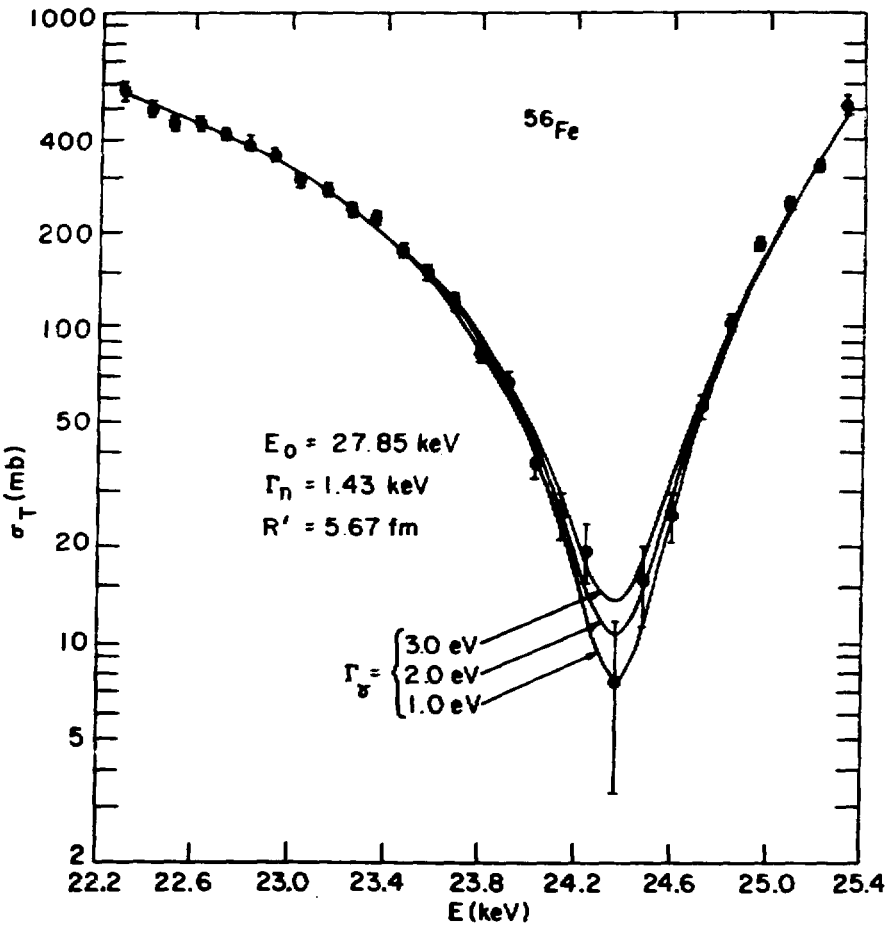

Fig. 7 The measured total cross section of ^{56}Fe near the 24.37-keV minimum region. The curves show the best fits for three different radiation widths using the reduced R-matrix theory. The measured minimum value of the cross section is 7.5 ± 4.2 mb [18].

Discussion

Mughabghab

I would like to point out that Bhat and Chrien (Phys. Rev. 155, 362, 1967) were aware of the problem of the tail of the resolution functions which was explicitly considered in the analysis of the resonance parameters of ^{232}Th.

Moore

You mentioned the importance of correlations of the neutron and radiation widths. This is a well known phenomenon; for example, in the ENDF/B-V resonance parameters of ^{238}U. Do you feel that this correlation is due to problems in the measurements or analysis, or is it in the physics?

Block

I was quoting the work of Olsen et al. (Nucl. Sci. and Eng. 62, 479, 1977) where they observe correlations in their fit to the potential scattering radius, a, and the Γ_n and Γ_γ of the first three s-wave levels of ^{238}U. This comes from their correlation matrix so I would say that this is the result of the analysis.

Lone

The structure observed in the subthermal region (which is due to Bragg scattering) depends crucially on the sample configuration and temperature. Also this structure is pronounced in measurements with well collimated directional neutron beams. In an isotropic or wide angle geometries the structure will not be the same. Under these circumstances, the observed cross section (transmission) will not be a representative of element cross section but rather relevant to that particular sample and environmental conditions. How can one take this into account in evaluations?

Block

I agree with what you say. In low energy transmission measurements there is an uncertainty which is due to a lack of knowledge of the structure of your sample.

SESSION VIII

UNRESOLVED RESONANCE REGION
Chairman: S.F. Mughabghab BNL

NEUTRON STRENGTH FUNCTIONS: THE LINK BETWEEN RESOLVED RESONANCES AND THE OPTICAL MODEL*

P. A. Moldauer

Applied Physics Division
Argonne National Laboratory
Argonne, Illinois 60439, U.S.A.

ABSTRACT

Neutron strength functions and scattering radii are useful as energy and channel radius independent parameters that characterize neutron scattering resonances and provide a connection between R-matrix resonance analysis and the optical model. The choice of R-matrix channel radii is discussed, as are limitations on the accuracies of strength functions. New definitions of the p-wave strength function and scattering radius are proposed. For light nuclei, where strength functions display optical model energy variations over the resolved resonances, a doubly reduced partial neutron width is introduced for more meaningful statistical analyses of widths. The systematic behavior of strength functions and scattering radii is discussed.

*This work performed under the auspices of the U.S. Department of Energy.

The neutron strength function provides a link between resonance scattering data and the optical model. Its usefulness in helping to determine optical potential parameters arises from the fact that a detailed analysis of resonance scattering resonances can provide separate determinations of the real and imaginary parts of the optical model s-wave scattering amplitude r_0 and the imaginary parts of the p-wave amplitudes $r_{1,1/2}$, $r_{1,3/2}$. These are four independent parameters describing the single parameter, a weighted sum of the real parts of the r_{lj}, which an average total cross section measurement over a sufficient energy interval determines. And if, in addition, d-wave resonances, or a p-wave background scattering phase shift can also be measured, the number of measurements exceeds the unknowns by one greater. For this reason, strength functions have played an important role in determining optical potentials from the inception of the model to the present [1-3]. Beyond this they have been applied to more detailed discussions of nuclear dynamics, such as intermediate structure, [4-9] and are useful for the construction of statistical resonance models of the optical potential.

There are also some disadvantages to the use of resonance parameters for the determination optical potential parameters. While average total cross sections can be measured over practically unlimited energy ranges with very high accuracies, resonance parameters can be determined only within a limited neutron energy interval that contains a limited number of resonances. Since strength functions are averages over resonance partial widths and since partial widths fluctuate according to the Porter-Thomas distribution [10] which has a root mean standard deviation of $\sqrt{2}$ relative to its average, the standard deviation of the average of a sample of N partial widths is $\sqrt{2/(N-1)}$ of its value. Therefore, a strength function derived from only 5 resonances has a 45% probable error, in addition to experimental uncertainties, and even 50 resonances can determine a strength function to within no better than 20%. In addition to this basic statistical error in strength function determination, there are also problems associated with energy and channel radius dependences of these parameters, which we shall discuss presently. Small energy variations may be large within the energy range of analyzable resonances, particularly in the case of lighter nuclei. Energy dependent strength functions may be useful in analyzing resonance widths for more reliable statistical analyses and intermediate structure determinations. I shall return to this point later also.

The only practical and generally applicable method for analyzing resonance data is the R-matrix method [11,12]. Such an analysis yields for each partial wave ℓj a set of resonance energies $E_\mu^{J(\ell j)}$ and a corresponding set of reduced amplitudes $\gamma_\mu^{\ell j}$. These R-matrix resonance parameters are theoretical constructs which have no directly measurable physical significance and their values depend on the more or less arbitrary choices of

channel radii $a_{c,j}$ and boundary conditions $B_{c,j}$. For resonance analysis purposes the most convenient choice of $B_{c,j}$ are those values which will cancel the channel shift functions at zero neutron energy and I will use that choice throughout.

When the R-matrix is calculated by solving the Schrödinger equation with a nuclear interaction Hamiltonian as was done for example by Takeuchi and Moldauer [13], it is essential that all channel radii be chosen, so as to be greater than the range of the nuclear interaction between the neutron and the target nucleus. However we are dealing here with an empirical R-matrix whose only function is to parameterize the resonances. Therefore we need not be concerned about such a restriction on channel radii and may choose the $a_{c,j}$ to be near the half falloff radius of the optical potential. That this is satisfactory is demonstrated in Fig. 1 where it is shown that the s and p wave strength functions and the R' parameter calculated for ^{58}Ni from an optical potential with half fall radius at 4.7 fm are all independent of channel radii for $a_{c,j}$ between 2 and 7 fm. Theoretically the use of small $a_{c,j}$ is justified by imagining that there exists some Hamiltonian whose interaction is confined within the $a_{c,j}$ and which yields exactly the E_μ and $\gamma_{\mu c}^2$ which lie within the analyzed energy interval. Since this is a finite number of parameters we should be able to construct the required equivalent Hamiltonian. The advantage of using channel radii of optical potential range is that this reduces the energy dependences of the strength functions and avoids the introduction of spurious optical model peaks, as demonstrated in Fig. 2. It would perhaps be useful to establish a standard channel radius for R-matrix fitting of resonance data. The standard adopted in the calculations reported here is $a = 1.25A^{1/3} + 0.5$ fm for all channels.

A single channel R-function resonance analysis of a total or elastic neutron cross section is obtained by fitting the measured cross section to the appropriate following formula

$$\sigma = \sum_{J,\pi,\ell,j} \frac{(2J+1)}{2(2I+1)} \sigma_{J,\pi,\ell,j} \quad , \tag{1}$$

$$\sigma^{\text{total}}_{J,\pi,\ell,j} = \frac{2\pi}{k^2} \left(1 - \text{Re}\, U_{J,\pi,\ell,j}\right) \quad , \tag{2}$$

$$\sigma^{\text{elastic}}_{J,\pi,\ell,j} = \frac{\pi}{k^2} \left|1 - U_{J,\pi,\ell,j}\right|^2 \quad , \tag{3}$$

where

$$U_{J,\pi,\ell,j} = e^{-2i\chi_{\ell j}} \frac{1 - L^{*}_{\ell j} R_{J,\pi,\ell,j}}{1 - L_{\ell j} R_{J,\pi,\ell,j}} \quad , \tag{4}$$

$$R_{J,\pi,\ell,j} = R^{\infty}_{J,\pi,\ell,j} + \frac{(\gamma^{J,\pi,\ell,j}_{\mu})^2}{E^{J,\pi}_{\mu} - E} \quad , \tag{5}$$

and for s and p waves and for our choice of boundary conditions

$$\chi_0 = \rho_0 \qquad L_0 = i\rho_0$$
$$\chi_{1j} = \rho_{1j} - \tan^{-1}\rho_{1j} \qquad L_{1j} = \frac{\rho_{1j}^2}{1 + \rho_{1j}^2}(1 + i\rho_{1j}) \tag{6}$$

where $\rho_{\ell j} = ka_{\ell j}$ and k is the channel wave number and $a_{\ell j}$ is the arbitrarily chosen channel radius. The object of such a fit is to obtain the background R-functions R^{∞}, the R-matrix poles E_{μ} and the pole channel amplitudes γ_{μ}. Where appropriate these formulas must be generalized to multichannel R-matrix formulas, but the final set of resonance parameters is of the same type.

At low enough energies $R_{1j} \times \mathrm{Re}L_{1j}$ is small enough compared to unity so that $\mathrm{Re}L_{1j}$ can be ignored. However, this is not always true for the whole range of analyzable resonances in lighter nuclei as is demonstrated in Fig. 3.

The connection between the R-matrix resonance parameters and the optical model amplitudes $\eta_{\ell j}$ is given by

$$\eta_{\ell j} = e^{-2i\chi_{\ell j}} \frac{1 - L^{*}_{\ell j} \tilde{R}_{\ell j}}{1 - L_{\ell j} \tilde{R}_{\ell j}} \tag{7}$$

where

$$\tilde{R}_{\ell j} = R^{\infty}_{\ell j} + i\pi s_{\ell j} \tag{8}$$

$$s_{\ell j} = \frac{(2j+1)}{2} \sum_{J} \frac{\langle (\gamma^{J,\pi,\ell,j}_{\mu})^2 \rangle}{D_{J,\pi,(\ell,j)}} \tag{9}$$

where $\langle\ \rangle$ indicates an average over resonance μ and D_J is the mean spacing of R-function poles E_{μ} of appropriate total angular momentum and parity. The coefficient and sum in Eq. (9) is

required when the optical model is independent of target spin I and total angular momentum J, as is assumed here. The same sum and coefficient defines $R^{\infty}_{\ell j}$ in terms of the $R^{\infty}_{J,\pi,\ell,j}$. The optical model η's are obtained from an integration of the Schrödinger equation with the optical potential interaction as is performed in all optical model computer programs.

Equations (7)-(9) define the background R-functions R^{∞} and the R-strength functions s in terms of the complex optical model scattering amplitudes η and the channel parameters λ and L. R^{∞} and s vary slowly with energy as a result of the optical model giant resonance energy variation. But these parameters depend strongly upon the choice of channel radius by virtue of the channel radius dependences of λ and L. To obtain a useful parameter independent of arbitrary radii, it is necessary to remove this channel radius dependence, without at the same time introducing the strong kinematical energy dependences of partial neutron widths. This is the purpose of the strength function definitions which are given below.

Solving Eq. (7) for $s_{\ell j}$ we get for low neutron energies

$$4\pi\, P_{\ell j}\, s_{\ell j} = T_{\ell j} \quad , \tag{10}$$

where $P_{\ell j} = \mathrm{Im}\, L_{\ell j}$ and the transmission coefficient

$$T_{\ell j} = 1 - |\eta_{\ell j}|^2 \quad . \tag{11}$$

At these low neutron energies the transmission coefficients can be related to the characteristics of cross section resonances by

$$T_{\ell j} = 2\pi\, \bar{\Gamma}_{\ell j}/D \quad , \tag{12}$$

where $\bar{\Gamma}_{\ell j}$ is the average partial neutron resonance width and D the resonance spacing. In contrast to the R-function parameters, these are real physical quantities that can be measured and that are independent of any channel radius. Moreover, their kinematical energy dependencies at low neutron energy are known. In particular $\bar{\Gamma}_{\ell j}/D$ behaves there as $E^{(\ell + 1/2)}$. Therefore the desired channel radius and energy independent definition of the strength function is obtained by dividing the left hand side of Eq. (10) by $E^{(\ell + 1/2)}$.

$$S_{\ell j} = \frac{2}{2\ell + 1} \frac{P_{\ell j}}{E^{\ell + 1/2}}\, s_{\ell j} \quad , \tag{13}$$

which includes a traditional factor of $(2\ell + 1)^{-1}$, and where, again by tradition, E is measured in electron volts. Equations (10), (12), (13) yield the traditional definition of the S-wave neutron strength function

$$S_0 = \frac{1}{\sqrt{E}} \frac{\bar{\Gamma}_o}{D} \quad . \tag{14}$$

For p-waves, we obtain by the same method

$$S_{lj} = \frac{2j+1}{3E^{3/2}} \frac{\bar{\Gamma}_{lj}}{D} \quad . \tag{15}$$

In contrast, the traditional formulation of the p-wave strength function

$$S_{lj}^{\text{traditional}} = \frac{2j+1}{3\sqrt{E}} \frac{1+(ka)^2}{(ka)^2} \frac{\bar{\Gamma}_{lj}}{D} = \frac{2}{3} \frac{ka}{\sqrt{E}} s_{lj} \tag{16}$$

does have the desired energy independence at low energies, but it also has a very strong and undesirable channel radius dependence which is demonstrated in Fig. 1. Therefore, to be interpretable, any value of $S_l^{\text{traditional}}$ must be supplemented by a channel radius value. In contrast the definition (15) of S_l is radius and energy independent up to energies where the value of $(ak)^2$ becomes appreciable compared to unity, that is, typically up to some tens of kilovolts. Above such energies other kinematical as well as dynamical effects such as optical model variability start coming into play, in any case. "I would therefore recommend that Eq. (15) be adopted as the definition of the p-wave strength function."

If E is measured in electron volts, then S_o is of order 10^{-4} and S_{lj} of Eq. (15) is of order 10^2.

In addition to the strength function, the background R-function R^∞ provides another channel parameter that can be connected with the optical model. Solving Eq. (7) for the s-wave R_o^∞, we obtain in the low energy limit the following connection with η_o, via the background scattering radius R'.

$$-\frac{\arg(\eta_o)}{2k} \equiv R' = a_o(1-R_o^\infty) \tag{17}$$

where the defining relationship is on the left and the connection with resonance analysis is on the right. R' is again an energy and radius independent parameter at low energies.

If we do the same for p-waves, we obtain the relation

$$R'_{lj} = \frac{P_{lj}}{k} \left(\frac{1}{3} - R^\infty_{lj}\right) \tag{18}$$

for the p-wave background scattering radii. These quantities are again independent of the channel radii a_{lj}, but they are obviously proportional to the neutron energy E at low energies. In order to obtain energy and radius independent p-wave potential scattering radii we must define the reduced p-wave scattering radii

$$R'^{o}_{lj} = R'_{lj}/E \quad , \tag{19}$$

which yield numbers in the vicinity of unity when E is measured in MeV. It should be noted that R'^{o}_{lj} may assume negative values in the vicinity of a p-wave strength function peak, as seen in Fig. 4. P-wave potential scattering radii have recently been measured [14].

In the lighter nuclei, A < 50, resonance cross sections can often be measured and analyzed by R-matrix parameters within energy regions where any or all of the corresponding strength functions $S_{\ell j}$ or $R'^{o}_{\ell j}$ display appreciable energy or radius dependences that cannot be removed. They are caused in part by the breakdown of low energy approximations and in part by optical model giant resonance effects. Moreover, the resonance spacings may be so large that no useful averages can be obtained within subintervals of small energy variability. In such circumstances it is useful to recognize these energy variabilities and build them explicitly into the definitions. For this purpose it is useful to consider a doubly reduced partial width parameter $\Gamma^{oo}_{\mu\ell j}$ from which both the kinematic channel energy dependence and the dynamical optical model energy dependence has been factored out:

$$\Gamma^{oo}_{\mu\ell j} = \frac{\Gamma_{\mu\ell j}\, S_{\ell j}(1\text{ eV})}{E_\mu^{\ell+1/2}\, S_{\ell j}(E_\mu)} \quad , \tag{20}$$

Alternately one could use reduced R-matrix amplitudes $\gamma^{\ell jo}_{\mu} = \gamma^{\ell j}_{\mu}\sqrt{s_{\ell j}(1\text{ eV})/s_{\ell j}(E_\mu)}$. Here $S_{\ell j}(E_\mu)$ or $s_{\ell j}(E_\mu)$ is determined by the optical potential and the latter can be adjusted in order to satisfy

$$\frac{2j+1}{2\ell+1}\,\frac{\bar{\Gamma}^{oo}_{\mu\ell j}}{D} = S_{\ell j}(1\text{ eV}) \quad . \tag{21}$$

This provides a systematic method of optical model fitting of resonance data in lighter nuclei.

In addition, the doubly reduced widths are convenient for statistical analyses in lighter nuclei. The $\Gamma^{oo}_{\mu\ell j}$ should be distributed according to the Porter-Thomas distribution, while the distributions of singly reduced widths $\Gamma^{o}_{\mu\ell j} = \Gamma_{\mu\ell j}/E_\mu^{\ell+1/2}$ may be distorted by optical model effects. Also the cumulative values

of doubly reduced widths $\Sigma_{E_\mu<E} \Gamma^{oo}_{\mu \ell j}$ give a more reliable indication of intermediate structure than do the customary stairway plots of unreduced or singly reduced widths. A case in point is the recent analysis of γ^2_μ for s and p-wave neutron resonances in ^{29}Si by Newson et al. [6], over a neutron energy range of up to 4.5 MeV. As indicated in Fig. 2, there is much optical model variation in the R-strength functions over this energy range. Moreover, this variation depends strongly upon the choice of channel radii. Thus the rapid rise in the s-wave strength above 3 MeV in Ref. (6) could possibly arise from the rapid rise of the s-wave R-strength function in the same region as shown in Fig. 2B. Similarly the apparent peak in the p-wave strength in Ref. [6] seems to be correlated with the optical model peak in the p1/2 strength in Fig. 2B. The appearance of spurious channel radius dependent peaks can be avoided by first obtaining an optical model fit to the resonance and other data as indicated in Eq. (21), and then constructing stairway plots with the doubly reduced widths of Eq. (20). Energy variations in the latter can then be interpreted as true intermediate resonances.

Finally, Fig. 4 displays the mass number dependence of the s and p-wave strength functions and (reduced) background scattering radii, as defined here, and as calculated from the overall optical potential of Ref. [2] with a fixed spin orbit potential of 7 MeV.

AFTERTHOUGHT: An alternative to the definition (13) might be the following

$$S'_{\ell j} = \frac{2}{2\ell+1} \frac{(ka)^{2\ell+1}}{E^{\ell+1/2}} s_{\ell j} \quad . \tag{13'}$$

This removes some of the kinematical energy dependence from the strength function at the expense of introducing an explicit channel radius dependence. The result of the definition (13') would be to introduce an additional factor of $1+(ka)^2$ into the definition (15) of the p-wave strength function. For the case of ^{28}Si, $S'_{1,1/2}$ and $S'_{1,3/2}$ are shown dotted in Fig. 2a.

REFERENCES

1. H. FESHBACH, C. E. PORTER and V. F. WEISSKOPF, Phys. Rev., 96, 448 (1954).

2. P. A. MOLDAUER, Nucl. Phys., 47, 65 (1963).

3. J. P. DELAROCHE, CH. LAGRANGE, J. SALVY, IAEA-190, VOL 1, p. 251 (1976).

4. B. BLOCK and H. FESHBACH, Ann. Phys., N.Y. 23, 47 (1963).

5. M. DIVADEENAM, W. P. BERES and H. W. NEWSON, Ann. Phys., N.Y., 69, 428 (1972); J. G. MALAN, W. F. E. PINEO, M. DIVADEENAM, B. H. CHOI, E. G. BILPUCH AND H. W. NEWSON, ibid. 89, 284 (1975), M. DIVADEENAM, W. P. BERES and H. W. NEWSON, ibid. 80, 231 (1973).

6. H. W. NEWSON, W. F. E. PINEO, B. H. CHOI, J. M. CLEMENT and M. DIVADEENAM, Ann. Phys., 103, 121 (1977).

7. H. I. LIOU, J. RAINWATER, G. HACKEN and U. N. SINGH, Phys. Rev. C, 12, 102 (1975).

8. H. S. CAMARDA, Phys. Rev. C, 16, 1803 (1977); ibid. 18, 1254 (1978).

9. D. J. HOREN, J. A. HARVEY and N. W. HILL, Phys. Rev. C, 20, 478 (1979).

10. C. E. PORTER and R. G. THOMAS, Phys. Rev., 104, 483 (1956).

11. E. P. WIGNER and L. EISENBUD, Phys. Rev., 72, 29 (1947).

12. A. M. LANE and R. G. THOMAS, Rev. Mod. Phys., 30, 257 (1958).

13. K. TAKEUCHI and P. A. MOLDAUER, Phys. Rev. C, 2, 925 (1970).

14. C. H. JOHNSON and R. R. WINTERS, Phys. Rev. C, 21, 2190 (1980).

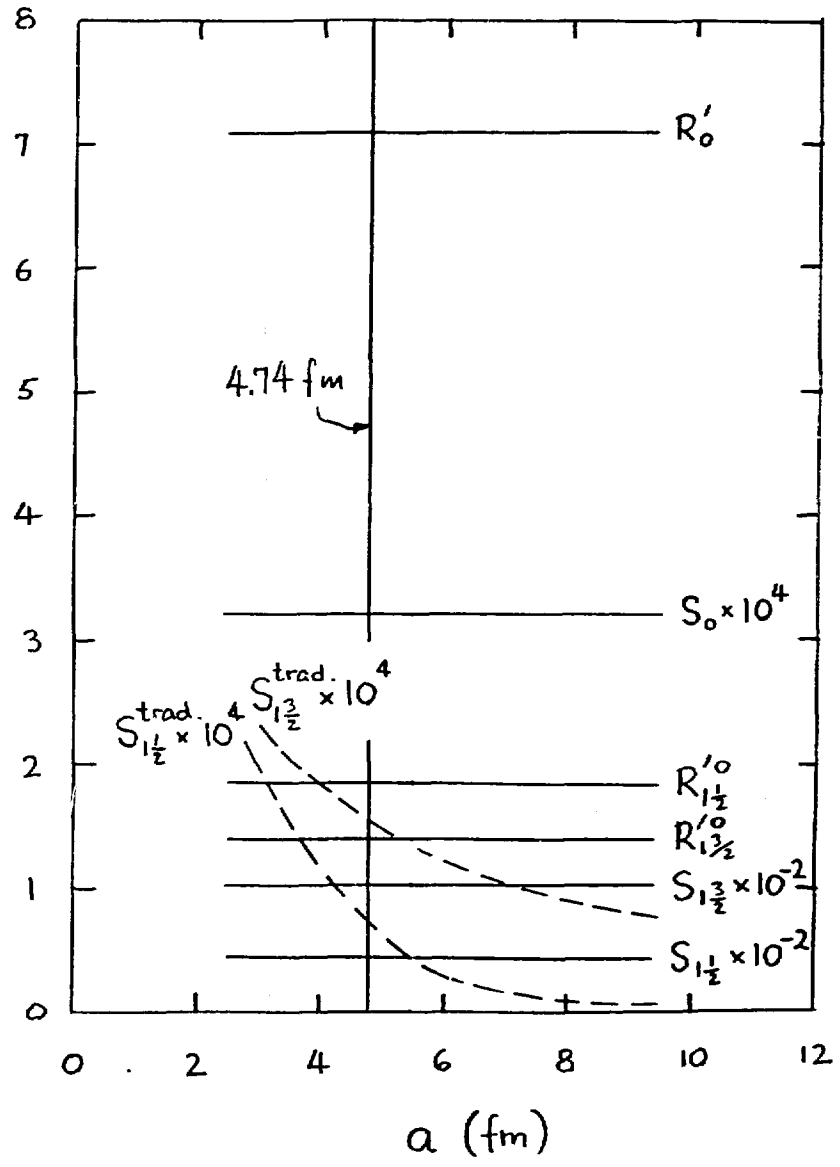

Fig. 1. Channel radius dependences of s and p-wave strength functions and (reduced) channel radii, Eqs. (14), (15), (17), (19), as well as traditional p-wave strength functions, Eq. (16), dashed lines, for an optical potential (^{60}Ni) with half falloff radius of 4.74 fm. (V = 53.1-0.3E, W = 7.9 + 0.25E, VSO = 8.0 MeV; R = $1.2A^{1/3}$, A = 0.6 fm).

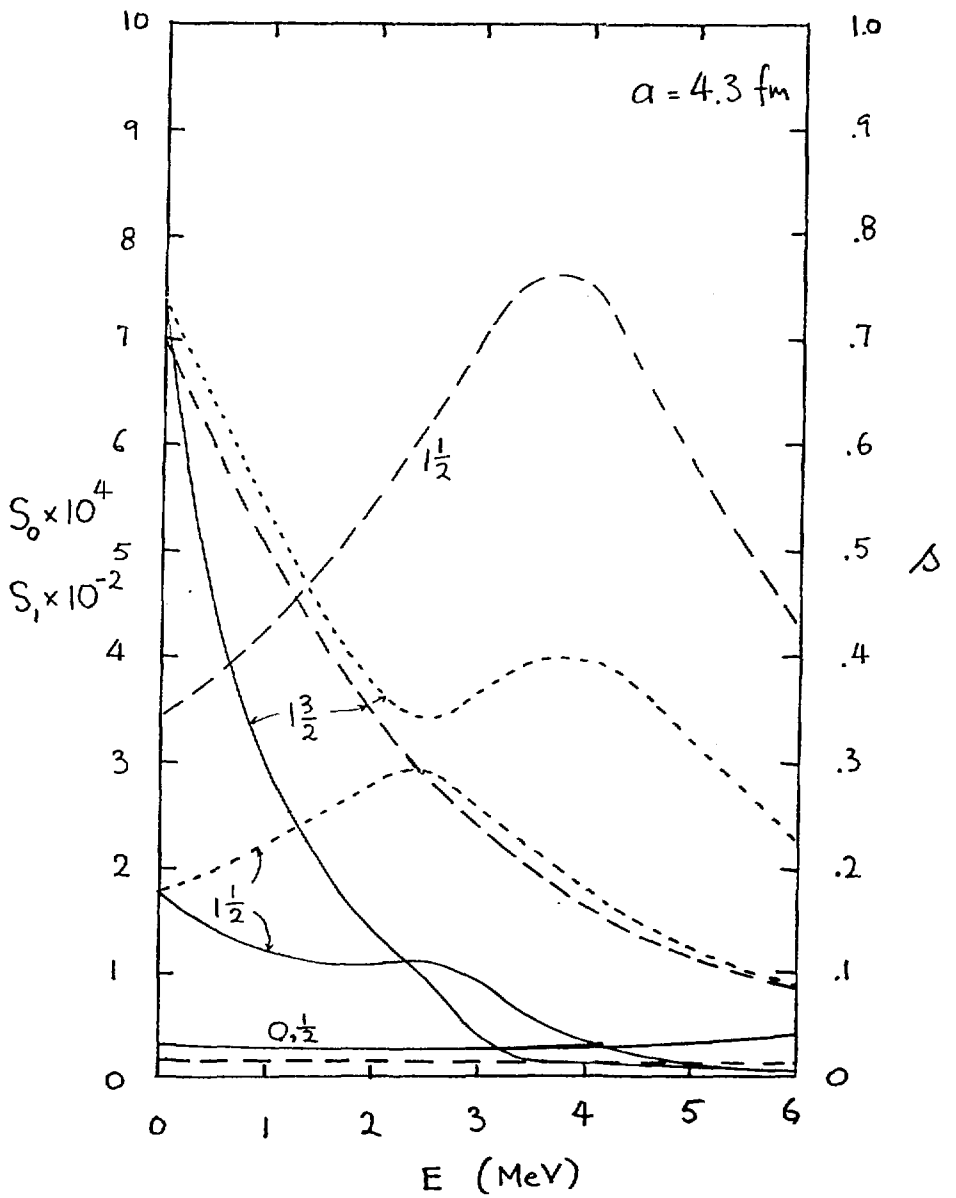

Fig. 2A. Energy dependences of s and p-wave R-strength functions Eq. (9), dashed lines, strength functions Eq. (13), full lines, and S_1, dotted lines, for a ^{28}Si optical model (V = 53.8, W = 3.0, VSO = 7.0 MeV; R = $1.21A^{1/3}$, A_V = 0.66, A_W = 0.48 fm) Channel radii a = 4.3 fm.

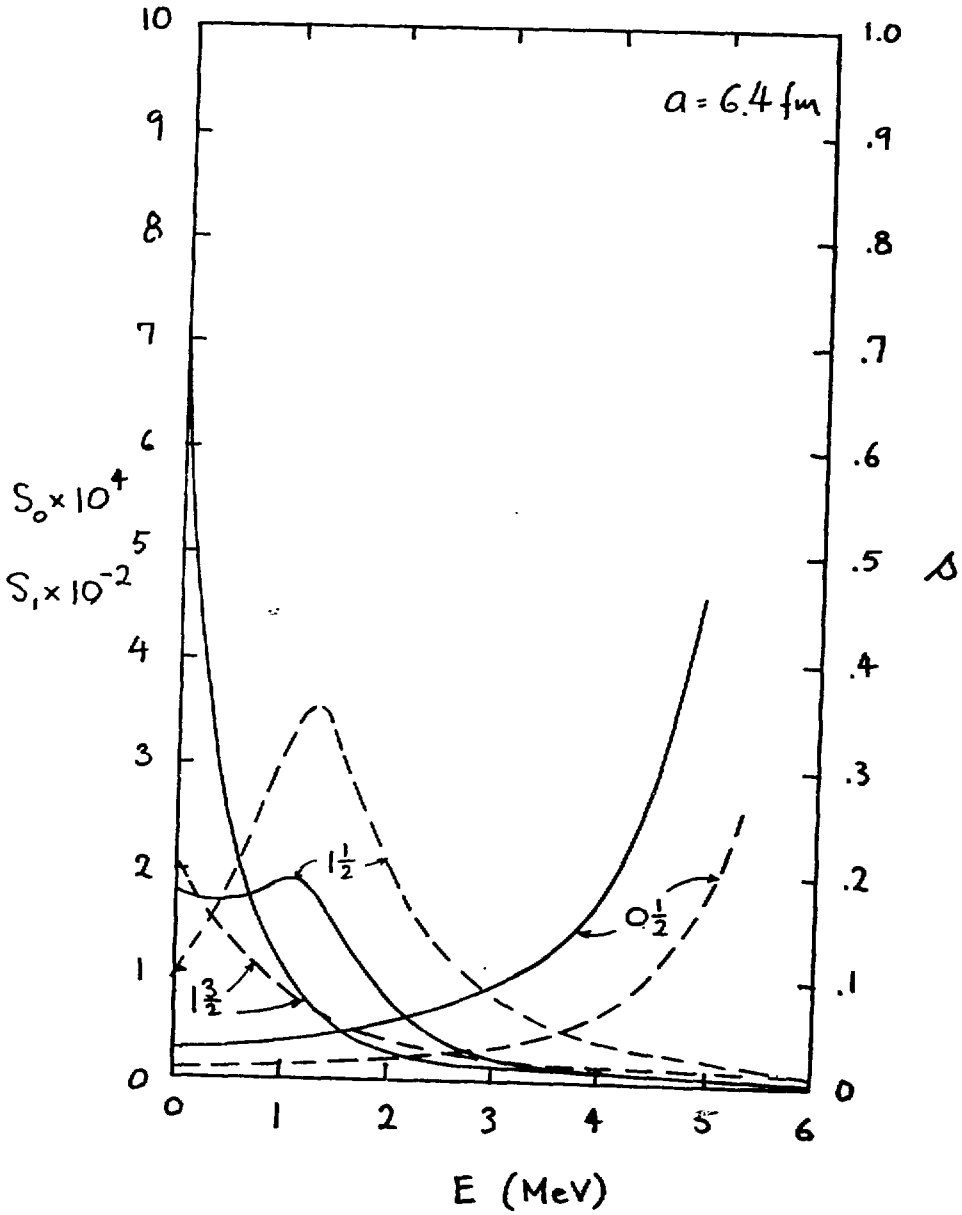

Fig. 2B. Same as 2A with a = 6.4 fm.

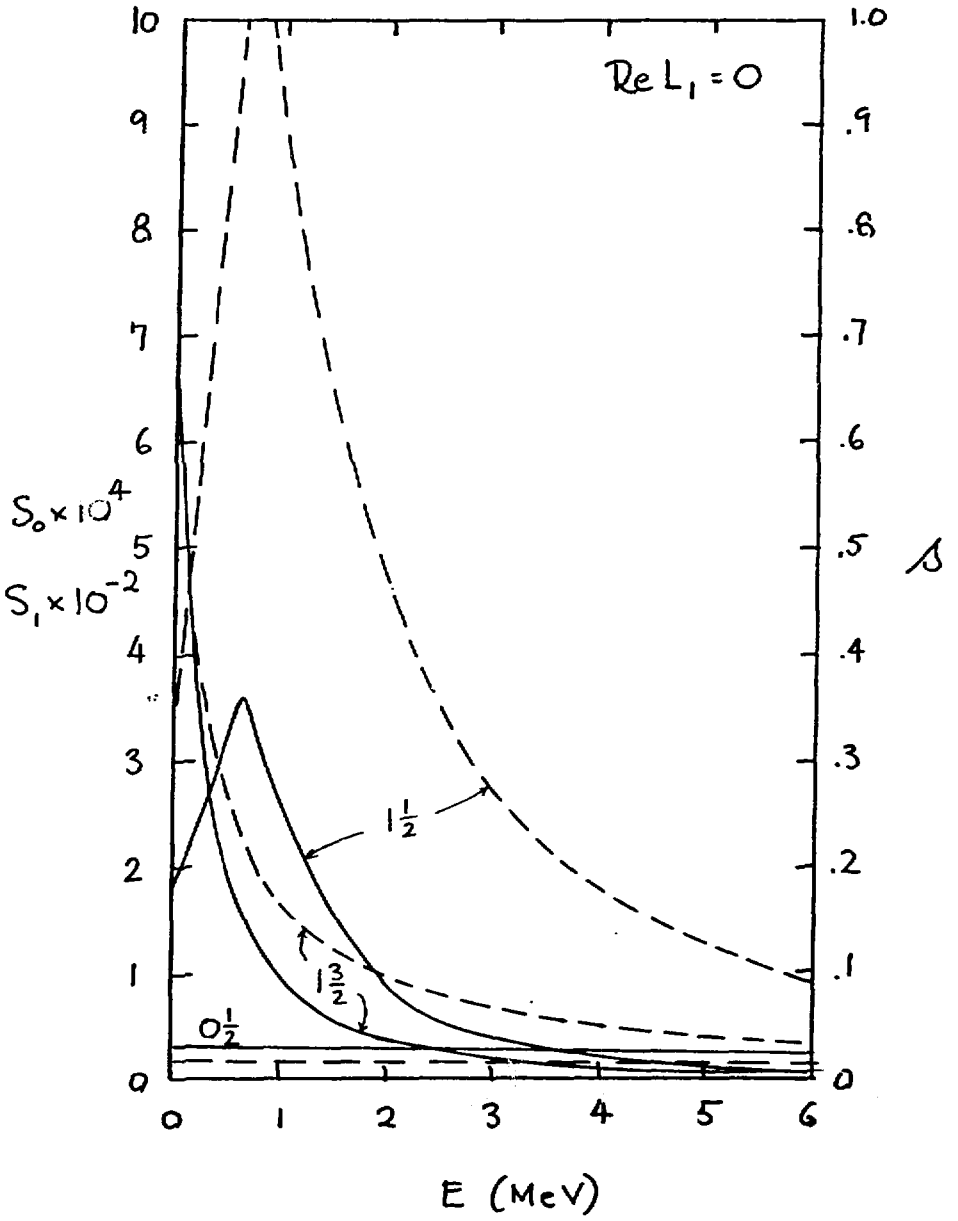

Fig. 2C. Same as 2A, but ignoring p-wave level shift factor ReL_{1j} in Eq. (7).

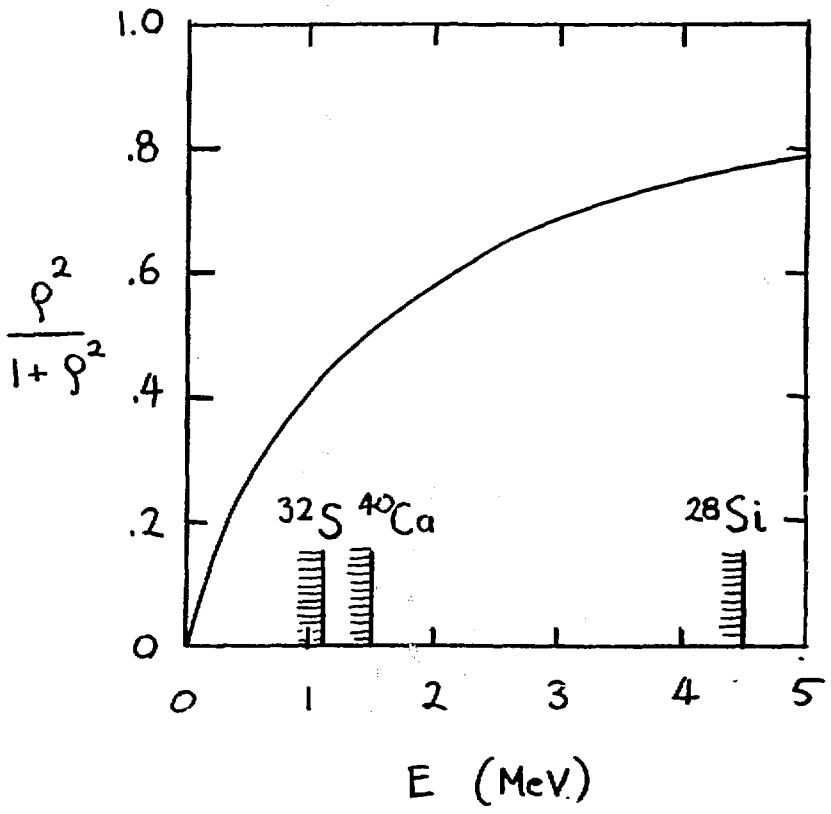

Fig. 3. Energy dependence of p-wave level shift factor ReL_{lj} for light nuclei compared to the limits of analyzable resolved p-wave resonances in ^{32}S, ^{40}Ca, and ^{28}Si.

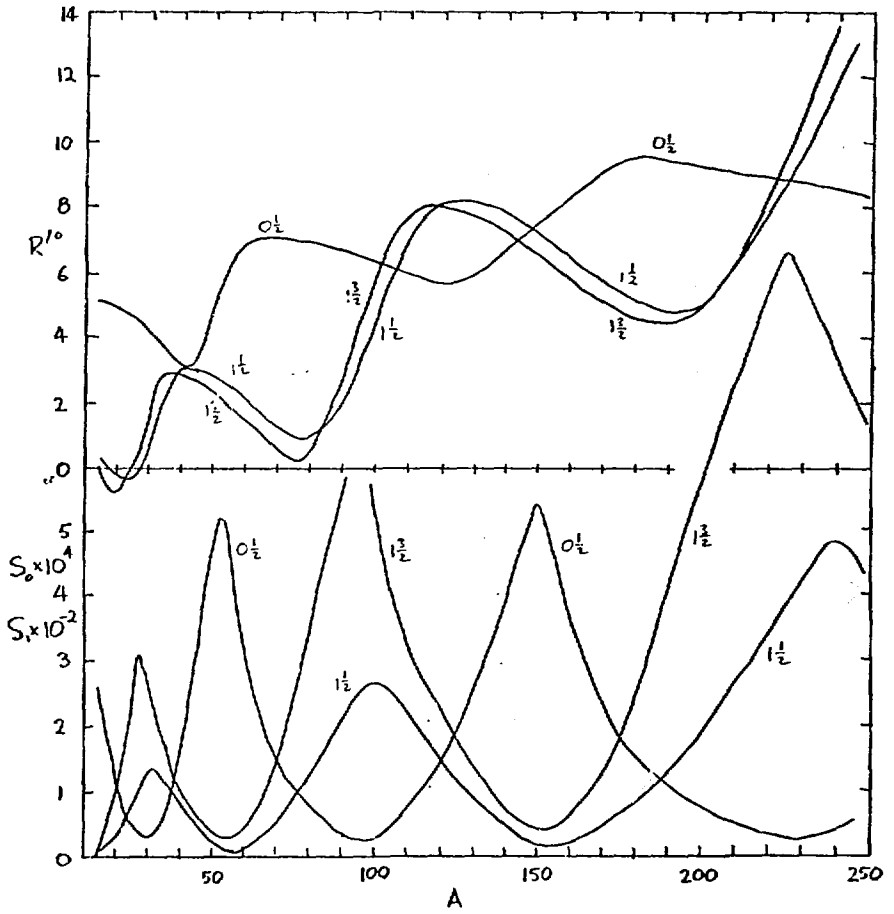

Fig. 4. Systematic mass number dependences of s and p-wave strength functions and (reduced) channel radii for an optical model with V = 46.0, W = 14.0, VSO = 7.0 MeV; $R_V = 1.37A^{1/3}$, $R_W = 1.447A^{1/3}$, $A_V = 0.62$, $A_W = 0.25$ fm.

Discussion

Froehner

I can see that taking the R-matrix channel radius inside the range of the nuclear interaction you can still establish a system of internal eigenfunctions and eigenvalues. But then the external wave functions are distorted near the channel radius. In the case of neutral incident particles, they are no longer Hankel functions from which we calculate our familiar hard sphere phase shifts and penetration factos. What are these latter now?

Moldauer

They are still Hankel functions because the equivalent Hamiltonian has no nuclear interaction of range greater than the chosen channel radius. This equivalent Hamiltonian is not required to describe or perscribe the optical potential.

Lagrange

Have you made calculations of the energy dependence of the strength functions for nuclei like niobium? From my optical model calculations of ^{93}Nb, I have observed a strong energy dependence of the p-wave strength functions.

Moldauer

Yes, I have made calculations near A=90 and found no energy variation of the strength functions over the range of resolved resonances.

Lagrange

What do you think of the strength functions deduced from an analysis of the average total cross sections. We refer to the work carried out in the past by Dr. Uttley and co-workers.

Moldauer

The strength function is directly determined by the optical model. If the average total cross section specifies the optical model well, then it also specifies the strength functions.

SYSTEMATICS OF S-AND P-WAVE RADIATION WIDTHS*

M. S. Moore

University of California
Los Alamos Scientific Laboratory

ABSTRACT

The question of calculating differences in s-and p-wave radiation widths as a valid evaluation tool is explored. A purely statistical approach such as that provided by the Brink-Axel formula depends upon two factors: 1) an adequate description of the giant dipole resonance shape at energies well below the resonance, and 2) an adequate description of the level densities between the ground state and the excitation of the compound nucleus near the neutron separation energy. Some success has been obtained in certain regions of the periodic table with this simple approach, e.g., in the actinides where all nuclei exhibit similar rigid permanent deformations. However, if the method is to be used as a general evaluation procedure throughout the periodic table and particularly in regions where the radiative transition probabilities are enhanced by direct processes, it appears that much more nuclear structure information needs to be incorporated into the calculations.

I. INTRODUCTION

The bulk of the information on s-and p-wave neutron reaction rates comes from the detailed study of neutron resonances. The average cross sections for compound nucleus formation can be described in terms of neutron transmission coefficients or strength functions (width-to-spacing ratios), which are essentially independent of the variation of the level density from nucleus to nucleus. Reduced neutron widths, then, are proportional to the spacings of the levels, or inversely proportional to the level density.

*Work supported by the U. S. Department of Energy Radiative

Radiative capture, on the other hand, involves a ratio of level densities, such that the radiative width varies only weakly with the level density. The level density enters in first order in the relative reaction rates, leading to pronounced differences, for example, in average radiative capture cross sections of even-even and even-odd targets. The same effect is found in low energy neutron resonance analysis. If the radiative width is small compared to the neutron width, one can in principle determine the radiative capture width to high accuracy from an analysis of the total and radiative capture cross sections. If the radiative width is dominant (as in the case of low-energy p-wave neutron capture), neither the total nor the capture cross sections are very dependent on the radiative capture width, and the accuracy with which it can be determined from low-energy neutron resonance analysis is not high. In this connection, it appears that a maximum likelihood technique for determining radiative widths from resonance areas developed by Caner [1] should be recommended.

At low energies, the accuracy of the p-wave radiation width may not be very important, in that the cross-section sensitivity is low. As the energy increases and the resonances become less well resolved, the p-wave and higher-partial-wave neutron widths increase strongly, and the radiative capture cross section becomes more sensitive to the radiative widths for these higher partial waves. For infinitely dilute concentrations, possible differences in s- and p-wave radiation widths are probably unimportant, but for strongly self-shielded configurations, the calculated reaction rates reflect such differences.

The experimental evidence for differences in s- and p-wave radiation widths was carefully considered in the excellent review article by Allen and Musgrove [2] who find significant differences primarily in the vicinity of the neutron size resonances near closed shells. Allen and Musgrove assumed that in the vicinity of the 3p size resonance, the total p-wave radiative width could be expressed as a sum of a statistical width plus a residual width that they attribute to non-statistical single-particle and collective effects. They then estimate that the statistical width is the same size as the s-wave width, where no non-statistical effects are expected. (In the vicinity of the 3s resonance, it is the s-wave radiation width that is systematically enhanced, and they evaluate the residual non-statistical width by using the p-wave width as the statistical reference value.) They next calculate the valence neutron contribution, finding that in the 3s and 3p size resonances, valence transitions account for a sizeable fraction of the total width. For certain nuclei, e.g., ^{54}Fe and ^{88}Sr, they find that virtually all the

residual radiative strength can be accounted for by valence transitions. However, for most 4s nuclei, they calculate that the valence process can play only a minor role in the capture mechanism.

Allen and Musgrove also consider correlations: in the initial state (Γ_n:Γ_γ), among the final states (Γ_{γ_a}:Γ_{γ_b}) and with the (d,p) spectroscopic factors. They conclude that the evidence for correlations is significant, and that in the 4s and 4p region, where valence effects are small, these correlations suggest an additional non-statistical capture process. They attribute these to doorway states. Destruction of two-quasiparticle doorways leads to final state correlations, and if only one of these is important, initial state correlations are expected. Where the nuclei are strongly deformed, they suggest that particle-vibrator doorways (a single particle coupled to a quadrupole, or, for p-wave capture, to an octupole-excited core) may be important. In any case, the channels may be observable through intermediate structure.

II. ASSUMPTIONS IN THE CALCULATION OF SPECTRAL SHAPES AND LEVEL DENSITIES

The statistical theory of nuclear reactions is based on the assumption of reciprocity, i.e., the equal probability of compound nucleus formation and decay at equal transition energies in a given channel. For neutron inelastic scattering, this leads to the familiar Hauser-Feshbach formula; for radiative capture, it leads to the Brink hypothesis [3]. The Brink-Axel formula [4,5] contains the additional assumption that the energy dependence of the spectral shape for E1 transitions can be accurately described by the tail of the Lorentzian fit to the giant dipole resonance. For nuclei with permanent quadrupole deformations, one expects the spectral shape to be the superposition of two Lorentzians with different vibrational frequencies [6]. For spherical vibrational nuclei (whose ground-state equilibrium deformation is zero but whose root-mean-square deformation is non-zero) one expects a superposition of Lorentzians modulated by a Gaussian probability distribution: the Kerman-Quang approach [7]. For transitional nuclei where nuclear-shape coexistence is found to occur [8], one expects the spectral shape to depend on the nuclear structure of the final state. Detailed nuclear structure information is also required to evaluate the probability that there is significant clustering of residual E1 strength around the unperturbed particle-hole energies. It is not clear whether one ought to use a single particle (energy-independent) representation for M1 strengths, or

whether there is a giant M1 resonance underlying the E1, the ratio of strengths being 7 ± 1 [9]. The contribution of other multipole resonances is generally neglected. The description of the giant resonance as a Lorentzian is open to question, as is the validity of the Brink hypothesis where direct processes are known to be important. The current state of the art is summarized in a study recently carried out by Gardner et al., [10] who prefer an energy-dependent Breit-Wigner representation of the giant dipole resonance, showing that this new parameterization yields satisfactory results.

The other factor, of equal importance in the calculation of radiative capture, is the energy and spin dependence of the level density. Level densities are well determined experimentally at only two points: near the ground state, and near the neutron separation energy where one counts resolved resonances. Interpolation and extrapolation from the neutron separation energy are often done by thermodynamic methods that give simple analytic representations of the level density. Calculation of the spectrum of levels in a 3-dimensional box leads to the Fermi-gas model; correction for pairing and fitting to observed densities at the two energy points leads to the back-shifted Fermi gas description. The constant-temperature model affords a particularly simple expression. For simplicity, many of the level density expressions contain a constant spin cut-off parameter, and odd- and even-parity levels are assumed to be equally probable. It is perhaps surprising that the calculation of radiative capture widths can be done reasonably well with these simple prescriptions. Lynn, [11] for example, estimated that capture calculations can be made to about 25% accuracy for actinide nuclides. The next step requires the use of combinatorial or microscopic descriptions based on a realistic nuclear potential. The review of Huizenga and Moretto [12] is a definitive summary of current techniques. In particular, they give an excellent description of the grand partition function of statistical mechanics, and show how the use of this powerful method leads to the microscopic level-density calculations that are only beginning to be used in evaluations.

III. STATISTICAL CALCULATIONS

C. H. Johnson [13] carried out statistical model calculations of radiation widths for $75 < A < 130$, using the Brink-Axel hypothesis with two free parameters for the normalization and A-dependence of the giant resonance tail, fitting known s-wave levels with a standard deviation of ~ ± 25%. Johnson noted that in the region of $A \simeq 90$ (in the region of the 50-neutron shell) the statistical model

calculations give excess p-wave radiation widths because the low lying states are mostly even parity. The excess is particularly large near A ≃ 90 because the level densities at the neutron binding energy are small, and the partial widths for transitions to these low-lying final states are distributed among fewer resonances. To describe the shape of the E1 and M1 strength Johnson used the Lorenzian expression

$$S_{E1}(E_\gamma) = \frac{1}{3}(2.6 \cdot 10^{-7}) \frac{\sigma_g \Gamma_g^2 E_\gamma}{\left(E_g^2 - E_\gamma^2\right)^2 + \Gamma_g^2 E_\gamma^2}$$

with $E_g = 76/A^{1/3}$ MeV, and $\Gamma_g\sigma_g = (40\pi e^2\hbar/Mc)(NZ/A)$. For Γ_g, he used 88A/NZ MeV, consistent with the level density description he chose, the backshifted Fermi gas model

$$\rho(U) = \exp\left(2\sqrt{aU}\right) / 12\sqrt{2}\, a^{1/4} U^{5/4} \sigma \quad ,$$

with the spin dependence given by

$$\rho_J(U) = \rho(U)(J + 1/2)(2\sigma^2)^{-1} \times \exp\left[-(J + 1/2)^2/2\sigma^2\right] \quad ,$$

where $U = E - \Delta$ and $\sigma^2 = 0.0888(aU)^{1/2} A^{2/3}$.

The radiation width was calculated as a sum over discrete and continuum final states,

$$\langle\Gamma_\lambda\rangle_{J\pi} = \left[\sum_{fE1} S_{E1}(E_\gamma)E_\gamma^3 + \sum_{fM1} S_{M1}(E_\gamma)E_\gamma^3\right] / \rho_{J\pi}(Ex) + \int_0^{E_\gamma - Ec} S(E_\gamma)E_\gamma^3 \sum_{I=J-1}^{J+1} \rho_I(Ex - E_\gamma)\, dE_\gamma / \rho_J(Ex) \quad ,$$

where $S(E_\gamma)$ in the second term is given by $S_{E1}(E_\gamma) + S_{M1}(E_\gamma)$. The second term is parity independent because the final states include equally both parities.

Johnson concluded that the statistical enhancement of p-wave widths for A ≃ 90 was roughly equal to the enhancement by valence capture calculated from observed reduced neutron widths and (d,p) spectroscopic factors, noting that below A = 88, there are predicted enhancements for s-wave

resonances rather than p-waves.

A similar study for the actinide region was reported by Moore at the Harwell conference [14], the major difference being that a combinatorial level density calculation was used instead of the Fermi-gas description. The situation in the actinides is very similar to that for $A \simeq 90$: the p-wave neutron widths are enhanced by the presence of the 4p resonance, and most of the low lying levels again have positive parity, so that the highest energy transitions are preferentially observed in p-wave resonances. This property was recognized by Corvi et al. and used successfully in assigning p-wave levels in ^{232}Th and ^{238}U [15,16]. The level density in the actinides is very much higher than for $A \simeq 90$, and a calculation using the Fermi-gas level-density description in the continuum would have shown that s- and p-wave radiation widths are negligibly different. However, the combinatorial level-density calculation suggested that the enhanced density of positive-parity states persists far enough into the continuum to give a significant difference in s- and p-wave radiation widths for even-even targets, where the level density at the neutron binding energy is least.

Johnson and Moore found that the Lorentzian parameters obtained by fitting the giant resonance overpredicted the neutron capture widths. In their review, Bartholemew et al. [17] noted that this result is a fairly general one: the Lorentzian shape generally overpredicts the radiative widths and gives a too soft capture spectrum. These difficulties led Gardner et al. [10] to adopt their energy dependent Breit-Wigner shape. Joly et al. [18] measured gamma-ray spectra from radiative capture for neutron energies below 3 MeV for rhodium, thulium, and gold. They compared their results with extrapolations of giant-dipole-resonance data and total radiative widths. Their results indicated that better agreement was obtained by using a depressed giant dipole resonance shape, a Lorentzian multiplied by a depression factor given by $\exp[\alpha(E_\gamma - E_0)]$ with parameters $\alpha = 0.164$ MeV^{-1} and $E_0 = 12.2$ MeV for gold, as suggested by Earle et al. [19], and $\alpha = 0.060$ MeV^{-1} and $E_0 = 13.4$ MeV for rhodium. It is perhaps unnecessary to remark that using such a depression factor for the $A \simeq 90$ and actinide calculations would lead to even larger differences in the predicted s- and p-wave radiation widths.

IV. NON-STATISTICAL EFFECTS

The definitive review of valence and doorway mechanisms in resonance neutron capture is that of Allen and Musgrove [2].

The valence model describes the change of state of the incident neutron in the entrance channel by the emission of dipole radiation in the field of a spectator target. The valence process is expected to be important when initial states have large reduced widths and when E1 transitions can excite final states with large spectroscopic factors near closed shells. In the valence process, the partial radiative width is proportional to the reduced neutron widths of both the initial and final states. Allen and Musgrove made valence model calculations across the periodic table, comparing these with s- and p-wave radiative widths. The pattern of width variations and correlations with mass number led them to the conclusion that there are other non-statistical processes that occur in addition to valence transitions. One of these gives neutron width and total radiation width correlations, and occurs in regions where valence capture is relatively unimportant. Another seems to give primarily final-state correlations but is non-correlated with neutron widths; this second single-particle mechanism seems to manifest itself in the region of the 3s shell and to interfere with valence capture. Allen and Musgrove conclude that the observed effects can be attributed to doorway states: large and symmetric initial and final state correlations are expected in the case of a single doorway with two-quasiparticle character; if there are n doorways, the initial-state correlations are reduced by a factor 1/n, but the final-state correlations remain large. Allen and Musgrove also discuss other doorway configurations, particle-vibrator doorways, and collective core transitions.

Neutron strength fluctuations, showing strong evidence for intermediate structure, are well established in the 3p and 4s size resonances, [20-22], and recently have been suggested by Perez et al. [23] for the capture cross section of ^{238}U in the 4p resonance. While one can speculate that radiative width enhancements and correlations with neutron widths are a general phenomenon associated with the neutron size resonances, it is not clear how one might include such effects in an evaluation, or in what cases it is essential to do so. Even in those cases where non-statistical effects appear to be well established, one should bear in mind that they may be neutron-energy dependent, in the same way as the intermediate structure fluctuations.

V. A LEVEL-DENSITY CALCULATION

The use of a thermodynamic level density description such as the back-shifted Fermi gas is probably the most deficient approximation made in the evaluation of s- and p-wave radiation widths in a purely statistical calculation. While a

combinatorial approach is cumbersome, it appears to offer a reasonable way of including certain nuclear structure information. The following features are to be incorporated in an independent particle calculation similar to that used in Ref. 14: 1) Use of a realistic one-body potential (Nilsson model) that includes the treatment of permanent quadrupole deformations. 2) Inclusion of the most important of the residual interactions, pairing correlations, by solving the BCS equation, or by the Wahlborn method [24] for those configurations that are only slightly affected by pairing. 3) Sequential calculation of densities according to the doorway-state hierarchy, which in principle permits the inclusion of valence neutron capture, precompound emission probabilities, and destruction of appropriate particle-hole pairs. 4) A realistic joining of discrete and continuum levels by replacing the lowest calculated levels with a given (E,J,π) by those that are known. 5) Calculation of partial radiative widths under the Brink-Axel hypothesis, modified as necessary by the depression factor described in Ref. 18 to give agreement with measured radiative widths. The code was written at the Central Bureau for Nuclear Measurements in Geel, Belgium. Preliminary tests have been made, but no production calculations were done. We hope to have the code operable on the LASL CDC-7600 in the near future.

VI. CONCLUSIONS AND RECOMMENDATIONS

The calculations of Johnson [13] showed that differences in s- and p-wave radiation widths are predicted by the statistical model in the region of $A \simeq 90$, and the results obtained by Moore [14] suggested that similar differences may exist in certain actinide nuclides. The use of the back-shifted Fermi-gas model to describe continuum level densities seems to preclude the use of Johnson's simple approach as a general evaluation tool. Results of a perhaps more realistic statistical calculation are not yet available.

We feel that the problem warrants further study. Non-statistical effects should be included in the evaluation of radiative widths, at least for those nuclides for which they are known to be important. It is not clear whether these effects may be rapidly energy dependent, or whether neutron and radiation-width correlations are of general enough importance that provision should be made for treating them in unresolved-resonance data evaluation.

ACKNOWLEDGEMENTS

The author would like to take this opportunity to thank his colleagues and the staff at the Central Bureau for Nuclear Measurements for their hospitality and interest in this problem, and D. M. Drake and S. Joly for illuminating discussions.

REFERENCES

1. M. CANER, Annals of Nuc. Energy 7, 403 (1980).

2. B. J. ALLEN and A. R. DE L. MUSGROVE, in "Advances in Nuclear Physics," (M. BARANGER and E. VOGT, eds.) Vol 10, p. 129 (1978).

3. D. M. BRINK, Ph.D. Thesis, Oxford (1955).

4. P. AXEL, Phys. Rev. 126, 671 (1962).

5. J. E. LYNN, The Theory of Neutron Resonance Reactions, Clarendon Press, Oxford (1968), p. 325.

6. See, for example recent measurements by J. T. CALDWELL, E. J. DOWDY, B. L. BERMAN, R. A. ALVAREZ, and P. MEYER, Phys. Rev. C21, 1215 (1980).

7. A. K. KERMAN and H. K. QUANG, Phys. Rev. 135, B883 (1964), see also B. L. BERMAN in "Photonuclear Reactions and Applications," Asilomar, CA CONF 730301 Vol. I, p. 567 (1973).

8. See, for example, R. G. LANIER, G. L. STRUBLE, L. G. MANN, I. C. ÖLRICH, I. D. PROCTOR, and D. W. HEIKKINEN, Phys. Rev. C22, 51 (1980).

9. L. M. BOLLINGER, in "Photonuclear Reactions and Applications, Asilomar, CA, CONF 730301, Vol II., p. 783 (1973).

10. D. GARDNER, M. A. GARDNER, and F. S. DIETRICH, Lawrence Livermore Laboratory Report UCID-18759, August 1980 (unpublished).

11. J. E. LYNN, Atomic Energy Research Establishment Report AERE-R7468 (1974).

12. J. R. HUIZENGA and L. G. MORETTO, Ann. Rev. Nuc. Sci. 22, 427 (1972).

13. C. H. JOHNSON, Phys. Rev. C16, 2238 (1977).

14. M. S. MOORE in "Neutron Physics and Nuclear Data for Reactors and Other Applied Purposes," OCED, Paris (1978), p. 313.

15. F. CORVI, G. PASQUARIELLO, and T. VAN DER VEEN, in "Neutron Physics and Nuclear Data for Reactors and Other Applied Purposes," OECD, Paris, (1978), p. 712.

16. F. CORVI, G. ROHR, and H. WEIGMANN, in "Nuclear Cross Sections and Technology," NBS Spec. Pub. 425 (1975), Vol. II, p. 733.

17. G. A. BARTHOLOMEW, E. D. EARLE, A. J. FERGUSON, J. W. KNOWLES, and M. A. LONE in "Advances in Nuclear Physics," (M. BARANGER and E. VOGT, eds.) Vol. 7, p. 229 (1973).

18. S. JOLY, D. M. DRAKE and L. NILSSON, Phys. Rev. C20, 2072 (1979).

19. E. D. EARLE, I. BERGQVIST, and L. NILSSON, A. B. Atomenergi Report AE-515 (1977).

20. G. ROHR, H. WEIGMANN, and J. WINTER, Nuc. Phys. A150, 97 (1970).

21. G. ROHR and H. WEIGMANN, Nuc. Phys. A264, 93 (1976).

22. H. WEIGMANN, S. RAMAN, J. A. HARVEY, R. L. MACKLIN, and G. G. SLAUGHTER, Phys. Rev. C20, 115 (1979).

23. R. B. PEREZ, G. DE SAUSSURE, R. L. MACKLIN, AND J. HALPERN, Phys. Rev. C20, 528 (1979).

24. S. WAHLBORN, Nuc. Phys. 37, 554 (1962).

Discussion

Lone

You warned against the use of a single Lorentzian term for calculation of the gamma-ray strength function. This certainly is not the practice. In my review talk at the Third International Conference on (n,γ) Spectroscopy held 1978 at BNL (published by Plenum Press, page 161), and our earlier review paper in Advances in Nuclear Phys. Vol. 7 (Editors: Vogt and Barranger), it is clearly pointed out that one uses the one or two term Lorenztian expressions which best fits the gamma-ray absorption cross section data across the giant dipole resonance region in the particular nucleus. Parameters for such fits are given by Berman and Fultz in their review paper published in the Review of Modern Physics. Deviations of the gamma strength function from Lorentzian extrapolations were also discussed in our review paper. You mentioned that from nucleus to nucleus the variation in the total radiative width is much less than the variation in the gamma ray strength function. Are you considering the same excitation energy in different nuclei?

Moore

Let me comment on your comment: My intent in mentioning the single and double Lorentzians was actually to point out the need for including nuclear structure information in transition nuclei where shape co-existence is known to exist. This is only illustrative of problems that arise in the GDR description. The answer to your question is that I was actually comparing neutron and radiative strength functions for neighboring nuclei at the same incident neutron energy, where neutron strengths are rather similar, but radiative strengths are quite different because of the difference in excitation energy.

Moldauer

With regard to the problem of level densities and level spacing distributions, there is a well developed theory based on the shell model which is due to Prof. Bruce French of the University of Rochester. Unfortunately, it is not too well documented in the open literature; it has been discussed for quite a number of years at various international meetings. This work may be of interest to evaluators.

Bhat

There was a conference at Iowa State in September 1979 dealing with the level density calculations of many fermion systems. The work of S. Grimes (LLL) and others in this connection is interesting.

Gruppelaar

Have you any preference for backward or forward - shifted level density prescription? These are the formulas which are still used by most of the evaluators at present.

Moore

My feeling is that any of the simple prescriptions currently used are open to question.

Peelle

Do I correctly infer from the last few talks that the evaluator can obtain little detailed guidance from resonance analysis for extension of the total and capture cross sections into the unresolved resonance region at higher neutron energy? (because of problems in separation of s-wave and p-wave levels, and the difficulties of knowing p-wave radiative width, for instance).

Moore

True. It appears that neutron strength fluctuations or intermediate structure is quite a general phenomenon, and one must be careful when extrapolating resolved resonance parameters to the unresolved region.

Froehner

I would like to respond also to Bob Peelle's question. It is difficult to extrapolate from the resolved resonance region beyond 100 or 200 keV, at least for me. I am impressed by the fits to ^{238}U capture data presented by Poenitz at the Knoxville Conference, which are good up to 1 MeV. I myself find difficulties when I try to estimate energy dependences of radiation widths or of inelastic scattering, e.g. with the Gilbert-Cameron formulae, because there is no good prescription for the E-dependence of the spin cut-off at low energies. It would be desirable to extract something like an improved Gilbert-Cameron formulae from the results of the BCS-type and combinatorial calculations so that the formulae become more useful near the ground state and over large energy ranges, of the order of 10 or 15 MeV.

Menapace

I agree on the fact that macroscopic formulas of level density should be improved in order to fit the results of microscopic models. A work in this direction is in progress at the Bologna Center, among others; and the first results were published (see Nuovo Cimento, 50A, 1979 and Sept. 80). A simple model ("black body" model by Benzi) utilizing the thermodynamic temperature from the microscopic calculations has been applied successfully to estimate average radiative widths.

Mughabghab

The work of Benzi and his collaborators appeared in 1978 Harwell Conference (p. 288) and the Proceedings of the Specialists' Meeting on Neutron Cross Sections of Fission Product Nuclei, Bologna 1979 (p. 215).

EVALUATIONS OF AVERAGE LEVEL SPACINGS

H. I. Liou

Brookhaven National Laboratory
Upton, New York 11973, U.S.A.

ABSTRACT

The average level spacing for highly excited nuclei is a key parameter in cross section formulas based on statistical nuclear models, and also plays an important role in determining many physics quantities. Various methods to evaluate average level spacings are reviewed. Because of the finite experimental resolution, to detect a complete sequence of levels without mixing other parities is extremely difficult, if not totally impossible. Most methods derive the average level spacings by applying a fit, with different degrees of generality, to the truncated Porter-Thomas distribution for reduced neutron widths. A method which tests both distributions of level widths and positions is discussed extensively with an example of ^{168}Er data.

INTRODUCTION

In the optical model and statistical model calculations for nuclear cross sections the s-wave average level spacing <D> of neutron resonances plays an important role along with other average parameters, such as the s- and p-wave neutron strength functions, and the average radiation widths. More knowledge about <D> leads to better understanding of the neutron reaction mechanisms. The average capture cross section in the resonance unresolved region is proportional to $1/\langle D\rangle$, and the average partial radiative capture width is proportional to <D> at capture state. The pairing energy, shell effects, and the level spacing of single particle states at Fermi surface energy can be determined by systematic study of <D> in the resonance region. Reactor fuel cycle and burn-up calculations also largely depends on the average level spacings of fission products.

Generally the average level spacings are obtained from the analysis of the resonance parameter sets. If one can measure a complete s-wave population of N levels in an energy interval ΔE, then $\langle D\rangle = \Delta E/N$. The Porter-Thomas (PT) single-channel distribution law [1],

$$P(X)dX = (2\pi X)^{-1/2}\,\mathrm{Exp}(-X/2)dX \quad \text{and} \quad X = g\Gamma_n^o/\langle g\Gamma_n^o\rangle$$

for reduced neutron width, however, is peaked at zero strength, and ~85% of the s-wave levels have $X \leq 10^{-2}$. The finite resolution and sensitivity of neutron experiments thus invariably result in a loss of weak levels. This has no practical consequence on determination of the strength functions, but the loss must be corrected to obtain a good value of the average spacing. The problem is even more complicated by the fact that p-wave levels may be detected, and usually are not distinguished from weak s-wave levels.

Various methods have been adopted to evaluate the average level spacings. Most of them are based on a fit in different degrees of generality to the upper portion of the PT distribution, which is undisturbed by spurious and missed s-wave levels. On the contrary the distributions and statistics concerning the level positions are distorted by these facts. An improvement of the results can, however, be achieved sometimes by a careful investigation of the level energy statistics combined with other considerations in an iteration procedure. We shall first summarize a few relevant statistical properties of level energies, then review briefly various methods used to extract the average level spacings. A discussion about the limitations of the methods and other remarks are given in the last section.

STATISTICAL PROPERTIES OF LEVEL ENERGIES

Wigner surmised in 1956 [2] that there should be a repulsion between levels of a single population, and suggested his famous spacing law,

$$P(X)dX = \frac{\pi X}{2} \mathrm{Exp}(-\pi X^2/4)dX \text{ and } X = D/\langle D\rangle .$$

He indicated that the levels for a single population should follow the same ordering behavior as do the eigenvalues of real square NxN symmetric matrices with random Gaussian-distributed elements (Gaussian Orthogonal Ensemble, G.O.E.). Later Gaudin [3] obtained a more exact distribution function of spacings as an infinite product rapidly converging. As shown in Fig. 1 the difference between his distribution and Wigner's surmise is less than what can be distinguished experimentally. The distribution shows that both small and large spacings (compared to $\langle D\rangle$) are equally improbable. When spurious levels are present, there tend to be too many small spacings. Figure 2 shows an example where two single populations are randomly mixed with a density ratio of 1.286. The smooth curve is an analytical prediction from G.O.E., and the histograms represent the Monte Carlo simulation. It is clear that the Wigner repulsion effect inhibiting small level spacings is largely removed.

Dyson [4] proposed a new circular orthogonal ensemble (C.O.E.) in which a compound nucleus system is represented by a NxN unitary matrix S instead of an hamiltonian H. The energy levels are related to the eigenvalues which are treated as points on a unit circle with joint probability proportional to the product of the chord length between all possible pairs of levels. Dyson and Mehta [5] were able to show that a long range correlation for level spacings is implied. In particular, their Δ_3 statistic, defined as the mean squire deviation of a best-fit straight line from the cumulative level count N(E), has the predicted mean and standard deviation (S.D.) for N levels as

$\langle \Delta_3 \rangle = (1/\pi^2)[\ln(N)-0.0687]$ and S.D. = 0.11.

Monte Carlo calculations of Δ_3 [6][7] based on G.O.E. showed that its mean and S.D. for various values of N are nearly the same as the analytical predictions of G.O.E. This indicates that the two models are indistinguishable.

It is evident that in the absence of long-range correlations Δ_3 should increase linearly with N instead of lnN. Monte Carlo calculations for sets of uncorrelated Wigner distribution spacings (U.W.) indeed showed that

$$\langle \Delta_3 \rangle = N/(55-210/N).$$

The mean and S.D. of Δ_3 values VS N are listed in Table I for both O.E. and U.W. single populations. It can be seen that the spread of Δ_3 values for U.W. distribution leads to an overlap between the correlated and uncorrelated cases for $N \leq 50$.

According to Mehta, the short range order expected from G.O.E. should have a correlation coefficient ρ of the adjacent level spacings equal to -0.27. Monte Carlo calculations [6][7] confirmed his result, and showed that the S.D. of ρ for a correlated level sequence of n spacings is of $0.92/(n)^{1/2}$. A test for the sum of Δ_3 and ρ gives a considerably better separation between the O.E. and U.W. distributions.

Dyson has developed an optimum statistic F [8][9] to diagnose the presence of spurious or missing levels in an otherwise perfect sequence of levels. For each level E_i in a series of levels, one calculates

$$F_i = \sum_{j \neq i} f(X_{ji}) \text{ and } X_{ji} = (E_j-E_i)/L,$$

where j runs through all levels between (E_i-L) and (E_i+L) excluding E_i, and

$$f(X) = 1/2 \ln\{[1+(1-X^2)^{1/2}]/[1-(1-X^2)^{1/2}]\}.$$

TABLE I

Comparison of Δ_3 values between the correlated (O.E.) and uncorrelated (U.W.) cases, both following the Wigner distribution.

N	Δ_3 (O.E.)	Δ_3 (U.W.)
10	0.23 ± 0.11	0.29 ± 0.12
20	0.30 ± 0.11	0.45 ± 0.23
30	0.34 ± 0.11	0.63 ± 0.35
50	0.39 ± 0.11	0.98 ± 0.58
100	0.46 ± 0.11	1.89 ± 1.16
200	0.53 ± 0.11	3.71 ± 2.32

Here $L = M\langle D \rangle$, M being an arbitrarily chosen integer (usually ~10). The mean and S.D. of F_i are

$$\langle F_i \rangle = n-\ln(n)-0.6[illegible] \text{ and S.D.} = (\ln n)^{1/2},$$

where n = [illegible]M. The expectation value of F_i for a spurious level in an otherwise perfect sequence of levels is $\langle F_i \rangle$ = n. This denotes that the presence of a spurious or missing level produces, on the average, a peak or a dip in F_i of magnitude ln(n), superposed on the natural fluctuation of F_i, $(\ln n)^{1/2}$.

Bohigas and Flores [10] have introduced the use of a statistic, $\sigma(k)$, which is the mean standard deviation of the spacing of levels having k levels between them in units of <D>. $\sigma(k)$ expresses the mean standard deviation of D/<D>. Monte Carlo calculations are required to obtain the mean and confidence limits of $\sigma(k)$ in O.E. case. In particular, the confidence limits are dependent on the total number of levels in the sequence.

If a single population chosen from imperfect data is required to agree with all the above tests plus other concernings, a strong constraint is placed on the manner of selection.

Dyson and Mehta [5] have derived an expression for the fractional statistical uncertainty of <D>,

$$\frac{0.450}{N}\left[\ln(2\pi N) + 0.343\right]^{1/2},$$

using the simplest statistic N, the total number of levels of a single population in the energy region. In the case where the optimum statistic [illegible] [5] can be applied in the evaluation of <D>, its statistical uncertainty is then slightly reduced.

METHODS OF EVALUATION OF <D>

Method of Level Number Staircase Plot

This is a method long used to obtain the average level spacing. One plots the cumulative number of levels versus energy, and takes the slope in its linearly increasing region as 1/<D> (usually in the lowest energy region). It is based on the assumption that the experimental sensitivity in the lowest energy region is sufficient to detect all s-wave levels. The assumption is, however, generally questionable, since a linear increase of the level number staircase can also result from the combined effect of missing s-wave levels and including spurious levels.

Method of Monte Carlo Simulation

The method has been applied by Derrien and Lucas [11] for ^{241}Am. They used Monte Carlo technique to generate a set of resonances with estimated values of <D> and $\langle g\Gamma_n^0 \rangle$ in the energy interval of interest. The level widths and spacings are chosen randomly from the PT and Wigner distributions. The Doppler and the experimental resolution effects on the cross sections are exactly simulated. The generated cross sections are then analyzed in the same way as for the real cross sections. The percentage of missed levels

can be found by a comparison of the observed number of levels to a priori given number of levels. The expectation value of the percentage is obtained by averaging over several sets of the simulated data, and its fluctuation provides the information of uncertainty. The method is valid only if its result is not sensitive to the guessed value of $\langle D \rangle$.

Method of Least Squares Fitting

This method, which was initiated at SACLAY [12], fits the portion of the integral distribution of $g\Gamma_n^o$ above a threshold to the PT distribution with a least squares procedure. The threshold is chosen in the sense that above the limit all s-wave levels are observed with no p-wave contamination. The s-wave strength function can be taken either as a fixed quantity or a free parameter fitted together with the total number of levels. One can vary the threshold to check how consistent the results are.

Method of Missing Level Estimator

The method [13] uses some results of the partial integration over a PT distribution P(X). They are

$$\int_{1/4}^{\infty} P(X)dX = 0.617 \text{ and } n \sum_{a}^{\infty} g\Gamma_n^o / (\sum_{a}^{\infty} \sqrt{g\Gamma_n^o})^2 = 1.206,$$

where $a = \langle g\Gamma_n^o \rangle / 4$, and n is the number of levels with $g\Gamma_n^o > g\Gamma_n^o > a$. The method consists in calculating the quantity $n g\Gamma_n^o / (\sum \sqrt{g\Gamma_n^o})^2$, starting with the largest value of $g\Gamma_n^o$ and adding one level at a time from larger to smaller until this quantity reaches 1.206. Then the total number of levels in the studied interval is n/0.617. It is quick and does not need any judgement. But its accuracy depends on the quality of the determination of the larger widths.

Method of Applying Bayes' Theorem to Set a Threshold

Rohr, Maisano and Shelly [14] have developed a method that applies Bayes' theorem to establish a threshold which virtually separates large s-wave levels from p-wave levels and small s-wave levels. It assumes that both ℓ=0 and 1 (s and p) populations obey the PT distribution,

$$P_\ell(X_\ell)dX_\ell = (2\pi X_\ell)^{-1/2} \mathrm{Exp}(-X_\ell/2)dX_\ell \text{ and } X_\ell = g\Gamma_n^\ell / \langle g\Gamma_n^\ell \rangle,$$

where $g\Gamma_n^o = g\Gamma_n / \sqrt{E(eV)}$, $g\Gamma_n^1 = g\Gamma_n [1+(ka)^2]/(ka)^2 \sqrt{E(eV)}$, and $k=\sqrt{E}$. $g\Gamma_n$ is the direct measurable quantity of a resonance without knowledge of its spin and ℓ values. The probability of a resonance with a given $g\Gamma_n$ to be ℓ=1 can be expressed by the Bayes' formula [15],

$$P(\ell=1, g\Gamma_n) = P_1 / (\pi_o P_o / \pi_1 + P_1),$$

where the ratio π_o/π_1 equals $\langle D_1 \rangle / \langle D \rangle$, depending on the spin of the target nucleus.

If a trial p-wave strength function $(S_1)_{bias}$ is chosen corresponding to a small p-wave probability (normally 10^{-3}), the bias threshold function $\ell(E)$, defined as $(g\Gamma_n)_{bias}/\sqrt{E(eV)}$, can be calculated in terms of preliminary values of <D> and S_o, using the above Eaves' formula. $\ell(E)$ is then fitted to a form $a\sqrt{E}$. Any observed resonance with $g\Gamma_n/\sqrt{E(eV)}$ above $\ell(E)$ is considered as s-wave. The S_o value and the total number of s-wave levels below $\ell(E)$ in the studied energy region are evaluated in an iterative way described in reference [14].

$(S_1)_{bias}$ does not have to be equal to the true p-wave strength function. This method works, as long as $(S_1)_{bias}$ is large enough so that the small p-wave probability above $\ell(E)$ is warranted. Normally three different $(S_1)_{bias}$ values ($S_1/3$, S_1, and $2S_1$) are chosen, and processed separately to check the consistency of the results for <D> and S_o. S_1 is taken from an optical model calculation or BNL 325 [17]. The uncertainty of <D> is determined from a large number of Monte Carlo data sets produced in a statistical fashion assuming the PT and Wigner distributions for the widths and spacings respectively.

Figure 3 shows an example applied to ^{238}U, where the three curves represent $\ell(E)$ for three given $(S_1)_{bias}$ values. The results for <D> and S_o are plotted in Fig. 4 for a series of $(S_1)_{bias}$ values, showing the influence of the bias. More than 240 nuclei have been processed using this method by Rohr et al. [14].

ESTIMA Method

According to references [18] and [19], an ESTIMA code was written for a simultaneous determination of <D> and $<g\Gamma_n^o>$ which maximizes the likelihood function defined as a product of the frequencies of each measured $g\Gamma_n^o$ value above a selected energy-independent threshold. It assumes: (1) reduced neutron widths follow the single-channel PT distribution, (2) unresolved doublet are unlikely in the studied energy interval, and (3) levels with $g\Gamma_n^o$ above the threshold are all s-wave resonances.

The threshold is varied. $<g\Gamma_n^o>$ and N_t (the total number of s-wave levels) are solved for each value of the threshold. Since the contamination by p-wave levels leads to a rapid variation of the two parameters, the adopted values for $<g\Gamma_n^o>$ and N_t are those which remain relatively stable when the threshold varies. The oscillation of N_t in the stable region suggests the experimental error in <D>, which is quadratically combined with the statistical uncertainty due to finite sample size. Figure 5, from reference [18], shows an application of ESTIMA code to ^{127}I. The two output parameters appear stable for the region where the square roots of the reduced width threshold are between 0.25 and 0.6 $meV^{1/2}$.

A check of the results is made by an investigation of the $g\Gamma_n^o$ distribution around $<g\Gamma_n^o>$. Let N_1, N_2 and N_3 represent the numbers of levels having $g\Gamma_n^o/<g\Gamma_n^o>$ value between 1 and ∞, 0.5 and 1, and 0.2 and 0.5 respectively. Then $N_1 \approx 2N_2 \approx 2N_3$ according to the PT distribution. In case these equalities are not approximately observed, a study is performed with a different value of $<g\Gamma_n^o>$.

Method of Maximum Likelihood with Variable Energy-Dependent Threshold

Goreva and Stefanon [20] and [21] have developed a maximum likelihood method to extract the parameters of <D>, S_o and S_1 with a variable energy-dependent threshold $\eta_\alpha(E)$. It is applied to zero-spin target nuclides, assuming (1) both s- and p-wave populations independently follow the PT distribution, (2) $p_{1/2}$ and $p_{3/2}$ sequences of p-wave levels have the same mean $\langle g\Gamma_n^1\rangle$, and (3) the average level spacing for each sequence is parity-independent, but proportional to $(2J+1)^{-1}$. The shape of $\eta_\alpha(E)$ is chosen according to the experimental conditions, with a parameter α to adjust its height. To obtain good results, the requirements are that all s- and p-wave resonances with $g\Gamma_n > \eta_\alpha(E)$ are observed, and that there are no unresolved doublets in the studied energy region.

The likelihood function is written as a product of probability functions over energy subintervals. The intervals are large enough to allow a Gaussian approximation of the distribution function of the number of levels for each sequence, and are also sufficiently narrow so that within each interval the energy variation of $\eta_\alpha(E)$ can be neglected. Maximization with respect to the parameters is obtained by means of a numerical algorithm based on stepwise variation of the parameters. A code, CAVE, was written for the fit that can perform with a free or fixed [illegible] function.

The method was carefully checked with Monte Carlo calculations. The results showed that the fractional uncertainty of <D> is $(0.8+n_s+n_p)^{1/2}/N_{obs}$, where N_{obs} is the number of observed levels above threshold, and n_s and n_p are the expected number of missed s-wave and mixed p-wave resonances respectively. This empirical formula demonstrates that one part of the uncertainty is due to the fluctuation of n_s and n_p following the Poisson distribution, and the rest is compatible with the prediction of Dyson-Mehta's linear statistic W [5].

In Fig. 6 the authors of reference [20] show a fit to ^{156}Gd resonances for different values of the threshold parameter α. The energy range consists of five subintervals, each being 400 eV wide and including about eleven s-wave resonances. The figure exhibits also mean values and S.D. of the simulated Monte Carlo results. While $\langle\Gamma_n^o\rangle$ is stable over the whole range of α, the estimated <D> and $\langle g\Gamma_n^1\rangle$ show a systematic variation for $\alpha<0.025$, possibly due to the fact that few resonances with $g\Gamma_n>\eta_\alpha(E)$ are missed for the lowest α-values. For larger α, $\langle g\Gamma_n^1\rangle$ begins to show stronger fluctuations because of the reduced information available. So above $\alpha=0.45$, a fixed $\langle g\Gamma_n^1\rangle$ (7.5 meV) is used. Figure 7 shows the expected numbers of N_{obs}, n_s and n_p versus α from the fit to the experimental data and Monte Carlo simulations.

Delfini and Gruppelaar [22] extended CAVE that it can be applied to a large number of fission product nuclides. A different procedure is adopted to determine the threshold function, since it is difficult to establish the experimental threshold functions in the analysis of those nuclides. The method selects the smallest value of $g\Gamma_n/\sqrt{E}$ from each ten resonances, then fits them to a function $\eta_o(E)=aE^b+c$, where a and b are free parameters, and c equals the minimum observed value of $g\Gamma_n/\sqrt{E}$. In practice the threshold function is varied by multiplying by a factor t ($\geq$1), $\eta(E)=t\eta_o(E)$. <D> may be over estimated for low values of t, since there may have significant number of missed resonances above the threshold. The final value of <D> is chosen from a region of t where the expected <D> values remain practically constant.

The extended code can be applied to non-zero spin targets, assuming two

different PT distributions, one for s-waves and one for p-waves. Since the sequences of the p-wave levels with J=I+1/2, (I+ 1/2 only, if I=1/2), are excited via two different entrance channels, their reduced neutron widths may follow a $\nu=2$ χ^2 distribution, and their average strength may be stronger than the other p-wave sequences. In addition, the simple relation $D_J=(2J+1)^{-1}$ becomes incorrect for values of $J\gtrsim 3$ because the exponential spin cut-off parameter can no longer be ignored. Thus this extension can only be applied in the cases where the number of p-wave levels is a small fraction of the observed resonances above the threshold.

In Fig. 8 the authors of [22] show a plot of $g\Gamma_n/\sqrt{E}$ for ^{127}I data as a function of neutron energy, together with the threshold function $\rho_o(E)$. The data are taken from reference [23]. Shown in Fig. 9 are the results of fit for values of t between 1 and 14, where the points marked with a cross are obtained with a fixed value of $\langle g\Gamma_n^1\rangle$. The expected value of $\langle D\rangle$ appears stable in the region of t between 2 and 5.

Method of Maximum Likelihood with the Observability Threshold

Froehner [24] [25] has derived a maximum likelihood method based on the observability threshold that is obtained via a fit to the observed level number staircase. The method eliminates all arbitrariness connected with artificial threshold, and discards no information of observation in the procedure.

Usually it is adequate to fit the level number staircase observed in an energy range between E_a and E_b with the parabolic form,

$$\bar{n}(E) = \int_{E_a}^{E} \bar{\rho}(E')dE' = a_o + a_1(E-E_a) + \frac{a_2}{2}(E^2-E_a^2).$$

Thus the observed level density $\bar{\rho}(E)=a_1+a_2E$. Define $G\equiv g\Gamma_n/\sqrt{E(eV)}$, and assume the reduced neutron widths $g\Gamma_n^\ell$ for each given ℓ-wave following the PT distribution. This leads to

$$P(G)dG = (2\pi G G_\ell V_\ell)^{-1/2}\mathrm{Exp}(-G/2G_\ell V_\ell),\quad 0<G<\infty,$$

where G_ℓ and V_ℓ denote $\langle g\Gamma_n^\ell\rangle$ and the ℓ-wave penetration factor per unit ka respectively. V_ℓ is energy dependent in case of $\ell>0$. Let ζ_ℓ express the level density ratio ρ_ℓ/ρ_o, which can be calculated with a reasonable guess of the spin cut-off σ.

Froehner has arrived at a general but concise expression for the distribution of G above the observability threshold,

$$P(G)dG = dG\,\frac{\rho_o}{\bar{N}}\sum_\ell \zeta_\ell \int_{E_a}^{E_L} P_\ell(G)\,\cdot$$

with

$$E_L = \begin{cases} \xi(G) \text{ if } \rho_o \sum_\ell \zeta_\ell \ \mathrm{erfc}\sqrt{G/2G_\ell V_\ell(E_b)} > \bar{\rho}(E_b), \\ E_b \text{ otherwise.} \end{cases}$$

$\bar{N}$ is the total number of the observed levels, and $\xi(G)$ can be solved from

$$\bar{\rho}(\xi) = \rho_o \sum_{\ell} \zeta_{\ell} \text{ erfc } \sqrt{G/2G_{\ell}V_{\ell}(E)}.$$

The derivation assumes that no level with a G value above the observability threshold is missed. The most likely set of level-statistical parameters, ρ_o and G_{ℓ}, can now be determined by maximization of the likelihood function $L=\prod_i P(G_i)$, using a numerical algorithm.

A code, STARA, has been written for the simplified case of pure s- or p-wave samples, and will be extended to the more general cases including mixed samples. The uncertainty of <D> ($=1/\rho_o$) is obtained by quadratically combining three contributions: (1) the square root of the estimated number of missed levels, (2) the statistical uncertainty from the orthogonal ensemble, and (3) the uncertainty from the parabolic fit to the level number staircase.

Figure 10 shows an application of STARA to the s-wave levels of ^{238}U, where the data are taken from reference [26]. The histograms express the observed reduced width distribution, and the smooth curves represent the integrated PT distributions calculated from best estimate of $<\Gamma_n^o>$ and from its confidence limits. The results are <D> =(20.4±0.3)eV, $10^4 S_o = 1.16^{+0.14}_{-0.11}$ and $10^4 S_1 = 1.86^{+0.26}_{-0.20}$. Figure 11 exhibits the distribution of u, defined as erfc $\sqrt{\Gamma_n^o/2<\Gamma_n^o>}$, versus level energy. The u-values, according to the PT distribution, should be uniformly distributed between 0 and 1 for complete samples, and between 0 and $\bar{\rho}(E)/\rho_o$ for a finite observability threshold. In the parabolic approximation of $\bar{n}(E)$, $\bar{\rho}(E)/\rho_o$ is a straight line in the E-u plane. The figures in the equal rectangles give the number of levels. The theoretical estimate is 14.7 ± 3.8.

Method of Testing both Level Widths and Positions

Several years ago the Columbia neutron physics group under Prof. Rainwater took great effort to search a complete single population of levels. Based on all possible tests and via an iteration procedure, they tried to single out the detected p-wave and missed s-wave levels in a measured sequence of resonances. While the selection is only good in a statistical sense, the determined <D> value becomes a useful byproduct of the procedure. The possible error in the final estimated number of s-wave levels may be kept less than $(n_s+n_p)^{1/2}$ (The expected fluctuation of Poisson distribution from a typical maximum likelihood method), especially in the case where n_s is small and n_p is large.

The s-wave strength function can be readily determined from a plot of the reduced neutron width staircase vs energy, if there is no intermediate structure. One then visually fits the experimental $\sqrt{\Gamma_R}$ histograms to the PT curve by varying the total number s-wave levels. Because of the weak level contamination, the first one or two histogram boxes are not included in fit. The result provides a starting value of <D>.

With known values of S_o and <D>, the number of missed s-wave levels can be calculated assuming estimated threshold of observability, which is energy dependent ($\alpha E^{1.5}$ for Columbia's neutron spectrometer). Using a guessed value

of the p-wave strength function S_1, one applies a Bayes' theorem calculation of a pasteriori probability that each observed weak level is p-wave. It is demanded that the sum of a posteriori probabilities agree with the estimated number of observed p-wave levels above the observability threshold within statistical fluctuation. The value of S_1 also has to fit the upper portion of the integral distribution of $g\Gamma_n^1$ for the levels favored as p-wave by the Bayes' theorem test. To fulfill these requirements, an adjustment of S_1 (sometimes with <D> together) is necessary.

After taking out all possible p-wave levels, the few missed s-wave levels are artificially added at middle of the largest level spacings in order to provide a better fit of level spacings to the Wigner distribution. Furthermore, the final set of the s-wave population must satisfy the Dyson-Mehta Δ_3 statistic, the adjacent level spacing correlation coefficient ρ, the Dyson's F statistic, and the $\sigma(k)$ in O.E. case. Most of the time this procedure requires an iteration of the total number of s-wave levels within the tolerance of keeping a good fit of $\sqrt{\Gamma_n^o}$ histograms to the PT distribution.

The procedure can be extended to non-zero spin targets by testing the statistics corresponding to a level sequence that has two populations randomly mixed with a given ratio of level density. The uncertainty of D includes two parts (combined quadratically): (1) the statistical uncertainty from the O.E. theory, (2) the error in the estimated number of (n_s-n_p) which can be determined from a judgment of the quality of the data and the goodness of over-all fits.

Since the procedure is trying to satisfy many different statistical tests instead of a best fit to the PT distribution, it is not practical to write the whole procedure into a computer code to avoid the necessity of judgment. An example for ^{168}Er from reference [7] is discussed in the following.

Figure 12 shows the plot of $\Sigma\Gamma_n^o$ vs energy up to 14.6 keV, which is insensitive to the contamination of weak levels. The slope of the average straight line determines $S_o=(1.50 \pm 0.21)10^{-4}$. The region chosen for a detailed statistical analysis is below 4.7 keV, having 72 observed levels. Shown in Fig. 13 are the $\sqrt{\Gamma_n^o}$ histograms where the dashed and solid curves represent the PT distributions separately with N=72 and 50. The final iteration value for the total number of s-wave levels is 50.

Figure 14 shows a plot of Γ_n vs E in log-log scale for weak levels, and the estimated threshold sensitivity, αE^{1-5}. About 2 s-wave levels are missed below the threshold. The results of a Bayes' theorem analysis for 32 weak levels are listed in Table II, using $S_o=1.5\times10^{-4}$ and $S_1=0.7\times10^{-4}$, the final adjusted values. A posteriori probabilities that each level is p-wave are shown in the last column with a sum of 24.03. The 24 levels denoted by superscript 'a' are likely to be p-wave. All of them have p-wave probabilities >0.79 except the one at 2900.5 eV that has p-wave probability equal to 0.587 and was chosen to avoid a concentration of three of the eight weakest s-wave choices in the 2500-to-3000 ev region. The 's-wave level' at 3751.6 ev (0.607 p-wave probability) was included to give 10 levels in the weakest $\sqrt{\Gamma_n^o}$ box of Fig. 13 after two more missed s-wave levels are added as suggested by the analysis of the threshold sensitivity. The separation between s- and p-wave levels according to a posteriori probabilities is great. The two missed s-wave levels were arbitrarily inserted at 646 and 2045 ev to equally

split the two largest spacings. Figure 15 shows the integral distribution of $\sqrt{g\Gamma_n^I}$ for the levels chosen as p-wave. Shown also is a fit of the PT integral curve for $S_1=0.7\times10^{-4}$ and $N_p=150$ (assuming $\langle D\rangle=3\langle D_1\rangle$).

Figure 16 exhibits histograms of the adjacent level spacings compared with the Wigner distribution. The dashed lines are for all measured levels, while the solid lines are for the selected s-wave levels. The Δ_3 straight-line-fits to all levels and to s-wave levels are separately shown in Fig. 17. The experimental value of Δ_3 for the 50 s-wave levels is 0.29 compared with the O.E. prediction of 0.39 ± 0.11. The value of ρ for s-wave levels equals -0.30 as compared to -0.27 ± 0.13, the O.E. expectation.

Figure 18 shows a plot of the F statistic test for the sequence of s-wave levels, where the ordinate expresses $F-\langle F\rangle$ in unit of the expected S.D. The fluctuation of F_i can be seen within the range of the O.E. prediction. The results of the $\sigma(k)$ test for the s-wave sequence are plotted in Fig. 19 up to $k=20$, compared with the O.E. expectations (solid curve) and the 90% confidence limits (dashed curves) which are obtained by Monte Carlo calculations. Shown also are the U.W. predicted $\sigma(k)$ values.

The average spacing $\langle D\rangle$ for ^{168}Er turns out to be (95.3 + 4.4) eV where the uncertainty is obtained based on the assumption that the error in the final adopted value of (n_s-n_p) is two.

DISCUSSION AND REMARKS

The problem in evaluation of average level spacings mainly depends on how to accurately estimate the numbers of spurious and missed s-wave levels after choosing a proper sequence of measured resonances. The method employing the level number staircase plot is a poor one. The method of Monte Carlo simulation is the only method that can quantitatively estimate the number of unresolved doublets, which often happen for non-spin target nuclides or in higher energy region. Since each generated sample must simulate the real experimental conditions, and many such samples are needed to extract a good average, it is inconvenient practically.

In view of the fact that spurious and missed s-wave levels have no influence on the upper part of the width distribution, most of the other methods are based on a fit to the truncated PT distribution above a specific threshold. The methods involving missing level estimators and least squares fitting are quick ones, but their accuracies depend on the quality of the larger width determination.

The standard method of maximum likelihood has been employed by several codes which are different mainly in the degree of generality and in use of threshold. The ESTIMA code chooses an energy-independent threshold of $g\Gamma_n^o$, and fits to s-wave set only.

The CAVE code, which was originally written for zero-spin targets and later extended to non-zero ones, deals with the energy-dependent threshold, and fits s- and p-wave levels together. In order to retain a sharp maximum in the likelihood function the number of missed s-wave or mixed p-wave levels should not be over 30% of the levels above threshold. The STARA code has an observability threshold automatically estimated, and eliminates all arbitrariness in connection with it. Since the threshold is rigidly set at the

observability level, an error can be induced, if some resonances are missed above the threshold by any reason including the unresolved doublets. This problem is handled more straightforwardly in CAVE, which can vary the threshold to check the stability of the output parameters.

The code developed by Rohr et al. sets an energy dependent threshold above virtually all expected p-wave levels, and fits S_0 and <D> via an iteration method. When it is applied to the case where S_1 ismuch larger than S_0, the data sample above threshold may become too small to extract an accurate mean level spacing.

Methods testing both level widths and positions may yield a result with less uncertainty, if the data to be analyzed have high quality, and miss only a small fraction of s-wave levels. The whole procedure is, however, very time consuming, and much depends on judgment.

In general, high quality data are required to obtain good results. If possible, it is helpful to examine the experimental conditions and the method used to extract the resonance parameters. Instrumental biases or using data sets which combine several authors' results may lead to reduced neutron widths which do not conform adequately to the PT distribution.

For non-zero spin target nuclides the problem of unresolved doublets may exist, and this can only be quantitatively estimated by Monte Carlo simulations. As the studied energy region extends higher, more s-(p-) wave resonances are misassigned. This may substantially broaden the maximum in the likelihood function. So sometimes one has to reduce the analyzed energy region to obtain a sample size with the necessary high quality.

The s-wave strength functions may have different values in different energy intervals due to non-statistical effects or intermediate structure. Rohr et al. [14] showed by an example of ^{177}Hf J=4 resonances where the value of <D> evaluated in the case having intermediate structure can be improved by dividing the energy range into 2 or 3 regions where the strength function remains constant.

ACKNOWLEDGMENTS

Valuable discussions with Dr. R. E. Chrien and Dr. S. Mughabghab on this subject are gratefully acknowledged. This work was performed under contract DE-AC-2-76CH00016 with the U.S. Department of Energy.

REFERENCES

1. C. E. Porter, R. G. Thomas, Phys. Rev. 104, 483 (1956).

2. E. P. Wigner, Conf. on Neutron Physics by time of flight, Gatlinburg 1956, ORNL Report 2309 (1957), p. 59.

3. M. Gaudin, Nucl. Phys. 25, 447 (1961).

4. F. J. Dyson, Journal of Math. Phys., Vol. 3, 140 (1962).

5. F. J. Dyson, M. L. Mehta, Journal of Math. Phys. Vol. 4, 701 (1963).

6. H. S. Camarda, H. I. Liou, F. Rahn, G. Hacken, M. Slagowitz, W. W. Havens, Jr., J. Rainwater, and S. Wynchank, in Statistical Properties of Nuclei, edited by J. B. Garg (Plenum, New York, 1972), p. 205.

7. H. I. Liou, H. S. Camarda, S. Wynchank, M. Slagowitz, G. Hacken, F. Rahn and J. Rainwater, Phys. Rev. C5, 974 (1972).

8. M. L. Mehta, in Statistical Properties of Nuclei, edited by J. G. Garg (Plenum, New York, 1972), p. 179.

9. H. I. Liou, H. S. Camarda and F. Rahn, Phys. Rev. C5, 1002 (1972).

10. O. Bohigas and J. Flores, in Statistical Properties of Nuclei, edited by J. B. Garg (Plenum, New York, 1972), p. 195.

11. H. Derrien and B. Lucas, Proc. of Conference, Nucl. Cross Sections and Technology, Washington, D.C. 1975, Vol. 2, p. 637.

12. E. Fort, H. Derrien and D. Lafond, Proc. of the Specialists Meeting on Neutron Cross Sections of Fission Product Nuclei, Bologna, Italy, 1979, p. 121.

13. G. A. Keyworth, M. S. Moore and J. D. Moses, ANL 7690, Argonne Conference (1976).

14. G. Rohr, L. Maisano and R. Shelly, Proc. of the Specialists Meeting on Neutron Cross Sections of Fission Product Nuclei, Bologna, Italy, 1979, p. 197.

15. L. M. Bollinger and G. E. Thomas, Phys. Rev. 171, 1293 (1968).

16. T. Fuketa and J. A. Harvey, Nucl. Instr. Meth., 33, 107 (1965).

17. S. F. Mughabghab and D. I. Garber, BNL 325 Neutron Cross Sections, Vol. I. Third Edition 1973.

18. P. Ribon, E. Fort, J. Krebs, Tran Quoc Thuong, CEA Report-CEA-N-1832, 167L (1975).

19. Tran Quoc Thuong, EANDC(E)-160AL.

20. C. Coceva and M. Stefanon, Nucl. Phys. A315, 1 (1979).

21. M. Stefanon, to be published.

22. G. Delfini and H. Gruppelaar, Proc. of the Specialists Meeting on Neutron Cross Sections of Fission Product Nuclei, Bologna, Italy, 1979, p. 169.

23. G. Rohr, R. Shelley and A. Brusegan, Neutron Resonances Studies of ^{127}I, to be published.

24. F. H. Froehner, Proc. of the Specialists Meeting on Neutron Cross Sections of Fission Product Nuclei, Bologna, Italy, 1979, p. 145.

25. F. H. Froehner, Report KFK 2669 (1978).

26. G. A. Keyworth and M. S. Moore, Neutron Physics and Nuclear Data, Harwell, 1978, p. 241.

Table II Bayes-theorem results for the weak levels of Er^{168} to 4.7 keV; $S_0 = 1.5 \times 10^{-4}$, $S_1 = 0.7 \times 10^{-4}$.

E_0 (eV)	Γ_n^0 (meV)	$g\Gamma_n^1$ (meV)	Prob. (p)
139.58 [a]	0.0093	23	0.975
145.71 [a]	0.0051	12	0.989
174.29 [a]	0.0114	23	0.973
296.67 [a]	0.0168	20	0.972
335.47 [a]	0.046	48	0.792
410.82	0.099	83	0.194
445.96	0.109	85	0.172
587.34 [a]	0.020	12	0.978
691.46 [a]	0.038	19	0.959
985.73 [a]	0.064	23	0.938
990.61 [a]	0.079	28	0.910
1022.4 [a]	0.054	18	0.954
1106.1 [a]	0.117	37	0.830
1193.2 [a]	0.064	19	0.949
1207.7 [a]	0.075	22	0.937
1342.8	0.24	65	0.384
1636.4 [a]	0.109	23	0.918
1681.3 [a]	0.073	15	0.953
2100.6 [a]	0.179	30	0.859
2325.9 [a]	0.089	13	0.952
2456.6 [a]	0.107	15	0.944
2544.0	0.58	79	0.121
2862.6	0.60	73	0.169
2900.5 [a]	0.39	47	0.587
3027.4 [a]	0.25	29	0.839
3202.8 [a]	0.15	16	0.931
3751.6	0.47	44	0.607
3849.9 [a]	0.23	21	0.900
4127.0 [a]	0.20	17	0.918
4284.3	0.93	76	0.116
4476.8 [a]	0.21	16	0.919
4643.6	0.72	54	0.395

[a] Considered to be $l = 1$.

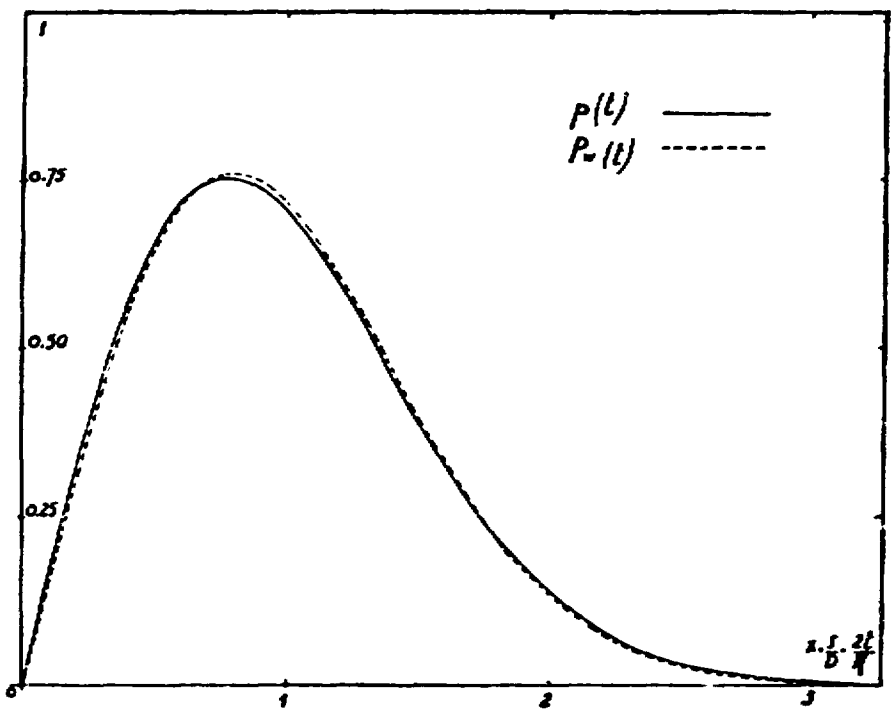

Fig. 1 Distribution of the nearest-neighbor level spacings for a single population, where the dashed and solid curves represent Wigner's surmise and Gaudin's more exact expression respectively. The difference is less than what can be distinguished experimentally.

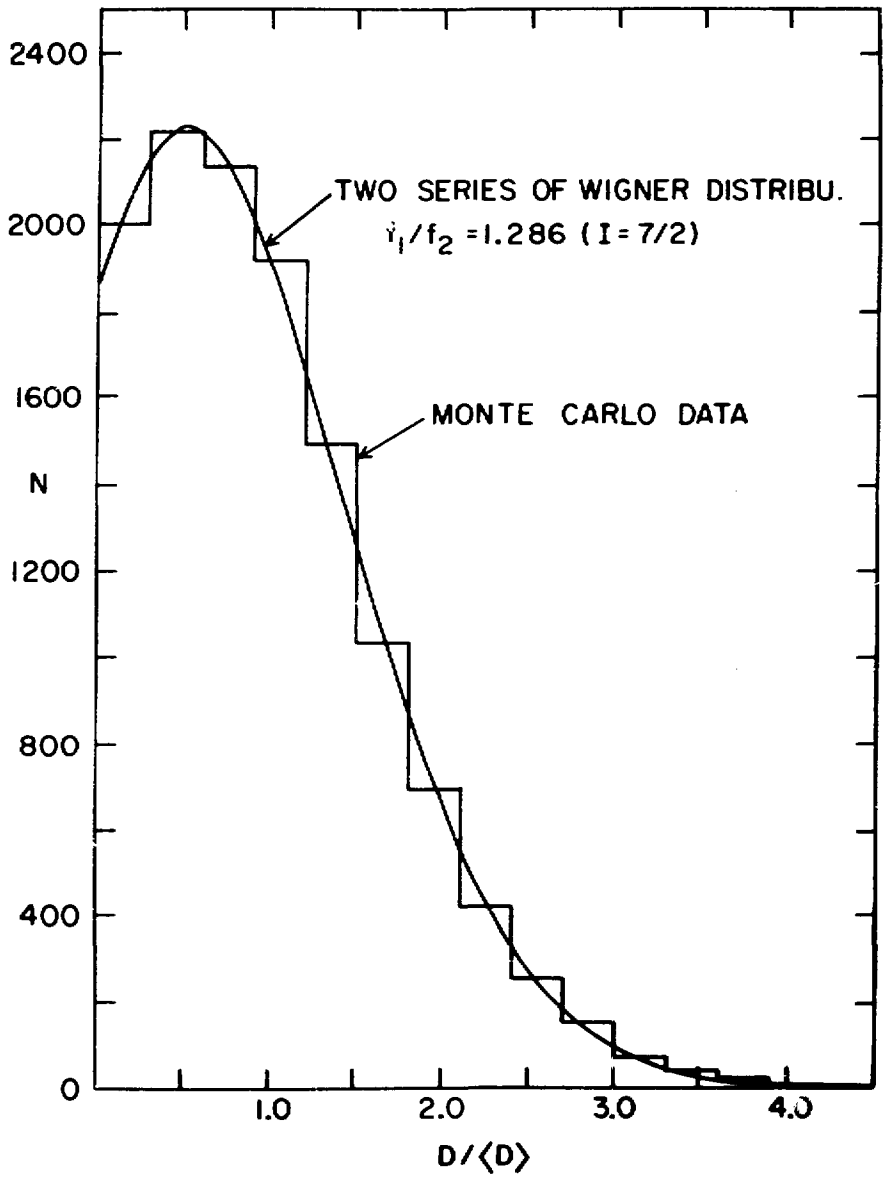

Fig. 2 Distribution of the adjacent level spacings for a level sequence having two single populations randomly mixed with a density ratio of 1.286. It is shown that the Wigner repulsion effect inhibiting small level spacings is largely removed.

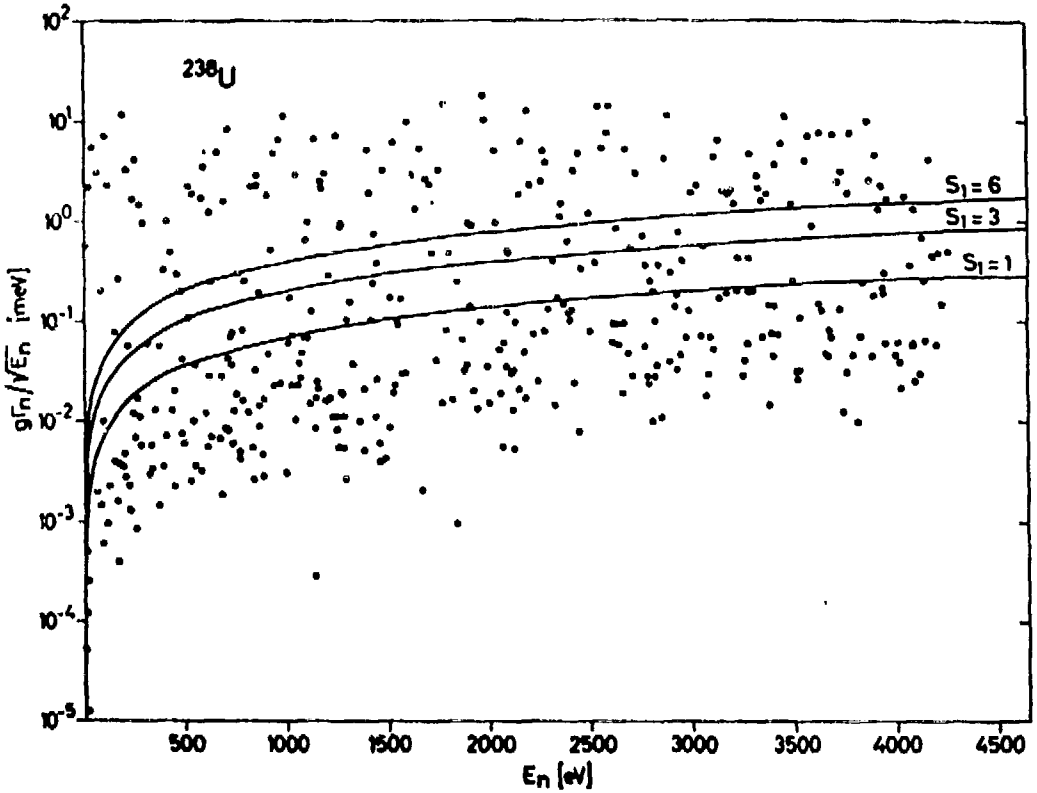

Fig. 3 The reduced neutron widths of ^{238}U resonances versus neutron energy. Shown are also three $\delta(E)$ functions corresponding to different $(S_1)_{bias}$ values.

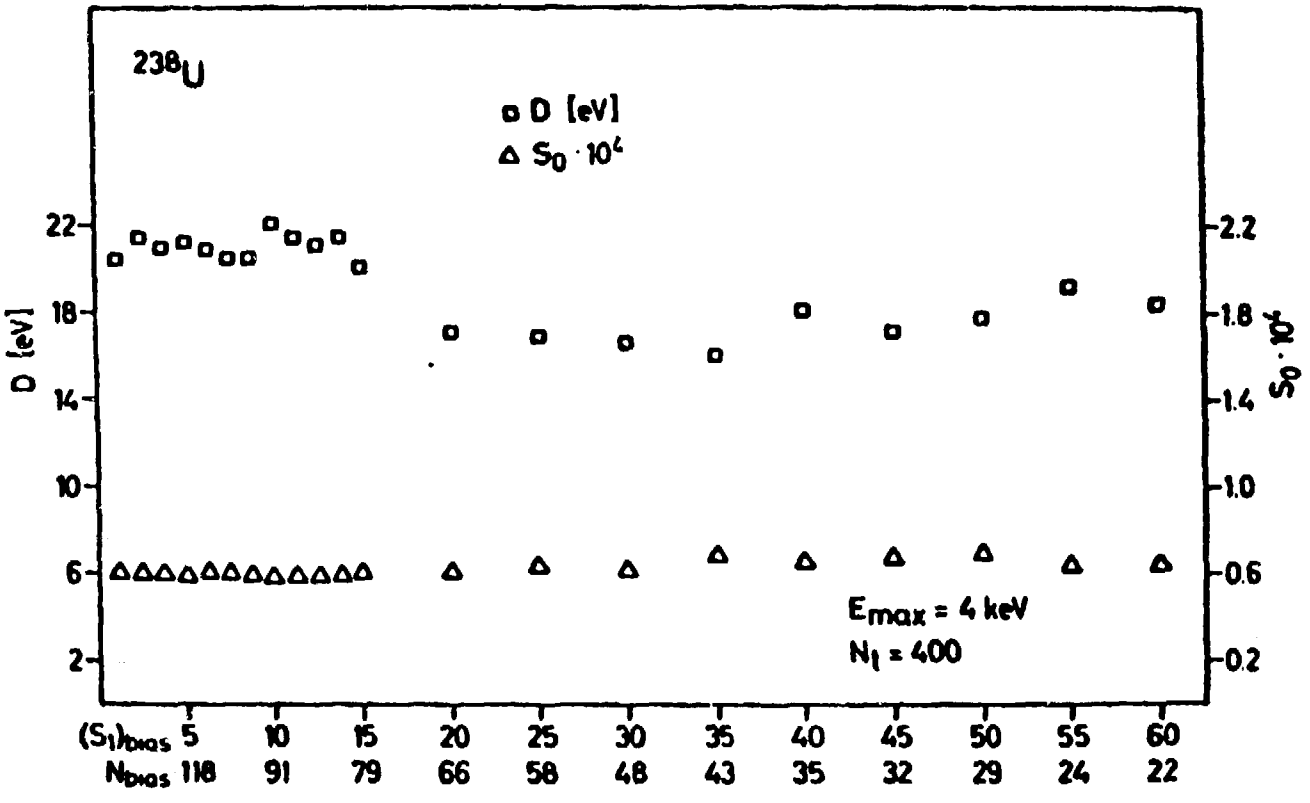

Fig. 4 Average level spacing D and strength function S_o for ^{238}U calculated for different bias values.

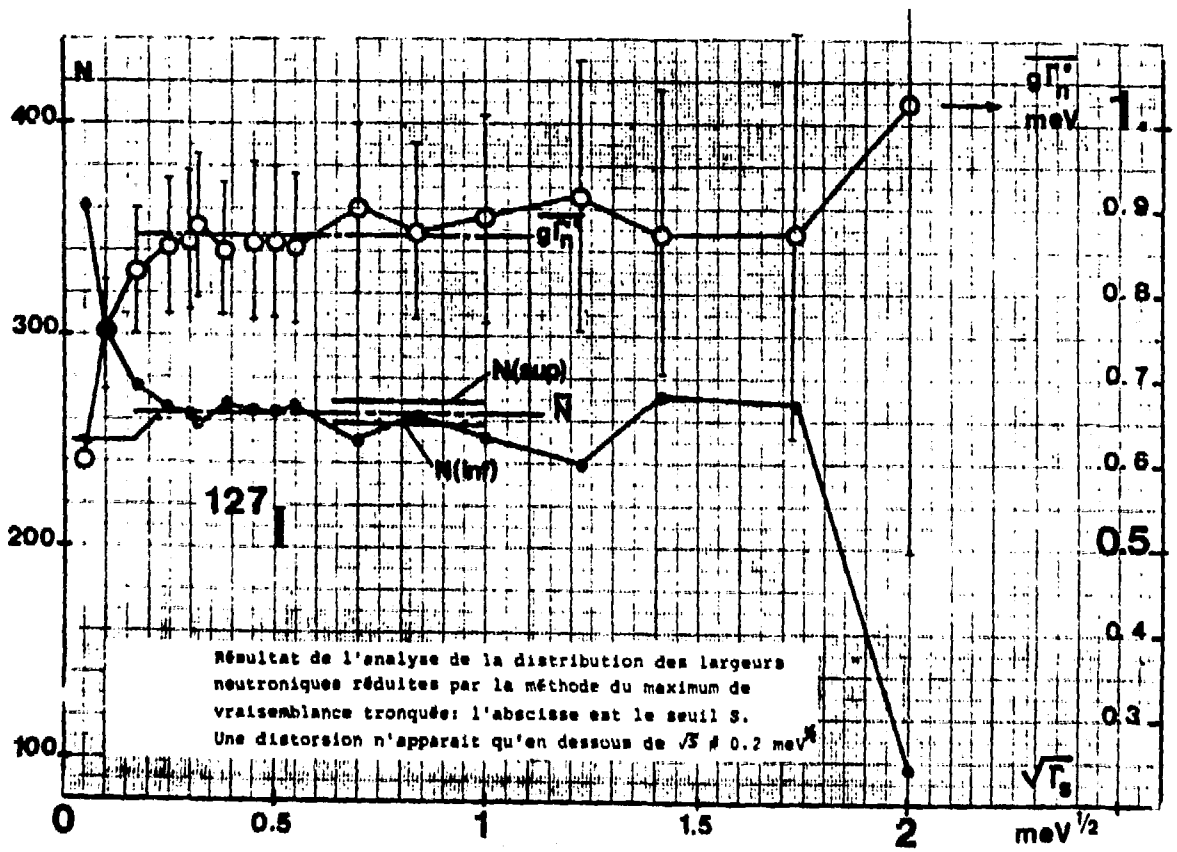

Fig. 5 Plot of an application of the ESTIMA code to ^{127}I.

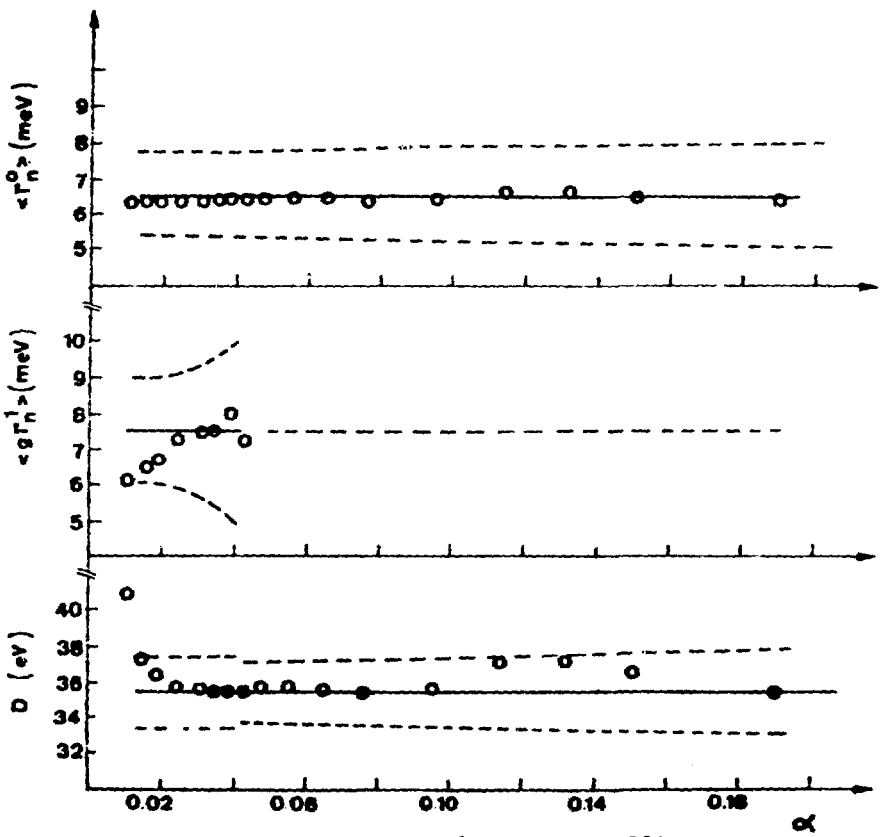

Fig. 6 Estimates of $\langle \Gamma_n^o \rangle$, $\langle g\Gamma_n^1 \rangle$ and D for ^{156}Gd versus threshold parameter α. Curves are Monte Carlo results for the averages and rms deviations.

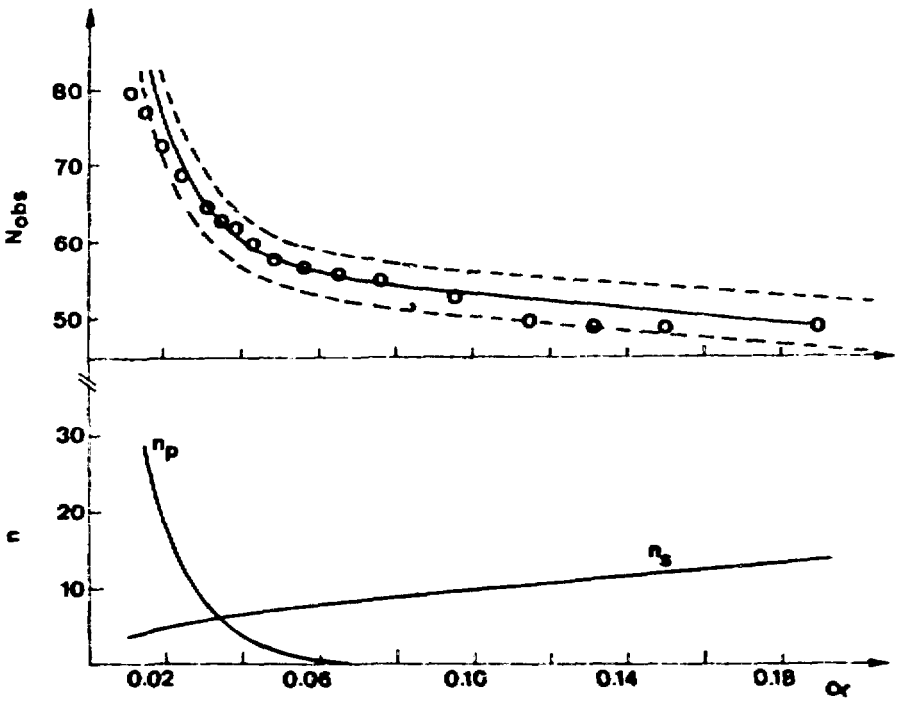

Fig. 7 The expected numbers of N_{obs}, n_s and n_p versus threshold parameter α from the fit to the experimental data of ^{156}Gd and Monte Carlo simulations.

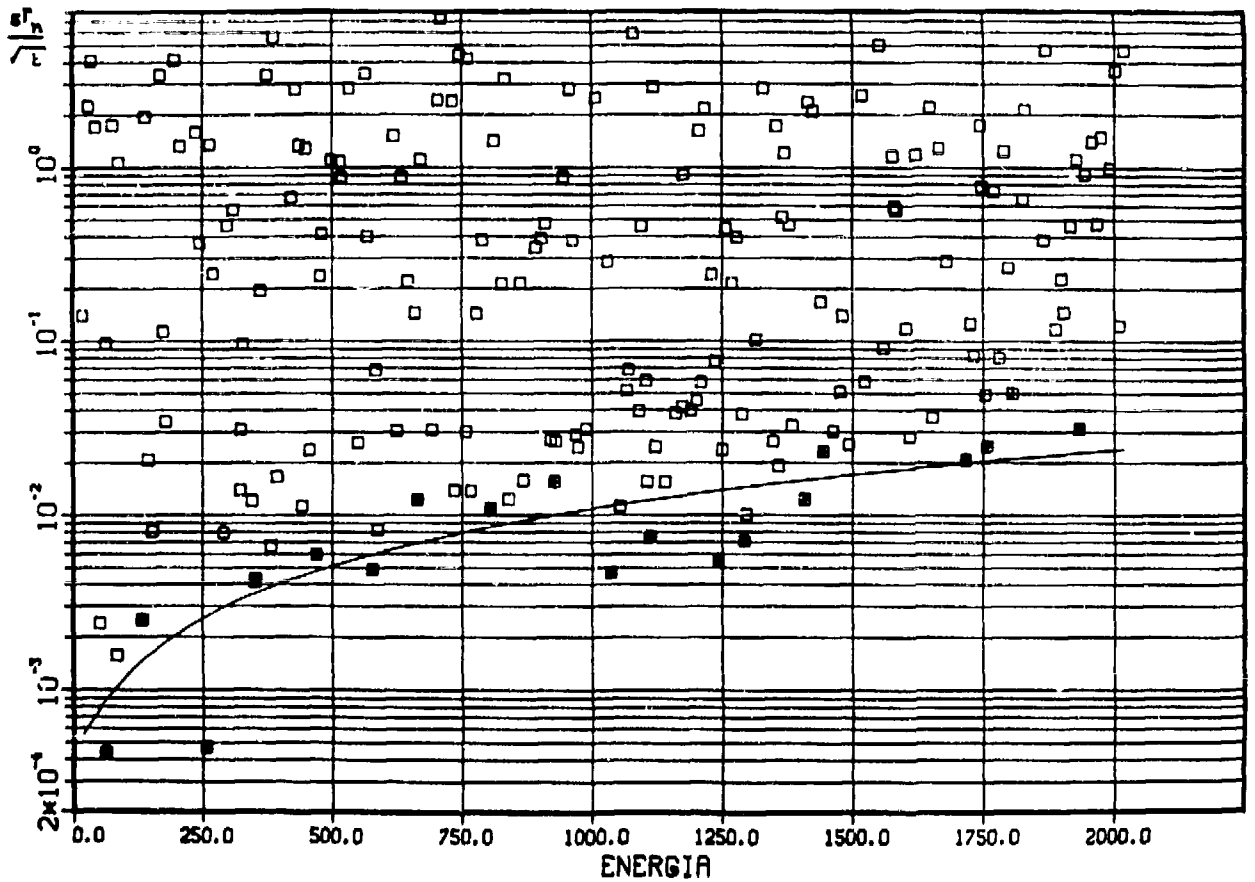

Fig. 8 Values of $g\Gamma_n/\sqrt{E}$ for ^{127}I. The threshold function $n_o(E)$ was fitted through the points indicated with a cross.

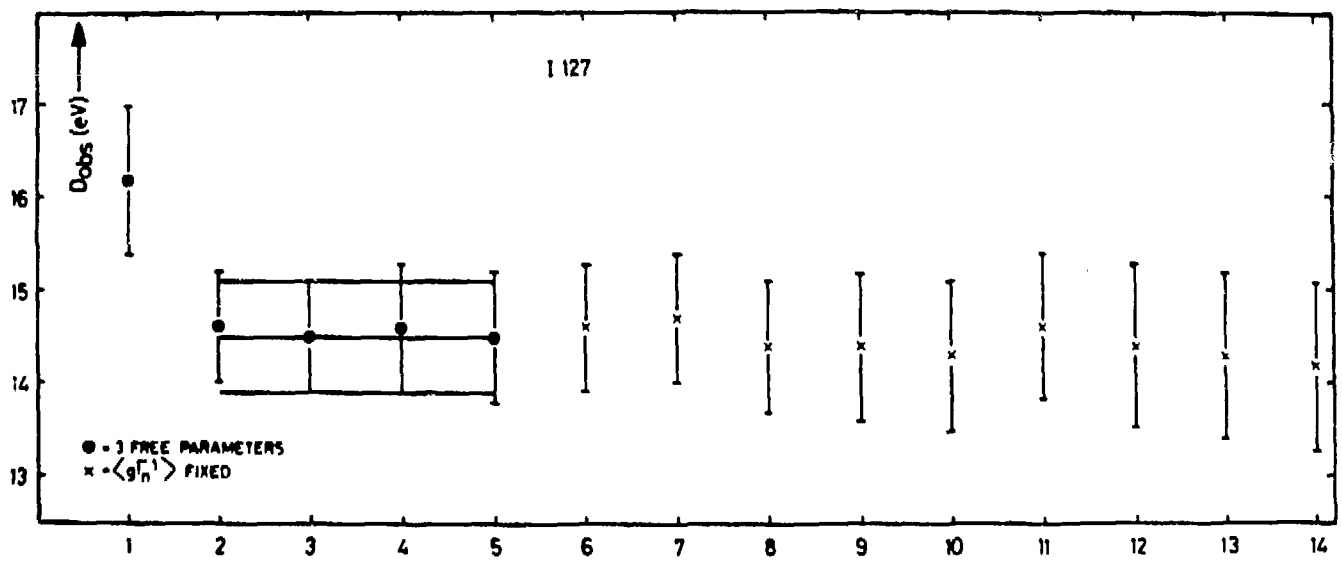

Fig. 9 Values of the average spacing D for ^{127}I versus the threshold multiplication factor t. Points marked with a circle were obtained without a fixed value of $sg\Gamma_n^1>$.

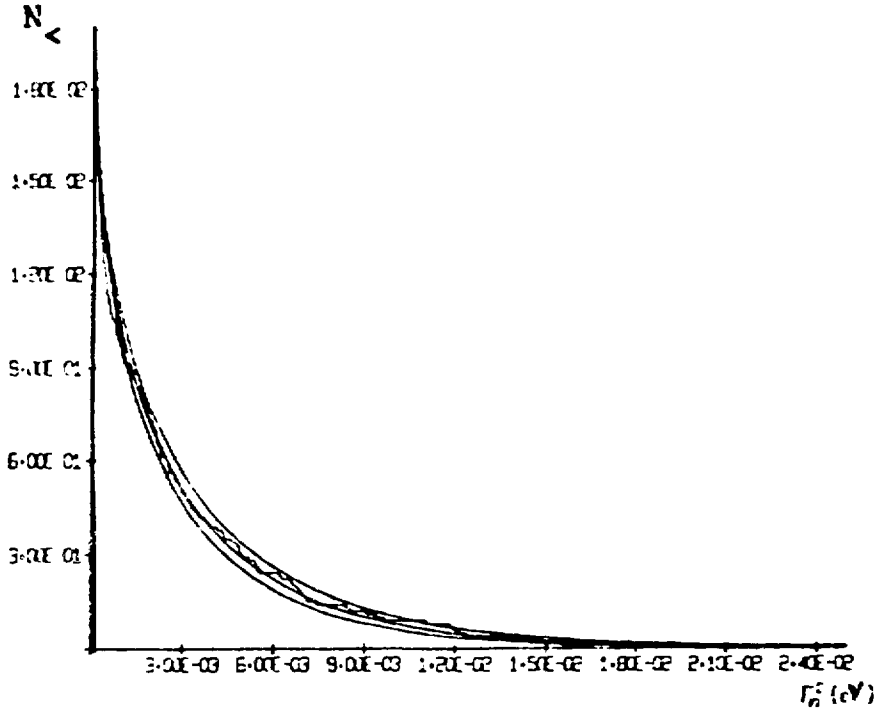

Fig. 10 Observed reduced neutron width distribution for ^{238}U (histogram) and integral Porter-Thomas distributions (smooth) calculated from best estimate of $\langle \Gamma_n^o \rangle$ and from its confidence limits (an application of the STARA code).

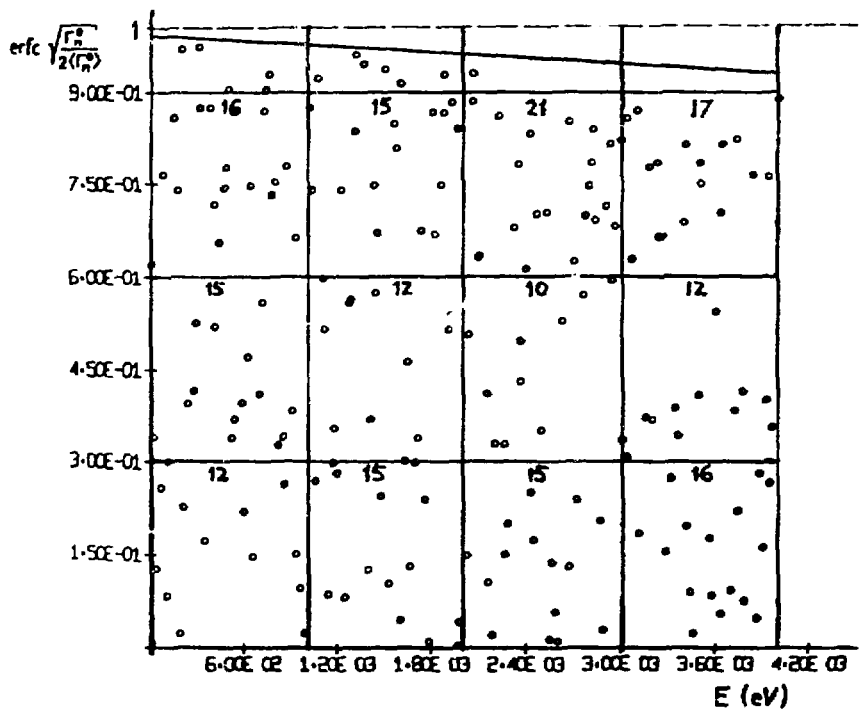

Fig. 11 Plot showing uniform distribution of levels in E-U plane and estimated observability threshold for ^{238}U.

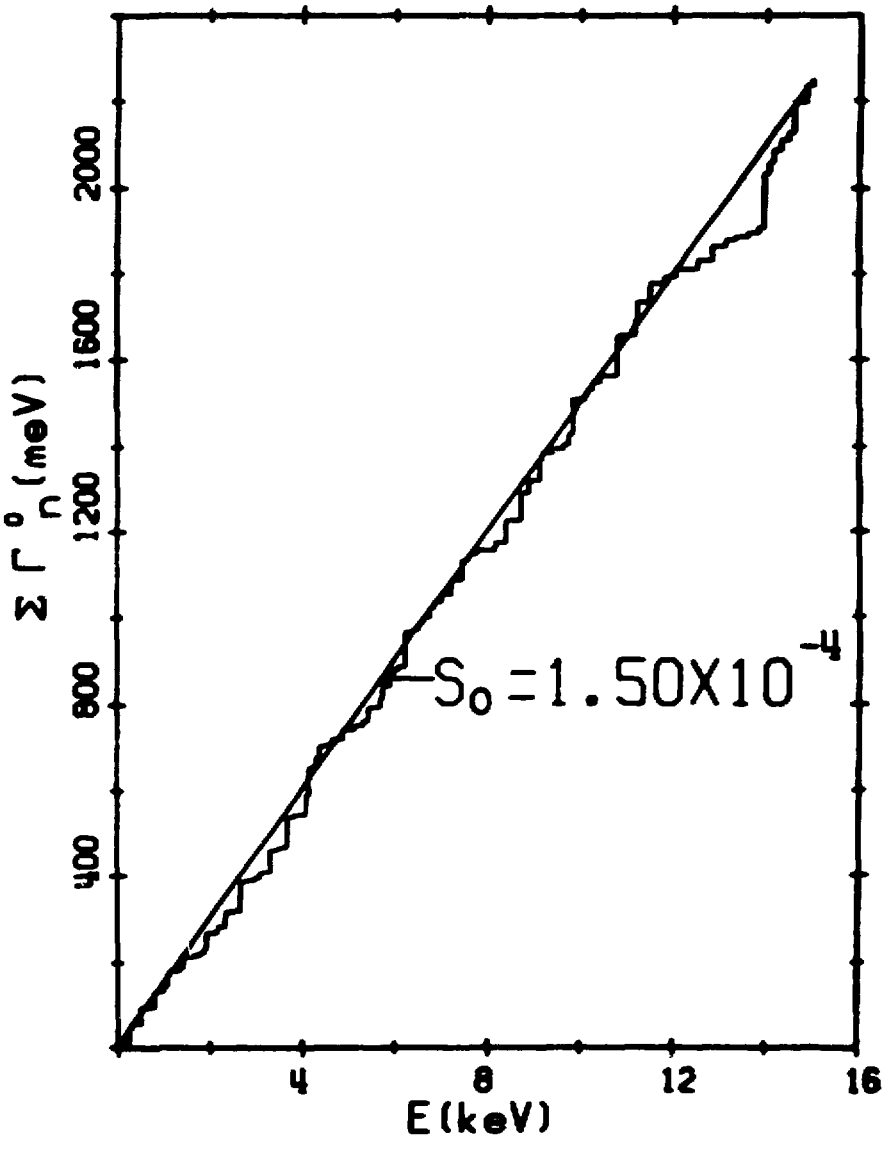

Fig. 12 Plot of $\Sigma\Gamma_n^o$ vs energy for ^{168}Er. The slope of the average straight line gives the s-wave strength function.

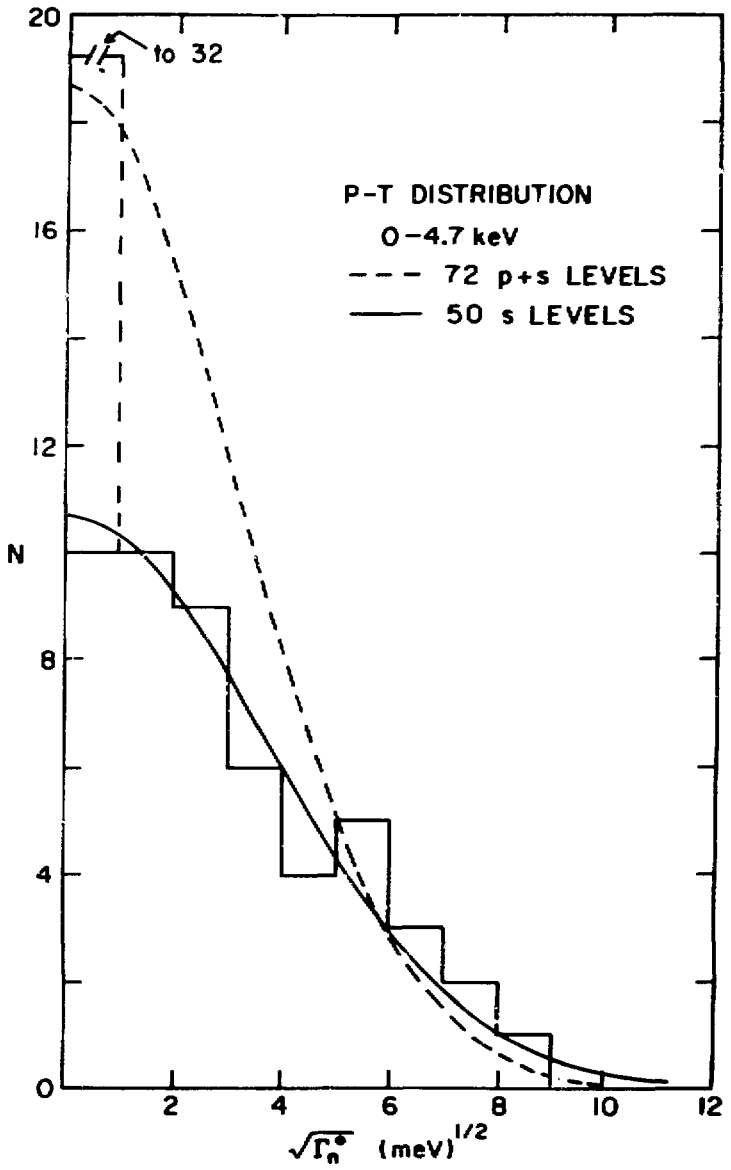

Fig. 13 Distribution of $\sqrt{\Gamma_n^o}$ values for ^{168}Er to 4.7 keV. The dashed and solid curves represent the Porter-Thomas distributions separately with N=72 and 50, subject to S_o= 1.5×10^{-4}. Fifty is the final iteration value for the total number of s-wave levels.

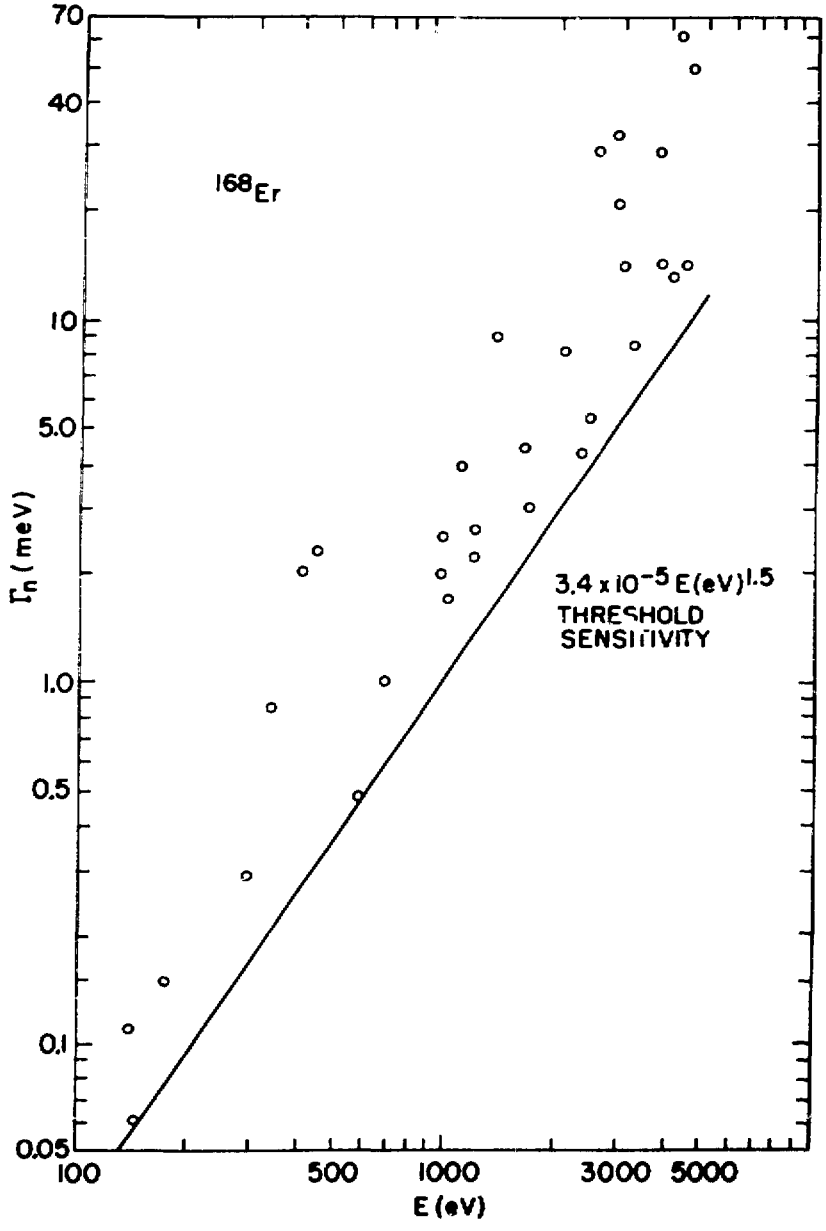

Fig. 14 Plot of Γ_n vs E for ^{168}Er weak levels to 4.7 kev. Shown also is a straight line representing the estimated threshold sensitivity (αE^{1-5}).

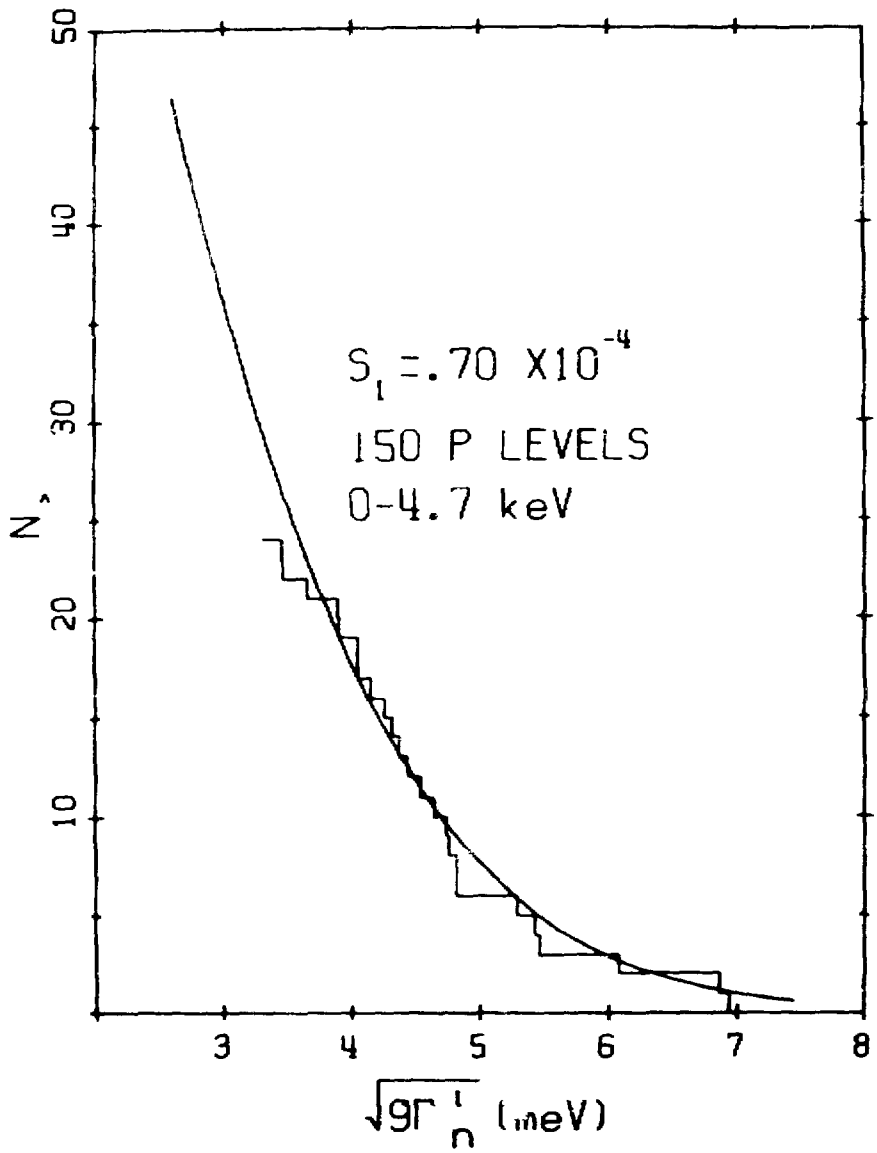

Fig. 15 Distribution of $\sqrt{g\Gamma_n^l}$ values for those ^{168}Er levels chosen as p-wave. The fit Porter-Thomas integral curve is subject to $S_1=0.7\times10^{-4}$ and $N_p=150$.

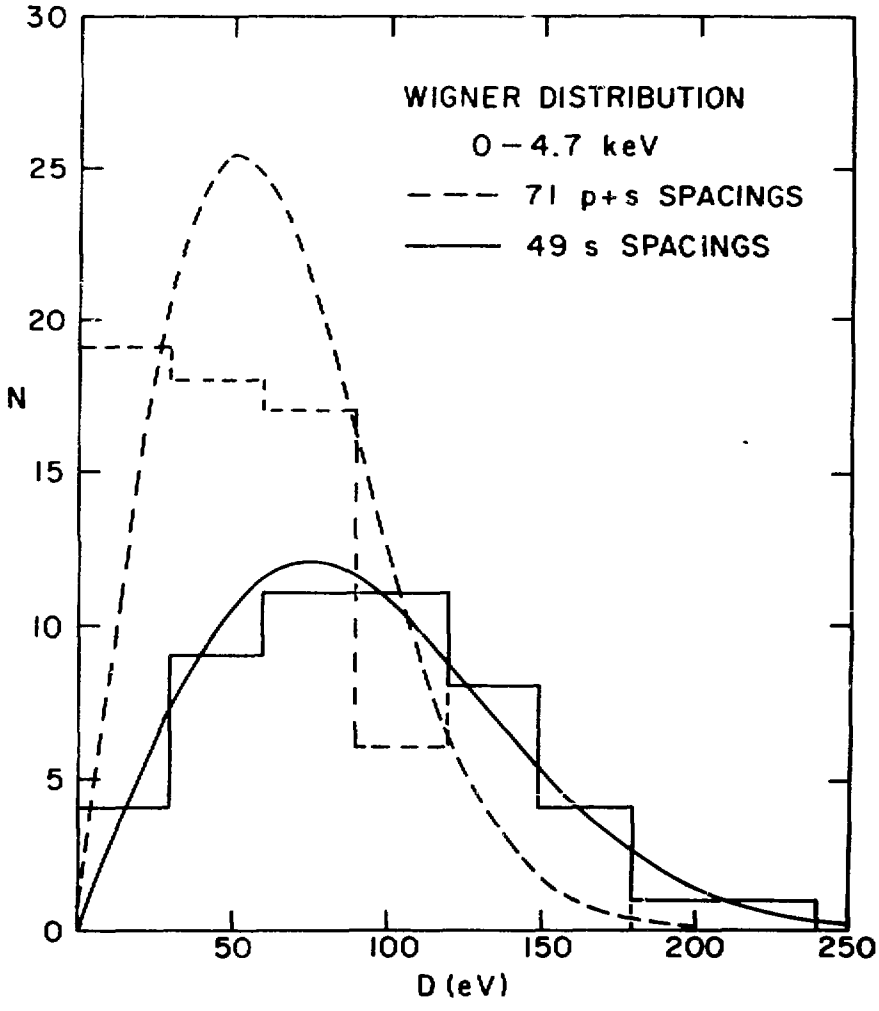

Fig. 16 Distributions of the adjacent level spacings for ^{168}Er to 4.7 kev, compared with the Wigner distributions. The dashed lines are for all measured levels, while the solid lines for the selected s-wave levels.

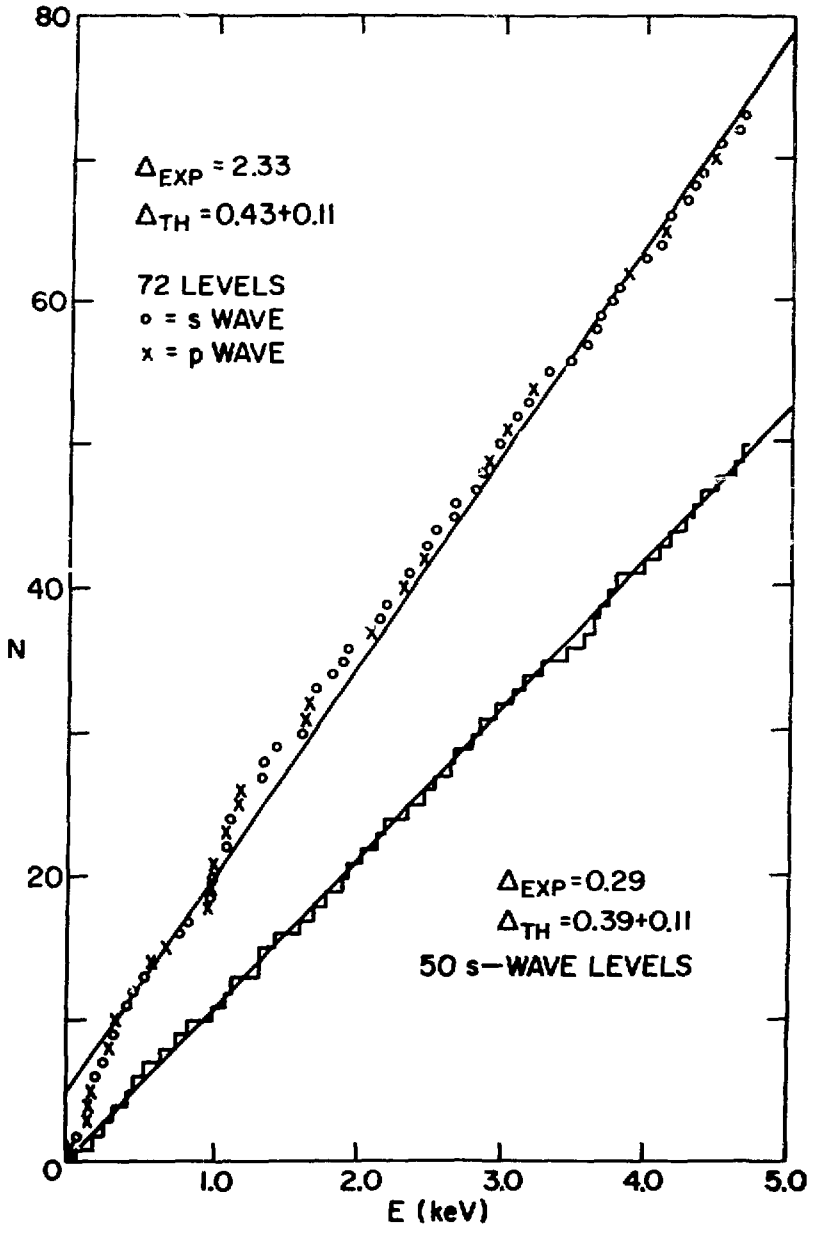

Fig. 17 Comparisons of N vs E for ^{168}Er with the best fitting straight lines for Δ_3 statistic. Shown are two cases fitted to all measured levels and to the selected s-wave levels.

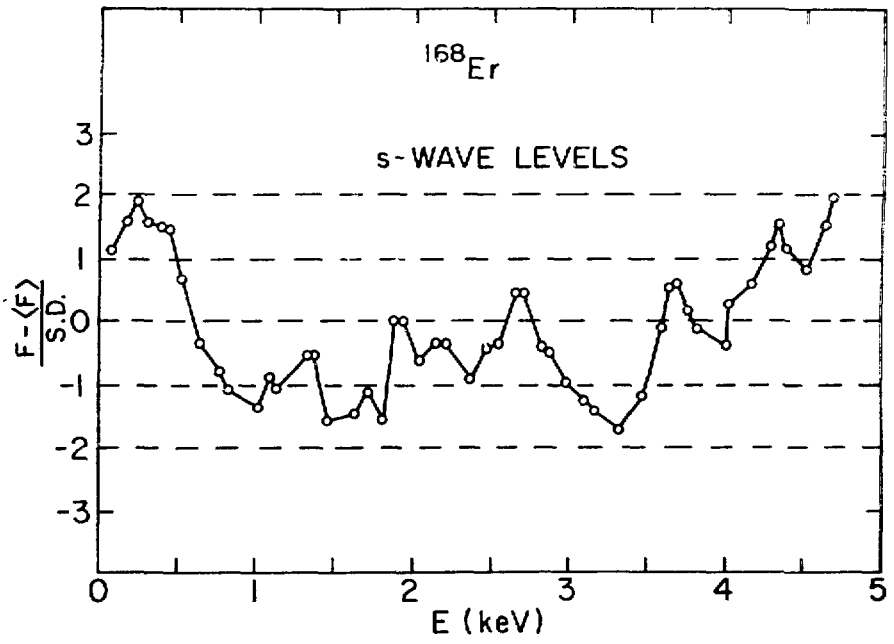

Fig. 18 Plot of the F statistic test for the 50 selected s-wave levels in ^{168}Er to 4.7 keV, where the ordinate expresses F-<F> in units of the expected S.D.

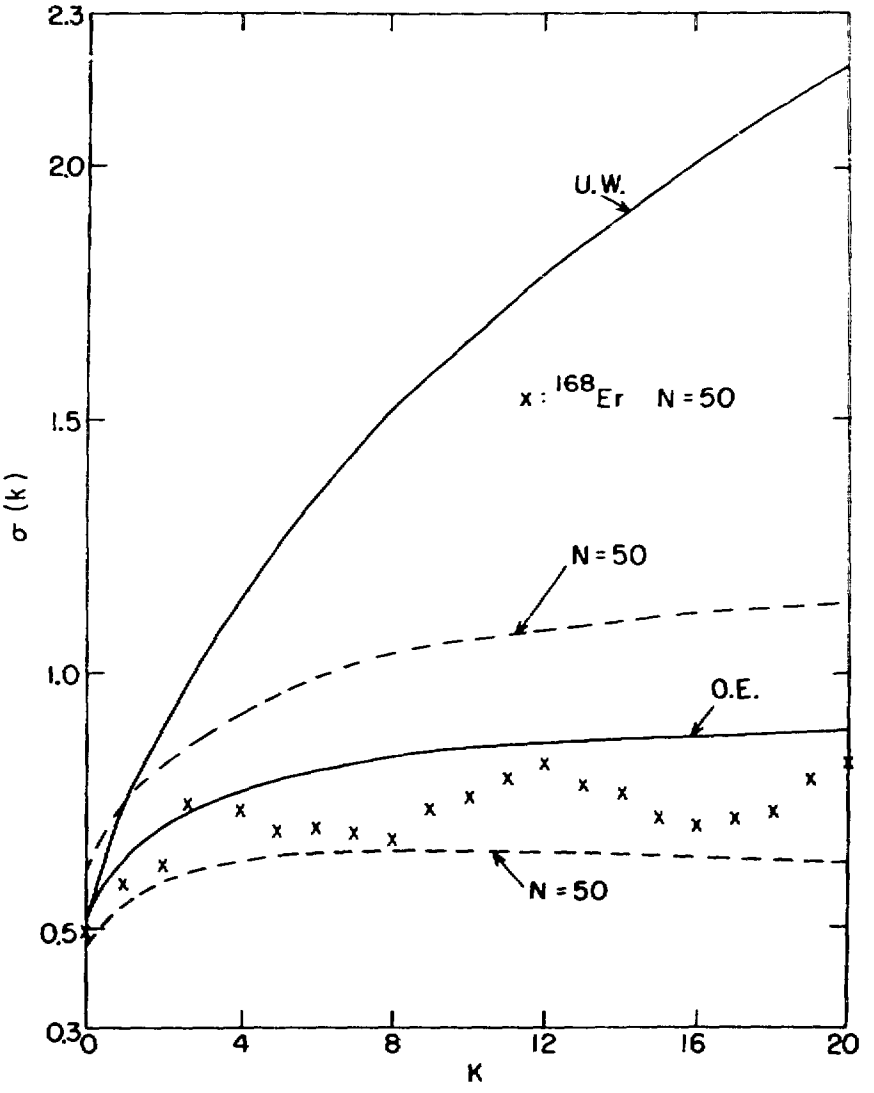

Fig. 19 Comparison of σ(k) vs k for the sequence of ^{168}Er s-wave levels with Monte Carlo results. σ(k) is the mean S.D. of the spacing of levels having k levels between them in units of <D>. The solid curves display the mean σ(k) corresponding to the O.E. and U.W. cases. The dashed curves represent the 10 and 90% confidence limits for the O.E. case.

Discussion

Menapace:

In the method utilized in the CAVE Code by Stefanon, a rigorously deduced expression of the error in the mean parameter estimate is given and the validity has been verified by Monte Carlo generation procedure. My question concerns the expression for the error in the other methods you mentioned and whether similar checking procedure was applied.

Liou

I believe that the error expression derived by Coceva and Stefanon can also be applied to other maximum likelihood methods provided that there are no unresolved resonances above the threshold. In the method of applying Bayes' theorem to set a threshold, the present author graphically expressed the fractional uncertainty of $\langle D \rangle$ in terms of S_{bias}/S and the total number of s-wave levels above threshold by using a similar Monte Carlo procedure. The method testing both level widths and positions may yield, in some favorable cases, less uncertainty than the maximum likelihood method. Methods of least squares fitting and missing level estimator are simpler procedures but may turn out larger uncertainties.

Menapace

I would like to comment that the CAVE code is made available to anybody upon request.

Froehner

I wish to make a remark concerning the Keyworth-Moore missing level estimator. As published and as shown by Liou it contains a cut-off value of 1/4. There is, in fact, nothing magic about this value, and one can easily generalize the prescription to other values which may more closely correspond to the observability threshold of a particular experiment.

Liou

I fully agree that the cut-off value, 1/4, is not a magic number. A user should adjust the value to fit his particular data.

Moore

I might remark that we have even generalized it to use a variable cut off. At any rate, the comment I want to make has to do with an exercise proposed by Pierre Ribon to test these various methods of determining level densities. Ribon proposes to generate a set of resonance energies by random matrix diagonalization, neutron widths by Monte Carlo samplings from the Porter Thomas distribution, and generation of a set of representative cross sections that will be analyzed to obtain resonance parameters. These data will be distributed and analyzed by various experimenters/evaluators, using their favorite techniques to obtain the level density. The results of this exercise should lead to a recommended method of data analysis.

Mughabghab

Thank you, Michael, for pointing out the Ribon exercise of average level spacings. (See Proceedings of the Specialists' Meeting on Neutron Cross Sections of Fission Product Nuclei held at Bologna, Italy Dec. 12-14, 1979, NEANDC(E)209 "L") I may remark that the National Nuclear Data Center has a copy of the generated data. Anybody interested in participating in this exercise can write to the NNDC and will be supplied with the data.

GENERAL REVIEW AND DISCUSSION (SESSIONS V-VIII)

J.J. Schmidt, IAEA

SUMMARY REVIEW SECOND DAY (23 September)

(Standards, Thermal Region, Resolved Resonance Region, Unresolved Energy Region)

J.J. Schmidt

Nuclear Data Section
International Atomic Energy Agency
Vienna, Austria

A wealth of material and a wealth of problems were brought together today. Let me start by dividing today's papers into two groups, one group consisting of the papers by Poenitz and Bhat and a second group consisting of all other papers (dealing essentially with resonance and thermal neutron cross section problems). The reasons for this split are twofold. First, the first two papers contain particularly "hot" material for discussion later. Second, the methods and requirements discussed by Poenitz and Bhat will very probably not be particularly applicable in the resonance range.

Let me start by reviewing some of the highlights of the second group of papers. In a lucid presentation, Mughabghab explained a number of good reasons why it is still interesting to study thermal neutron cross sections. Classical areas of importance are certainly the thermal reactor fuel cycle and burnup and the normalization of relative cross section measurements at energies above the thermal. Two other fruitful areas of research are the relationship between thermal neutron cross sections and fundamental nuclear structure properties (such as the properties of light nuclei levels below neutron binding energy) and the derivation of astonishingly reliable thermal neutron capture cross section values from measured γ-ray transition strengths.

In the ensuing discussion, Lone emphasized the need for a reliable chemical analysis of the samples used in thermal capture research since an unknown or inaccurately known admixture of a material with a high thermal capture cross section could lead to a serious interpretation problem.

Froehner gave a concise and systematic review of the current progress in numerical resonance analysis. His most important message can be put into one short statement: use the Reich-Moore formula! The multi-level Breit-Wigner formula and the Adler-Adler formula have the distinct drawback of not fulfilling the unitarity condition, whereas the Reich-Moore approach is very close to unitarity. The open problem in the practical use of the Reich-Moore formula, i.e. that it did not allow the use of the well known Voigt profiles for the description of resonance Doppler broadening, could be overcome by using a method developed by Turing almost 40 years ago. The method allows much faster

calculations of Doppler-broadened resonance cross sections with the Reich-Moore formula. Froehner also demonstrated, in several cases, the possibility of a fit of the energy dependence of neutron cross sections in the thermal range with the assumption of only one "negative" resonance per spin state as opposed to two or more "negative" resonances used in the past.
In a vivid talk, Block gave an insight into all the intricacies connected with converting measured transmission into total cross sections, i.e. sample thickness, background, resolution, dead time in electronics and other corrections needed and last but not least, the formalism used to interprete transmission data. The conclusions from his talk are essentially questions. Is it important in evaluation for a reactor application to consider Bragg scattering at low neutron energies? He showed examples of evaluations where this was simply ignored with the result that the evaluated data differed significantly from experiment at very low neutron energies. Another question one should pay attention to: are there real correlations between neutron capture widths and the scattering radius?

Block then stressed the importance of measurements in the energy range of unresolved resonances which could be used as "semi-integral" data to determine average resonance parameters for s- and p-wave neutrons. While this is a rather classical method, more information can be drawn from today's more detailed and sophisticated measurements (e.g., the recent spin-dependent ^{235}U fission cross section measurements performed at LASL). In addition, filtered beams could be used as a sort of benchmark for high resolution time-of-flight resonance measurements (e.g., the 2 keV filtered beam for a sequence of ^{232}Th resonances).

In the context of average resonance parameters, Moldauer's review talk centered around the problem of removing the dependence on energy and channel radius from s- and p-wave neutron strength functions. Liu gave a short summary on nine different methods for the evaluation of nuclear level densities, their merits and faults. The discussion did not lead to a conclusion as to the best method to be used. The hope was expressed that the NEANDC-supported "Ribon-project" for the derivation of average level spacings from resolved resonance data will shed some light on this problem. Moore emphasized the desirable properties of nuclear level density calculations such as an appropriate single particle potential, pairing correlations, configuration mixing, residual forces (e.g., quadrupole interactions) and others. Moldauer drew our attention to a new approach to level density calculations by French et al., which is still not as well known as it deserves to be. In summary, as Peelle and Froehner put it, we still do not have concise ideas about the energy dependence of nuclear level densities nor the spin dependence of the capture widths, and resolved resonance investigations do not provide much guidance to the cross sections and average parameters in the unresolved resonance range.

Now let me come back to the first two papers by Poenitz and Bhat. After having listened to these two talks and all the other talks I discussed before, I feel compelled to stay with my assertion of yesterday evening that evaluation is not only an art, but also a science in the sense that it uses scientific criteria, judgement and methods. Poenitz and Bhat put the whole problem clearly into perspective. In a nutshell, both of them aim at systematizing the evaluation process, replacing subjectivity in judgement and methods by objective criteria and mathematical procedures. This is certainly necessary and may go a long way. However, one should not forget that sometimes the judgement of a good physicist experienced in a given area of research without any mathematical inference, may come closer to the truth than a scientist who has to rely on second-hand information, though having all the mathematical machinery on hand.

Let me now briefly go through what Poenitz detailed in his talk. What one needs in an evaluation first, is carefully prepared input, i.e.,all data on all types of relevant measurements including differential cross sections and cross section shapes, average cross sections, cross section ratios and ratio shapes, standards etc. Normally, one has more measurements, i.e. more information available, than one actually needs and one is faced with an overdetermined problem that has to be put into mathematical terms. As a second step in input preparation one has to detail all types of statistical and systematic errors, the most important and simultaneously the most difficult ones being the unknown, accidental, and psychological errors. I should like to stress the importance of the psychological error, which, according to Poenitz, consists of the fear of an experimenter, who measures a quantity for the $(n+1)^{th}$ time, that he will deviate from his n predecessors outside experimental error, with the consequence that he will either neglect searching for additional error sources or he will search for mono-directional corrections only. Another type of psychological error can very easily influence the evaluator himself. He may, even subconsciously, differentiate between friends and others, or, on a more objective level, between whom he considers to be good physicists and bad physicists. Incidentally, the evaluator may eventually be right, but he should certainly try to be more objective.

While systematic errors such as psychological errors are very difficult or impossible to assess, there exist factual correlations between different measurements e.g. common normalization, detectors, or samples, which principally should be taken into account and, which can be quantified and cast into physically meaningful variance-covariance matrices. The remaining part of the evaluation is then essentially mathematics where the classical least squares estimation continues to be the best recommendable method. However, here we run into a size problem. Biased and subset estimations will have to be introduced in order to reduce the monstrous variance-covariance matrices to a size still manageable on today's largest computers.

Bhat first gave an outline of three commonly used, partially theory-based evaluation methods; the phase shift method (as applied for example to the hydrogen scattering cross section), the R-matrix theory (as applied for example by Hale to the consistent interpretation of light nuclei cross sections) and the coupled-channel method (as applied for example in inelastic excitation cross section calculations). For each method, he specified a physical model, the data types to be used, the calculational model and some associated problems. I would like to stress the importance of the physical model since, as Bhat explained, it may allow discovery of discrepant data sets and inconsistencies in the evaluation

Bhat then went on to discuss three areas of problems and needs for a successful implementation of the above evaluation schemes. He first requested the experimenter to provide full documentation, including variance-covariance matrices for his experiments. While agreeing with the need for full documentation, strong doubts were expressed in the audience as to whether variance-covariance matrices should be provided by the experimenter. I shall come back to this point in a moment. The second requirement which I would strongly underline is to make an in-depth error analysis in the experimental planning phase. Third, Bhat requested that future evaluations use variance-covariance information, present an objective analysis, produce variance-covariance matrix files, analyze cross section standards in a consistent manner, and finally, be fully documented. While agreeing with most of this I should like to re-iterate that subjectivism may not always be fully avoidable and occasionally may even be desirable. I would again put a question mark on the variance-covariance argument.

In conclusion I feel that we are faced with three major problems.

1. Should experimentalists in the future be asked to produce variance-covariance matrices from their own experiments? I strongly concur with Poenitz and Peelle that the experimentalist should not provide variance-covariance matrices, but a component breakdown of his statistical and systematic errors. These error components should be compiled by the data centers and made available to evaluators who would convert them to variance-covariance matrices. Even here a slow pace is recommended with selected important but limited data areas such as neutron standard reference cross sections, where the need for a detailed specification of error components and correlations is apparent. If the measurer provides variance-covariance matrices, this would have the decisive drawback that information will be lost which will be very difficult, if not impossible to recover when comparing and evaluating different measured data. This would also put a heavy additional burden on all neutron data centers, i.e. to devise a non-trivial extension of the present EXFOR system

to compile and exchange variance-covariance matrices, thus overloading the EXFOR files.

2. This latter remark leads me to the second problem. Most of present-day experiments are rather complex and, as appropriate as it may be to have all conceivable detail on all experiments, should an experimentalist really specify all the information behind what Alan Smith called an "airplane crash" i.e., a finished experiment? There are limits, one should be practical, and one has to set priorities.
3. The third problem concerns the decision between re-evaluation of a given set of experiments or a new much more accurate experiment, when the users are not satisfied with the available data. A more accurate experiment is usually very expensive these days and may need a lot of development work. Because of finite resources and manpower one would choose this solution only in important cases. On the other hand the value of a reevaluation of a given set of experiments is intimately bound to the detection and elimination of more systematic errors inherent in the experiments than in previous evaluations. To quote an example: about ten years ago Poenitz performed an evaluation of the ^{235}U fission cross section. It was a brilliant work, because it turned out in his re-evaluation ten years later with incorporation of the lot of measurements performed in the meantime, that he was right ten years earlier. Then the question inevitably arises; what was the worth of all these measurements if they did not lead to a real gain in knowledge? One positive answer to this question is that the errors were brought down, and one has gained confidence in the previously evaluated data.

The whole problem resides in the existence of systematic errors, which I think are the real concern and stimulus behind Perey's theory. Take the ideal case when all experimenal errors would be only statistical. In that case, one could advise doing as many measurements as could be afforded, and if the next experiment is statistically more accurate than the last one, even better, because every new experiment will help to bring the combined error down. The real situation is closer to the opposite extreme. The situation in today's experiments is often that the statistical errors are rather small and that systematic errors are predominant. If that is the case, then a new experiment may risk adding to the systematic errors and thus not help the situation unless the experiment is extremely carefully planned and proven to be much better than the previous ones. Here again, we run into the problems of prioritization according to users' needs in view of resource limitations. So far we have only scattered attempts to develop a systematic theory of experiment planning. Professor Usachev and co-workers at

Obninsk in the Soviet Union were the first to start the development of such a theory (which you can study in several INDC reports translated by the IAEA from Russian into English (INDC(CCP)-19/U, -33/L, -46/L and -109/U)). I would like to end the present day's summary by expressing the hope that these developments and those of Perey and others may eventually provide us with a handle for the treatment of systematic errors and the planning of experiments.

R.W. Peelle With new facilities and techniques, it is not hard to find important cross section areas where experiments can be planned that can be expected to have a significant impact on the corresponding evaluations. Since no experimenter is so rich as to wish to waste his life, experiments try to focus on such cases. To have significant impact on the world situation following the experiment, it is necessary to anticipate that

a) In an important interval the new experiment will have uncertainties no larger than would a current evaluation of pre-existing information, or

b) The new experiment is sufficiently different from previous ones that important systematic errors would not likely be the same as in older experiments

Note that it is unnecessary and unrealistic to ask a new experiment to be 5 times better than previous ones! Also note the importance of seeking new experimental techniques even in times of diminishing support.

J.J. Schmidt: I should like to express my gratefulness to Mike Moore and Francis Perey for pointing out the time dependence of errors. An evaluator has to look into the question of whether errors quoted by experimentalists are really credible before he starts his mathematical procedures. We have had very good examples in the past, e.g. measurements of ^{252}Cf-$\bar{\nu}$, where various method-dependent errors in the individual experiments were discovered with the consequence that the measured values come to a closer agreement. I could quote a number of other examples, where careful evaluation helped to solve discrepancies.

U.S. GOVERNMENT PRINTING OFFICE: 624-090-854